

2018

The Sedimentary Record Of Eocene Deformation In The Interior Of The Southern Canadian Cordillera

Erica May Rubino
University of South Carolina

Follow this and additional works at: <https://scholarcommons.sc.edu/etd>

 Part of the [Geology Commons](#)

Recommended Citation

Rubino, E. M.(2018). *The Sedimentary Record Of Eocene Deformation In The Interior Of The Southern Canadian Cordillera*. (Master's thesis). Retrieved from <https://scholarcommons.sc.edu/etd/4649>

This Open Access Thesis is brought to you by Scholar Commons. It has been accepted for inclusion in Theses and Dissertations by an authorized administrator of Scholar Commons. For more information, please contact dillarda@mailbox.sc.edu.

THE SEDIMENTARY RECORD OF EOCENE DEFORMATION IN THE INTERIOR OF
THE SOUTHERN CANADIAN CORDILLERA

by

Erica May Rubino

Bachelor of Science
Bucknell University, 2015

Submitted in Partial Fulfillment of the Requirements

For the Degree of Master of Science in

Geological Sciences

College of Arts and Sciences

University of South Carolina

2018

Accepted by:

Andrew Leier, Director of Thesis

David Barbeau, Reader

James Kellogg, Reader

Cheryl L. Addy, Vice Provost and Dean of the Graduate School

© Copyright by Erica May Rubino, 2018
All Rights Reserved.

ACKNOWLEDGEMENTS

I would like to extend my thanks and appreciation to my advisor, Dr. Andrew Leier, for his support, encouragement, and guidance throughout the progression of this project. I would also like to thank my committee members, Dr. David Barbeau, and Dr. James Kellogg, as well as my collaborators including Dr. Elizabeth Cassel, and Dr. Bruce Archibald for their guidance and comments. Thank you to my fellow graduate students and friends at the University of South Carolina, especially John Chesley for his assistance with the collection of this data in the field. Thank you also to my family and friends, who have supported me throughout my academic career.

Additional funding for this project was provided by the Geological Society of America Graduate Student Research Grant, and the Suzanne Takken Memorial Grant from AAPG.

ABSTRACT

Eocene sedimentary strata exposed in the interior of the southern Canadian Cordillera (SCC) in British Columbia (BC) and northernmost Washington (WA) record a poorly understood history of extension-related deformation in the hinterland of the orogen. Today these strata are exposed in isolated, distinct outcrop belts, although the nature of the original basin(s) is unknown. We examined 650 m of Eocene strata, analyzed 2,995 detrital zircons for uranium-lead (U-Pb) ages, and measured 67 detrital zircons for Hf isotope systematics in an effort to better understand the physiography of the SCC during this time period. Eocene strata consist of clast- and matrix-supported conglomerates, very fine- to very coarse-grained sandstones, mudstones, and coal that were deposited in fluvial, alluvial fan, lacustrine, and paludal environments. Sandstone samples from across the region contain large populations of detrital zircons with Eocene (ca. 51 Ma) and/or Jurassic (ca. 160) U-Pb ages, which are interpreted to have been derived from the erosion of the Eocene Challis-Kamloops volcanics, and Mesozoic-age batholiths, respectively. Maximum depositional ages (MDA) of the Eocene strata are relatively uniform throughout the region, with most MDA between 47-50 Ma. ϵ_{Hf} values of ~50 Ma detrital zircons extracted from samples collected in 3 locations (Merritt, BC, Kelowna, BC, and Republic, WA) across the SCC vary between -16 to +14. Detrital zircons from strata in Republic, WA, in the east of the study area, have primarily negative ϵ_{Hf} values, with one positive value (-16 to +7), indicating derivation from relatively evolved sources. Detrital zircons from strata in Merritt, BC, in the west of the study area,

have positive ϵ_{Hf} values, with one negative value (-2 to +13), indicating relatively juvenile sources. Detrital zircons from Kelowna, BC, in the central part of the study area have bimodal ϵ_{Hf} values, with both positive and negative populations (-10 to +12). ϵ_{Hf} values correspond to the depositional location relative to the strontium (Sr) 0.706 isopleth. The localized changes in sedimentary facies, the variability in ϵ_{Hf} values of 50 Ma detrital zircons, and the local variations in detrital zircon U-Pb ages indicate Eocene sedimentary strata in the hinterland of the SCC were deposited in multiple, isolated basins separated by paleotopographic highs, and not in a single continuous hinterland basin. The MDA data and existing constraints suggest these basins formed across the SCC at approximately the same time, although the basins to the east formed in traditional grabens, those in the central portion formed in a supradetachment basin, and those in the west are associated with strike-slip faulting. The regional transtensional stress field is attributed to the subduction of an oceanic spreading center beneath the SCC during the Eocene, which resulted in oblique subduction along this portion of the North American margin.

TABLE OF CONTENTS

Acknowledgements	iii
Abstract	iv
List of Figures	ix
List of Abbreviations	xi
Chapter 1: Introduction	1
Chapter 2: Background	12
2.1 Regional tectonic setting	12
2.2 Cordilleran hinterland and deformation	14
2.3 Eocene strata	16
2.4 Climate and paleoelevation estimates	17
Chapter 3: Methods	19
3.1 Field data and sampling	19
3.2 Detrital zircon U-Pb geochronology	19
3.3 Detrital zircon Hf systematics	21
Chapter 4: Results	33
4.1 U-Pb results	33
4.2 Hf results	43
Chapter 5: Analysis	46
5.1 U-Pb age populations and sediment sources	46
5.2 Maximum depositional ages	49

5.3 Comparing age populations.....	50
5.4 ϵ_{Hf} interpretations.....	52
Chapter 6: Discussion	59
6.1 Southern Canadian Cordillera Intermontane Basins	59
6.2 Provenance	61
6.3 Implications for geodynamic and tectonic models.....	63
6.4 Modern Analogue.....	66
Chapter 7: Conclusion.....	71
References.....	73
Appendix A: USC Rock Preparation Laboratory & CEMS U-Pb Analyses	95
A.1 Sample Preparation.....	95
A.2 Laser-Ablation Mass Spectrometry	97
A.3 Post-Acquisition Processing & Data Reduction.....	98
A.4 References	100
Appendix B: CEMS Detrital Zircon U-Pb Analyses Data Table	101
Appendix C: Detrital Zircon U-Pb KDE (blue) & PDP (black) plots separated by sample (0-500 Ma, and 0-2,400 Ma).....	120
Appendix D: Detrital Zircon U-Pb KDE (blue) and PDP (black) plots separated by location (0-2,400 Ma)	164
Appendix E: Arizona LaserChron Center U-Pb and Hf Analyses.....	175
E.1 U-Pb geochronologic analyses of detrital zircon (Nu HR ICPMS).....	175
E.2 Hf analytical methods at the Arizona LaserChron Center	178
E.3 References.....	180
Appendix F: Arizona LaserChron Center Detrital Zircon U-Pb Analyses Data Table ...	182

Appendix G: Arizona LaserChron Center Detrital Zircon Hf Analyses Data Table196

Appendix H: Detrital Zircon U-Pb Maximum Depositional Age Data and Graphs198

LIST OF FIGURES

Figure 1.1 Southern Canadian Cordillera overview	5
Figure 1.2 Tectonic setting ca 50 Ma.....	6
Figure 1.3 Structural setting of the southern Canadian Cordillera	7
Figure 1.4 Eocene formation chart.....	8
Figure 1.5 Lithologic photographs.....	9
Figure 1.6 Measured sections part I.....	10
Figure 1.7 Measured sections part II.....	11
Figure 3.1 KDE and PDP for all U-Pb data from Republic, WA	22
Figure 3.2 KDE and PDP for all U-Pb data from Midway, BC	23
Figure 3.3 KDE and PDP for all U-Pb data from White Lake, BC	24
Figure 3.4 KDE and PDP for all U-Pb data from Summerland, BC	25
Figure 3.5 KDE and PDP for all U-Pb data from Kelowna, BC	26
Figure 3.6 KDE and PDP for all U-Pb data from Princeton, BC.....	27
Figure 3.7 KDE and PDP for all U-Pb data from Blakeburn, BC	28
Figure 3.8 KDE and PDP for all U-Pb data from Kamloops, BC	29
Figure 3.9 KDE and PDP for all U-Pb data from McAbee, BC	30
Figure 3.10 KDE and PDP for all U-Pb data from Merritt, BC.....	31
Figure 3.11 KDE and PDP for all U-Pb data from Coldwater, BC	32
Figure 4.1 Detrital zircon Hf data	44
Figure 4.2 Detrital zircon Hf data, separated by location	45

Figure 5.1 Map of SCC with pie charts of U-Pb ages	55
Figure 5.2 MDAs vs. Longitude	56
Figure 5.3 MDS plot of all U-Pb data, separated by location.....	57
Figure 5.4 MDS plot of all U-Pb data, separated by location, with synthetic ages	58
Figure 6.1 KDE and PDP for sample WLR1 from White Lake, BC	68
Figure 6.2 KDE and PDP for sample WLR2 from White Lake, BC	69
Figure 6.3 Paleogeography diagram of SCC during the Eocene	70

LIST OF ABBREVIATIONS

ALC.....	Arizona LaserChron Center
BC	British Columbia
CEMS.....	Center for Elemental Mass Spectrometry
Hf	Hafnium
KDE	Kernel Density Estimation
K-S	Kolmogorov-Smirnoff
LA-HR-SC-ICP-MS ..	Laser-ablation high-resolution single-collector inductively-coupled mass-spectrometry
MDA	Maximum Depositional Age
MDS.....	Multi-Dimensional Scaling
MSWD	Mean Square Weighted Deviation
OVSZ	Okanagan Valley Shear Zone
PDP	Probability Density Plot
SCC.....	Southern Canadian Cordillera
SL.....	Sri Lanka
Sr.....	Strontium
U-Pb	Uranium-Lead
USC.....	University of South Carolina
WA.....	Washington
Yb.....	Ytterbium

CHAPTER 1

INTRODUCTION

The Southern Canadian Cordillera (SCC; Figure 1.1) resulted from ocean-continent convergence and terrane accretion along the western margin of North America, and today represents one of the classic cordilleran orogenic systems in the world (Bally et al., 1966; Dahlstrom, 1970; Price, 1981; Armstrong, 1982; Monger et al., 1982; Brown and Read, 1983; Okulitch, 1984). Although the geologic history of the fold-thrust belt and foreland basin in the SCC is well documented (e.g., Price, 1981, 1986; Leckie and Smith, 1992; Miall, 1995), far less is known about the evolution of the hinterland of the orogen. This is particularly true for the Paleogene Period, a time when compressive stresses in the interior of the SCC gave way to extension and transtension. During this time, the SCC was located above a slab window associated with a subducted ocean spreading center (Figure 1.2; Thorkelson and Taylor, 1989; Breitsprecher et al., 2003). To the south, in the United States, the Farallon plate rolled back to the south-southwest (Figure 1.2; Dickinson, 1979, 2004; Humphreys, 1995, 2009); however near the SCC, the northern plate of the ocean spreading center (Resurrection plate) subducted obliquely beneath the North American margin with dextral relative slip (Haeussler et al., 2003; Madsen et al., 2006; Groome and Thorkelson, 2009; Eddy et al., 2016). A variety of deformation occurred in the SCC in response to the changing tectonic boundary conditions, including detachment faulting and core complex formation (Coney, 1980; Coney and Harms, 1984; Bardoux, 1985; Tempelman-Kluit and Parkinson, 1986;

McNulty and Farber, 2002; McClaughry and Gaylord, 2005; Giovanni et al., 2010; Brown et al., 2012), strike-slip faulting (Ewing, 1980, 1981a; Fyles, 1990; Schiarizza and Israel, 2001; Eddy et al., 2016), and high-angle normal faulting (Ewing, 1980, 1981a; Thorkelson, 1989; Suydam and Gaylord, 1997; Beatty et al., 2006). However, our understanding of the linkages between these features and the ancient physiography of the SCC hinterland during this period is limited, due in large part to the sparse amount of geologic data from this area.

The interior of the SCC contains outcrops of Eocene strata that were deposited concomitant with upper crustal faulting and extension (Figure 1.3). Today, these strata occur in discontinuous outcrops across the area (Figure 1.4) and consist of clastic sediments, ranging from boulder-conglomerates to mudstones and coal (Figures 1.4, 1.5, 1.6, and 1.7). Detailed and regional provenance data from these sediments do not exist, which prohibit reconstructions of hinterland physiography. Deposition in the hinterlands of modern cordilleran margins occurs in a variety of regional and isolated basins, and in an assortment of depositional systems (Horton, 2012). Although the outcrops in the hinterland are now isolated from one another, it is unclear if this was always the case. Similarly discontinuous outcrops of Eocene strata in the forearc of the SCC were once part of a single regional basin and were subsequently separated along strike-slip faults (Eddy et al., 2016).

We examined 16 outcrops across southern British Columbia (BC) and northernmost Washington (WA; which we include as part of the SCC) in order to better understand the Eocene history of this region. The specific aims of this study are to: 1) determine sediment provenance of the Eocene strata in the hinterland of the SCC; 2)

determine if the strata were deposited in isolated basins or one regional and continuous basin; and 3) determine maximum depositional ages (MDAs) of the strata in order to constrain the history of basin formation and upper crustal deformation. We collected 22 samples of Eocene strata from 11 locations (Figure 1.1; Table 1.1), and measured ~650 m of strata in the field, collecting information on grain-size and facies. Detrital zircons from the samples were analyzed using uranium-lead (U-Pb) geochronology and hafnium (Hf) isotopes, yielding a total of 2,995 U-Pb ages and 67 ϵ Hf values. In total, these data record a complex history of upper crustal deformation in the hinterland of the SCC during the Eocene.

Table 1.1 Table of all 22 samples, the location where they were collected, the location of analysis (ALC = Arizona LaserChron Center; CEMS = Center for Elemental Mass Spectrometry), the number of detrital zircon grains analyzed, and how many measured sections were collected at each location.

Sample	Location	N	W	U-Pb Analysis Location	Number of U-Pb grains analyzed	Hf Analysis Location	Number of Hf grains analyzed	Number of Measured Sections collected
15Ca01B	Republic, WA	48.643628	-118.737	ALC	308	ALC	15	2
15Ca03A	Republic, WA	48.6504	-118.74004	ALC	303	ALC	15	
15Ca04A	Republic, WA	48.80054	-118.641146	CEMS	99			
CAN-BC-1024K	Midway, BC	49.017517	-118.851738	CEMS	116			0
CAN-BC-1024L	Midway, BC	49.041733	-118.874149	CEMS	100			
WLR1	White Lake, BC	49.33061	-119.63216	CEMS	117			1
WLR2	White Lake, BC	49.32906	-119.62995	CEMS	111			
SKEL1	Summerland, BC	49.62039	-119.68225	CEMS	117			1
SKEL2	Summerland, BC	49.61897	-119.68025	CEMS	106			
CAN-BC-1023H	Kelowna, BC	49.8202	-119.649614	ALC	105	ALC	15	2
SAWMILL1	Kelowna, BC	49.8177	-119.65308	CEMS	100			
15Ca18A	Kelowna, BC	49.820189	-119.652825	CEMS	114			
PB2	Princeton, BC	49.537332	-120.52024	CEMS	108			4
15CAN10B	Princeton, BC	49.536941	-120.519624	CEMS	119			
15Ca15A	Princeton, BC	49.454832	-120.51075	CEMS	105			
Prince1A	Princeton, BC	49.45525	-120.51083	CEMS	115			
15Ca13B	Blakeburn, BC	49.483636	-120.744793	CEMS	123			0
AbbeyRd2	Kamloops, BC	50.69157	-120.57502	CEMS	105			1
15Ca23B	McAbee, BC	50.797026	-121.142149	CEMS	103			0
CAN-BC-1022Gab	Merritt, BC	50.088573	-120.8008	ALC	311	ALC	22	0
CAN-BC-1022Gbb	Merritt, BC	50.088573	-120.8008	CEMS	111			
Coldwater1	Coldwater, BC	49.95673	-120.92689	CEMS	99			0

4



Figure 1.1 Overview map of the southern Canadian Cordillera, showing the location of the five-morphogeological belts (Monger, 1989; Monger and Price, 2002), and the locations of the 11 areas where measured sections and samples were collected from southern British Columbia and northern Washington.

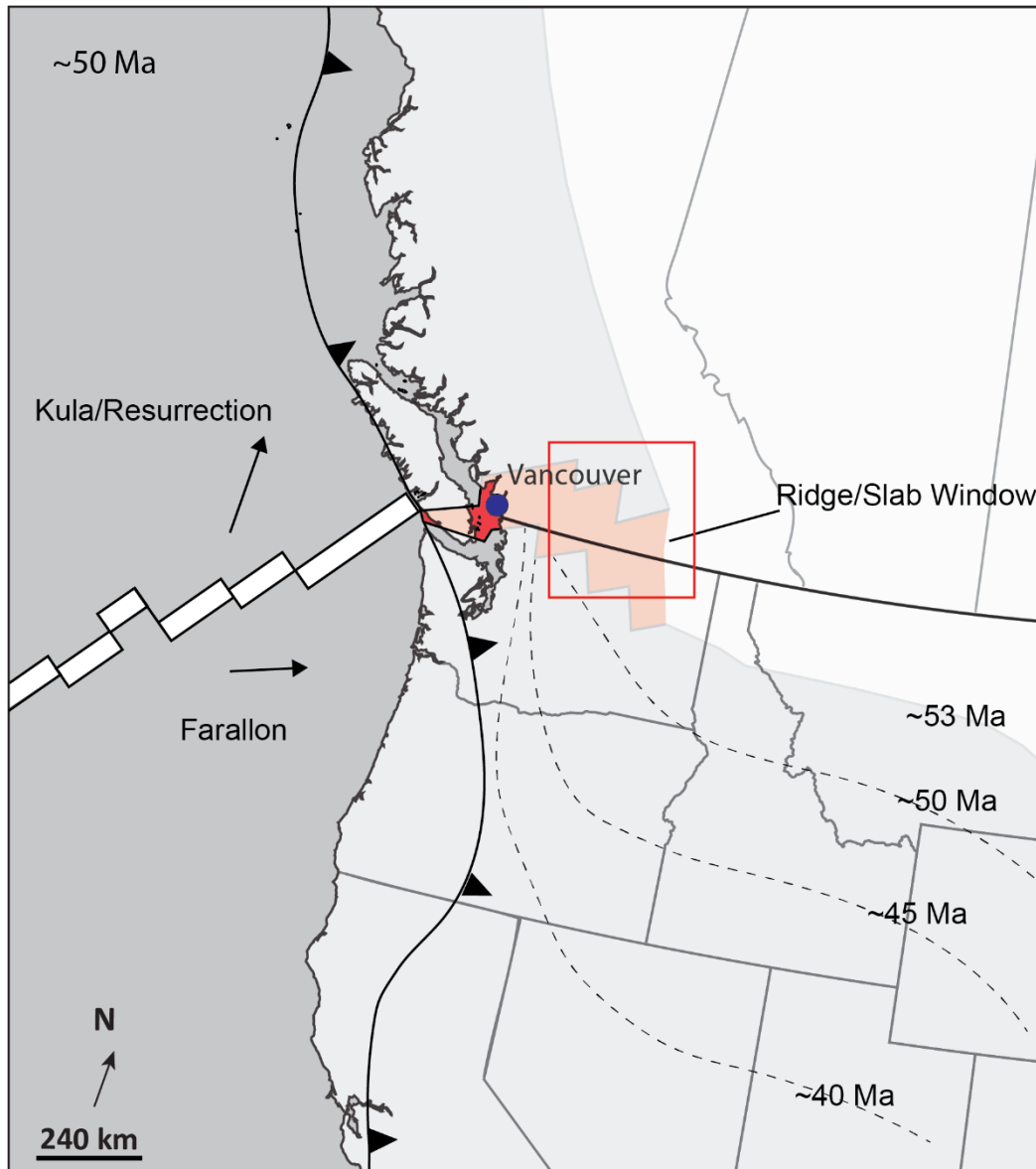


Figure 1.2 Eocene (~50 Ma) paleotectonic map of the Canadian Cordillera and adjacent areas. Red shading represents the approximate geometry of the Kula/Resurrection-Farallon slab window underneath the southern Canadian Cordillera, due to the subducted spreading center of the diverging Kula/Resurrection and Farallon plates (Breitsprecher et al., 2003; Haeussler et al., 2003). Vectors shown for oceanic plates represent motion relative to North America (Breitsprecher et al., 2003; Haeussler et al., 2003). Dotted lines in the western United States represent the approximate location, through time, of the northern part of the Farallon plate as it foundered and as slab rollback occurred (Armstrong, 1988; Dickinson, 2006; Smith et al., 2014). Red box highlights the general study area.

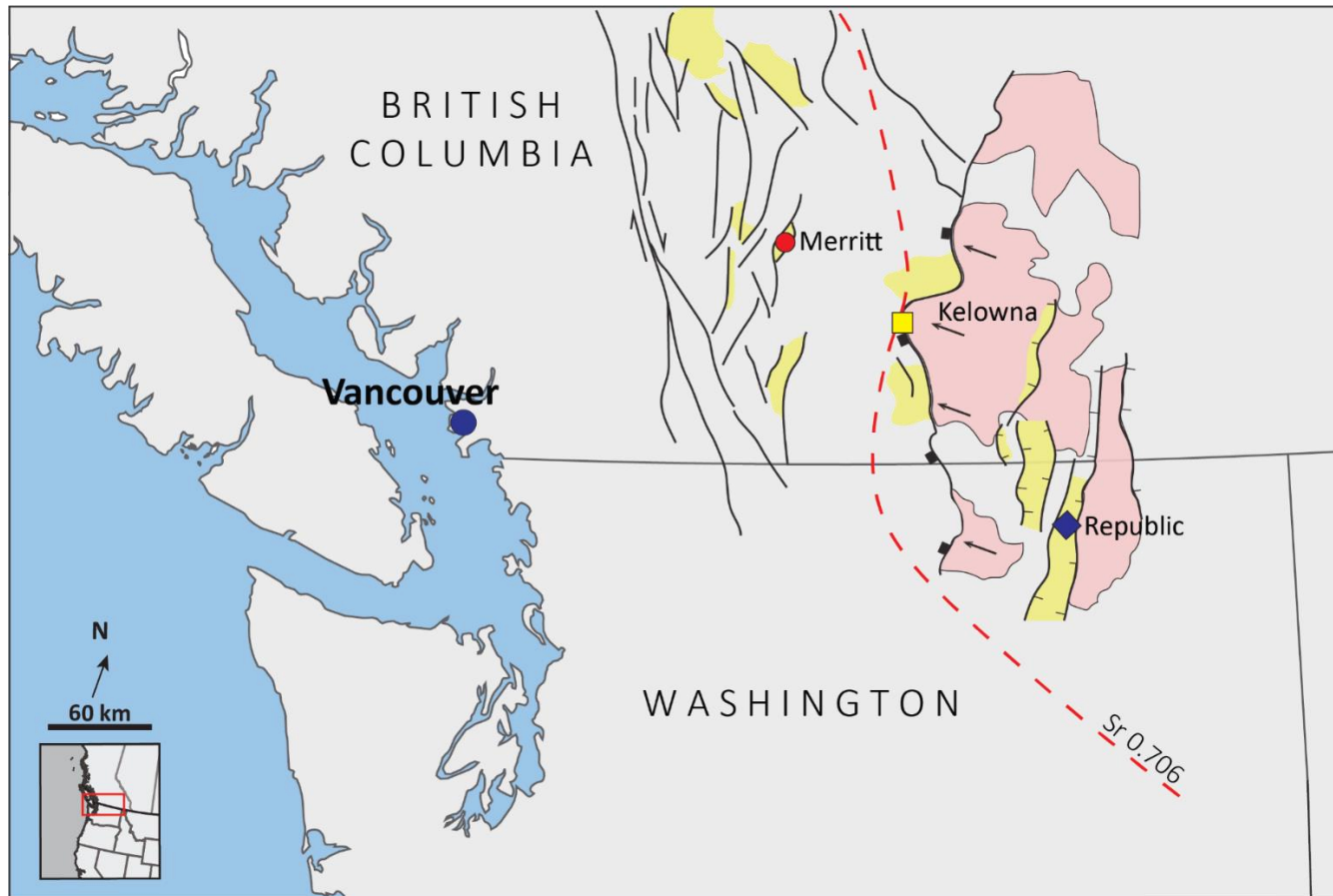


Figure 1.3 Map showing the structural setting of the SCC. In the eastern part of the hinterland, deformation is dominated by the OVSZ and the Shuswap Metamorphic Core Complex (pink). In the west, the SCC is more affected by transtensional strike-slip faulting. Basins formed in graben, strike-slip, and pull-apart structures, as well as supradetachment basins along the metamorphic core complex. The red dotted line is the approximate Sr 0.706 isotope boundary line, separating cratonic North America from accreted terranes. In both this figure and Figures 4.1 and 4.2, the red circle represents Merritt, BC; the yellow square represents Kelowna, BC; the black square represents Princeton, BC; and the blue diamond represents Republic, WA.

Eocene Strata													
Epoch	Age	Ma	Location										
			Republic, WA	Midway, BC	White Lake, BC	Summerland, BC	Kelowna, BC	Princeton, BC	Blakeburn, BC	Kamloops, BC	McAbee, BC	Merritt, BC	Coldwater, BC
Eocene	Lutetian	41.2											
	Ypresian	47.8	Klondike Mtn Formation	Penticton Group	Penticton Group	Penticton Group	Penticton Group	Allenby Formation	Allenby Formation	Kamloops Group	Kamloops Group	Allenby Formation	Kamloops Group
		56.0											

Walker, J.D., Geissman, J.W., Bowring, S.A., and Babcock, L.E., compilers, 2012, Geologic Time Scale v. 4.0: Geological Society of America, doi: 10.1130/2012.CTS004R3C.

Figure 1.4 Generalized formation chart presenting the names, ages, and locations of the Eocene formations studied in the southern Canadian Cordillera (Mathews, 1964; Ewing, 1980; Hora and Church, 1985; Thorkelson, 1989; Gaylord et al., 1996; Read, 2000; Wolfe et al., 2003).

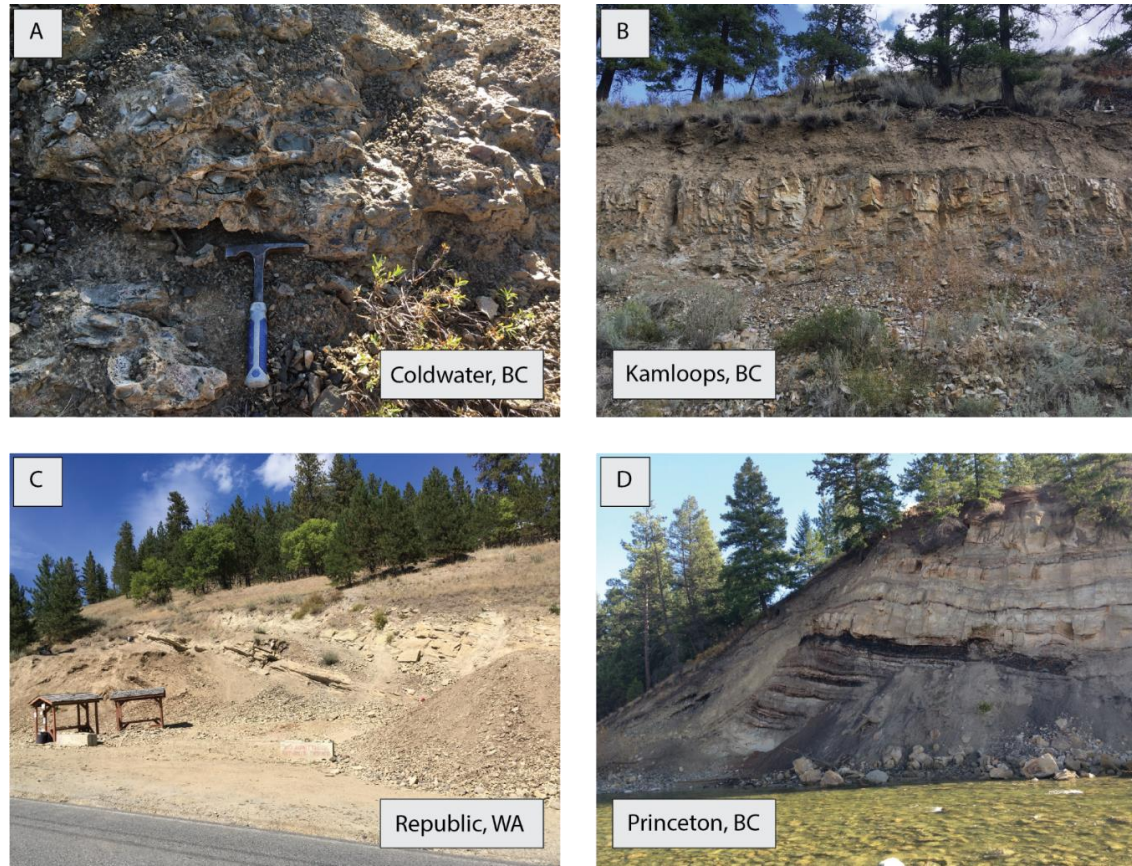


Figure 1.5 Photos showing range of lithologies and grain size in the Eocene sedimentary strata of southern British Columbia. (A) Subrounded to rounded pebble conglomerate from our Coldwater, BC, location, which is a part of the Kamloops Group of the Fig Lake Graben. (B) Interbedded sandstone, siltstone, and shale of the Kamloops Group, located on Abbey Rd. west of Kamloops, BC. Flora in foreground approximately 0.5 m high. (C) Interbedded mudstone, siltstone, and sandstone of the Klondike Mountain Formation, located at the Stonerose Interpretative Center and Eocene Fossil Site in Republic, WA. Scale is provided by 2 m structure in foreground. (D) Interbedded sandstones, mudstones, and coals located in the Allenby Formation, located in Princeton, BC. Thick black coal seam is approximately 0.5 m.

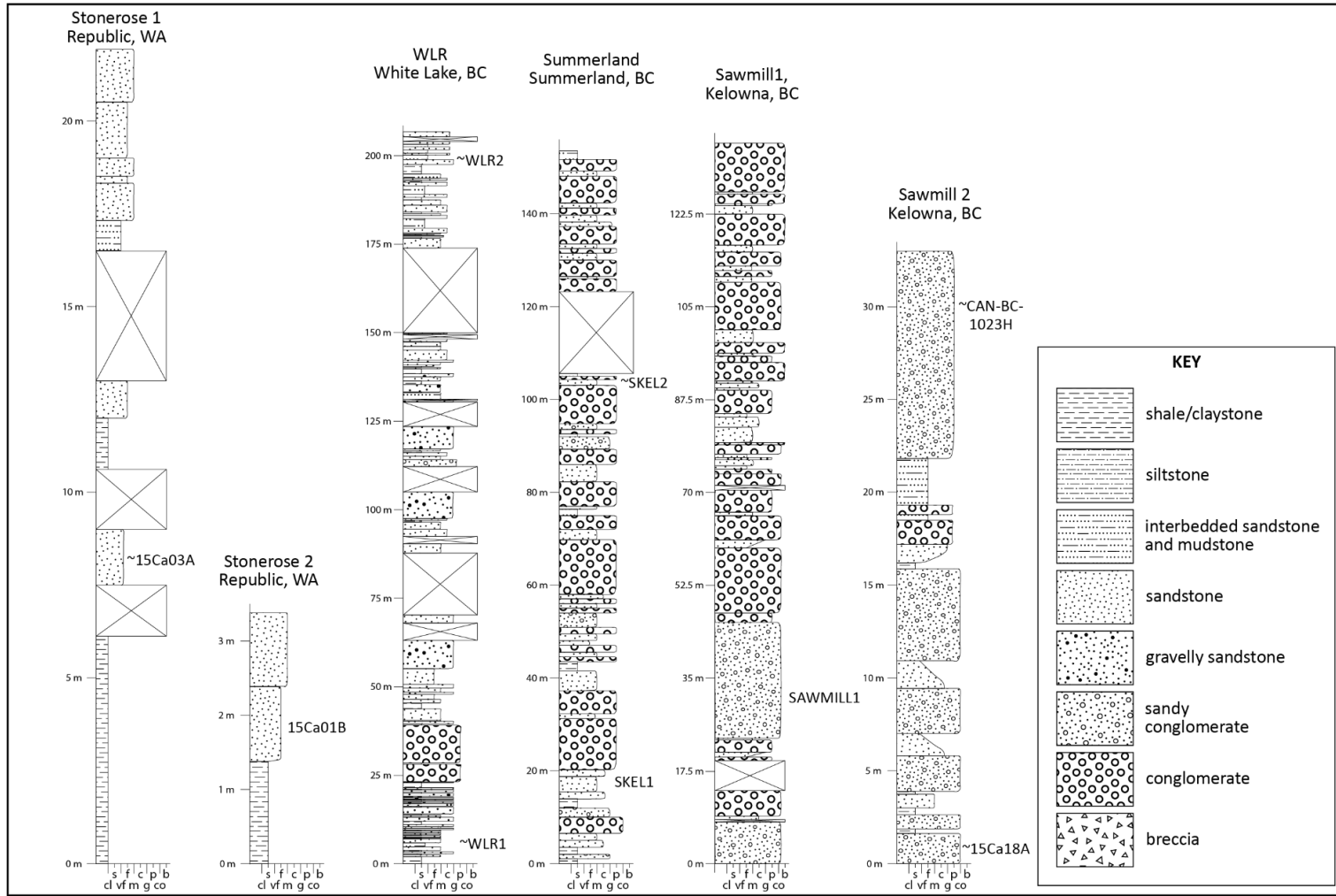


Figure 1.6 Measured sections from Republic, WA (N=2), White Lake, BC (N=1), Summerland, BC (N=1), and Kelowna, BC (N=2). Strata that sample was collected from is marked next to respective measured section. Areas marked by “X” are covered sections, where no strata could be measured.

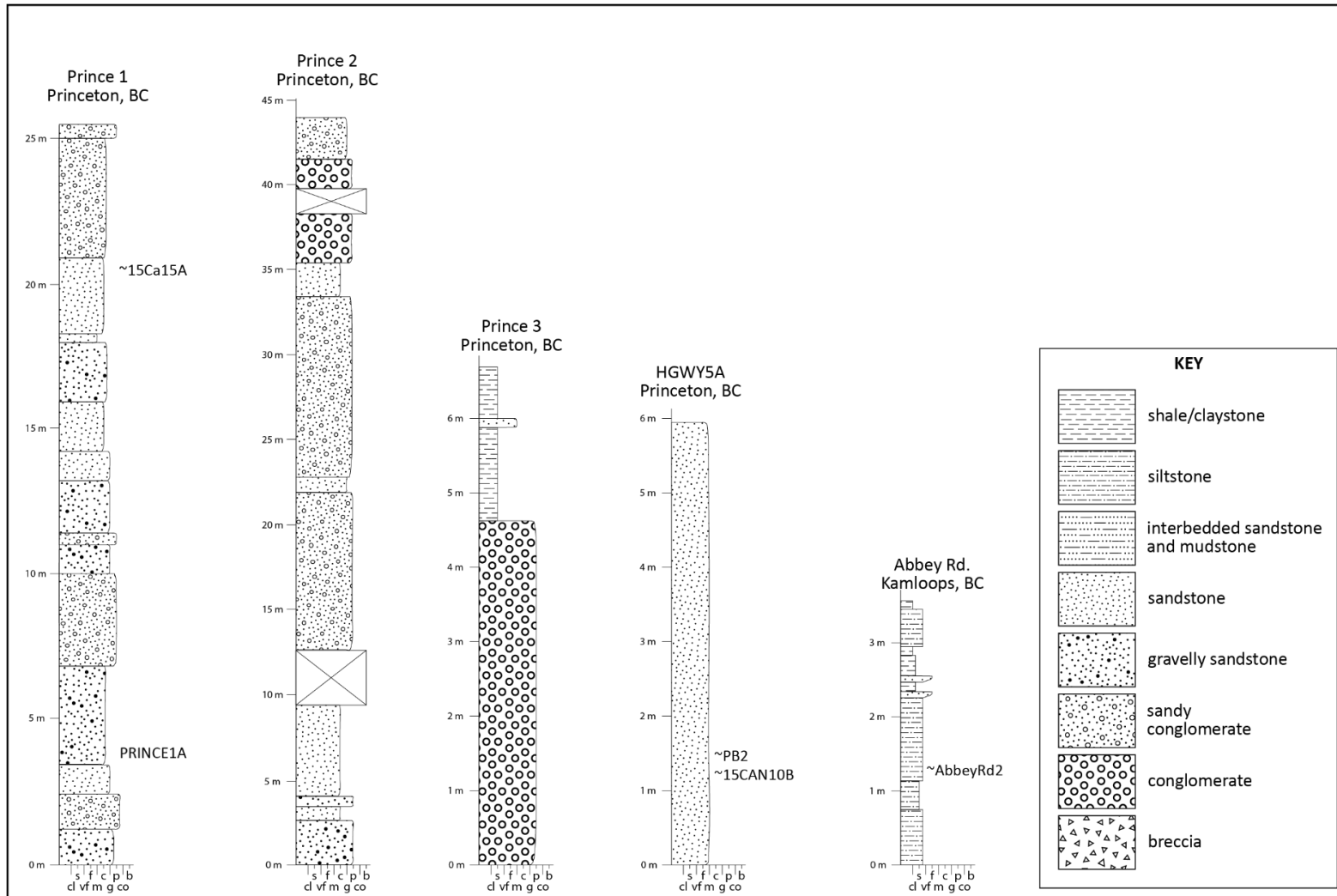


Figure 1.7 Measured sections from Princeton, BC (N=4), and Kamloops, BC (N=1). Strata that sample was collected from is marked next to respective measured section. Areas marked by “X” are covered sections, where no strata could be measured.

CHAPTER 2

BACKGROUND

2.1 REGIONAL TECTONIC SETTING

Subduction of oceanic material along the southern margin of Canada began by at least Early Jurassic time (Gabrielse and Yorath, 1991; Engebretson et al., 1992; Monger and Price, 2002; Cook et al., 2012) and was accompanied by the accretion of oceanic and intraoceanic arc rocks of Paleozoic and younger age onto the Archean-Paleoproterozoic basement of western North America (Monger, 1977; Monger and Irving, 1980; Porter et al., 1982; Okulitch, 1984; Price, 1986; Monger, 1989, Gabrielse et al., 1991; Roed et al., 1995; Monger and Price, 2002; Haeussler et al., 2003; Simony and Carr, 2011).

Convergence and subduction over this period resulted in an eastward propagating orogenic wedge (Price, 1981; Yorath, 1991) that records a total of at least ~200-350 km of NE-SW horizontal shortening by the early Cenozoic (Brown et al., 1993; Johnson and Brown, 1996). Prior to Cenozoic extension, parts of the SCC are estimated to have reached a total crustal thickness of ~50-60 km (Price and Mountjoy, 1970; Brown et al., 1986; Bardoux and Mareschal, 1994; Brown and Gibson, 2006; Gibson et al., 2008).

Terminal phases of contraction in the easternmost fold-thrust belt between ~60-40 Ma (Van Der Pluijm et al., 2006) coincided with the onset of ESE-WNW oriented extension in the interior of the mountain belt (Ewing, 1980; Monger, 1985; Parrish et al., 1988; Thorkelson, 1989; Monger et al., 1991; Wingate and Irving, 1994; Monger and Price,

2002; Brown and Gibson, 2006; Glombick et al., 2006; Gervais and Brown, 2011). Extension in the hinterland was associated with core complex exhumation, strike-slip faulting, sediment deposition, and volcanism (e.g., Ewing, 1981a; Coney and Harms, 1984; Monger, 1985; Armstrong, 1988; Parrish et al., 1988; Roaed et al., 1995; Constenius, 1996; Brown et al., 2012). The volcanism is part of the Challis-Kamloops volcanic episode, which occurred primarily between Early to Middle Eocene time (Monger et al., 1982; Armstrong, 1988; Dostal et al., 2003).

Several tectonic models have been proposed to explain the onset of extension in the SCC hinterland. In the regions south of the SCC, extension and volcanism during the Cenozoic is attributed to slab foundering and rollback (e.g., Humphreys, Dickinson); however, such processes do not seem consistent with the geologic record in the SCC (e.g., Armstrong 1988). The composition and distribution of volcanism in the SCC, as well as plate reconstruction models suggest that the SCC overrode a subducted ocean-spreading center (slab window) during the Eocene (Thorkelson and Taylor, 1989; Lawver and Scotese, 1990; Breitsprecher et al., 2003; Haeussler et al., 2003), which amongst other things, resulted in oblique (right-lateral) subduction north of the slab window (Haeussler et al., 2003; Madsen et al., 2006; Groome and Thorkelson, 2009; Eddy et al., 2016). Oblique subduction likely produced a northwest-southeast oriented extensional stress field (e.g. Price, 1979; Price et al., 1981; Monger, 1985; Price and Carmichael, 1986; Thorkelson, 1989; Harms and Price, 1992), which is reflected in the orientation of upper crustal features in the hinterland of the SCC (Price and Carmichael, 1986). Bao et al. (2014) recently proposed an alternative (although not mutually exclusive) model of

SCC Eocene geodynamics involving delamination and the removal of dense mantle lithosphere from beneath the SCC.

2.2 CORDILLERAN HINTERLAND AND DEFORMATION

The Canadian Cordillera is commonly separated into five geomorphological belts that from east to west include the Foreland, Omineca, Intermontane, Coast, and Insular Belts (Gabrielse and Yorath, 1989; Price, 1994; Monger and Price, 2002). Eocene sedimentary strata in the hinterland of the SCC occur almost entirely within the Intermontane Belt; an area characterized by relatively low elevations and minimal relief. Geologically, this region consists of Devonian to Early Jurassic sedimentary rocks and Devonian to early Cenozoic volcanic rocks (Haggart and Richstad, 1998; Monger and Price, 2002). West of the Intermontane Belt is the Coast Belt, which consists primarily of Jurassic-Cretaceous granite and volcanic rocks (Gehrels et al., 1992; Haggart and Richstad, 1998; Monger and Price, 2002). The Omineca Belt lies to the east of the Intermontane Belt and consists of Paleoproterozoic continental crust, Neoproterozoic rift-related clastics and volcanics, Paleozoic clastic and volcanic rocks, local late Paleozoic to Mesozoic volcanic rocks, and early Cenozoic continental volcanic and sedimentary rocks (Monger and Price, 2002). The boundary between accreted terranes and Precambrian crystalline basement of North America is marked by the north-south trending strontium (Sr) 0.706 isotope boundary, which is located near the boundary of the Intermontane and Omineca belts in the SCC (Armstrong, 1988; Souther, 1991; Gosh, 1995; Dostal et al., 2003).

Extensional deformation in the hinterland of the SCC began approximately 60 million years ago (Monger et al., 1991; Wingate and Irving, 1994; Brown and Gibson,

2006; Glombick et al., 2006; Gervais and Brown, 2011) and resulted in the Okanagan Valley shear zone (OVSZ); a part of the greater Shuswap Metamorphic Core Complex (Bardoux, 1993; Johnson, 1994). The OVSZ is a ~1.5 km thick zone that consists of high-grade footwall gneisses juxtaposed against low-grade to nonmetamorphosed hanging-wall rocks across a detachment surface that dips ~10°-30° to the west (Tempelman-Kluit and Parkinson, 1986; Brown et al., 2012). Exhumation along the OVSZ is speculated to have lasted from 56-48 Ma, with its peak between 53-50 Ma (Brown et al., 2012). During the Eocene, the OVSZ is estimated to have undergone 64-90 km of WNW-directed horizontal extension (~291°), with an original shear zone angle of ~15° (Tempelman-Kluit and Parkinson, 1986; Brown et al., 2012). Supradetachment basins formed to the west of and above the OVSZ, including the White Lake Basin (e.g., Pearson and Obradovich, 1977; Mathews, 1981; Wingate and Irving, 1994; Suydam and Gaylord, 1997; McClaughry and Gaylord, 2005).

Extensional and strike-slip related deformation occurred in other parts of the SCC hinterland coincident with the activity along the OVSZ. To the east of the OVSZ, high-angle (~60°) normal faulting resulted in the Republic and Toroda Creek Grabens, linear basins which are oriented approximately NNE-SSW (e.g., Gaylord, 1989; Suydam and Gaylord, 1997). Deformation to the west of the OVSZ typically has a greater component of strike-slip motion (Ewing, 1981a). Examples include the Princeton Basin, which is the site of a N-trending half-graben, formed by steeply dipping strike-slip and dip-slip faults (Read, 2000), and the Fig Lake Graben, which originated as a pull-apart basin resulting from Eocene dextral faulting (Ewing, 1981a; Thorkelson, 1989).

2.3 EOCENE STRATA

Eocene strata in the SCC consist of clastic, nonmarine deposits interbedded with volcanic and volcanoclastic units. Most Eocene strata are considered to be part of the Penticton Group (e.g., Hamblin, 2011; Mustoe, 2011, 2015), which is a 0-2,500 m thick succession, composed of volcanic and sedimentary rocks, and commonly divided into several local 6 formations (Church, 1981; Hora and Church, 1985). Clastic units consist of immature sandstones, mudstones, conglomerates, and coals (Church, 1981; Hora and Church, 1985; Tribe, 2005; Hamblin, 2008), deposited in environments including: alluvial fan, debris flow, fluvial, lacustrine, and paludal settings (Williams and Ross, 1979; Suydam and Gaylord, 1993; Tribe, 2005; Hamblin, 2011; Mustoe, 2011, 2015). Although there are local variations, the strata typically lie on Paleozoic-Mesozoic granitoids and Paleozoic-Mesozoic meta-sedimentary and meta-volcanic rocks in unconformable-disconformable relationships. In most locations in the Intermontane Belt, the Eocene strata are unconformably overlain by Miocene basalt (Church, 1981; Mathews, 1988, 1989).

Several formations are exposed across the Intermontane Belt, and therefore warrant additional discussion. Eocene strata in the Republic, WA area belong to the Klondike Mountain Formation (Pearson and Obradovich, 1977; Suydam and Gaylord, 1997). These Eocene strata consist of debris-flow breccias, conglomerates, sandstones, and mudstones, and were deposited in the Republic graben, and the adjacent Toroda Creek half-graben in alluvial fan and lacustrine environments (Gaylord et al., 1987; Gaylord et al., 1996; Mustoe, 2015). The White Lake Formation is exposed around the city of Kelowna, BC, and consists of up to ~3,500 m of volcanic breccia and

conglomerates deposited by debris flows, mudstones, and sandstones deposited in lacustrine and fluvial environments (Church, 1981; Hora and Church, 1985; McClaughry and Gaylord, 2005; Hamblin, 2011). The Allenby Formation is exposed in the central part of the Intermontane Belt and consists of fault-bounded conglomerates, sandstones, shales, and coals deposited in alluvial fan, fluvial, and paludal settings (e.g., McMechan, 1983; Read, 2000; Mustoe, 2005, 2011). The Kamloops Group is exposed near the city of Kamloops, BC, and consists of up to 2,000 m of volcano-clastic and volcanic strata (Mathews, 1964; Ewing, 1981a). Within the Kamloops Group are the Tranquille Formation and the McAbee Beds, both of which were deposited primarily in lacustrine environments (Ewing, 1981a; Souther, 1991). Conglomerate beds of the Kamloops Group are exposed within the Coldwater fault system (strike-slip) and consist of up to 2,000 m of pebble- to cobble-conglomerate that were deposited in the transtensional Fig Lake Graben (Thorkelson, 1989).

2.4 CLIMATE AND PALEOELEVATION ESTIMATES

During the Eocene, the Intermontane Belt in the SCC was much warmer than present, with mean annual temperatures $>10^{\circ}\text{C}$ and mean coldest month temperatures $\sim 8^{\circ}\text{C}$ (Wolfe and Weher, 1991; Wolfe et al., 1998; Greenwood et al., 2005; Archibald et al., 2014). Paleoelevation of the SCC during the Eocene is poorly constrained, but the majority of the estimates suggest elevations higher than current values. Paleoaltimetry data including stable isotopes and paleoflora assemblages from Mix et al. (2011) support a high elevation for the central Intermontane Belt, with elevations of 4 km or more. Mathews (1991) speculated the SCC may well have exceeded 5 km. Mulch et al. (2007) reconstructed paleoelevations of 3-4 km in the Kettle metamorphic core complex, and 4-5

km in the Shuswap metamorphic core complex, both located in the adjacent Omineca Belt. In contrast, Tribe (2005) suggested more modest paleoelevations of 400-1500 m for the Eocene Intermontane Belt. Most recently, Foster-Baril (2017) used hydrated volcanic glass (δD_{glass}) values from ignimbrites from the western Cordilleran hinterland to estimate that the hinterland of the SCC was $2.8\text{-}3.0 \text{ km} \pm 0.3 \text{ km}$ during the Eocene.

CHAPTER 3

METHODS

3.1 FIELD DATA AND SAMPLING

Over 600 m of stratigraphic sections of Eocene sedimentary units were measured and described in detail across the SCC including two sections near Republic, WA, one in the White Lake, BC area, one in the Summerland, BC area, two in the Kelowna, BC area, four from the Princeton, BC area, and one from Kamloops, BC (Figures 1.6 and 1.7). Sections were measured at the centimeter to decimeter-scale with grain-size, sedimentary structures, fossils, bedding, stratigraphic surfaces, and other salient features recorded.

Twenty-two ~4 kg samples of sandstone were collected from outcrop exposures at 11 locations for detrital zircon U-Pb geochronology and ϵ Hf analyses (Table 1.1; Figure 1.1). Detrital zircons were extracted through mechanical disaggregation, and density and magnetic differentiation in the Rock Preparation Laboratory at the University of South Carolina (USC), following standard procedures described in Gehrels et al. (2006).

3.2 DETRITAL ZIRCON U-PB GEOCHRONOLOGY

Detrital zircon U-Pb geochronology of 18 samples (Table 1.1) was performed at the USC Center for Elemental Mass Spectrometry (CEMS) using laser-ablation high-resolution single-collector inductively coupled plasma mass-spectrometry (LA-HR-SC-ICP-MS). For each sample, ~100-120 randomly selected zircon grains were ablated using

a PhotonMachines Analyte G2 193 nm (deep ultraviolet) ArF exciplex laser with accompanying HelEx ablation chamber. Ablated material was transported via argon gas to the plasma source of a Thermo Scientific Element2 high-resolution SC-ICP-MS. An analysis of the zircon standard 91500 (1062.4 ± 0.4 Ma; Wiedenbeck et al., 1995) and Sri Lanka Zircon (SL; ID-TIMS age 563.5 ± 3.2 Ma; Gehrels et al., 2008) was collected after every fifth unknown analysis. Data was reduced and processed in the Iolite add-on U-Pb Geochronology 3 data reduction scheme for WaveMetrics' IgorPro software package (Paton et al., 2011). Additional details can be found in Appendix A.

Four additional samples were analyzed at the Arizona LaserChron Center (ALC). For these particular samples, approximately 300 zircon grains were randomly selected from each sample and ablated with a PhotonMachines Analyte G2 excimer laser equipped with HelEx ablation cell. Ablated material was carried in helium into the plasma source of a Thermo Scientific Element2 high-resolution inductively-coupled-multi-collector-plasma-mass-spectrometer. An analysis of zircon standard SL, FC-1 (1099 ± 2 Ma; Paces and Miller, 1993; Wiedenbeck et al., 1995), and R33 (ID-TIMS age 419.3 ± 0.4 Ma; Black et al., 2004) was collected after every fifth unknown analysis. Post-processing data reduction was performed with an ALC Python decoding routine and Excel spreadsheet (E2agecalc). Additional details can be found in Appendix E.

All U-Pb results are presented in Figure 3.1 as Kernel Density Estimations (KDE), Probability Density Plots (PDP), histograms, and individual ages following procedures outlined in Vermeesch (2012). Additional KDE, PDP, and histograms for samples separated by location can be found in Appendix D. Raw data for all analyses can be found in the Appendix B and Appendix F.

3.3 DETRITAL ZIRCON HF SYSTEMATICS

Hf isotope analyses were conducted on four detrital zircon samples (CAN-BC-1023H; 15Ca01B; 15Ca03A; CAN-BC-1022Gab) at the ALC (Table 1.1). Hf isotope analyses were conducted with a Nu HR ICP-MS connected to a Photon Machines Analyte G2 excimer laser following procedures described in Gehrels and Pecha (2014). Analyses of unknowns are bracketed by analyses of standard solutions and zircon standards to ensure interference corrections are conducted accurately. The standards used include: Mud Tank (Black and Gulson, 1978; Woodhead and Hergt, 2005); 91500 (Wiedenbeck et al., 1995), Temora-2 (Black et al., 2004), R33 (Black et al., 2004), FC-52 (similar to FC-1; see above), Plešovice (Sláma et al., 2008), and SL (Gehrels et al., 2008). Solution analyses were run with a 60-second background, followed by 3 blocks of 20 measurements, separated by 20-second background measurements, with an integration period of 5 seconds. Laser ablation occurred on U-Pb analysis pits, with a laser beam diameter of 40 μm , and a laser pulse frequency of 7 Hz. Zircon standards were analyzed at the start of the session, between every ~25 unknown analyses, and at the end of the session. At the end of the session, all analyses from solutions and standard zircons were plotted together, and the cutoff for the use of ytterbium (βYb) versus βHf was evaluated. Additional details and raw data are included in Appendix E and Appendix G.

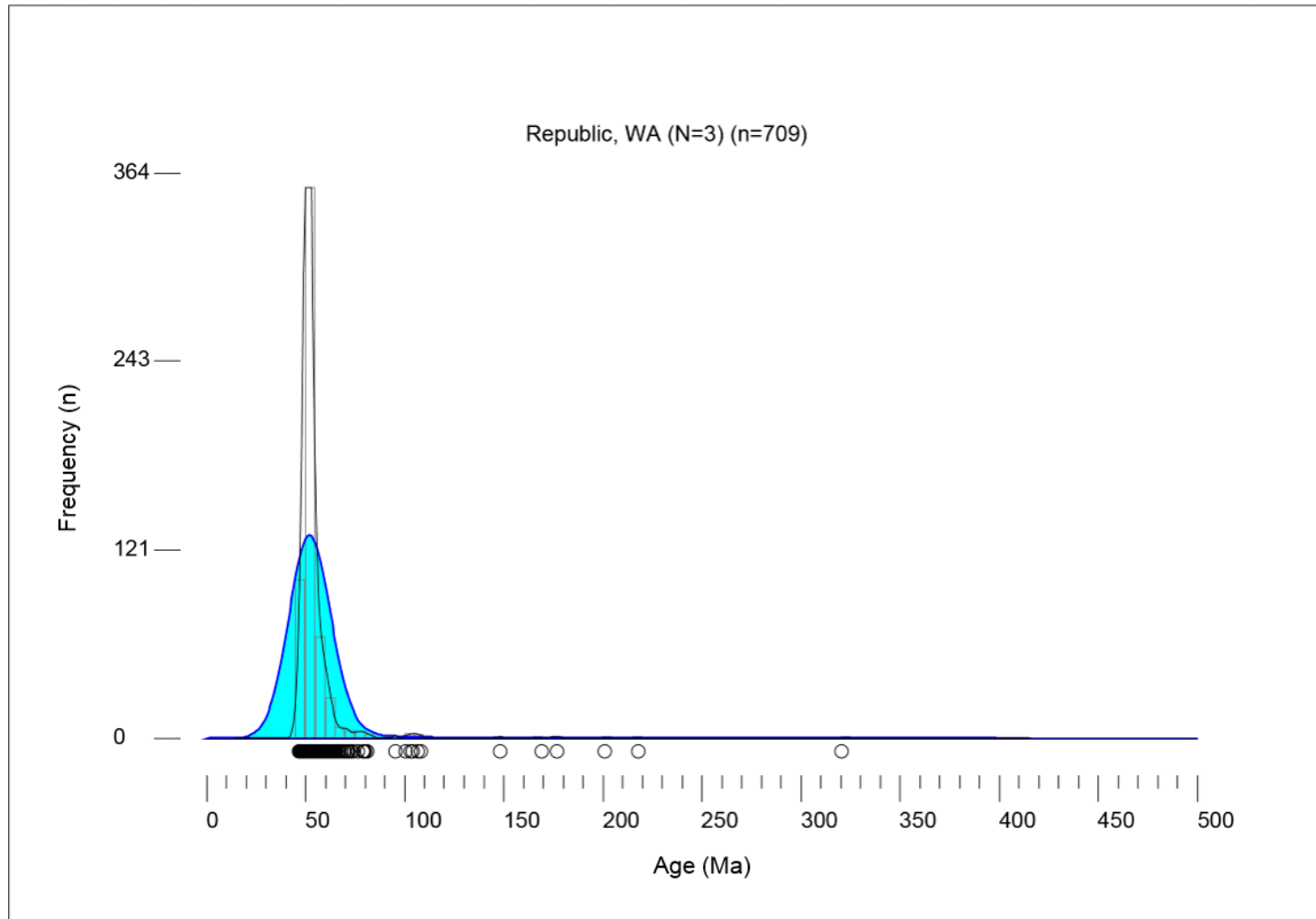


Figure 3.1 Detrital zircon U-Pb KDE (blue) and PDP (black) plot for all Republic, WA, samples, from 0-500 Ma. KDE has a bandwidth of 10, and a normalized area of 0.02. Histogram is represented by gray boxes, which have a bin width of 5.

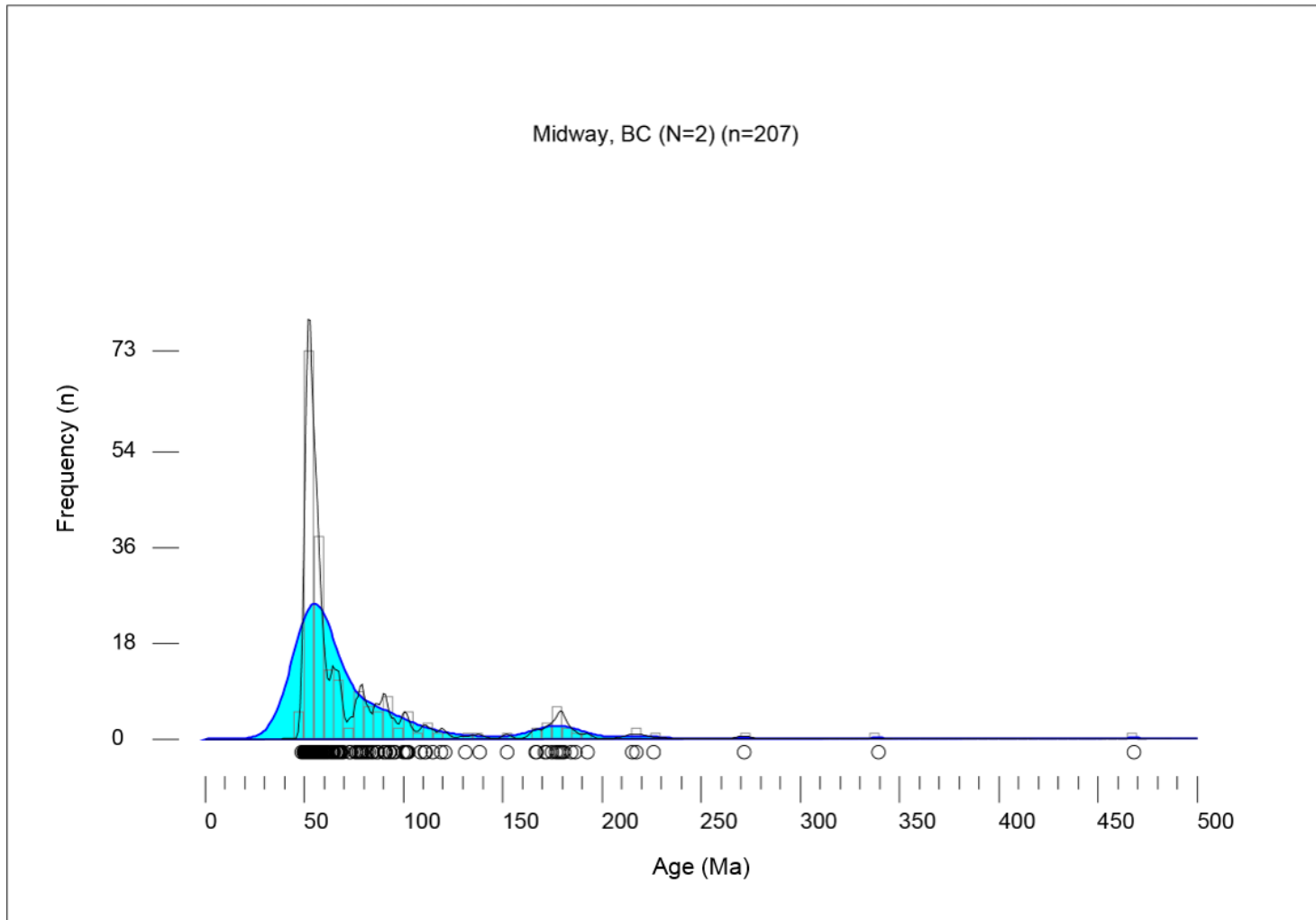


Figure 3.2 Detrital zircon U-Pb KDE (blue) and PDP (black) plot for all Midway, BC, samples, from 0-500 Ma. KDE has a bandwidth of 10, and a normalized area of 0.02. Histogram is represented by gray boxes, which have a bin width of 5.

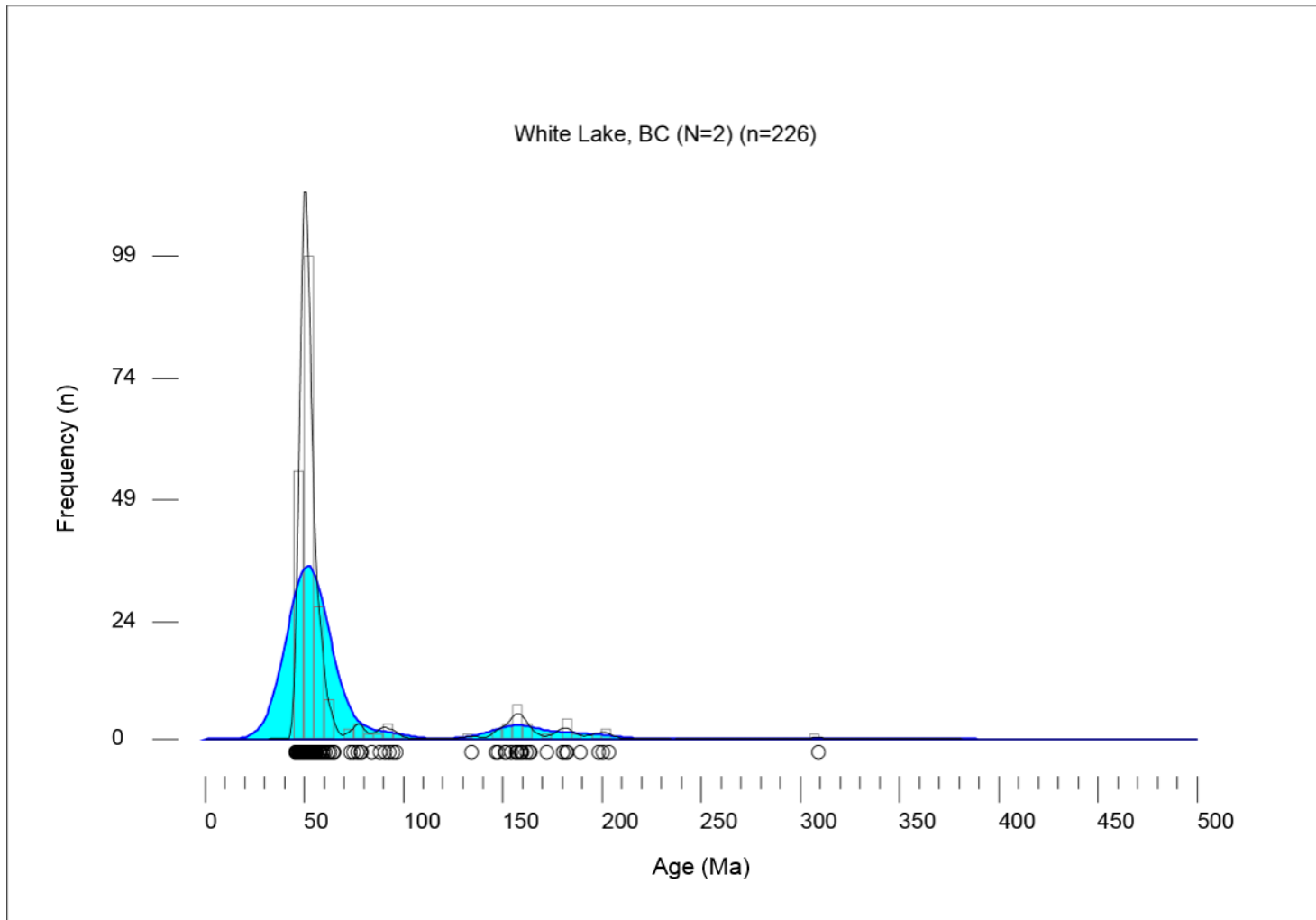


Figure 3.3 Detrital zircon U-Pb KDE (blue) and PDP (black) plot for all White Lake, BC, samples, from 0-500 Ma. KDE has a bandwidth of 10, and a normalized area of 0.02. Histogram is represented by gray boxes, which have a bin width of 5.

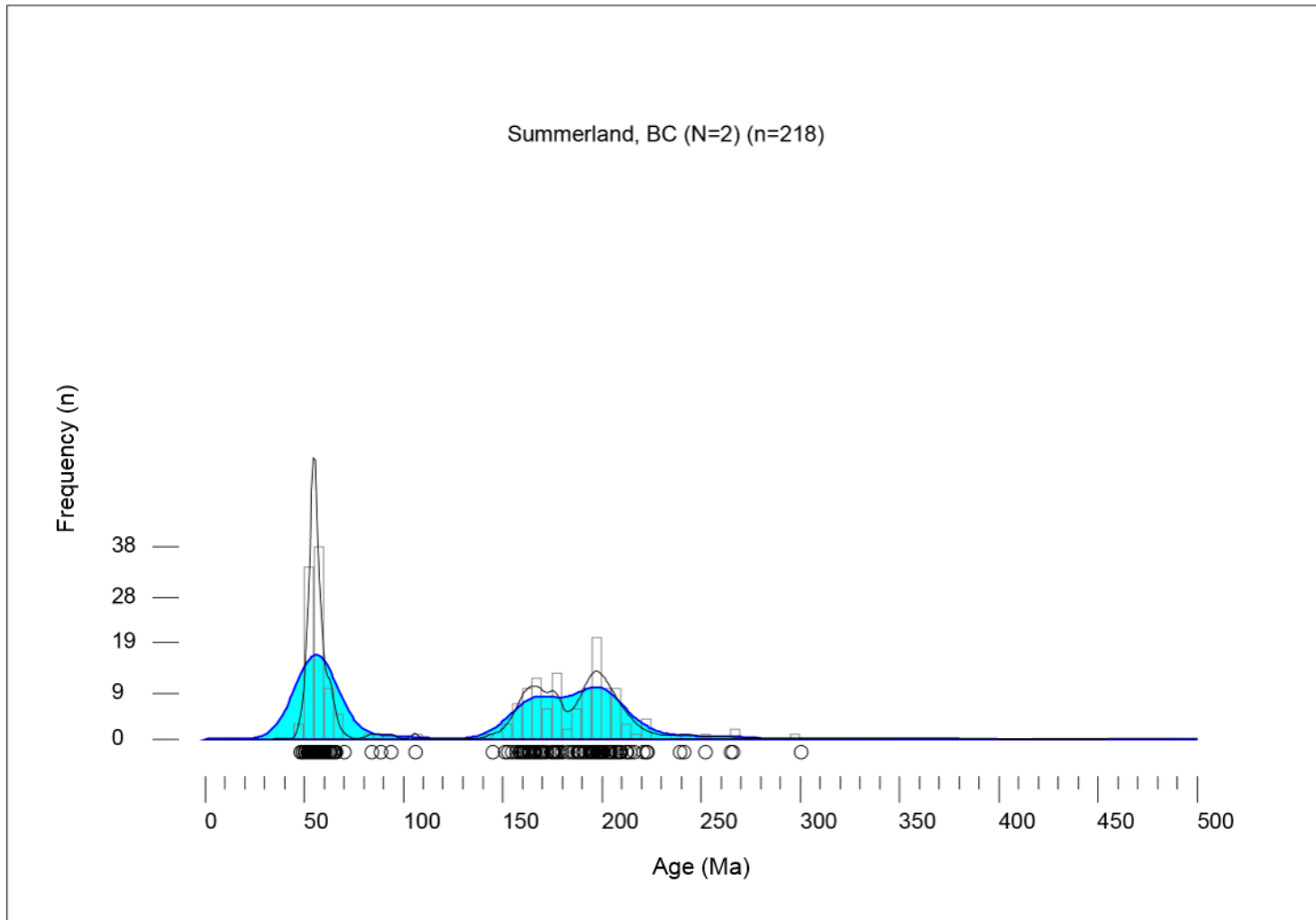


Figure 3.4 Detrital zircon U-Pb KDE (blue) and PDP (black) plot for all Summerland, BC, samples, from 0-500 Ma. KDE has a bandwidth of 10, and a normalized area of 0.02. Histogram is represented by gray boxes, which have a bin width of 5.

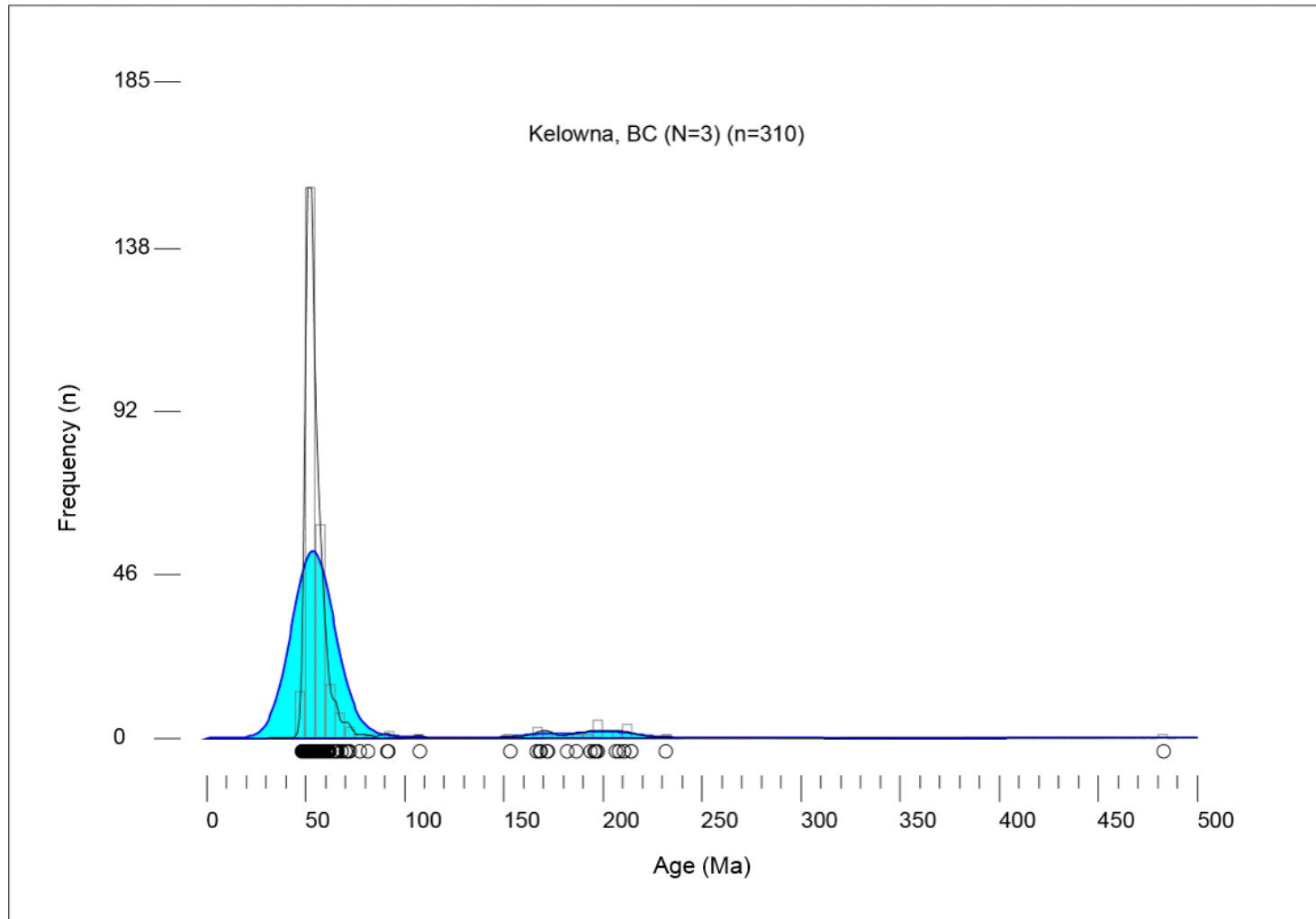


Figure 3.5 Detrital zircon U-Pb KDE (blue) and PDP (black) plot for all Kelowna, BC, samples, from 0-500 Ma. KDE has a bandwidth of 10, and a normalized area of 0.02. Histogram is represented by gray boxes, which have a bin width of 5.

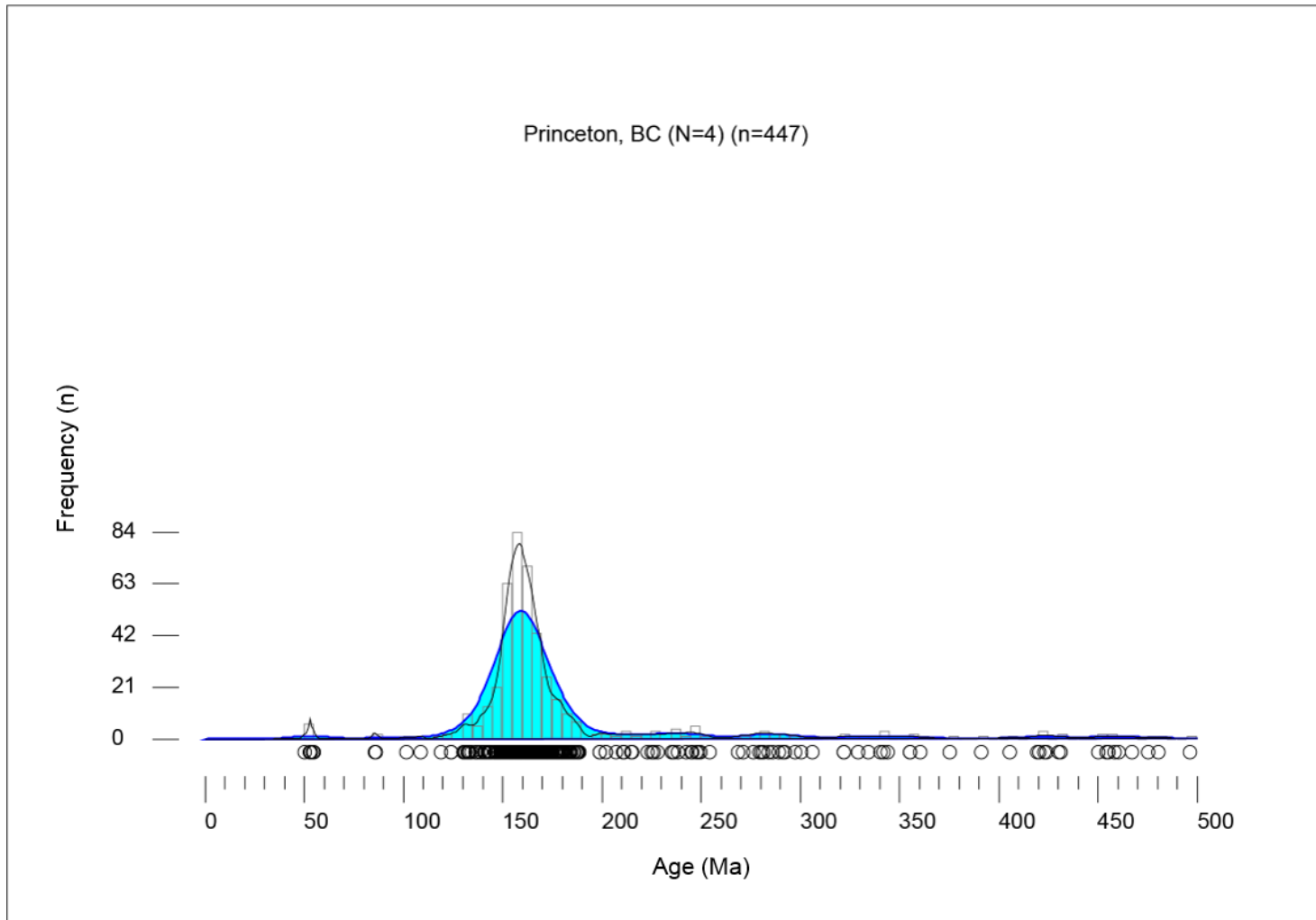


Figure 3.6 Detrital zircon U-Pb KDE (blue) and PDP (black) plot for all Princeton, BC, samples, from 0-500 Ma. KDE has a bandwidth of 10, and a normalized area of 0.02. Histogram is represented by gray boxes, which have a bin width of 5.

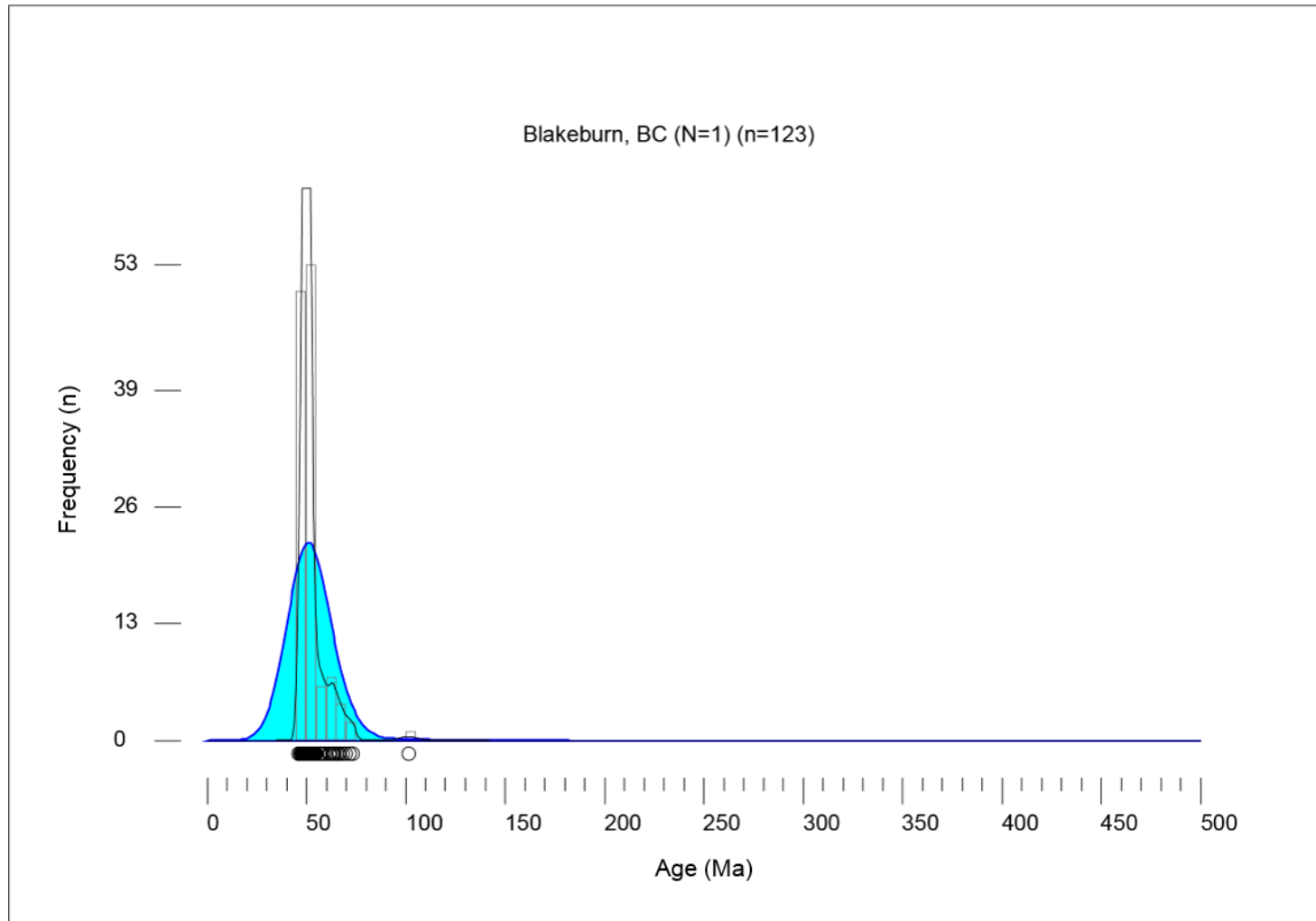


Figure 3.7 Detrital zircon U-Pb KDE (blue) and PDP (black) plot for all Blakeburn, BC, samples, from 0-500 Ma. KDE has a bandwidth of 10, and a normalized area of 0.02. Histogram is represented by gray boxes, which have a bin width of 5.

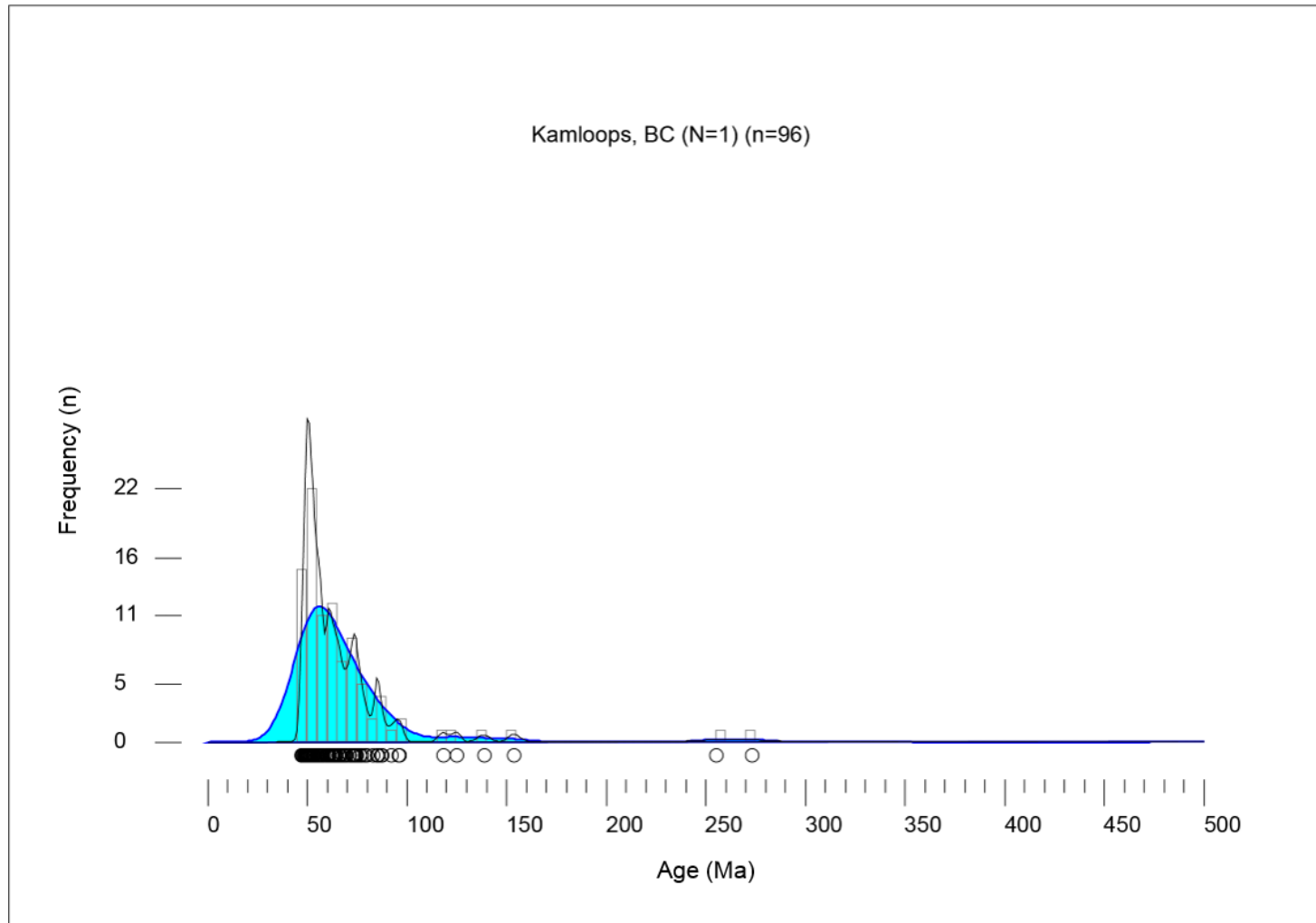


Figure 3.8 Detrital zircon U-Pb KDE (blue) and PDP (black) plot for all Kamloops, BC, samples, from 0-500 Ma. KDE has a bandwidth of 10, and a normalized area of 0.02. Histogram is represented by gray boxes, which have a bin width of 5.

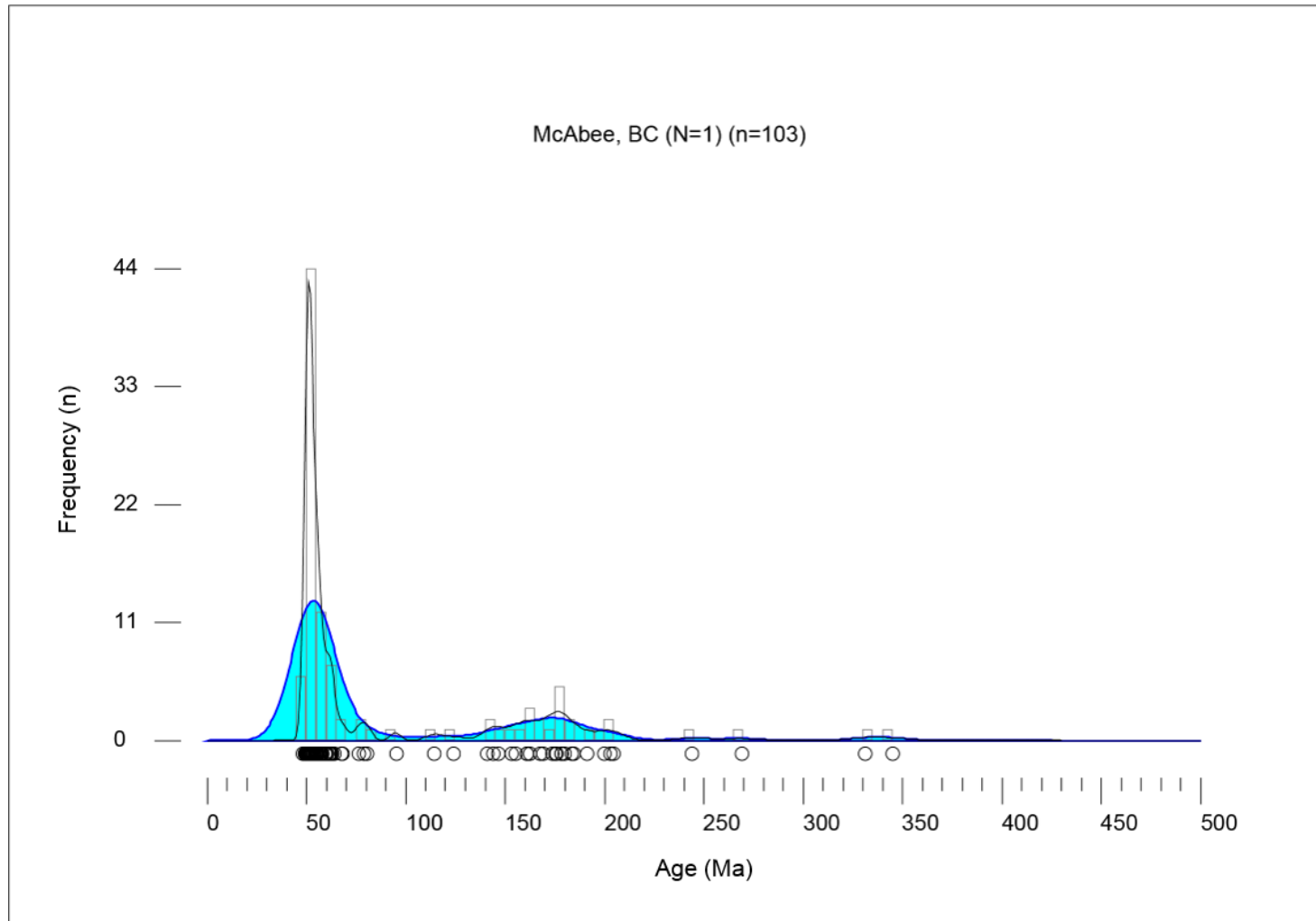


Figure 3.9 Detrital zircon U-Pb KDE (blue) and PDP (black) plot for all McAbee, BC, samples, from 0-500 Ma. KDE has a bandwidth of 10, and a normalized area of 0.02. Histogram is represented by gray boxes, which have a bin width of 5.

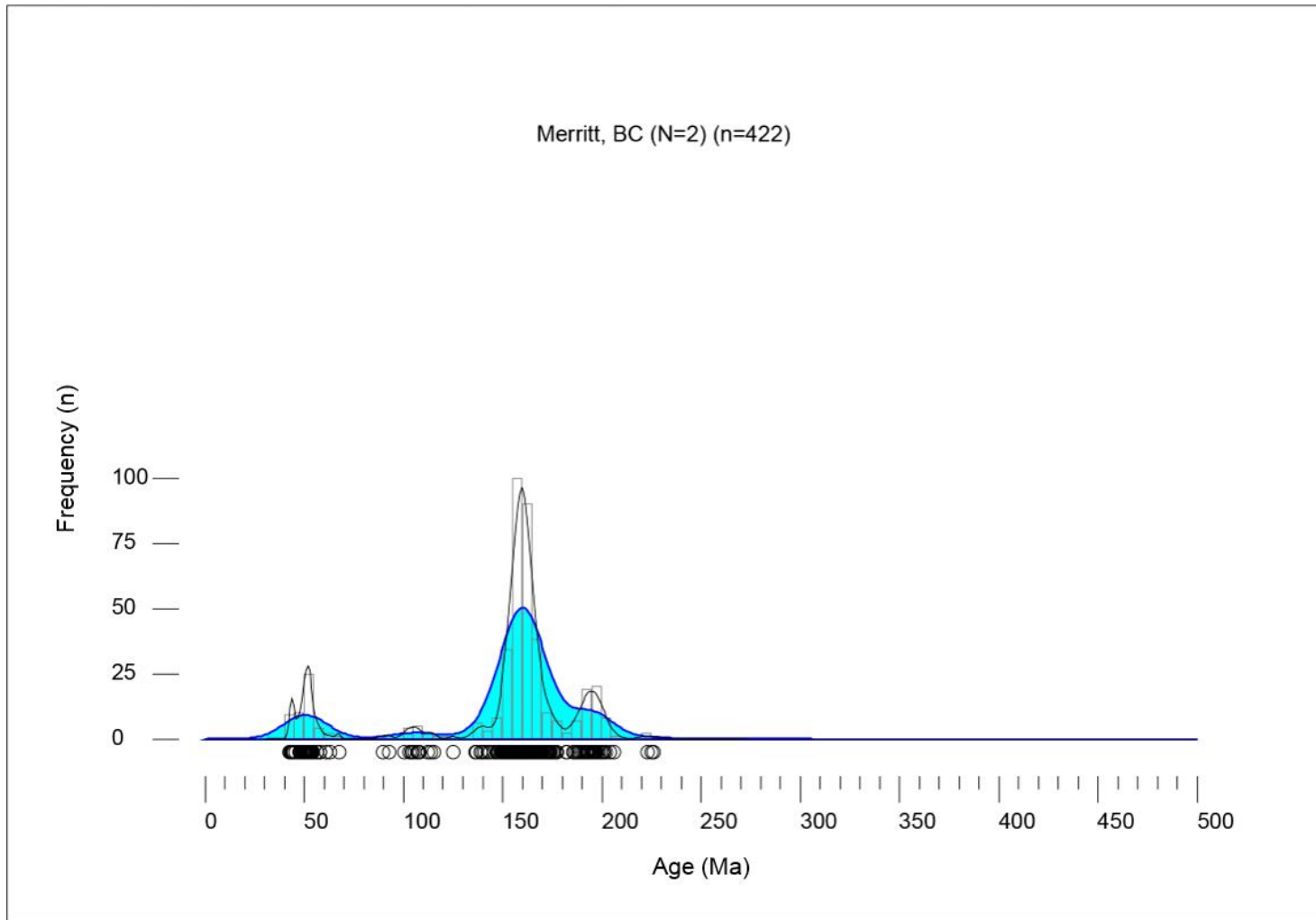


Figure 3.10 Detrital zircon U-Pb KDE (blue) and PDP (black) plot for all Merritt, BC, samples, from 0-500 Ma. KDE has a bandwidth of 10, and a normalized area of 0.02. Histogram is represented by gray boxes, which have a bin width of 5.

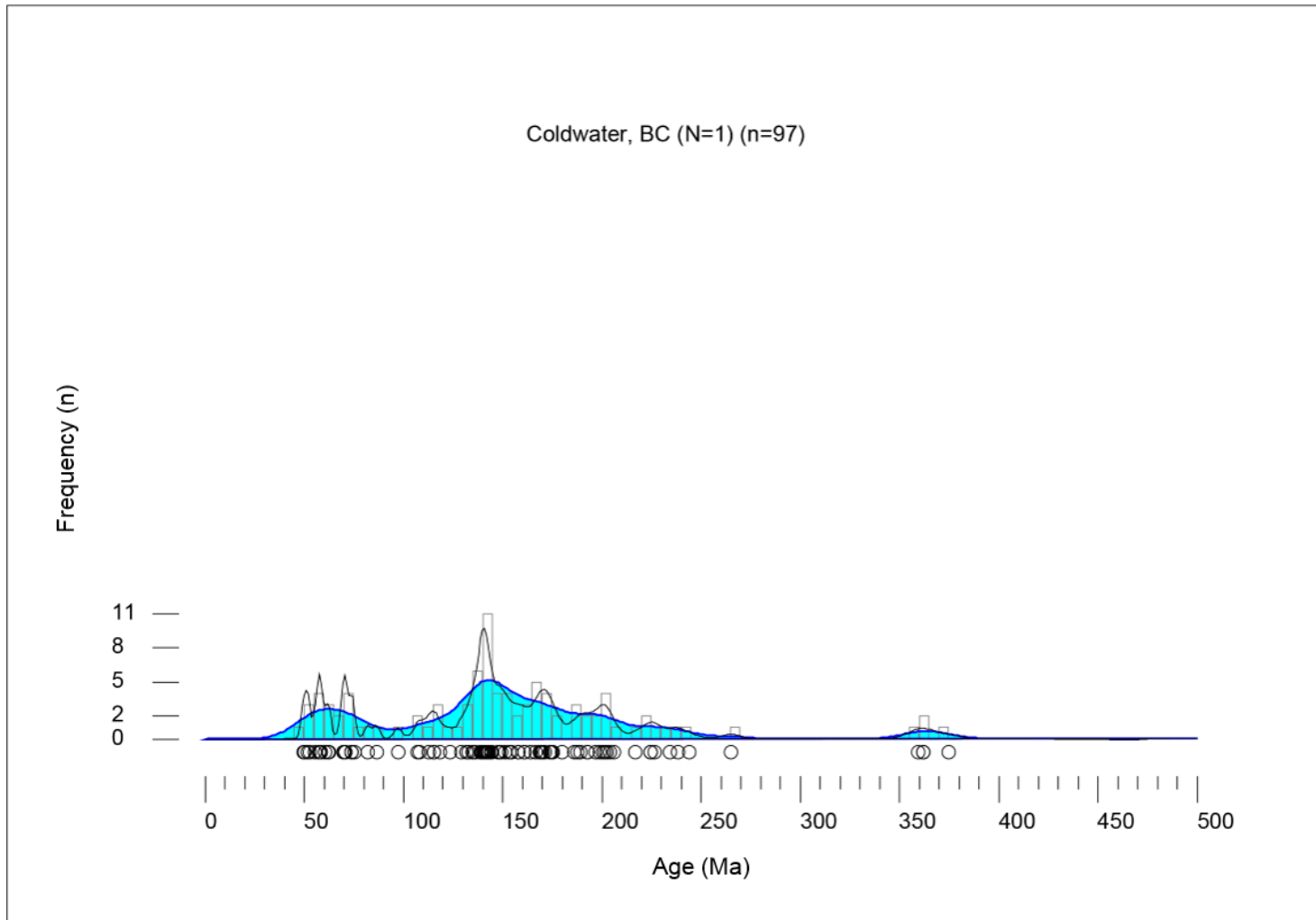


Figure 3.11 Detrital zircon U-Pb KDE (blue) and PDP (black) plot for all Coldwater, BC, samples, from 0-500 Ma. KDE has a bandwidth of 10, and a normalized area of 0.02. Histogram is represented by gray boxes, which have a bin width of 5.

CHAPTER 4

RESULTS

4.1 U-PB RESULTS

The 22 analyzed samples of Eocene strata from the SCC yielded 2,995 acceptable U-Pb ages (Appendix B and Appendix F). Samples analyzed at CEMS are corrected to the standard 91500, whereas those from the ALC are corrected to the SL standard. For the purposes of clarity and brevity, we grouped multiple samples from adjacent outcrops into single locations (e.g., Republic) and discuss the data within this framework.

Youngest U-Pb ages from each sample are shown with: 1) the youngest age and the particular standard used to determine that age; 2) the MDA of the youngest two-to-three grains that have overlapping 2σ standard deviation; 3) the mean square weighted deviation (MSWD) provided for the same two-three grains used to determine the MDA; 4) the youngest peak ages from PDP and KDE plots. All raw data and graphs are available in Appendix H.

4.1.1 Republic, WA

Three samples from fine- to medium-grained sandstone were collected from the Klondike Mountain Formation near Republic, WA, and were analyzed for detrital zircon U-Pb ages (n=710) (Figure 3.1). Strata in Republic, WA, were measured in two sections (Figure 1.6), and consist primarily of interbedded mudstone, siltstone and sandstone, although local conglomerates are reported (Suydam and Gaylord, 1997). The best

exposures of Eocene strata are located in the town of Republic, where the strata consist of shale and mudstone, with very thin to thick beds of fine- to medium-grained sandstone (i.e. Mustoe, 2015). The ~20 m thick succession in Republic, WA consists of a coarsening upward succession as laminated mudstones are progressively replaced by fine- to medium-grained sandstone beds near the top of the exposure. The sandstone beds are laterally continuous and contain multiple planar laminations, asymmetric ripples, rip-up clasts, and flame structures, with interbedded, thinly laminated shale, carbonized wood fragments, and leaf, insect, and fish fossils. Overall, we interpret these beds as prograding lacustrine delta deposits, similar to Mustoe (2015).

Sample 15Ca01B ($n=308$) was analyzed at the ALC and contains a single population with a peak at 51 Ma (range: 45-70 Ma), which constitutes 97% of the analyzed grains. The youngest U-Pb age from the sample is 47 ± 2 Ma (SL standard), the MDA (SL standard) is 47 ± 1 Ma (MSWD 0.043), and the youngest peak is 51 Ma. Sample 15Ca03A ($n=303$) was analyzed at the ALC and contains a single population with a peak at 51 Ma (range: 45-60 Ma), which constitutes 98% of the analyzed grains. The youngest U-Pb age from the sample is 46 ± 2 Ma (SL standard), the MDA (SL standard) is 47 ± 1 Ma (MSWD 0.64), and the youngest peak is 51 Ma. Sample 15Ca04A ($n=99$) was analyzed at CEMS and contains a single population with a peak at 55 Ma (range: 45-80 Ma), which constitutes 93% of the analyzed grains. Four grains have U-Pb ages between 90-110 Ma. The youngest U-Pb ages from the sample are 48 ± 2 Ma (91500 standard) and 45 ± 2 Ma (SL standard), the MDA (91500 standard) is 51 ± 3 Ma (MSWD 5.2), and the youngest peak is 55 Ma.

4.1.2 Midway, BC

Two samples of fine- to medium-grained sandstone were collected from road cuts of the Penticton Group along Canadian Highway 3 near the town of Midway, BC (Figure 3.2). Sandstone beds in the area are planar and laterally continuous, but due to poor exposures, no section was measured at this location.

Sample CAN-BC-1024K ($n=116$) was analyzed at CEMS and contains a single population with a peak at 52 Ma (range: 47-73 Ma), which constitutes 90% of the analyzed grains. Additional grains have U-Pb ages between 74 Ma – 2.6 Ga. The youngest age from the sample is 49 ± 1 Ma (both 91500 and SL standards), the MDA (91500 standard) is 49 ± 1 Ma (MSWD 1.19), and the youngest peak is 51 Ma. Sample CAN-BC-1024L ($n=100$) was analyzed at CEMS and contains a primary population with a peak at 56 Ma (range: 51-104 Ma), which constitutes 68% of the analyzed grains. An additional population includes 163-196 Ma (12% of total grains). The youngest ages from the sample are 52 ± 1 (91500 standard), and 50 ± 1 Ma (SL standard), the MDA (91500 standard) is 52 ± 2 Ma (MSWD 0.15), and the youngest peak is 55 Ma.

4.1.3 White Lake, BC

Two samples from fine- to medium-grained sandstone exposures were collected from the Penticton Group on White Lake Road, south of Penticton, BC (Figure 3.3). One measured section (Figure 1.6) was collected along White Lake Road, where strata consist of interbedded matrix- and clast-supported conglomerate, very fine- to very coarse-grained sandstone, and black and green mudstones with abundant organic material, and lesser coals. Conglomerates include subangular to subrounded pebble-size clasts, while

sandstones include abundant volcanic rock fragments, trough cross strata, rip-up clasts, and horizontal laminations. Carbonaceous mudstones include *Metasequoia* fragments (Church, 1973), and other fossilized plant detritus. The depositional environments of these deposits are interpreted as debris flow, braided fluvial, meandering fluvial and floodplain deposits (e.g., Church, 1981; McClaughry and Gaylord, 2005; Hamblin, 2011).

Sample WLR1 ($n=117$) was analyzed at CEMS and contains a single population with a peak at 51 Ma (range: 44-68 Ma), which constitutes 91% of the analyzed grains. The youngest ages from the sample are 46 ± 1 Ma (91500 standard), and 48 ± 1 Ma (SL standard), the MDA (91500 standard) is 46 ± 1 Ma (MSWD 0.57), and the youngest peak is 51 Ma. Sample WLR2 ($n=111$) was analyzed at CEMS and contains a primary population with a peak at 50 Ma (range: 44-67 Ma), which constitutes 74% of the analyzed grains. The secondary population in the sample includes 142-169 Ma (14% of total grains). The youngest ages from the sample are 46 ± 1 Ma (91500 standard), and 48 ± 1 Ma (SL standard), the MDA (91500 standard) is 46 ± 2 Ma (MSWD 1.5), and the youngest peak is 50 Ma.

4.1.4 Summerland, BC

Two samples from fine- to medium-grained sandstone exposures were collected from the Penticton Group outside Summerland, BC (Figure 3.4). One measured section (Figure 1.6) was collected outside Summerland, where strata consist primarily of interbedded organic-rich mudstones, fine- to very coarse-grained sandstones, and subangular to subrounded, matrix-supported conglomerates and breccias. Sandstones are

very fine- to very coarse-grained, and include pebble clasts. The depositional environments for these strata are interpreted as braided fluvial, floodplain, and debris flow settings.

Sample SKEL1 ($n=117$) was analyzed at CEMS and contains a prominent peak at 55 Ma (range: 49-67 Ma), which constitutes 57% of the analyzed grains. Additional populations include grains with 157-183 Ma (16% of total grains) and 185-228 Ma (18% of total grains). The youngest ages from the sample are 51 ± 1 Ma (91500 standard), and 48 ± 1 Ma (SL standard), the MDA (91500 standard) is 51 ± 1 Ma (MSWD 1.4), and the youngest peak is 55 Ma. Sample SKEL2 ($n=106$) was analyzed at CEMS and contains two chief populations with peaks at 52 Ma (range: 46-72 Ma) and 195 Ma (range: 146-216 Ma), which constitute 22% and 71% of the analyzed grains, respectively. The youngest ages from the sample are 48 ± 2 Ma (91500 standard), and 49 ± 2 Ma (SL standard), the MDA (91500 standard) is 49 ± 1 Ma, and the (MSWD 0.83), and the youngest peak is 52 Ma.

4.1.5 Kelowna, BC

Three samples from fine- to medium-grained sandstone were collected from the Penticton Group near Kelowna, BC (Figure 3.5). Two measured sections (Figure 1.6) were collected in the Kelowna area, where the strata consist of interbedded matrix- and clast-supported conglomerates, fine- to coarse-grained sandstones, and shale. Conglomerates include pebble- to cobble-size clasts, with poor imbrication locally, while sandstones have both normal and inverse grading. Mudstones include organic matter and

abundant plant fossils. The depositional environments of these strata are interpreted as debris-flows, lacustrine, braided fluvial, and floodplain environments.

Sample CAN-BC-1023H ($n=105$) was analyzed at ALC and contains a single population with a peak at 52 Ma (range: 46-58 Ma), which constitutes 89% of the analyzed grains. The youngest age from the sample is 48 ± 2 Ma (SL standard), the MDA (SL standard) is 48 ± 1 Ma (MSWD 0.046), and the youngest peak is 51 Ma. Sample SAWMILL1 ($n=100$) was analyzed CEMS and contains a single prominent population with a peak at 55 Ma (range: 47-80 Ma), which constitutes 84% of the analyzed grains. A lesser population of grains with ages of 161-204 Ma constitutes 16% of the total grains. The youngest ages from the sample are 49 ± 1 Ma (91500 standard) and 48 ± 1 Ma (SL standard), the MDA (91500 standard) is 50 ± 2 Ma (MSWD 1.3), and the youngest peak is 55 Ma. Sample 15Ca18A ($n=114$) was analyzed at CEMS and contains a single population with a peak at 52 Ma (range: 46-64 Ma), which constitutes 83% of the analyzed grains. The additional grains have ages of 65-73 Ma, 87-97 Ma, 201-213 Ma, 481-530 Ma, and 619-681 Ma. The youngest age from the sample is 48 ± 1 Ma (both 91500 and SL standards), the MDA (91500 standard) is 50 ± 1 Ma (MSWD 0.029), and the youngest peak is 52 Ma.

4.1.6 Princeton, BC

Four samples from fine- to medium-grained sandstone were collected from the Allenby Formation near Princeton, BC (Figure 3.6). Four measured sections (Figure 1.7) were collected in Princeton, where strata consist primarily of interbedded medium- to very coarse-grained sandstones, siltstones and mudstones with organic matter, with lesser

pebble- to cobble-conglomerates and coals. Sandstone strata include local sources, lenticular beds, trough cross-stratification, and normal grading. Conglomerates are both matrix- and clast-supported. The depositional environments of these strata are interpreted as braided and meandering fluvial systems and lacustrine environments.

Sample PB2 ($n=108$) was analyzed at CEMS and contains a prominent population with a peak at 155 Ma (range: 138-171 Ma), which constitutes 52% of the analyzed grains. Lesser populations include 174-186 Ma (6% of the total grains), 194-255 Ma (15% of the total grains), 263-305 Ma (8% of the total grains), and 316-349 Ma (6% of the total grains). The youngest age from the sample is 131 ± 2 Ma (91500 standard), the MDA (91500 standard) is 142 ± 1 Ma (MSWD 0.88), and the youngest peak is 130 Ma. Sample 15CAN10B ($n=119$) was analyzed at CEMS and contains a primary population with a peak at 167 Ma (range: 151-192 Ma), which constitutes 77% of the analyzed grains. The youngest age from sample 15CAN10B is 53 ± 1 Ma (91500 standard), the MDA (91500 standard) is 53 ± 1 Ma (MSWD 0.39), and the youngest peak is 53 Ma. Sample 15Ca15A ($n=105$) was analyzed at CEMS and contains a single population with a peak at 156 Ma (range: 126-185 Ma), which constitutes 97% of the analyzed grains. The youngest age from the sample is 50 ± 1 (both 91500 and SL standards), the MDA (91500 standard) is 52 ± 5 Ma (MSWD 8.4), and the youngest peak is 51 Ma. Sample Prince1A ($n=115$) was analyzed at CEMS and contains a single population with a peak at 159 Ma (range: 114-190 Ma), which constitutes 97% of the analyzed grains. The youngest ages from the sample are 86 ± 1 (91500 standard) and 88 ± 1 Ma (SL standard), the MDA (91500 standard) is 86 ± 1 Ma (MSWD 0.116), and the youngest peak is 85 Ma.

4.1.7 Blakeburn, BC

One sample from a tuffaceous sandstone exposed between coal beds was collected from the Allenby Formation near Blakeburn, BC (Figure 3.7). Eocene strata in the Blakeburn area contain thick (~30 m) coal beds as well as lesser sandstone and mudstone. Exposures are poor and no section was measured in this locality. However, based on the lithologies the sediments were likely deposited in fluvial and paludal settings (e.g., McMechan; 1983; Read, 2000; Mustoe, 2005, 2011).

Sample 15Ca13B ($n=123$) was analyzed at CEMS and contains a single population with a peak at 50 Ma (range: 44-76 Ma), which constitutes 99% of the analyzed grains. The youngest zircon ages from the sample are 46 ± 1 Ma (91500 standard) and 48 ± 1 Ma (SL standard), the MDA from the (91500 standard) is 49 ± 1 Ma (MSWD 0.86), and the youngest peak is 50 Ma.

4.1.8 Kamloops, BC

One sample from fine- to medium-grained sandstone was collected from the Kamloops Group near Kamloops, BC (Figure 3.8). One small section was measured (Figure 1.7), and consists of interbedded, thin, tuffaceous sandstone beds, siltstone, and shale. Individual sandstone and siltstone beds are laterally continuous and many are normally-graded. Mudstone beds are thinly laminated and contain well-preserved fossil leaves. We interpret these beds as having been deposited in a lacustrine environment.

Sample ABBEYRD2 ($n=105$) was analyzed at CEMS and contains a single population with a peak at 50 Ma (range: 47-100 Ma), which constitutes 86% of the analyzed grains. The remaining grains have ages between 115-660 Ma. The youngest

ages from the sample are 47 ± 1 Ma (91500 standard) and 49 ± 1 Ma (SL standard), the MDA (91500 standard) is 47 ± 1 Ma (MSWD 0.25), and the youngest peak is 50 Ma.

4.1.9 McAbee, BC

One sample from fine-grained tuffaceous sandstone was collected from the McAbee Beds from the Kamloops Group (Figure 3.9). The McAbee Beds consist of ash-fall tuffs interbedded with thin beds of siltstones, sandstones, and localized clast-supported and matrix-supported cobble-conglomerates. These strata are interpreted to have been deposited in lacustrine environments adjacent to alluvial fans (e.g., Ewing, 1981a; Foster-Baril, 2017).

Sample 15Ca23B ($n=103$) was analyzed at CEMS and contains a primary population with a peak at 51 Ma (range: 46-71 Ma), which constitutes 69% of the analyzed grains, and a secondary population with ages between 135 and 200 Ma that constitute 21% of the analyzed grains. The youngest age from the sample is 48 ± 1 Ma (both 91500 standard and SL standard), the MDA (91500 standard) is 49 ± 1 Ma (MSWD 0.89), and the youngest peak is 51 Ma.

4.1.10 Merritt, BC

Two samples from fine- to medium-grained sandstone were collected from the Allenby Formation, near Merritt, BC (Figure 3.10). Due to poor exposures no sections were measured in this location. Previous interpretations indicate these strata were deposited in fluvial-paludal environments (Ewing, 1981a).

Sample CAN-BC-1022Gab ($n=311$) was analyzed at ALC and contains a prominent population with a peak at 159 Ma (range: 133-182 Ma), which constitutes 69% of the analyzed grains. Lesser populations have ages of 41-59 Ma (11.5% of total grains) and 181-210 Ma (15% of total grains). The youngest age from the sample is 43 ± 1 (SL standard), the MDA (SL standard) is 43 ± 2 Ma (MSWD 2.8), and the youngest peak is 44 Ma. Sample CAN-BC-1022Gbb ($n=111$) was analyzed at CEMS and contains a prominent population with a peak at 163 Ma (range: 133-187 Ma), which constitutes 76% of the analyzed grains. Less prominent populations have ages of 40-64 Ma (12% of total grains) and 187-207 Ma (7% of total grains). The youngest ages from sample CAN-BC-1022Gbb are 43 ± 1 (91500 standard) and 41 ± 1 Ma (SL standard), the MDA (91500 standard) is 43 ± 1 Ma, (MSWD 0.55), and the youngest peak is 43 Ma.

4.1.11 Coldwater, BC

One sample from a clast-supported pebble conglomerate was collected from the Kamloops Group in the Fig Lake Graben along Coldwater Creek, BC (Figure 3.11). Due to poor exposures, no section was measured in this location; however, the beds are typically interpreted as having been deposited in a braided, fluvial to fluviolacustrine environment (Thorkelson, 1989).

Sample COLDWATER1 ($n=99$) was analyzed at CEMS and contains a prominent population with a peak at 140 Ma (range: 100-218 Ma), which comprises 66% of the analyzed grains. Less prominent populations have ages of 47-100 Ma (22% of the analyzed grains), and 220-265 Ma (7% of the analyzed grains). The youngest age from

the sample is 49 ± 1 Ma (both 91500 standard and SL standard), the MDA (91500 standard) is 50 ± 3 Ma (MSWD 4.1), and the youngest peak is 51 Ma.

4.2 HF RESULTS

ϵ_{Hf} detrital zircon values ($n=67$) were analyzed for 4 of the samples collected from the SCC (Table 1.1; Figure 4.1); all ϵ_{Hf} analyses were performed at the ALC. ϵ_{Hf} values vary from -16 to +14 for zircons with U-Pb ages of ~50 Ma. These data are presented on Hf-evolution diagrams (Figure 4.2), which depict ϵ_{Hf} values at the time of crystallization.

Sample CAN-BC-1022Gab ($n=22$) from Merritt, BC, contains primarily positive ϵ_{Hf} values, with values between -3 and +14. Sample CAN-BC-1023H ($n=15$) from Kelowna, BC, contains both positive and negative values, with a total range in values of -10 to +14. This sample contains two distinct ϵ_{Hf} populations, one with positive ϵ_{Hf} values, the other with negative ϵ_{Hf} values. Samples 15Ca01B and 15Ca03A from Republic, WA ($n=30$), contain almost exclusively negative values, with values between -16 and +7.

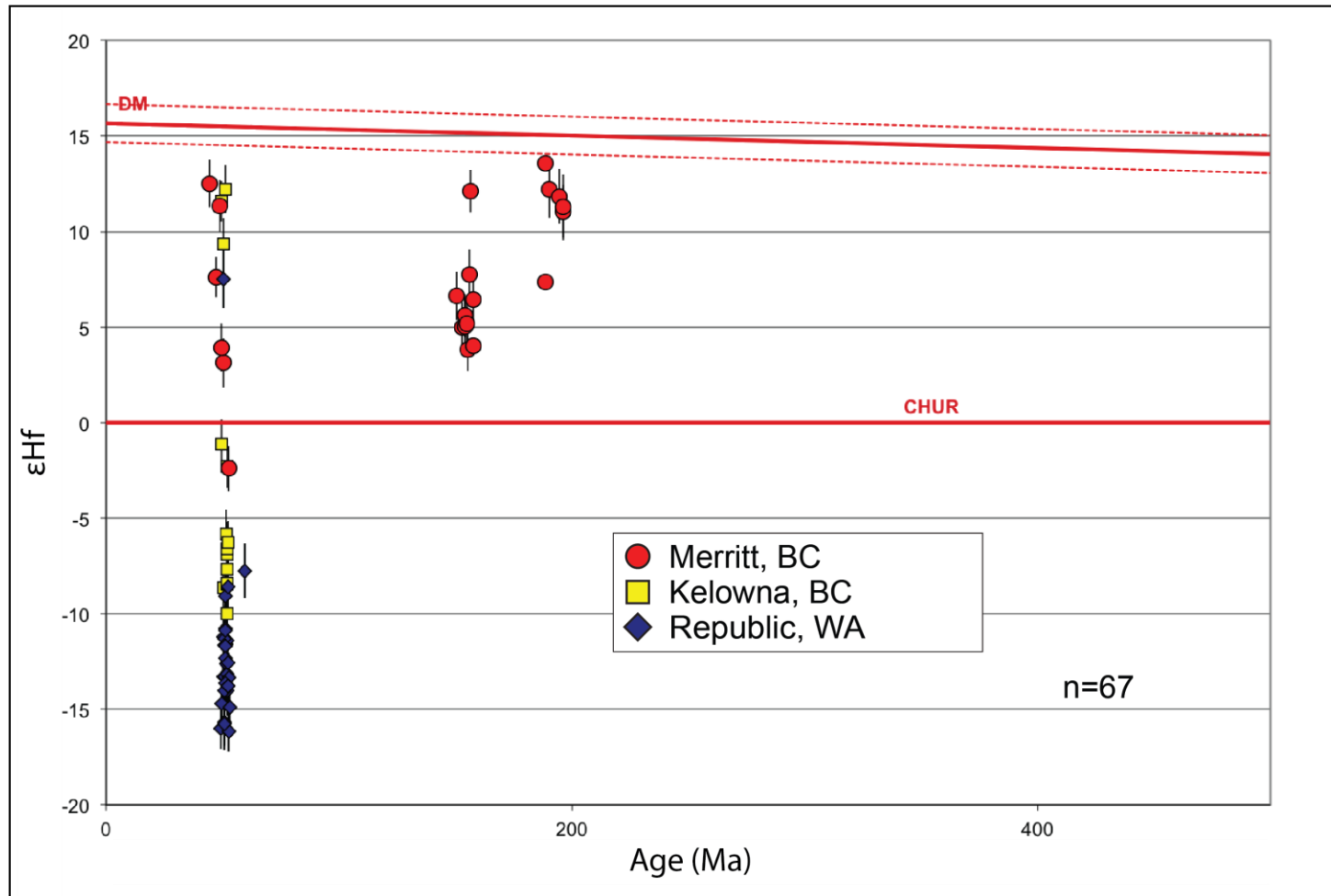


Figure 4.1 Detrital zircon Hf isotope data with detrital zircon U-Pb ages of 0-500 Ma. ϵ_{Hf} values vary between -16 to 14 for $n=67$ grains taken Merritt, BC ($N=1$), Kelowna, BC ($N=1$), and Republic, WA ($N=2$), with a widespread distribution of ϵ_{Hf} values for detrital zircons with U-Pb ages of ~ 50 Ma. Positive and negative ϵ_{Hf} values for detrital zircons with ages of ~ 50 Ma correlate to the Sr 0.706 isotope boundary.

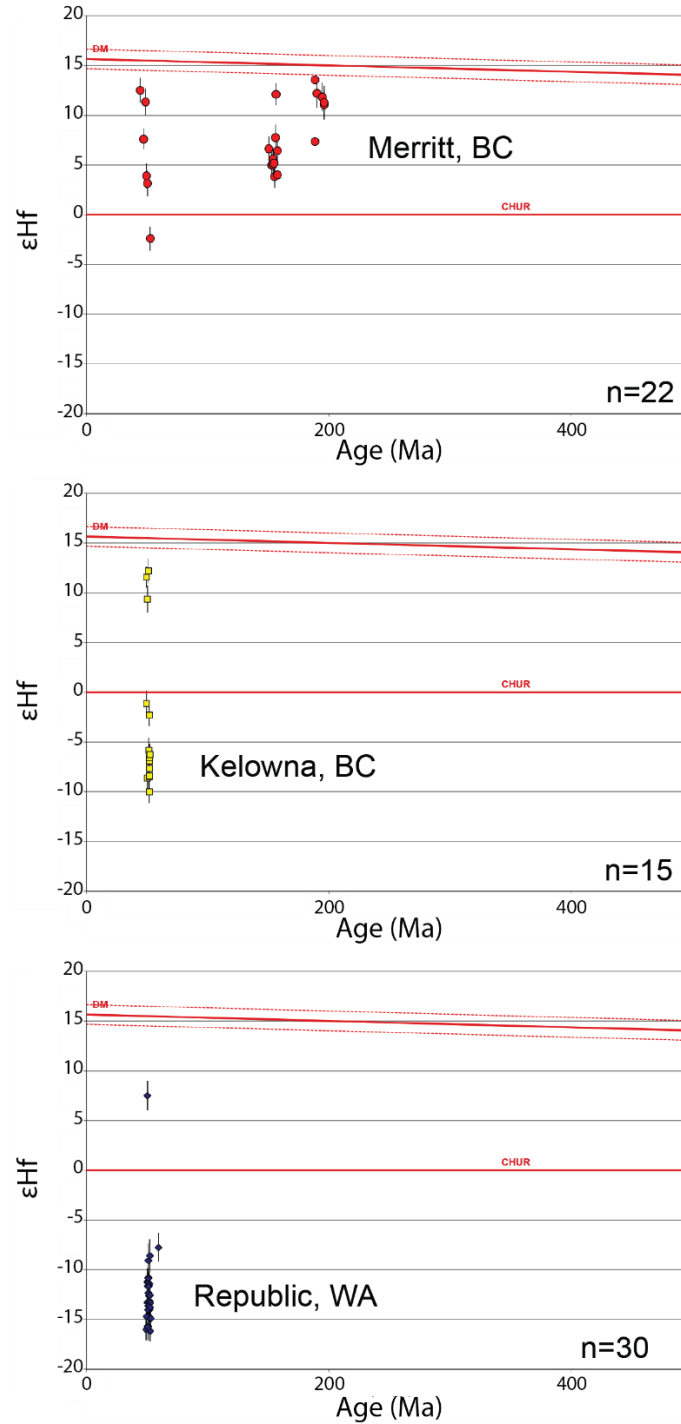


Figure 4.2 Detrital zircon Hf isotope data, separated by location, with detrital zircon U-Pb ages of 0-200 Ma. The ϵ_{Hf} data discussed is primarily for detrital zircons dated ~ 50 Ma from U-Pb dating. ϵ_{Hf} values for detrital zircons aged ~ 50 Ma range from positive to negative, differing by geographic location. Detrital zircons from Merritt, BC (N=1), have primarily positive ϵ_{Hf} values from 14 to -3, zircons from Kelowna, BC (N=1) have two distinct ϵ_{Hf} populations, with ϵ_{Hf} values from 14 to -10, and zircons from Republic, WA (N=2), have primarily negative ϵ_{Hf} values from 8 to -16.

CHAPTER 5

ANALYSIS

5.1 U-PB AGE POPULATIONS AND SEDIMENT SOURCES

Eocene sandstone from the SCC contain a variety of detrital zircon U-Pb age populations, but several populations are more prevalent than others. The most common age population consists of Eocene-age (ca. 51 Ma) detrital zircons: of all of the zircons analyzed, nearly 50% have U-Pb ages that correspond to the Eocene Epoch, with the next most common populations being Jurassic (29%), Paleocene (10%), Cretaceous (8%), and Triassic (3%) in age (Figure 5.1). Zircons with Permian-Archean age are also present in the samples, but at a relatively small percentage.

Eocene-age detrital zircons, particularly those with ca. 50 Ma ages are interpreted to have been derived from the voluminous Challis-Kamloops volcanics, which were deposited across the SCC between ca. 55 and 42 Ma (e.g. Pearson and Obradovich, 1977; Ewing, 1980; Armstrong, 1988; Armstrong and Ward, 1991; Morris et al., 2000; Madsen et al., 2006). Record of this volcanic episode is present throughout the North American Cordillera, but is particularly common in the areas of Idaho, WA, and southern BC (Souther, 1991; Breitsprecher et al., 2003; Dostal et al., 2003; Ickert et al., 2009). The Challis-Kamloops volcanics consists of calc-alkaline igneous rocks in the west, and alkaline igneous rocks in the east (Armstrong and Ward, 1991; Ickert et al., 2009); the volcanic units in the south are alkaline in nature (Madsen et al., 2006), while the middle

of the Challis-Kamloops volcanics in southern BC and northern United States represents a geochemical transition zone. This transition zone includes adakitic, alkalic, and arc rocks (Ewing, 1981a; Breitsprecher et al., 2003; Madsen et al., 2006). Today, many of the sedimentary basins in the SCC are interstratified with volcanic units related to the Challis-Kamloops series (Dostal et al., 2003; Ickert et al., 2009). The ubiquity of ca. 50 Ma volcanics in the area limits the use of these grains as provenance indicators; however, ϵHf isotopes of these ~50 Ma grains are useful for interpreting provenance and sediment source areas (below).

Mesozoic-age detrital zircons are interpreted to have been derived from the erosion of local Cretaceous, Jurassic, and Triassic intrusive intermediate-to-felsic rocks, which are common across the SCC (Armstrong, 1988; Armstrong and Ward, 1991). Examples of Jurassic-Cretaceous igneous rocks in the area include the Okanagan and Similkameen batholiths, which are exposed adjacent to Eocene sedimentary strata. Igneous rocks of Triassic- to very early Jurassic-age in the area include the Iron Mask and Cherry Creek plutons (Ewing, 1981a; Armstrong, 1988). In addition, it is possible that Triassic-Cretaceous age detrital zircons in the Eocene sedimentary strata were recycled from Triassic-Cretaceous sedimentary strata in the SCC. Examples of these strata include the Sophie Mountain Conglomerate and clastic units of the Rossland Group (Tipper, 1984; Monger et al., 1991; Beatty et al., 2006) in southern BC. Although these units are far smaller volumetrically than the igneous rocks, they may have contributed some Jurassic-Cretaceous zircons. Once again, the widespread nature of these rocks in the SCC makes them difficult to use for provenance studies, although the ϵHf data

described below provides some possible avenues for future research and improved provenance reconstructions.

Paleozoic-age detrital zircons are present in several samples, particularly in the Princeton and Merritt areas, although the relative percentage of these grains to the total grains analyzed is small (Figure 3.1). The specific origin of these detrital zircons is difficult to determine due to the fact that many of these grains may have been recycled once or more times prior to deposition as Eocene sediments. Samples with $n \geq 3$ of Permian-, Carboniferous-, Devonian-, Silurian-, and Ordovician-age detrital zircons are restricted to samples 15CAN10B and PB2 from Princeton, BC; sample COLDWATER1, from a sample collected south of Merritt, BC, also has $n \geq 3$ of Devonian-age detrital zircons. Possible sources of Paleozoic grains include the rocks that accreted onto western North America during the Mesozoic-early Cenozoic. These terranes are located in the Omineca, Intermontane, and Coast Belts, and include the Bridge River (Carboniferous-Upper Jurassic), Cache Creek (Carboniferous-Lower Jurassic), Chilliwack (Devonian-Lower Jurassic), Quesnel (Upper Paleozoic-Lower Jurassic), Slide Mountain (Devonian-Permian), and Kootenay (Proterozoic-Paleozoic) terranes (Gabrielse et al., 1991; Massey et al., 2005; Beatty et al., 2006).

Proterozoic-age detrital zircons with $n \geq 3$ are present in several samples (CAN-BC-1024L, SKEL1, 15Ca18A, and ABBEYRD2), including Midway, Summerland, Kelowna, and Kamloops, BC (Figures 3.2, 3.4, 3.5, and 3.8). Proterozoic detrital zircons are interpreted to have been derived originally from ancestral North America, although the potential for the recycling of these grains between Proterozoic and Eocene times is very high. In particular, the Belt-Purcell Group is a widespread and voluminous

sedimentary/metasedimentary unit that contains Proterozoic-age detrital zircons (Evans et al., 2000; Luepke and Lyons, 2001; Ross and Villeneuve, 2003; Lemieux et al., 2007).

5.2 MAXIMUM DEPOSITIONAL AGES

The youngest detrital zircon ages constrain the timing of deposition (Rainbird et al., 2001; Stewart et al., 2001; Surpless et al., 2006; Brown and Gehrels, 2007). The youngest-grain measures can only define the MDAs, not the actual depositional ages (Dickinson and Gehrels, 2009), but MDAs can be useful for evaluating regional trends, particularly in areas like the SCC where sedimentation was accompanied by coeval volcanism.

Dickinson and Gehrels (2009) determined the most statistically robust method to estimate MDA was to measure the mean age of the youngest two or more grains that overlap in age at 2σ . Using this technique, the majority of the 22 samples for this study have an MDA of 47-50 Ma, without any regional trends dependent on longitude (Figure 5.2). There are a few samples with outlying MDAs, including Princeton (described below), which has MDAs dating to the Mesozoic (PRINCE1A & PB2). Despite the ages, we know these samples are younger than their MDAs indicate, based on previous paleobiology studies in the area (McMechan, 1983; Read, 2000; Greenwood et al., 2005; Mustoe, 2011).

Merritt samples also have outlying MDAs, with both samples having MDAs of 43 Ma. A 43 MDA is younger than those from surrounding areas, but consistent with fossils in the area, which date the strata of the Merritt Basin as Eocene to Miocene in age (Rouse

et al., 1971; Piel, 1971, 1977; Clague, 1974; Rouse and Mathews, 1979; Mathews and Rouse, 1984; Read, 2000).

5.3 COMPARING AGE POPULATIONS

Comparing the U-Pb ages between samples and sampling areas can provide insights into the depositional history and the paleogeography of a region. The difficulty of such comparisons lies in the large number of U-Pb ages (e.g., Vermeesch, 2013; Spencer and Kirkland, 2015). Visual comparison using traditional KDE or PDP curves is next to impossible with all 22 samples. Vermeesch (2013) proposed a new visual display, multi-dimensional scaling (MDS), which involves a two-dimensional map of points. MDS is based on a dissimilarity matrix for a series of samples derived from the D values of the Kolmogorov-Smirnoff (K-S) test. The K-S test converts detrital zircon probability spectrum to a cumulative density arrangement, which is the sum of probabilities with increasing age, based on the D values from each sample. The closer that outputs are plotted on the MDS plot to each other, the more similar they are; the farther away they are plotted, the more dissimilar they are. A solid line is drawn from each point in the plot to its “closest” neighbor in dissimilarity-space, and a dotted line is drawn to the second “closest” neighbor (Vermeesch, 2013).

All U-Pb data are separated by location and are plotted using the MDS technique in Figure 5.3 (for KDEs and PDPs of U-Pb data for all 22 individual samples, see Appendix C). On this plot, there are two principal groups: the first group consists of Princeton, Merritt, Summerland, and Coldwater, while the second group consists of Blakeburn, Republic, White Lake, McAbee, Kelowna, Midway, and Kamloops. These two groups appear to reflect the relative proportion of ca. 51 Ma grains to ca. 160 Ma

grains. Alternatively, an argument could be made that three groups exist, with Blakeburn, Republic, and White Lake representing a distinct group (Figure 5.3).

Proximity in MDS space is not always consistent with proximity in geographical space. KDEs for Midway and Kamloops, BC (Figure 5.3), are nearly identical, even though they are located 200 km apart. Samples from both locations show widespread age populations between ~50-100 Ma. In MDS space, Midway and Kamloops are plotted almost on top of one another, as well are connected by a solid line, suggesting they are highly similar to one another. In contrast, Samples from Princeton and Blakeburn were collected less than 20 km apart, but are plotted far apart in MDS space (Figure 5.3). Detrital zircons in Princeton samples have markedly older, Mesozoic U-Pb ages, while detrital zircons from Blakeburn consist primarily of Cenozoic U-Pb ages.

Adding synthetic age populations to MDS evaluations can highlight principal sediment source areas for different samples (Spencer and Kirkland, 2015). Based on the two largest detrital zircon age populations from our samples, we plotted two “synthetic” source areas, one with an age of 51 ± 5 Ma, which approximates the Challis-Kamloops volcanics and associated rocks, and the other with an age of 160 ± 5 Ma, which approximates the Jurassic-age population present in several samples (Figure 5.4). The addition of synthetic age populations does not alter the relative similarity/dissimilarity between sample locations, but those locations with greater similarity to 51 Ma or 160 Ma source areas will group nearer these endmembers. With the synthetic source areas added to the MDS plot (Figure 5.4), the sample locations continue to be separated into distinguishable groups: Merritt, Princeton, Summerland, and Coldwater plot more closely to the 160 Ma endmember, while the remaining sample locations plot more closely to the

51 Ma endmember. We interpret this as indicating that locations such as Blakeburn, BC, received the majority of its sediment from the Challis-Kamloops volcanics (i.e., 51 Ma), whereas the Princeton, Merritt, Summerland and Coldwater area received a greater proportion of sediment from Jurassic-age sources (or younger if the grains were recycled).

5.4 ϵ_{Hf} INTERPRETATIONS

The abundance of ca. 50 Ma detrital zircons in the Eocene strata of the SCC combined with the widespread ca. 50 Ma Challis-Kamloops volcanics makes provenance interpretations difficult. For example, a 50 Ma detrital zircon within a particular succession could have been derived from either a local or distant exposure of Challis-Kamloops volcanics. Moreover, it is impossible to determine if two sedimentary successions containing ca. 50 Ma grains were once part of a continuous sedimentary basin, or if they were originally two separate basins with similar sediment source rocks in the surrounding area. ϵ_{Hf} data from these analyses offers a way of examining the abundant ca. 50 Ma grains in the Eocene strata in a different space.

ϵ_{Hf} values from the 4 collected samples vary between -16 to +14 for detrital zircons with ca. 50 Ma U-Pb ages (Figure 4.1). In general, zircons from Republic, WA, have the most negative ϵ_{Hf} values, those from Merritt have the most positive ϵ_{Hf} values, and those from Kelowna have primarily negative values as well as some positive values (Figure 4.2). We interpret the negative ϵ_{Hf} values in the Republic area as indicating the ca. 50 Ma zircons crystallized from relatively evolved igneous sources (e.g., Amelin et al., 1999; Bodet and Schärer, 2000; Kinny and Maas, 2003; Augustsson et al., 2006; Bahlburg et al., 2011; Cecil et al., 2011). Gashnig et al. (2011) measured zircons with

similar ϵ_{Hf} values in the Idaho Batholith, south-southeast of Republic, WA. We interpret the positive ϵ_{Hf} values in the Merritt area as indicating the ca. 50 Ma grains were derived from relatively juvenile sources (e.g., Amelin et al., 1999; Bodet and Schärer, 2000; Kinny and Maas, 2003; Augustsson et al., 2006; Bahlburg et al., 2011; Cecil et al., 2011). Similar ϵ_{Hf} values were measured in the Coastal Batholiths of BC by Cecil et al. (2011). We interpret the ϵ_{Hf} values of detrital zircons in the Kelowna area as a bimodal population, and therefore likely from two different sources. The positive and negative ϵ_{Hf} values in the Kelowna area are interpreted to reflect derivation from both relatively evolved and juvenile sources.

The variability in ϵ_{Hf} values between detrital zircons of the same age correspond to their depositional locations relative to the presumed margin of ancestral North America. The changes in ϵ_{Hf} values correspond to the general location of the Sr 0.706 isopleth, which separates the younger, accreted terranes in the west from ancestral North American crust to the east (Figure 1.3; Armstrong, 1988; Souther, 1991; Gosh, 1995; Dostal et al., 2003). Zircons with primarily positive ϵ_{Hf} values are located west of the Sr 0.706 isopleth, whereas zircons with negative ϵ_{Hf} values are located to the east of the same isotopic boundary. The Kelowna sampling location lies nearly atop the Sr 0.706 isopleth and has zircons with both positive and negative ϵ_{Hf} values.

The differences in ϵ_{Hf} values of detrital zircons have important implications for reconstructing the dimensions and continuity of the Eocene sedimentary basins. If during the Eocene, one large basin, or several smaller basins that were in communication, were receiving sediment from the same or similar sources at the time of deposition, we would expect similar ϵ_{Hf} values, independent of their geographical location and distance from

the Sr 0.706 isopleth. Instead, we see relatively distinct ϵ_{Hf} populations for samples from Merritt, Kelowna, and Republic, dependent on their proximity and position to the Sr 0.706 isotope boundary. The distinct ϵ_{Hf} populations are consistent with the strata of isolated basins, which received no sediment communication at the time of deposition.

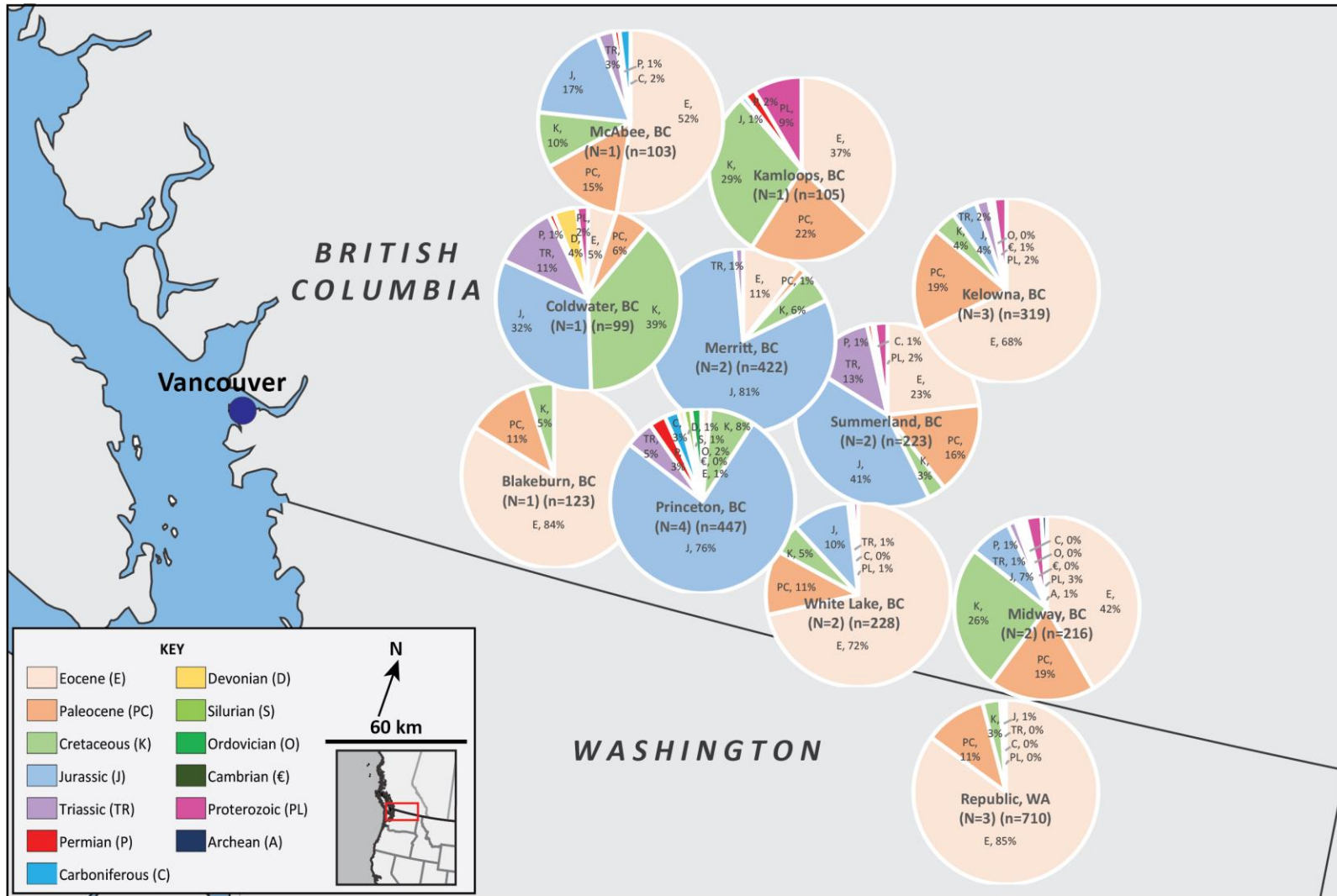


Figure 5.1 Map of the SCC with pie charts displaying the distribution of detrital zircon U-Pb ages, separated by location.

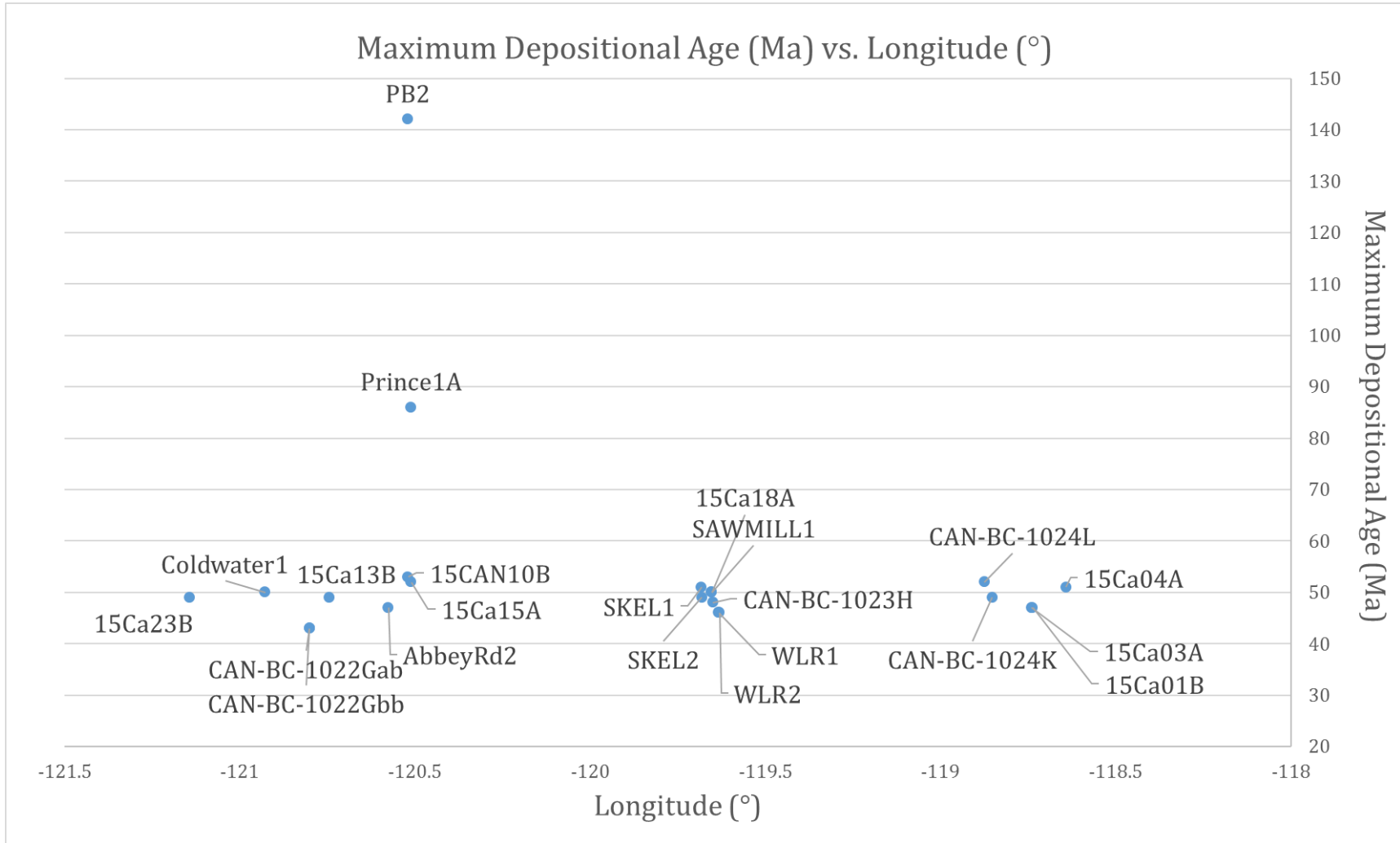


Figure 5.2 Graph showing maximum depositional age (MDA) of N=22 samples versus the longitudinal position where each sample was collected. Most samples have MDAs ~47-50 Ma, with no regional trends dependent on longitude.

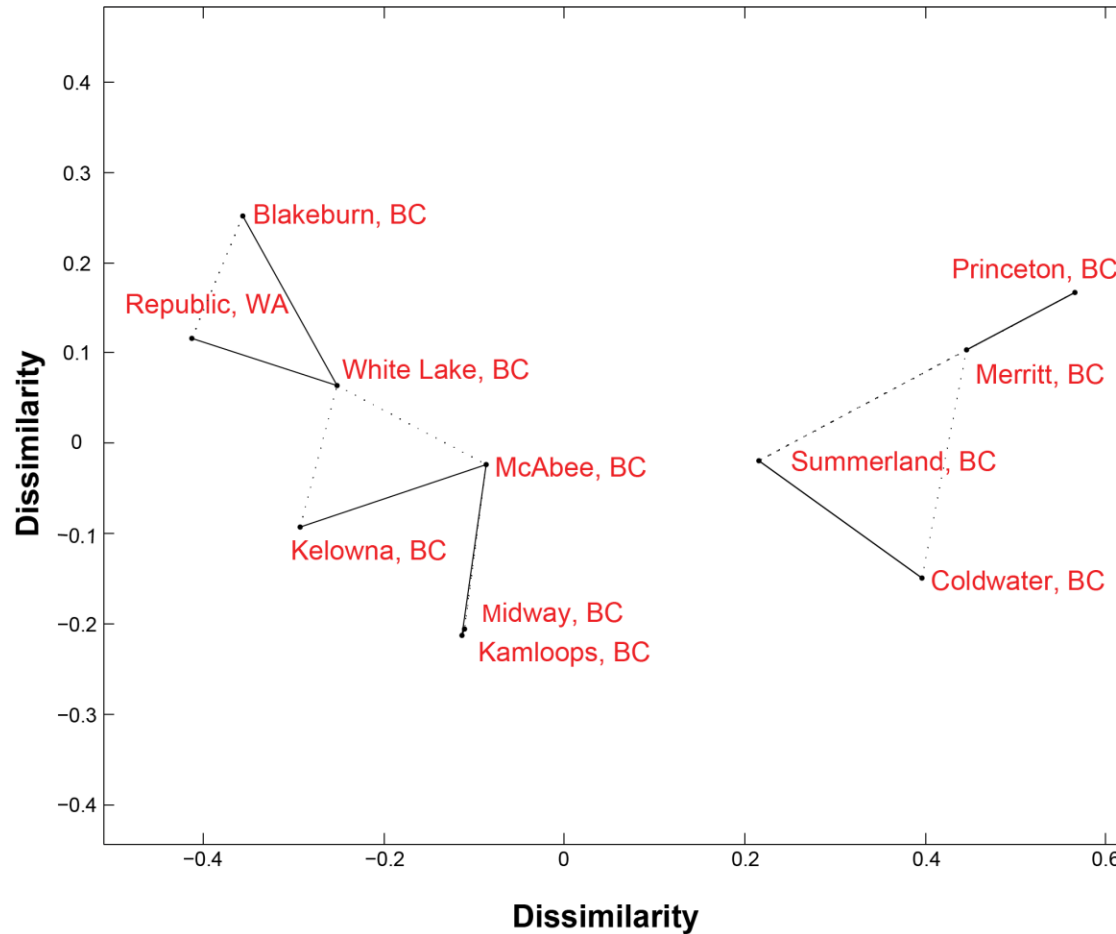


Figure 5.3 MDS plot of all 22 samples, separated by location. This MDS plot shows the similarities and dissimilarities between detrital zircon U-Pb age population data between sample locations. This may be observed through the distance each location is plotted relative to one another in Euclidean space. Solid lines mark the closest neighbors in dissimilarity-space, while dashed lines show the second closest neighbors. In this plot, for example, Midway, BC, and Kamloops, BC, contain statistically similar detrital zircon U-Pb age populations.

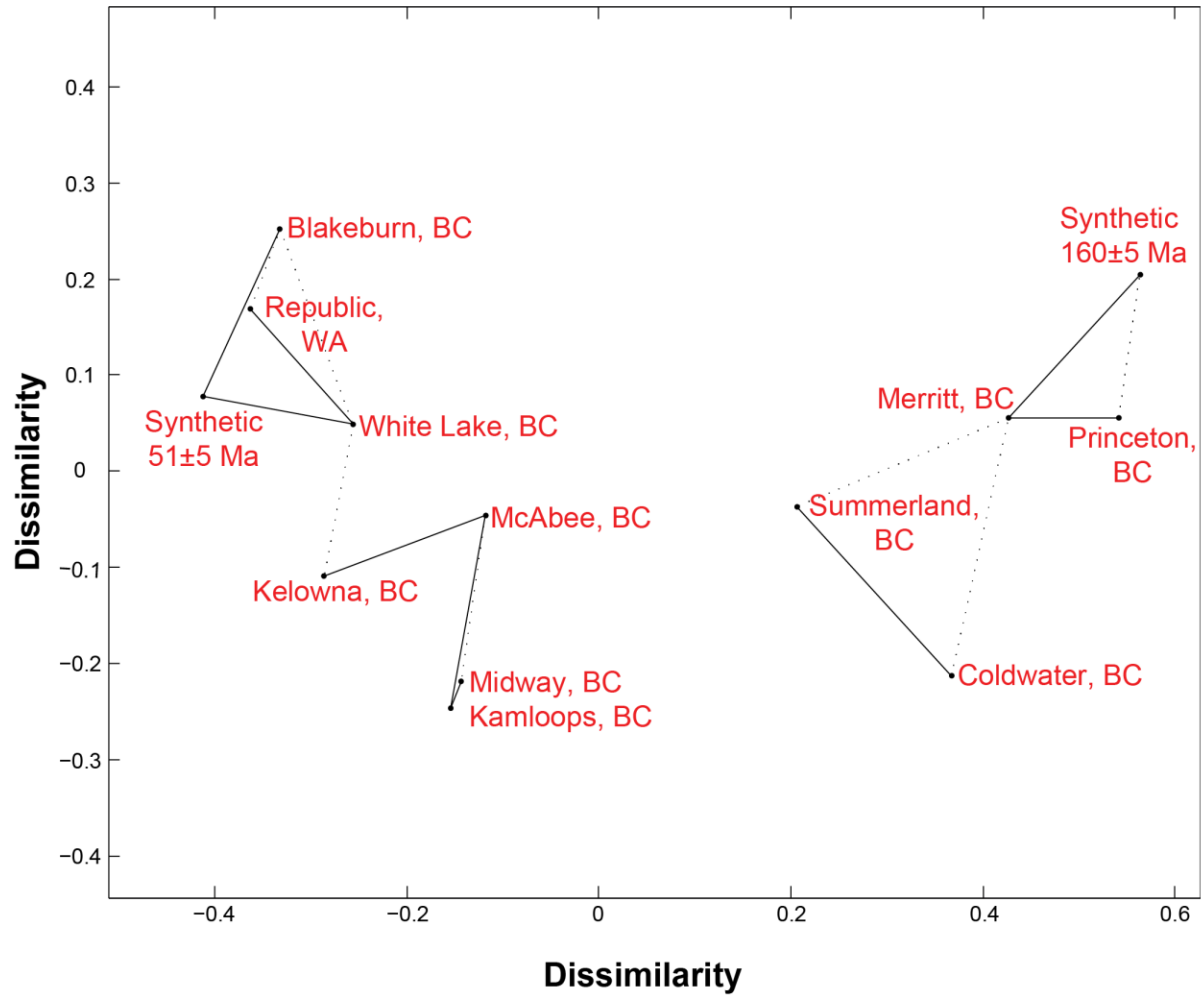


Figure 5.4 MDS plot of all 22 samples, separated by location, with synthetic, normally-distributed 51 ± 5 Ma, and 160 ± 5 Ma age populations. The synthetic age populations show the increasing contributions of detrital zircons with those age components, providing more information on the primary source of sediments at locations plotted closely to a synthetic age.

CHAPTER 6

DISCUSSION

6.1 SOUTHERN CANADIAN CORDILLERA INTERMONTANE BASINS

Deposition in intermontane regions of cordilleran margins takes place in a variety of tectonic and structural settings (Horton, 2012). In the South American Cordillera today there are intermontane basins associated with compression (Horton, 1998, 2012), extension (McNulty and Farber 2002), strike-slip faulting (Toussaint and Restrepo, 1994; Winkler et al., 2005), and mantle processes (DeCelles et al., 2009). These basins are manifested as everything from single, relatively continuous depocenters like the Altiplano (Horton, 2012), to multiple, isolated basins like those in the Puna Plateau (Allmendinger et al., 1997). The style and nature of intermontane deposits record important insights into the tectonic mechanisms responsible for sediment accumulation (e.g., DeCelles et al., 2009), but can be difficult to reconstruct from ancient sedimentary successions due to the poor preservation potential in intermontane areas (Horton, 2012).

A basic question regarding the Eocene strata in the SCC hinterland is whether these deposits were once associated with one single hinterland basin (i.e., was sediment transport and water flow in communication throughout the area), or multiple isolated basins. Although the Eocene-age deposits in the SCC hinterland are exposed today in discrete locations across the area, this does not mean that they were originally deposited in isolated basins. Approximately coeval sedimentary strata preserved to the west of the

SCC hinterland are exposed today in a series of discrete exposures over a ~200 km distance in the state of WA. Eddy et al. (2016) demonstrated that despite the isolated and discrete nature of these exposures, the Eocene sediments in all of these locales were originally deposited in a single depositional basin, which was segmented by later faulting. The similar ages of the Eocene strata in the SCC hinterland (Figure 1.4), the similar MDAs (Figure 5.2), the consistent lithofacies, and the similarity in many of the detrital zircon populations (Figure 3.1) suggest the possibility of a similar history for these strata.

Our data indicate the Eocene sedimentary units exposed across the SCC hinterland were deposited at approximately the same time, but in multiple, isolated basins. Although the lithofacies in each Eocene exposure in the SCC are similar, the physical sedimentology suggests local derivation, proximal provenance, and minimal distances of sediment transport. Strata in many of the exposures in the SCC consist of matrix-supported conglomerates, suggesting these units were deposited by debris-flow processes. Debris-flows typically cease moving when local slope diminishes below several degrees, indicating proximal source areas and local paleorelief (e.g., Blair and McPherson, 1994). Localized topography and sediment sources is more consistent with multiple basins and local relief. Similarly, the angularity of the conglomerate and sandstone beds indicate proximal deposition and minor sediment transport. Abrupt changes in grain size or facies across relatively small geographic distances (e.g., 25 km), as well as local facies changes within Eocene exposures are also more consistent with localized depocenters versus a single, continuous basin. The paleoflora throughout the area also suggest localized basins and transport (Greenwood et al. 2005) as the fossil

leaves in the strata are not known to transport more than a few hundred meters down streams (Greenwood, 1992; Steart et al., 2002).

ϵ_{Hf} data provide additional evidence the Eocene sediment in the SCC were derived from different sources and did not mix within a continuous regional basin. Many of the detrital zircons in the Eocene strata of the SCC have U-Pb ages of ~50 Ma, but have distinct ϵ_{Hf} values between locations. The distinct ϵ_{Hf} values between samples is more consistent with multiple sediment sources and multiple basins. If the SCC hinterland were occupied by a single regional basin where sediment and water were in communication, a greater variety of ϵ_{Hf} values would be expected within each location.

6.2 PROVENANCE

The majority of the samples collected in the SCC contain high percentages of ca. 50 Ma detrital zircon grains; however there are several that deviate from this trend. Samples from Princeton, Merritt, and Coldwater, which are all in relatively close proximity to one another (Figure 1.1), contain relatively large percentages of 150-160 Ma detrital zircons and few with ca. 50 Ma ages (Figures 3.6, 3.10, and 3.11). The most obvious interpretation from these numbers is that the small population of ca. 50 Ma detrital zircons reflects a relatively small contribution of zircons from the Eocene Challis-Kamloops volcanics during deposition, but the reason for this is not entirely clear. We postulate that either the Eocene volcanic units were not widespread in this area of the SCC and/or that these volcanic units were eroded prior to deposition of the sedimentary strata in this region. The Princeton Group, from which samples were collected in the Princeton area, is interstratified with volcanic and volcanoclastic units (McMechan, 1983; Read, 2000), and areas adjacent to these specific locations in the SCC contain large

populations of ca. 50 Ma detrital zircons (e.g., Blakeburn, Figure 3.7), suggesting the absence of Eocene volcanic rocks in this area is an unlikely explanation for the small population of Eocene detrital zircons. We propose that the likely explanation is that the Challis-Kamloops volcanic strata in this part of the SCC were eroded prior to deposition in the Princeton, Merritt, and Coldwater areas, leaving the underlying Jurassic igneous rocks in the region as the principal sediment source to these basins. The samples from the Merritt, Princeton, and Coldwater areas were collected from the middle-to-upper portion of the respective stratigraphic successions, leaving open the possibility that by the time of deposition, the surrounding volcanic strata had already been eroded from the contributing sediment source areas. This hypothesis implies that strata from the lowermost portion of these successions would have larger populations of ca. 50 Ma detrital zircons.

Samples from the White Lake location demonstrate this trend of increasing proportions of 150-160 Ma detrital zircons up-section, which we interpret as an unroofing signal (Figure 1.1). Sample WLR1 was collected from a lower portion of the White Lake succession and WLR2 was collected from higher in the section (Figure 1.6). Sample WLR1 contains a large population of ca. 50 Ma detrital zircons and only few with ages >150 Ma (Figure 6.1), whereas sample WLR2 contains larger populations of 150-160 Ma detrital zircons (Figure 6.2). WLR1 and WLR2 samples were collected from Penticton Group strata, deposited in half-grabens and supradetachment basins, which formed adjacent to the Okanagan Valley fault system (McClaughry and Gaylord, 2005; Hamblin, 2011). The volcanic rocks in the Penticton Group of the White Lake Basin are associated with Challis-Kamloops volcanic episode; Eocene strata in the basin rest non-conformably on Mesozoic-Cenozoic igneous and metamorphic rocks (Dostal et al., 2003). The

increase in ~155 Ma detrital zircons up-section may indicate progressive erosion of the Challis-Kamloops volcanic carapace from the surrounding region, which was replaced by exposures of the surrounding bedrock. Determining provenance from the relative percentage of detrital zircons is tenuous without large numbers of zircons (e.g., Pullen et al., 2014); however, similar unroofing trends are noted within the White Lake Basin by detailed sedimentary and stratigraphy analyses by McClaughry and Gaylord (2005), as well as by detrital provenance on conglomerates and breccias by Suydam and Gaylord (1997) in the nearby Toroda Creek half graben.

The fact that the three areas with relatively large populations of 150-160 Ma detrital zircons are relatively close to one another geographically suggests some genetic relationship. The two most likely scenarios are that the Coldwater, Princeton, and Merritt strata were deposited in a continuous basin (sediment mixing) or shared similar source rocks. Facies from each of the locations suggests sediment was derived and deposited in proximal systems (e.g., alluvial fan), which is inconsistent with a continuous sedimentary basin, although it does not exclude this hypothesis. We surmise that the hypothesis of similar source rocks in the regions surrounding these areas is the primary cause of the similar detrital zircon signatures.

6.3 IMPLICATIONS FOR GEODYNAMIC AND TECTONIC MODELS

Sedimentation in the hinterland of Cordilleran margins records information on topography, physiography, and tectonics. Several models have been proposed to explain the Eocene evolution of the SCC hinterland, focusing in particular on the mechanisms that changed the stresses from compression to extension. Bao et al. (2014) proposed Eocene delamination of the lower lithosphere in the SCC. This model involves the

removal of dense mantle lithosphere from beneath the SCC and upwelling of asthenosphere, which would have resulted in surface uplift in the overlying SCC hinterland and subsequent extension. One of the primary pieces of evidence for this is the absence of mantle lithosphere beneath the SCC hinterland today (Bao et al., 2014). It is difficult to test this model with sedimentary strata alone, however the data we have are not consistent with at least some aspects of this hypothesis. Delamination or drip models predict that prior to the removal of the dense mantle lithosphere and eclogitic lower crust, the overlying region becomes topographically depressed, forming a regional “drip basin” (DeCelles et al., 2009). Such a process is thought to lead to deposition (typically fine-grained deposits) in one, regionally continuous basin in the hinterland of cordilleran margins, which is subsequently segmented by upper crustal normal-faulting following drip-removal (DeCelles et al., 2009). We observed no evidence of a continuous, correlatable stratigraphic unit at or near the base of the sedimentary successions in the SCC hinterland, as would be expected in a removal scenario. It is possible that such strata were eroded prior to deposition of the Eocene sedimentary strata in the SCC, and therefore not preserved, or that current ideas about drip basins are over-simplified. Either way, our current data set does not contain evidence to support mantle delamination or drip from beneath the SCC during the Eocene.

Slab rollback or steepening of the down-going slab beneath the SCC during the Eocene could be used to explain the transition from compression and extension in the SCC (e.g., Horton and Fuentes, 2016). In this model, the decrease in the subduction angle beneath the SCC during the Eocene could have resulted in reduced compressive stresses, allowing for extension. The rollback of the subducted Farallon Plate to the south of the

SCC, in the US Cordillera, was accompanied by significant topographic, sedimentary, and volcanic changes and occurred at roughly the same time as extensional deformation and deposition in the SCC (e.g., Humphreys, 1995; Dickinson, 2002, 2006; Smith et al., 2014). The data from the SCC, however, is not consistent with a slab rollback model. Rollback is generally associated with a margin-directed shift in volcanic activity (Humphreys, 2009; Smith et al., 2014), which is not observed in the geologic record of the SCC (e.g., Armstrong, 1988). In addition, deformation in the overriding plate tends to mimic the margin-directed shift in the volcanic arc, which in this case would result in an east-to-west trend in deformation and sedimentation (e.g., Smith et al., 2014). Existing paleontological constraints, coupled with our MDA data, suggest all of the basins in the SCC hinterland formed at approximately the same time, without any spatial-temporal trend (Figure 5.2).

The data from this study are consistent with models proposing that an oceanic-spreading center (i.e., slab window) was subducted beneath the SCC during the Eocene. Tectonic and volcanic studies suggest that a slab window was located underneath the hinterland of the SCC during the Eocene, as the Resurrection/Kula-Farallon ridge subducted along western North America (Thorkelson and Taylor, 1989; Lawver and Scotese, 1990; Breitsprecher et al., 2003; Groome et al., 2003; Haeussler et al., 2003; Madsen et al., 2006; Ickert et al., 2009). South of this slab window, the Farallon Plate experienced slab rollback directed to the south-southwest (present-day coordinates), whereas to the north, the Resurrection/Kula plate subducted obliquely to the north-northeast (Humphreys, 1995; Thorkelson and Taylor, 1989; Breitsprecher et al., 2003). In the SCC hinterland, the slab window and the oblique subduction resulted in a wide zone

of transtension with extension oriented roughly northwest-southeast (Figure 6.3; Ewing, 1981a; Price and Carmichael, 1986). Our data suggest the upper crust in the SCC hinterland responded to this stress field through strike-slip faulting in the western hinterland (e.g., Princeton Basin), detachment faulting in the central hinterland (OVSZ), and high-angle normal faulting in the eastern hinterland (Republic; Figure 6.3). The transtension and the upper crustal deformation resulted in the coeval formation of strike-slip and pull-apart basins, supradetachment basins, and grabens. The en-echelon nature of the grabens, the direction of slip along the detachment fault hanging wall and the strike slip basins are consistent with right-lateral transtension in the hinterland (Ewing, 1981a; Price and Carmichael, 1986). Similar right-lateral deformation occurred in the forearc region of the SCC during the same time (Eddy et al., 2016). These numerous basins formed at approximately the same time (the OVSZ may have been active prior to this; Parrish et al., 1988; Brown et al. 2012), in a hinterland area that was ~3-4 km above sea-level (Mix et al., 2011; Foster-Baril 2017).

6.4 MODERN ANALOGUE

A modern tectonic analogue of the SCC is the southern Chilean margin of South America. The forearc of the southern Andes consists of the Chile Triple Junction, the location where the Nazca, Antarctic, and South American Plates meet. North of the Chile Triple Junction, the Nazca plate is obliquely subducting under South America, resulting in the structural decoupling and northward motion of the Chiloé block from the rest of the Andes, along the Liquiñe-Ofqui fault zone (Cembrano et al., 1996; Rosenau et al., 2006; Melnick et al., 2009; Georgieva et al., 2016). This fault zone consists of a crustal-scale intra-arc, dextral-transpressional fault system, which accommodates the margin-parallel

component of oblique subduction, and is associated with volcanic activity, rock uplift, exhumation, and enhanced cooling (Cembrano et al., 2002; Thomson, 2002; Rosenau et al., 2006). The collision of three relatively short ridge segments of the Chile Rise in the Golfo de Penas region has resulted in the opening of an areally-extensive asthenospheric slab window beneath southern Patagonia (Cande and Leslie, 1986; Cande et al., 1987; Murdie et al., 1993; Breitsprecher and Thorkelson, 2009; Russo et al., 2010a). The northward motion of the Chiloé block is accommodated by extension in the Golfo de Penas basin (Forsythe and Nelson, 1985; Nelson et al., 1994).

East of the Chile Triple Junction, the Northern Patagonian Icefield is characterized by abrupt paleotopographic elevations and relief. This area consists of localized extension along normal faults, tectonic subsidence, and lower elevations along the Andean crest line to the south, which is characterized by fjord landscapes and anomalously low elevation regions along the axis of the Andes (Georgieva et al., 2016). Margin-parallel right-lateral strike-slip deformation along the eastern flank of the Northern Patagonian Icefield is enhanced by the oblique collision of the oceanic ridge segments of the Chile Rise over the past 6 Ma.

The SCC during the Eocene also experienced regional transtensional and dextral strike-slip faulting, attributed to the subduction of the Resurrection-Farallon spreading center. There was also oblique subduction along the western margin of southern British Columbia and northern Washington during the Eocene.

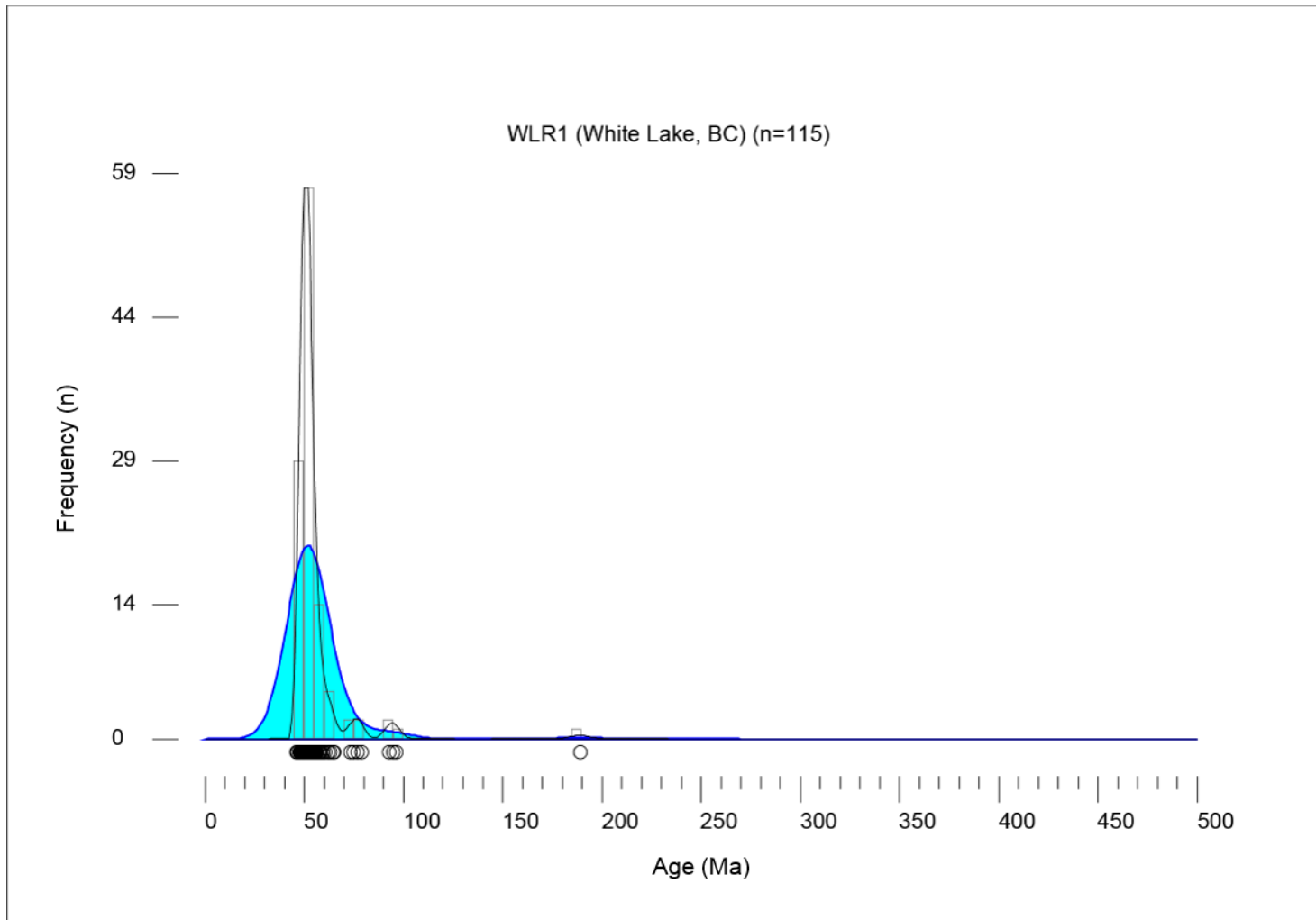


Figure 6.1 Detrital zircon U-Pb KDE (blue) and PDP (black) plot for WLR1 from White Lake, BC, from 0-500 Ma. KDE has a bandwidth of 10, and a normalized area of 0.02. Histogram is represented by gray boxes, which have a bin width of 5.

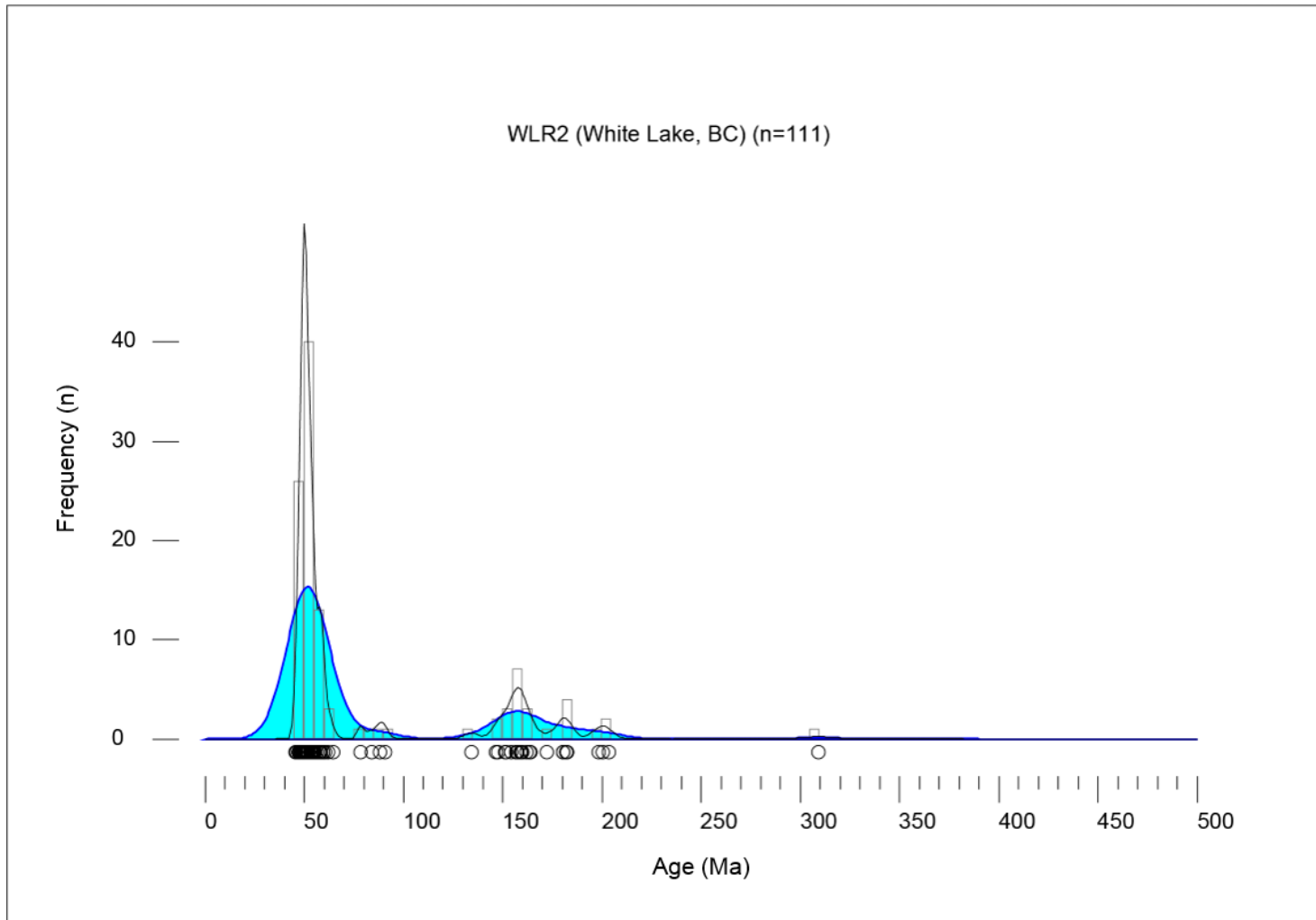


Figure 6.2 Detrital zircon U-Pb KDE (blue) and PDP (black) plot for WLR2 from White Lake, BC, from 0-500 Ma. KDE has a bandwidth of 10, and a normalized area of 0.02. Histogram is represented by gray boxes, which have a bin width of 5.

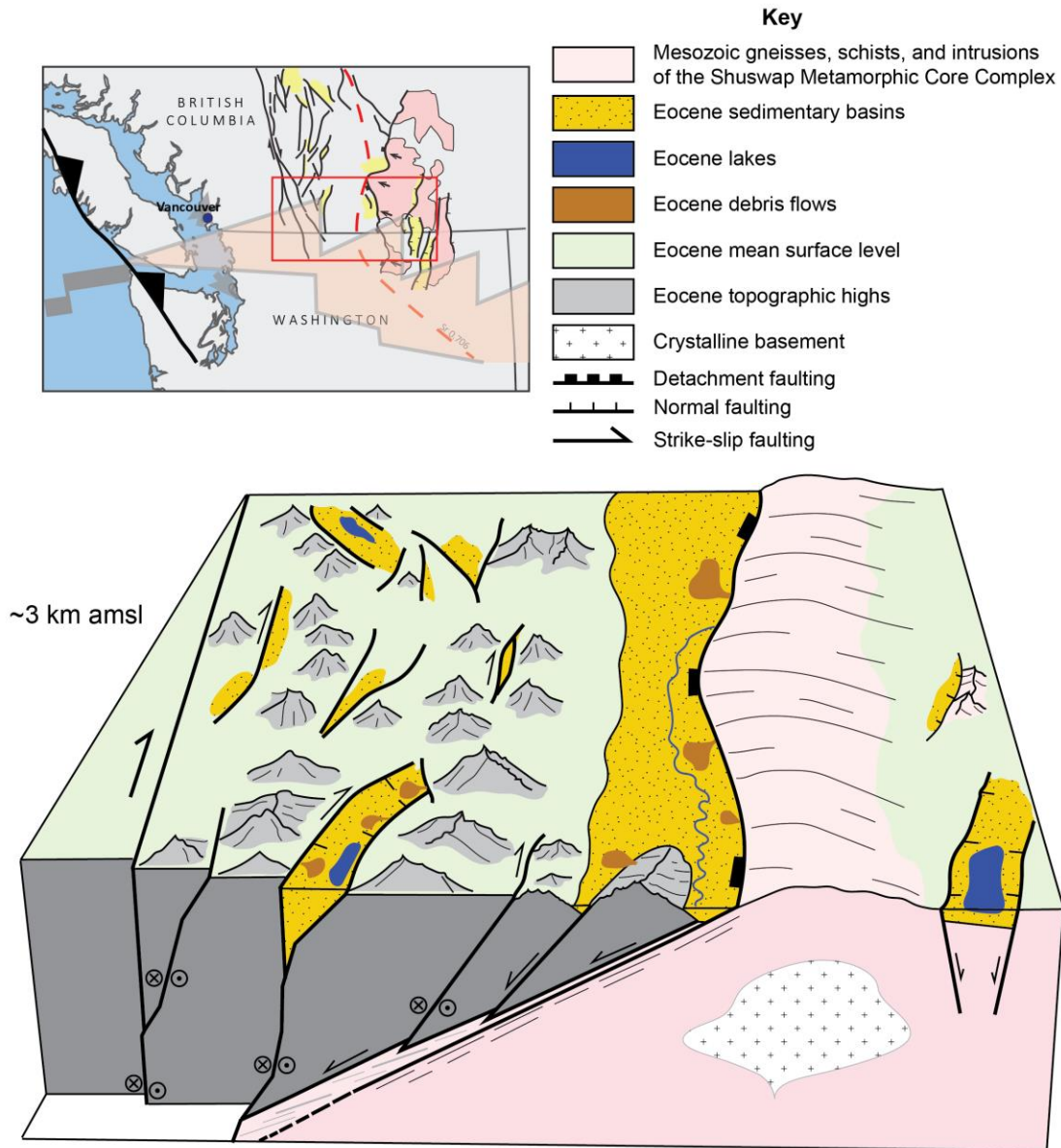


Figure 6.3 3D diagram of the surface manifestation and basin formation above the complicated structural and tectonic setting in the hinterland of the SCC (represented in the inset map view). Due to the regional dextral transtension during the Eocene, strike-slip faulting and the exhumation of the Shuswap Metamorphic Core Complex caused multiple, isolated basins, separated by local paleohighs, to form. In the east, supradetachment basins formed along the metamorphic core complex, while in the west, normal and strike-slip faulting caused basins to form in pull-apart, graben, and half-graben structures.

CHAPTER 7

CONCLUSION

The transition from compression to extension and transtensional stress along the western margin of BC and WA during the Eocene caused the formation of several basins in the hinterland of the SCC. The regional transtensional stress and dextral strike-slip faulting is attributed to the subduction of the Resurrection-Farallon spreading center, resulting in oblique subduction along the western margin of this part of North America during this time. Today, Eocene strata are exposed in separate outcrops, and consist of clast- and matrix-supported pebble and cobble conglomerates, very coarse- to very fine-grained sandstones, mudstones, and coals, which were deposited in fluvial, alluvial fan, lacustrine, and paludal environments. This study measured ~650 m of Eocene strata, analyzed 2,995 detrital zircons for U-Pb ages, and analyzed 67 detrital zircons for ϵ_{Hf} values in order to determine the sediment provenance, MDAs, and whether strata were deposited in isolated basins or one regional and continuous basin during this complicated tectonic and structural setting.

Twenty-two sandstone samples were collected from 11 locations throughout the SCC; these samples contain primarily Eocene U-Pb ages (ca. 51 Ma), interpreted to derive from the erosion of the Eocene Challis-Kamloops volcanics, and Jurassic U-Pb ages (ca. 160 Ma), interpreted to derive from Mesozoic-age batholiths. MDAs of the Eocene sandstones are relatively similar throughout the region, with ages 47-50 Ma,

suggesting widespread deposition throughout the study area at approximately the same time. ϵ_{Hf} values for detrital zircons with U-Pb ages of ~50 Ma were obtained from samples in 3 locations (Merritt, Kelowna, and Republic) across the SCC, and vary between -16 and +14. Detrital zircons from Merritt, BC, in the west of the study area, have primarily positive ϵ_{Hf} values, with one negative value (-2 to +13), indicating relatively juvenile sources. Detrital zircons from Republic, WA, in the east of the study area, have primarily negative ϵ_{Hf} values, with one positive value (-16 to +7), indicating relatively evolved sources. Detrital zircons from Kelowna, BC, in the central part of the study area, have two populations of ϵ_{Hf} values; one positive and one negative (-10 to +12). ϵ_{Hf} values coincide geographically to their location relative to the Sr 0.706 isotope boundary, which separates ancestral North American crust to the east from accreted terranes to the west.

Together, the localized changes in stratigraphy throughout the interior of the SCC, the variability in ϵ_{Hf} values of detrital zircons with ~50 Ma U-Pb ages geographically, and the local variation of U-Pb ages indicate Eocene sedimentary strata were deposited in multiple, isolated basins, and not in a single, continuous basin, during the Eocene (Figure 6.3). These basins were separated by local paleotopographic highs, and were not connected or in communication with one another. Basin formation varied from east to west: in the east of the study area, basins formed in traditional grabens and half-grabens; in the central part of the study area, basins formed in a supradetachment basin; and in west of the study area, basins area associated with strike-slip faulting.

REFERENCES

- Allmendinger, R.W., Jordan, T.E., Kay, S.M., and Isacks, B.L., 1997, The evolution of the Altiplano-Puna plateau of the Central Andes: *Annual Review of Earth and Planetary Sciences*, v. 25, p. 139-174.
- Amelin, Y., Lee, D.-C., Halliday, A.N., and Pidgeon, R.T., 1999, Nature of the Earth's earliest crust from hafnium isotopes in single detrital grains: *Nature*, v. 399, p. 252-255.
- Archibald, S.B., Morse, G.E., Greenwood, D.R., and Mathewes, R.W., 2014, Fossil palm beetles refine upland winter temperatures in the Early Eocene Climatic Optimum: *Proceedings of the National Academy of Sciences*, v. 111, p. 8095-8100.
- Armstrong, R.L., 1982, Cordilleran metamorphic core complexes—From Arizona to southern Canada: *Annual Review of Earth and Planetary Sciences*, v. 10, p. 129-154, doi: 10.1146/annurev.ea.10.050182.001021.
- Armstrong, R.L., 1988, Mesozoic and early Cenozoic magmatic evolution of the Canadian Cordillera: *Geological Society of America Special Papers* 218, p. 55-92.
- Armstrong, R.L., and Ward, P., 1991, Evolving Geographic Patterns of Cenozoic Magmatism in the North American Cordillera: The temporal and spatial association of magmatism and metamorphic core complexes: *Journal of Geophysical Research*, v. 96, no. B8, p. 13,201-13,224.
- Augustsson, C., Münker, M., Bahlburg, H., and Fannin, M., 2006, Provenance of Late Paleozoic metasediments of the SW South American Gondwana margin from combined U-Pb and Hf isotope compositions of single detrital zircons: *Journal of the Geological Society, London*, v. 163, p. 983-995.

Bahlburg, H., Vervoort, J.D., DuFrane, S.A., Carlotto, V., Reimann, C., and Cárdenas, J., 2011, The U-Pb and Hf isotope evidence of detrital zircons of the Ordovician Ollantaytambo Formation, southern Peru, and the Ordovician provenance and paleogeography of southern Peru and northern Bolivia: *Journal of South American Earth Sciences*, v. 32, p. 196-209.

Bally, A. W., Gordy, P., and Stewart, G. A., 1966, Structure, seismic data, and orogenic evolution of southern Canadian Rocky Mountains: *Bulletin of Canadian Petroleum Geology*, v. 14, p. 337-381.

Bao, X., Eaton, D.W., and Guest, B., 2014, Plateau uplift in western Canada caused by lithospheric delamination along a craton edge: *Nature Geoscience*, v. 7, p. 830-833.

Bardoux, M., 1985, The Kelowna detachment zone, Okanagan Valley, south-central British Columbia. Geological Survey of Canada, Current research, Part A, Paper 85-1A, p. 333-339.

Bardoux, M., 1993, The Okanagan Valley Normal Fault from Penticton to Enderby, South-Central British Columbia [Ph.D. thesis]: Ottawa, Ontario, Carleton University, 292 p.

Bardoux M., and Mareschal, J.C., 1994, Extension in south-central British Columbia: mechanical and thermal controls, *Tectonophysics*, v. 238, p. 451-470.

Beatty, T.W., Orchard, M.J., and Mustard, P.S., 2006, Geology and tectonic history of the Quesnel terrane in the area of Kamloops, British Columbia: *Canadian and Alaskan Cordillera: Geological Association of Canada*, p. 483-504.

Black, L.P., and Gulson, B.L., 1978, The age of the Mud Tank carbonatite, Strangways Range, Northern Territory: *BMR Journal of Australian Geology and Geophysics*, v. 3, pg. 227-232.

Black, L., Kamo, S., Allen, C., Davis, D., Aleinikoff, J., Valley, J., Mundil, R., Campbell, I., Korsch, R., Williams, I., and Foudoulis, C., 2004, Improved $^{206}\text{Pb}/^{238}\text{U}$ microprobe geochronology by monitoring of a trace-element-related matrix effect; SHRIMP, ID-TIMS, ELA-ICP-MS and oxygen isotope documentation for a series of zircon standards: *Chemical Geology*, v. 205, p. 115-140.

Blair, T.C., and McPherson, J.G., 1994, Alluvial fans and their natural distinction from rivers based on morphology, hydraulic processes, sedimentary processes, and facies assemblages: *Journal of Sedimentary Research*, v. A64, p. 450-489.

Bodet, F., and Schärer, U., 2000, Evolution of the SE-Asian continent from U-Pb and Hf isotopes in single grains of zircon and baddeleyite from large rivers: *Geochimica et Cosmochimica Acta* 64, p. 2067-2091.

Breitsprecher, K. and Thorkelson, D.J., 2009, Neogene kinematic history of Nazca-Antarctic-Phoenix slab windows beneath Patagonia and the Antarctic Peninsula: *Tectonophysics*, v. 464, no. 1-4, p. 10-20, doi: 10.1016/j.tecto.2008.02.013.

Breitsprecher, K., Thorkelson, D., Groome, W., and Dostal, J., 2003, Geochemical confirmation of the Kula-Farallon slab window beneath the Pacific Northwest in Eocene time: *Geology*, v. 31, p. 351-354.

Brown, E.R., and Gehrels, G.E., 2007, Detrital zircon constraints on terrane ages and affinities and timing of orogenic events in the San Juan Islands and North Cascades, Washington: *Canadian Journal of Earth Sciences*, v. 44, p. 1375-1396.

Brown, R.L., and Read, P.B., 1983, Shuswap Terrane of British Columbia: A Mesozoic "core complex." *Geology*, v. 11, p. 164-168, doi: 10.1130/0091-7613(1983)11<164:STOBKA>2.0.CO;2.

Brown, R.L., and Gibson, H.D., 2006, An argument for channel flow in the southern Canadian Cordillera and comparison with Himalayan tectonics, *in* Law, R.R., Searle, M.P., and Godin, L., eds., *Channel Flow, Ductile Extrusion and Exhumation in Continental Collision Zones: Geological Society of London Special Publication 268*, p. 543-559.

Brown, R.L., Journeay, J.M., Lane, L.S., Murphy, D.C., and Rees, C.J., 1986, Obduction, backfolding and piggyback thrusting in the metamorphic hinterland of the southeastern Canadian Cordillera: *Journal of Structural Geology*, v. 8, p. 255-268, doi:10.1016/0191-8141(86)90047-7.

Brown, R.L., Beaumont, C., and Willet, S.D., 1993, Comparison of the Selkirk fan structure with mechanical models: Implications for interpretation of the southern Canadian Cordillera: *Geology*, v. 21, p. 1015-1018.

Brown, S.R., Gibson, H.D., Andrews, G.D.M., Thorkelson, D.J., Marshall, D.D., Vervoort, J.D., and Rayner, N., 2012, New constraints on Eocene extension within the Canadian Cordillera and identification of Phanerozoic protoliths for footwall gneisses of the Okanagan Valley shear zone: *Lithosphere*, v. 4, p. 354-377.

Cande, S.C., and Leslie, R.B., 1986, Late Cenozoic tectonics of the southern Chile trench: *Journal of Geophysical Research*, v. 91, p. 471-496, doi: 10.1029/JB091iB01p00471.

Cande, S.C., Leslie, R.B., Parra, J.C., and Hobart, M., 1987, Interaction between the Chile Ridge and Chile Trench: Geophysical and geothermal evidence: *Journal of Geophysical Research*, v. 92, p. 495-520, doi: 10.1029/JB092iB01p00495.

Cecil, M. R., Gehrels, G., Ducea, M. N., and Patchett, P. J., 2011, U-Pb-Hf characterization of the central Coast Mountains batholith: Implications for petrogenesis and crustal architecture: *Lithosphere*, v. 3, no. 4, p. 247-260, doi:10.1130/L134.1.

Cembrano, J., Herve, F., and Lavenu, A., 1996, The Liquine Ofqui fault zone: A long-lived intra-arc fault system in southern Chile: *Tectonophysics*, v. 259, p. 55-66, doi: 10.1016/0040-1951(95)00066-6.

Cembrano, J., Lavenu, A., Reynolds, P., Arancibia, G., Lopez, G., and Sanhueza, A., 2002, Late Cenozoic transpressional ductile deformation north of the Nazca-South America-Antarctica triple junction: *Tectonophysics*, v. 354, p. 289-314, doi: 10.1016/S0040-1951(02)00388-8.

- Chamberlain C.P., Mix, H.T., Mulch, A., Hren, M.T., Kent-Corson, M.L., Davis, S.J., Horton, T.W., and Graham, S.A., 2012, Cenozoic climatic and topographic evolution of the western North American Cordillera: *American Journal of Science*, v. 312, p. 213-262, doi: 10.2475/02.2012.05.
- Church, B.N., 1973, Geology of the White Lake Basin. British Columbia Department of Mines and Petroleum Resources, Bulletin 61, 120p.
- Church, B.N., 1981, Notes on the Penticton Group: A progress report on a new stratigraphic subdivision of the Tertiary south-central British Columbia: *British Columbia Geological Survey, Geological Fieldwork 1981*, p. 12-16.
- Church, B.N., 1985, Volcanology and structure of the Tertiary outliers in south-central British Columbia, Trip 5, *in* Tempelman-Kluit, D., ed., *Field Guides to Geology and Mineral Deposits in the Southern Canadian Cordillera*: Geological Survey of Canada, p. 1-46.
- Clague, J.J., 1974, The St. Eugene Formation and the development of the southern Rocky Mountain Trench: *Canadian Journal of Earth Sciences*, v. 11, p. 916-938.
- Coney, P.J., 1980, Cordilleran metamorphic core complexes: An overview *in* Crittenden, M.D., Coney, P.J., and Davis, G.H., eds., *Cordilleran Metamorphic Core Complexes*: Geological Society of America Memoir 153, p. 7-13.
- Coney, P.J., and Harms, T.A., 1984, Cordilleran metamorphic core complexes: Cenozoic extensional relics of Mesozoic compression: *Geology*, v. 12, p. 550-554.
- Constenius, K.N., 1996, Late Paleogene extensional collapse of the Cordilleran foreland fold and thrust belt: *Geological Society of America Bulletin*, v. 108, no. 1, p. 20-39.
- Cook, F.A., Erdmer, P., and van der Velden, A.J., 2012, The evolving Cordilleran lithosphere, *in* Percival, J.A., Cook, F.A., and Clowes, R.M. eds., *Tectonic styles in Canada: The Lithoprobe perspective*: Geological Survey of Canada, Special Paper 49, 89 p.

Dahlstrom, C.D., 1970, Structural geology in the eastern margin of the Canadian Rocky Mountains: *Bulletin of Canadian Petroleum Geology*, v. 18, p. 332-406.

DeCelles, P.G., Ducea, M.N., Kapp, P., Zandt, G., 2009, Cyclicity in Cordilleran orogenic systems: *Nature Geoscience*, v. 2, p. 251-257, doi: 10.1038/NGEO469.

Dickinson, W.R., 1979, Cenozoic plate tectonic setting of the cordilleran region in the United States, *in* Armentrout, J.M., Cole, M.R., and TerBest, H., Jr., eds., *Cenozoic paleogeography of the western united States: Pacific Section, Society of Economic Paleontologists and Mineralogists Pacific Coast Paleogeography Symposium 3*, p. 1-13.

Dickinson, W.R., 2002, The Basin and Range Province as a composite extensional domain: *International Geology Review*, v. 44, p. 1-38.

Dickinson, W.R., 2004, Evolution of the North American Cordillera: *Annual Review of Earth and Planetary Sciences*, v. 32, p. 13-45, doi: 10.1146/annurev.earth.32.101802.120257.

Dickinson, W.R., 2006, Geotectonic evolution of the Great Basin: *Geosphere*, v. 2, no. 7, p. 353-368, doi: 10.1130/GES00054.1.

Dickinson, W.R., and Gehrels, G.E., 2009, Use of U-Pb ages of detrital zircons to infer maximum depositional ages of strata: A test against a Colorado Plateau Mesozoic database: *Earth and Planetary Science Letters*, v. 288, p. 115-125, doi: 10.1016/j.epsl.2009.09.013.

Dostal, J., Breitsprecher, K., Church, B.N., Thorkelson, D., and Hamilton, T.S., 2003, Eocene melting of Precambrian lithospheric mantle: Analcime-bearing volcanic rocks from the Challis-Kamloops belt of south central British Columbia: *Journal of Volcanology and Geothermal Research*, vol. 126, p. 303-326.

- Eddy, M.P., Bowring, S.A., Umhoefer, P.J., Miller, R.B., McLean, N.M., and Donaghy, E.E., 2016, High-resolution temporal and stratigraphic record of Siletzia's accretion and triple junction migration from nonmarine sedimentary basins in central and western Washington: *Geological Society of America Bulletin*, v. 128, no. 3/4, p. 425-441, doi: 10.1130/B31335.1.
- Engebretson D.C., Kelley, L., Cashman, H., and Richards, M., 1992, 180 million years of subduction, *GSA Today*, v. 2, p. 93-100.
- Evans, K.V., Aleinikoff, J.N., Obradovich, J.D., and Fanning, J.M., 2000, SHRIMP U-Pb geochronology of volcanic rocks, Belt Supergroup, western Montana: Evidence for rapid deposition of sedimentary strata: *Canadian Journal of Earth Sciences*, v. 37, p. 1287-1300.
- Ewing, T.E., 1980, Paleogene tectonic evolution of the Pacific Northwest: *The Journal of Geology*, v. 88, no. 6, p. 619-638.
- Ewing, T.E., 1981a, Regional stratigraphy and structural setting of the Kamloops Group, south-central British Columbia: *Canadian Journal of Earth Sciences*, v. 18, p. 1464-1477.
- Ewing, T.E., 1981b, Petrology and geochemistry of the Kamloops Group volcanics, British Columbia: *Canadian Journal of Earth Sciences*, v. 18, p. 1478-1491.
- Forsythe, R., and Nelson, E., 1985, Geological manifestation of ridge collision: Evidence from the Golfo de Penas-Taitao basin, Southern Chile: *Tectonics*, v. 4, p. 477-495, doi: 10.1029/TC004i005p00477.
- Foster-Baril, Z., 2017, Eocene basin records of volcanism, topography, and tectonics in southern British Columbia, Canada [Master's thesis]: University of Idaho, 84 p.
- Fyles, J.T., 1990, Geology of Greenwood—Grandforks area, British Columbia, NTS 82E/1, 2: British Columbia Ministry of Energy, Mines, and Petroleum Resources, Open File 1990-25.

- Gabrielse, H., and Yorath, C.J., 1989, DNAG 4 The cordilleran orogen in Canada: Geoscience Canada, vol. 16, no. 2, p. 67-83.
- Gabrielse, H., and Yorath, C.J., 1991, Tectonic synthesis, *in* Gabrielse, H., and Yorath, C.J., eds., Geology of the Cordilleran Orogen in Canada: Geological Survey of Canada, Geology of Canada, no. 4, p. 677-705.
- Gabrielse, H., Monger, J.W.H., Wheeler, J.O., and Yorath, C.J., 1991, Part A. Morphogeological belts, tectonic assemblages, and terranes, *in* Gabrielse, H., and Yorath, C.J., eds., Geology of the Cordilleran Orogen in Canada: Geological Survey of Canada, Geology of Canada, no. 4, p. 15-28.
- Gashnig, R.M., Vervoort, J.D., Lewis, R.S., and Tikoff, B., 2011, Isotopic evolution of the Idaho Batholith and Challis Intrusive Province, northern US Cordillera: Journal of Petrology, v. 52, no. 12, p. 2397-2429, doi: 10.1093/petrology/egr050.
- Gaylord, D.R., 1989, Eocene sedimentation in the Republic graben, north-central Washington: Geological Society of America Abstracts with Programs, v. 21, no. 5, p. 82.
- Gaylord, D.R., Theissen, R.L., and Mohl, G.B., 1987, Geology of Republic graben and implications for Eocene sedimentation in north-central portions of the Columbia Basin, *in* Proceedings of the American Association of Petroleum Geologists Rocking Mountain Meeting, Boise, Idaho, 13-16 September.
- Gaylord, D.R., Suydam, J.D., Price, S.M., Matthews, J., and Lindsey, K.A., 1996, Depositional history of the uppermost Sanpoil Volcanics and Klondike Mountain Formation in the Republic basin: Washington Geology, v. 24, p. 5-18.
- Gehrels, G., and Pecha, M., 2014, Detrital zircon U-Pb geochronology and Hf isotope geochemistry of Paleozoic and Triassic passive margin strata of western North America: Geosphere, v. 10, n. 1, p. 49-65, doi: 10.1130/GES00889.1.

- Gehrels, G.E., McClelland, W.C., Samson, S.D., Patchett, J., and Orchard, M.J., 1992, Geology of the western flank of the Coast Mountains between Cape Fanshaw and Taku Inlet, southeastern Alaska: *Tectonics*, v. 11, no. 3, p. 567-585, doi: 10.1029/92TC00482.
- Gehrels, G., Valencia, V., and Pullen, A., 2006, Detrital zircon geochronology by Laser-Ablation-Multicollector ICPMS at the Arizona LaserChron Center: *Paleontological Society Papers*, v. 12, p. 67-76.
- Gehrels, G.E., Valencia, V.A., and Ruiz, J., 2008, Enhanced precision, accuracy, efficiency, and spatial resolution of U-Pb ages by laser ablation-multicollector-inductively coupled plasma-mass spectrometry: *Geochemistry, Geophysics, Geosystems*, v. 9, Q03017, doi:10.1029/2007GC001805.
- Georgieva, V., Melnick, D., Schildgen, T.F., Ehlers, T.A., Lagabrielle, Y., Enkelmann, E., and Strecker, M.R., 2016, Tectonic control on rock uplift, exhumation, and topography above an oceanic ridge collision: Southern Patagonian Andes (47°S), Chile: *Tectonics*, v. 35, p. 1317-1341, doi: 10.1002/2016TC004120.
- Gervais, F., and Brown, R.L., 2011, Testing modes of exhumation in collisional orogens: Syn-convergent channel flow in the southeastern Canadian Cordillera: *Lithosphere*, v. 3, no. 1, p. 55-75, doi: 10.1130/L98.1.
- Gibson, H.D., Brown, R.L., and Carr, S.D., 2008, Tectonic evolution of the Selkirk fan, southeastern Canadian Cordillera: A composite Middle Jurassic-Cretaceous orogenic structure: *Tectonics*, v. 27, doi:10.1029/2007TC002160.
- Giovanni, M.K., Horton, B.K., Garzzone, C.N., McNulty, B., and Grove, M., 2010, Extensional basin evolution in the Cordillera Blanca, Peru: Stratigraphic and isotopic records of detachment faulting and orogenic collapse in the Andean hinterland: *Tectonics*, v. 29, TC6007, doi: TC2010TC002666.

Glombick, P., Thompson, R., Erdmer, P., Heaman, L., Friedman, M., Villeneuve, M., and Daughtry, K., 2006, U-Pb constraints on the thermotectonic evolution of the Vernon antiform and the age of the Aberdeen gneiss complex, southeastern Canadian Cordillera: *Canadian Journal of Earth Sciences*, v. 43, p. 213-244, doi: 10.1139/e05-096.

Gosh, D.K., 1995, Nd-Sr constraints on the interactions of the Intermontane Superterrane with the western edge of North America in the southern Canadian Cordillera: *Canadian Journal of Earth Sciences*, v. 32, no. 10, p. 1740-1758.

Greenwood, D.R., 1992, Taphonomic constrains on foliar physiognomic interpretations of Late Cretaceous and Tertiary palaeoclimates: Review of Palaeobotany and Palynology, v. 71, p. 142-196.

Greenwood, D.R., Archibald, S.B., Mathewes, R.W., and Moss, P.T., 2005, Fossil biotas from the Okanagan Highlands, southern British Columbia and northern Washington state: Climates and ecosystems across an Eocene landscape: *Canadian Journal of Earth Sciences*, v. 42, p. 167-185, doi: 10.1139/E04-100.

Groome, W.G., and Thorkelson, D.J., 2009, The three-dimensional thermos-mechanical signature of ridge subduction and slab window migration: *Tectonophysics*, v. 464, p. 70-83, doi: 1.1016/j.tecto.2008.07.003.

Groome, W.G., Thorkelson, D.J., Friedman, R.M., Mortensen, J.K., Massey, N.W.D., Marshall, D.D., and Layer, P.W., 2003, Magmatic and tectonic history of the Leech River complex, Vancouver Island, British Columbia: Evidence for ridge-trench intersection and accretion of the Crescent terrane, *in* Sisson, V.B., Roeske, S.M., and Pavlis, T.L., eds., *Geology of a Transpressional Orogen Developed During Ridge-Trench Interaction Along the North Pacific Margin: Geological Society of America Special Paper 371*, p. 327-353, doi:10.1130/0-8137-2371-X.327.

Haeussler, P.J., Bradley, D.C., Wells, R.E., and Miller, M.L., 2003, Life and death of the Resurrection plate: Evidence for its existence and subduction in the northeastern Pacific in Paleocene-Eocene time: *Geological Society of America Bulletin*, v. 115, p. 867-880.

Haggart, J.W., and Richstad, R.L., 1998, Paleontological Resources of the Lillooet Land Resource Management Plan (LRMP) Area, British Columbia: Geological Survey of Canada, Open File 3588, 42 p.

Hamblin, A.P., 2008, Hydrocarbon potential of the Tertiary succession of Intermontane basins of the Cordillera: preliminary conceptual synthesis of background data. Geological Survey of Canada, Open File 5732, 1 CD.

Hamblin, A.P., 2011, Detailed outcrop measured sections of the Eocene White Lake Formation, southern Okanagan Valley, British Columbia: Geological Survey of Canada, Open File 6857, 18 p., doi: 10.4095/288673.

Harms, T.A., and Price, R.A., 1992, The Newport fault: Eocene listric normal faulting, mylonitization, and crustal extension in northeast Washington and northwest Idaho: Geological Society of America Bulletin, v. 104, p. 745-761.

Hora, Z.D., and Church, B.N., 1985, Zeolites in Eocene rocks of the Penticton Group, Okanagan-boundary region south-central British Columbia: British Columbia Ministry of Energy, Mines and Petroleum Resources, Geological Fieldwork, paper 1986-1, p. 51-56.

Horton, B.K., 1998; Sediment accumulation on top of the Andean orogenic wedge: Oligocene to late Miocene basins of the Eastern Cordillera, southern Bolivia: Geological Society of America Bulletin, v. 110, no. 9, p. 1174-1192.

Horton, B.K., 2012, Cenozoic evolution of hinterland basins in the Andes and Tibet, *in* Busby, C., and Azor, A., eds., *Tectonics of Sedimentary Basins: Recent Advances* (first edition): West Sussex, UK, Wiley-Blackwell, p. 427-444.

Horton, B.K., and Fuentes, F., 2016, Sedimentary record of plate coupling and decoupling during growth of the Andes: *Geology*, v. 44, no. 8, p. 647-650.

Humphreys, E.D., 1995, Post-Laramide removal of the Farallon slab, western United States: *Geology*, v. 23, no. 11, p. 987-990.

- Humphreys, E., 2009, Relation of flat subduction to magmatism and deformation in the western United States: Geological Society of America Memoirs, v. 204, p. 85-98.
- Ickert, R.B., Thorkelson, D.J., Marshall, D.D., and Ullrich, T.D., 2009, Eocene adakitic volcanism in southern British Columbia: Remelting of arc basalt above a slab window: Tectonophysics, v. 464, p. 164-185, doi:10.1016/j.tecto.2007.10.007.
- Johnson, B., 1994, Structure and tectonic setting of the Okanagan Valley Fault system in the Shuswap Lake area, southern British Columbia [Ph.D. thesis]: Ottawa, Ontario, Canada, Carleton University, 266 p.
- Johnson, B., and Brown, R., 1996, Crustal structure and Early Tertiary extensional tectonics of the Omineca belt at 51° N latitude, southern Canadian Cordillera: Canadian Journal of Earth Sciences, v. 33, p. 1596-1611, doi:10.1139/e96-121.
- Kinny, P.D., and Maas, R., 2003, Lu-Hf and Sm-Nd isotope systems in zircon. In: Hanchar, J.M., Hoskin, P.W.O. (Eds.), Zircon. Reviews in Mineralogy and Geochemistry, vol. 53, pp. 327-341.
- Lawver, L.A., and Scotese, C.R., 1990, A review of tectonic models for the evolution of the Canada Basin, in Grantz, A., et al., eds., The Arctic Ocean region: Boulder, Colorado, Geological Society of America, Geology of North America, v. L, p. 593-618.
- Leckie, D.A., and Smith, D.G., 1992, Regional setting, evolution, and depositional cycles of the western Canada foreland basin, in Macqueen, R.W., and Leckie, D.A., eds., Foreland Basins and Fold Belts: American Association of Petroleum Geologists, p. 9-46, doi: 10.1306/M55563C2.
- Lemieux, Y., Thompson, R. I., Erdmer, P., Simonetti, A., and Creaser, R.A., 2007, Detrital zircon geochronology and provenance of Late Proterozoic and mid-Paleozoic successions outboard of the miogeocline, southeastern Canadian Cordillera: Canadian Journal of Earth Sciences, v. 44, no. 12, p. 1675–1693, doi:10.1139/E07-048.

- Luepke, J.J., and Lyons, T.W., 2001, Pre-Rodinian (Mesoproterozoic) supercontinental rifting along the western margin of Laurentia: geochemical evidence from the Belt-Purcell Supergroup: *Precambrian Research*, v. 111, p. 79-90
- Madsen, J.K., Thorkelson, D.J., Friedman, R.M., and Marshall, D.D., 2006, Cenozoic to recent plate configuration in the Pacific Basin: Ridge subduction and slab window magmatism in western North America: *Geosphere*, v. 2. P. 11-34, doi:10.1130/GES00020.1.
- Massey, N.W.D., MacIntyre, D.G., Desjardins, P.J., and Cooney, R.T., 2005, Digital geology map of British Columbia: Whole Province: British Columbia Ministry of Energy, Mines and Petroleum Resources, Geological Survey Branch, GeoFile 2005-1.
- Mathews, W.H., 1964, Potassium-argon age determinations of Cenozoic volcanic rocks from British Columbia: *Geological Society of America Bulletin*, vol. 75, p. 465-468.
- Mathews, W.H., 1981, Early Cenozoic resetting of potassium-argon dates and geothermal history of north Okanagan area, British Columbia: *Canadian Journal of Earth Sciences*, v. 18, p. 1310-1319, doi: 10.1139/e81-121.
- Mathews, W.H., 1988, Neogene geology of the Okanagan Highland, British Columbia: *Canadian Journal of Earth Sciences*, v. 25, p. 725-731.
- Mathews, W.H., 1989, Neogene Chilcotin basalts in south-central British Columbia: *Canadian Journal of Earth Sciences*, v. 26, p. 969-982.
- Mathews, W.H., 1991, Physiographic evolution of the Canadian Cordillera, *in* Gabrielse, H., and Yorath, C.J., eds., *Geology of the Cordilleran Orogen in Canada: Geological Survey of Canada, Geology of Canada*, no. 4, p. 403-418.
- Mathews, W.H., and Rouse, G.E., 1984, The Gang Rang-Big Bar area, south-central British Columbia: Stratigraphy, geochronology, and palynology of the Tertiary Beds and their relationship to the Fraser Fault: *Canadian Journal of Earth Sciences*, v. 21, p. 1132-1144.

McClaghry, J.D., and Gaylord, D.R., 2005, Middle Eocene sedimentary and volcanic infilling of an evolving supradetachment basin: White Lake Basin, south-central British Columbia: *Canadian Journal of Earth Sciences*, v. 42, p. 49-66, doi: 10.1139/E04-105.

McMechan, R.D., 1983, *Geology of the Princeton Basin*: British Columbia Ministry of Energy, Mines and Petroleum Resources, Paper 1983-3, 61 p.

McNulty, B., and Farber, D., 2002, Active detachment faulting above the Peruvian flat slab: *Geology*, v. 30, p. 567-570.

Melnick, D., Bookhagen, B., and Strecker, M.R., 2009, Segmentation of megathrust rupture zones from fore-arc deformation patterns over hundreds of millions of years, Arauco peninsula, Chile: *Journal of Geophysical Research*, v. 114, B01407, doi: 10.1029/2008JB005788.

Miall, A.D., 1995, Collision-related foreland basins, *in* Busby, C.J., and Ingersoll, R.V., eds., *Tectonics of sedimentary basins*: Oxford, Blackwell Science, p. 393-424.

Mix, H.T., Mulch, A., Kent-Corson, M.L., and Chamberlain, C.P., 2011, Cenozoic migration of topography in the North American Cordillera: *Geology*, v. 39, no. 1, p. 87-90, doi:10.1130/G31450.1.

Monger, J.W.H., 1977, Upper Paleozoic rocks of the western Canadian Cordillera and their bearing on Cordilleran evolution: *Canadian Journal of Earth Sciences*, v. 14, no. 8, p. 1832-1859, doi:10.1139/e77-156.

Monger, J.W.H., 1985, Structural evolution of the southwestern Intermontane belt, Ashcroft and Hope map areas, British Columbia *in* *Current research, part A*: Geological Survey of Canada, Paper 85-1A, p. 349-358.

Monger, J.W.H., 1989: Overview of Cordilleran geology, *in* *Western Canada Sedimentary Basin: A Case History*, B.D. Ricketts (ed.), p. 9-32.

Monger, J.W.H., and Irving, E., 1980, Northward displacement of north-central British Columbia: *Nature*, v. 285, p. 289-294.

Monger, J., and Price, R., 2002, The Canadian Cordillera: Geology and Tectonic Evolution: Canadian Society of Exploration Geophysics, February, p. 17-36.

Monger, J.W.H., Price, R.A., and Tempelman-Kluit, D.J., 1982, Tectonic accretion and the origin of the two major metamorphic and plutonic belts in the Canadian Cordillera: *Geology*, v. 10, p. 70-75, doi: 10.1130/0091-7613(1982)10<70:TAATOO>2.0.CO;2.

Monger, J.W.H., Wheeler, J.O., Tipper, H.W., Gabrielse, H., Harms, T., Struik, L.C., Campbell, R.B., Dodds, C.J., Gehrels, G.E., and O'Brien, J., 1991, Upper Devonian to Middle Jurassic assemblages, *in* Gabrielse, H., and Yorath, C.J., eds., *Geology of the Cordilleran Orogeny in Canada: Geological Survey of Canada, Geology of Canada, Series 4*, p. 281-317 (also Geological Survey of America, *The Geology of North America*, v. G-2).

Morris, G.A., Larson, P.B., and Hooper, P.R., 2000, "Subduction style" magmatism in a non-subduction setting: the Colville Igneous Complex, NE Washington State, USA: *Journal of Petrology*, vol. 41, p. 43-67.

Mulch, A., Teyssier, C., Cosca, M., and Chamberlain, C., 2007, Stable isotope paleoaltimetry of Eocene core complexes in the North American Cordillera: *Tectonics*, v. 26, 13 p.

Murdie, R.E., Prior, D.J., Styles, P., Flint, S.S., Pearce, R.G., and Agar, S.M., 1993, Seismic responses to ridge-transform subduction: Chile triple junction: *Geology*, v. 21, no. 12, p. 1095-1098, doi: 10.1130/0091-7613(1993)021<1095:SRTRTS>2.3.CO;2.

Mustoe, G.E., 2005, Diatomaceous origin of siliceous shale in Eocene lake beds of central British Columbia: *Canadian Journal of Earth Sciences*, v. 42, p. 231-241, doi: 10.1139/E04-099.

Mustoe, G.E., 2011, Cyclic sedimentation in the Eocene Allenby Formation of south-central British Columbia and the origin of the Princeton Chert fossil beds: *Canadian Journal of Earth Sciences*, v. 48, p. 25-43.

Mustoe, G.E., 2015, Geologic History of Eocene Stonerose Fossil Beds, Republic, Washington, USA: *Geosciences*, v. 5, p. 243-263.

Nelson, E., Forsythe, R., and Arit, I., 1994, Ridge collision tectonics in terrane development: *Journal of South American Earth Sciences*, v. 7, no. 3-4, p. 271-278, doi: 10.1016/0895-9811(94)90013-2.

Okulitch, A.V., 1984, The role of the Shuswap metamorphic complex in Cordilleran tectonism: A review: *Canadian Journal of Earth Sciences*, v. 21, p. 1171-1193, doi:10.1139/e84-123.

Paces, J.B., and Miller, J.D., 1993, Precise U-Pb ages of Duluth Complex and related mafic intrusions, northeastern Minnesota: Geochronological insights to physical, petrogenetic, Paleomagnetic, and tectomagmatic processes associated with the 1.1 Ga midcontinent rift system: *Journal of Geophysical Research*, v. 98, p. 13997-14013.

Parrish, R.R., Carr, S.D., and Parkinson, D.L., 1988, Eocene extensional tectonics and geochronology of the southern Omineca Belt, British Columbia and Washington: *Tectonics*, v. 7, no. 2, p. 181-222.

Paton, C., Hellstrom, J., Paul, B., Woodhead, J., and Hergt, J., 2011, Iolite: Freeware for the visualisation and processing of mass spectrometric data: *Journal of Analytical Atomic Spectrometry*, v. 26, p. 2508-2518.

Pearson, R.C., and Obradovich, J.D., 1977, Eocene Rocks in Northwest Washington – Radiometric Ages and Correlation: *United States Geological Survey Bulletin* 1433, 41 p.

Piel, K.M., 1971, Palynology of Oligocene sediments from central British Columbia: *Canadian Journal of Botany*, v. 49, p. 1885-1920.

- Piel, K.M., 1977, Miocene palynological assemblages from central British Columbia: American Association of Stratigraphic Palynologists, Contribution Series 5A, p. 91-110.
- Porter, J.W., Price, R.A. and McCrossan, R.G., 1982, The Western Canada Sedimentary Basin: Philosophical Transactions of the Royal Society of London, Series A, v. 305, p. 169-192.
- Price, R.A., 1979, Intracontinental ductile crustal spreading linking the Fraser River and Northern Rocky Mountain Trench transform fault zones, south-central British Columbia and Northeast Washington: Geological Society of America, Abstracts with Programs, v. 11, p. 499.
- Price, R.A., 1981, The Cordilleran Foreland Thrust and Fold Belt in the Southern Canadian Rocky Mountains, in McClay, K. R., and Price, N. J., eds., Thrust and Nappe Tectonics, The Geological Society, p. 427-448.
- Price, R.A., 1986, The southeastern Canadian Cordillera: Thrust faulting, tectonic wedging, and delamination of the lithosphere: Journal of Structural Geology, v. 8, p. 239-254.
- Price, R.A., 1994, Cordilleran tectonics and the evolution of the Western Canada sedimentary basin, in Mossop, G., and Shestin, I., eds., Geological Atlas of the Western Canada Sedimentary Basin: Calgary, Alberta, Canadian Society of Petroleum Geologists and Alberta Research Council, p. 13-24.
- Price, R.A., and Mountjoy, E.W., 1970, Geologic structure of the Canadian Rocky Mountains between Bow and Athabasca Rivers-A progress report: Geological Association of Canada Special Paper 6, p. 7-25.
- Price, R.A., and Carmichael, D.M., 1986, Geometric test for Late Cretaceous-Paleogene intracontinental transform faulting in the Canadian Cordillera: Geology, v. 14, p. 468-471.

- Price, R.A., Archibald, D., and Farrar, E., 1981, Eocene stretching and necking of the crust and tectonic unroofing of the Cordilleran metamorphic infrastructure, southeastern British Columbia and adjacent Washington and Idaho: Geological Association of Canada Abstracts, v. 6, p. A-47.
- Pullen, A., Ibáñez-Mejía, M., Gehrels, G.E., Ibáñez-Mejía, J.C., and Pecha, M., 2014, What happens when $n=100$? Creating large- n geochronological datasets with LA-ICP-MS for geologic investigations: Journal of Analytical Atomic Spectrometry, v. 29, p. 971-980, doi: 10.1039/C4JA00024B.
- Rainbird, R.H., Hamilton, M.A., and Young, G.M., 2001, Detrital zircon geochronology and provenance of the Torridonian, NW Scotland: Journal of Geological Sciences (London), v. 158, p. 15-27.
- Read, P.B., 2000, Geology and industrial minerals of the Tertiary basins, south-central British Columbia: British Columbia Ministry of Energy and Mines, Geological Survey Branch, GeoFile 2000-3.
- Roed, M., Dobson, D., Greenough, J., Ewonus, G., Hughes, B., Luttermerding, H., Peto, P., and Williams, N., 1995, Geology of the Kelowna area and origin of the Okanagan Valley, British Columbia: Kelowna Geology Committee, 183 p.
- Rosenau, M., Melnick, D., and Echtler, H., 2006, Kinematic constraints on intra-arc shear and strain partitioning in the southern Andes between 38 degrees S and 42 degrees S latitude: Tectonics, v. 25, TC4013, doi: 10.1029/2005TC001943.
- Ross, G.M., and Villeneuve, M., 2003, Provenance of the Mesoproterozoic (1.45 Ga) Belt basin (western North America): Another piece in the pre-Rodinia paleogeographic puzzle: Geological Society of America Bulletin, v. 115, no. 10, p. 1191-1217.
- Rouse, G.E., and Mathews, W.H., 1979, Tertiary Geology and Palynology of the Quesnel Area, British Columbia: Bulletin of Canadian Petroleum Geology, v. 27, p. 418-445.

Rouse, G.E., Hopkins, W.S., and Piel, K.M., 1971, Palynology of some Late Cretaceous and Early Tertiary deposits in British Columbia and adjacent Alberta: Geological Society of America, Special Paper 127, p. 213-246.

Russo, R.M., Gallego, A., Comte, D., Mocanu, V.I., Murdie, R.E., and VanDecar, J.C., 2010, Source-side shear wave splitting and upper mantle flow in the Chile Ridge subduction region: *Geology*, v. 38, p. 707-710, doi: 10.1130/G30920.1.

Schiarizza, P., and Israel, S., 2001, Geology and mineral occurrences of the Nehalliston Plateau, south-central British Columbia (92P/7, 8, 9, 10), in *Geological Fieldwork 2000: British Columbia Ministry of Energy and Mines, Paper 2001-1*, p. 1-30.

Simony, P.S., and Carr, S.D., 2011, Cretaceous to Eocene evolution of the southeastern Canadian Cordillera: Continuity of Rocky Mountain thrust systems with zones of “in-sequence” mid-crustal flow: *Journal of Structural Geology*, v. 33, no. 9, p. 1417-1434.

Sláma, J., Košler, J., Condon, D.J., Crowley, J.L., Gerdes, A., Hanchar, J.M., Horstwood, M.S.A., Morris, G.A., Nasdala, L., Norberg, N., Schaltegger, U., Schoene, B., Tubrett, M.N., and Whitehouse, M.J., 2008, Plešovice zircon – a new natural reference material for U-Pb and Hf isotopic microanalysis: *Chemical Geology*, v. 249, p. 1-35.

Smith, M.E., Carroll, A.R., Jicha, B.R., Cassel, E.J., and Scott, J.J., 2014, Paleogeographic record of Eocene Farallon slab rollback beneath western North America: *Geology*, v. 42, no. 12, p. 1039-1042, doi: 10.1130/G36025.1.

Souther, J.G., 1991, Volcanic Regimes, in Gabrielse, H., Yorath, C.J., eds., *Geology of the Cordilleran Orogen in Canada: Geological Survey of Canada, Geology of Canada*, no. 4, p. 457-490.

Spencer, C.J., and Kirkland, C.L., 2015, Visualizing the sedimentary response through the orogenic cycle: A multidimensional scaling approach: *Lithosphere*, v. 8, no. 1, p. 29-37, doi:10.1130/L479.1.

- Stewart, D.C., Boon, P.I., Greenwood, D.R., and Diamond, N.T., 2002, Transport of leaf litter in upland streams of south-eastern Australian *Eucalyptus* and *Nothofagus* forests: *Archiv für Hydrobiologie*, v. 156, p. 43-61.
- Stewart, J.H., Gehrels, G.E., Barth, A.P., Link, P.K., Christie-Blick, N., and Wrucke, C.T., 2001, Detrital zircon provenance of Mesoproterozoic to Cambrian arenites in the western United States and northwestern Mexico: *Geological Society of America Bulletin*, v. 113, p. 1343-1356.
- Surpless, K.D., Graham, S.A., Covault, J.A., and Wooden, J.L., 2006, Does the Great Valley Group contain Jurassic strata? Reevaluation of the age and early evolution of a classic foreland basin: *Geology*, v. 34, p. 21-24.
- Suydam, J.D., and Gaylord, D.R., 1993, Sedimentary and stratigraphic evidence of Eocene extension in the Okanogan Highlands, Washington [abstract]: *Geological Society of America Abstracts with Programs*, v. 23, no. 5, p. 68.
- Suydam, J.D., and Gaylord, D.R., 1997, Toroda Creek half graben, northeast Washington: Late-stage sedimentary infilling of a synextensional basin: *Geological Society of America Bulletin*, v. 109, no. 10, p. 1333-1348.
- Tempelman-Kluit, D., and Parkinson, D., 1986, Extension across the Eocene Okanogan crustal shear in Southern British Columbia: *Geology*, v. 14, p. 318-321.
- Thomson, S.N., 2002, Late Cenozoic geomorphic and tectonic evolution of the Patagonian Andes between latitudes 42 degrees S and 46 degrees S: An appraisal based on fission-track results from the transpressional intra-arc Liquine-Ofqui fault zone: *Geological Society of America Bulletin*, v. 114, no. 9, p. 1159-1173, doi: 10.1130/0016-7606(2002)114<1159:LCGATE>2.0.CO;2.
- Thorkelson, D.J., 1989, Eocene sedimentation and volcanism in the Fig Lake Graben, southwestern British Columbia: *Canadian Journal of Earth Sciences*, v. 26, p. 1368-1373.

Thorkelson, D.J., and Taylor, R.P., 1989, Cordilleran slab windows: *Geology*, v. 17, p. 47-63.

Toussaint, J.F., and Restrepo, J.J., 1994, The Colombian Andes during Cretaceous times, *in* Salfity, J.A., ed., *Cretaceous tectonics of the Andes*: Braunschweig, Wiesbaden, Vieweg, p. 61-100.

Tipper, H.W., 1984, The age of the Jurassic Rossland Group of southeastern British Columbia: *Geological Survey of Canada Paper 84-1A*, p. 631-632.

Tribe, S., 2005, Eocene paleo-physiography and drainage directions, southern Interior Plateau, British Columbia: *Canadian Journal of Earth Sciences*, v. 42, p. 215-230.

Van der Pluijm, B., Vrolijk, P.J., Pevear, D.R., Hall, C.M., and Solum, J., 2006, Fault dating in the Canadian Rocky Mountains: evidence for late Cretaceous and early Eocene orogenic pulses: *Geology*, v. 34, no. 10, p. 837-840, doi: 10.1130/G22610.1.

Vermeesch, P., 2012, On the visualization of detrital age distributions: *Chemical Geology*, v. 312-313, p. 190-194, doi: 10.1016/j.chemgeo.2012.04.021

Vermeesch, P., 2013, Multi-sample comparison of detrital age distributions: *Chemical Geology*, vol. 341, p. 140-146.

Wiedenbeck, M., Alle, P., Corfu, F., Griffin, W.L., Meier, M., Oberli, F., von Quadt, A., Roddick, J.C., and Spiegel, W., 1995, 3 Natural zircon standards for U-Th-Pb, Lu-Hf, trace-element and REE analyses: *Geostandards Newsletter*, v. 19, p. 1-23.

Williams, V.E., and Ross, C.A., 1979, Depositional setting and coal petrology of Tulameen Coalfield, south-central British Columbia: *The American Association of Petroleum Geologists Bulletin*, v. 63, no. 11, p. 2058-2069.

Wingate, W.T.D., and Irving, E., 1994, Extension in high-grade terranes of the southern Omineca Belt, British Columbia: Evidence from paleomagnetism: tectonics, v. 13, p. 686-711, doi: 10.1029/93TC03490.

Winkler, W., Villagomez, D., Spikings, R., Abegglen, P., Tobler, S., and Egeuz, A., 2005, The Chota basin and its significance for the inception and tectonic setting of the inter-Andean depression in Ecuador: Journal of South American Earth Science, v. 19, p. 5-19.

Wolfe, J.A., and Wehr, W.C., 1991, Significance of the Eocene fossil plants at Republic, Washington: Washington Geology, v. 19, no. 3, p. 18-24.

Wolfe, J.A., Forest, C.E., and Molnar, P., 1998, Paleobotanical evidence of Eocene and Oligocene paleoaltitudes in midlatitude western North America: Geological Society of America Bulletin, v. 110(5), p. 664-678. Woodhead, J., Hergt, J., Shelley, M., Eggins, S., and Kemp, R., 2004, Zircon Hf-isotope analysis with an excimer laser, depth profiling, ablation of complex geometries, and concomitant age estimation: Chemical Geology, v. 209, p. 121-135.

Wolfe, J.A., Gregory-Wodzicki, K.M., Molnar, P., and Mustoe, G., 2003, Rapid uplift and then collision in the Eocene of Okanagan? Evidence from paleobotany: Geological Association of Canada-Mineralogical Association of Canada-Society of Economic Geologists, Joint Annual Meeting, Vancouver, Abstracts 28, 533. [CD-ROM]

Woodhead, J.D., and Hergt, J.M., 2005, A preliminary appraisal of seven natural zircon reference materials for in situ Hf isotope determination: Geostandards and Geoanalytical Research, v. 29, p. 183-195.

Yorath, C.J., 1991, Upper Jurassic to Paleogene assemblages, in Geology of the Cordilleran Orogen in Canada, Gabrielse, H., and Yorath, C.J., eds., Geological Survey of Canada, Geology of Canada, no. 4, p. 329-371.

APPENDIX A
USC ROCK PREPARATION LABORATORY &
CEMS U-PB ANALYSIS

A.1 SAMPLE PREPARATION

Zircon separates were acquired through mechanical disaggregation and density and magnetic differentiation in the Rock Preparation Facility and Sedimentary Geology Laboratory at the University of South Carolina, using protocols adapted from previous, well-established methods (Gehrels et al., 2006).

Samples were progressively disaggregated using a Bico Braun WD Chipmunk jaw crusher and Bico Braun UA Pulverizer disc mill. At the end of each milling step, all material finer than 500 μm was removed from further disaggregation steps via single-use Sefar NITEX nylon filament mesh mounted by hose clamp to an 8" diameter polyvinyl chloride cylinder.

Resulting disaggregated grains were further separated by hydrodynamic characteristics using a MD Mineral Technologies MK-2 Gemini shaking water table, and then further separated using a manually operated ABS gold pan. Grains retained within the gold pan were dried in an $\sim 30^\circ\text{C}$ oven, and proceeded to further processing; splits exiting the gold pan were examined to confirm the absence of zircon, and archived.

Retained grains were then progressively separated by their effective magnetic susceptibility first with a hand magnet, and then an L-1 Frantz isodynamic magnetic

separator operating at horizontal and vertical angles of 15° and 10° degrees, respectively. Grains were progressively removed in 0.3 ampere increments up to 1.2 amperes. The magnetic fraction was removed and stored for possible heavy-mineral analysis; the nonmagnetic fractions at 1.2 amperes proceeded to further processing (below).

Resulting nonmagnetic dense mineral fractions were combined with Lithium Metatungstate (LMT; Specific gravity=2.95) in 15 mL centrifuge tubes, agitated and left to settle, until grains separated into fully floating and sunken fractions with an intervening clear heavy liquid window. Centrifuge tubes were then placed vertically into liquid nitrogen to a sufficient depth to submerge one-half of the heavy liquid window. Upon complete freezing of the submerged liquid and sunken fraction, the remaining liquid and floating fraction were poured off into a 11 cm pore-diameter filter paper cone, rinsed repeatedly with de-ionized water, transferred to a second filter paper, re-rinsed, dried, and archived. The frozen sunken separate and remaining liquid were thawed in a 30°C oven, and poured off into a separate 11 cm pore-diameter filter paper cone, and rinsed repeatedly with de-ionized water, transferred to a second filter paper, re-rinsed, and then dried in a 30°C oven. All samples later analyzed at CEMS were sent to GeoSep Services for further Methl Iodide (MI) density separation of zircon and apatite, except for samples PB2 and 15Ca10b.

To avoid possible biases associated with hand-picking, when possible each sample's resulting zircon-rich separate was poured onto double-sided tape attached to a 6" square glossy ceramic tile, and within the bounds of a 1" Buehler circular ring form. These mounted grains were then bound in place using Buehler Epo-Thin epoxy resin. Upon 48-72 hours of curing, the resulting mounts were pried from their tiles, and gently

ground using wet sandpaper of 600 grit in order to expose the grain cores, followed by polishing using 1 μm abrasive alumina solution polishing powder suspended in de-ionized water and a Buehler MINIMET auto-polisher. Such procedure was repeated in 15-30 minute increments, until a reflected light microscope revealed an absence of scratches in target zircons. Mounts were then sonicated in a de-ionized water bath for 15 minutes, and then dried in a 30°C oven.

A.2 LASER-ABLATION MASS-SPECTROMETRY

U-Pb detrital-zircon geochronology was conducted by laser-ablation high-resolution single-collector inductively coupled plasma mass-spectrometry (LA-HR-SC-ICPMS) at the University of South Carolina's Center for Elemental Mass Spectrometry (CEMS) in 3 sample runs during December 2015 to March 2017.

Analysis involved grain-ablation with a PhotonMachines Analyte G2 193 nm (deep ultraviolet) ArF exciplex laser with a spot diameter of 25 μm , with a 6.5 J/cm² energy fluence, aimed at the centers of individual sample ('unknown') and reference (aka 'standard') zircon grains, mounted in 1" polished epoxy resin pucks (see 1.1 above). For each sample, 105-120 unknown zircon grains were targeted, with the goal of recovering ~100 usable ages. Unknown zircons were selected randomly from each mounted aliquot analyzed in batches of five grains each, separated by the analysis of natural reference zircons of known and well-constrained U-Pb isotope-dilution thermal ionization mass-spectrometry (ID-TIMS) ages after every five to ten 'unknown' analyses.

In this study reference material 91500 (1062.4 \pm 0.4 Ma; Wiedenbeck et al., 1995) was analyzed after every 4-5 'unknown' analyses and was used as the primary reference material for all samples analyzed at CEMS. In this study reference material Sri Lanka

(SL; ID-TIMS age 563.5 ± 3.2 Ma; Gehrels et al., 2008) was analyzed after every 4-5 'unknown' analyses and was used as the monitor reference material for all samples analyzed at CEMS.

Prior to each analytical session, the coupled LA-HR-SC-ICP-MS system was manually tuned to optimize performance using the NIST 612 synthetic glass standard and the SL natural zircon reference material. Typical tuning optimization routines involved adjusting torch position, then sample and HelEx (MFC) gas flows to maximize signal (^{139}La and ^{238}U) while minimizing oxide formation and inter-elemental fractionation.

A.3 POST-ACQUISITION PROCESSING & DATA REDUCTION

Post-acquisition processing of data utilized the *UPbGeochronology3* data reduction scheme (DRS) of the Iolite (v. 6.36) software package, employed in the cross-platform WaveMetrics IgorPro computational environment.

Processing began with the import of individual .FIN2 files acquired from analysis of each unknown or reference zircon and its associated baseline and washout signals into the time-constrained reference frame of the IgorPro environment. Following data import, integration windows for baseline and ablatant signals were selected by trimming from the start and end of each data file for baseline integrations, and from the start and end of each data file for ablation signals. In addition to removing the baseline signal for the ablatant signal, the latter data trimming removes any surface contamination incorporated into the mount surface during grinding, polishing and storage. Small offsets in analytical start times caused by operator error or computational delays in compiling prior analyses' data occasionally yielded inaccurately auto-selected integration windows; the ablation of epoxy in insufficiently ground zircons and/or small zircons drilled through during

standard ablation durations yielded similarly inappropriate windows. Adjustment of these windows was achieved by manual grain-by-grain data inspection, as was the elimination of analyses of grains known not to be zircon (e.g., by low U signals, etc.). In the case of the former, care was taken to ensure that the start time of each ablation integration window was spatially equivalent to those of grains with auto-selected windows in order to optimize the accuracy of down-hole fraction correction models (see below).

Following data import, selection, and inspection of integration windows, Iolite-based data reduction involved: (1) subtraction of background signals from an automatic (best-fit: see Paton et al. 2010) interpolation model; (2) determination of an appropriate downhole-fractionation correction model by separately stacking the $^{206}\text{Pb}/^{238}\text{U}$, $^{207}\text{Pb}/^{235}\text{U}$ and $^{208}\text{Pb}/^{232}\text{Th}$ downhole ratios of each of the approximately two primary reference zircon analyses, calculating best-fit exponential curves to those stacked datasets, and applying the resulting models to transform the isotopic ratios of analyzed ‘unknown’ zircons, ideally to optimize ratio steadiness; (3) estimation and correction of instrumental age-offsets and drift by comparison of determined (raw) and accepted (i.e., ID-TIMS) isotopic ratios of the primary reference zircon; and (4) calculation of final ages and values, including (a) propagated uncertainties determined from analyses of the primary reference zircon as pseudo-secondary standards, progressively removing them individually from the dataset, reprocessing the data, and calculating uncertainty, and (b) error correlations using the IgorPro StatsCorrelation function. See Paton et al. (2010) for further clarification and discussion of methods of Iolite data reduction of U-Pb zircon data.

A.4 REFERENCES

Gehrels, G., Valencia, V., and Pullen, A., 2006, Detrital zircon geochronology by Laser-Ablation-Multicollector ICPMS at the Arizona LaserChron Center: Paleontological Society Papers, v. 12, p. 67-76.

APPENDIX B

CEMS DETRITAL ZIRCON U-PB ANALYSES DATA TABLE

analysis	ISOTOPIC RATIOS						ELEMENTAL CONCENTRATIONS		AGES								conc. (%)					
	207/206	prop. 2s	206/238 vs 207/206 error correlation	prop. 2s	208/206 vs 207/206 error correlation	prop. 2s	U (ppm)	U/Th	207/238 age (Ma)	prop. 2s (Myr)	206/238 age (Ma)	prop. 2s (Myr)	207/206 age (Ma)	prop. 2s (Myr)	208/232 age (Ma)	prop. 2s (Myr)						
X15CA04A_1	0.068	0.014	0.00957	0.00059	0.14031	0.055	0.012	0.24753	0.00213	0.00092	73.7	0.7	64	13	55	3.7	420	380	63	19	13%	
X15CA04A_2	0.052	0.02	0.00484	0.00077	0.11147	0.04	0.016	-0.097184	0.0039	0.0019	37.7	1.0	50	19	54.4	4.9	-90	540	70	30	-60%	
X15CA04A_3	0.051	0.017	0.00951	0.00061	-0.08943	0.035	0.013	0.43004	0.0031	0.00089	52.8	0.8	50	16	61	3.9	-440	440	62	20	-14%	
X15CA04A_4	0.111	0.021	0.00831	0.00026	0.59404	0.089	0.016	-0.44483	0.00343	0.00079	750	0.9	105	19	53.3	1.6	1090	330	69.2	16	5%	
X15CA04A_5	0.281	0.057	0.01021	0.0008	-0.085382	0.183	0.037	0.099638	0.0049	0.0017	240	0.9	243	44	65.5	3.8	2420	400	98	34	3%	
X15CA04A_6	0.117	0.022	0.00928	0.00063	0.30978	0.096	0.026	0.000000	0.000000	0.000000	320	2.1	109	27	53	4.1	1160	480	119	24	5%	
X15CA04A_7	0.164	0.031	0.00966	0.00054	0.20661	0.114	0.021	0.12718	0.00496	0.0014	144.5	0.9	151	27	61.9	3.5	1030	360	100	28	4%	
X15CA04A_8	0.0723	0.0096	0.00817	0.00028	0.095978	0.0603	0.0078	0.31726	0.00305	0.00071	1030	1.7	70.6	9.1	52.5	1.8	500	270	61.0	14	11%	
X15CA04A_9	0.294	0.067	0.01022	0.00092	0.29554	0.177	0.036	-0.000006	0.00009	0.00017	77.4	0.8	250	51	68	5.9	2640	340	131	34	3%	
X15CA04A_10	0.1127	0.013	0.01483	0.00041	-0.026601	0.0506	0.0093	0.14668	0.00033	0.00019	416	2.2	108.1	12	94.9	2.6	300	230	107	26	32%	
X15CA04A_11	0.083	0.023	0.00862	0.00041	0.093167	0.071	0.02	-0.040892	0.00092	0.00095	75	1.1	79	21	55.3	2.6	450	490	59	19	12%	
X15CA04A_12	0.0688	0.0079	0.00872	0.00029	0.031915	0.0525	0.0061	0.36907	0.00325	0.00082	478	1.8	64.5	7.5	56	1.8	260	230	65.5	17	22%	
X15CA04A_15	0.089	0.028	0.00828	0.00063	0.051456	0.083	0.034	0.041811	0.0052	0.0016	46.7	0.7	81	35	53.2	4	330	580	105	33	16%	
X15CA04A_16	0.0599	0.0092	0.00801	0.0002	0.36519	0.0493	0.0044	0.19546	0.00278	0.00068	1893	6.2	53.2	5	51.68	1.3	171	190	56.1	14	30%	
X15CA04A_17	0.051	0.0051	0.00804	0.00026	0.35734	0.0474	0.0044	0.14833	0.00237	0.00055	1251	2.7	50.5	4.9	51.6	1.7	60	190	47.8	11	86%	
X15CA04A_18	0.048	0.018	0.00839	0.00056	0.14727	0.048	0.018	-0.067083	0.00408	0.0019	47.4	0.7	47	17	53.9	3.6	-320	510	82	26	-17%	
X15CA04A_19	0.061	0.016	0.00804	0.00041	0.0249107	0.06	0.016	0.10222	0.003	0.00086	121	0.8	59	15	51.6	2.6	310	438	60	17	17%	
X15CA04A_20	0.039	0.005	0.00974	0.00068	-0.1509	0.076	0.024	0.26701	0.00596	0.0012	55.2	1.0	91	30	62.5	4.4	440	580	72	23	14%	
X15CA04A_21	0.142	0.042	0.00921	0.00084	0.52204	0.121	0.031	-0.11961	0.0045	0.0015	96	0.8	129	35	59	5.4	1470	510	91	31	4%	
X15CA04A_22	0.085	0.019	0.00843	0.00043	-0.16518	0.076	0.017	0.20931	0.00299	0.00085	104.2	0.8	82	17	54.1	2.8	740	380	60	17	7%	
X15CA04A_23	0.089	0.019	0.00853	0.00033	-0.10089	0.085	0.016	0.27682	0.00317	0.00087	144.6	0.8	93	17	54.7	2.1	1240	380	84	18	4%	
X15CA04A_25	0.086	0.019	0.00971	0.00045	-0.07959	0.071	0.016	0.20434	0.00407	0.0012	226	1.9	82	18	62.3	2.9	620	430	82	25	10%	
X15CA04A_26	0.077	0.02	0.00833	0.00043	-0.1371	0.068	0.018	0.24818	0.0027	0.00071	146.1	0.7	74	18	53.5	2.8	530	430	54.4	14	10%	
X15CA04A_27	0.244	0.062	0.00964	0.00072	-0.046377	0.195	0.064	0.35026	0.0047	0.0017	72.2	1.1	204	61	62.8	4.9	1140	580	94	34	4%	
X15CA04A_28	0.237	0.029	0.0043	0.0013	0.25649	0.051	0.0059	0.089068	0.0119	0.0028	408	2.6	215	23	217.5	8.4	200	220	239	55	109%	
X15CA04A_29	0.085	0.026	0.00863	0.00044	0.2486	0.07	0.02	-0.10612	0.00342	0.00096	113.8	0.8	80	23	55.4	2.8	590	540	69	19	10%	
X15CA04A_30	0.096	0.024	0.00947	0.00046	-0.074501	0.072	0.018	0.19456	0.0044	0.0003	200	8.9	90	21	60.7	2.9	640	430	126	65	3%	
X15CA04A_31	0.135	0.02	0.00926	0.00045	0.15905	0.11	0.017	0.16627	0.00444	0.0003	268	1.1	128	17	59.4	2.9	1680	280	80	27	4%	
X15CA04A_35	0.084	0.036	0.00931	0.0008	0.037918	0.08	0.037	-0.038972	0.0101	0.006	68.1	1.3	77	32	59.7	5.1	190	270	200	120	31%	
X15CA04A_36	0.061	0.009	0.00844	0.00041	-0.074887	0.0503	0.0271	0.50114	0.00345	0.0004	458	0.8	60	8.5	54.2	2.6	160	240	49.4	12	30%	
X15CA04A_37	0.088	0.016	0.00951	0.00033	0.16249	0.053	0.011	-0.071571	0.0045	0.0019	269	1.8	66	15	58.4	2.1	160	330	90	38	37%	
X15CA04A_38	0.106	0.042	0.00936	0.00056	-0.01499	0.081	0.031	0.14794	0.004	0.0013	103	1.1	96	35	60	3.6	360	600	80	26	17%	
X15CA04A_39	0.0678	0.0078	0.00822	0.00032	-0.039555	0.0567	0.0064	0.34473	0.00274	0.00089	1039	2.0	66.5	7.4	54.7	2	460	250	55.2	14	12%	
X15CA04A_40	0.112	0.019	0.01146	0.0009	0.039373	0.056	0.011	0.1815	0.0066	0.0017	693	3.7	114	17	73.4	6.7	960	300	134	36	4%	
X15CA04A_41	0.0808	0.0092	0.01234	0.00046	0.52084	0.0476	0.0049	0.0097579	0.00366	0.001	873	3.4	78.7	8.6	79.1	2.9	90	200	74	20	88%	
X15CA04A_43	0.0681	0.011	0.00851	0.0004	0.08478	0.0953	0.009	0.17082	0.00293	0.00082	389	1.1	64.6	11	54.6	2.6	320	310	69	16	17%	
X15CA04A_44	0.118	0.027	0.00842	0.00045	-0.14744	0.104	0.034	-0.030385	0.0042	0.0014	160	1.3	108	32	54	2.9	540	540	84	28	6%	
X15CA04A_45	0.001	0.037	0.00882	0.00047	-0.022342	0.07	0.028	0.092499	0.0033	0.00096	77.1	0.6	83	33	56.8	3	450	690	86	19	13%	
X15CA04A_46	0.093	0.013	0.00880	0.00047	0.041414	0.0736	0.011	0.38719	0.00369	0.0009	427	0.9	90	12	57.6	3	1040	310	74.4	18	6%	
X15CA04A_47	0.057	0.03	0.0089	0.0006	-0.01895	0.046	0.026	-0.020152	0.0046	0.0017	70.8	1.4	92	28	57.1	3.8	60	730	93	34	95%	
X15CA04A_48	0.107	0.023	0.0094	0.00045	0.0098	0.1012	0.014	0.055	-0.000151	0.005	0.0084	49.8	0.9	13	35	61.3	5.7	-1260	910	100	68	-5%
X15CA04A_50	0.107	0.023	0.0094	0.00045	0.0098	0.1012	0.014	0.055	-0.000151	0.005	0.0084	49.8	0.9	13	35	61.3	5.7	-1260	910	100	68	-5%
X15CA04A_51	0.123	0.069	0.00999	0.00085	-0.000886	0.1	0.051	0.29341	0.001	0.0013	55.2	0.7	100	57	64.1	5.4	150	120	123	60	43%	
X15CA04A_52	0.235	0.084	0.00956	0.00089	0.020316	0.1	0.063	0.09012	0.006	0.0041	84.7	1.3	63	62	48.1	3.6	100	1100	14	25	48%	
X15CA04A_53	0.080	0.013	0.00979	0.00048	0.20119	0.0595	0.016	-0.064411	0.00294	0.00068	460	0.9	64.8	12	62.8	3.1	670	270	53.4	94	9%	
X15CA04A_54	0.52	0.12	0.0108	0.001	0.36908	0.316	0.074	-0.1343	0.0062	0.0019	76.3	0.7	393	81	69.2	6.4	3400	430	124	39	2%	
X15CA04A_55	0.0568	0.0071	0.00899	0.00029	0.38129	0.0454	0.0053	-0.089939	0.00309	0.00089	1064	1.5	56	6.8	57.7	1.9	-10	210	62.3	14	-577%	
X15CA04A_56	0.044	0.007	0.00957	0.00039	0.08854	0.07	0.025	-0.152	0.00548	0.001	77.6	0.9	25	4	55.4	4.7	470	350	64	15	20%	
X15CA04A_57	0.1199	0.013	0.01662	0.00053	0.14609	0.0223	0.0058	0.31776	0.00562	0.0013	56.7	1.9	114.6	12	106.3	3.3	260	230	113	26	41%	
X15CA04A_58	0.135	0.026	0.0127	0																		

analysis	ISOTOPIIC RATIOS										ELEMENTAL CONCENTRATIONS		AGES										conc. (%)
	206/238 vs 207/235 correlation		206/238 vs 207/235 correlation		208/232 vs 207/235 correlation		208/232 vs 207/235 correlation		U (ppm)	U/Th	207/235 age (Ma)		206/238 age (Ma)		208/232 age (Ma)		208/232 age (Ma)						
	prop. 2s	prop. 2s	prop. 2s	prop. 2s	prop. 2s	prop. 2s	prop. 2s	prop. 2s			prop. 2s	prop. 2s	prop. 2s	prop. 2s	prop. 2s	prop. 2s	prop. 2s	prop. 2s	prop. 2s				
CANBC1024K_7	0.087	0.02	0.00947	0.00044	0.74162	0.081	0.02	-0.31692	0.0034	0.0003	470	1.0	83	18	54.3	2.8	780	330	68.7	6	7%		
CANBC1024K_8	3.08	0.25	0.0339	0.0021	0.85726	0.653	0.02	0.19356	0.0611	0.0039	221	1.1	1420	63	215	13	4830	46	1198	74	5%		
CANBC1024K_9	0.134	0.024	0.00956	0.00044	0.87407	0.116	0.017	-0.43751	0.00504	0.00081	700	1.3	126	21	55.6	2.8	1710	270	102	16	3%		
CANBC1024K_10	0.0623	0.0052	0.00797	0.00038	0.19664	0.675	0.0035	0.10225	0.00292	0.0016	677	1.3	5	61.3	5	50.5	2.4	470	130	56.9	3.7	11%	
CANBC1024K_11	0.143	0.048	0.00837	0.0005	0.26309	0.113	0.035	-0.24545	0.00524	0.00074	114.6	1.0	128	40	53.8	3.2	1260	590	95	15	4%		
CANBC1024K_12	0.0692	0.0056	0.00934	0.00044	0.2794	0.0541	0.0029	0.092175	0.00288	0.00025	1065	2.2	67.9	5.3	59.9	2.8	350	110	58.1	5.1	17%		
CANBC1024K_13	0.073	0.0066	0.00796	0.00034	0.035471	0.0682	0.0077	0.22052	0.00258	0.00017	659	0.9	71.3	8.1	51.3	2.2	740	200	52	3.5	7%		
CANBC1024K_14	0.279	0.029	0.00995	0.00056	0.64353	0.204	0.013	-0.16939	0.00649	0.00061	308	0.9	248	22	63.8	3.6	2049	99	131	12	2%		
CANBC1024K_15	0.384	0.055	0.01081	0.00087	0.75995	0.208	0.027	-0.099151	0.0008	0.0013	451	1.3	261	42	68.1	4.3	2890	240	176	25	3%		
CANBC1024K_16	0.09	0.015	0.00785	0.00008	-0.032997	0.082	0.012	0.22086	0.0028	0.00036	345	1.1	87	13	50.4	2.4	1050	260	56.5	7.2	5%		
CANBC1024K_17	0.503	0.099	0.01206	0.00093	0.85423	0.275	0.04	-0.59158	0.011	0.0025	141	1.1	393	67	77.3	6	3200	290	221	49	2%		
CANBC1024K_18	0.091	0.02	0.00796	0.00038	0.7325	0.07	0.014	-0.05041	0.00322	0.0005	715	1.4	77	18	51.1	2.4	630	320	65	10	8%		
CANBC1024K_19	0.228	0.037	0.00978	0.00043	0.64261	0.329	0.042	-0.13973	0.00449	0.00055	262	0.8	206	29	58.3	3.2	2260	200	306	11	2%		
CANBC1024K_20	0.119	0.019	0.00808	0.00048	0.37186	0.098	0.013	0.068587	0.00469	0.00049	179	2.2	113	17	51.9	3.1	1680	240	95	18	3%		
CANBC1024K_21	0.0486	0.0043	0.00769	0.00035	0.241	0.0452	0.0029	0.093287	0.00226	0.00014	791	1.1	48.2	4.2	49.4	2.2	10	110	46	2.9	494%		
CANBC1024K_22	0.0526	0.0058	0.00819	0.00042	0.46829	0.061	0.0042	0.015366	0.00288	0.0002	461	0.8	51.9	5.5	52.6	2.7	10	160	58.2	4.1	526%		
CANBC1024K_23	0.095	0.015	0.0081	0.00057	0.28226	0.063	0.012	-0.015976	0.00345	0.00037	585	1.4	91	14	52	2.4	1080	260	69.7	7.4	5%		
CANBC1024K_24	0.0538	0.006	0.00923	0.00043	0.02889	0.0465	0.0036	-0.051559	0.00257	0.0002	627	1.2	53	5.8	52.8	2.6	-10	110	51.8	4.5	-528%		
CANBC1024K_25	0.0788	0.0063	0.00834	0.00038	0.044913	0.0667	0.0052	0.28812	0.00333	0.00043	401	1.3	76.8	7.8	53.5	2.4	750	160	67.2	6	7%		
CANBC1024K_26	0.093	0.017	0.00814	0.00034	-0.053984	0.081	0.014	0.15669	0.00277	0.00043	376	1.1	89	15	52.3	2.2	920	290	55.9	8.7	6%		
CANBC1024K_27	0.108	0.018	0.0085	0.00039	0.41118	0.089	0.013	-0.25748	0.00367	0.00051	451	1.3	104	16	54.5	2.5	1230	260	74	10	4%		
CANBC1024K_28	0.065	0.0045	0.00827	0.00034	0.016375	0.0445	0.0035	0.22553	0.00261	0.00018	375	1.0	738	70	102.4	7	4156	97	420	50	2%		
CANBC1024K_29	0.142	0.015	0.0087	0.00039	-0.17915	0.117	0.011	0.35251	0.0036	0.0003	496	1.2	134	13	55.9	2.5	1830	150	72.5	6	3%		
CANBC1024K_30	0.095	0.012	0.00843	0.00039	0.17679	0.0779	0.008	0.013307	0.00286	0.00036	395	1.0	91.5	11	54.1	2.5	1100	220	57.7	7.3	5%		
CANBC1024K_31	0.0919	0.0072	0.00807	0.00034	0.18372	0.0811	0.004	0.21076	0.00294	0.00022	498	1.1	89.2	6.6	51.8	2.2	1194	97	59.3	4.3	4%		
CANBC1024K_32	0.0819	0.009	0.00815	0.00039	0.29204	0.0734	0.0081	-0.025193	0.0031	0.00028	247	1.2	79.6	9.3	52.3	2.5	900	200	62.5	5.7	6%		
CANBC1024K_33	0.358	0.055	0.00987	0.00045	0.89886	0.137	0.033	-0.79107	0.008	0.0022	296	1.1	176	47	64.8	4.8	2130	430	120	43	3%		
CANBC1024K_34	0.376	0.045	0.0107	0.00059	0.33062	0.235	0.02	0.01913	0.0087	0.0012	260	1.1	320	33	68.6	3.7	3120	140	176	25	2%		
CANBC1024K_35	0.132	0.014	0.00834	0.00041	-0.019703	0.1144	0.0096	0.30812	0.00425	0.00032	578	1.3	125	13	53.5	2.6	1790	160	85.7	6.4	3%		
CANBC1024K_36	0.138	0.017	0.00863	0.00039	0.39953	0.102	0.01	-0.15159	0.00434	0.00057	635	1.3	122	15	55.4	2.5	1600	220	97	12	3%		
CANBC1024K_37	0.085	0.0045	0.00827	0.00034	0.016375	0.0445	0.0035	0.22553	0.00261	0.00018	375	1.0	738	70	102.4	7	4156	97	420	50	2%		
CANBC1024K_38	0.0532	0.0043	0.00815	0.00041	0.1716	0.0469	0.0031	0.34341	0.00251	0.00019	438	1.1	52.6	4.1	52.3	2.6	80	130	50.7	8.9	65%		
CANBC1024K_39	0.0691	0.0069	0.00826	0.00037	0.16077	0.0594	0.0049	0.15547	0.00219	0.00017	364	1.0	67.7	6.5	53	2.4	620	160	44.2	3.3	9%		
CANBC1024K_40	9.06	0.27	0.0397	0.0025	0.83461	0.623	0.015	0.22854	0.0815	0.0074	333	1.4	1408	67	236	16	4567	39	1980	140	5%		
CANBC1024K_41	0.084	0.009	0.00811	0.00039	0.53863	0.079	0.01	-0.26862	0.00326	0.0004	381	1.4	82	12	52.1	2.7	960	250	65.3	8.9	5%		
CANBC1024K_42	0.0568	0.0048	0.00797	0.00038	0.017017	0.0521	0.0047	0.16133	0.00287	0.00033	483	1.2	59.1	4.7	51.2	2.4	240	160	53.8	4.1	21%		
CANBC1024K_43	0.098	0.015	0.0088	0.00044	0.10433	0.081	0.011	-0.006072	0.00308	0.00035	245	0.9	94	14	56.5	2.8	1010	240	62.2	7	6%		
CANBC1024K_44	0.051	0.0048	0.00814	0.00034	0.2298	0.0451	0.0031	0.054667	0.00259	0.00024	340	1.4	50.5	4.6	52.2	2.2	-20	130	52.3	4.9	-261%		
CANBC1024K_45	0.106	0.013	0.00905	0.00051	0.8601	0.0814	0.0063	-0.6668	0.0049	0.001	480	1.5	102	12	58.1	3.3	1190	170	100	21	5%		
CANBC1024K_46	0.077	0.007	0.00814	0.00035	0.45166	0.069	0.011	-0.10162	0.00286	0.00033	298	1.4	75	12	52.2	2.2	300	380	89.7	6.7	3%		
CANBC1024K_47	0.18	0.043	0.01041	0.00052	-0.14363	0.122	0.029	0.19775	0.00569	0.00048	83.4	0.8	164	34	68.8	3.3	1620	390	74.5	9.7	4%		
CANBC1024K_48	0.0536	0.0057	0.00807	0.00037	-0.014037	0.0489	0.0047	0.21999	0.00248	0.00025	434	1.5	52.9	5.5	52.1	2.3	80	160	50.1	5	65%		
CANBC1024K_49	0.079	0.009	0.00938	0.00066	0.21237	0.06	0.028	-0.23425	0.0038	0.0011	55.9	1.3	72	32	60.2	4.2	-50	630	76	30	-120%		
CANBC1024K_50	3.259	0.16	0.02789	0.0018	0.82861	0.604	0.014	-0.002668	0.0038	0.0008	270	1.4	117	49	117.5	8.3	4521	190	1549	72	4%		
CANBC1024K_51	0.125	0.013	0.00845	0.00038	-0.014446	0.1059	0.009	0.062435	0.00384	0.00056	600	1.1	119	12	54.2	2.4	1650	150	77	11	3%		
CANBC1024K_52	0.052	0.0057	0.00798	0.00036	0.013472	0.0481	0.0051	0.22798	0.00257	0.00028	424	1.1	51.4	5.4	51.2	2.3	40	160	51.9	5.7	128%		
CANBC1024K_53	0.0709	0.0074	0.00807	0.00037	0.081143	0.0634	0.006	0.13408	0.00291	0.00026	500	1.0	69.4	7	51.8	2.4	620	190	58.8	5.2	8%		
CANBC1024K_54	0.079	0.019	0.00871	0.0006	0.088419	0.071	0.021	0.063474	0.00293	0.00048	106.6	0.9	76	17	58.9	3.9	390	380	99.1	9.6	14%		
CANBC1024K_55	0.0722	0.0072	0.00817	0.00037	0.27722	0.0707	0.0047	0.34509	0.00256	0.00021	417	1.1	79.8	7.1	52.5	2.6	950	260	60.6	4.5	6%		
CANBC1024K_56	0.194	0.015	0.00941	0.0004	0.24862	0.08	0.012	-0.048632	0.00344	0.0003	385	1.4	90	13	54	2.5	960	250	69.4	6	6%		
CANBC1024K_57	0.073	0.017	0.00909	0.0004	0.45926	0.1395	0.0091	-0.067681	0.0063	0.00044	218.9	1.8	166	14	58.3	2.5	2200	120	62.7	8.7	3%		
CANBC1024K_58	0.076	0.013	0.00901	0.00049	-0.20232	0.064	0.012	0.44019	0.00393	0.00028	190	4.3	74	12	57.8	3.1	530	320	79	16	11%		
CANBC1024K_59	0.071	0.0078	0.00819	0.00037	0.07861	0.0632	0.0041	-0.050722	0.00316	0.00022	186	1.6	176	6	58.5	3.5	630	150	62.8	4.2	4%		
CANBC1024K_60	0.071	0.0078	0.00819	0.00037	0.15716	0.0652	0.0068	0.13802	0.00316	0.00022	402	1.5	69.4	7.5	52.6	2.4	780	210	63.8	5.4	3%		
CANBC1024																							

analysis	ISOTOPE RATIOS										ELEMENTAL CONCENTRATIONS		AGES								conc. (%)
	206/238 vs 207/235 error correlation		206/238 vs 207/235 error correlation		208/232 vs 207/235 error correlation		208/232 vs 207/235 error correlation		U (ppm)	U/Th	207/235 age (Ma)		206/238 age (Ma)		207/235 age (Ma)		208/232 age (Ma)				
	prop. 2s	prop. 2s	prop. 2s	prop. 2s	prop. 2s	prop. 2s	prop. 2s	prop. 2s			prop. 2s	prop. 2s	prop. 2s	prop. 2s	prop. 2s	prop. 2s	prop. 2s	prop. 2s	prop. 2s		
CANBC1024K_116	1.02	0.17	0.0159	0.0014	0.865	0.411	0.035	-0.65434	0.0147	0.00019	82	0.8	680	63	101.6	8.8	3910	130	295	38	3
CANBC1024K_117	0.0847	0.0078	0.00795	0.00034	0.26623	0.0763	0.0053	0.054686	0.00271	0.00021	581	1.2	82.3	7.3	51	2.2	1110	130	54.6	4.2	5
CANBC1024K_118	0.113	0.026	0.00659	0.0005	0.82984	0.099	0.02	-0.67021	0.00363	0.00064	477	1.2	107	23	55.1	3.2	1430	350	73	13	4
CANBC1024L_1	0.0593	0.0099	0.00886	0.00039	0.47289	0.0505	0.0073	0.028266	0.00335	0.00068	458	1.7	98.2	9.4	56.9	2.5	200	260	67.5	14	28
CANBC1024L_2	0.273	0.041	0.01028	0.00037	0.29485	0.191	0.021	-0.01049	0.008	0.00022	220.7	0.9	240	33	65.9	2.4	2680	200	160	41	2
CANBC1024L_3	0.1303	0.012	0.01859	0.0005	0.64893	0.0504	0.0029	0.33541	0.00694	0.00021	3020	5.1	124.1	11	118.8	3.2	201	190	140	24	59
CANBC1024L_4	0.121	0.016	0.01795	0.00058	0.46097	0.0505	0.005	-0.12784	0.0066	0.00016	600	1.4	115	11	110.9	3.7	230	200	52	36	50
CANBC1024L_5	0.0995	0.011	0.01289	0.00033	0.20445	0.0478	0.0047	0.19411	0.0081	0.00023	828	17.3	86.6	10	82.5	2.1	90	130	162	46	92
CANBC1024L_6	0.731	0.062	0.0831	0.002	0.78721	0.061	0.0035	0.22983	0.0246	0.00038	690	2.0	555	38	514	12	626	120	430	75	82
CANBC1024L_7	0.1025	0.011	0.01556	0.00044	0.40098	0.0476	0.0034	0.12446	0.00459	0.00075	1189	1.6	100.2	9.8	99.6	2.8	90	140	92.5	15	111
CANBC1024L_8	0.08	0.023	0.0106	0.00049	0.13593	0.055	0.014	0.089399	0.00465	0.0011	203	1.5	76	21	68	3.1	230	430	34	22	23
CANBC1024L_9	0.19	0.049	0.0158	0.00092	0.20486	0.093	0.022	-0.017676	0.0082	0.00012	140	1.0	169	40	101	5.8	1030	470	105	25	10
CANBC1024L_10	0.209	0.026	0.02823	0.00075	0.18497	0.0552	0.0062	0.50591	0.00886	0.0016	460	2.0	191	21	179.5	4.7	330	210	178	32	54
CANBC1024L_11	4.83	0.39	0.3025	0.0076	0.80574	0.1085	0.0055	0.31651	0.0916	0.014	483	2.1	1803	69	1703	37	1772	92	1768	270	96
CANBC1024L_12	0.0598	0.01	0.01413	0.00045	0.45252	0.0489	0.0041	0.48928	0.0087	0.0015	873	5.5	90.8	9.3	90.2	2.9	140	170	135	29	65
CANBC1024L_13	0.173	0.025	0.01409	0.00053	0.023585	0.093	0.013	0.17884	0.0074	0.0018	462	2.0	159	29	92.3	3.3	1000	330	148	35	8
CANBC1024L_14	0.0575	0.0068	0.00867	0.00023	0.32053	0.049	0.0051	0.1937	0.00251	0.00052	1135	2.9	56.7	6.5	55.7	1.5	180	210	50.6	10	31
CANBC1024L_15	0.059	0.014	0.00817	0.00038	0.26278	0.05	0.012	0.015806	0.00323	0.00073	224	0.7	58	13	52.5	2.5	150	410	65	15	35
CANBC1024L_16	0.197	0.025	0.01795	0.00048	0.40297	0.0767	0.0078	0.089568	0.00863	0.0015	630	1.4	181	21	114.7	3	1070	200	174	30	11
CANBC1024L_17	0.013	0.012	0.00524	0.00035	0.3628	0.0579	0.0075	-0.05542	0.00351	0.00076	511	1.0	72	12	68.1	2.3	410	270	71	15	14
CANBC1024L_18	0.1137	0.012	0.01581	0.00046	0.22357	0.049	0.0041	0.33701	0.00518	0.00095	705	1.1	109	11	101.1	2.9	190	170	104	19	53
CANBC1024L_19	0.0831	0.01	0.01144	0.00032	0.13216	0.0503	0.0057	0.2146	0.00362	0.00078	613	1.7	80.7	9.7	73.3	2.1	170	220	73	16	43
CANBC1024L_20	0.0824	0.0096	0.01224	0.00041	0.13777	0.0486	0.0048	0.098956	0.0057	0.0018	608	14.3	80.2	8.9	78.4	2.6	120	190	115	37	65
CANBC1024L_21	0.186	0.032	0.022	0.0022	0.68954	0.0481	0.0048	-0.012745	0.0048	0.00021	330	2.0	170	26	171	34	100	190	227	40	17
CANBC1024L_22	0.0661	0.011	0.01319	0.00049	0.29786	0.0478	0.0053	0.25081	0.00403	0.00076	576	1.7	82.6	9.9	84.2	2.6	90	200	61.3	13	106
CANBC1024L_23	0.21	0.028	0.02808	0.00067	0.22272	0.0598	0.0071	0.016646	0.0115	0.0024	264	2.2	191	23	178.5	4.2	330	230	231	48	54
CANBC1024L_24	0.014	0.024	0.01236	0.00046	0.0034107	0.081	0.013	0.0042146	0.00479	0.00011	242	1.9	131	21	81.1	2.9	990	310	37	22	8
CANBC1024L_25	0.0976	0.01	0.01423	0.00052	0.29662	0.0435	0.0044	0.39987	0.0054	0.0018	633	15.8	85	9.8	91.1	3.3	80	170	108	35	-114
CANBC1024L_26	0.194	0.018	0.0226	0.0015	0.60383	0.0705	0.005	-0.035356	0.00768	0.00013	610	2.4	180	15	151	9.6	350	240	155	27	14
CANBC1024L_27	0.061	0.0077	0.00963	0.00029	0.21315	0.0516	0.0058	0.22894	0.004	0.0013	587	6.4	59.9	7.3	55.4	1.9	250	210	90	26	22
CANBC1024L_28	8.99	1	0.375	0.022	0.86626	0.1687	0.0083	0.1936	0.1048	0.016	268	2.0	2317	110	2050	100	2524	84	2011	300	81
CANBC1024L_29	0.205	0.022	0.02708	0.00068	0.30005	0.0549	0.0046	0.22503	0.00986	0.0016	515	2.0	189	19	172.3	4.3	360	170	180	31	48
CANBC1024L_30	0.024	0.014	0.00955	0.00036	0.0073524	0.018	0.011	0.23531	0.00282	0.00057	131	1.0	23	14	54.8	2.3	-1020	420	57	13	-5
CANBC1024L_31	0.103	0.028	0.00034	0.00039	0.2015	0.093	0.013	-0.13463	0.0033	0.00013	243	1.9	86	25	68.1	2.3	107	30	107	30	9
CANBC1024L_32	0.054	0.0072	0.00837	0.00024	0.20185	0.0468	0.0056	0.049895	0.00226	0.00042	648	1.0	54.5	6.9	53.7	1.5	30	210	47.7	8.5	179
CANBC1024L_33	0.06	0.01	0.00889	0.00024	0.14057	0.0492	0.007	0.00042601	0.00236	0.00075	417	2.5	58.8	9.5	57.1	1.6	110	260	60	15	52
CANBC1024L_35	0.073	0.1	0.1	0.0063	0.92301	0.0613	0.0055	0.24891	0.036	0.0057	331	2.8	62.7	6.7	61.3	37	637	120	694	110	96
CANBC1024L_36	0.0582	0.0082	0.0082	0.00029	0.061987	0.0483	0.0036	0.17267	0.00284	0.00018	433	1.2	64.8	8	62.7	1.8	80	240	54.7	12	20
CANBC1024L_37	0.0571	0.0081	0.00906	0.0003	0.17595	0.0457	0.0057	0.11472	0.00341	0.00056	585	1.7	56.2	7.7	58.1	1.9	20	230	68.9	13	29
CANBC1024L_38	0.0801	0.0079	0.0119	0.00025	0.32717	0.0475	0.0033	0.17405	0.00345	0.00016	1513	3.1	78.1	7.4	76.2	1.6	83	140	69.6	12	92
CANBC1024L_39	0.087	0.034	0.00918	0.00059	-0.24933	0.079	0.031	0.48836	0.0042	0.0017	80	1.1	80	30	58.9	3.6	230	660	85	34	26
CANBC1024L_40	0.0722	0.0091	0.01368	0.00034	0.18886	0.048	0.0054	0.057894	0.00346	0.00067	460	7.9	70.5	8.6	65.6	2.1	90	200	92	29	76
CANBC1024L_41	0.541	0.054	0.054	0.0038	0.81478	0.0718	0.0061	0.58631	0.0332	0.0066	1270	4.3	440	36	339	23	380	150	637	130	36
CANBC1024L_42	0.0694	0.0091	0.00963	0.00037	0.20276	0.051	0.0059	0.23551	0.00302	0.00063	609	2.7	67.9	8.6	61.8	2.4	190	200	60.9	13	33
CANBC1024L_43	0.0543	0.0078	0.00936	0.00031	0.11597	0.0428	0.0051	0.19059	0.00269	0.00022	536	4.8	55.8	7.5	60	2	-110	200	54	16	-55
CANBC1024L_44	0.0567	0.0077	0.00888	0.00034	-0.13314	0.0443	0.0069	0.32075	0.00311	0.00059	391	1.4	53.5	7.5	57	2.2	-30	260	62.7	12	-190
CANBC1024L_45	0.0512	0.0072	0.00995	0.00036	0.5287	0.0451	0.0047	0.04632	0.00271	0.00056	676	1.5	60.1	7.7	63.8	3.3	460	240	54.7	12	20
CANBC1024L_46	0.21	0.023	0.03036	0.00071	0.62941	0.0491	0.0036	-0.1153	0.0097	0.00022	416	1.8	193	20	192.8	4.5	170	150	196	40	113
CANBC1024L_48	0.086	0.032	0.00892	0.00048	0.018406	0.078	0.028	0.093981	0.00333	0.00077	211	1.0	80	29	57.2	3.1					

analysis	ISOTOPIC RATIOS										ELEMENTAL CONCENTRATIONS		AGES							conc. (%)	
	207/235		206/238 vs 207/235 correlation		208/232 vs 207/235 correlation		208/232 vs 206/238 correlation		208/232		U (ppm)	U/Th	207/235 age (Ma)		206/238 age (Ma)		208/232 age (Ma)		prop. 2s (Myr)		
	prop. 2s	prop. 2s	prop. 2s	prop. 2s	prop. 2s	prop. 2s	prop. 2s	prop. 2s	prop. 2s	prop. 2s	prop. 2s	prop. 2s	prop. 2s	prop. 2s	prop. 2s	prop. 2s	prop. 2s	prop. 2s	prop. 2s		
WLRI_1	0.075	0.014	0.00831	0.00059	0.4708	0.0653	0.0093	-0.25408	0.00283	0.00033	468	0.8	73	13	53.4	3.8	6.10	260	57.1	6.7	9%
WLRI_2	0.66	0.13	0.01142	0.00096	0.40289	0.379	0.057	-0.15382	0.00655	0.0013	117	0.8	488	77	73.2	6.1	3680	260	172	25	2%
WLRI_3	0.283	0.045	0.0101	0.00075	0.31889	0.188	0.027	-0.17289	0.00615	0.0011	252	0.8	230	37	64.8	4.8	2620	240	134	21	2%
WLRI_4	0.237	0.028	0.02973	0.0016	0.37119	0.0666	0.0466	-0.1389	0.0121	0.0017	371	2.7	215	22	109.9	11	420	180	225	34	45%
WLRI_5	0.082	0.021	0.0079	0.00051	0.12768	0.075	0.019	-0.06984	0.0041	0.0015	360	0.7	78	19	50.7	3.2	110	370	91	31	8%
WLRI_6	0.15	0.04	0.00792	0.00056	0.018725	0.131	0.035	0.12757	0.00369	0.00056	154.2	1.0	137	34	50.8	3.6	1940	440	74.4	11	3%
WLRI_7	0.044	0.014	0.00903	0.00054	0.10471	0.039	0.012	0.12303	0.0034	0.0011	171.4	1.4	43	13	51.8	3.5	360	380	66	21	-14%
WLRI_9	0.085	0.026	0.00828	0.00053	0.19912	0.077	0.024	-0.15187	0.0042	0.0023	224	3.2	81	23	53.1	3.4	530	430	63	15	10%
WLRI_10	0.026	0.021	0.00826	0.00059	-0.13889	0.053	0.019	0.28789	0.0048	0.002	196	1.2	57	20	53	3.8	110	460	97	40	-6%
WLRI_11	0.127	0.038	0.00872	0.0007	0.12585	0.107	0.03	-0.023699	0.00369	0.001	185	1.2	116	32	56	4.5	1250	570	74	21	4%
WLRI_12	0.169	0.048	0.00857	0.00065	-0.13137	0.148	0.042	0.25176	0.0042	0.0015	201	1.1	151	39	55	4.1	1950	560	84	30	3%
WLRI_13	0.094	0.02	0.00943	0.00059	0.29975	0.079	0.015	0.35411	0.0041	0.0005	291	1.1	90	19	54.1	3.7	960	400	83	17	6%
WLRI_18	0.138	0.051	0.00796	0.00053	0.042490	0.123	0.047	-0.027186	0.00289	0.00055	225	1.1	116	40	51.2	3.4	1120	500	66	13	5%
WLRI_15	0.096	0.034	0.00807	0.00065	0.042899	0.099	0.038	0.001643	0.00317	0.00042	228	1.0	89	29	51.8	3.5	670	530	64	14	8%
WLRI_16	0.088	0.013	0.00797	0.00049	-0.098415	0.077	0.0081	0.29941	0.00311	0.00071	429	1.2	82.6	10	51.2	3.1	1010	200	62.7	8.3	5%
WLRI_17	0.187	0.03	0.00835	0.00058	0.35422	0.136	0.022	-0.17068	0.0055	0.0013	295	1.2	146	26	53.6	3.7	2150	330	111	26	2%
WLRI_19	0.067	0.02	0.00752	0.00053	-0.162571	0.065	0.019	0.19093	0.00249	0.00071	201	1.1	64	18	48.3	3.4	270	440	50	14	18%
WLRI_20	0.114	0.021	0.008	0.00054	0.073795	0.104	0.017	0.15185	0.00357	0.00057	263	1.0	109	19	51.4	3.6	1480	290	72	11	3%
WLRI_21	0.057	0.018	0.00786	0.00053	0.019747	0.055	0.017	0.028622	0.00277	0.00049	195.3	1.1	55	17	50.5	3.4	80	480	55.8	9.9	63%
WLRI_22	0.094	0.026	0.00824	0.00073	0.32466	0.088	0.022	-0.027452	0.005	0.0014	169.7	1.2	89	24	52.9	4.7	1040	530	102	28	5%
WLRI_23	0.066	0.02	0.00801	0.00057	-0.20389	0.063	0.022	0.27855	0.00292	0.00047	308	0.8	63	18	51.4	3.6	1110	370	58.8	9.4	47%
WLRI_24	0.125	0.035	0.00749	0.00056	-0.10127	0.115	0.027	0.3105	0.00303	0.00062	126.6	0.7	115	30	48.1	3.6	1310	510	61.2	12	4%
WLRI_25	0.0544	0.006	0.00819	0.00052	0.13679	0.0498	0.0098	0.2343	0.00293	0.00039	1507	3.9	53.7	5.8	52.6	3.3	160	140	59.1	7.9	33%
WLRI_26	0.074	0.011	0.00737	0.00045	0.38973	0.0736	0.031	-0.2293	0.00291	0.00046	859	0.9	72.1	11	47.3	2.9	900	250	58.8	9.2	5%
WLRI_27	0.186	0.03	0.011	0.0007	0.70224	0.0709	0.003	0.33909	0.0019	0.001	448	1.0	673	54	651	49	965	87	815	80	88%
WLRI_28	0.063	0.033	0.00846	0.00053	0.4638	0.082	0.017	-0.21352	0.00279	0.0005	266	1.0	89	20	50.5	3.4	440	460	68.2	10	11%
WLRI_29	0.0821	0.01	0.00863	0.00054	0.067001	0.0713	0.0077	0.14401	0.00354	0.00055	429	1.0	79.9	9.7	55.4	3.4	850	190	71.5	11	7%
WLRI_30	0.051	0.014	0.00754	0.00048	0.1233	0.053	0.014	0.16441	0.00339	0.00038	217.9	1.4	49	13	48.4	3.1	50	90	68	18	97%
WLRI_31	0.059	0.027	0.00771	0.00059	-0.0007681	0.077	0.036	0.13029	0.0042	0.0014	137	1.5	56	25	49.5	3.8	20	630	84	29	248%
WLRI_32	0.067	0.024	0.00779	0.00047	0.64427	0.062	0.01	-0.12042	0.00222	0.0004	206.2	0.4	50	5.2	46.2	3	265	130	44.7	4.5	15%
WLRI_33	0.0948	0.01	0.00766	0.00047	0.23448	0.082	0.0078	0.14725	0.00291	0.00036	839	1.0	82.4	9.8	49.2	3	1180	190	58.6	7.1	4%
WLRI_34	0.0444	0.007	0.00796	0.0005	-0.069722	0.0406	0.004	0.20144	0.00251	0.00031	612	1.3	44	5.5	51.1	3.2	200	160	50.7	6.2	-26%
WLRI_35	0.068	0.016	0.00771	0.00049	0.42451	0.063	0.013	-0.31006	0.00278	0.00038	553	0.8	86	15	49.5	3.1	390	360	56.2	7.7	13%
WLRI_36	0.078	0.023	0.00793	0.00053	0.26688	0.068	0.019	-0.23588	0.00318	0.00053	198.5	1.1	73	21	50.9	3.4	380	470	64.1	11	14%
WLRI_37	0.063	0.033	0.00843	0.00053	0.06403	0.131	0.021	-0.42738	0.0029	0.0005	395.7	0.9	160	28	50.6	3.4	1900	30	160	16	11%
WLRI_38	0.034	0.012	0.00736	0.00053	-0.15006	0.04	0.017	0.30745	0.00267	0.00065	160	1.0	33	12	47.2	3.4	-440	440	54	13	-11%
WLRI_39	0.064	0.014	0.00851	0.00056	-0.10661	0.054	0.011	0.19660	0.00303	0.00045	289	1.2	62	13	54.6	3.6	180	300	66.5	9.1	30%
WLRI_40	0.056	0.011	0.00746	0.00046	0.37116	0.0539	0.0086	-0.26346	0.00254	0.00036	508	2.2	54.9	10	47.9	3	230	260	51.2	7.4	21%
WLRI_41	0.061	0.022	0.00793	0.00053	-0.11356	0.067	0.018	0.12964	0.00308	0.00042	199	1.2	56	18	50.8	3.4	150	480	78	23	34%
WLRI_42	0.082	0.021	0.00779	0.00052	-0.1587	0.076	0.019	0.35148	0.0039	0.0011	147	1.3	79	19	50	3.3	710	210	78	22	7%
WLRI_43	0.041	0.011	0.00788	0.00051	0.050908	0.041	0.011	0.00045448	0.00225	0.00037	225	1.3	40	11	50.6	3.2	-290	560	45.3	7.5	-17%
WLRI_44	0.046	0.0077	0.00747	0.00061	0.54975	0.0457	0.0048	-0.13012	0.00225	0.00025	700	0.8	47	6.6	48	3.9	10	170	45.5	5.1	-80%
WLRI_45	0.048	0.016	0.00763	0.00053	-0.028182	0.046	0.015	0.048005	0.00272	0.00052	158.4	1.0	42	12	50.3	3.4	270	340	55	19	5%
WLRI_46	0.852	0.56	0.2595	0.016	0.81782	0.1098	0.0044	0.67833	0.0532	0.005	414	1.9	1617	67	487	80	756	73	1048	110	7%
WLRI_47	0.094	0.013	0.00763	0.00049	0.15021	0.0911	0.01	0.16456	0.00237	0.00044	485	1.3	90.5	12	49	3.1	1910	220	65.9	8.9	4%
WLRI_48	0.0724	0.0097	0.00798	0.00049	-0.036718	0.0654	0.007	0.36682	0.00282	0.00029	987	1.0	70.8	9	51.3	3.1	690	190	58.9	7.9	7%
WLRI_49	0.064	0.015	0.00762	0.00055	0.0071408	0.062	0.015	0.26549	0.0038	0.0012	233	1.0	62	14	48.9	3.5	540	410	76	24	9%
WLRI_50	0.0821	0.004	0.00716	0.00045	0.14873	0.0626	0.002	-0.0019763	0.0004	0.00042	84.4	0.8	60	8.9	45.1	2.8	360	280	49.3	6.4	8%
WLRI_51	0.152	0.045	0.00854	0.00058	0.42443	0.115	0.028	-0.21285	0.00343	0.00068	264	1.4	137	36	54.8	3.7	1950	400	69.2	12	4%
WLRI_52	0.093	0.013	0.00791	0.00049	-0.016672	0.0839	0.0094	0.39482	0.0026	0.0003	845	0.5	89.9	12	50.8	3.1	1150	220	56.5	6.1	4%
WLRI_53	0.174	0.033	0.00839	0.00055	0.19224	0.142	0.022	0.24053	0.00443	0.00073	303	1.0	160	28	53.8	3.5	2070	270	89	15	3%
WLRI_54	0.060	0.029	0.00807	0.0005	0.064242	0.085	0.027	-0.029455	0.00226	0.00033	140.8	1.0	64	25	51.4	3.6	900	640	65.7	10	3%
WLRI_55	0.088	0.01	0.00759	0.00046	0.47825	0.066	0.0088	-0.39981	0.00277	0.00032	774	1.0	67.1	11	48.7	2.9	740	290	65.9	6.5	7%
WLRI_56	0.071	0.013	0.00794	0.00053	0.033108	0.066	0.011	0.11921	0.00392	0.00092	382	1.5	70	12	51	3.4	690	300	79	18	7%
WLRI_57	0.303	0.086	0.00872	0.00062	0.4745	0.231	0.056	-0.37589	0.00344	0.00047	208	0.6	251	63	55.9	3.9	2430	490	69.4	9.6	2%
WLRI_58	0.0997	0.012	0.00791	0.00047	0.36475	0.0645	0.0096	-0.25532	0.00261	0.00032	980	1.1	68	11							

analysis	ISOTOPIC RATIOS										ELEMENTAL CONCENTRATIONS		AGES							conc. (%)	
	206/238 vs 207/235 correlation					208/232 vs 207/235 correlation					U (ppm)	U/Th	207/235 age (Ma)	prop. 2s (Myr)	206/238 age (Ma)	prop. 2s (Myr)	207/235 age (Ma)	prop. 2s (Myr)	208/232 age (Ma)		prop. 2s (Myr)
	207/235	prop. 2s	206/238	prop. 2s	207/235 error	207/235	prop. 2s	208/232	prop. 2s												
WLR1_111	0.069	0.012	0.00757	0.00051	0.89882	0.066	0.0084	-0.73796	0.00307	0.00044	590	1.1	67.7	11	48.6	3.3	660	210	61.9	8.8	7%
WLR1_112	0.074	0.017	0.00816	0.00054	0.35404	0.065	0.013	-0.27102	0.00296	0.00045	184	1.3	72	15	52.4	3.5	520	330	59.7	9.1	10%
WLR1_113	0.119	0.027	0.00837	0.00059	0.027247	0.119	0.03	0.16174	0.00341	0.00072	100.8	1.1	112	23	53.9	3.7	1400	390	69	14	4%
WLR1_114	0.077	0.037	0.00895	0.00061	0.83675	0.135	0.022	-0.59912	0.00407	0.00092	222	1.2	154	27	57.4	3.9	2010	340	93	18	3%
WLR1_115	0.089	0.015	0.00776	0.0005	0.020742	0.082	0.013	0.15105	0.00321	0.00062	269	1.4	86	14	49.8	3.2	1000	290	65	12	5%
WLR1_116	0.31	0.079	0.01162	0.001	0.34846	0.18	0.038	-0.27922	0.0057	0.0012	86	0.7	258	59	74.5	6.6	2150	450	114	25	3%
WLR1_117	0.0502	0.079	0.008	0.0005	0.22057	0.052	0.0065	-0.087198	0.00234	0.00043	443	1.2	54.4	7.5	51.3	3.2	160	190	47.2	6.1	32%
WLR1_118	0.063	0.015	0.00828	0.00058	0.063622	0.055	0.012	0.054001	0.00263	0.00057	138.1	1.1	62	14	53.2	3.7	340	360	53	12	16%
WLR1_119	0.078	0.017	0.00796	0.00051	0.073897	0.073	0.0157	0.034957	0.00278	0.00043	181	1.1	76	15	51.1	3.3	170	360	56.3	8.6	7%
WLR1_120	0.116	0.023	0.00873	0.00066	0.23834	0.093	0.015	-0.1001	0.00442	0.00075	223	1.3	110	21	56	4.2	1950	310	99	15	4%
WLR2_1	0.0577	0.009	0.00796	0.00039	-0.19088	0.034	0.0095	0.35245	0.00322	0.00071	272.3	3.3	56.6	8.5	51.1	2.5	210	260	85	14	24%
WLR2_2	0.214	0.021	0.02498	0.0011	0.30419	0.0616	0.0095	-0.10986	0.01111	0.0012	1018	2.5	196	17	159	6.6	580	160	223	24	27%
WLR2_3	0.28	0.019	0.03151	0.0013	0.38301	0.0655	0.0035	0.0034966	0.01351	0.0013	305	2.3	250	15	200	8.4	810	93	271	26	25%
WLR2_4	0.0487	0.0061	0.00758	0.0003	-0.0070403	0.0487	0.0056	0.089332	0.00267	0.00037	359	1.3	48.1	5.9	48.7	1.9	20	190	53.9	7.4	244%
WLR2_5	0.1307	0.01	0.02374	0.001	0.59762	0.0515	0.0022	0.21458	0.00793	0.00056	1160	1.8	159.8	9	151.2	6.5	255	95	159.5	19	60%
WLR2_6	0.0572	0.052	0.00792	0.00038	0.44743	0.0514	0.0039	0.070288	0.00391	0.00029	849	1.1	86.4	5	60.8	2.4	230	150	59.8	5.8	22%
WLR2_7	0.0593	0.0084	0.00801	0.00037	-0.21602	0.0531	0.0086	0.44807	0.00293	0.00043	367	1.5	58.1	8.9	51.4	2.4	190	280	59.2	8.6	27%
WLR2_8	0.0567	0.058	0.0076	0.00033	-0.021099	0.0549	0.0052	0.24625	0.00305	0.00036	871	2.9	55.9	5.5	48.8	2.1	370	190	61.6	7.3	13%
WLR2_9	0.0576	0.0658	0.00803	0.00036	-0.11113	0.052	0.0055	0.31719	0.00312	0.00038	748	2.8	56.7	5.5	51.6	2.3	210	180	62.9	7.7	25%
WLR2_10	0.0564	0.063	0.00783	0.00035	0.03013	0.0488	0.0065	0.062265	0.00263	0.00024	576	0.6	49.8	6	49.3	2.3	30	210	53.2	4.9	165%
WLR2_11	0.0483	0.004	0.00744	0.00025	0.23233	0.0472	0.0036	0.20253	0.00287	0.00038	926	2.8	47.9	3.8	47.8	2.2	60	140	57.9	7.7	80%
WLR2_12	0.351	0.023	0.023	0.0013	0.011016	0.1125	0.0081	0.70055	0.01432	0.0011	2360	1.9	305	18	146.6	8.4	1820	140	287	22	8%
WLR2_13	0.1692	0.0097	0.02208	0.00096	0.36238	0.0487	0.0019	0.14594	0.00868	0.00067	1379	1.8	158.6	8.4	159.7	6.1	134	82	174.6	13	119%
WLR2_14	0.062	0.016	0.008	0.00029	-0.058953	0.056	0.015	0.22722	0.00314	0.00073	271	3.2	60	15	51.3	2.5	120	360	53	15	43%
WLR2_15	0.163	0.052	0.0082	0.00048	0.8273	0.148	0.031	-0.43227	0.011	0.0034	446	2.2	189	43	59	3	2110	180	246	61	3%
WLR2_16	0.2275	0.014	0.02466	0.00099	0.73878	0.0664	0.0025	0.018288	0.01064	0.00078	1550	1.8	209	11	157	6.2	808	79	212	16	19%
WLR2_17	0.047	0.0034	0.00746	0.0003	0.0023067	0.0459	0.0031	0.33116	0.00273	0.00032	1500	1.5	46.6	3.3	47.9	1.9	10	130	55.1	6.4	473%
WLR2_18	0.0623	0.0098	0.00727	0.0003	0.001864	0.0613	0.0095	0.17473	0.00261	0.00028	529	1.1	61	9.3	46.7	1.8	450	280	52.7	5.7	10%
WLR2_19	0.054	0.0063	0.00763	0.00035	0.03013	0.0488	0.0065	0.062265	0.00263	0.00024	576	0.6	49.8	6	49.3	2.3	30	210	53.2	4.9	165%
WLR2_20	0.1159	0.011	0.0089	0.00033	-0.061463	0.0943	0.0017	0.21446	0.00564	0.00061	569	2.9	111	9.8	57.1	2.1	1500	160	113.6	12	4%
WLR2_21	0.185	0.036	0.00909	0.00049	0.84208	0.137	0.017	-0.68495	0.00683	0.001	560	2.1	155	21	58.3	3.2	2090	170	137	20	3%
WLR2_22	0.1904	0.013	0.02492	0.0012	0.59274	0.0739	0.0028	0.27972	0.00928	0.00062	669	2.5	178.4	11	158.7	7.7	602	110	187	17	32%
WLR2_23	0.348	0.035	0.0284	0.0011	0.1489	0.0852	0.0081	0.11173	0.011	0.0034	301	1.7	301	26	180.5	7	1300	150	265	14	14%
WLR2_24	0.022	0.0046	0.00048	0.0001	0.79729	0.137	0.014	-0.46287	0.00726	0.0011	949	2.3	153	20	54.3	2.4	2120	190	146	21	3%
WLR2_25	0.168	0.037	0.00861	0.00025	0.28216	0.139	0.03	-0.15893	0.008	0.002	535	2.0	153	32	55.3	2.3	1760	440	183	42	3%
WLR2_26	0.266	0.06	0.01	0.00062	0.62236	0.184	0.034	-0.55418	0.0071	0.0016	362	1.0	229	46	64.2	4	2390	340	143	31	3%
WLR2_27	0.056	0.012	0.00837	0.00038	-0.1555	0.049	0.011	0.21393	0.00328	0.00041	300	0.9	55	12	53.7	2.4	10	340	86.1	8.3	537%
WLR2_28	0.05	0.005	0.0076	0.00032	0.03341	0.049	0.014	-0.036889	0.00284	0.00042	234	1.6	48	13	48.8	2.7	110	360	59.3	4.9	45%
WLR2_29	0.0537	0.0042	0.00775	0.0003	0.32449	0.0508	0.0032	-0.024073	0.00268	0.00024	1659	1.1	53.1	4	49.8	1.9	210	120	54	4.8	24%
WLR2_30	0.093	0.011	0.00794	0.00036	0.5273	0.0846	0.0086	-0.27395	0.00397	0.00054	830	2.4	89.7	10	51	2.3	1160	220	80	11	4%
WLR2_31	0.0395	0.0048	0.00832	0.00038	0.30888	0.0346	0.0035	-0.12525	0.00321	0.00069	445	3.1	39.2	4.7	53.4	2.4	-430	140	65	14	-12%
WLR2_32	0.1953	0.01	0.0083	0.00035	0.15267	0.056	0.027	0.68079	0.00663	0.00068	520.0	1.7	61.6	12.5	54	6	480	180	171	14	33%
WLR2_33	0.167	0.034	0.00919	0.00051	0.45242	0.128	0.022	-0.31701	0.005	0.00055	222	1.1	163	28	59	3.2	1760	300	101	13	3%
WLR2_34	0.42	0.041	0.01223	0.00053	0.89356	0.249	0.016	-0.54194	0.00648	0.00051	2960	0.4	353	29	78.3	3.4	3180	100	110.4	10	2%
WLR2_35	0.132	0.077	0.00829	0.00048	0.047245	0.103	0.059	0.011533	0.0049	0.00015	82.2	2.1	93	54	53.2	3.1	100	900	88	29	53%
WLR2_36	0.0627	0.01	0.00766	0.00035	-0.2619	0.036	0.01	0.40915	0.00413	0.00075	561	2.5	61.3	9.6	49.2	2.2	520	320	83	15	9%
WLR2_37	0.272	0.017	0.0256	0.0013	0.70891	0.073	0.025	0.41686	0.01093	0.0006	1620	1.9	244.9	15	164	6.4	1147	210	219.5	12	14%
WLR2_38	0.174	0.016	0.02465	0.001	0.030305	0.0521	0.0046	0.12508	0.00879	0.0011	407	1.7	162	14	157	6.3	240	160	177	22	65%
WLR2_39	0.1961	0.013	0.0284	0.0015	0.57078	0.0509	0.0024	0.2481	0.01043	0.001	648	5.7	181.5	11	180.3	9.5	223	99	210	20	81%
WLR2_40	0.0438	0.0062	0.00763	0.00041	0.15643	0.0409	0.0046	0.092844	0.00249	0.00026	569	1.1	43.4	6	49	2.6	-190	180	50.3	5.3	-26%
WLR2_41	0.0675	0.01	0.0083	0.00037	-0.24598	0.062	0.011	0.36711	0.00343	0.00083	473	3.5	65.8	9.6	53.3	2.3	430	280	67	17	12%
WLR2_42	0.0618	0.0041	0.00832	0.00034	0.18161	0.0535	0.0033	0.38872	0.00296	0.00027	1787	1.6	60.9	3.9	53.4	2.2	300	130	59.8	5.4	17%
WLR2_43	0.047	0.0064	0.0076	0.00035	0.21864	0.0473	0.0066	0.01644	0.0044	0.0021	434	3.0	46.5	6.2	48.8	2.3	30	200	88	42	163%
WLR2_44	0.1716	0.012	0.02461	0.0011	0.46185	0.0518	0.0028	0.13575	0.00871	0.00074	625	2.1	160.5	10	156.7	7	300	130	175.3	15	52%
WLR2_45	0.073	0.0059	0.00827	0.00037	0.79023	0.0336	0.0033	-0.50248	0.00243	0.00018	3590	0.4	71.5	5.6	53.1	2.4	699	110	49.1	3.6	8%
WLR2_46	0.073	0.022	0.00923																		

analysis	ISOTOPIC RATIOS										ELEMENTAL CONCENTRATIONS		AGES							conc. (%)	
	207/235		206/238 vs 207/235 error correlation		208/232		208/232 vs 207/235 error correlation		208/232		U (ppm)		207/235 age (Ma)		206/238 age (Ma)		208/232 age (Ma)		prop. 2s (Ma)		
	prop. 2s	prop. 2s	prop. 2s	prop. 2s	prop. 2s	prop. 2s	prop. 2s	prop. 2s	prop. 2s	prop. 2s	prop. 2s	prop. 2s	prop. 2s	prop. 2s	prop. 2s	prop. 2s	prop. 2s				
WLR2_97	0.106	0.03	0.01305	0.0008	0.21484	0.06	0.018	0.069736	0.0051	0.0013	116	2.9	99	26	83.6	5.1	200	380	103	26	42%
WLR2_98	0.0587	0.0069	0.00774	0.00037	0.17374	0.0549	0.0057	0.096301	0.00309	0.00083	667	3.0	57.7	6.6	49.7	2.3	300	200	62	17	16%
WLR2_99	0.065	0.014	0.00784	0.00039	-0.023764	0.061	0.013	0.091412	0.00233	0.00031	262	1.6	63	13	50.4	2.5	330	340	47.1	6.2	15%
WLR2_100	0.0553	0.0073	0.00789	0.00039	0.18219	0.0498	0.006	0.15562	0.00252	0.00051	671	2.8	52.5	12	53.7	2.5	130	210	53.9	5.2	42%
WLR2_101	0.0617	0.0067	0.00764	0.00035	-0.081345	0.0581	0.0064	0.27241	0.0027	0.00033	712	1.8	60.7	6.4	49.1	2.2	470	210	54.5	6.6	10%
WLR2_102	0.0472	0.0041	0.00828	0.00042	0.37924	0.0428	0.0035	0.055135	0.0026	0.00033	630	2.3	46.8	4	53.1	2.7	-110	140	52.4	6.6	-68%
WLR2_103	0.1893	0.012	0.02316	0.00084	0.23866	0.0579	0.0027	0.045139	0.00668	0.00026	1156	2.1	172.4	10	147.6	5.3	503	100	174	16	29%
WLR2_104	0.228	0.051	0.00899	0.00032	0.51109	0.194	0.043	-0.40085	0.00429	0.00059	4680	0.6	201	40	57.72	2.1	2410	380	96	12	2%
WLR2_105	0.153	0.01	0.02462	0.00093	0.46982	0.1616	0.0021	0.10838	0.006	0.00062	924	2.0	161.8	9.1	156.8	5.9	269	87	161.1	13	59%
WLR2_106	0.267	0.023	0.00764	0.00049	0.69626	0.243	0.018	-0.42652	0.0231	0.00027	1680	5.1	239	19	49	3.1	3140	110	462	53	2%
WLR2_107	0.0648	0.0078	0.00751	0.00029	0.12524	0.0817	0.0068	0.15462	0.0003	0.00016	611	2.9	82.5	7.3	48.2	1.8	1340	170	106	31	4%
WLR2_108	0.0565	0.006	0.00733	0.00036	-0.27139	0.0554	0.006	0.40265	0.00258	0.00025	690	0.6	59.7	5.7	47.1	2.3	390	190	52.1	5.1	13%
WLR2_109	0.142	0.008	0.00851	0.00033	0.19021	0.098	0.0095	0.18889	0.00506	0.00061	762	2.1	110.9	8.2	54.7	2.1	1620	120	102	12	3%
WLR2_110	0.0552	0.0046	0.00793	0.00037	0.2651	0.0499	0.0039	0.12013	0.00261	0.00028	459	1.2	54.5	4.4	50.9	2.3	210	140	52.7	5.7	24%
WLR2_111	0.658	0.054	0.02658	0.0011	-0.39911	0.172	0.016	0.74407	0.01526	0.00124	2540	0.8	514	34	181.6	7.2	2220	150	306	28	7%
WLR2_112	0.14	0.037	0.0085	0.00043	0.3391	0.112	0.025	-0.1747	0.00418	0.00061	150.8	1.0	128	31	54.6	2.6	1390	340	94	12	4%
SHELL_1	0.75	0.13	0.0314	0.0018	-0.19077	0.179	0.034	0.44977	0.0212	0.007	61.2	2.0	542	74	199	11	2290	340	120	140	9%
SHELL_2	0.2142	0.02	0.02746	0.00079	0.16041	0.0562	0.0049	0.23039	0.00955	0.0018	386	1.5	196.7	17	174.6	4.9	435	190	420	36	40%
SHELL_3	1.69	0.18	0.02273	0.00097	0.76799	0.527	0.044	-0.070647	0.0273	0.0058	343	0.8	999	64	144.8	6.1	4309	120	543	110	3%
SHELL_4	0.0708	0.0085	0.00875	0.00039	-0.080874	0.0192	0.0068	0.86152	0.00367	0.00049	802	3.9	626.1	7.9	54.9	2.5	430	200	69	14	11%
SHELL_5	0.32	0.065	0.02494	0.00067	-0.32524	0.091	0.018	0.7601	0.01023	0.002	234.6	1.6	272	46	159.6	4.7	1190	330	206	41	13%
SHELL_7	1.686	0.16	0.0382	0.0014	0.18662	0.319	0.027	0.43219	0.039	0.00073	54.7	1.2	1000	58	241.5	8.9	3548	140	773	140	7%
SHELL_8	0.71	0.25	0.0278	0.0017	0.88739	0.156	0.04	-0.67306	0.0187	0.0058	133.1	1.8	490	120	177	10	1920	400	372	110	9%
SHELL_9	0.227	0.026	0.00959	0.00035	0.56667	0.164	0.016	-0.26111	0.0046	0.00059	435	0.8	204	22	61.5	2.2	2480	180	92.7	18	2%
SHELL_10	0.098	0.013	0.00889	0.00039	-0.180296	0.1714	0.01	0.27441	0.00514	0.0011	151.7	3.3	85.5	11	57.7	2.3	920	390	104	23	19%
SHELL_11	0.0714	0.01	0.00939	0.0005	-0.045157	0.0542	0.0074	0.26448	0.00259	0.00058	317	0.8	69.8	9.6	60.3	3.2	310	240	60.4	12	19%
SHELL_12	0.0816	0.0087	0.00851	0.00031	0.17256	0.0735	0.0088	0.23961	0.00317	0.00075	529	0.9	73.5	8.1	54.6	2	340	230	63.9	12	6%
SHELL_13	0.079	0.016	0.00858	0.00032	-0.16361	0.072	0.016	0.20089	0.0035	0.0005	110	1.2	80	16	55.1	2.1	630	340	70.5	15	9%
SHELL_14	0.262	0.026	0.0324	0.0015	0.45366	0.3534	0.0469	0.00659	0.018	0.0034	161.1	2.3	219	21	211.8	9.6	350	220	350	61	11%
SHELL_15	0.214	0.027	0.0311	0.0012	0.26578	0.0482	0.005	-0.006595	0.0106	0.0023	120	2.3	195	21	197.3	7.5	140	230	213	46	141%
SHELL_16	0.0544	0.0055	0.00834	0.00024	0.22563	0.048	0.0044	0.16573	0.00288	0.00055	695	0.9	53.9	5.3	53.6	1.5	100	180	58.2	11	54%
SHELL_17	0.179	0.031	0.00904	0.00045	0.68985	0.135	0.019	-0.41164	0.00629	0.0014	383	1.6	165	26	58	2.6	2050	240	127	28	3%
SHELL_18	0.0609	0.0089	0.00833	0.00033	-0.11739	0.0513	0.0086	0.31953	0.0025	0.00045	157	0.7	59.7	9.4	54.9	2.1	210	350	50.4	93	26%
SHELL_19	0.0582	0.013	0.00919	0.00021	-0.46712	0.072	0.012	0.85903	0.00323	0.00063	617	1.1	73	12	62.6	1.8	780	270	52.3	10	1%
SHELL_20	0.0611	0.0072	0.00866	0.00028	0.105	0.0508	0.0056	0.061511	0.00295	0.00058	439	1.2	60.1	6.8	55.6	1.8	200	210	59.6	12	28%
SHELL_21	0.087	0.013	0.00907	0.0003	-0.24262	0.07	0.011	0.51527	0.00387	0.00085	340.1	1.6	84	12	58.2	1.9	800	300	78	17	7%
SHELL_22	0.1974	0.017	0.02307	0.00089	0.24472	0.0508	0.0041	0.32925	0.00949	0.0018	704	1.4	182.8	15	178.4	5.6	1220	180	341	36	80%
SHELL_23	0.652	0.062	0.0341	0.0011	0.66589	0.253	0.012	-0.23914	0.00384	0.00061	221	2.5	466	43	216.9	6.9	1803	190	656	130	1%
SHELL_24	0.47	0.086	0.0275	0.0012	0.6034	0.12	0.019	-0.40958	0.0171	0.0037	289	2.4	378	56	174.6	7.5	2750	270	192	74	10%
SHELL_25	0.22	0.024	0.02753	0.00077	0.30556	0.0567	0.0054	0.059245	0.0107	0.0022	265	2.4	201	19	175.1	4.8	460	210	216	44	38%
SHELL_27	0.025	0.024	0.03122	0.00087	-0.029121	0.0543	0.0051	-0.10725	0.012	0.0022	151.9	3.2	214	19	188.2	5.4	350	190	241	53	57%
SHELL_28	0.037	0.013	0.00868	0.00036	0.077872	0.0561	0.01	-0.07054	0.00276	0.00058	320	1.0	65	12	55.7	2.4	270	280	55.8	11	21%
SHELL_29	0.069	0.0072	0.00862	0.00031	-0.29813	0.0581	0.0056	0.85125	0.00351	0.00069	775	1.7	68.7	7.4	55.3	2	480	300	70.9	14	12%
SHELL_30	2.03	0.43	0.0476	0.0041	0.86728	0.306	0.044	-0.50185	0.062	0.024	436	1.5	1110	140	300	25	3140	220	190	420	9%
SHELL_31	0.109	0.018	0.00893	0.00027	0.33714	0.088	0.013	-0.16154	0.00344	0.00077	585	0.9	104	16	57.3	1.7	1270	270	69.4	13	5%
SHELL_32	0.0718	0.011	0.00883	0.00029	-0.26203	0.0621	0.01	0.38623	0.00366	0.00079	303	2.0	70	10	55.4	1.9	470	280	73.7	16	12%
SHELL_33	0.058	0.008	0.00825	0.00034	0.45423	0.0716	0.0067	0.2243	0.00254	0.00047	154.0	0.8	57.3	5.7	51.3	2	310	190	61.4	40	18%
SHELL_35	0.1956	0.019	0.02759	0.00086	0.61856	0.051	0.043	-0.0254557	0.01011	0.002	524	1.9	181.1	16	175.4	5.4	233	180	300	40	75%
SHELL_36	11.96	1.1	0.1138	0.0047	0.90865	0.759	0.058	0.30472	0.14	2.9	67.2	60.7	2995	84	694	27	4870	130	5420	3900	14%
SHELL_37	0.233	0.024	0.0326	0.0011	0.28428	0.0517	0.0047	0.10428	0.01127	0.0022	268	1.9	212	19	206.8	7.2	250	190	227	43	83%
SHELL_38	0.284	0.038	0.028	0.0017	0.28985	0.0736	0.0051	0.11139	0.0022	0.0005	305	1.4	252	29	196	1.8	1100	200	300	44	1%
SHELL_39	0.082	0.009	0.00809	0.00031	0.7586	0.148	0.054	-0.54863	0.00419	0.0011	380	1.1	176	67	88.3	5.3	1960	760	85	22	4%
SHELL_41	0.192	0.019	0.026	0.0011	0.6047	0.053	0.0044	0.047301	0.0108	0.0023	1082	3.9	177.8	16	165.7	7.2	315	180	216	46	53%
SHELL_42	0.234	0.057	0.01014	0.00059	0.48062	0.164	0.038	-0.28559	0.0024	0.0003	245	1.1	209	46	65	3.8	2440	410	106	25	3%
SHELL_43	0.216	0.052	0.00852	0.00064	0.12043	0.174	0.032	0.84196	0.00472	0.001	621	0.8	194	42	54.7	4.1	2380	410	216	20	2%
SHELL_44	0.263	0.028	0.02678	0.00074	0.45423	0.0716	0.0067	0.10732	0.0106	0											

analysis	ISOTOPIC RATIOS										ELEMENTAL CONCENTRATIONS		AGES							conc. (%)		
	207/235	prop. 2s	206/238	prop. 2s	206/238 vs 207/235 error correlation	207/236	prop. 2s	208/232 vs 207/236 error correlation	208/232	prop. 2s	[U] (ppm)	U/Th	207/235 age (Ma)	prop. 2s (Myr)	206/238 age (Ma)	prop. 2s (Myr)	207/236 age (Ma)	prop. 2s (Myr)	208/232 age (Ma)		prop. 2s (Myr)	
SHELL_102	0.1663	0.017	0.0291	0.00085	0.43899	0.0523	0.0043	0.17428	0.00919	0.0018	312	2.5	173.3	15	164.9	5.3	282	180	185	35	58%	
SHELL_103	0.216	0.021	0.03655	0.0011	0.33784	0.0512	0.0046	0.11147	0.01201	0.0024	169	1.1	198.1	18	194	6.8	240	190	241	47	81%	
SHELL_104	0.411	0.043	0.02708	0.00094	0.6074	0.1097	0.0099	-0.16485	0.01394	0.0025	155.7	0.9	348	31	172.2	5.9	1764	160	269	50	10%	
SHELL_106	12.81	1.2	0.1189	0.0056	-0.02024	0.169	0.016	0.45265	0.0513	0.0091	54.7	0.2	292	96	729	33	4890	180	1010	150	15%	
SHELL_107	0.174	0.035	0.00967	0.00033	0.52493	0.143	0.027	-0.29212	0.0042	0.00088	400	0.9	159	30	55.6	2.1	1850	390	84.7	18	3%	
SHELL_108	0.68	0.12	0.0138	0.0013	0.92605	0.328	0.044	-0.80919	0.0163	0.0039	371	1.1	500	79	88.5	8.1	3460	290	339	85	3%	
SHELL_109	0.0885	0.0093	0.01311	0.00091	0.73751	0.0491	0.0041	0.63172	0.00222	0.0011	1104	7.3	86	6.6	83.9	5.6	167	190	105.3	21	50%	
SHELL_110	0.226	0.041	0.00976	0.0005	0.50811	0.165	0.028	-0.13573	0.00587	0.0021	117.6	1.0	202	34	62.6	3.2	2240	390	111	25	3%	
SHELL_111	0.1869	0.017	0.0266	0.00094	0.25679	0.0606	0.0042	0.52094	0.00918	0.0019	99	3.1	173.8	15	169.2	5.3	235	230	195	35	72%	
SHELL_112	0.22	0.021	0.02996	0.00083	0.23608	0.0607	0.0055	0.6623	0.0097	0.0012	333	2.0	201.5	18	165.2	5.2	620	210	195	39	27%	
SHELL_113	0.133	0.018	0.00926	0.00038	-0.26447	0.106	0.015	0.53743	0.00369	0.00031	665	0.7	126	16	59.4	2.4	1950	240	74.4	14	4%	
SHELL_114	0.383	0.038	0.03089	0.0011	0.43693	0.0894	0.0081	0.12671	0.0147	0.003	343	2.4	328	28	196.1	6.7	1381	160	294	59	14%	
SHELL_116	0.1022	0.01	0.0091	0.00024	0.39162	0.0626	0.0075	0.34291	0.00336	0.00062	2520	0.8	88.7	9.2	57.8	2.2	1228	170	67.8	13	5%	
SHELL_117	0.149	0.025	0.00983	0.00036	0.70905	0.12	0.017	-0.53634	0.00461	0.001	625	1.0	140	22	56.7	2.3	1740	310	33	20	3%	
SHELL_118	1.16	0.2	0.03352	0.0011	0.1036	0.244	0.041	0.070368	0.0345	0.0068	378	1.8	758	73	212.5	7.1	3010	210	85	130	7%	
SHELL_119	0.249	0.029	0.01008	0.00045	0.5743	0.179	0.017	-0.09808	0.00489	0.001	370	0.7	225	23	64.7	2.9	2600	170	100	21	2%	
SHELL_120	0.299	0.032	0.0349	0.0026	0.75573	0.0621	0.0054	0.46961	0.01013	0.002	687	3.5	264	25	221	16	650	170	204	40	34%	
SHELL_122	0.178	0.051	0.00524	0.00043	0.8643	0.138	0.033	-0.70929	0.00459	0.001	338	0.9	168	45	59.3	2.7	1790	380	88	20	15%	
SHELL_123	0.0733	0.011	0.00802	0.00024	0.016458	0.0655	0.0089	0.18066	0.00314	0.00064	336	1.0	71.5	10	51.5	1.5	700	290	63.4	13	7%	
SHELL_124	0.0629	0.0085	0.00817	0.00031	-0.3554	0.0557	0.0079	0.70607	0.00295	0.00061	205	0.7	63.4	8.9	52.4	2	430	280	59.8	12	12%	
SHELL_125	0.256	0.024	0.02773	0.00079	-0.42601	0.0683	0.0064	0.91518	0.01154	0.0022	712	1.5	230.6	19	176.3	4.9	440	170	322	44	21%	
SHELL_126	0.1713	0.018	0.02785	0.00063	0.63247	0.0602	0.0041	0.14559	0.00925	0.0018	621	3.8	157.3	15	177.2	5.2	202	180	186	36	86%	
SHELL_127	11.59	1.2	0.1048	0.0057	0.96319	0.813	0.073	0.02486	0.0427	0.0025	5.24	0.2	255.5	100	642	33	4991	170	844	160	13%	
SHELL_129	0.162	0.022	0.00893	0.0004	0.79184	0.134	0.016	-0.57067	0.0038	0.00078	300	0.6	156	21	57.3	2.6	2110	200	76.7	16	3%	
SHELL_131	0.1982	0.018	0.02225	0.00086	0.61816	0.0505	0.004	0.22745	0.01045	0.002	709	1.7	181.8	15	179.6	5.4	212	180	210	39	85%	
SHELL_132	0.74	0.76	0.0866	0.0066	0.24141	0.604	0.06	0.7876	0.1261	0.024	10.6	0.7	221.6	86	608	38	4480	160	2390	430	13%	
SHELL_133	1.05	0.29	0.033	0.0029	0.7583	0.198	0.041	-0.69993	0.0102	0.0036	68.1	4.8	840	130	209	16	2430	390	1940	840	4%	
SHELL_135	0.952	0.091	0.0328	0.0013	0.24368	0.212	0.019	0.42599	0.0175	0.0034	45	0.9	676	48	208.3	8.2	2996	150	390	68	7%	
SHELL_1	0.71	0.091	0.02029	0.0018	0.32268	0.175	0.018	-0.24279	0.0171	0.0021	45.1	1.1	533	52	179.8	11	2660	180	342	42	7%	
SHELL_2	0.578	0.082	0.0302	0.0019	0.0096829	0.197	0.018	0.20569	0.00965	0.0012	84.9	0.9	458	51	191.5	12	2110	230	194	24	9%	
SHELL_3	0.357	0.054	0.03166	0.0018	0.56773	0.086	0.013	-0.38611	0.00909	0.0011	159	1.4	304	37	200.9	11	1120	240	183	22	18%	
SHELL_4	0.234	0.017	0.03161	0.0018	0.039798	0.0398	0.0029	0.17655	0.011	0.0015	222	2.2	213	24	200.6	11	340	110	222	31	59%	
SHELL_5	0.33	0.031	0.03259	0.0018	0.22951	0.0791	0.006	-0.03432	0.075	0.0027	204	1.1	287	24	206.1	11	950	170	351	54	22%	
SHELL_6	0.093	0.003	0.02022	0.0002	-0.1253	0.087	0.02	0.1942	0.01	0.002	18.6	0.5	165.000	203	60	140	10	110	200	600	2200	195%
SHELL_7	0.129	0.025	0.00827	0.00063	0.21306	0.111	0.02	-0.10378	0.00388	0.00067	69.2	0.9	121	22	53.1	4	1690	390	78	13	3%	
SHELL_8	0.2224	0.013	0.02954	0.0017	0.37045	0.0541	0.002	0.28996	0.01035	0.001	835	1.5	203.8	11	167.7	11	360	80	208.2	21	52%	
SHELL_9	0.2261	0.015	0.03044	0.0018	0.35752	0.053	0.002	0.06673	0.01037	0.0011	416	2.2	206.7	12	196.6	11	316	83	208	23	62%	
SHELL_10	0.228	0.035	0.03008	0.00054	0.9078	0.173	0.022	-0.17185	0.00871	0.00091	697	1.3	203	29	65.3	3.1	420	230	136	16	4%	
SHELL_11	0.2281	0.014	0.03194	0.0019	0.23146	0.0922	0.002	0.088178	0.01005	0.0011	171	1.2	216	24	183	11	1430	140	322	21	13%	
SHELL_12	0.242	0.017	0.03081	0.0017	0.22263	0.0574	0.0031	0.12487	0.0144	0.0012	283	2.5	219.6	14	196.6	11	480	110	230	39	41%	
SHELL_13	0.226	0.017	0.03035	0.0018	0.18579	0.0534	0.0029	0.094445	0.0135	0.0016	200	2.7	206.5	14	193.7	11	298	110	272	33	65%	
SHELL_14	0.228	0.035	0.03008	0.00054	0.9078	0.173	0.022	-0.17185	0.00871	0.00091	697	1.3	203	29	65.3	3.1	420	230	136	16	4%	
SHELL_16	0.2423	0.015	0.03261	0.0019	0.84084	0.0925	0.0016	0.078137	0.0111	0.0011	1340	4.1	220.1	12	206.8	12	300	71	223	22	65%	
SHELL_17	0.387	0.025	0.03135	0.0019	0.22645	0.0892	0.004	0.040708	0.0143	0.0019	288	2.2	331	18	199	12	1990	86	296	37	14%	
SHELL_18	0.118	0.039	0.00806	0.00055	-0.031737	0.095	0.026	0.056022	0.00337	0.00088	117.2	1.2	90	26	51.8	3.5	950	510	68	18	5%	
SHELL_19	0.414	0.034	0.03131	0.0018	0.14202	0.0952	0.0062	0.19893	0.0132	0.0016	246	1.7	350	24	198.7	11	1530	120	266	32	13%	
SHELL_20	0.187	0.011	0.02759	0.0015	0.30675	0.0451	0.0017	-0.10287	0.0101	0.0011	896	4.3	97	17.7	9.7	161.6	9.1	140	73	201	21	154%
SHELL_21	0.247	0.018	0.03207	0.0018	0.31612	0.0599	0.0025	0.016036	0.01198	0.0014	620	2.3	223.7	14	203.4	11	408	81	229	27	50%	
SHELL_22	0.243	0.019	0.03116	0.0018	0.026091	0.0574	0.0036	0.22429	0.0108	0.0018	162.1	2.5	220	15	197.8	11	470	130	217	36	42%	
SHELL_23	0.182	0.027	0.02472	0.0015	-0.19439	0.053	0.0081	0.30682	0.01008	0.0022	59.3	2.1	188	22	166.6	11	250	250	212	43	79%	
SHELL_24	0.242	0.15	0.026	0.002	0.42182	0.0465	0.0024	0.4699	0.0096	0.0008	458	0.8	167	53	166	13	4121	200	543	79	4%	
SHELL_25	0.2033	0.014	0.02993	0.0014	0.25225	0.0568	0.0027	0.04465	0.00608	0.00066	518	1.6	187.7	11	165.4	8.5	489	100	162.8	17	34%	
SHELL_26	0.278	0.023	0.0327	0.0021	0.61082	0.0628	0.0035	-0.17165	0.0127	0.0023	151	4.4	248	18	207.3	13	660	120	254	46	31%	
SHELL_27	0.229	0.016	0.02605	0.0015	0.40931	0.0634	0.003	0.025891	0.00946	0.00092	699	2.1	210.8	14	165.8	9.3	739	97	170.2	18	22%	
SHELL_28	0.313	0.029	0.02791	0.0016	0.1128	0.0811	0.0063	0.093031	0.0106	0.0019	103.3	2.2	274	22	177.4	10	1150	190	313	38	15%	
SHELL_29	0.0906	0.01	0.00998	0.0005	0.2018	0.071	0.0065	0.022106	0.00334	0.00045	365	1.3	87.7	9.2	57.62	3.2						

analysis	ISOTOPE RATIOS										ELEMENTAL CONCENTRATIONS		AGES								conc. (%)
	207/235		206/238		206/238 vs 207/235 correlation		208/206 vs 207/235 correlation		208/232		[U] (ppm)	U/Th	207/235 age (Ma)		206/238 age (Ma)		207/235 age (Ma)		208/232 age (Ma)		
	prop. 2s	prop. 1s	prop. 2s	prop. 1s	prop. 2s	prop. 1s	prop. 2s	prop. 1s	prop. 2s	prop. 1s	prop. 2s	prop. 1s	prop. 2s	prop. 1s	prop. 2s	prop. 1s	prop. 2s	prop. 1s	prop. 2s	prop. 1s	
SHEL2_84	0.2183	0.013	0.03126	0.0018	0.34565	0.0505	0.0017	0.17337	0.01188	0.0013	572	4.6	300.4	11	198.4	11	212	74	239	26	94%
SHEL2_85	0.1637	0.0098	0.02393	0.0014	0.61627	0.0505	0.0015	0.086082	0.00842	0.00093	2459	9.1	153.9	8.6	152.5	8.5	211	69	170	19	72%
SHEL2_86	0.1983	0.015	0.03657	0.0018	0.46096	0.0484	0.0026	0.0054581	0.01088	0.0013	166	2.6	183.4	12	194.1	11	120	110	221	26	162%
SHEL2_87	0.3689	0.054	0.03562	0.0027	0.26272	0.144	0.0019	-0.075769	0.03163	0.0016	96	0.5	150.2	6.6	223	17	4030	180	624	70	5%
SHEL2_88	1.3	0.15	0.0421	0.0034	0.26134	0.236	0.024	0.19675	-140	170	13.8	44.0	863	68	266	21	3060	180	11200	2100	9%
SHEL2_89	0.102	0.016	0.00852	0.00052	0.29677	0.084	0.012	-0.1483	0.00382	0.00053	296	1.2	98	14	54.7	3.3	1210	280	77.1	11	5%
SHEL2_90	0.1645	0.011	0.02425	0.0014	0.52188	0.0497	0.0018	0.05836	0.00881	0.00093	590	1.9	145.4	8.9	154.5	9	174	79	177.4	19	89%
SHEL2_91	0.2946	0.017	0.03226	0.0018	0.30127	0.0625	0.0021	0.050501	0.01191	0.0022	712	7.0	254.1	14	206.8	11	697	66	383	44	30%
SHEL2_92	2.539	0.11	0.2107	0.0012	0.51617	0.0969	0.003	0.36663	0.0572	0.0069	419	2.8	136.1	44	122	64	1568	57	1314	130	75%
SHEL2_93	0.305	0.025	0.03195	0.0019	0.53852	0.0687	0.004	-0.31436	0.0133	0.0016	269.1	2.3	269	19	202.7	12	850	120	266	32	24%
SHEL2_94	0.0616	0.0097	0.00835	0.00051	0.22902	0.0514	0.0069	-0.070879	0.00213	0.00034	139	0.8	60.3	9.1	53.6	3.3	230	230	43.1	6.9	23%
SHEL2_95	0.1791	0.012	0.02529	0.0014	0.64843	0.0519	0.0026	-0.29747	0.00941	0.0011	452	2.1	167.1	11	161	8.9	256	100	189	22	63%
SHEL2_96	0.2297	0.019	0.02948	0.0013	-0.04849	0.0393	0.0029	-0.10397	0.00913	0.0018	270	2.7	215	15	157.3	10	480	120	184	22	35%
SHEL2_97	1.43	0.27	0.042	0.0041	0.13323	0.241	0.048	0.092553	0.5	0.14	6.84	16.8	880	100	265	25	2990	330	7900	1700	9%
SHEL2_98	0.1726	0.01	0.02566	0.0015	0.43212	0.0488	0.0015	0.089085	0.00842	0.00082	1330	1.3	161.6	9	163.3	9.4	138	66	169.5	16	118%
SHEL2_99	0.202	0.035	0.01016	0.00074	0.53302	0.139	0.02	-0.44952	0.0057	0.0021	225	0.7	183	29	65.2	4.7	2020	260	114	43	3%
SHEL2_100	0.2473	0.016	0.03014	0.0018	0.4552	0.0502	0.0023	0.24534	0.00826	0.0009	568	1.9	224.2	13	191.4	11	607	86	166.2	18	32%
SHEL2_101	0.254	0.015	0.02079	0.00087	0.20181	0.0557	0.0031	0.34882	0.0077	0.0008	448	1.4	174.4	13	174.4	10	400	120	155.1	16	44%
SHEL2_102	0.1741	0.011	0.02494	0.0014	0.35593	0.0504	0.0018	0.23683	0.00806	0.00082	1031	1.6	162.9	9	158.8	9.1	205	78	162.3	16	77%
SHEL2_103	0.0773	0.01	0.00826	0.00047	0.37329	0.0682	0.008	-0.20046	0.00297	0.00032	845	0.9	9.4	53	3	750	220	60	6.5	7%	
SHEL2_104	0.214	0.03	0.01003	0.00071	0.22223	0.155	0.023	0.14582	0.00394	0.00065	138	0.8	194	24	64.3	4.5	2330	220	80	13	3%
SHEL2_105	0.278	0.023	0.03175	0.00156	-0.04849	0.0393	0.0027	-0.19664	0.00846	0.00098	333	2.0	232	18	199.6	11	420	130	160.2	20	41%
SHEL2_106	0.0536	0.0039	0.00509	0.00046	0.33755	0.0485	0.0025	-0.19146	0.0025	0.00026	1300	1.0	83	3.8	51.92	2.9	120	50.4	5.2	43%	
SHEL2_107	0.2305	0.015	0.03075	0.0018	0.090867	0.0544	0.0022	0.059092	0.00842	0.0009	367	1.8	210.3	12	195.2	11	371	84	169.4	18	53%
SHEL2_108	0.1987	0.014	0.02923	0.0016	0.43005	0.0493	0.0021	-0.1778	0.0102	0.0011	492	1.8	183.8	11	187.7	10	159	90	205	22	117%
SHEL2_109	0.348	0.025	0.02562	0.0015	0.36252	0.0697	0.0056	-0.1784	0.00623	0.00094	390	1.2	227	21	163	9.1	860	180	166	19	19%
SHEL2_110	0.1978	0.012	0.02509	0.00082	0.24389	0.0552	0.0023	0.69175	0.00899	0.00071	1500	2.0	183.1	10	183.9	10	402	49	138.5	44	40%
SHEL2_111	0.1747	0.011	0.02495	0.0015	0.09886	0.0508	0.0018	0.045322	0.00713	0.00072	1228	1.5	163.3	9.8	158.8	9.3	225	80	143.5	14	71%
SHEL2_112	0.075	0.013	0.00909	0.0005	0.58516	0.0682	0.01	-0.39348	0.00272	0.00034	484	1.1	72	12	51.9	3.2	700	270	54.9	6.9	7%
SAWMILL1_1	0.063	0.013	0.00856	0.00049	0.32822	0.0505	0.0086	-0.2569	0.00299	0.00051	393	1.0	61	12	55.1	3.1	110	270	60.3	10	50%
SAWMILL1_2	0.056	0.012	0.00845	0.00053	0.011829	0.0475	0.0089	0.1197	0.0042	0.00016	260	1.3	55.1	11	54.2	3.4	10	290	85	33	542%
SAWMILL1_3	0.095	0.012	0.00835	0.00049	0.16811	0.0491	0.011	-0.10719	0.00085	0.00093	373	0.9	54	11	53.6	3.1	20	320	57.6	11	268%
SAWMILL1_4	0.2556	0.012	0.02995	0.00051	0.35562	0.0621	0.0089	-0.079355	0.00301	0.00053	206.1	1.2	57.4	11	57.4	3.3	630	270	60.7	11	9%
SAWMILL1_5	0.2102	0.012	0.03035	0.00047	0.42104	0.0507	0.0089	-0.079355	0.00084	0.0004	193.9	1.2	193.9	11	193.6	11	218	190	97.8	29	85%
SAWMILL1_7	0.0612	0.012	0.00866	0.00052	0.10179	0.0509	0.0085	0.087108	0.00331	0.00061	857	1.4	59.8	11	55.6	3.3	150	280	66.9	12	37%
SAWMILL1_8	0.0634	0.011	0.00782	0.00041	0.093301	0.059	0.0092	0.015333	0.00265	0.00042	306	0.9	62	9.9	50.2	2.6	360	240	53.6	8.4	14%
SAWMILL1_9	0.062	0.013	0.0083	0.00049	0.042955	0.0546	0.011	-0.02098	0.00315	0.00059	654	0.8	60	12	53.3	3.1	210	320	63.6	12	25%
SAWMILL1_10	0.0564	0.0095	0.00863	0.00049	-0.2626	0.0493	0.0086	0.47416	0.00296	0.00044	264	1.0	57.4	7.5	64.8	3.1	150	220	57.7	8.9	3%
SAWMILL1_11	0.053	0.014	0.00987	0.00049	0.051438	0.0485	0.0056	0.25017	0.003	0.00048	494	1.5	54.3	7.1	56.9	3.2	30	220	60.5	9.6	190%
SAWMILL1_12	0.081	0.015	0.01122	0.00062	-0.17793	0.0517	0.0092	0.301	0.00376	0.00076	615	1.2	79	13	71.9	4	90	230	76	15	80%
SAWMILL1_13	0.0563	0.0098	0.008	0.00045	0.14589	0.0501	0.0078	0.10718	0.00241	0.00037	211	0.7	55.3	9.3	51.4	2.9	270	310	46.7	74	19%
SAWMILL1_14	0.0569	0.0074	0.00865	0.00052	-0.086732	0.041	0.00873	0.03103	0.00263	0.00051	393	1.2	48.3	7.1	55.5	3.3	-160	230	57.1	31	31%
SAWMILL1_15	0.0559	0.0066	0.0086	0.00052	0.98205	0.0504	0.0054	-0.19204	0.00317	0.00052	304	1.7	55.2	6.4	55.2	4	150	170	54	10	37%
SAWMILL1_16	0.075	0.016	0.00922	0.00054	-0.0034142	0.062	0.013	0.15776	0.00284	0.00056	1010	1.4	73	15	59.1	3.4	420	330	59.3	11	14%
SAWMILL1_17	0.063	0.013	0.00838	0.00054	0.13002	0.055	0.011	0.0624	0.00282	0.00051	343	0.9	62	12	53.8	3.5	220	300	58.8	10	24%
SAWMILL1_18	0.0721	0.0093	0.00868	0.0005	0.4885	0.0526	0.0067	-0.18933	0.00327	0.00041	312	0.9	70.5	8.8	58.7	3.2	630	210	54.5	8.2	9%
SAWMILL1_19	0.0524	0.0095	0.00863	0.00047	0.052727	0.045	0.0095	0.10156	0.00297	0.00057	650	1.0	61.4	10	53.5	3.4	260	220	59.8	11	41%
SAWMILL1_20	0.222	0.028	0.03039	0.0018	0.25042	0.0521	0.0098	-0.15523	0.0106	0.00118	271.5	1.9	202	23	196.4	11	260	210	212	36	79%
SAWMILL1_21	0.0588	0.0093	0.00831	0.00045	0.026177	0.053	0.0082	0.034082	0.00295	0.00049	182.1	1.4	57.8	8.8	53.4	2.9	230	260	59.5	9.9	23%
SAWMILL1_22	0.0524	0.0072	0.00817	0.00																	

analysis	ISOTOPIC RATIOS										ELEMENTAL CONCENTRATIONS		AGES							conc. (%)	
	206/238 vs 207/235 correlation					238/206 vs 208/232 correlation					U (ppm)	U/Th	207/235 age (Ma)		206/238 age (Ma)		208/232 age (Ma)		prop. 2s (Myr)		
	207/235	prop. 2s	206/238	prop. 2s	207/235	prop. 2s	208/232	prop. 2s	207/235	prop. 2s			207/235	prop. 2s	206/238	prop. 2s	208/232	prop. 2s			
SAWMLL1_83	0.123	0.034	0.00969	0.0006	0.46174	0.082	0.016	-0.31341	0.00405	0.0007	426	1.3	114	28	61.5	3.9	950	310	81.7	14	6%
SAWMLL1_84	0.052	0.016	0.00884	0.0006	-0.1612	0.051	0.021	0.25785	0.00289	0.00052	955	0.9	51	15	56.7	3.8	-180	440	58.3	10	-32%
SAWMLL1_85	0.0595	0.0098	0.0085	0.00051	0.24254	0.051	0.0071	-0.15541	0.00273	0.00049	269	0.9	58.4	9.3	54.5	3.2	190	250	55.1	9.8	29%
SAWMLL1_86	0.25	0.029	0.0311	0.0021	0.70288	0.027	0.046	-0.23916	0.00896	0.0013	521	2.4	335	24	197.4	13	296	200	103	27	67%
SAWMLL1_87	0.0555	0.0064	0.00873	0.0005	0.26416	0.0465	0.0045	0.24847	0.00271	0.00045	948	0.9	54.8	6.2	56	3.2	40	190	54.8	9	140%
SAWMLL1_88	0.328	0.039	0.02864	0.0016	-0.14168	0.0841	0.0092	0.88951	0.01233	0.0019	132	1.9	287	30	182	9.8	1230	200	251	35	15%
SAWMLL1_89	0.06	0.0092	0.00947	0.00047	-0.039403	0.0521	0.0079	0.10519	0.00279	0.00051	309	0.8	58.9	8.6	54.4	3	140	200	56.3	10	39%
SAWMLL1_90	0.1943	0.021	0.02694	0.0014	0.45544	0.0522	0.0044	0.16755	0.00087	0.00019	101.1	1.3	100.2	18	171.3	8.9	206	190	175	26	60%
SAWMLL1_91	0.077	0.015	0.00947	0.00058	-0.03265	0.0614	0.011	0.2122	0.00389	0.00077	326	0.8	75	13	60.8	3.7	450	290	78	16	14%
SAWMLL1_92	0.0584	0.0068	0.00908	0.00046	0.16356	0.052	0.0066	-0.052879	0.00279	0.00045	374	1.7	57.5	8.2	51.8	2.9	240	240	56.4	9	22%
SAWMLL1_93	0.111	0.02	0.00868	0.00053	0.14468	0.092	0.014	-0.028235	0.00361	0.00062	1170	1.0	106	18	55.7	3.4	1260	290	72.9	12	4%
SAWMLL1_94	0.1	0.025	0.00979	0.00055	0.17208	0.081	0.019	-0.077889	0.00295	0.00047	497	0.9	89	18	56.4	3.6	780	330	59.6	9.4	7%
SAWMLL1_95	0.1987	0.022	0.0231	0.0016	0.5635	0.087	0.0043	0.52739	0.00879	0.0013	489	2.0	103.8	49	106.2	9.9	145	190	110.9	26	128%
SAWMLL1_96	0.094	0.018	0.00893	0.0005	0.30272	0.068	0.013	-0.23005	0.00286	0.00046	979	1.0	81	16	57.3	3.2	500	230	58.1	9.3	11%
SAWMLL1_97	0.115	0.027	0.00918	0.00056	0.50563	0.09	0.019	-0.27624	0.00338	0.00062	237	1.1	109	24	58.9	3.5	1090	380	68.3	12	5%
SAWMLL1_98	0.674	0.11	0.0366	0.0023	0.56376	0.129	0.018	-0.48992	0.0319	0.0062	910	2.8	507	69	231.7	14	2020	260	633	120	11%
SAWMLL1_100	0.079	0.013	0.00836	0.00047	0.051837	0.0668	0.0099	0.099272	0.0048	0.001	374	2.7	76.8	12	53.6	3.2	680	280	59	23	8%
SAWMLL1_101	0.0786	0.011	0.00916	0.00051	0.54675	0.0609	0.0076	-0.18761	0.00316	0.00055	366	0.8	74.7	10	58.8	3.2	540	240	63.8	11	11%
SAWMLL1_102	0.165	0.024	0.0103	0.00061	0.62591	0.118	0.014	-0.30896	0.00411	0.00071	588	0.8	154	21	66.1	3.9	1850	220	82.9	14	4%
SAWMLL1_103	0.0567	0.0077	0.00949	0.00045	0.10296	0.0477	0.0057	0.15934	0.00302	0.00046	509	1.4	55.9	7.4	54.5	2.9	110	240	60.9	9.2	50%
SAWMLL1_104	0.074	0.012	0.00898	0.00053	-0.26151	0.0808	0.009	0.44872	0.00316	0.00052	388	0.9	72.1	11	57.6	3.4	440	260	63.6	11	13%
SAWMLL1_105	0.0522	0.0088	0.00893	0.00055	0.46802	0.0812	0.0054	-0.15219	0.00273	0.00048	369	2.0	65.7	8.3	57.3	3.7	220	210	60.6	9.6	26%
SAWMLL1_106	0.061	0.0077	0.00946	0.00049	0.0080471	0.0518	0.0059	0.41885	0.00262	0.00059	122	0.9	60.1	7.3	54.3	3.1	250	210	52.9	7.8	22%
SAWMLL1_107	0.0641	0.0092	0.00856	0.00048	0.16639	0.055	0.0073	0.063484	0.00281	0.00043	197.3	1.0	62.9	8.7	54.9	3.1	330	240	56.8	8.7	17%
X15CA18A_1	0.163	0.048	0.00939	0.00076	0.8276	0.122	0.031	-0.68183	0.0054	0.0012	556	1.1	156	44	60.2	4.8	1360	450	109	23	4%
X15CA18A_2	0.067	0.011	0.00802	0.00036	0.17787	0.0626	0.0096	0.024704	0.00374	0.001	382	3.3	65	10	51.5	2.3	480	280	75	20	11%
X15CA18A_3	0.251	0.032	0.02649	0.0012	0.67792	0.0673	0.0066	-0.354	0.00978	0.0012	541	1.4	225	25	168.5	7.7	740	190	197	25	23%
X15CA18A_4	0.0596	0.0068	0.00813	0.0004	0.39604	0.0468	0.0027	0.45484	0.00259	0.00025	1630	0.7	52.9	3.5	52.2	2.5	70	120	52.3	5	75%
X15CA18A_5	0.129	0.06	0.00914	0.00045	0.72889	0.154	0.05	-0.1348	0.00377	0.0006	132	1.5	118	60	58.7	4.6	1310	570	126	16	4%
X15CA18A_6	0.0813	0.011	0.00859	0.00037	0.2255	0.0727	0.0087	0.036585	0.00249	0.00027	777	0.7	78.9	9.8	53.9	2.4	840	250	50.3	5.4	6%
X15CA18A_7	0.082	0.015	0.00849	0.00044	0.092638	0.073	0.014	0.20037	0.00309	0.00079	242	1.7	79	14	54.5	2.6	770	330	79	16	7%
X15CA18A_8	0.066	0.0064	0.0078	0.00037	0.13165	0.0549	0.0063	-0.025713	0.00292	0.00063	623	1.3	55.2	6.1	50.1	2.4	310	200	59	13	16%
X15CA18A_9	0.052	0.022	0.00807	0.00061	0.13928	0.079	0.019	0.02488	0.00269	0.00055	139.6	1.4	87	20	55.8	3.9	610	380	58	11	7%
X15CA18A_10	0.125	0.01	0.0084	0.00037	0.13004	0.0684	0.011	0.0038937	0.00291	0.00051	540	1.3	540	20	54	3	540	260	58.7	10	10%
X15CA18A_11	0.0618	0.01	0.00804	0.00041	0.13183	0.0579	0.0094	0.045839	0.00321	0.00059	208.1	1.6	60.5	9.5	51.6	2.6	420	300	65	12	12%
X15CA18A_12	0.07	0.013	0.008	0.00041	0.14006	0.062	0.014	0.024388	0.00405	0.00071	336	1.6	68	12	56.5	2.6	440	320	62	14	13%
X15CA18A_14	0.164	0.013	0.00815	0.00035	0.00028592	0.058	0.011	0.16686	0.00272	0.00054	549	1.4	62	12	52.4	2.2	500	300	59	6.8	15%
X15CA18A_15	0.029	0.00919	0.00945	0.0005	-0.076899	0.11	0.014	0.28036	0.00364	0.0013	369	2.0	116	16	59	2.4	610	380	125	16	4%
X15CA18A_17	0.076	0.014	0.00892	0.00051	0.56206	0.142	0.017	-0.20953	0.00442	0.00054	578	1.0	163	20	57.2	3.2	2060	240	89.1	11	3%
X15CA18A_18	0.0593	0.0099	0.00792	0.00033	0.69688	0.0504	0.0028	-0.19477	0.00291	0.00035	2500	5.7	54.8	3.7	50.8	2.1	201	120	58.8	7.1	25%
X15CA18A_19	0.0525	0.0034	0.00828	0.00036	0.38175	0.046	0.0025	0.25837	0.00264	0.00024	3470	0.7	52.5	3.6	53.1	2.3	15	100	53.3	4.8	354%
X15CA18A_20	0.057	0.007	0.00826	0.00035	0.24231	0.047	0.0025	0.14861	0.00269	0.00034	2630	0.5	53	5.3	50	2.2	55	100	54.3	4.8	36%
X15CA18A_22	0.0865	0.0067	0.00853	0.00037	0.14289	0.0789	0.0086	0.33021	0.00299	0.0003	826	0.6	84.1	6.3	53.5	2.4	1100	160	60.3	6.1	5%
X15CA18A_23	0.105	0.015	0.00847	0.00042	0.15068	0.092	0.013	-0.0082523	0.00354	0.00043	353	1.4	100	14	54.3	2.7	1000	220	71.4	8.7	4%
X15CA18A_24	0.061	0.011	0.00813	0.00041	-0.11658	0.0561	0.0098	0.19065	0.00303	0.00055	218	0.8	60	11	52.2	2.6	280	290	61	11	19%
X15CA18A_26	0.088	0.029	0.00866	0.0005	-0.22333	0.079	0.029	0.34905	0.00321	0.00064	145	0.8	83	24	54.9	3.2	490	440	65	13	11%
X15CA18A_27	0.04	0.12	0.0127	0.0012	0.68276	0.243	0.061	-0.47321	0.0032	0.0019	265	0.8	478	61	51.3	7.6	2200	430	165	36	3%
X15CA18A_28	0.0977	0.0059	0.00894	0.00039	0.14356	0.0889	0.041	0.44764	0.00434	0.00054	765	2.7	85.3	5.5	56.8	2.5	890	130	87.5	11	6%
X15CA18A_29	0.094	0.014	0.0082	0.00033	-0.093564	0.079	0.012	0.21847	0.00291	0.00056	261	0.6	91	13	52.6	2.1	1010	300	58.7	7.3	5%
X15CA18A_31	0.83	0.17	0.0143	0.0014	0.93149	0.366	0.055	-0.8365	0.0105	0.0021	190.2	0.6	671	96	91.7	8.8	3510	340	210	42	3%
X15CA18A_32	0.328	0.022	0.0257	0.00176	0.68782	0.0867	0.0081	0.56783	0.00778	0.0017	497	0.7	80	16	54.5	2.9	1550	680	1504	130	88%
X15CA18A_33	0.0593	0.0068	0.00794	0.00038	0.15805	0.0553	0.0068	0.017739	0.00265	0.00021	434	0.7	58.4	6.4	51	2.4	380	230	53.4	6	13%
X15CA18A_34	0.0486	0.0055	0.00804	0.00037	0.14523	0.0428	0.0046	-0.044518	0.00284	0.00042	360	1.5	49.1	5.3	52.9	2.4	-110	180	57.3	8.5	-48%
X15CA18A_35	0.0512	0.0032	0.00797	0.00033	0.30115	0.0458	0.0024	0.31481	0.00237	0.00022	2220	0.7	50.7	3.1	51.2	2.1	10	100	47.8	4.3	512%
X15CA18A_36	0.0752	0.0082	0.00855	0.00037	0.41142	0.0642	0.0062	0.022891</													

analysis	ISOTOPIC RATIOS										ELEMENTAL CONCENTRATIONS		AGES							conc. (%)	
	206/238 vs 207/235 correlation		206/238 vs 207/235 correlation		206/238 vs 207/235 correlation		206/238 vs 207/235 correlation		206/238 vs 207/235 correlation		[U] (ppm)	U/Th	207/235 age (Ma)	prop. 2s (Myr)	206/238 age (Ma)	prop. 2s (Myr)	207/235 age (Ma)	prop. 2s (Myr)	208/232 age (Ma)		prop. 2s (Myr)
	207/235	prop. 2s	206/238	prop. 2s	207/235	prop. 2s	206/238	prop. 2s	207/235	prop. 2s	208/232	prop. 2s	207/235	prop. 2s	206/238	prop. 2s	207/235	prop. 2s	208/232		prop. 2s
X15CA18A_101	0.212	0.075	0.00909	0.00077	0.92478	0.15	0.045	-0.83729	0.0093	0.0032	495.4	2.3	178	08	58.3	4.9	1990	540	187	63	4%
X15CA18A_102	0.077	0.014	0.00879	0.00044	0.13735	0.068	0.111	0.07861	0.00278	0.00047	261	1.3	75	13	56.4	2.8	630	300	56.1	9.5	9%
X15CA18A_104	0.0788	0.0065	0.00396	0.00061	-0.42676	0.0651	0.0072	0.83955	0.0126	0.003	603	2.12	74.1	6.1	61.6	3.9	680	230	252	60	9%
X15CA18A_106	0.108	0.021	0.00855	0.00044	0.53331	0.093	0.0117	-0.27573	0.00279	0.0039	355	0.9	102	19	54.9	2.8	1150	330	56.4	7.9	5%
X15CA18A_107	12.43	1.1	0.1293	0.011	0.119	0.722	0.056	0.68937	0.0466	0.0068	3.78	0.2	2620	73	795	67	4780	130	900	130	17%
X15CA18A_108	0.0586	0.0052	0.00813	0.00038	0.172	0.0549	0.0045	0.1981	0.00241	0.00025	803	0.9	57.8	4.9	52.2	2.4	390	180	48.6	5.1	13%
X15CA18A_109	0.0533	0.0031	0.00562	0.00038	0.54663	0.0468	0.0022	0.54588	0.00346	0.00023	4400	0.4	52.7	3	54.7	2.4	51	95	49.7	4.6	107%
X15CA18A_110	0.0541	0.0063	0.00782	0.00039	0.29811	0.0496	0.0045	0.17231	0.00229	0.00029	513	1.0	53.4	5.1	50.2	2.5	150	170	46.3	5.9	33%
X15CA18A_113	0.0562	0.0033	0.00538	0.00034	0.47746	0.0479	0.0023	0.31191	0.00242	0.00022	3460	0.6	55.5	3.2	53.6	2.2	37	100	48.9	4.4	55%
X15CA18A_114	0.0505	0.0068	0.00902	0.00041	0.2617	0.0706	0.0058	0.060608	0.00314	0.00037	633	1.1	87.7	8.2	57.9	2.6	880	160	63.4	7.5	7%
X15CA18A_115	9.04	0.77	0.0836	0.0044	0.024471	0.779	0.061	0.38339	0.0331	0.0059	7.02	0.2	2335	82	51.7	26	4910	140	658	68	11%
X15CA18A_116	0.156	0.024	0.00899	0.00041	0.56823	0.119	0.016	-0.40124	0.0041	0.00059	392	1.2	145	21	57.7	26	1740	240	82.6	12	3%
X15CA18A_117	0.182	1.1	0.0317	0.0079	0.74219	0.251	0.015	0.20334	0.0336	0.0051	8.3	0.2	2300	110	526	47	4890	140	656	99	10%
X15CA18A_118	0.0571	0.0039	0.00946	0.00033	0.17306	0.0471	0.0025	0.16033	0.00242	0.00023	1660	1.1	56.3	3.4	54.3	2.1	66	110	49	4.6	82%
X15CA18A_119	10.42	0.7	0.097	0.0056	0.098935	0.76	0.052	0.5172	0.0388	0.0041	6.87	0.2	2463	65	596	33	4870	120	709	80	12%
X15CA18A_120	0.0992	0.0044	0.00835	0.0004	0.4698	0.0488	0.0028	0.23293	0.00241	0.00021	4000	0.3	58.3	4.2	53.6	2.5	150	130	48.6	4.3	36%
X15CA18A_122	0.0555	0.0038	0.00539	0.00039	0.57744	0.0471	0.0024	-0.05884	0.00244	0.00022	2610	0.4	54.9	3.3	53.8	2.5	69	100	49.2	4.4	85%
X15CA18A_123	11.82	0.84	0.1052	0.0081	0.11893	0.787	0.065	0.2165	0.0422	0.0059	6.15	0.2	2953	69	643	47	4910	180	833	110	13%
X15CA18A_124	0.0568	0.006	0.00814	0.00033	0.28554	0.0506	0.0047	-0.089427	0.00232	0.00027	375	0.5	56	5.7	52.2	2.1	230	190	46.8	5.4	24%
X15CA18A_125	0.0518	0.0038	0.008	0.00034	0.31227	0.0478	0.0031	0.18010	0.00244	0.00023	1163	1.0	51.2	3.5	51.4	2.2	90	130	49.4	4.6	57%
X15CA18A_126	0.0529	0.0032	0.0082	0.00033	0.16244	0.0474	0.0026	0.44769	0.00293	0.00021	1168	0.7	52.3	3.1	52.6	2.1	75	110	47	4.2	70%
X15CA18A_127	0.0541	0.0043	0.00867	0.00038	0.67078	0.0522	0.003	0.06745	0.00258	0.00023	4620	0.5	44	4.1	52.7	2.4	400	120	62.1	4.7	14%
X15CA18A_129	0.0539	0.0038	0.00834	0.00035	0.44613	0.0469	0.0034	0.23607	0.00293	0.00023	2010	0.6	53.3	3.4	53.6	2.3	55	100	53.1	4.7	97%
X15CA18A_130	0.0535	0.004	0.00745	0.00031	0.15521	0.0525	0.0036	0.30049	0.00245	0.00024	1219	0.7	52.9	3.8	47.8	2	280	140	49.5	4.8	7%
X15CA18A_131	0.081	0.012	0.00831	0.00037	0.56389	0.0697	0.0094	-0.38991	0.00308	0.00033	959	0.9	78	11	53.4	2.4	720	250	62.2	6.7	17%
X15CA18A_132	0.131	0.031	0.00888	0.0005	0.67471	0.111	0.024	-0.48029	0.00481	0.00087	177	1.0	171	37	55.7	3.2	1300	400	87	14	4%
X15CA18A_134	0.1099	0.0071	0.01079	0.00077	0.21908	0.0478	0.0036	0.25242	0.00566	0.00071	972	3.9	105.8	6.5	107.3	4.8	94	94	118	116	114%
X15CA18A_135	0.0533	0.003	0.00827	0.00033	0.48176	0.0475	0.0027	0.32277	0.00265	0.00024	4000	0.8	52.6	3.2	53.9	2.5	25	90	51.9	4.6	216%
X15CA18A_136	0.0532	0.0033	0.00839	0.0004	0.81078	0.0483	0.0021	0.17734	0.00257	0.00023	4660	0.8	52.6	3.2	53.9	2.5	25	90	51.9	4.6	216%
X15CA18A_137	0.0712	0.0062	0.00797	0.00034	0.15186	0.0649	0.0051	0.098325	0.00304	0.00035	635	1.8	69.7	5.9	51.2	2.2	710	170	61.4	7.1	7%
X15CA18A_138	0.0566	0.0038	0.00831	0.00037	0.36579	0.0491	0.0029	0.27309	0.00295	0.00027	1960	0.3	55.1	3.7	52.7	2.3	147	120	53.7	3.6	36%
X15CA18A_139	0.0538	0.0045	0.00811	0.00037	0.15891	0.0478	0.0037	-0.037744	0.00293	0.00026	711	0.7	53.1	4.3	52.1	2.3	80	140	53.1	5.2	65%
X15CA18A_140	0.0511	0.048	0.0325	0.0016	0.2655	0.1123	0.0093	0.002588	0.01129	0.0011	65.4	0.2	416	32	206.3	9.9	1780	150	230	25	12%
PB2_1	0.1603	0.033	0.02451	0.0009	0.64365	0.0475	0.0096	-0.072372	0.00764	0.0031	770	2.8	190.7	29	156.1	5.7	94	420	163.8	63	166%
PB2_2	1.259	0.27	0.0361	0.0024	0.70739	0.262	0.054	0.19558	0.0667	0.028	58.8	2.9	827	110	228	15	3266	330	1304	520	7%
PB2_4	5.51	1.1	0.0732	0.003	0.51480	0.545	0.111	0.29076	0.0333	0.015	17.03	0.3	1899	190	458	18	4356	300	700	280	10%
PB2_5	6.54	1.2	0.0725	0.0055	0.78007	0.576	0.12	-0.2226	0.206	0.086	14.08	0.2	1937	210	450	33	4436	300	3770	1400	10%
PB2_6	0.331	0.03	0.02465	0.00071	0.19521	0.0766	0.022	0.28689	0.0148	0.0069	153.4	1.7	209	32	158.9	4.5	1560	370	387	120	13%
PB2_7	3.98	0.85	0.0574	0.003	0.90177	0.498	0.1	-0.42018	0.171	0.072	128	2.2	1627	180	380	18	4234	290	3170	1300	9%
PB2_8	0.37	0.077	0.0251	0.00079	0.15657	0.1047	0.021	0.11651	0.01259	0.0052	150.3	1.3	314	48	159.8	5	1676	370	253	100	10%
PB2_9	0.173	0.036	0.02364	0.00078	0.36137	0.0525	0.011	-0.016433	0.00748	0.0031	638	1.0	161.8	31	150.6	4.9	254	380	150.6	61	59%
PB2_10	0.255	0.052	0.02375	0.00087	0.39846	0.0767	0.016	0.39099	0.01063	0.0044	765	1.5	230	42	151.3	5.5	1111	420	213.8	87	14%
PB2_12	0.52	1.1	0.0592	0.0027	0.25822	0.573	0.12	0.45869	0.0432	0.017	132.5	0.3	1923	180	431	16	4443	300	387	340	10%
PB2_13	0.1645	0.033	0.02394	0.00072	0.55895	0.0496	0.01	-0.067579	0.00793	0.0033	1245	2.6	154.4	29	152.5	4.5	170	430	160.1	65	90%
PB2_14	1.207	0.25	0.0318	0.0014	0.31054	0.278	0.058	0.31365	0.0402	0.017	28.3	1.6	805	110	202.6	8.7	3341	300	735	320	6%
PB2_15	0.12	0.04	0.0512	0.0018	0.63677	0.44	0.089	0.020209	0.0367	0.019	29.2	0.5	1490	160	321	11	4057	310	738	290	8%
PB2_16	0.764	0.36	0.0389	0.0019	0.68159	0.286	0.059	-0.05972	0.0271	0.011	61.2	1.0	819	120	198.9	9.4	3385	380	56.2	64	13%
PB2_17	0.93	0.22	0.0284	0.0014	0.68369	0.225	0.05	-0.39151	0.01017	0.0042	84.5	0.2	646	110	180.5	9	2970	370	205	64	6%
PB2_18	0.186	0.038	0.0234	0.00078	0.42718	0.0592	0.012	-0.061													

analysis	ISOTOPIC RATIOS										ELEMENTAL CONCENTRATIONS		AGES							conc. (%)		
	206/238 vs 207/235 correlation		206/238 vs 207/235 correlation		206/238 vs 207/235 correlation		206/238 vs 207/235 correlation		206/238 vs 207/235 correlation		U (ppm)	U/Th	207/235 age (Ma)		206/238 age (Ma)		207/235 age (Ma)		206/238 age (Ma)		207/235 age (Ma)	206/238 age (Ma)
	207/235	prop. 2s	206/238	prop. 2s	207/235	prop. 2s	206/238	prop. 2s	207/235	prop. 2s			207/235 age (Ma)	prop. 2s (Myr)	206/238 age (Ma)	prop. 2s (Myr)	207/235 age (Ma)	prop. 2s (Myr)				
FB2_81	4.77	0.97	0.0672	0.0028	0.48005	0.517	0.11	0.32317	0.0288	0.012	20.2	0.3	1786	170	419	17	4296	310	573	230	10%	
FB2_82	4.93	1	0.0649	0.0017	0.099073	0.544	0.11	0.40046	0.0465	0.019	17.02	0.4	1907	170	405.2	10	4372	320	899	360	9%	
FB2_83	0.472	0.1	0.02515	0.00068	0.085227	0.1327	0.028	0.096432	0.00833	0.0034	87.3	0.2	382	53	160.1	4.3	2090	360	167.6	69	8%	
FB2_84	0.163	0.031	0.02343	0.00058	0.37865	0.4694	0.0092	0.21629	0.00887	0.0038	1520	1.8	144.4	27	143	3.7	162	430	138.4	57	85%	
FB2_85	0.1514	0.03	0.02204	0.0006	0.36577	0.4474	0.0096	0.16929	0.00776	0.0032	421	1.4	143	27	146.2	3.8	75	410	156.3	64	150%	
FB2_86	3.27	0.69	0.0513	0.0029	0.61657	0.435	0.09	-0.0020275	0.0278	0.011	25.19	0.4	1478	160	322	18	4080	330	553	230	8%	
FB2_87	0.1811	0.037	0.02428	0.00078	0.47254	0.5547	0.011	0.20415	0.00818	0.0034	795	2.1	168.7	32	154.7	4.9	375	360	164.7	67	41%	
FB2_88	0.1699	0.034	0.02454	0.00064	0.61457	0.4084	0.0097	0.10917	0.00867	0.0036	922	1.9	159.1	29	159.8	4	116	430	174	72	137%	
FB2_89	4.61	0.92	0.0599	0.003	0.64051	0.556	0.12	-0.14514	0.16	0.069	35.6	1.9	1746	180	375	8	4360	330	2900	1200	9%	
FB2_90	3.96	0.82	0.0567	0.0019	0.48139	0.494	0.1	-0.080545	0.0292	0.012	26.2	0.3	1619	170	355	12	4213	300	591	240	8%	
FB2_91	5.11	1	0.069	0.003	0.24613	0.522	0.11	0.46579	0.0335	0.014	16.7	0.3	1827	170	430	18	4276	310	668	270	10%	
FB2_92	0.828	0.18	0.02881	0.00087	0.5961	0.21	0.044	-0.30177	0.0238	0.0099	671	1.3	608	98	183.1	5.5	2880	330	475	200	6%	
FB2_93	2.85	0.54	0.0461	0.0014	0.09568	0.422	0.086	0.48522	0.0261	0.011	35.2	0.4	1316	150	281.1	8.4	3371	330	521	210	7%	
FB2_94	0.1497	0.03	0.02235	0.00076	0.40506	0.4492	0.01	0.22711	0.00767	0.0051	669	2.0	141.5	27	142.5	4.8	153	420	154.3	63	93%	
FB2_95	3.34	0.7	0.0523	0.0023	0.63251	0.458	0.095	0.023762	0.142	0.059	21.05	2.3	1481	160	329	14	4121	300	2670	1000	8%	
FB2_97	0.162	0.034	0.02362	0.00092	0.38904	0.4491	0.01	-0.046383	0.00755	0.0031	430	2.4	152	30	150.5	5.6	140	410	152	62	108%	
FB2_98	0.194	0.041	0.02415	0.00073	0.42678	0.598	0.012	-0.010775	0.0159	0.0072	209	6.6	180	34	153.8	4.6	520	450	316	140	30%	
FB2_99	0.162	0.032	0.02201	0.00093	0.26895	0.4696	0.01	-0.03086	0.00777	0.0032	145.1	1.6	145.1	27	143.9	5.2	170	420	186.4	64	83%	
FB2_100	0.1529	0.031	0.02298	0.00064	0.45586	0.4497	0.01	0.1736	0.00769	0.0032	1192	2.3	144.3	27	146.5	4	177	440	154.3	63	83%	
FB2_101	0.411	0.085	0.02506	0.0007	0.36816	0.1194	0.025	0.013333	0.00847	0.0035	121.2	0.3	348	61	159.5	4.4	1918	370	170.5	69	8%	
FB2_102	1.87	0.4	0.0387	0.0021	0.56922	0.339	0.017	0.15262	0.0307	0.013	50.7	0.9	1070	140	245	13	3620	320	611	250	7%	
FB2_103	3.57	0.74	0.0524	0.0027	0.68482	0.468	0.086	0.12664	0.0338	0.014	95.5	0.4	1026	170	340	18	4130	330	671	270	8%	
FB2_104	0.253	0.058	0.02423	0.001	-0.21376	0.5745	0.017	0.35523	0.0132	0.0058	35.3	1.7	226	44	154.3	6.5	910	370	264	120	17%	
FB2_105	0.1618	0.033	0.02457	0.00064	0.47896	0.4478	0.0097	0.057417	0.00809	0.0033	716	2.4	152.1	29	156.5	4	94	420	162.9	67	166%	
FB2_107	5.07	1	0.068	0.0027	0.31993	0.541	0.11	0.34736	0.0326	0.013	15.59	0.3	1832	170	424	16	4358	320	648	260	10%	
FB2_108	1.73	0.36	0.0361	0.0014	0.37465	0.318	0.066	0.045113	0.0239	0.0097	50.6	0.6	1022	120	245.4	8.8	3556	300	470	190	7%	
FB2_109	0.459	0.093	0.02598	0.00072	0.06839	0.1281	0.026	0.39173	0.0136	0.0047	114.6	0.6	382	64	165.3	4.5	2041	330	226	83	8%	
FB2_110	0.1683	0.034	0.02425	0.00063	0.33193	0.5005	0.01	0.3436	0.00949	0.0035	808	4.4	157.8	29	154.5	4	210	440	171	70	74%	
FB2_112	0.163	0.034	0.02458	0.00076	0.2625	0.4499	0.011	0.17184	0.00802	0.0033	225	1.8	153	30	156.5	4.8	170	400	161	66	92%	
FB2_113	0.1681	0.034	0.02483	0.00076	0.51026	0.4995	0.011	0.18926	0.00807	0.0034	1930	24.3	157.6	29	158.1	4.8	163	430	162	69	97%	
FB2_114	2.46	0.51	0.0423	0.002	0.52986	0.416	0.086	0.45685	0.0359	0.017	32.5	1.9	1265	160	276	12	3564	290	1740	630	7%	
FB2_115	0.721	0.15	0.0294	0.0019	0.45002	0.184	0.038	0.007125	0.00946	0.0059	57.1	0.2	546	90	180.3	8.3	2130	340	190.3	78	7%	
FB2_117	0.474	0.1	0.0259	0.00086	0.78514	0.1344	0.028	-0.44999	0.01272	0.0052	388	0.8	391	69	164.8	5.4	2130	370	255	100	8%	
FB2_118	0.1603	0.032	0.02417	0.00072	0.59949	0.4488	0.0099	-0.053881	0.00739	0.003	926	2.0	150.8	28	153.9	4.6	150	440	148.7	61	103%	
FB2_120	1.238	0.25	0.0393	0.0013	0.26172	0.2333	0.047	0.54413	0.0323	0.013	70.7	1.1	814	110	246.5	8.2	3075	320	641	260	8%	
FB2_121	0.76	0.16	0.029	0.0011	0.14701	0.198	0.041	0.14741	0.00884	0.0037	69.7	0.1	370	90	178.2	6.9	2770	330	162	74	6%	
X15CAN108_1	3.182	0.625	0.02628	0.00079	0.10446	0.0505	0.0689	0.12391	0.00718	0.002	376	2.2	169	21	167.2	5	180	260	145	39	93%	
X15CAN108_2	0.1755	0.022	0.02676	0.00062	0.45613	0.4771	0.0056	0.08927	0.00753	0.002	775	2.3	163.9	19	170.2	3.9	61	240	142	40	275%	
X15CAN108_3	0.212	0.026	0.02675	0.00063	0.38725	0.5688	0.0068	0.12184	0.00881	0.0024	792	1.6	195	22	170.2	3.3	460	270	177	48	37%	
X15CAN108_4	0.1697	0.021	0.02537	0.00066	0.337	0.4666	0.0056	0.068689	0.00734	0.0019	559	2.1	155.4	18	161.5	4.1	43	230	148	39	376%	
X15CAN108_5	3.65	0.48	0.0349	0.0029	-0.050440	0.488	0.014	0.47115	0.0257	0.0088	16.95	0.3	154.7	100	154	18	4240	330	513	140	8%	
X15CAN108_6	1.54	0.21	0.0356	0.0014	-0.087527	0.516	0.047	0.3546	0.0094	0.0067	33.5	0.7	835	78	225.7	9	3510	230	479	130	6%	
X15CAN108_7	0.183	0.033	0.02561	0.00058	0.09331	0.053	0.0099	0.10578	0.00747	0.002	193	1.2	169	27	163	3.7	210	320	190	41	78%	
X15CAN108_8	3.28	0.56	0.0487	0.0037	0.90386	0.461	0.059	-0.51286	0.0171	0.0047	60.5	0.2	1440	140	306	23	4092	190	342	93	7%	
X15CAN108_9	5.72	0.74	0.0752	0.0052	-0.041209	0.549	0.082	0.64386	0.096	0.026	14.24	0.9	1922	110	467	31	4320	240	1930	480	11%	
X15CAN108_10	0.1581	0.023	0.02586	0.001	0.60811	0.576	0.067	0.7833	0.0092	0.0019	2640	1.4	162.9	18	161.4	6.3	486	230	142	39	101%	
X15CAN108_12	0.1714	0.022	0.026	0.00059	0.31754	0.4477	0.0058	0.20812	0.00701	0.0019	568	2.2	160.4	19	165.5	3.7	90	240	141	38	184%	
X15CAN108_13	0.1756	0.021	0.02564	0.00051	0.48826	0.4485	0.0055	0.28396	0.00633	0.0016	1920	1.3	164.2	18	163.2	3.2	121	260	127.3	33	135%	
X15CAN108_14	0.216	0.028	0.02605	0.00061	0.036335	0.6001	0.0078	0.17078	0.00784	0.0021	308	1.3	188	23	165.8	3.9	560	270	158	41	30%	
X15CAN108_15	0.1718	0.021	0.02581	0.00054	0.30887	0.691	0.054	0.28715	0.00867	0.0026	846	0.3	2182	120	196	3	4702	330	609	240	11%	
X15CAN108_16	0.204	0.031	0.02615	0.00074	-0.017342	0.3555	0.0084	0.12192	0.00851	0.0022	970	1.2	187	26	164.4	4.6	340	280	167	44	49%	
X15CAN108_18	0.175	0.021	0.02583	0.00067	0.040611	0.4479	0.0056	0.41233	0.00703	0.0018	848	1.1	163.6	18	164.4	4.2	96	240	142	37	171%	
X15CAN108_19	0.1693	0.02	0.02498	0.00058	0.43808	0.4492	0.0057	0.16809	0.00722	0.0019	785	2.0	158.7	17	159	3.6	167	260	145	38	95%	
X15CAN108_20	0.187	0.023	0.0255	0.00059	0.71282	0.5333	0.0064	-0.2956	0.00627	0.0016	1170	1.8	174	20	162.3	3.7	319	250	126	33	51%	
X15CAN108_21	0.1804	0.021	0.02559	0.00062	0.85251	0.4936	0.0055	0.23083	0.00733	0.002	2340	2.0	1									

analysis	ISOTOPIC RATIOS										ELEMENTAL CONCENTRATIONS		AGES							conc. (%)	
	206/238 vs 207/235 correlation		206/238 vs 207/235 correlation		206/238 vs 207/235 correlation		206/238 vs 207/235 correlation		206/238 vs 207/235 correlation		U (ppm)	U/Th	207/235 age (Ma)		206/238 age (Ma)		206/238 age (Ma)		206/238 age (Ma)		206/238 age (Ma)
	prop. 2s	prop. 2s	prop. 2s	prop. 2s	prop. 2s	prop. 2s	prop. 2s	prop. 2s	prop. 2s	prop. 2s			prop. 2s	prop. 2s	prop. 2s	prop. 2s	prop. 2s	prop. 2s			
X15CAN108_71	0.1775	0.02	0.02686	0.00069	0.35056	0.0448	0.0051	0.579	0.0083	0.0022	1340	2.8	165.9	18	181.6	4.3	-38	230	167	43	-478%
X15CAN108_72	0.1925	0.023	0.02421	0.00049	0.34598	0.0574	0.0068	0.030086	0.00721	0.0022	1930	1.2	179.9	21	154.2	3.1	482	250	145	38	32%
X15CAN108_73	0.18	0.021	0.02562	0.00049	0.39172	0.05	0.0058	0.15329	0.00744	0.0072	504.4	1.5	169.1	17	164.3	3.1	189	250	150	40	87%
X15CAN108_74	0.1667	0.02	0.02619	0.0006	0.37393	0.0466	0.0053	0.011743	0.00731	0.0019	2270	1.5	156.4	17	166.6	3.8	469	230	147.8	36	417%
X15CAN108_75	0.0504	0.007	0.00963	0.00026	-0.076396	0.0443	0.0062	0.24955	0.00259	0.00073	392	1.3	49.8	6.8	54.7	1.7	-50	240	52	15	-103%
X15CAN108_77	0.1661	0.02	0.02538	0.00073	0.37469	0.0484	0.0055	0.10539	0.00681	0.0018	1450	1.7	155.9	17	161.6	4.6	122	260	139	37	132%
X15CAN108_78	0.1787	0.022	0.02662	0.00061	0.061428	0.0506	0.0064	0.25291	0.00678	0.0018	330	1.2	166.6	19	169.4	3.8	200	250	137	36	85%
X15CAN108_79	0.1495	0.017	0.02473	0.00049	0.47636	0.0456	0.0052	0.24817	0.00692	0.0018	1126	2.2	141.4	15	157.5	3.1	-6	230	139	37	-2625%
X15CAN108_80	0.1519	0.019	0.02468	0.00062	0.22475	0.0469	0.0059	0.30447	0.00614	0.0016	718	1.2	192.3	17	157.2	3.9	152	260	124	33	103%
X15CAN108_81	0.307	0.086	0.0296	0.0017	0.88491	0.07	0.014	-0.070556	0.0095	0.0028	690	1.0	259	57	198	11	740	280	191	55	25%
X15CAN108_82	0.1614	0.019	0.02178	0.00042	0.50984	0.0564	0.0064	0.28995	0.0067	0.0017	4022	1.6	151.9	16	138.9	2.6	460	250	134.9	35	30%
X15CAN108_83	0.166	0.02	0.02723	0.00066	0.44367	0.0499	0.0063	0.37381	0.00705	0.0019	625	2.9	155.9	17	173.2	4.1	-2	240	142	38	-8650%
X15CAN108_84	0.1553	0.018	0.02311	0.00062	0.32999	0.0447	0.0052	0.41053	0.00388	0.0027	511	2.3	146.5	16	166.1	3.9	-39	220	177	54	-425%
X15CAN108_85	0.2	0.02	0.02687	0.00058	0.40313	0.0475	0.0054	0.52272	0.00763	0.002	898	1.5	159.4	17	170.9	3.6	67	260	154	41	255%
X15CAN108_87	0.1706	0.02	0.02656	0.00066	0.58905	0.0477	0.0054	0.4344	0.00679	0.0018	1789	1.2	161.4	16	169.1	4.1	86	240	137	36	192%
X15CAN108_88	0.1458	0.0061	0.0052	0.00023	0.24474	0.0444	0.0055	0.29189	0.00199	0.00055	495	1.2	48.9	6.2	52.8	1.4	-80	240	40	11	-65%
X15CAN108_89	0.158	0.019	0.02595	0.0007	0.52104	0.0481	0.0061	0.23195	0.00632	0.0017	2563	1.8	148.8	16	165.1	4.4	-25	220	127	34	-660%
X15CAN108_90	0.166	0.02	0.02746	0.00081	0.74466	0.0448	0.0051	0.18185	0.00718	0.0019	1580	1.6	155.8	17	174.6	5.1	-35	210	145	38	-493%
X15CAN108_91	0.23	0.032	0.0282	0.00084	0.089689	0.062	0.0091	0.20157	0.0111	0.0021	252	3.5	209	26	179.3	5.3	620	300	223	61	29%
X15CAN108_92	0.192	0.026	0.0281	0.0014	0.7184	0.0478	0.0055	0.02638	0.00739	0.0019	1320	1.1	178	21	178.8	8.7	94	240	148	39	190%
X15CAN108_93	0.1787	0.023	0.02705	0.00055	0.68564	0.0543	0.0063	0.4029	0.01005	0.0028	2985	4.0	184.1	19	172.1	3.7	379	250	137	56	42%
X15CAN108_94	0.1635	0.02	0.02596	0.00081	0.54344	0.0471	0.0054	0.22128	0.00668	0.0018	904	1.7	153.5	18	165.2	5.1	53	250	135	37	312%
X15CAN108_95	2.2	0.34	0.0454	0.0026	0.6469	0.34	0.045	-0.23695	0.0198	0.0052	28.9	0.4	1168	110	206	16	3660	220	395	100	8%
X15CAN108_96	5.37	0.71	0.0766	0.0043	0.5344	0.521	0.066	0.25511	0.0299	0.0083	10.02	0.3	1875	120	480	25	4321	190	959	160	11%
X15CAN108_98	0.1664	0.026	0.02566	0.00095	0.45156	0.0476	0.0056	-0.14237	0.00664	0.0018	400	0.3	156.2	17	163.3	5.3	87	240	134	36	108%
X15CAN108_99	0.2057	0.025	0.02944	0.00054	0.47423	0.0534	0.0064	-0.14277	0.0074	0.0019	789	1.5	189.6	21	180.9	3.3	320	270	149	38	57%
X15CAN108_100	0.1863	0.022	0.02895	0.00073	0.23387	0.0469	0.0053	0.20021	0.00739	0.002	689	2.3	173.3	19	194	4.5	48	240	149	40	383%
X15CAN108_102	4.57	0.56	0.0669	0.0029	0.43831	0.496	0.059	0.43633	0.0269	0.0069	14.9	0.2	1736	110	420	18	4241	160	536	140	10%
X15CAN108_103	1.6	0.3	0.0357	0.0023	0.80015	0.326	0.047	-0.57889	1.66	0.48	41.2	89.0	980	130	226	19	3590	240	1900	360	6%
X15CAN108_104	0.1872	0.023	0.02719	0.0011	0.76104	0.0469	0.0057	0.2625	0.00764	0.0021	1470	1.9	179.6	21	177.6	6.8	136	260	166	42	9%
X15CAN108_105	0.1872	0.023	0.02776	0.00087	0.32423	0.0485	0.0057	0.11994	0.0082	0.0023	347	1.8	173.9	20	176.5	5.5	123	250	165	47	143%
X15CAN108_106	0.1889	0.023	0.02791	0.00085	0.56265	0.0493	0.0058	0.017218	0.00754	0.0021	428	1.9	175.4	20	177.4	5.3	155	280	152	42	114%
X15CAN108_107	0.1917	0.023	0.0292	0.0011	0.71448	0.0484	0.0055	0.38214	0.00688	0.0023	1070	2.1	177.9	20	185.5	6.8	106	260	175	45	177%
X15CAN108_108	0.2142	0.026	0.03315	0.0007	0.51787	0.0507	0.0059	0.077667	0.00927	0.0025	905	1.3	196.8	21	196.8	6.1	221	270	166	50	90%
X15CAN108_109	0.1841	0.022	0.02661	0.00092	0.47423	0.0534	0.0064	0.40418	0.0091	0.0021	567	1.9	171.4	18	169.3	3.2	250	190	134	51	60%
X15CAN108_110	0.1508	0.023	0.02707	0.00057	0.59478	0.0513	0.0059	0.11788	0.00787	0.0021	793	2.2	178.2	20	172.1	3.6	244	260	158	42	71%
X15CAN108_111	0.1748	0.021	0.02612	0.00066	0.54885	0.0489	0.0055	0.32983	0.00719	0.0019	1319	1.8	163.5	18	166.2	4.2	133	270	145	39	125%
X15CAN108_112	0.1815	0.022	0.02639	0.00075	0.70999	0.0501	0.0057	0.23095	0.00787	0.0021	908	1.4	169.2	18	167.9	4.7	194	250	138	42	87%
X15CAN108_113	0.198	0.027	0.02723	0.00071	0.1477	0.062	0.0071	0.046484	0.0091	0.0021	130	1.0	181	23	173.8	4.8	290	250	184	51	60%
X15CAN108_114	0.1829	0.022	0.02681	0.00064	0.53836	0.0506	0.0059	0.05385	0.00727	0.0019	672	2.8	170.4	19	170.5	4	214	250	146	39	80%
X15CAN108_115	0.1998	0.025	0.02943	0.00097	0.6665	0.0497	0.0059	-0.10655	0.00788	0.0021	1190	1.3	184.7	21	187	6.1	190	260	159	43	98%
X15CAN108_116	0.1736	0.021	0.02744	0.00082	0.33324	0.0463	0.0055	0.37507	0.00756	0.002	355	1.7	164.2	18	174.5	5.1	13	220	152	40	1342%
X15CAN108_117	5.72	0.73	0.074	0.0026	0.48795	0.568	0.066	-0.063717	0.0097	0.006	408	0.2	1928	110	460	15	4068	180	610	160	10%
X15CAN108_118	2.42	0.3	0.0443	0.0018	0.6295	0.354	0.047	0.28289	0.0234	0.0062	31.8	0.4	1250	96	279	11	3874	80	457	120	8%
X15CAN108_119	1.93	0.24	0.0402	0.0015	0.38279	0.347	0.042	0.13985	0.0078	0.0021	35.9	2.2	1087	81	254.3	9.2	3693	180	1510	390	7%
X15CAN108_120	1.92	0.26	0.02749	0.00099	0.32834	0.0495	0.0062	0.20716	0.00805	0.0022	226	1.1	178	22	174.8	6.2	220	290	162	44	79%
X15CAN108_121	6.33	0.64	0.0729	0.0029	0.22042	0.532	0.065	0.58007	0.0423	0.011	14.33	0.3	1876	110	454	18	4330	170	836	220	10%
X15CAN108_122	0.14281	0.01	0.0211	0.0004	0.14281	0.1771	0.018	0.242	0.00816	0.0021	61.9	0.1	46	24	109.6	3	210	100	61	42	9%
X15CAN108_124	0.1887	0.023	0.02662	0.00084	0.29338	0.0507	0.006	0.169													

analysis	ISOTOPIIC RATIOS										ELEMENTAL CONCENTRATIONS		AGES							conc. (%)		
	206/238 vs 207/235 correlation		206/238 vs 207/235 correlation		208/232 vs 207/235 correlation		208/232 vs 207/235 correlation		208/232 vs 207/235 correlation		U (ppm)	U/Th	207/235 age (Ma)		206/238 age (Ma)		208/232 age (Ma)		prop. 2s			
	207/235	prop. 2s	206/238	prop. 2s	207/235	prop. 2s	208/232	prop. 2s	208/232	prop. 2s	U (ppm)	U/Th	207/235 age (Ma)	prop. 2s	206/238 age (Ma)	prop. 2s	208/232 age (Ma)	prop. 2s	prop. 2s			
X15CA15A_57	0.1604	0.0096	0.02295	0.0011	0.06072	0.0007	0.0024	0.11203	0.00745	0.00046	1066	2.0	151	8.4	146.2	6.8	220	110	150.1	9.2	66%	
X15CA15A_58	0.1628	0.0095	0.0241	0.0012	0.72186	0.0495	0.0021	0.37537	0.00762	0.00039	2350	1.3	153.1	8.2	153.5	7.3	175	97	153.5	7.8	85%	
X15CA15A_59	0.1695	0.012	0.02508	0.0013	0.89915	0.0495	0.0024	-0.006209	0.00709	0.00045	935	1.4	158.8	10	159.7	7.9	169	110	142.8	9	94%	
X15CA15A_60	0.161	0.012	0.02336	0.0011	0.46282	0.0559	0.0031	0.25183	0.00859	0.00045	3304	1.6	166.7	9	149.8	6.7	439	120	172.3	8.7	34%	
X15CA15A_61	0.342	0.045	0.02207	0.0011	0.68232	0.11	0.012	-0.45887	0.00892	0.00082	1582	0.7	294	32	140.7	6.9	1689	200	179	16	8%	
X15CA15A_62	0.0977	0.0084	0.0084	0.00074	0.87995	0.0838	0.004	0.37282	0.00284	0.00022	10400	1.4	84.5	7.7	53.9	4.8	1282	93	57.2	4.4	4%	
X15CA15A_63	0.1771	0.012	0.0214	0.0019	0.44393	0.0597	0.005	0.8617	0.00756	0.00073	1980	1.7	165.3	10	136	12	520	160	152	15	26%	
X15CA15A_64	0.1693	0.011	0.02489	0.0011	0.45425	0.0499	0.0026	0.45793	0.00812	0.00047	1249	2.4	158.6	9.3	158.5	7.1	197	110	163.4	9.4	80%	
X15CA15A_65	0.1695	0.011	0.02414	0.0013	0.4789	0.0508	0.0027	0.37368	0.00778	0.00065	659	2.1	158.8	9.3	153.7	8.3	236	120	157	13	65%	
X15CA15A_66	0.1679	0.01	0.02376	0.0012	0.56422	0.0502	0.0022	0.13081	0.00774	0.00064	1410	2.4	157.9	9.1	151.4	7.3	199	98	163	13	76%	
X15CA15A_67	0.1595	0.0098	0.02427	0.0011	0.49355	0.0474	0.0023	0.16241	0.00834	0.00055	571	1.4	150.2	8.6	154.6	7	75	99	167.9	11	200%	
X15CA15A_68	0.165	0.013	0.02313	0.0011	0.04566	0.0505	0.0035	0.30003	0.00867	0.00074	424	1.8	154.9	12	147.4	6.8	200	140	172	15	74%	
X15CA15A_69	0.1674	0.01	0.02393	0.001	0.42787	0.0613	0.0027	0.27557	0.00825	0.00067	509	2.2	157	9.1	152.5	6.6	240	120	166	13	54%	
X15CA15A_70	0.1693	0.011	0.02467	0.0012	0.49625	0.0494	0.0025	0.082759	0.00866	0.00057	767	2.4	158.6	9.6	157.1	7.3	163	110	174.3	11	96%	
X15CA15A_72	0.1454	0.0099	0.0204	0.0013	0.89355	0.0513	0.0022	0.40602	0.00883	0.00047	3990	1.9	138.5	8.7	130.4	8.4	246	96	137.5	9.5	53%	
X15CA15A_73	0.1751	0.01	0.02506	0.0012	0.61931	0.0496	0.0023	0.40977	0.00836	0.00046	956	1.8	163.8	8.9	159.6	7.3	170	100	168.2	9.2	94%	
X15CA15A_80	0.162	0.011	0.02439	0.0011	0.30715	0.049	0.0028	0.47963	0.00804	0.00052	457	1.5	153.2	8.7	155.3	7.2	161	120	161.9	10	96%	
X15CA15A_76	0.1774	0.011	0.02497	0.0011	0.28683	0.0606	0.0026	0.24624	0.00881	0.00062	801	1.6	159.3	9.9	153.9	7	215	110	173	12	71%	
X15CA15A_76	0.1632	0.01	0.02368	0.001	0.63764	0.0496	0.0023	-0.1111	0.00804	0.00042	1053	1.5	153.3	9	150.9	6.5	171	100	161.8	8.4	88%	
X15CA15A_77	0.1711	0.01	0.02514	0.0012	0.56469	0.0492	0.0023	0.25817	0.00884	0.00057	876	1.8	160.2	8.7	160.1	7.4	155	99	177.8	11	103%	
X15CA15A_78	0.1722	0.012	0.0256	0.0015	0.70517	0.0473	0.0022	0.31629	0.00792	0.00053	930	1.4	161.1	10	163.2	9.4	69	97	159	13	237%	
X15CA15A_79	0.182	0.013	0.02577	0.0012	0.43923	0.0502	0.0021	-0.13025	0.00803	0.00065	473	1.5	161.7	11	157	7.5	150	120	162	13	83%	
X15CA15A_80	0.1771	0.012	0.02535	0.0011	0.52508	0.0498	0.0024	0.10649	0.00818	0.00058	655	2.1	166.4	11	161.3	7.2	183	100	165	12	88%	
X15CA15A_81	0.1921	0.012	0.02487	0.0012	0.77141	0.0547	0.0023	0.13977	0.00872	0.00034	956	1.3	178.3	10	159.3	7.2	423	100	136.4	6.8	37%	
X15CA15A_82	0.18	0.011	0.02517	0.0012	0.41351	0.0518	0.0027	0.26271	0.00888	0.00073	337	2.3	167.9	9.7	160.2	7.3	262	110	179	15	15%	
X15CA15A_83	0.158	0.015	0.02366	0.0012	0.55167	0.0507	0.0024	-0.015716	0.00835	0.00058	1970	1.2	191.7	13	150.7	7.5	600	130	168.2	7.7	25%	
X15CA15A_84	0.1524	0.015	0.02484	0.0012	0.61263	0.0568	0.0027	0.2229	0.00863	0.00062	1186	2.5	160.8	11	164.5	7.3	424	110	194	13	48%	
X15CA15A_85	0.1766	0.012	0.026	0.0013	0.49867	0.0505	0.0027	0.12757	0.0089	0.00085	448	2.0	164.9	11	165.4	7.9	211	110	179	13	78%	
X15CA15A_86	0.1719	0.01	0.02697	0.0012	0.40599	0.0478	0.0022	0.23579	0.00839	0.00052	656	1.7	161	9	171.6	7.7	96	169	10	175%		
X15CA15A_87	0.1751	0.01	0.02195	0.001	0.61526	0.0574	0.0027	0.5474	0.00932	0.00038	317	1.0	163.8	8.8	140	6.5	490	100	107.2	7.6	29%	
X15CA15A_88	0.182	0.013	0.02577	0.0012	0.38395	0.0629	0.0026	0.19739	0.00864	0.00053	512	1.3	176.7	11	164	7.5	323	110	172	15	13%	
X15CA15A_89	0.1854	0.011	0.02478	0.0011	0.71243	0.054	0.0023	0.13677	0.00854	0.00046	1010	1.5	172.5	9.7	157.8	7.1	361	95	172	13	44%	
X15CA15A_90	0.1687	0.011	0.02492	0.0012	0.634	0.0497	0.0024	0.065173	0.00854	0.00048	854	1.5	158.1	9.4	158.7	7.7	175	100	171.8	9.7	91%	
X15CA15A_91	0.1682	0.011	0.02473	0.0011	0.39029	0.0494	0.0026	0.36827	0.00777	0.00052	636	1.8	157.7	9.2	157.5	7.2	164	110	156.5	10	96%	
X15CA15A_92	0.232	0.018	0.02363	0.0014	0.43636	0.0516	0.0023	-0.05501	0.00765	0.00074	457	1.4	156.2	13	179.3	8.9	280	130	154	15	5%	
X15CA15A_93	0.1774	0.016	0.0239	0.0015	0.63036	0.0527	0.0023	0.078699	0.00787	0.00053	538	1.4	164	13	151	5.0	290	130	154	13	52%	
X15CA15A_94	0.0716	0.011	0.0083	0.00042	-0.15604	0.0614	0.0082	0.28383	0.00367	0.00052	314	3.4	69.8	9.7	53.3	2.7	500	230	74	10	11%	
X15CA15A_95	0.1705	0.012	0.02461	0.001	0.12527	0.0524	0.0023	0.064201	0.00778	0.00044	1103	1.7	164.8	10	156.7	6.4	280	120	156.6	8.8	56%	
X15CA15A_96	0.1902	0.012	0.02577	0.0012	0.28776	0.0542	0.0028	0.39177	0.00784	0.0005	1160	1.6	176.6	9.9	164	7.6	360	110	157.9	10	46%	
X15CA15A_97	0.1685	0.009	0.02484	0.0012	0.61263	0.0568	0.0027	0.2229	0.00863	0.00062	1186	2.5	160.8	11	164.5	7.3	424	110	194	13	48%	
X15CA15A_98	0.1685	0.011	0.02409	0.0013	0.60763	0.0506	0.0029	0.54084	0.00822	0.00054	986	1.3	157.9	9.8	153.5	8.2	215	120	165.5	11	71%	
X15CA15A_99	0.239	0.016	0.02291	0.00098	0.24856	0.0758	0.0042	0.17075	0.00817	0.00056	504	1.1	171.1	13	146	6.2	1062	110	164.4	11	14%	
X15CA15A_100	0.1919	0.013	0.02705	0.0013	0.89188	0.0521	0.0027	-0.04571	0.00973	0.00076	514	2.2	177.9	11	172.1	7.9	285	120	196	15	60%	
X15CA15A_101	0.174	0.011	0.02461	0.0011	0.64446	0.0504	0.0025	0.18327	0.00823	0.00046	1261	1.4	162.7	9.7	156.7	6.8	208	100	167.3	10	77%	
X15CA15A_102	0.182	0.012	0.02594	0.0012	0.38319	0.0512	0.0027	0.38235	0.00875	0.00051	847	1.6	165.5	10	165.1	7.7	249	120	176.1	10	66%	
X15CA15A_104	0.174	0.015	0.024	0.0011	0.14436	0.0537	0.0042	0.098643	0.0095	0.0014	314	3.3	162	13	152.9	6.7	340	170	191	29	45%	
X15CA15A_105	0.1578	0.0094	0.02234	0.001	0.61981	0.0521	0.0023	0.18274	0.00832	0.00055	1467	2.5	148.6	8.3	142.4	6.6	280	98	127	11	51%	
X15CA15A_106	0.1639	0.012	0.02397	0.0011	0.39063	0.0509	0.0023	0.035005	0.00761	0.0005	324	8	20	153.8	11	152.7	7.1	210	130	153	12	73%
X15CA15A_107	0.15423	0.009	0.0244	0.0011	0.45453	0.0534	0.0024	0.34654	0.00837	0.00054	1540	1.3	157.4	8	166.6	6.7	306	120	163.3	10	45%	
X15CA15A_108	0.1764	0.011	0.0256	0.0011	0.34002	0.0513	0.0025	0.45549	0.00946	0.00054	836	1.8	164.8	9.4	162.9	7.1	246	110	170.3	11	66%	
PRINCE1A_1	0.173	0.0078	0.02986	0.00099	0.45133	0.0492	0.0024	0.83032	0.00778	0.0011	606	1.5	162	6.5	164.6	6.2	153	100	156.6	20	100%	
PRINCE1A_2	0.1764	0.0083	0.0221	0.00095	0.61568	0.0506	0.0021	0.2512	0.00626	0.0011	828	2.0	164.8	7.2	159.8	6	227	97	166.3	22	70%	
PRINCE1A_3	0.1754	0.0091	0.02525	0.00093	0.41802	0.0495	0.0024	0.38781	0.00828	0.0011	697	2.1	163.9	7.8	160.7	5.9	167	100	166.7	23	96%	
PRINCE1A_4																						

analysis	ISOTOPIC RATIOS										ELEMENTAL CONCENTRATIONS		AGES							conc. (%)	
	207/235		206/238		206/238 vs 207/235 error correlation		208/232		207/206 error correlation		U (ppm)	U/Th	207/235 age (Ma)		206/238 age (Ma)		207/206 age (Ma)		208/232 age (Ma)		
	prop. 2s	prop. 2s	prop. 2s	prop. 2s	prop. 2s	prop. 2s	prop. 2s	prop. 2s	prop. 2s	prop. 2s			prop. 2s	prop. 2s	prop. 2s	prop. 2s	prop. 2s	prop. 2s	prop. 2s		prop. 2s
PRINCE1A_56	0.1606	0.0098	0.02382	0.00093	0.21319	0.0498	0.0028	0.28987	0.00785	0.0011	948	1.5	150.9	8.5	151.7	5.8	174	120	158	21	87%
PRINCE1A_57	0.174	0.014	0.02492	0.00092	0.049708	0.0523	0.0047	0.19313	0.00888	0.0015	420	2.2	162	12	158.7	5.8	180	140	179	29	86%
PRINCE1A_58	0.1613	0.0068	0.02312	0.00078	0.43716	0.0513	0.0024	0.14784	0.00701	0.00095	1850	1.8	151.7	7.4	147.3	4.9	244	100	141	1	60%
PRINCE1A_59	0.162	0.0084	0.02306	0.00087	0.45845	0.0494	0.0022	0.045199	0.00754	0.00099	1940	1.5	152.3	7.3	152	5.5	136	96	151.3	20	53%
PRINCE1A_60	0.173	0.013	0.02326	0.0018	0.85407	0.0544	0.0027	0.59234	0.00778	0.0012	1150	1.5	161.7	11	150	11	368	110	157	25	41%
PRINCE1A_62	0.174	0.0096	0.02556	0.001	0.56411	0.0491	0.0022	0.14405	0.00877	0.0014	688	1.9	162.6	8.3	162.8	6.6	153	96	176	28	106%
PRINCE1A_63	0.1755	0.01	0.02581	0.0009	0.41422	0.0507	0.0028	0.068118	0.00948	0.0011	834	1.9	165.9	9	164.3	5.6	211	110	170	22	78%
PRINCE1A_64	0.1615	0.0085	0.02415	0.00097	0.34619	0.0492	0.0025	0.11612	0.00793	0.0011	1019	1.5	151.9	7.4	153.2	6.1	152	110	157.5	21	101%
PRINCE1A_66	0.1698	0.0096	0.02496	0.0008	0.56515	0.0503	0.0024	-0.062131	0.00728	0.0011	935	1.7	159	8.3	158.9	5	138	100	160	20	80%
PRINCE1A_68	0.1495	0.0091	0.02404	0.00082	0.23464	0.0452	0.0026	0.16381	0.00772	0.0011	638	1.9	140.4	8	153.2	5.1	38	94	155	22	-403%
PRINCE1A_67	0.1668	0.0082	0.02429	0.00086	0.59813	0.0494	0.0022	0.3158	0.00723	0.00098	1270	1.9	156.5	7.1	154.7	5.4	162	97	146.6	20	95%
PRINCE1A_68	0.176	0.011	0.02584	0.0011	0.5024	0.0498	0.0027	0.0050559	0.00798	0.0011	1210	1.4	164.4	9.8	164.4	7.2	178	110	160.7	22	92%
PRINCE1A_73	0.191	0.014	0.02514	0.00092	-0.39789	0.055	0.0041	0.61172	0.00826	0.0012	752	2.1	177.2	11	160	5.8	360	140	166	24	44%
PRINCE1A_70	0.175	0.013	0.0245	0.00091	-0.19121	0.0525	0.0053	0.3197	0.00685	0.00093	1210	1.7	163.2	11	156	5.7	190	86	137.9	19	82%
PRINCE1A_71	0.1798	0.009	0.02518	0.00093	0.56257	0.0515	0.0023	0.31317	0.00791	0.0011	1171	2.3	167.7	7.7	160.3	5.8	252	97	159.3	22	64%
PRINCE1A_72	0.1657	0.0073	0.02475	0.00084	0.27916	0.0483	0.0021	0.48475	0.00752	0.0011	1377	2.2	155.6	6.4	157.6	5.3	116	93	151.5	20	136%
PRINCE1A_74	0.206	0.014	0.0208	0.0015	-0.46148	0.0757	0.0096	0.88318	0.00694	0.0011	1520	1.3	189	12	132.8	9.3	930	230	140	21	14%
PRINCE1A_75	0.1772	0.0095	0.02365	0.00088	0.31386	0.0538	0.0027	0.27251	0.00725	0.00095	1806	1.5	165.4	8.2	150.7	5.5	325	97	146.1	19	46%
PRINCE1A_76	0.1593	0.0098	0.02345	0.00096	0.61822	0.0494	0.0025	-0.099993	0.00688	0.00095	664	1.1	149.9	8.3	149.4	6	162	110	138.6	19	92%
PRINCE1A_77	0.19	0.013	0.02555	0.00097	0.10209	0.0531	0.0035	0.27874	0.00906	0.0014	644	3.2	176	11	162.6	6.1	300	130	152	27	54%
PRINCE1A_78	0.1787	0.01	0.02519	0.0011	0.45479	0.0502	0.0028	0.24209	0.00805	0.0011	601	2.7	164.1	8.8	160.3	6.8	197	120	162.1	22	81%
PRINCE1A_79	0.1793	0.011	0.02554	0.0011	0.55676	0.0493	0.0026	0.20126	0.00728	0.00098	726	1.8	167.2	9.1	162.6	6.7	172	110	146.7	20	95%
PRINCE1A_80	0.1654	0.0083	0.02407	0.00094	0.18173	0.0489	0.0025	0.27849	0.00752	0.0011	942	1.6	155.3	7.3	153.3	5.9	141	110	151.4	20	109%
PRINCE1A_81	0.1526	0.0076	0.0211	0.0012	0.7047	0.0524	0.0027	0.78736	0.00534	0.00075	1830	0.8	144.1	6.7	134.3	7.8	299	110	107.6	15	45%
PRINCE1A_82	0.1653	0.0085	0.02296	0.00091	0.52980	0.0492	0.0025	0.23751	0.00694	0.0011	1090	1.4	156	8.2	150.2	6.6	146	97	138.5	20	401%
PRINCE1A_83	0.1721	0.009	0.02394	0.00096	0.41198	0.051	0.0025	0.22321	0.00693	0.00094	1520	2.0	161	7.8	162.5	6	246	110	139.5	19	62%
PRINCE1A_84	0.1836	0.011	0.02242	0.0011	0.57241	0.0503	0.0024	0.424751	0.00743	0.0011	1808	2.0	168	8.1	159.9	6.5	201	100	149.6	20	79%
PRINCE1A_85	0.1744	0.0094	0.02496	0.001	0.54171	0.0503	0.0024	0.24751	0.00743	0.0011	1808	2.0	168	8.1	159.9	6.5	201	100	149.6	20	79%
PRINCE1A_86	0.1686	0.011	0.0247	0.0013	0.54885	0.0487	0.0026	0.27997	0.00784	0.0011	727	1.5	158	9.2	157.3	8.3	130	110	158	22	121%
PRINCE1A_89	0.1714	0.008	0.02468	0.00098	0.34176	0.0498	0.0025	0.24209	0.00791	0.0011	1056	1.6	166.7	8.6	162.6	6.2	154	92	155.3	19	62%
PRINCE1A_88	0.1055	0.0044	0.01335	0.00046	0.54486	0.0567	0.0023	0.5026	0.00412	0.00054	2620	1.6	101.8	4.1	85.5	2.9	472	89	83.1	11	18%
PRINCE1A_99	0.1677	0.011	0.02523	0.00092	0.54213	0.0472	0.0025	0.071786	0.00829	0.0013	629	2.1	158.6	9.6	160.6	5.8	67	100	167	25	240%
PRINCE1A_90	0.1943	0.011	0.02653	0.0009	0.2224	0.0494	0.0026	-0.002693	0.00905	0.0014	757	2.1	171.9	9.1	168.8	5.7	164	110	132	28	103%
PRINCE1A_91	0.196	0.014	0.02529	0.001	0.25887	0.0503	0.0027	-0.01462	0.0094	0.0012	797	2	179.3	12	179.3	10	180	140	159	36	100%
PRINCE1A_92	0.1435	0.0082	0.02088	0.0011	0.60181	0.05	0.0025	0.36355	0.00662	0.00099	2220	1.9	137	6.9	133.2	7	181	110	133	20	74%
PRINCE1A_93	0.1671	0.0081	0.02469	0.001	0.72597	0.0488	0.0021	0.43538	0.00748	0.0011	1631	1.6	156.8	7	157.2	6.6	126	95	170	20	125%
PRINCE1A_94	0.1936	0.011	0.02657	0.001	0.48724	0.0519	0.0026	0.19889	0.00864	0.0012	776	1.5	178.1	8.3	169	6.6	264	110	153.9	23	64%
PRINCE1A_95	0.1745	0.0098	0.02484	0.001	0.41225	0.0513	0.0026	0.12674	0.00743	0.0011	682	1.6	163.1	8.5	159.9	6.6	239	110	149.7	21	68%
PRINCE1A_96	0.1714	0.009	0.02591	0.00099	0.47184	0.0492	0.0025	0.25418	0.00791	0.0011	762	2.0	165.2	7.7	164.4	6.2	154	94	153.2	21	107%
PRINCE1A_97	0.1717	0.0086	0.02582	0.001	0.49901	0.0487	0.0022	0.51306	0.00763	0.0011	2500	1.6	160.7	7.5	164.3	6.5	132	96	159.6	20	124%
PRINCE1A_98	0.1566	0.011	0.01941	0.00097	0.84129	0.0579	0.0027	-0.1857	0.00407	0.00063	2060	1.1	147.4	9.9	123.9	6.1	532	100	82	13	23%
PRINCE1A_99	0.147	0.015	0.0194	0.0014	0.85742	0.0564	0.0032	-0.2886	0.00651	0.0011	1090	1.8	143	13	124.1	8.6	461	120	131	22	27%
PRINCE1A_100	0.1683	0.0081	0.02376	0.00095	0.51025	0.0525	0.0024	0.46235	0.00723	0.0011	930	1.4	154.1	7.1	151.3	5.8	234	100	145.6	16	51%
PRINCE1A_101	0.1653	0.0088	0.02549	0.00099	0.51234	0.048	0.0023	0.26963	0.0077	0.0011	1053	1.2	155.2	7.4	162.2	6.2	104	100	155.1	15	156%
PRINCE1A_102	0.177	0.0089	0.02543	0.00094	0.099556	0.0513	0.0026	0.25405	0.00796	0.0011	884	1.9	165.3	7.7	161.8	5.9	241	110	160.2	22	67%
PRINCE1A_103	0.163	0.0084	0.02468	0.001	0.32706	0.0475	0.0025	0.39335	0.00765	0.0011	645	2.2	153.1	8.2	157.2	6.5	80	110	154	22	197%
PRINCE1A_104	0.229	0.015	0.0291	0.00094	0.02967	0.0673	0.0045	0.46202	0.00849	0.0012	342	1.2	209	13	160	5.9	830	140	171	24	15%
PRINCE1A_105	0.1426	0.0074	0.02349	0.00088	0.70231	0.0504	0.0021	0.28621	0.00688	0.00084	2870	2.2	136.2	6.6	130.7	6.2	210	94	128.6	17	62%
PRINCE1A_106	0.1675	0.0079	0.02422	0.00092	0.32981	0.052	0.0026	0.33161	0.00774	0.0011	1160	1.2	157.2	6.9	154.3	5.8	269	100	155.9	21	57%
PRINCE1A_107	0.179	0.012	0.025	0.00096	0.46802	0.0529	0.0029	-0.14066	0.00774	0.0011	1807	1.9	166.9	10	159.2	6.1	304	110	156	23	52%
PRINCE1A_108	0.1893	0.011	0.0255	0.00092	0.38273	0.0489	0.0029	0.104002	0.008	0.0011	582	2.1	158.4	9.8	162.3	5.8	116	110	161	23	140%
PRINCE1A_109	0.18181	0.0092	0.02524	0.00091	0.81911	0.0524	0.0023	0.33723	0.00791	0.0011	939	1.6	164.1	8.9	162.6	6.2	200	110	155.3	19	62%
PRINCE1A_110	0.1596	0.0072	0.02259	0.00088	0.7829	0.052	0.0022	0.41966	0.00666	0.00087	3440	1.3	150.3	6.3	144	5.6	278	89	134.2	18	52%
PRINCE1A_111	0.1668	0.007	0.02488	0.00086	0.5853	0.049															

analysis	ISOTOPIIC RATIOS										ELEMENTAL CONCENTRATIONS		AGES							conc. (%)	
	206/238 vs 207/235 correlation		206/238 vs 207/235 correlation		208/232 vs 207/235 correlation		208/232 vs 207/235 correlation		U (ppm)	U/Th	207/235 age (Ma)		206/238 age (Ma)		207/235 age (Ma)		208/232 age (Ma)				
	prop. 2s	prop. 2s	prop. 2s	prop. 2s	prop. 2s	prop. 2s	prop. 2s	prop. 2s			prop. 2s	prop. 2s	prop. 2s	prop. 2s	prop. 2s	prop. 2s	prop. 2s	prop. 2s	prop. 2s		
unk15CA13b_48	0.202	0.05	0.00886	0.00059	0.8424	0.144	0.024	-0.62143	0.0127	0.003	988	3.6	179	39	56.9	3.7	3120	300	254	59	3%
unk15CA13b_49	0.157	0.035	0.0085	0.00048	0.79433	0.131	0.025	-0.67259	0.0102	0.0023	566	4.3	144	29	54.6	3.1	1890	320	206	46	3%
unk15CA13b_50	1.07	0.26	0.0199	0.0016	0.99663	0.467	0.065	-0.25749	0.062	0.011	490	3.7	710	110	101.4	10	4050	200	1210	210	3%
unk15CA13b_51	0.22	0.031	0.00905	0.00041	0.73144	0.195	0.02	-0.23932	0.0163	0.002	331	3.9	205	26	58.1	3	2460	150	205	54	2%
unk15CA13b_52	0.0489	0.0054	0.00759	0.00038	0.1097	0.0469	0.0045	0.10964	0.00256	0.00032	617	2.9	48.4	5.2	48.7	2.4	50	170	51.6	6.4	97%
unk15CA13b_53	0.077	0.011	0.00773	0.00042	0.48523	0.0737	0.0091	-0.34055	0.00483	0.001	677	4.0	75.4	10	49.7	2.7	880	220	97	21	6%
unk15CA13b_54	0.065	0.012	0.00795	0.00043	-0.14147	0.061	0.011	0.32153	0.00459	0.00069	206	3.7	64	11	51	2.7	580	350	32	14	9%
unk15CA13b_55	0.0599	0.0074	0.00799	0.00044	0.11603	0.0546	0.0054	0.14024	0.00249	0.00058	289	5.3	98.9	7	51.3	2.8	310	230	50	12	17%
unk15CA13b_56	0.138	0.038	0.00891	0.00061	0.80836	0.108	0.02	-0.40993	0.0093	0.0028	750	3.9	126	28	67.2	3.9	1540	240	187	55	4%
unk15CA13b_57	0.0929	0.0091	0.00774	0.00037	-0.052816	0.0878	0.0065	0.31783	0.00782	0.00021	6660	6.3	92.8	8.3	49.7	2.4	1320	130	157	14	4%
unk15CA13b_58	0.065	0.012	0.00753	0.00043	-0.19308	0.061	0.011	0.34387	0.00367	0.00028	346	4.9	63	11	48.4	2.8	340	250	74	16	14%
unk15CA13b_59	0.19	0.052	0.0092	0.00063	0.93933	0.153	0.033	-0.79847	0.0108	0.0028	295	3.5	170	42	52.6	4	2130	470	216	56	2%
unk15CA13b_60	0.0496	0.005	0.00775	0.00037	0.14907	0.0479	0.0054	-0.02079	0.00281	0.00035	544	4.4	49.3	4.8	47.8	2.4	80	140	48.8	7.1	60%
unk15CA13b_61	0.153	0.02	0.00834	0.00043	0.52016	0.126	0.013	-0.26501	0.0102	0.0016	420	4.4	144	18	53.5	2.8	1860	190	206	32	3%
unk15CA13b_62	0.059	0.0056	0.00784	0.00039	0.33327	0.0549	0.0038	-0.050451	0.00312	0.00039	1472	3.3	59	5.9	50.3	2.5	360	140	62.9	7.8	14%
unk15CA13b_63	0.125	0.013	0.00824	0.00041	0.62918	0.1104	0.0087	-0.33424	0.00661	0.00076	811	3.3	119.2	11	52.9	2.6	1770	140	133	15	3%
unk15CA13b_64	0.073	0.013	0.00757	0.00045	0.61289	0.0619	0.0048	-0.33409	0.00372	0.00053	1750	3.9	62.8	6.7	48.6	2.9	580	140	75	11	8%
unk15CA13b_65	0.081	0.015	0.00799	0.00044	0.49377	0.083	0.011	-0.39795	0.0052	0.0012	386	4.3	78	14	51.3	2.8	1100	330	105	24	6%
unk15CA13b_66	0.0495	0.0069	0.00729	0.00039	0.019371	0.0474	0.0054	0.15587	0.00248	0.00034	645	4.2	48.9	6.6	46.8	2.5	50	190	50.1	6.9	94%
unk15CA13b_67	0.1025	0.0092	0.00812	0.00045	0.33382	0.0918	0.0061	0.099918	0.00572	0.00063	1105	3.6	98.9	8.4	52.1	2.8	1440	130	115	13	4%
unk15CA13b_68	0.0961	0.011	0.00819	0.00042	0.12227	0.0848	0.0086	-0.044881	0.00624	0.00096	523	4.3	92.8	10	52.6	2.7	1220	170	126	19	4%
unk15CA13b_69	0.0581	0.0089	0.00803	0.00044	0.17659	0.0535	0.0073	-0.04092	0.0034	0.00052	427	5.2	57	6.5	49.9	2.8	240	240	48	13	21%
unk15CA13b_70	0.076	0.014	0.00755	0.0004	0.31569	0.079	0.015	-0.096902	0.0044	0.0011	903	4.2	74	13	48.5	2.5	890	330	99	23	5%
unk15CA13b_71	0.0768	0.0089	0.00797	0.00041	0.51415	0.069	0.009	-0.20955	0.00432	0.00096	1060	3.7	75.3	8.7	51.2	2.6	840	180	87	20	6%
unk15CA13b_72	0.0525	0.0039	0.00762	0.00039	0.22103	0.0481	0.002	0.36645	0.00259	0.00031	2037	4.7	51.9	3.8	50.2	2.5	109	88	52.2	6.2	46%
unk15CA13b_73	0.073	0.013	0.00816	0.00042	0.65044	0.064	0.01	-0.05291	0.00276	0.00045	594	4.7	71	12	52.5	2.7	500	260	55.6	8.1	11%
unk15CA13b_74	0.0647	0.0074	0.00782	0.00043	0.29181	0.0579	0.0054	-0.059431	0.00349	0.00047	970	3.8	63.5	7.2	60.2	2.8	440	190	68.8	8.4	11%
unk15CA13b_75	0.156	0.018	0.00928	0.00046	0.12396	0.121	0.012	0.19299	0.00738	0.00089	727	2.9	146	16	59.6	2.9	1860	200	149	18	3%
unk15CA13b_76	0.0568	0.0079	0.00759	0.00045	-0.49973	0.0533	0.0063	0.81908	0.00286	0.00032	675	3.7	54.9	7.5	48.7	2.9	210	190	58	16	23%
unk15CA13b_77	0.228	0.033	0.00955	0.00064	0.79689	0.169	0.016	-0.57507	0.0084	0.0013	1800	2.4	207	27	61.2	4.1	2550	160	170	27	2%
unk15CA13b_78	0.0513	0.0032	0.00785	0.00038	0.11615	0.0569	0.0047	0.19457	0.00238	0.00034	1020	2.9	50.9	4.9	47.8	2.4	190	170	47	6	8%
unk15CA13b_79	0.0689	0.01	0.00785	0.00038	0.047962	0.0629	0.0087	0.042161	0.00349	0.00079	662	4.9	64.8	8.3	50.4	2.5	480	230	78	16	11%
unk15CA13b_80	0.0707	0.01	0.0077	0.00039	0.0079494	0.0678	0.0097	0.10801	0.0034	0.00034	1000	3.0	69	9.5	49.4	2.5	650	280	87	19	8%
unk15CA13b_81	0.0495	0.035	0.01139	0.00065	0.73616	0.26	0.012	-0.40076	0.0195	0.0015	782	2.0	391	26	73	4.2	3344	84	311	31	2%
unk15CA13b_82	0.0915	0.011	0.00808	0.00043	0.15791	0.0759	0.0078	0.10929	0.00345	0.00055	800	4.7	63	8.7	50.3	2.6	1100	330	118	13	5%
unk15CA13b_83	0.0415	0.011	0.00808	0.00043	0.1456	0.0895	0.0092	0.059179	0.00494	0.00047	320	3.0	96	10	51.9	2.6	910	390	91.1	11	4%
unk15CA13b_84	0.141	0.044	0.00845	0.00054	0.77339	0.131	0.037	-0.65778	0.0086	0.0011	971	3.6	128	36	54.2	3.4	1460	420	172	62	4%
unk15CA13b_85	0.0574	0.0046	0.00816	0.00044	-0.34688	0.0513	0.0041	0.80257	0.00311	0.00059	1460	2.7	56.6	4.4	52.4	2.8	250	160	63	12	21%
unk15CA13b_86	0.0568	0.0043	0.00807	0.00039	0.43836	0.0502	0.002	0.021895	0.00255	0.00021	5270	5.0	56.1	4.1	51.78	2.5	198	88	51.4	4.3	26%
unk15CA13b_87	0.0514	0.0032	0.00789	0.00039	0.0939257	0.0464	0.0028	0.14876	0.00266	0.00068	643	4.9	50.9	5	60.7	2.6	310	150	94	12	16%
unk15CA13b_88	0.0562	0.0051	0.00756	0.00036	0.021888	0.0525	0.0035	0.14685	0.00255	0.00027	2057	2.8	55.5	4.9	48.85	2.3	270	130	51.5	5.4	18%
unk15CA13b_89	0.0761	0.007	0.00794	0.0004	0.074362	0.0689	0.0049	0.24358	0.0036	0.0004	2110	2.9	74.4	6.6	51	2.6	860	140	72.7	8	6%
unk15CA13b_90	0.0892	0.0083	0.00767	0.0004	-0.056267	0.0533	0.0071	0.26265	0.0039	0.00067	787	3.8	58.2	7.9	50.5	2.5	230	230	79	13	22%
unk15CA13b_91	0.0526	0.004	0.00771	0.00045	0.27386	0.0495	0.0025	-0.20991	0.00269	0.00061	520	4.0	53	5.9	49.6	2.6	105	180	54.3	6.5	30%
unk15CA13b_92	0.0592	0.0045	0.00776	0.0004	0.38529	0.0553	0.002	0.23887	0.00259	0.00033	1869	5.2	57.5	4.3	50.1	2.6	430	120	66.5	6.7	12%
unk15CA13b_93	0.0502	0.0042	0.00775	0.00039	0.28992	0.0469	0.0028	-0.016505	0.0028	0.00036	1256	3.0	49.7	4.1	49.8	2.5	50	110	56.5	7.2	100%
unk15CA13b_94	0.342	0.043	0.00992	0.00047	0.79546	0.238	0.019	-0.61804	0.0231	0.0017	890	3.9	295	32	63.7	3.6	3110	140	462	53	2%
unk15CA13b_95	0.112	0.016	0.0082	0.00045	0.080347	0.0596	0.012	0.12893	0.0087	0.0026	399	5.1	107	14	52.6	2.9	1650	280	174	31	3%
unk15CA13b_96	0.0514	0.004	0.00767	0.00037	0.12826	0.0489	0.004	0.292	0.00248	0.0002	2410										

analysis	ISOTOPIC RATIOS										ELEMENTAL CONCENTRATIONS		AGES										conc. (%)
	207/235		206/238		206/238 vs 207/235 error correlation		208/232		208/232 vs 207/235 error correlation		U (ppm)	U/Th	207/235 age (Ma)		206/238 age (Ma)		208/232 age (Ma)		208/232 age (Ma)				
	prop. 2s	prop. 2s	prop. 2s	prop. 2s	prop. 2s	prop. 2s	prop. 2s	prop. 2s	prop. 2s	prop. 2s			prop. 2s	prop. 2s	prop. 2s	prop. 2s	prop. 2s	prop. 2s	prop. 2s	prop. 2s			
ABBEYRD_22	0.0589	0.0046	0.00882	0.00038	0.093845	0.0482	0.004	0.15805	0.00297	0.0004	884	2.1	98.1	4.4	57	26	100	160	80	8.1	57%		
ABBEYRD_23	0.0481	0.0065	0.00763	0.0004	-0.03755	0.0445	0.0061	0.27304	0.003	0.0005	299	0.9	47.5	6.0	49	2.5	60	220	60.5	10	-82%		
ABBEYRD_25	0.066	0.013	0.00793	0.00033	0.082135	0.059	0.011	-0.000161	0.0033	0.00057	397	2.6	60.2	9.6	50.9	2.1	230	190	66.5	12	22%		
ABBEYRD_26	0.065	0.018	0.00978	0.00039	0.26285	0.044	0.013	-0.23253	0.0089	0.0005	123	3.1	57	62.4	5.6	-250	420	176	99	-26%			
ABBEYRD_27	0.0772	0.0049	0.01163	0.00041	0.077039	0.0484	0.0032	0.16002	0.00426	0.00056	1022	2.5	75.5	4.6	73.9	2.6	130	190	85.9	11	62%		
ABBEYRD_28	0.0624	0.004	0.00949	0.00039	0.46139	0.0468	0.0027	0.063316	0.005	0.0016	702	10.7	61.4	3.8	60.9	2.5	49	120	100	31	124%		
ABBEYRD_39	0.0828	0.0041	0.00934	0.00045	0.50885	0.0491	0.0031	0.3212	0.00418	0.00065	978	6.1	61.8	3.9	59.9	2.9	153	130	84.3	13	39%		
ABBEYRD_40	0.093	0.011	0.01296	0.00063	-0.061938	0.0519	0.0064	0.18715	0.00482	0.00075	355	3.0	89.5	9.9	60	4	150	160	97	15	55%		
ABBEYRD_41	0.0651	0.01	0.00789	0.00031	-0.03675	0.0606	0.0053	0.14812	0.00254	0.00035	421	0.7	63.6	9.3	63.7	2	450	290	51.3	7	11%		
ABBEYRD_42	0.08	0.012	0.00895	0.00042	-0.14647	0.068	0.012	0.2645	0.00384	0.00069	215	1.0	77	11	57.4	2.7	650	290	79	14	9%		
ABBEYRD_43	0.066	0.023	0.00858	0.0006	-0.13208	0.059	0.024	0.23262	0.0072	0.0037	80	1.0	63	21	55.1	3.8	-130	460	143	73	-42%		
ABBEYRD_44	0.0525	0.0056	0.00626	0.00035	-0.12304	0.046	0.048	0.28811	0.00251	0.00034	465	0.9	51.8	5.3	53	2.3	-50	130	50.7	6.8	-106%		
ABBEYRD_45	0.074	0.036	0.0434	0.0044	0.30384	0.079	0.0055	-0.019764	0.0283	0.0043	813	4.4	460	4.4	273	27	1572	100	524	84	17%		
ABBEYRD_46	0.0645	0.006	0.0099	0.00043	0.060496	0.0473	0.0046	0.17941	0.00296	0.00048	354	1.0	63.3	5.7	63.5	2.8	70	180	59.8	9.6	91%		
ABBEYRD_47	0.064	0.012	0.00784	0.00034	0.22477	0.06	0.011	-0.09551	0.00265	0.00049	413	1.8	62	11	50.4	2.2	350	290	53.5	9.8	14%		
ABBEYRD_48	0.147	0.047	0.01507	0.00068	0.25995	0.06	0.013	-0.18169	0.00454	0.00081	354	4.5	120	25	96.4	4.3	320	260	92	16	30%		
ABBEYRD_49	0.081	0.022	0.00775	0.00042	-0.11597	0.078	0.023	0.11961	0.00355	0.00081	167	1.1	77	20	49.8	2.7	570	400	71	16	9%		
ABBEYRD_50	0.071	0.016	0.00795	0.00041	0.1569	0.063	0.012	-0.063301	0.00381	0.00091	170.9	1.0	85	10	48.5	2.6	450	340	73	18	11%		
ABBEYRD_51	0.076	0.014	0.00996	0.00043	0.15169	0.0555	0.0097	-0.027142	0.0041	0.00072	153	1.9	73	13	63.9	2.8	260	280	83	15	25%		
ABBEYRD_52	1.752	0.096	0.1527	0.0069	0.9042	0.0836	0.0039	0.24004	0.0167	0.0035	1110	14.6	1025	35	915	39	1267	85	334	63	71%		
ABBEYRD_53	0.0602	0.0068	0.00822	0.00037	0.17855	0.0533	0.0059	0.12184	0.00291	0.00053	581	3.6	59.2	6.5	52.8	2.4	270	210	58.7	11	20%		
ABBEYRD_54	0.123	0.025	0.00976	0.0005	-0.18893	0.104	0.0045	0.51675	0.00271	0.00078	151	1.7	115	25	65.2	3.2	1300	460	97	31	4%		
ABBEYRD_55	0.0567	0.0038	0.00529	0.00032	0.14544	0.0495	0.0032	0.25332	0.00296	0.00037	1193	2.3	56	3.4	53.2	2	162	130	57.8	7.5	33%		
ABBEYRD_56	0.0577	0.0054	0.00847	0.00033	-0.19306	0.0517	0.0065	0.3182	0.00338	0.00068	498	7.4	56.9	5.2	54.4	2.1	140	160	60	14	39%		
ABBEYRD_57	0.145	0.025	0.0136	0.00067	0.01972	0.079	0.014	0.096946	0.00566	0.00088	1030	2.8	135	21	87	4.3	950	310	114	18	9%		
ABBEYRD_59	0.095	0.014	0.01147	0.00074	0.13356	0.0606	0.0038	0.06893	0.0057	0.0019	206.2	3.4	91	11	73.5	4.7	470	290	116	31	16%		
ABBEYRD_60	0.1423	0.061	0.01027	0.00049	0.1423	0.0489	0.0038	0.14516	0.00324	0.00046	524	1.9	67.7	4.9	65.9	2.6	140	140	54.7	9.3	41%		
ABBEYRD_62	0.093	0.015	0.01084	0.00049	0.143036	0.063	0.011	0.10794	0.00383	0.00059	223.1	1.6	89	14	69.5	3.1	490	290	77.3	12	14%		
ABBEYRD_63	0.0661	0.0073	0.00852	0.00039	-0.005082	0.057	0.007	0.18141	0.00272	0.00049	459	2.4	68.9	6.9	54.7	2.5	380	230	54.8	9.9	14%		
ABBEYRD_64	0.0879	0.0078	0.01332	0.00047	0.13989	0.0499	0.0042	0.13205	0.00387	0.00056	481	3.1	85.3	7	89.3	3	130	160	78.1	11	66%		
ABBEYRD_65	0.067	0.006	0.00868	0.00038	0.13289	0.0521	0.0049	0.51675	0.00271	0.00078	526	1.3	62.5	5.3	62.5	2.4	300	210	54.6	8	1%		
ABBEYRD_66	0.091	0.021	0.00924	0.00043	0.24719	0.088	0.021	-0.16202	0.00304	0.00062	173	0.8	87	19	52.9	2.7	1050	420	51	12	5%		
ABBEYRD_67	0.114	0.024	0.00975	0.00057	0.23072	0.083	0.017	-0.18501	0.0041	0.0014	161	1.2	107	21	62.6	3.6	880	370	83	27	7%		
ABBEYRD_68	0.077	0.027	0.00948	0.00043	-0.06309	0.067	0.023	0.05238	0.00274	0.00049	214	1.1	79	24	54.4	2.8	110	400	150	10	49%		
ABBEYRD_69	0.0566	0.006	0.01187	0.00054	-0.13313	0.0476	0.0088	0.18407	0.0034	0.00072	222	2.9	65.2	8.4	58.4	4.1	100	240	66	24	6%		
ABBEYRD_70	0.0949	0.0063	0.01189	0.00047	0.28407	0.092	0.0038	0.069573	0.0077	0.0031	1095	27.6	61	19	62	3	240	150	59.2	60	32%		
ABBEYRD_71	0.091	0.02	0.00749	0.00036	0.18605	0.088	0.019	-0.14636	0.0029	0.00043	285	0.9	87	18	48.1	2.3	1000	340	58.4	8.7	5%		
ABBEYRD_72	0.0625	0.0084	0.00799	0.0003	-0.021285	0.0567	0.0095	0.039562	0.00278	0.00041	282	0.8	81.2	8.6	51.3	1.9	270	180	56	8.2	19%		
ABBEYRD_73	0.183	0.046	0.01	0.00057	0.11923	0.141	0.041	0.143056	0.00381	0.00063	123	0.5	164	36	64.2	3.7	1750	420	77	17	4%		
ABBEYRD_74	0.185	0.018	0.01017	0.00063	-0.0038825	0.134	0.015	0.28711	0.0038	0.0017	147	2.2	171	16	65.2	4	2360	210	166	34	1%		
ABBEYRD_75	0.079	0.017	0.00935	0.00047	0.22679	0.068	0.014	-0.0072055	0.00239	0.00039	197	0.8	76	16	53.6	3	550	370	48.2	7.9	10%		
ABBEYRD_76	0.089	0.007	0.01138	0.00046	-0.25137	0.0663	0.0063	0.36558	0.00384	0.00058	506	2.5	86.3	8	72.9	2.9	420	200	77.4	12	17%		
ABBEYRD_77	0.0542	0.0031	0.00909	0.00031	0.27884	0.0493	0.0028	0.32642	0.00258	0.00033	1770	1.2	53.6	3	51.9	2	157	120	52.2	6.7	33%		
ABBEYRD_78	0.0635	0.006	0.00945	0.00036	0.42361	0.0468	0.0027	0.3305	0.0032	0.00045	630	5.0	43.5	3.2	60.7	3	790	240	64.5	9.1	44%		
ABBEYRD_79	0.154	0.021	0.01135	0.00055	0.08819	0.098	0.014	-0.0073811	0.00358	0.00062	150	0.7	143	18	72.8	3.5	1450	300	10.6	13	5%		
ABBEYRD_80	0.122	0.0064	0.01368	0.00063	0.52757	0.065	0.041	-0.14954	0.00802	0.0013	2360	10.3	1167	7.6	87.6	4	747	120	161	25	12%		
ABBEYRD_81	0.0561	0.0054	0.00809	0.00035	0.20007	0.0515	0.0056	0.025149	0.00269	0.00043	381	0.7	55.3	5.2	52	2.3	210	180	54.2	8.6	25%		
ABBEYRD_82	0.0708	0.0078	0.00946	0.00048	0.44296	0.0536	0.0048	-0.17125	0.00383	0.0006	740	2.9	69.2	7.3	60.7	3.1	320	200	77.2	12	19%		
ABBEYRD_83	0.067	0.008	0.01325	0.00046	0.040556	0.047	0.0041	0.16184	0.0037	0.00072	524	3.7	64.6	5.9	65.5	2.9	90	160	96	14	142%		
ABBEYRD_84	0.08	0.024	0.00776	0.00041	-0.041773	0.076	0.025	0.11478	0.00355	0.00084	184	1.0	76	21	49.9	2.6	320	380	72	17	16%		
ABBEYRD_85	0.059	0.011	0.00777	0.00032	0.27977	0.0554	0.01	-0.19851	0.00364	0.00084	332	2.1	58	11	49.9	2	240	290	73	17	21%		
ABBEYRD_86	0.172	0.027	0.00996	0.00045	0.56432	0.137	0.018	-0.24193	0.00518	0.00088	380	1.3	159	23	57.5	2.9	2040	270	104	18	3%		
ABBEYRD_87	0.093	0.01	0.00784	0.00035	0.39565	0.0679	0.0081	-0.0678	0.00281	0.00061	510	1.1	94	11	61.6	4.9	610	180	48.4	7.1	36%		
ABBEYRD_88	0.108	0.025	0.01004	0.00078	0.0032218	0.077	0.019	0.20333	0.00485	0.00095	199	4.1	102	22	64.4	4.6	870	320	98	19	10%		
ABBEYRD_89	0.106	0.032	0.00988	0.00055	0.084866	0.076	0.021	0.0034361	0.0047	0.00091	128.2	1.7	99	27	63.4	3.5							

analysis	ISOTOPIC RATIOS										ELEMENTAL CONCENTRATIONS		AGES							conc. (%)	
	206/238 vs 207/235 correlation		206/238 vs 207/235 correlation		206/238 vs 207/235 correlation		206/238 vs 207/235 correlation		206/238 vs 207/235 correlation		U (ppm)	U/Th	207/235 age (Ma)		206/238 age (Ma)		207/235 age (Ma)		206/238 age (Ma)		
	prop. 2s	prop. 2s	prop. 2s	prop. 2s	prop. 2s	prop. 2s	prop. 2s	prop. 2s	prop. 2s	prop. 2s			prop. 2s	prop. 2s	prop. 2s	prop. 2s	prop. 2s	prop. 2s	prop. 2s		prop. 2s
X15CA23B_29	0.0541	0.0059	0.00797	0.00047	0.35784	0.0493	0.0049	-0.05203	0.00287	0.00041	810	2.7	93.5	5.7	51.2	3	135	190	57.9	8.2	38%
X15CA23B_30	0.422	0.09	0.01057	0.00092	0.23885	0.262	0.051	0.08504	0.0112	0.0025	66.5	1.6	341	65	67.8	5.9	3270	380	276	50	2%
X15CA23B_31	0.141	0.049	0.008	0.00065	0.89689	0.112	0.03	-0.12445	0.0039	0.00078	448	10	127	40	51.3	4.1	1520	480	79	16	3%
X15CA23B_32	0.069	0.02	0.02659	0.0016	0.39574	0.0469	0.0049	-0.049387	0.0036	0.0013	263	1.9	159	17	169.1	16	60	200	173	25	262%
X15CA23B_33	0.0536	0.008	0.00783	0.00054	0.06621	0.049	0.0069	0.071275	0.00247	0.00041	634	1.0	52.8	7.5	50.3	3.4	60	200	49.8	8.3	84%
X15CA23B_34	0.059	0.012	0.00838	0.00053	-0.13499	0.0509	0.01	0.23882	0.00267	0.00069	188	2.1	57.6	11	53.8	3.4	110	310	54	14	49%
X15CA23B_35	0.2	0.022	0.0301	0.0019	0.35131	0.0486	0.0047	0.17701	0.01082	0.0015	270	2.7	184.7	19	191.1	12	127	200	217	30	150%
X15CA23B_36	0.1754	0.018	0.02526	0.0015	0.017279	0.0487	0.0047	0.52162	0.0033	0.0011	503	3.7	162.2	15	160.8	9.5	132	200	167	29	122%
X15CA23B_37	0.0546	0.0068	0.00786	0.00049	-0.16398	0.0621	0.0099	0.31475	0.0026	0.00039	254	0.7	53.7	9.5	60.5	3.2	160	310	52.6	7.8	32%
X15CA23B_38	0.07	0.014	0.00785	0.0005	-0.12943	0.064	0.013	0.19698	0.0026	0.00057	143.7	0.8	68	13	50.4	3.2	550	330	64.5	12	9%
X15CA23B_39	0.768	0.092	0.0426	0.0035	0.92678	0.1282	0.012	-0.2805	0.0289	0.0039	490	3.4	573	52	269	21	2081	160	576	76	13%
X15CA23B_40	0.207	0.026	0.02502	0.0017	0.14433	0.0531	0.0066	-0.00089105	0.0089	0.0013	224	2.6	190	22	178.1	10	280	240	179	25	64%
X15CA23B_41	0.056	0.022	0.00953	0.00069	0.38975	0.067	0.014	-0.17695	0.0048	0.00072	406	1.3	110	18	61.9	3.8	1170	330	30	14	5%
X15CA23B_42	0.056	0.009	0.00962	0.0006	0.25125	0.0488	0.0064	0.040308	0.0026	0.00051	347	2.1	54.7	8.5	54.7	3.8	-50	210	56.6	10	-109%
X15CA23B_43	0.219	0.025	0.0286	0.002	0.80721	0.0527	0.0049	-0.17115	0.0101	0.00013	840	2.7	202	20	180.4	13	305	200	203	26	60%
X15CA23B_44	0.186	0.019	0.02733	0.0018	0.22661	0.0481	0.0047	0.3371	0.00945	0.0014	354	1.8	173	17	173.8	11	109	200	190	29	159%
X15CA23B_45	0.2173	0.022	0.03199	0.0019	0.59985	0.0493	0.0047	-0.016954	0.00571	0.0013	710	2.6	199.4	16	203	12	157	200	186	25	125%
X15CA23B_46	0.0561	0.0084	0.00806	0.00054	0.11671	0.0472	0.0052	0.31248	0.0034	0.00031	1193	1.3	54.4	6.1	53	3.6	70	200	49.9	6.3	76%
X15CA23B_47	0.063	0.019	0.00808	0.00057	-0.065712	0.056	0.017	0.073448	0.0028	0.00058	143.9	1.4	61	17	51.9	3.6	130	400	57.8	12	40%
X15CA23B_48	0.062	0.028	0.00841	0.00069	0.12572	0.051	0.024	-0.055553	0.0036	0.00056	57	1.9	58	26	54	4.4	-190	650	63	17	-28%
X15CA23B_49	0.0502	0.0058	0.00786	0.00047	0.30489	0.0456	0.0049	0.064637	0.0034	0.00029	412.7	3.9	49.7	5.6	50.5	3	120	200	49	12	500%
X15CA23B_50	0.071	0.014	0.0079	0.00052	0.078492	0.063	0.012	-0.14407	0.00365	0.00076	197.6	1.0	49	14	60.7	3.4	640	390	70	16	8%
X15CA23B_51	0.0651	0.01	0.00597	0.00095	0.64246	0.0486	0.0056	-0.14202	0.0053	0.00021	301	3.5	63.7	9.7	60.1	6	130	220	106	42	50%
X15CA23B_52	0.0566	0.0063	0.00815	0.00053	0.49163	0.0503	0.0051	0.028553	0.0029	0.00044	779	3.8	55.8	6.1	52.4	3.4	200	210	56.6	8.9	26%
X15CA23B_53	0.1205	0.013	0.01784	0.0013	0.75446	0.0434	0.0046	0.02781	0.0026	0.0011	990	4.0	115.3	12	114	8.3	162	200	166	21	70%
X15CA23B_54	0.0097	0.022	0.00895	0.00074	0.57447	0.076	0.015	-0.27083	0.00368	0.00039	471	1.7	83	20	57.5	4.7	790	340	14	7%	
X15CA23B_55	0.562	0.087	0.01227	0.0011	0.14774	0.359	0.047	-0.01213	0.0189	0.0035	54.8	1.7	438	65	78.6	7.1	3360	70	377	69	2%
X15CA23B_56	0.0503	0.0056	0.00791	0.00049	0.29892	0.0469	0.0049	0.13286	0.0026	0.00038	694	0.8	49.8	5.4	50.8	3.1	60	200	53.6	7.8	85%
X15CA23B_57	0.0493	0.0056	0.00815	0.0005	0.43912	0.0437	0.0045	-0.115	0.00317	0.00075	409	5.9	48.8	5.4	52.3	3.2	-70	190	64	15	-75%
X15CA23B_58	0.061	0.021	0.00524	0.00068	0.18576	0.055	0.019	-0.1308	0.0029	0.0011	58	2.1	59	19	52.9	4.3	60	550	29	21	106%
X15CA23B_59	0.0515	0.0059	0.00772	0.00048	0.073889	0.0491	0.0053	0.018589	0.0027	0.00037	801	2.2	50.8	5.7	49.6	3.1	150	210	54.4	7.4	33%
X15CA23B_60	0.1954	0.019	0.02759	0.0016	0.40957	0.0506	0.0046	0.36945	0.0096	0.0011	608	2.8	181.1	16	175.5	10	207	210	180	23	85%
X15CA23B_61	0.0617	0.0098	0.00886	0.00082	0.79634	0.0495	0.0062	-0.17856	0.0035	0.00085	440	4.1	60.5	9.2	57.5	5.2	150	240	71	17	38%
X15CA23B_62	0.0843	0.0085	0.00966	0.00059	0.17383	0.049	0.0062	0.063996	0.0041	0.00073	439	1.6	63.1	8.1	62	3.7	120	230	83	15	52%
X15CA23B_63	0.0478	0.0068	0.00747	0.00053	0.04829	0.0482	0.0048	0.16623	0.00242	0.00041	537	2.7	46.7	5.7	46.7	2.8	-20	190	46.8	6.3	-240%
X15CA23B_64	0.053	0.008	0.00777	0.00046	-0.01219	0.0462	0.0054	0.02191	0.0025	0.00037	466	1.0	49.5	5.8	49.9	2.9	60	300	50.8	7.4	4%
X15CA23B_65	0.051	0.01	0.00787	0.00053	0.088017	0.0474	0.0092	-0.062019	0.004	0.0013	107.2	2.0	50.2	9.6	50.5	3.4	70	340	81	27	72%
X15CA23B_66	0.1508	0.016	0.02208	0.0015	0.65185	0.0434	0.0044	-0.12737	0.0072	0.00089	1370	2.0	142.4	14	140.7	9.7	162	200	145.1	18	87%
X15CA23B_67	0.0608	0.0061	0.00581	0.00058	0.61347	0.0471	0.0043	0.27037	0.00282	0.00038	1940	6.4	59.9	5.8	59.7	3.7	52	190	56.9	7.7	115%
X15CA23B_68	0.1178	0.01	0.02526	0.0011	0.81187	0.061	0.0047	-0.026207	0.00672	0.0011	658	3.3	165.8	16	160.7	9.4	231	270	176	22	20%
X15CA23B_69	0.186	0.038	0.00885	0.00066	0.46948	0.145	0.0027	-0.35292	0.0066	0.0015	82.6	1.3	169	32	56.8	4.2	2190	340	133	30	3%
X15CA23B_70	0.044	0.013	0.00803	0.00059	0.084677	0.041	0.012	0.0044687	0.00274	0.00061	90.5	1.5	42	13	51.6	3.8	-290	410	55	12	-18%
X15CA23B_71	0.128	0.017	0.00971	0.00063	0.46183	0.0864	0.012	-0.1812	0.00446	0.00067	162	1.2	122	15	62.3	4	1500	230	30	13	4%
X15CA23B_72	0.0784	0.0088	0.00899	0.00055	0.37884	0.0469	0.0063	0.16561	0.0025	0.00046	549	2.5	60.3	6.5	57.7	3.1	170	210	65.6	23	34%
X15CA23B_73	0.093	0.014	0.00827	0.00056	0.16545	0.0782	0.011	0.12019	0.0046	0.00063	296	1.4	13	53.1	3.2	1070	290	81.8	13	5%	
X15CA23B_74	0.203	0.023	0.02825	0.0018	0.17058	0.0525	0.0059	0.076536	0.0101	0.0014	244	2.5	187	19	179.6	11	270	230	209	29	67%
X15CA23B_75	0.067	0.0077	0.00799	0.00051	-0.00668	0.0555	0.007	0.29467	0.00286	0.00046	870	1.3	59.7	7.3	51.3	3.3	370	260	178	9.2	14%
X15CA23B_76	0.066	0.025	0.00778	0.00052	-0.18964	0.06	0.024	0.22628	0.00254	0.00071	81.1	1.7	61	22	50	3.4	-40	410	51	14	-125%
X15CA23B_77	0.0525	0.006	0.00778	0.00047	0.072119	0.061	0.022	0.14162	0.00296	0.00049	393	1.4	66.7								

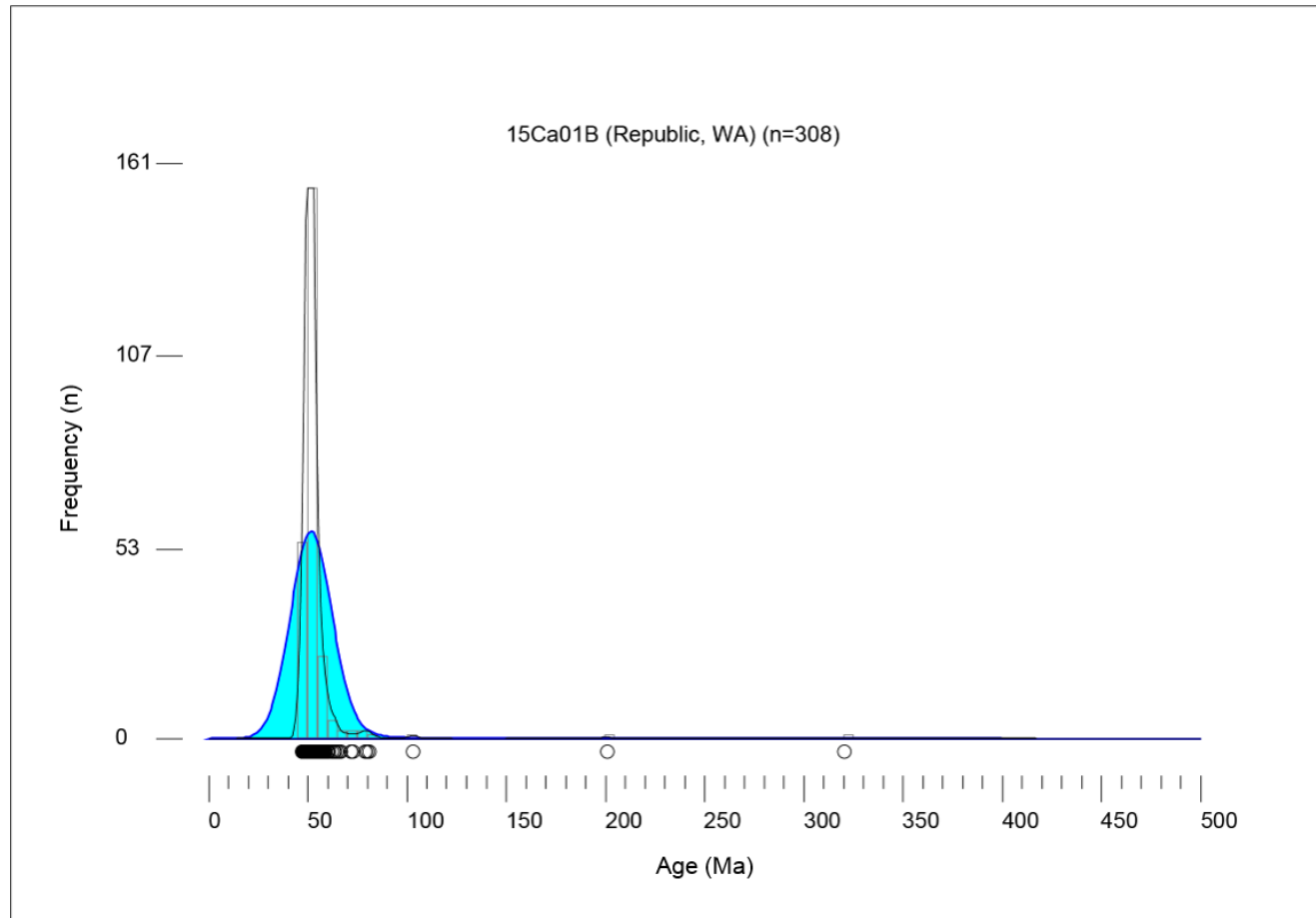
analysis	ISOTOPIC RATIOS										ELEMENTAL CONCENTRATIONS		AGES								conc. (%)
	206/238 vs 207/235 correlation		208/206 vs 207/206 correlation		208/206 vs 208/232 correlation		prop. 2s		[U] (ppm)	U/Th	207/235 age (Ma)		206/238 age (Ma)		208/232 age (Ma)		prop. 2s				
	207/235	prop. 2s	207/235	prop. 2s	208/232	prop. 2s	208/232	prop. 2s			207/235	prop. 2s	206/238	prop. 2s	208/232	prop. 2s	208/232				
CANBC1022G6B_30	0.1827	0.015	0.02971	0.0012	0.31754	0.0474	0.0035	0.19606	0.01021	0.00088	248	1.2	170.1	12	182.4	7.7	70	150	205	18	261%
CANBC1022G6B_31	0.1767	0.014	0.02642	0.00097	0.70763	0.049	0.003	-0.26433	0.008	0.00055	611	1.3	166.4	13	168.1	6.1	148	130	161	11	114%
CANBC1022G6B_32	0.043	0.0061	0.00709	0.00029	-0.11691	0.0455	0.0067	0.20718	0.00279	0.00039	232	2.5	42.6	5.9	45.5	1.8	-30	250	56.2	7.9	-152%
CANBC1022G6B_33	0.1638	0.011	0.02512	0.00095	0.58138	0.0491	0.0027	0.2796	0.0079	0.00051	2041	2.2	159.2	9.8	159.9	5.9	160	120	159	10	100%
CANBC1022G6B_35	0.1214	0.02	0.03178	0.0012	0.11986	0.05	0.0045	0.27316	0.0109	0.00015	132	4.2	196	16	201.7	7.5	160	170	218	30	126%
CANBC1022G6B_36	0.1821	0.013	0.02612	0.001	0.44963	0.0507	0.0029	0.32655	0.00883	0.00055	509	1.9	169.7	11	166.2	6.4	218	130	177.6	11	76%
CANBC1022G6B_37	0.1636	0.013	0.02455	0.00091	0.42204	0.0486	0.0031	0.071289	0.00772	0.0003	374	1.5	163.6	11	156.4	5.7	128	130	156.5	10	122%
CANBC1022G6B_38	0.1626	0.013	0.02397	0.00092	0.24059	0.0493	0.0033	0.31011	0.00976	0.0002	634	1.5	170.2	11	171.6	5.6	160	130	176.3	12	107%
CANBC1022G6B_40	0.38	0.1	0.0276	0.0021	0.89638	0.083	0.015	-0.79907	0.011	0.0013	376	1.0	304	67	175	13	1060	340	221	26	16%
CANBC1022G6B_41	0.121	0.016	0.0168	0.0016	0.75788	0.0518	0.0046	0.044428	0.006	0.0011	294	4.5	117	15	107	10	260	180	122	22	41%
CANBC1022G6B_42	0.1728	0.013	0.02511	0.0009	0.40773	0.0508	0.0034	0.07414	0.00872	0.00064	461	1.7	161.6	11	159.9	5.6	212	140	179.5	13	75%
CANBC1022G6B_43	0.176	0.013	0.02368	0.00095	0.45896	0.0492	0.0033	0.10267	0.00956	0.00064	765	1.6	166.2	10	161.6	5.1	161	120	160.7	11	100%
CANBC1022G6B_44	0.172	0.015	0.0251	0.0013	0.71579	0.0506	0.0031	0.091484	0.00967	0.00083	371	2.7	160.6	13	159.6	8.5	229	120	175	17	70%
CANBC1022G6B_45	0.324	0.024	0.02556	0.0009	0.12894	0.0938	0.0065	0.29226	0.01655	0.0012	522	2.1	287	19	162.7	5.7	1473	130	332	24	11%
CANBC1022G6B_46	0.1716	0.013	0.02362	0.00079	0.11662	0.052	0.0032	0.40789	0.0083	0.00056	898	1.7	160.6	11	150.5	5	288	140	167	11	53%
CANBC1022G6B_47	0.1737	0.013	0.02351	0.00087	0.50622	0.0508	0.0029	0.21689	0.00869	0.00067	578	2.5	162.5	11	161.1	6.1	210	130	173	13	77%
CANBC1022G6B_48	0.1744	0.013	0.02378	0.00084	0.46593	0.0493	0.0032	0.33871	0.00906	0.00065	802	3.1	163.2	9.7	164.1	5.7	198	120	162.3	13	104%
CANBC1022G6B_49	0.1987	0.013	0.0275	0.0013	0.81455	0.053	0.0029	0.81633	0.00979	0.00069	1980	2.2	184	11	175	8.4	322	120	156.8	14	54%
CANBC1022G6B_50	0.204	0.016	0.0272	0.0013	0.64192	0.0545	0.0033	0.20091	0.00907	0.00028	402	2.0	197.9	13	173	8.1	388	130	182	16	45%
CANBC1022G6B_51	0.1845	0.013	0.02507	0.00094	0.45723	0.0524	0.0031	0.17828	0.00864	0.00069	673	2.3	171.8	11	165.9	5.8	302	130	173.8	12	55%
CANBC1022G6B_52	0.1708	0.016	0.02303	0.00082	0.45896	0.0492	0.0033	0.16931	0.00778	0.00077	222	1.6	160.9	10	161.6	5.1	161	120	160.7	11	100%
CANBC1022G6B_53	0.1439	0.011	0.0214	0.0013	0.82378	0.0519	0.0029	0.62585	0.00661	0.00058	2090	1.8	141.7	5.3	136.6	7.9	272	120	131	14	50%
CANBC1022G6B_54	0.176	0.014	0.02553	0.00091	-0.17135	0.0506	0.0039	0.37957	0.00875	0.00077	380	2.1	164.3	12	162.5	5.7	200	150	176	15	81%
CANBC1022G6B_55	0.175	0.012	0.0266	0.00094	0.75603	0.048	0.0026	-0.090194	0.0083	0.00051	1380	2.3	165.6	11	169.2	5.9	100	120	167	10	169%
CANBC1022G6B_56	0.1939	0.012	0.0245	0.0012	0.32628	0.0564	0.0039	0.47038	0.00862	0.00072	278	1.1	176	14	147	7.7	440	150	187.8	17	33%
CANBC1022G6B_57	0.1744	0.012	0.02569	0.00096	0.60285	0.0496	0.0028	-0.068682	0.00874	0.00066	567	2.3	163.1	11	163.5	5.4	171	20	175.9	13	96%
CANBC1022G6B_58	0.254	0.034	0.02684	0.0009	0.20031	0.0751	0.01	-0.030845	0.0097	0.00087	670	1.7	227	26	164.4	5.7	930	250	196	17	18%
CANBC1022G6B_59	0.1714	0.012	0.0254	0.00083	0.53889	0.0486	0.0027	0.06111	0.00814	0.00052	1375	1.4	160.5	10	161.7	5.2	129	120	163.9	11	125%
CANBC1022G6B_60	0.0988	0.0049	0.00635	0.00031	0.24104	0.0501	0.0034	0.14084	0.00914	0.00033	691	1.4	88	4.7	53.6	2	189	140	63.4	6.6	28%
CANBC1022G6B_61	0.1621	0.011	0.02546	0.00095	0.4465	0.0479	0.0027	0.51552	0.009	0.0011	1309	33.4	167.7	10	162.2	6	236	120	162	23	162%
CANBC1022G6B_62	0.167	0.012	0.02521	0.00086	0.32455	0.0481	0.0028	0.39981	0.00788	0.00053	1028	1.0	156.7	10	160.5	5.4	109	120	158.7	11	147%
CANBC1022G6B_63	0.236	0.026	0.0286	0.0017	-0.12887	0.0605	0.0074	0.57415	0.01015	0.00076	593	1.7	214	21	181.6	11	590	280	204	15	31%
CANBC1022G6B_64	0.295	0.022	0.0168	0.0013	-0.2508	0.125	0.012	0.75936	0.00967	0.00066	3100	1.6	254	17	107.9	7.9	2020	200	192.4	13	5%
CANBC1022G6B_65	0.2063	0.016	0.0261	0.0011	0.2063	0.0588	0.0027	0.073138	0.00862	0.00072	278	1.1	176	14	163.4	6.6	260	150	173	15	65%
CANBC1022G6B_66	0.1734	0.012	0.02567	0.00096	0.59793	0.0489	0.0027	-0.087615	0.00874	0.00066	567	2.3	163.1	11	163.5	5.4	171	20	175.9	13	96%
CANBC1022G6B_67	0.1809	0.014	0.02598	0.0009	0.58224	0.0498	0.003	-0.029496	0.00851	0.00061	569	2.3	168.6	12	163.5	5.6	207	140	171.3	12	80%
CANBC1022G6B_68	0.1724	0.013	0.02489	0.00087	0.187	0.0504	0.003	0.19049	0.0092	0.00012	754	2.4	161.3	11	159.1	5.5	200	130	186	25	80%
CANBC1022G6B_69	0.1789	0.012	0.02517	0.00083	0.2673	0.0517	0.0031	0.31596	0.00798	0.00056	527	1.7	167.9	11	160.2	5.2	261	130	160.7	10	61%
CANBC1022G6B_70	0.1777	0.012	0.02561	0.00091	0.46781	0.0508	0.0033	0.032695	0.00786	0.00056	676	2.3	163.1	11	163.5	5.4	226	130	162.3	13	75%
CANBC1022G6B_71	0.199	0.017	0.02586	0.0011	0.22596	0.0527	0.0039	0.024536	0.00983	0.00063	573	1.8	175.6	14	164.6	6.9	280	150	179.3	13	59%
CANBC1022G6B_72	0.219	0.018	0.0311	0.0014	0.25211	0.0519	0.0039	0.30999	0.0107	0.0011	195	2.6	200.6	15	197.1	8.5	280	150	214	23	70%
CANBC1022G6B_73	0.0462	0.0065	0.00674	0.00031	0.39683	0.0511	0.0059	-0.13522	0.00247	0.0004	259	2.6	45.7	5.3	43.3	2	270	230	49.9	8	16%
CANBC1022G6B_74	0.2243	0.016	0.0321	0.0011	0.60675	0.0508	0.0027	0.07294	0.00862	0.00072	850	2.3	205.4	12	203.6	6.9	234	120	212	13	91%
CANBC1022G6B_75	0.1759	0.014	0.02519	0.0011	0.56789	0.0504	0.0033	0.024597	0.00801	0.00055	464	1.1	154.1	12	164.4	6.9	202	140	161.3	11	75%
CANBC1022G6B_76	0.0539	0.0051	0.00734	0.00038	0.16311	0.0498	0.0045	0.16564	0.00249	0.0002	584	1.0	53.3	4.8	51	2.4	130	160	50.2	4.1	39%
CANBC1022G6B_77	0.1642	0.012	0.02467	0.00086	0.22616	0.0494	0.0034	0.34089	0.00756	0.00056	347	1.6	154.2	11	157.1	5.4	170	140	152.2	11	92%
CANBC1022G6B_78	0.1668	0.014	0.02389	0.00092	-0.060103	0.0501	0.0039	0.24115	0.00864	0.00062	132	1.1	156.3	12	152.8	5.8	190	160	174	17	80%
CANBC1022G6B_79	0.175	0.015	0.0256	0.0011	0.91261	0.0467	0.0029	0.07919	0.00729	0.00022	1700	0.9	105.2	64	163.6	10	423.2	71	655	43	8%
CANBC1022G6B_80	0.2126	0.016	0.03152	0.0011	-0.010444	0.0487	0.0033	0.40335	0.01039	0.0011	311	2.8	195.4	14	200.1	6.7	135	140	209	20	146%
CANBC1022G6B_81	0.1665	0.013	0.02455	0.00087	0.21228	0.0493	0.0036	0.070707	0.00844	0.0006	333	1.5	156.1	11	156.4	5.5	150	140	169.8	12	104%
CANBC1022G6B_82	0.1079	0.008	0.01605	0.00054	0.85487	0.048	0.0028	-0.24104	0.00607	0.00047	765	2.8	103.9	7.3	102.6	3.4	99	120	122.2	11	104%
CANBC1022G6B_83	0.1743	0.012	0.02563	0.00095	0.17692	0.051	0.0031	0.029982	0.00802	0.00055	527	1.7	167.9	11	160.2	5.2	261	130	160.7	10	61%
CANBC1022G6B_84	0.1548	0.012	0.02137	0.00091	0.80881	0.0526	0.0029	0.26116	0.00604	0.00048	2000	0.9	145.9	10	138.3	5.8					

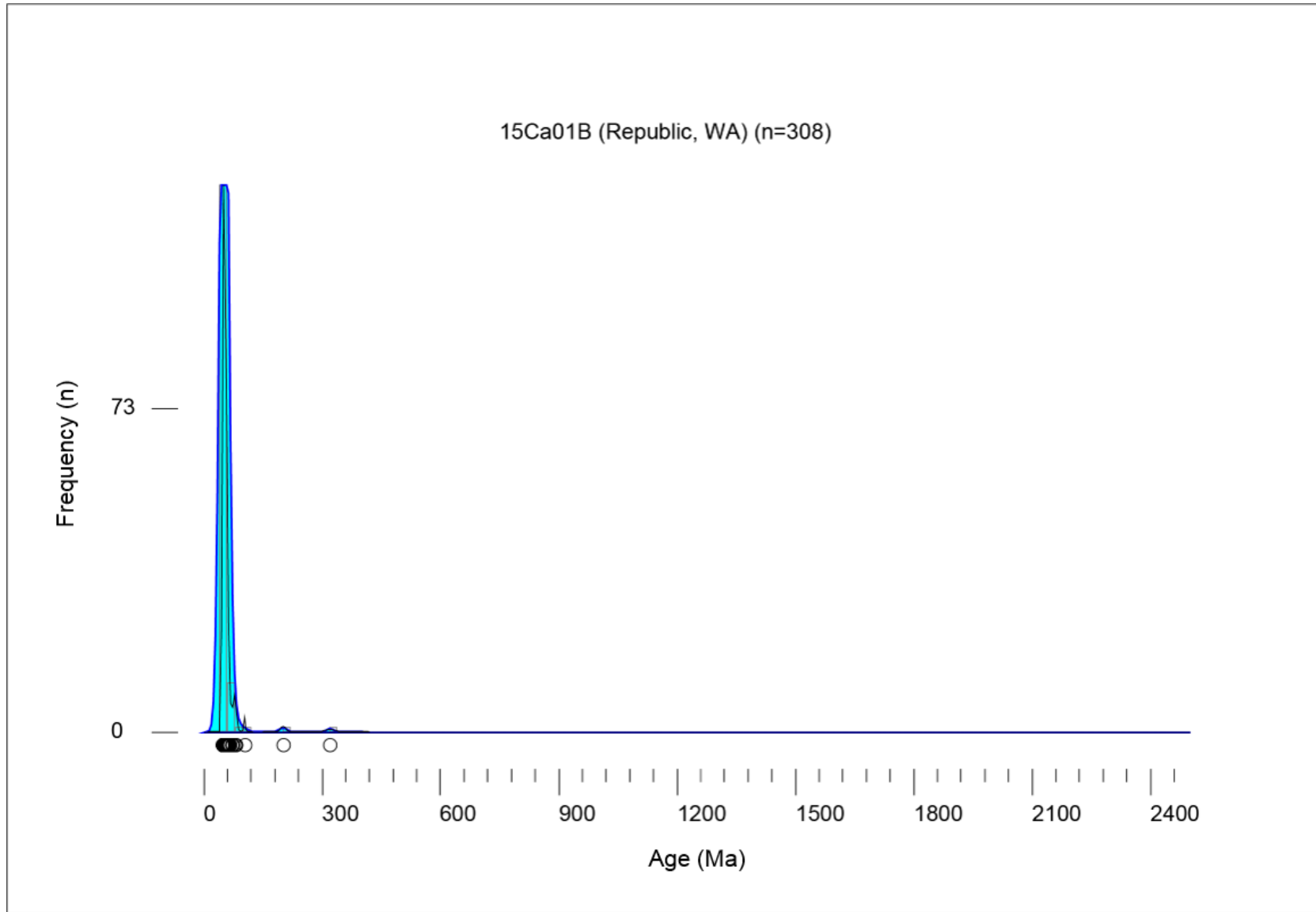
analysis	ISOTOPIC RATIOS										ELEMENTAL CONCENTRATIONS		AGES							conc. (%)		
	207/235	206/238	206/238 vs 207/235 error correlation	206/238 vs 207/235 error correlation	207/235	207/235 error correlation	208/232	207/235 error correlation	208/232	prop. 2s	[U] (ppm)	U/Th	207/235 age (Ma)	prop. 2s (Myr)	206/238 age (Ma)	prop. 2s (Myr)	207/235 age (Ma)	prop. 2s (Myr)	208/232 age (Ma)		prop. 2s (Myr)	
	prop. 2s	prop. 2s	prop. 2s	prop. 2s	prop. 2s	prop. 2s	prop. 2s	prop. 2s	prop. 2s	prop. 2s	prop. 2s	prop. 2s	prop. 2s	prop. 2s	prop. 2s	prop. 2s	prop. 2s	prop. 2s	prop. 2s		prop. 2s	
COLDWATER_1_25	0.0512	0.0022	0.00003	0.00032	0.18995	0.0461	0.0023	0.66141	0.00271	0.0004	860	1.3	90.6	2.1	51.5	2.1	29	96	54.7	8.1	170%	
COLDWATER_1_26	0.199	0.045	0.01799	0.00089	0.82047	0.076	0.0123	-0.67764	0.0091	0.0018	591	1.8	179	35	115	5.7	980	310	183	35	12%	
COLDWATER_1_27	0.1329	0.0059	0.02021	0.00073	0.36775	0.0473	0.0023	0.070021	0.00662	0.0011	520	3.8	126	5.3	129	4.6	79	97	138	21	163%	
COLDWATER_1_29	0.164	0.013	0.02342	0.00033	0.39887	0.0512	0.0034	-0.084518	0.0084	0.0015	392	4.3	154	11	149.2	5.2	230	130	170	29	65%	
COLDWATER_1_30	0.265	0.017	0.0385	0.0018	0.31667	0.0454	0.0029	0.28355	0.0115	0.002	144	3.0	240	13	243.7	11	80	110	242	38	487%	
COLDWATER_1_31	0.215	0.008	0.0321	0.0012	0.11695	0.0466	0.0019	0.42057	0.0105	0.0016	543	4.2	197.6	6.7	203.7	7.4	31	84	212	32	657%	
COLDWATER_1_32	0.1879	0.0093	0.02736	0.0011	0.36685	0.048	0.0024	0.27368	0.00941	0.0014	543	2.3	174.5	7.9	174	6.8	103	100	189	27	169%	
COLDWATER_1_33	0.1776	0.0081	0.02669	0.001	0.35702	0.0464	0.002	0.25134	0.00832	0.0011	305	1.5	165.8	7	169.8	6.4	53	88	167	22	320%	
COLDWATER_1_34	0.21	0.014	0.03189	0.0012	0.23351	0.0479	0.0033	0.07675	0.0108	0.0016	346	2.6	195	12	202.3	7.6	100	130	217	30	202%	
COLDWATER_1_35	0.4	0.075	0.0206	0.0013	0.22518	0.14	0.027	0.11241	-3700	1400	47.2	-924000.0		336	56	131.6	8.5	1950	390	24300	1600	7%
COLDWATER_1_36	0.5672	0.0097	0.0578	0.0021	0.81288	0.0717	0.0016	0.8759	0.01184	0.0013	5270	0.9	456	6.3	362	13	979	46	237.9	26	37%	
COLDWATER_1_37	0.0578	0.0031	0.0097	0.00039	0.43866	0.0437	0.0024	0.045902	0.00372	0.00063	710	5.5	57.1	3	62.2	2.5	85	96	75	13	-73%	
COLDWATER_1_38	0.0884	0.0037	0.011	0.00041	0.21425	0.0451	0.0025	0.16285	0.00317	0.00039	1140	1.6	67.2	3.5	70.5	2.6	-17	100	54	7.6	-415%	
COLDWATER_1_39	0.142	0.0048	0.02225	0.00082	0.26844	0.0471	0.002	0.39642	0.00719	0.0011	747	4.3	134.8	4.3	141.9	5.2	62	90	145	23	273%	
COLDWATER_1_40	0.638	0.065	0.0226	0.0014	0.31031	0.203	0.012	0.23401	0.0431	0.0044	47.8	4.1	494	40	144.3	8.8	2860	150	850	180	5%	
COLDWATER_1_41	0.1472	0.0062	0.02207	0.00084	0.45346	0.0491	0.002	0.22999	0.00772	0.001	695	2.9	139.2	5.5	140.7	5.3	137	89	155	20	103%	
COLDWATER_1_42	0.0561	0.0047	0.00818	0.00037	-0.044511	0.0485	0.0042	-0.44012	0.00277	0.0005	250	1.7	95.3	4.5	52.5	2.4	140	170	95	10	38%	
COLDWATER_1_43	0.213	0.018	0.0195	0.0009	-0.15883	0.0784	0.0073	0.4223	0.00504	0.0011	152.7	1.0	195	15	123.2	5	1110	200	166	22	11%	
COLDWATER_1_44	0.269	0.015	0.02076	0.00083	0.13889	0.0502	0.0062	0.26713	0.00821	0.0013	151.8	0.8	241	12	132.4	5.3	1430	120	165	26	9%	
COLDWATER_1_45	0.1521	0.0099	0.02111	0.00081	0.38625	0.053	0.0034	-0.0010522	0.0084	0.0014	311	4.1	143.4	8.7	134.7	5.1	300	130	170	28	45%	
COLDWATER_1_46	0.221	0.01	0.03134	0.0012	0.1937	0.0499	0.0024	0.31214	0.01022	0.0014	316	2.1	202.3	6.5	189.9	7.2	184	100	205	28	106%	
COLDWATER_1_47	0.1589	0.0085	0.02121	0.00089	0.40806	0.0529	0.0029	0.22794	0.0108	0.0026	422	3.0	149.6	7.4	155.3	5.5	380	120	211	52	36%	
COLDWATER_1_48	0.218	0.012	0.03081	0.0012	0.3478	0.0525	0.0028	0.12663	0.0113	0.002	219.5	3.6	201.7	9.6	192.4	7.6	310	110	227	40	62%	
COLDWATER_1_49	0.1589	0.0069	0.02404	0.0009	0.087479	0.0486	0.0025	0.44022	0.0077	0.0013	478	4.8	149.5	6	153.1	5.7	110	110	156	26	139%	
COLDWATER_1_50	0.1522	0.0047	0.0221	0.00077	-0.0016209	0.0502	0.0019	0.45811	0.0079	0.0012	927	3.9	143.8	4.1	140.9	4.8	200	81	159	23	70%	
COLDWATER_1_51	0.208	0.0097	0.02755	0.0013	0.30514	0.0554	0.0031	0.66889	0.0067	0.0017	213	319.0	192.4	8.2	175.2	8	430	130	350	430	41%	
COLDWATER_1_52	0.0577	0.0056	0.01353	0.00054	0.083246	0.0461	0.0032	0.23816	0.00445	0.00067	424	2.5	85.2	6.2	66.1	3.4	50	80	94	34	173%	
COLDWATER_1_53	0.233	0.082	0.0096	0.00005	0.92587	0.143	0.039	-0.8174	0.0069	0.0023	287	1.1	193	6.1	61.8	5.4	1510	510	139	46	4%	
COLDWATER_1_54	0.433	0.024	0.0573	0.0023	0.23867	0.0545	0.0032	0.25572	0.0183	0.003	170	2.4	364	17	399.4	14	380	130	366	61	95%	
COLDWATER_1_55	0.2693	0.0088	0.0342	0.0015	0.70947	0.0551	0.0016	0.18532	0.01049	0.0012	1577	1.6	234.6	7	216.5	9.2	408	68	211	25	53%	
COLDWATER_1_56	0.1657	0.0041	0.02476	0.00087	0.62868	0.049	0.0014	0.37014	0.0074	0.00084	3910	2.9	158.3	5.5	157.8	6.1	146	65	145	17	103%	
COLDWATER_1_57	0.1506	0.0074	0.02254	0.00089	0.50675	0.0494	0.002	0.19276	0.00842	0.00098	1120	1.2	142.2	6.5	143.7	6.2	162	84	169.4	20	89%	
COLDWATER_1_58	0.1775	0.007	0.02613	0.00096	0.33052	0.0488	0.0021	0.22031	0.00823	0.001	809	1.8	165.7	6	166.3	6	153	92	166	20	103%	
COLDWATER_1_59	0.0726	0.0036	0.01145	0.00045	0.51361	0.0464	0.0023	-0.024652	0.00347	0.00046	1116	1.9	71.1	3.4	73.4	2.8	99	97	70.1	9.3	188%	
COLDWATER_1_60	0.0655	0.0055	0.00862	0.00038	0.4441	0.0555	0.0071	-0.22752	0.00283	0.00038	360	0.9	64.3	8.2	55.3	2.4	320	240	57.1	7.7	17%	
COLDWATER_1_61	0.0577	0.0056	0.01332	0.00077	0.21908	0.0498	0.0022	0.24654	0.00724	0.0011	875	3.3	138	4.6	136	4.9	170	146	23	146	23	
COLDWATER_1_63	0.0565	0.0021	0.00895	0.00034	0.34457	0.0465	0.0019	0.2824	0.00307	0.00057	2450	8.4	55.8	2.1	57.4	2.1	29	85	62	12	196%	
COLDWATER_1_64	0.1479	0.0044	0.02216	0.0008	0.33715	0.0484	0.0017	0.17091	0.00762	0.00084	1150	2.6	140	3.9	141.3	5	117	75	153	19	121%	
COLDWATER_1_65	0.1519	0.0079	0.02325	0.00091	0.34869	0.048	0.0026	0.20054	0.00743	0.0011	335	3.3	143.4	7	148.2	5.7	130	110	150	23	114%	
COLDWATER_1_66	0.239	0.013	0.0293	0.001	0.29596	0.0489	0.0041	0.24680	0.01025	0.0014	248	1.3	217	11	161	6.6	870	120	206	28	19%	
COLDWATER_1_67	0.23	0.012	0.02962	0.0011	0.18193	0.0575	0.0032	0.25346	0.00967	0.0014	331	1.9	203.7	9.9	187.6	6.8	480	120	194	28	39%	
COLDWATER_1_69	0.0707	0.0073	0.01091	0.0005	0.47244	0.0476	0.0044	-0.10281	0.0043	0.0017	260	17.7	69.1	6.9	69.9	3.2	80	170	87	35	87%	
COLDWATER_1_70	0.194	0.012	0.02925	0.0011	0.23003	0.0503	0.0031	0.11455	0.011	0.0017	233	3.4	180	10	179.6	6.8	210	130	220	34	86%	
COLDWATER_1_71	0.218	0.012	0.03103	0.0013	0.26848	0.0519	0.0029	0.24856	0.01033	0.0014	353	1.9	201.3	9.7	186.9	7.6	260	110	208	28	76%	
COLDWATER_1_72	0.057	0.0055	0.011	0.00042	0.098145	0.0511	0.0028	0.35342	0.00332	0.00046	925	2.0	74.8	3.5	70.5	2.7	330	110	67	9.2	31%	
COLDWATER_1_73	0.1562	0.0056	0.02416	0.0009	0.032827	0.0472	0.002	0.48862	0.00663	0.0013	618	7.1	148.1	4.7	153.9	5.7	70	86	174	26	220%	
COLDWATER_1_74	0.308	0.022	0.03764	0.0014	0.46827	0.0582	0.0035	-0.099109	0.0123	0.0017	312.7	2.2	271	17	238.2	8.9	540	140	246	34	44%	
COLDWATER_1_75	0.153	0.012	0.02309	0.00087	0.15693	0.0486	0.004	0.16103	0.0086	0.0017	260	4.0	144	11	147.2	5.5	180	170	173	33	82%	
COLDWATER_1_76	0.225	0.013	0.03154	0.0013	0.19454	0.0529	0.0029	0.32621	0.0104	0.0016	296.7	2.2	205	11	200.2	8.2	190	120	209	32	105%	
COLDWATER_1_77	0.1124	0.0075	0.01693	0.00068	-0.16259	0.048	0.0037	0.51235	0.00614	0.001	260	2.3	109.1	6.6	108.2	4.3	130	150	124	21	83%	
COLDWATER_1_78	0.1475	0.0059	0.02181	0.00082	0.20017	0.0492	0.0022	0.33424	0.007	0.0013	564	4.7	139.6	5.2	139.1	5.2	167	98	140	25	83%	
COLDWATER_1_79	0.1869	0.0073	0.02667	0.0011	0.15627	0.0508	0.0023	0.086298	0.00848	0.001	820	1.5	172.9	6.3	169.6	6.6	220	96	170.8	20	77%	
COLDWATER_1_80	0.272	0.014	0.0354	0.0014	0.33621	0.0569	0.0027	0.27181	0.0135	0.0027	325	6.6	244	11	224.2	8.9	459	100	271	54	45%	
COLDWATER_1_81	0.1467	0.0066	0.02207	0.00078	0.20349	0.0482	0.0024	0.1508	0.00749	0.0012												

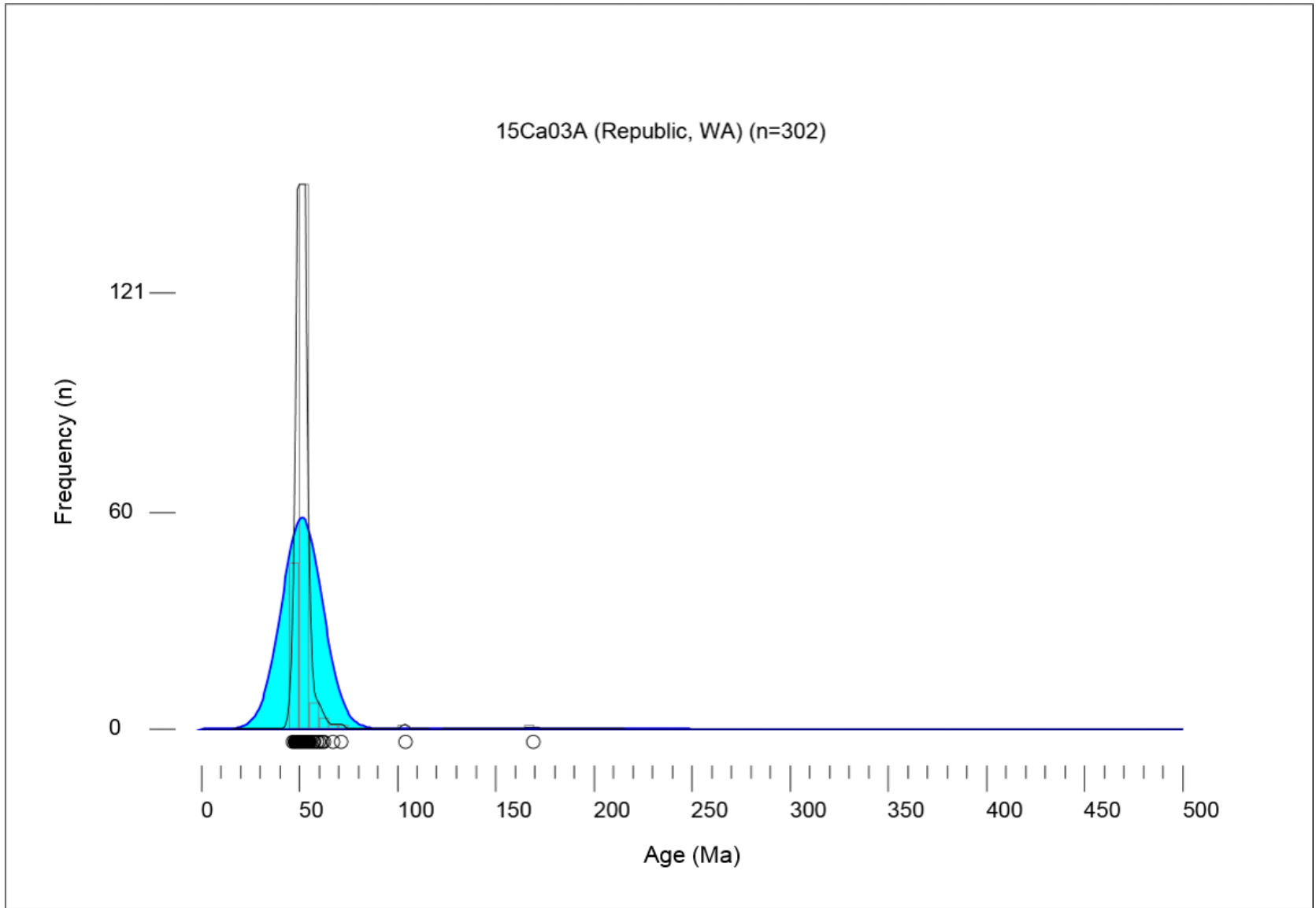
APPENDIX C

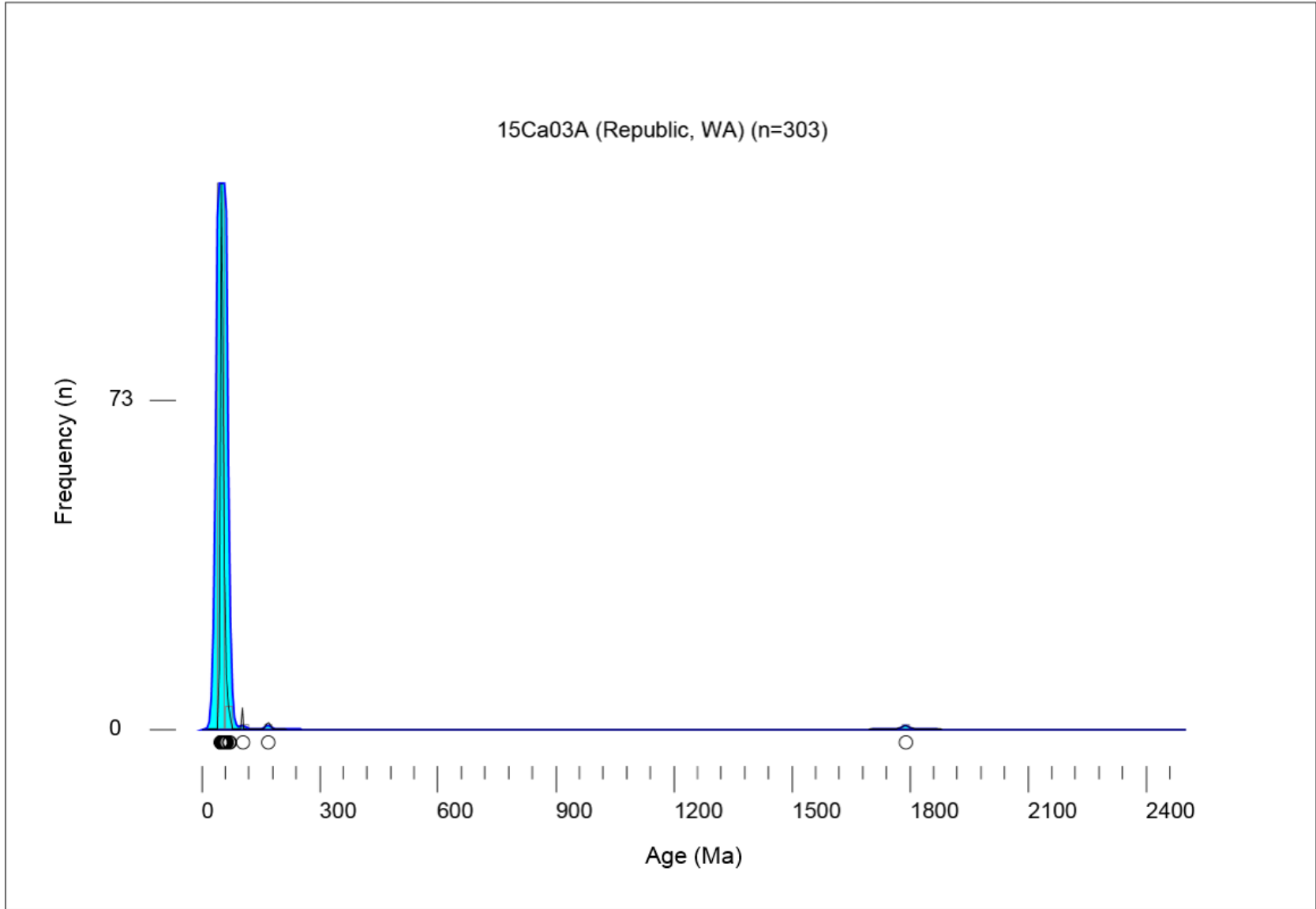
DETRITAL ZIRCON U-PB KDE (BLUE) & PDP (BLACK) PLOTS

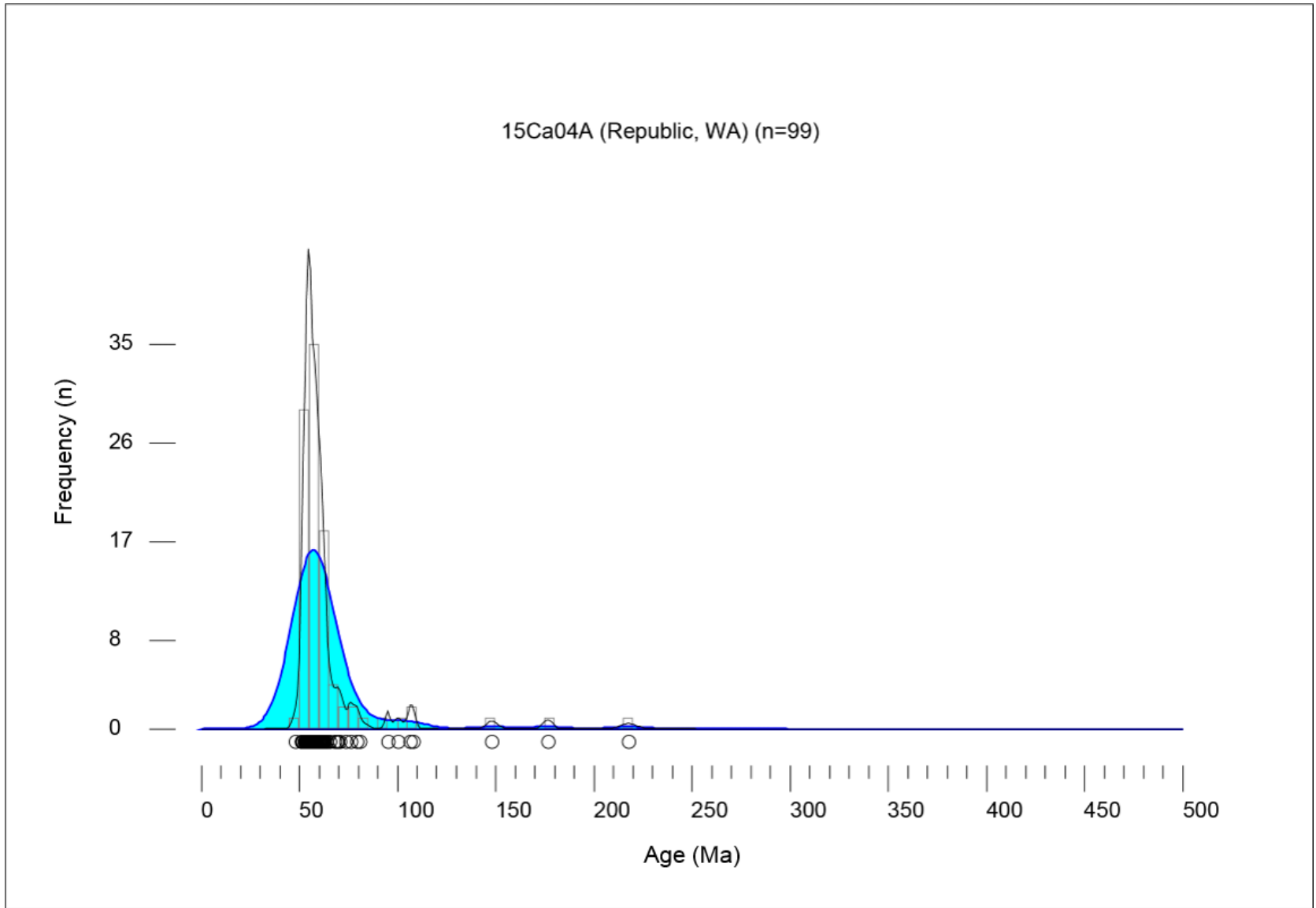
SEPARATED BY SAMPLE (0-500 MA, & 0-2,400 MA)

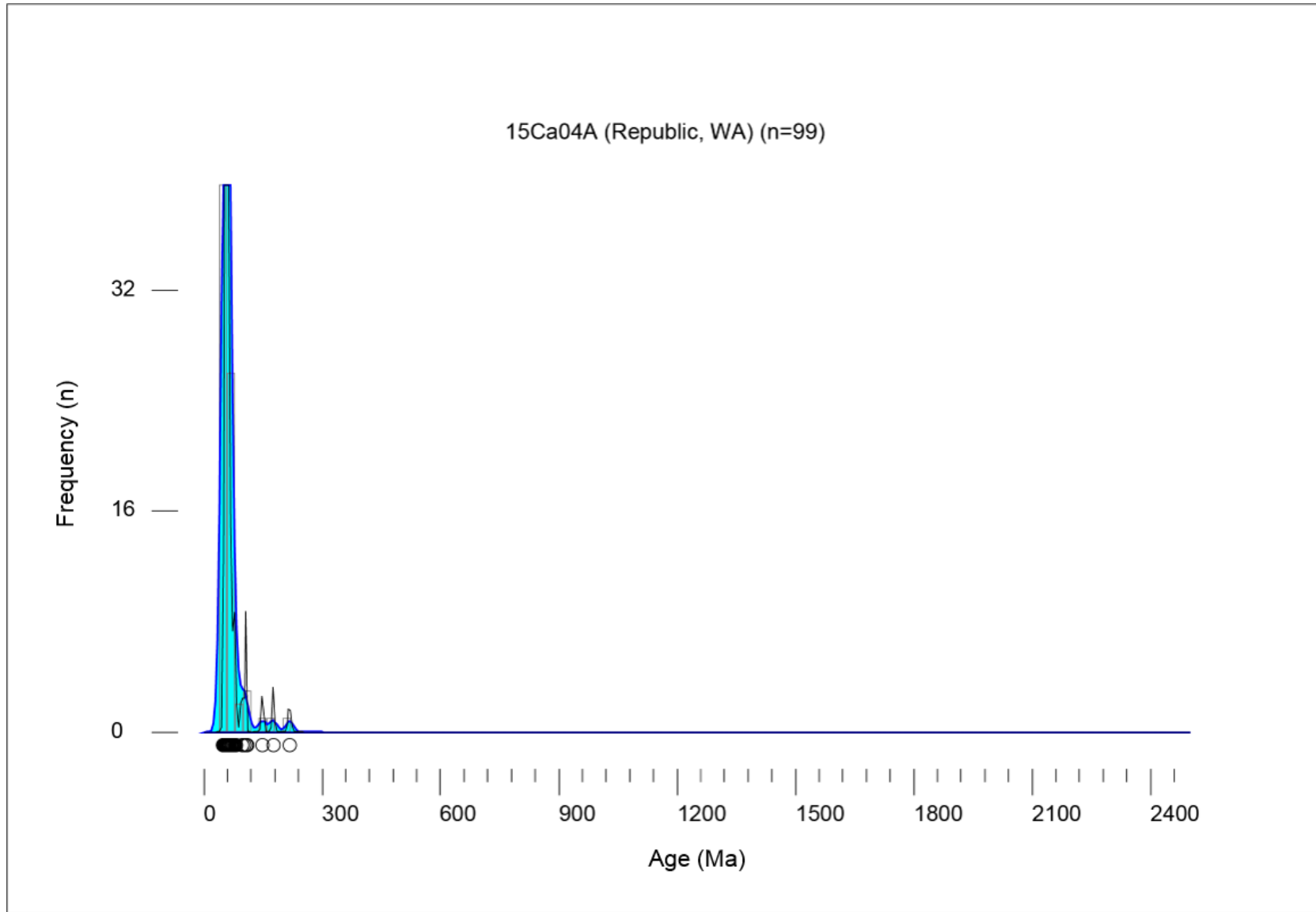


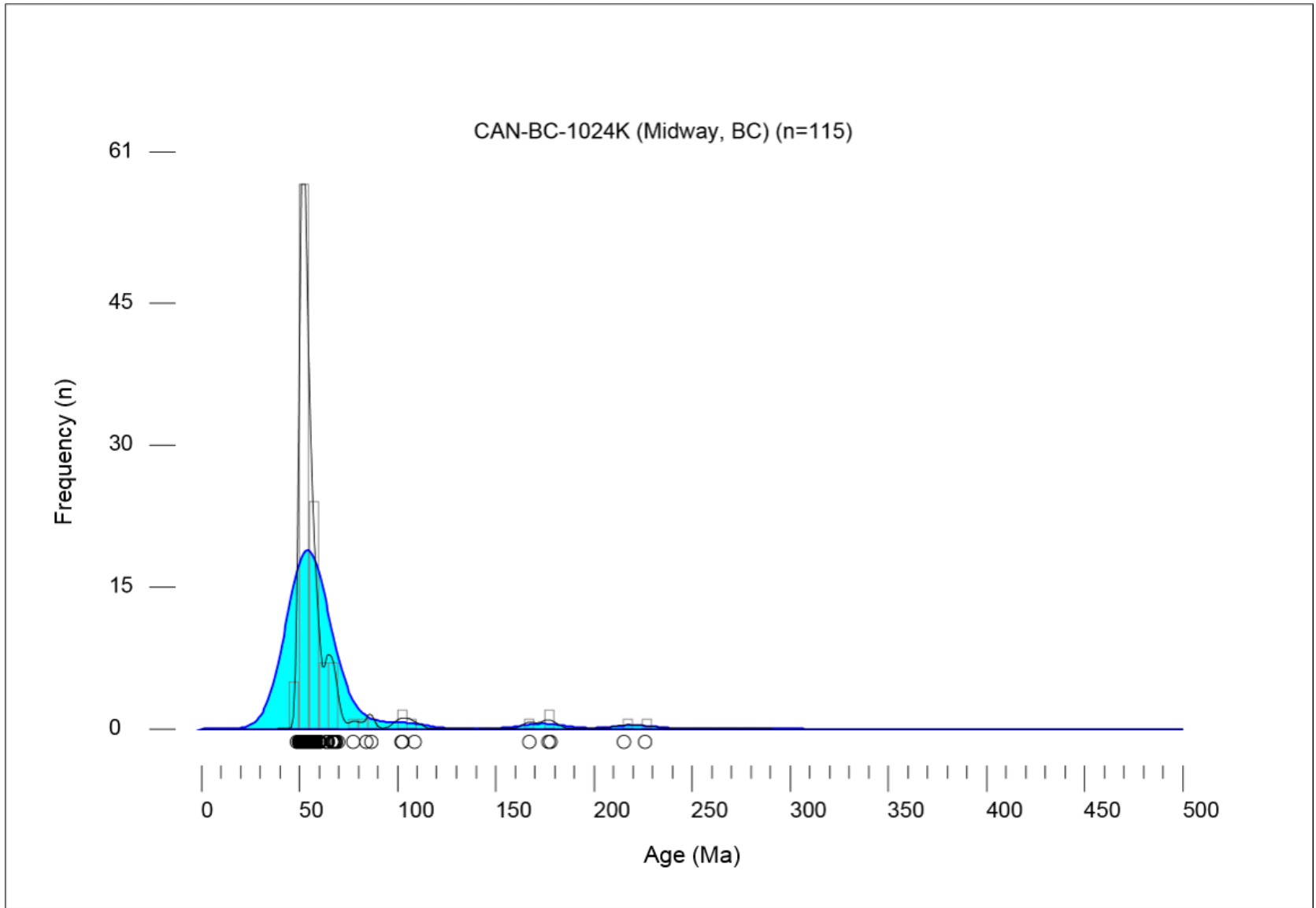


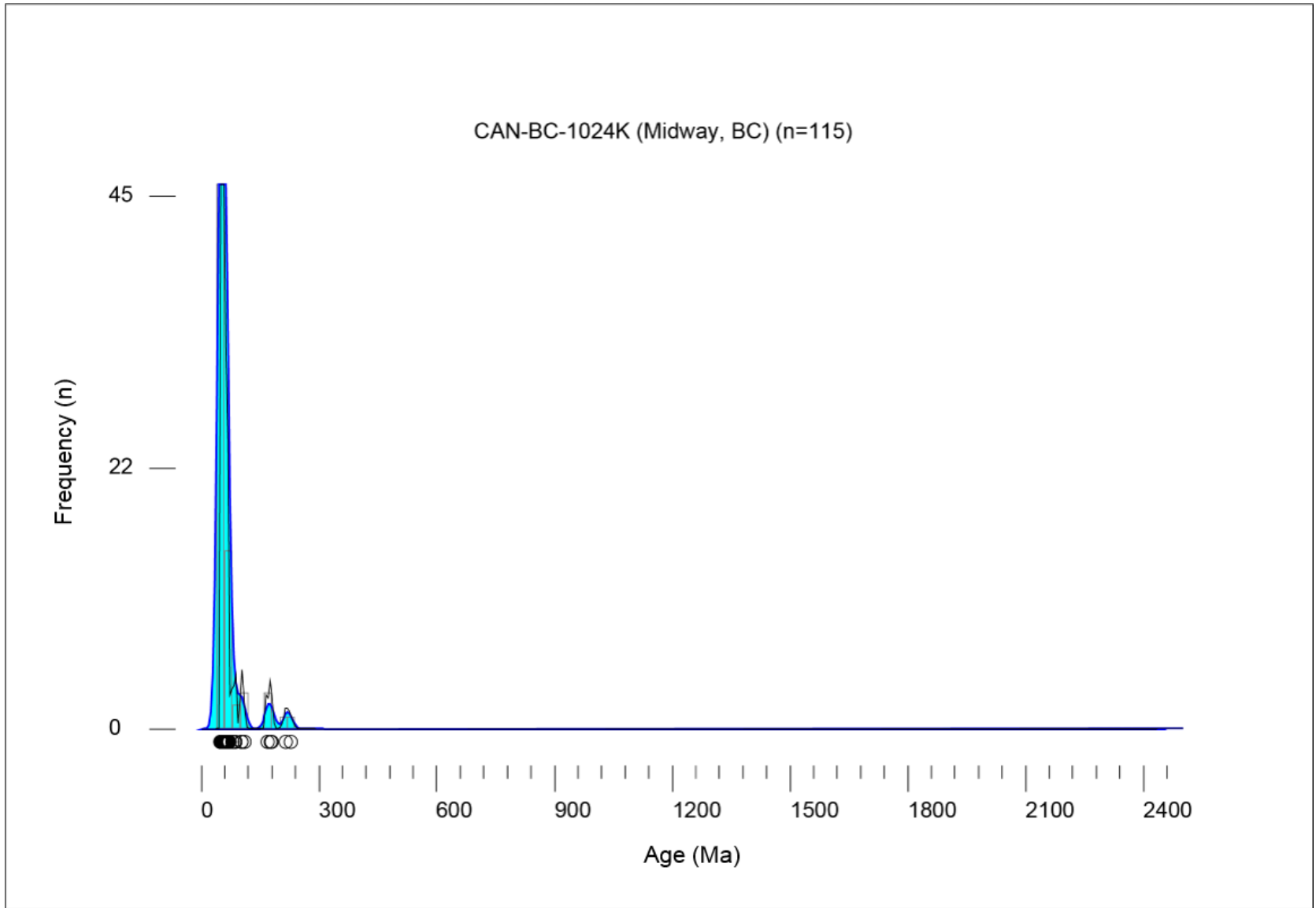


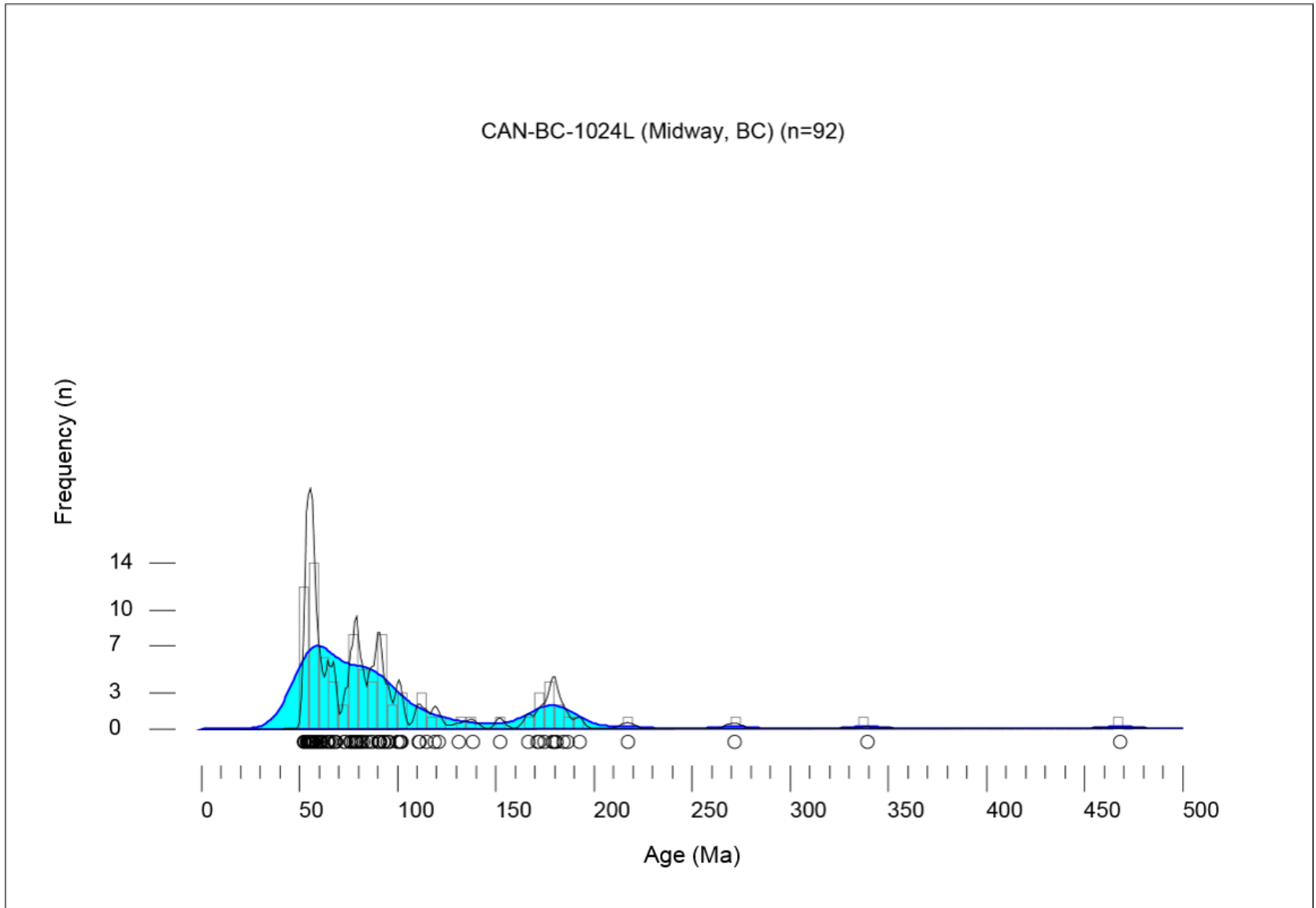


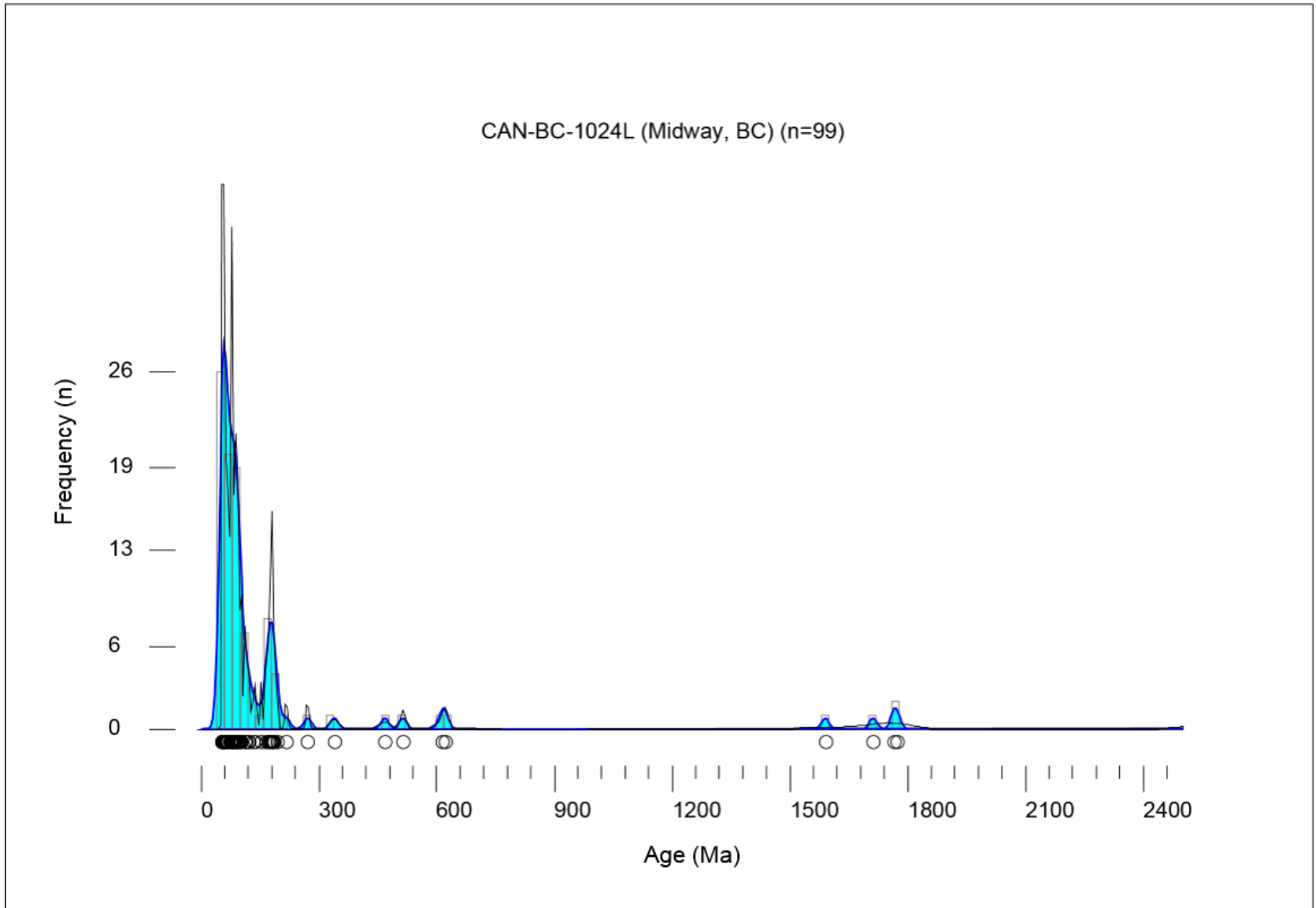


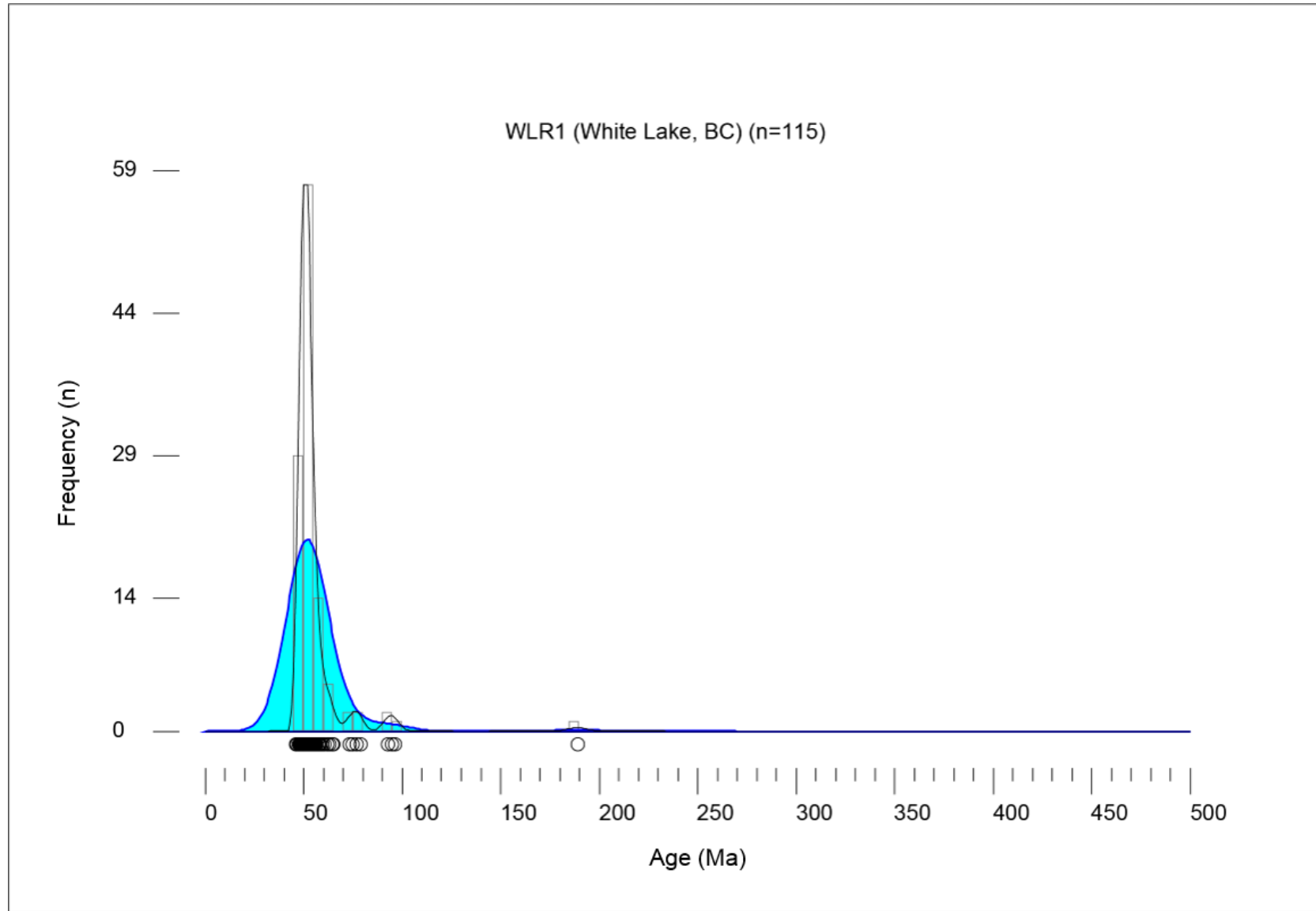


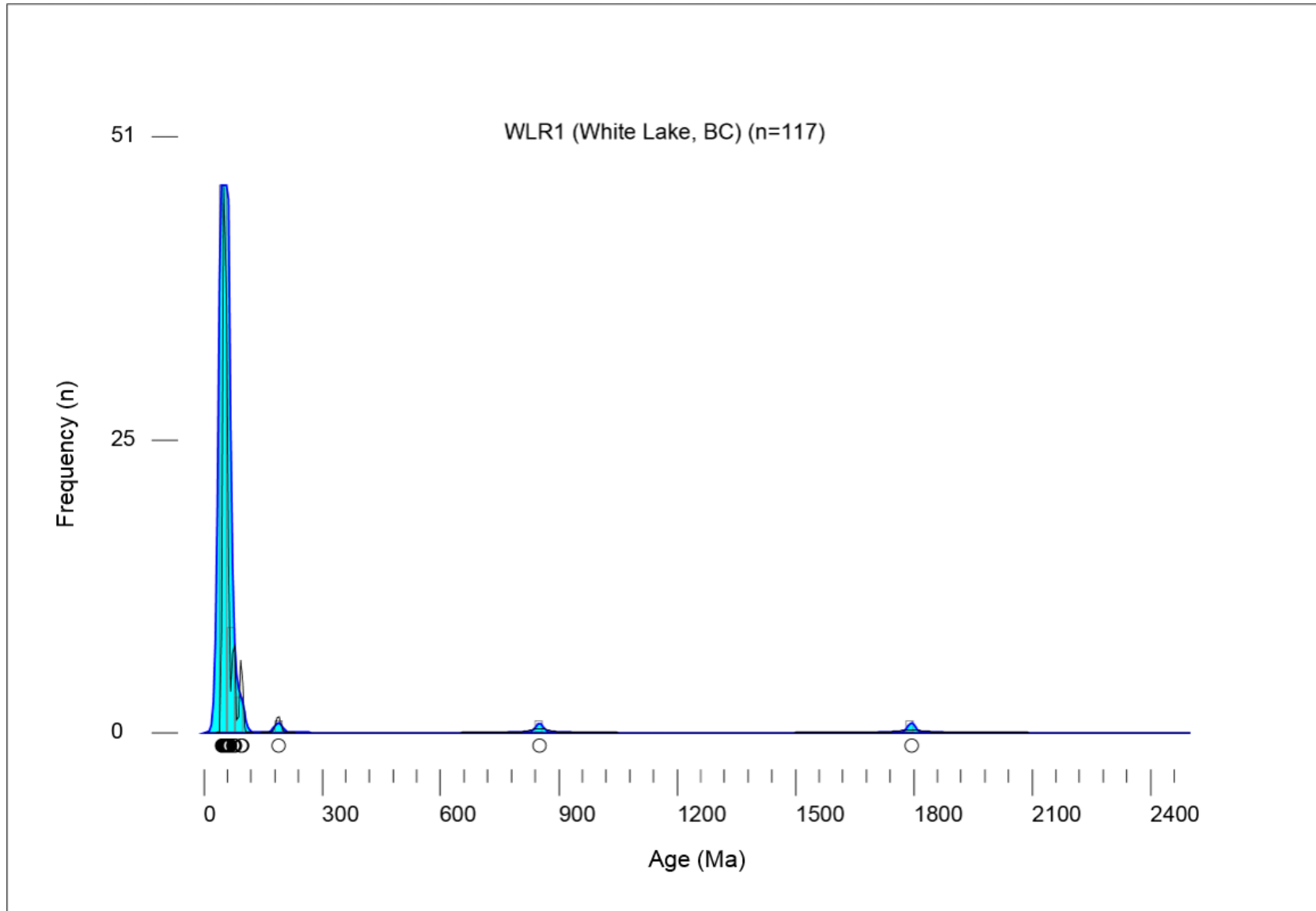


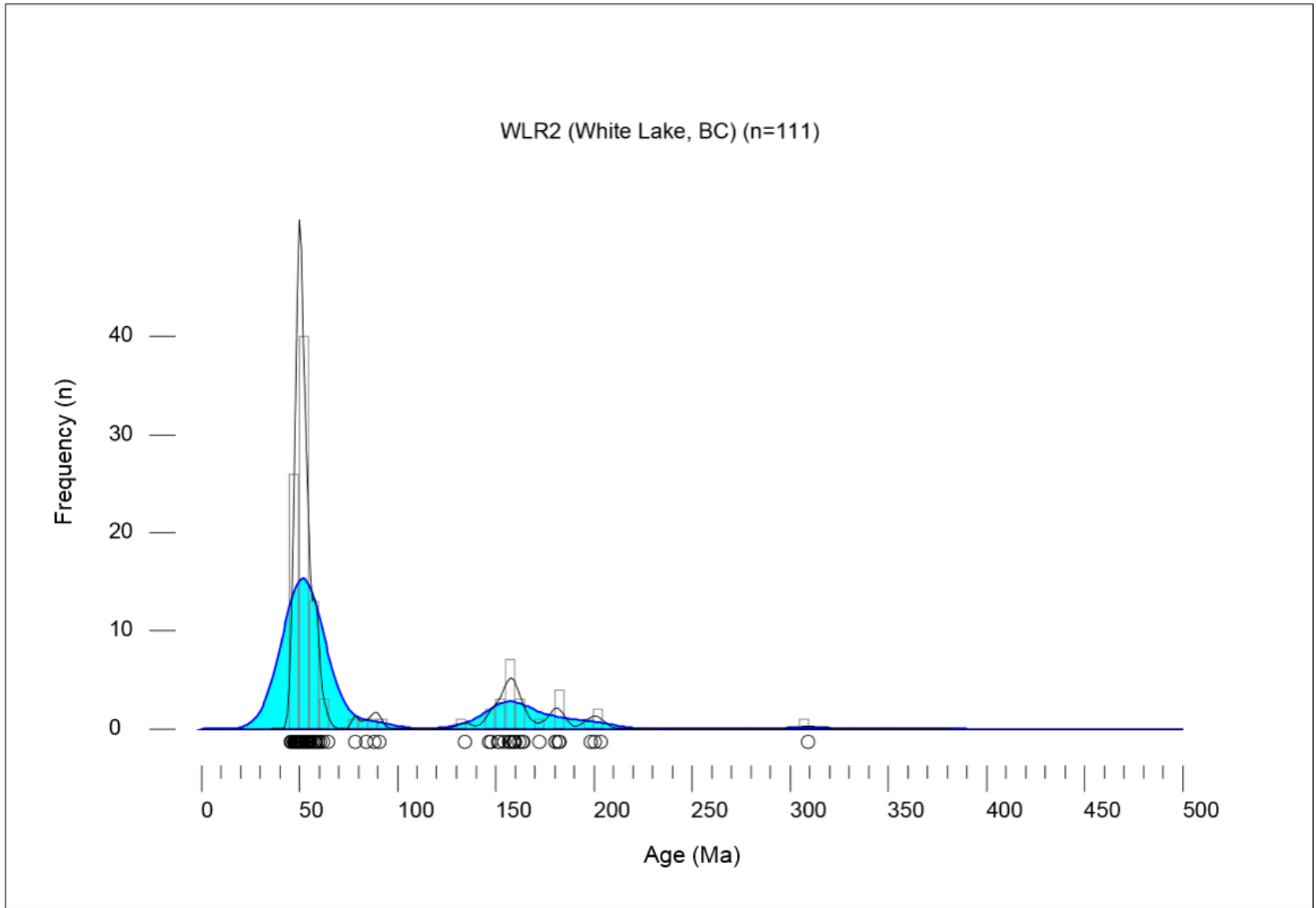


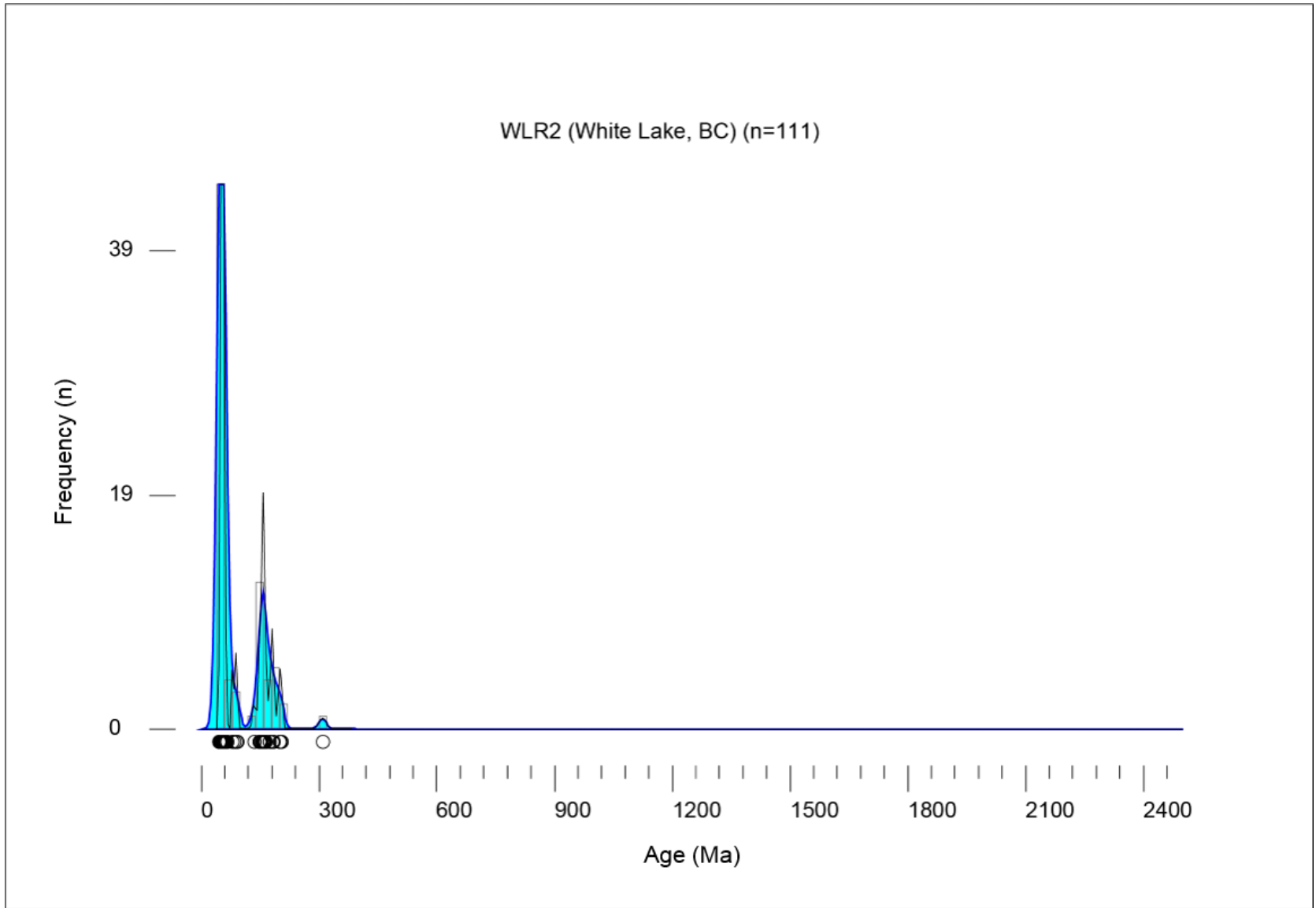


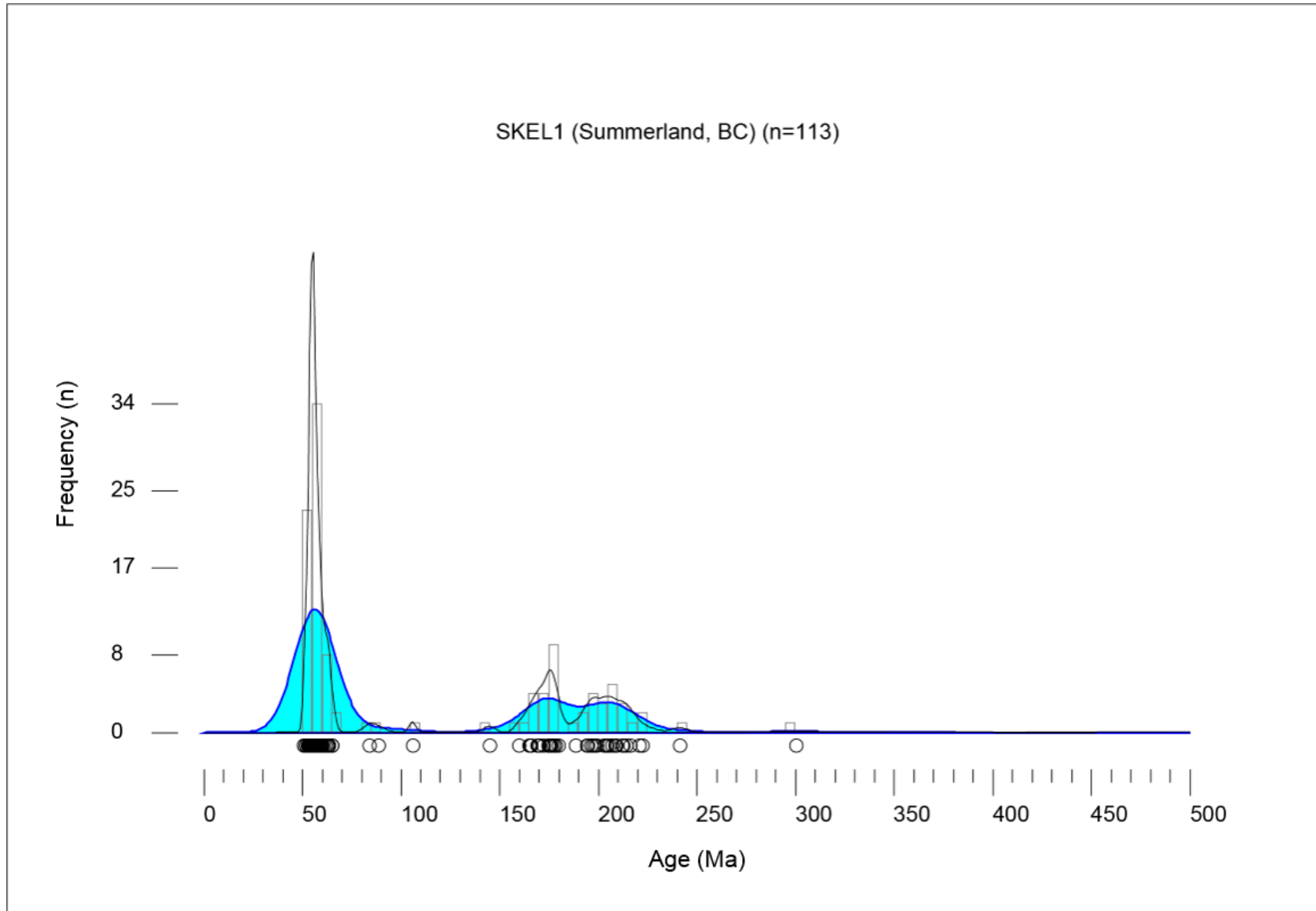


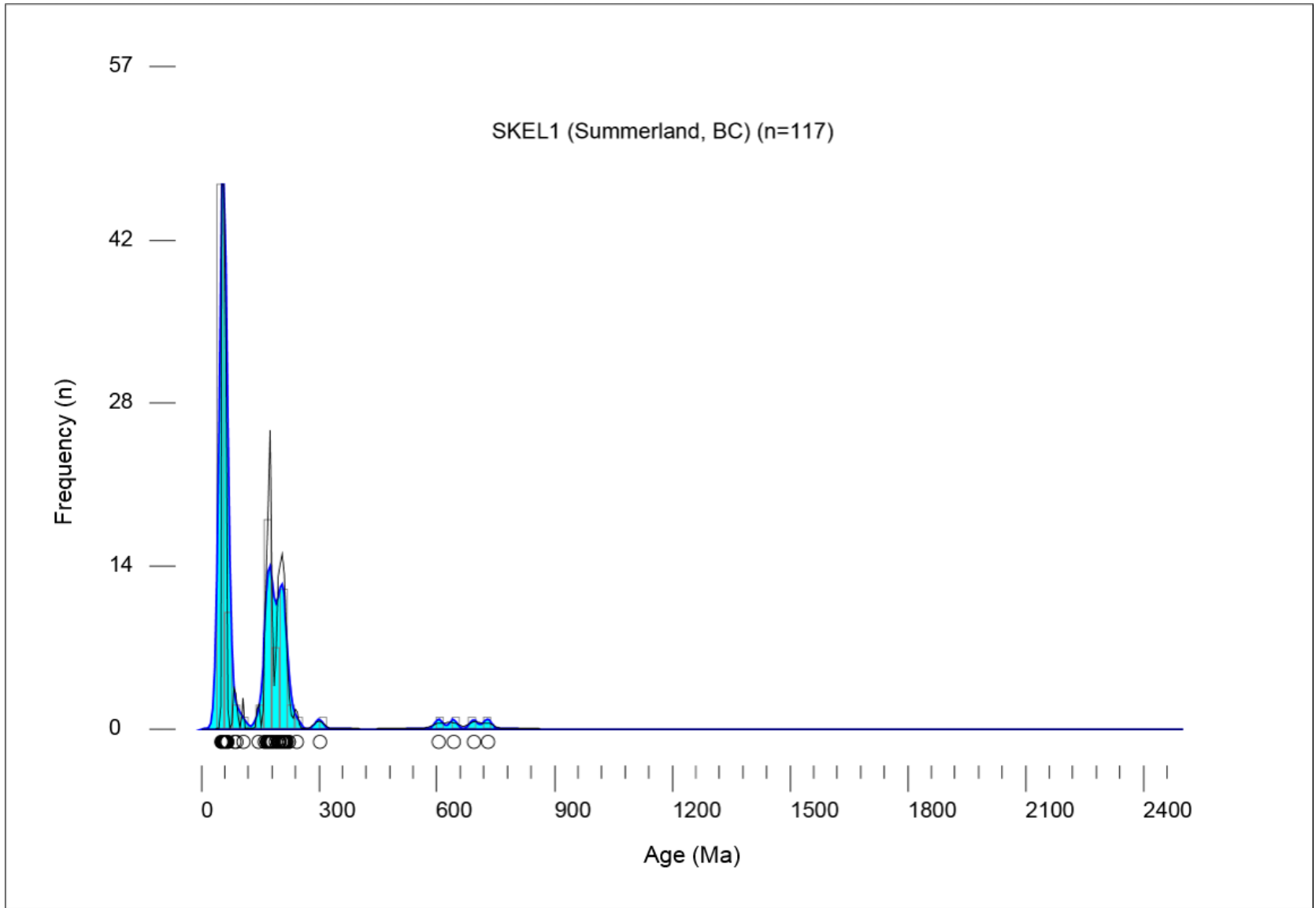


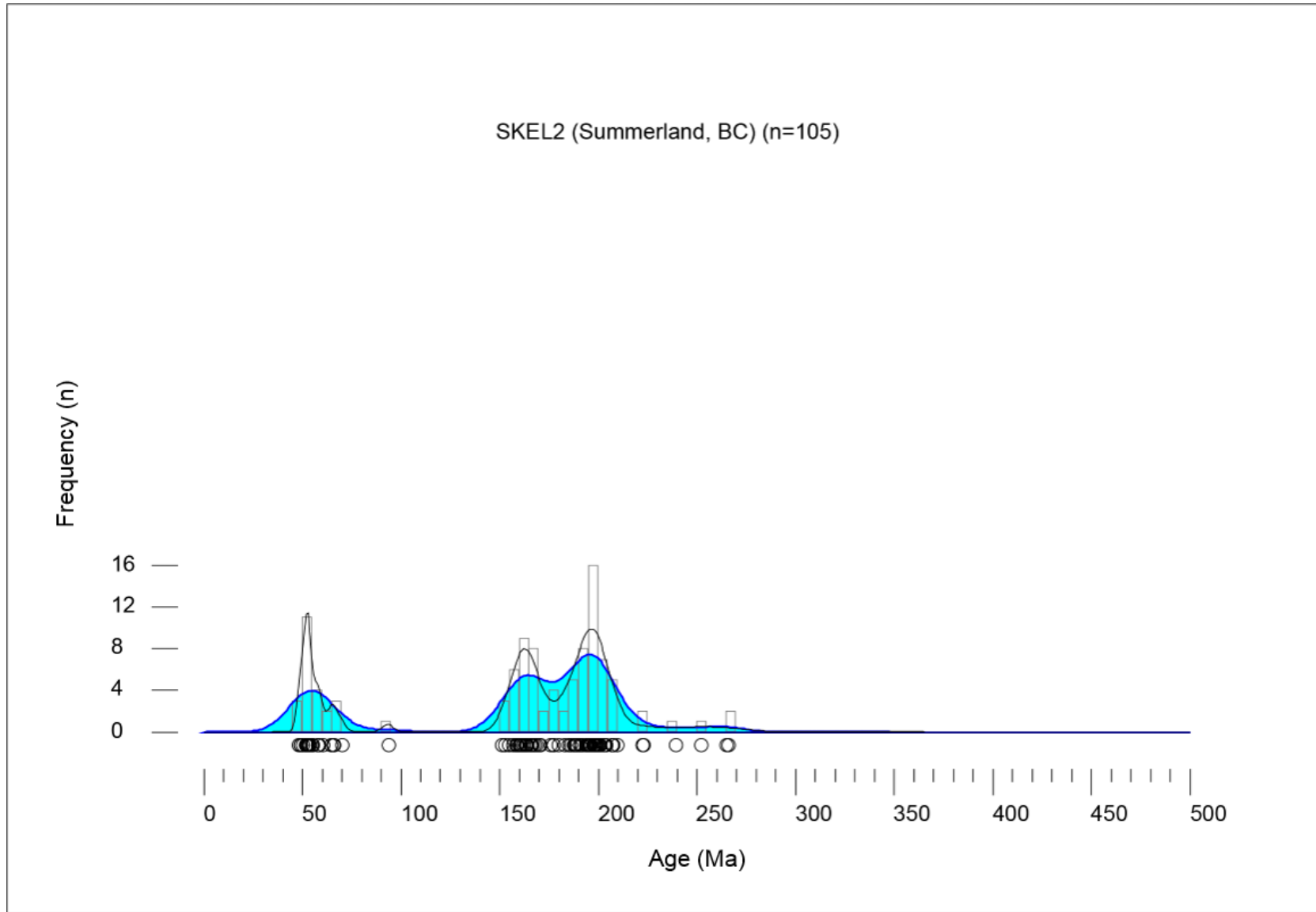


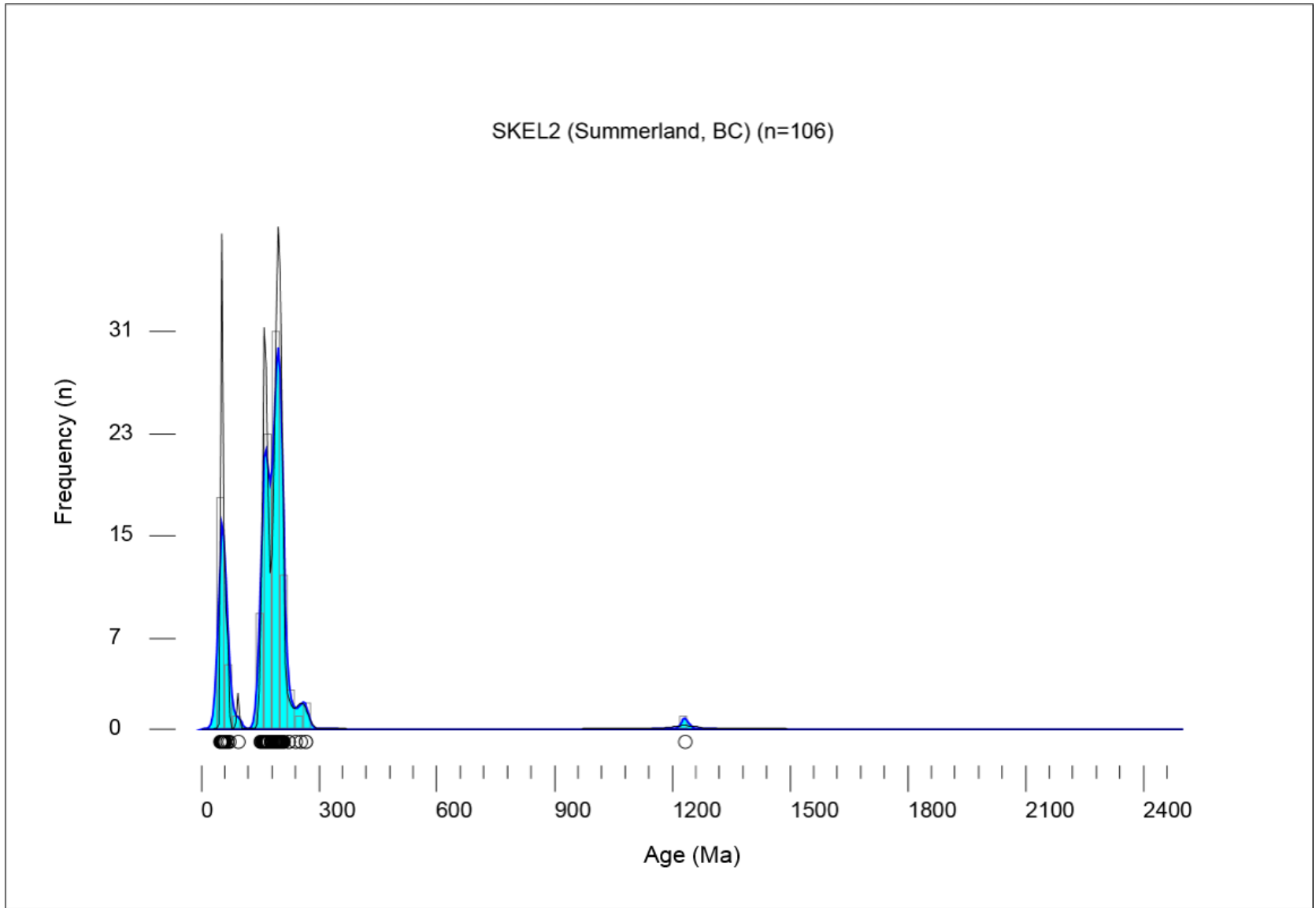


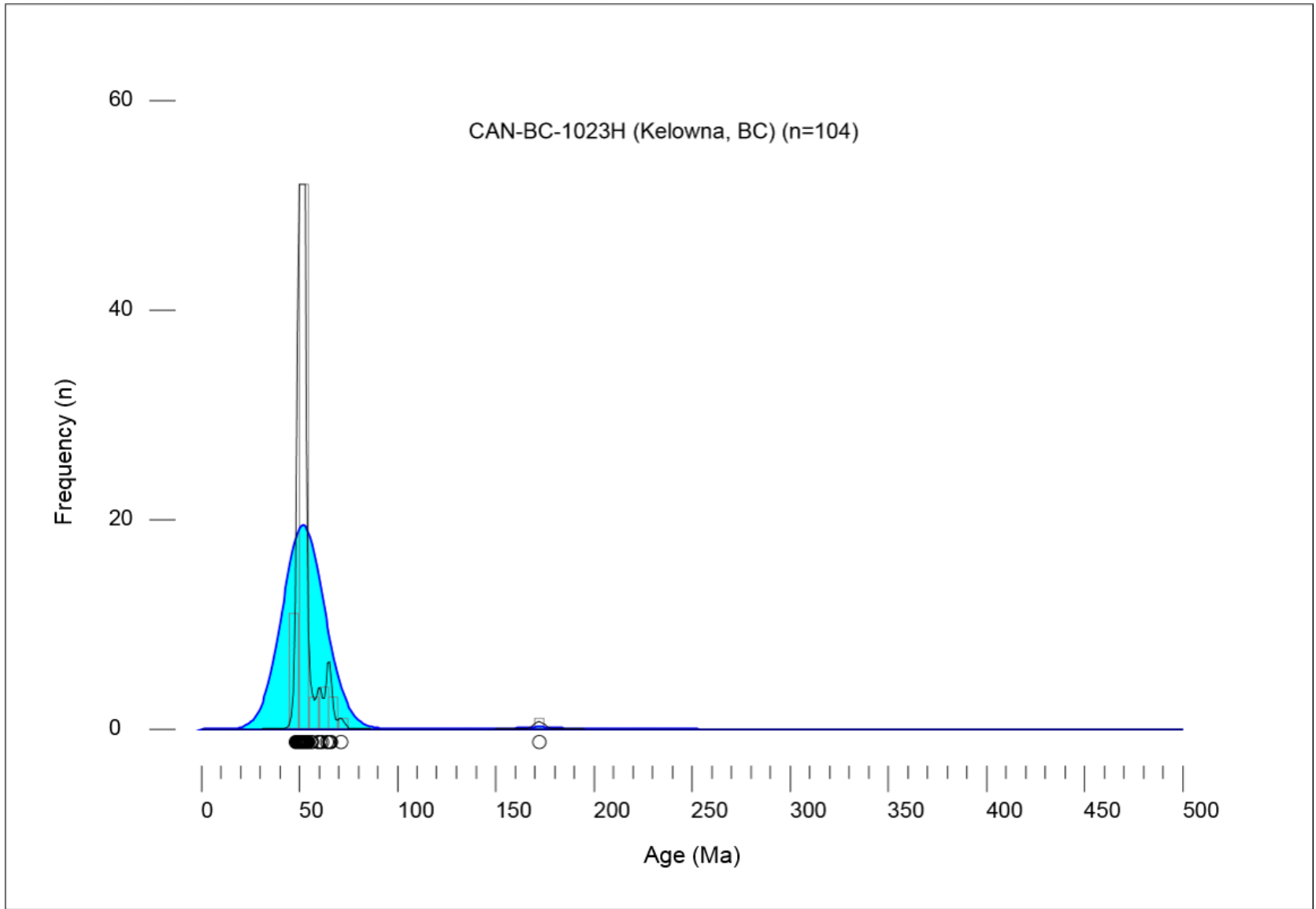


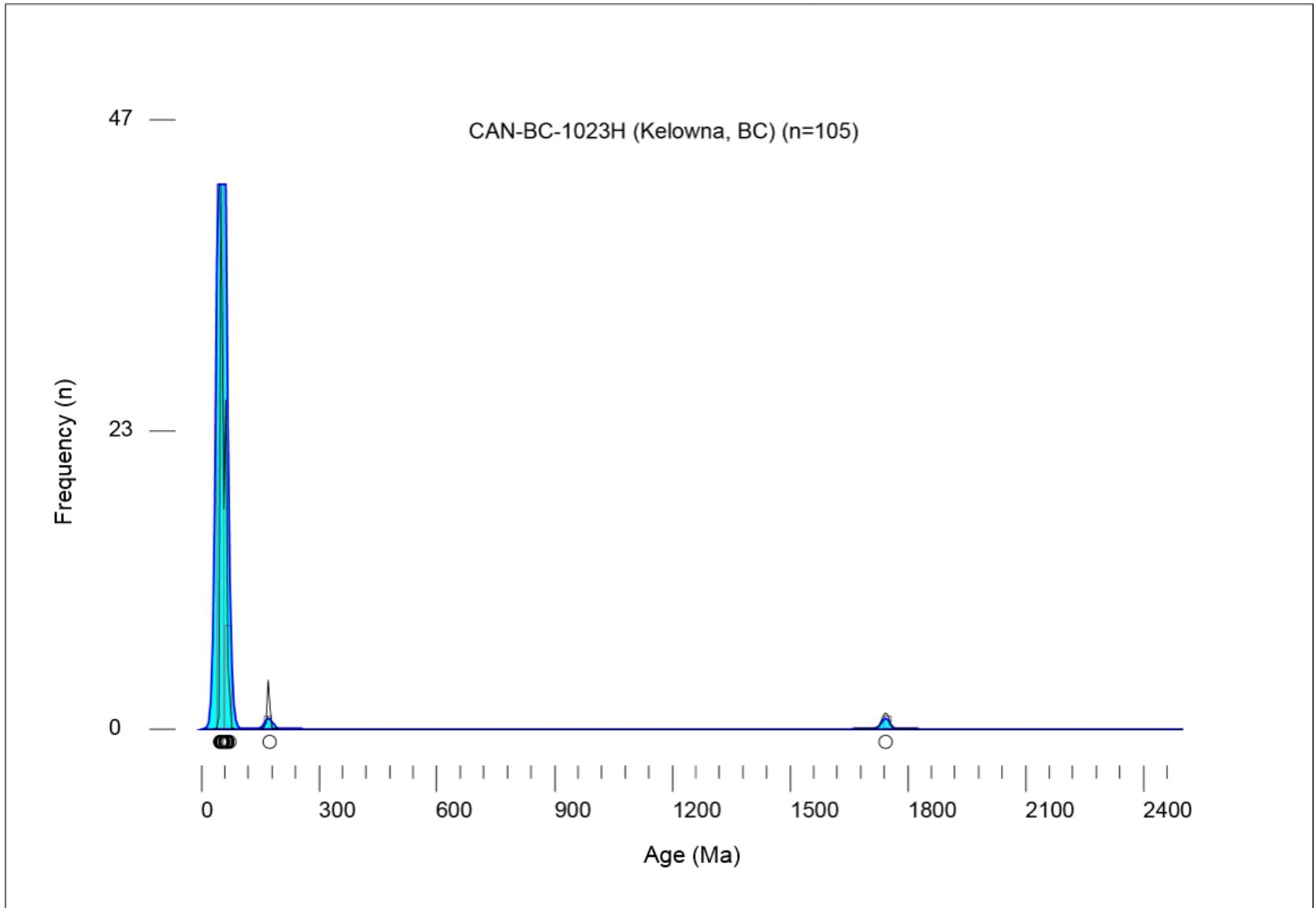


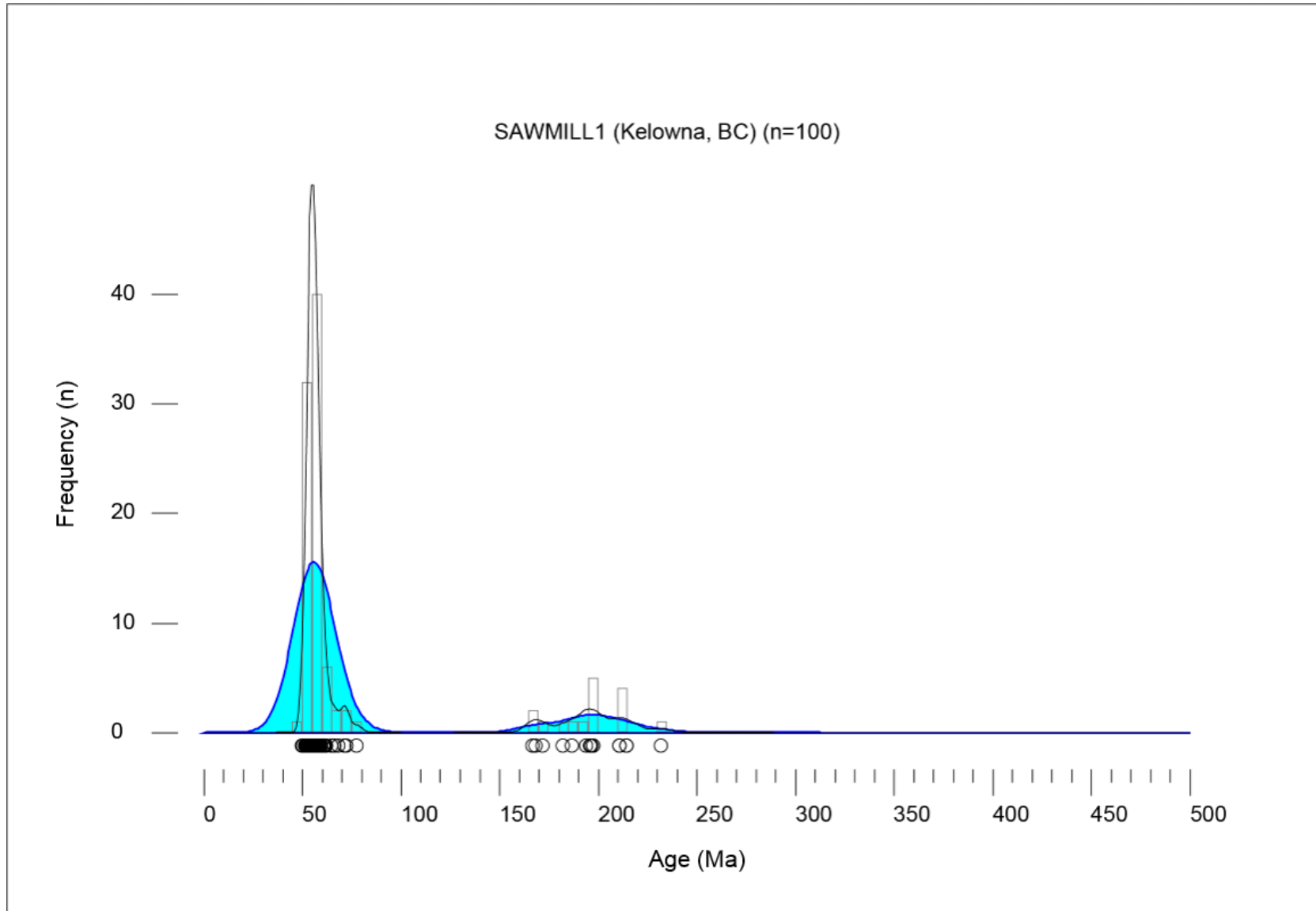


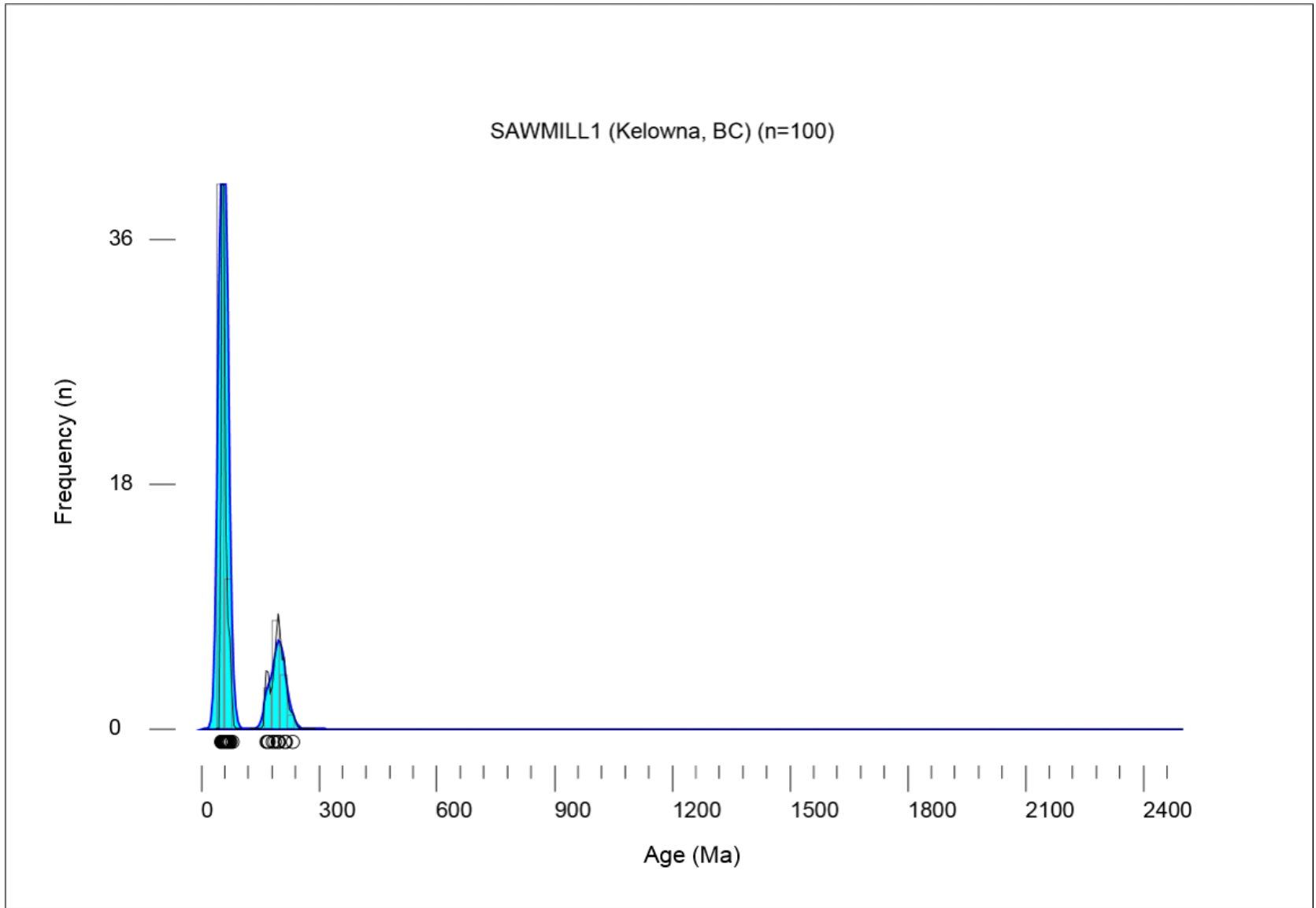


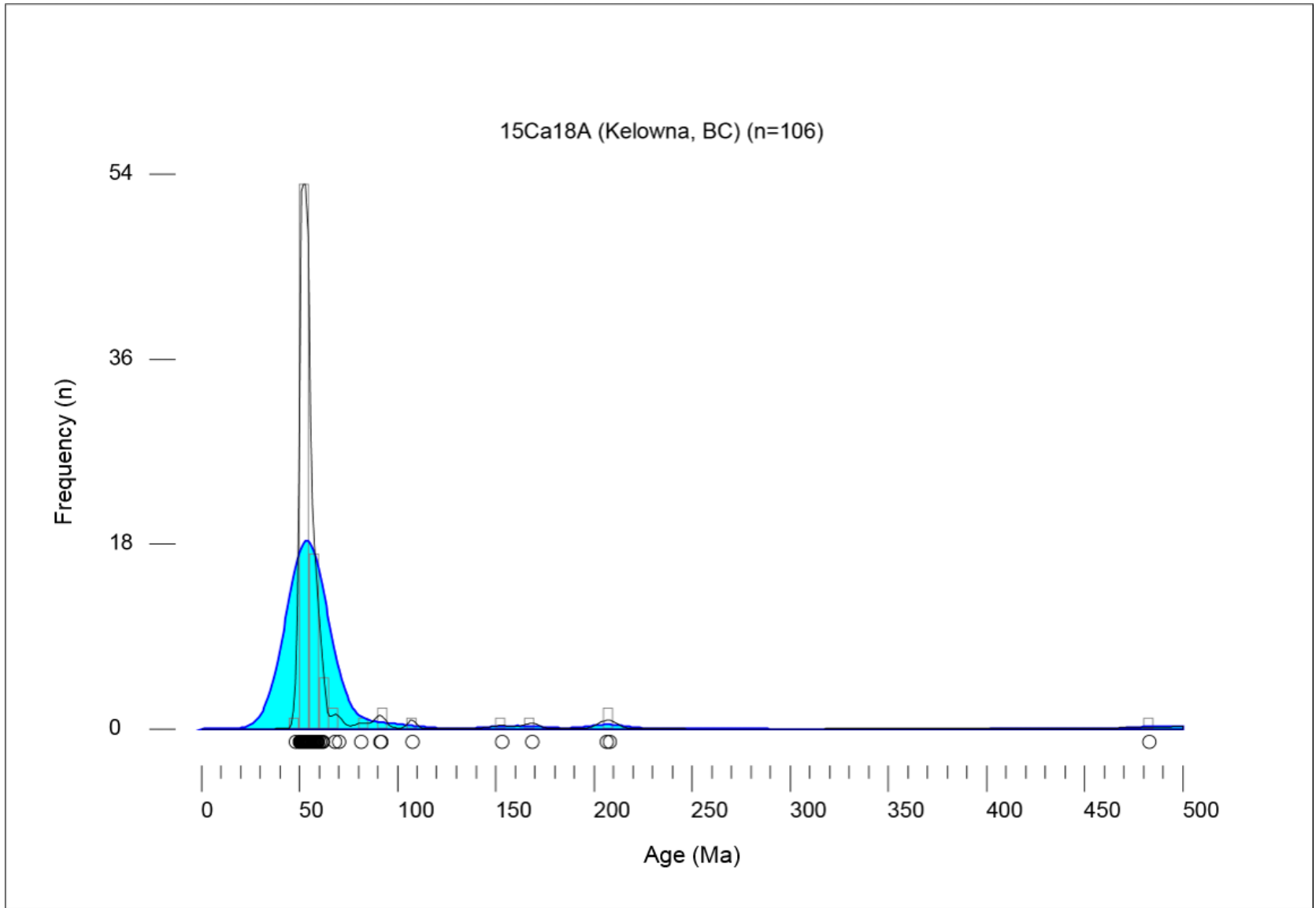


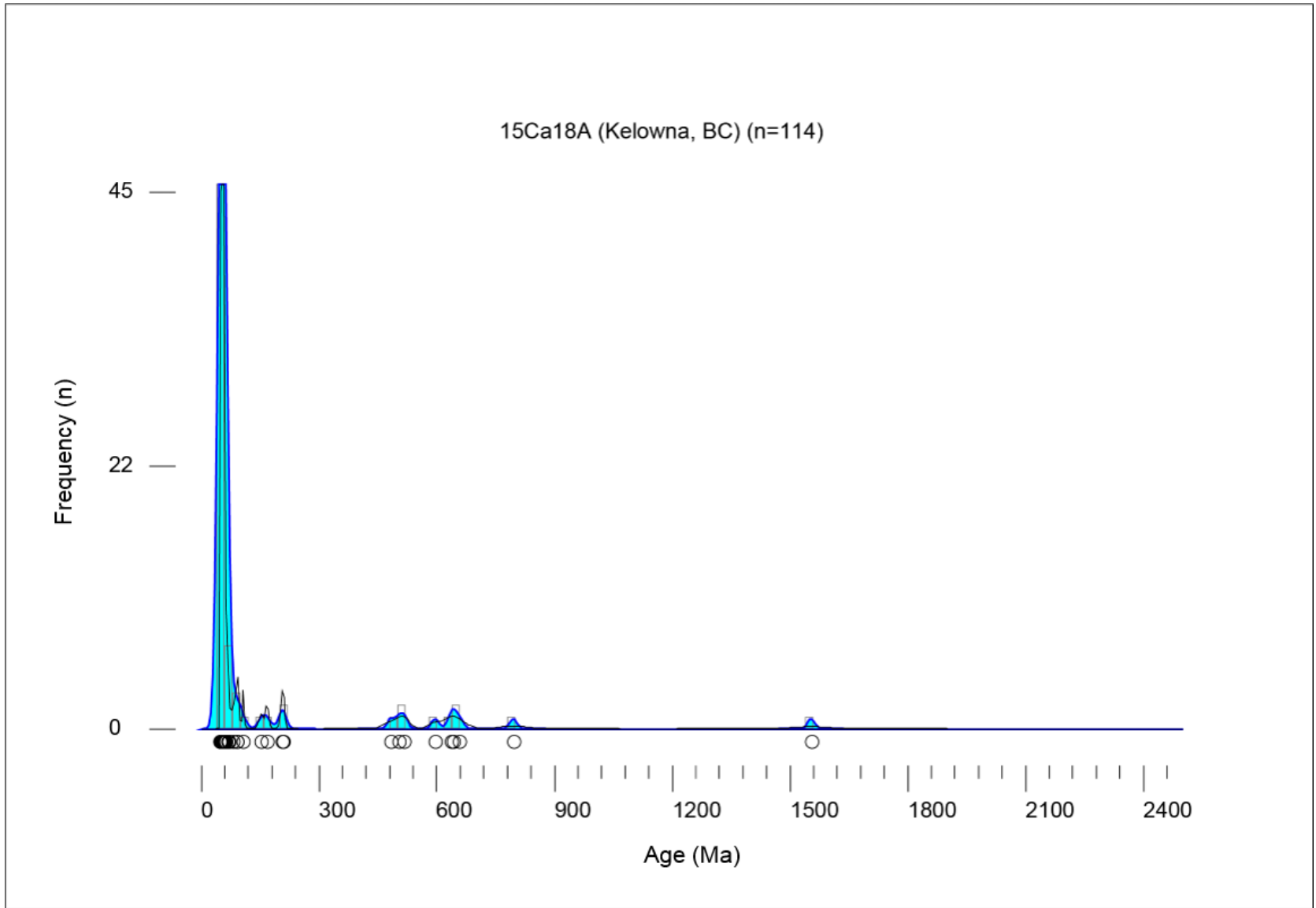


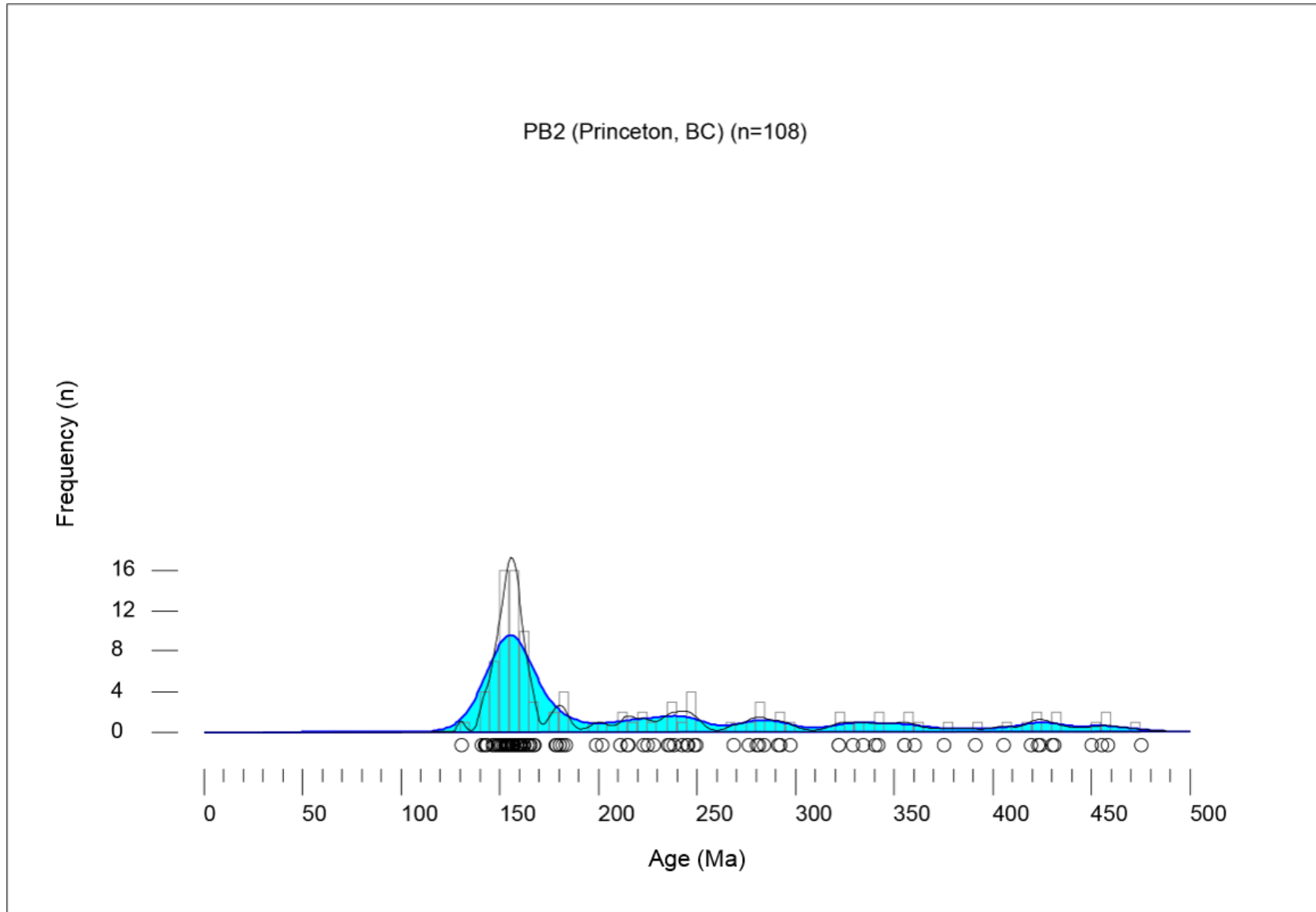


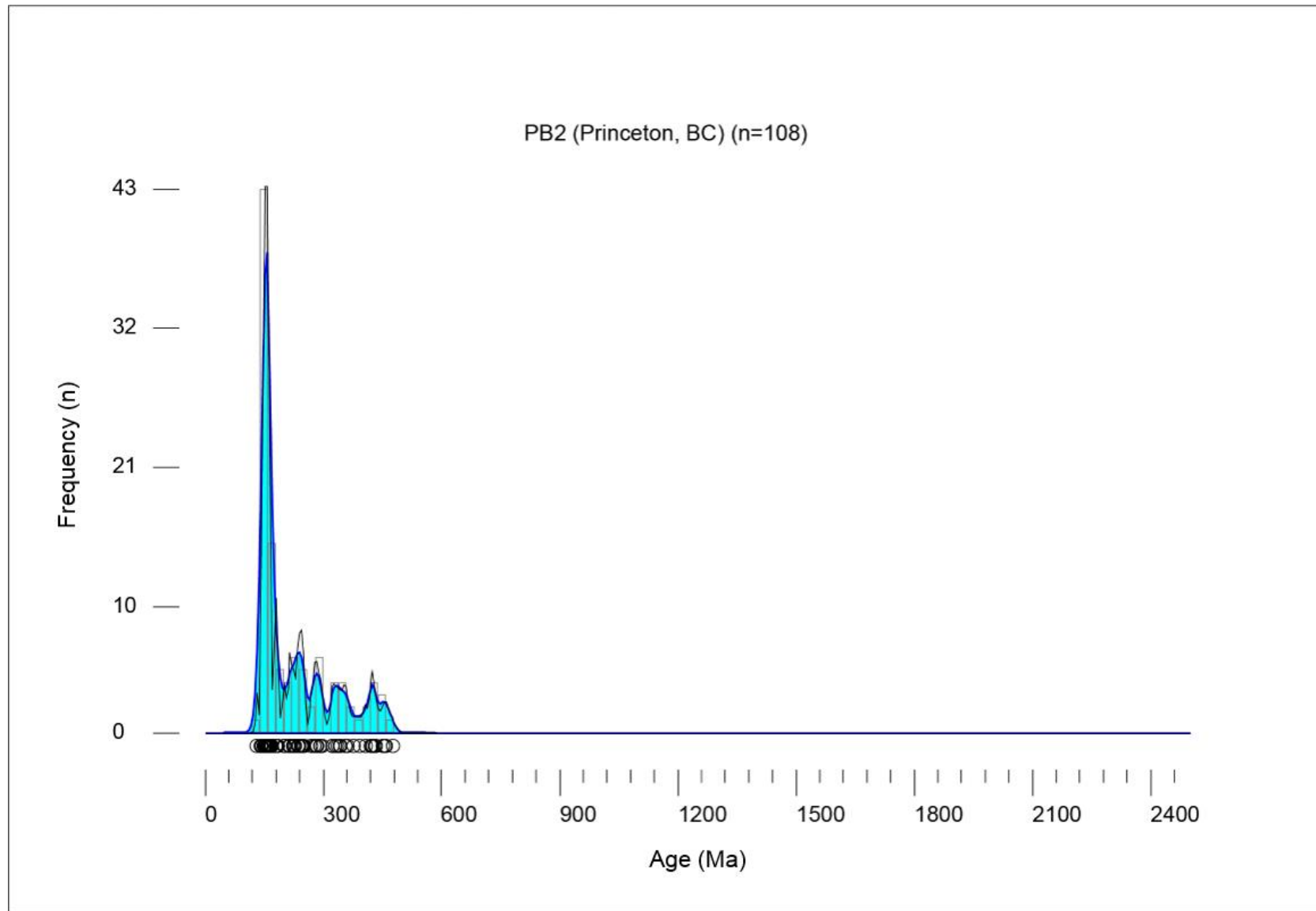


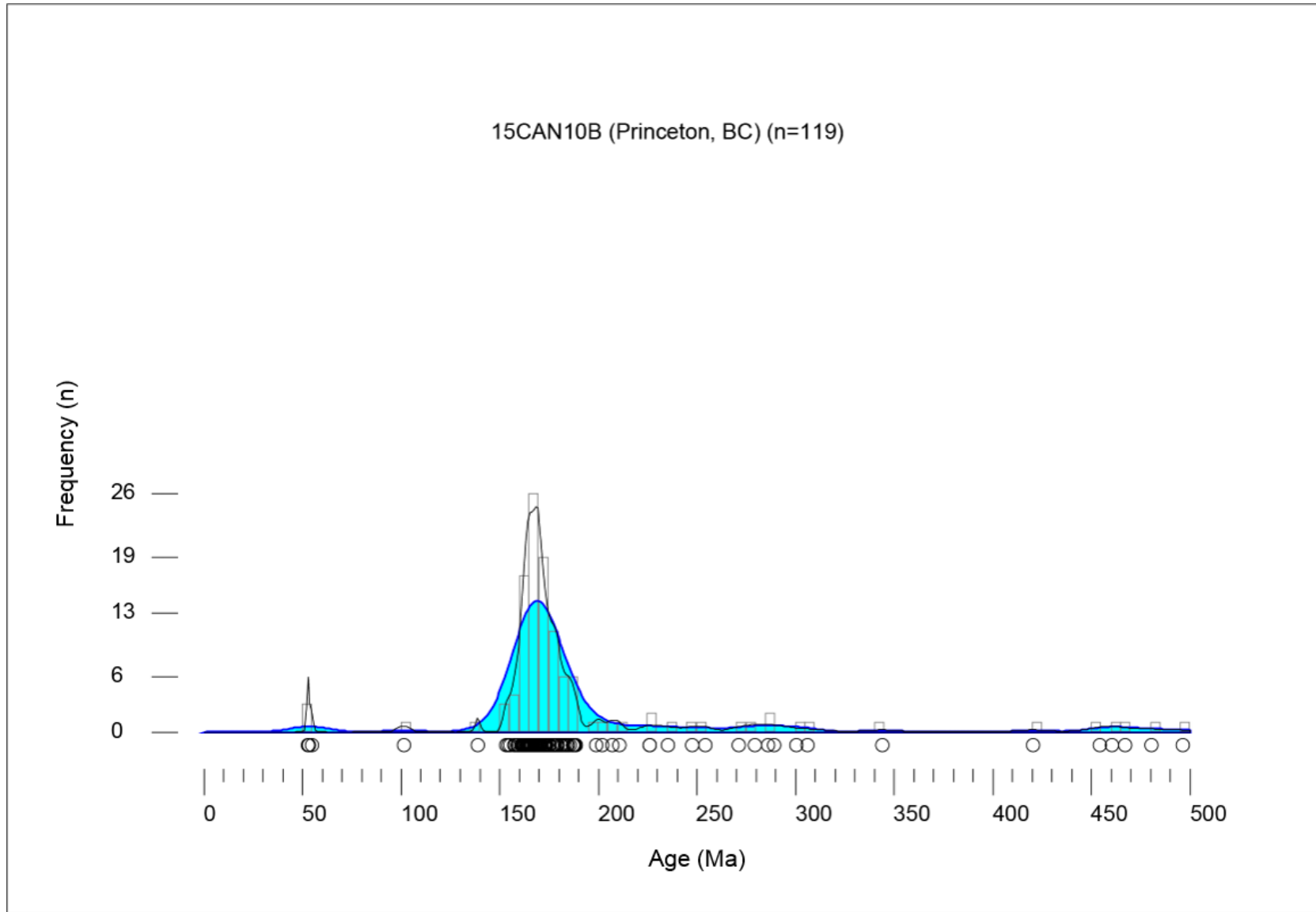


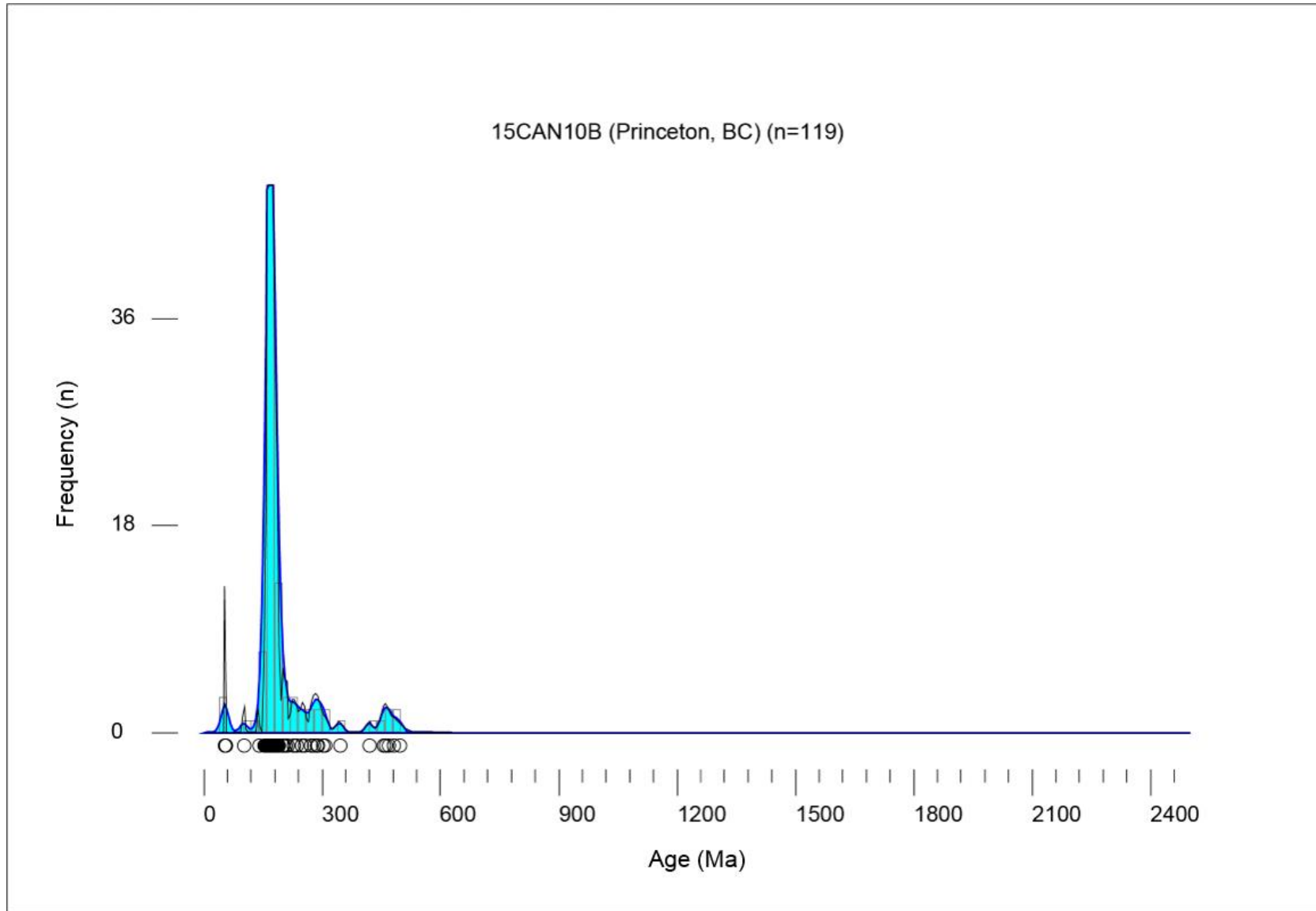


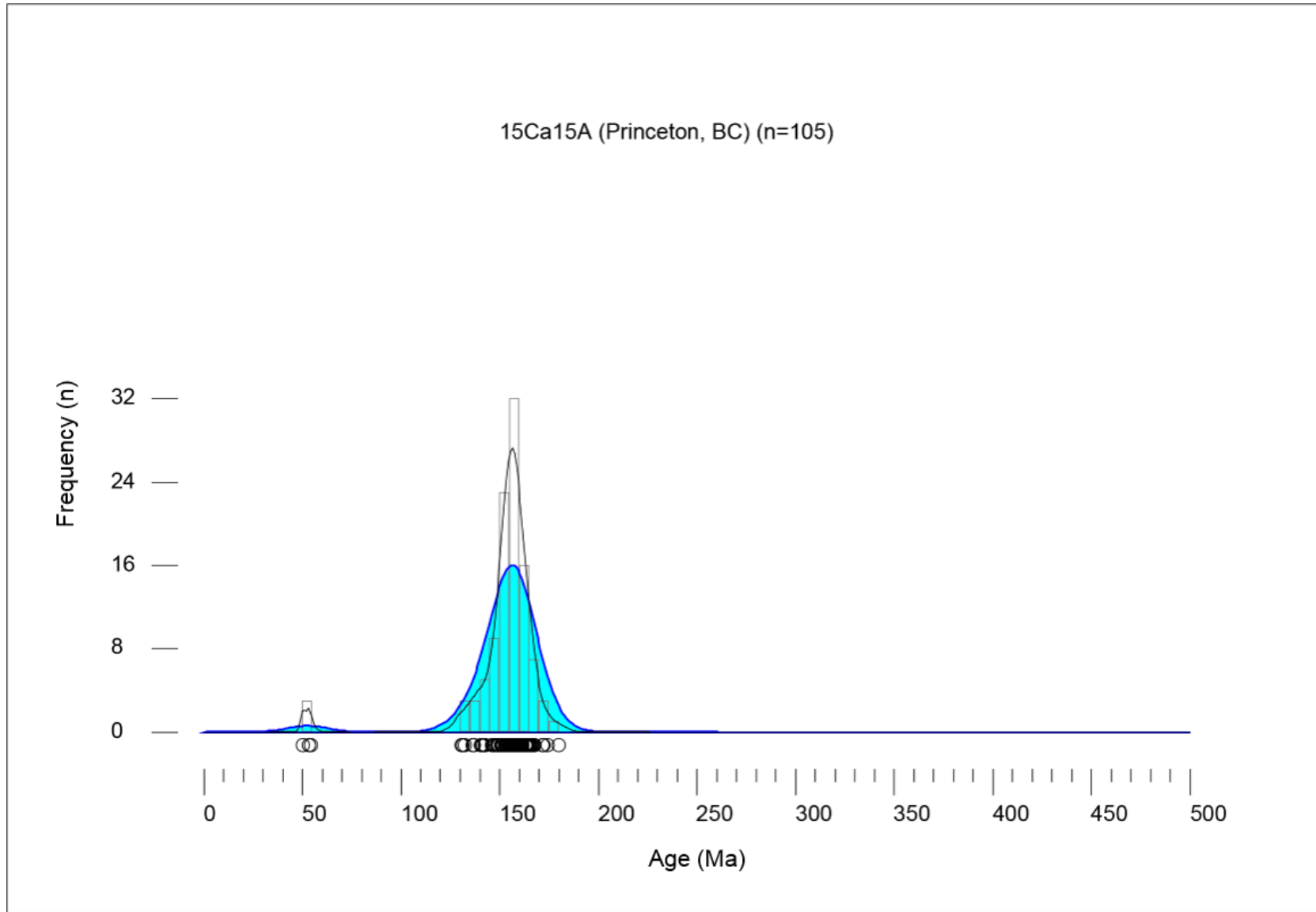


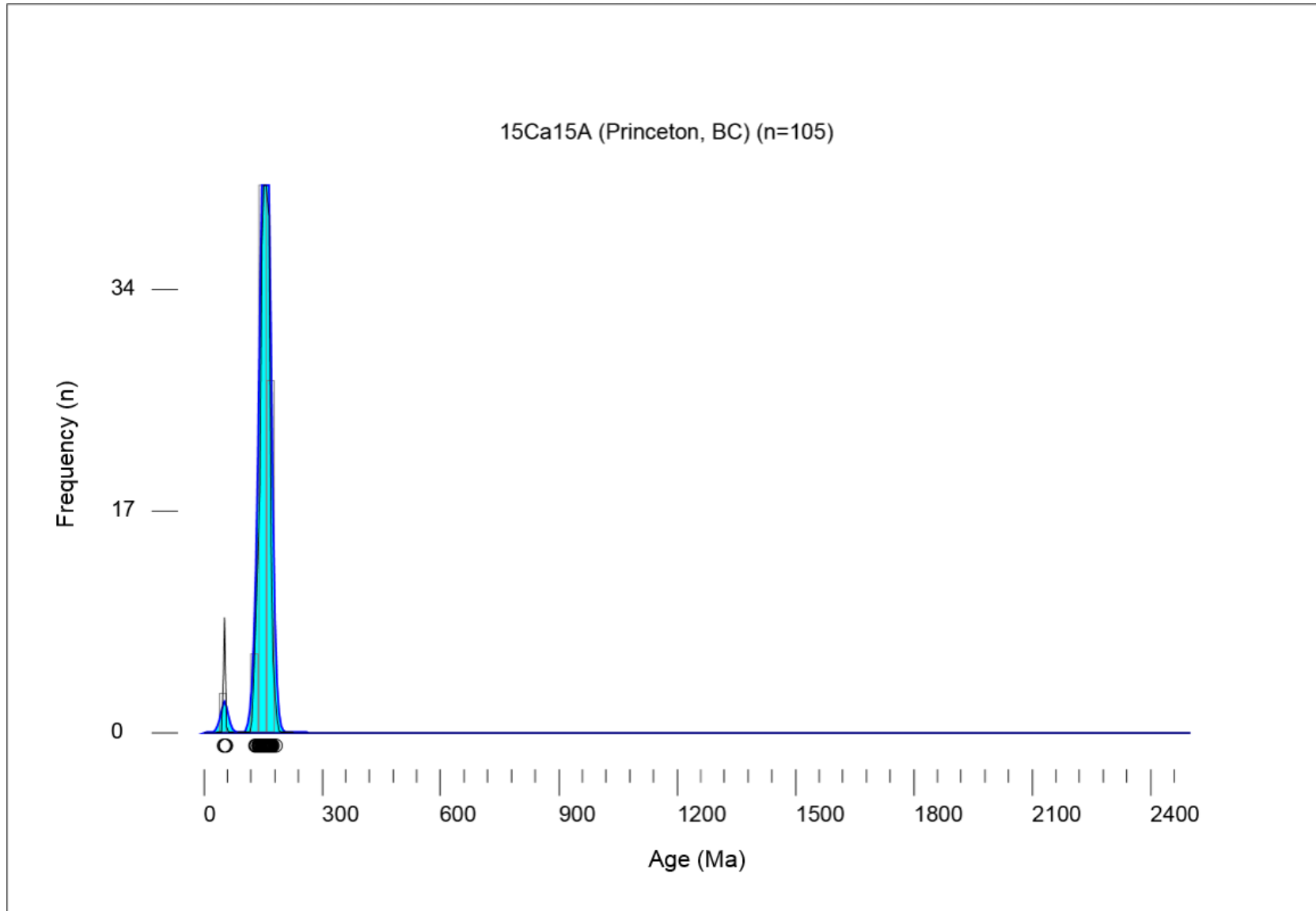


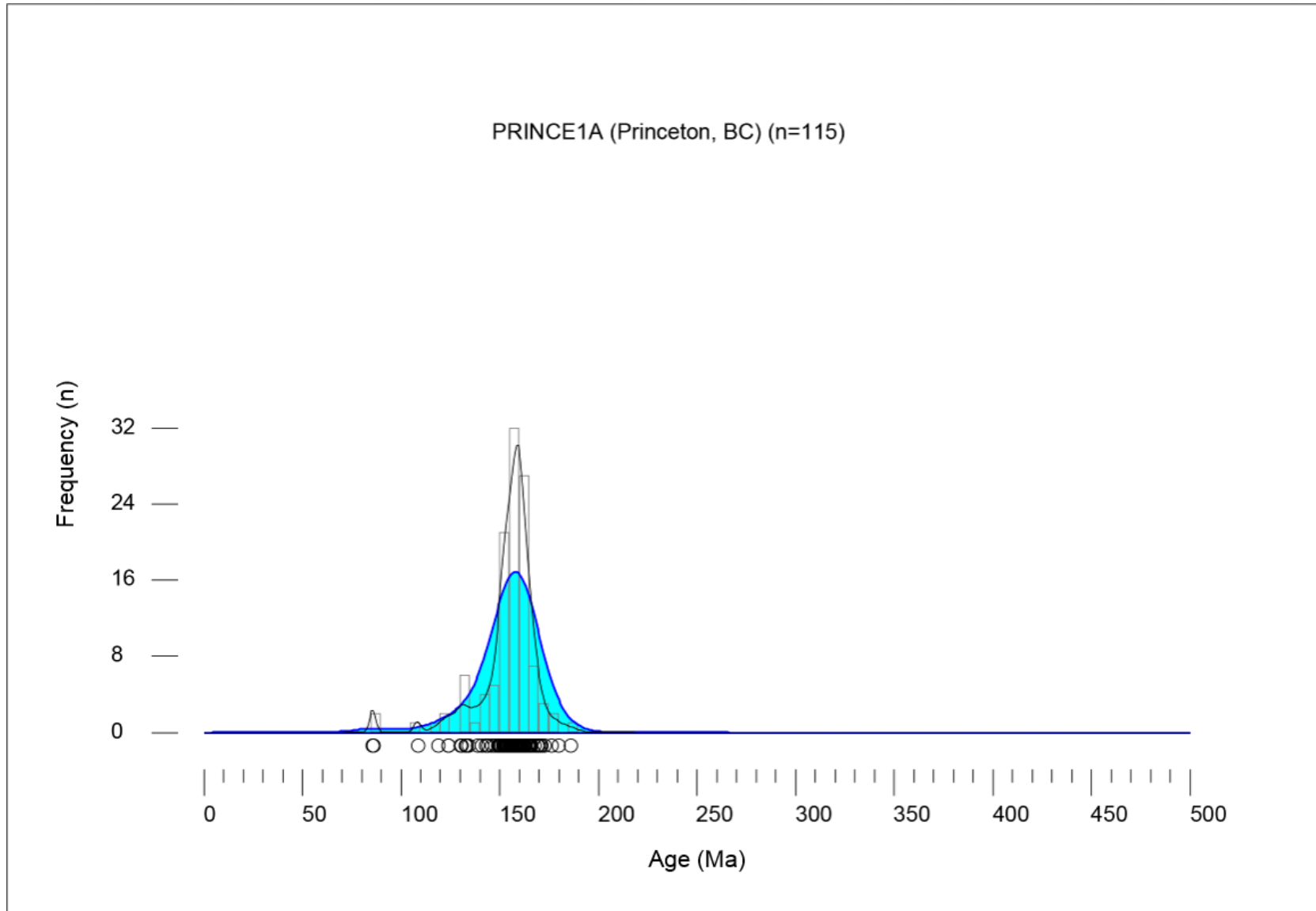


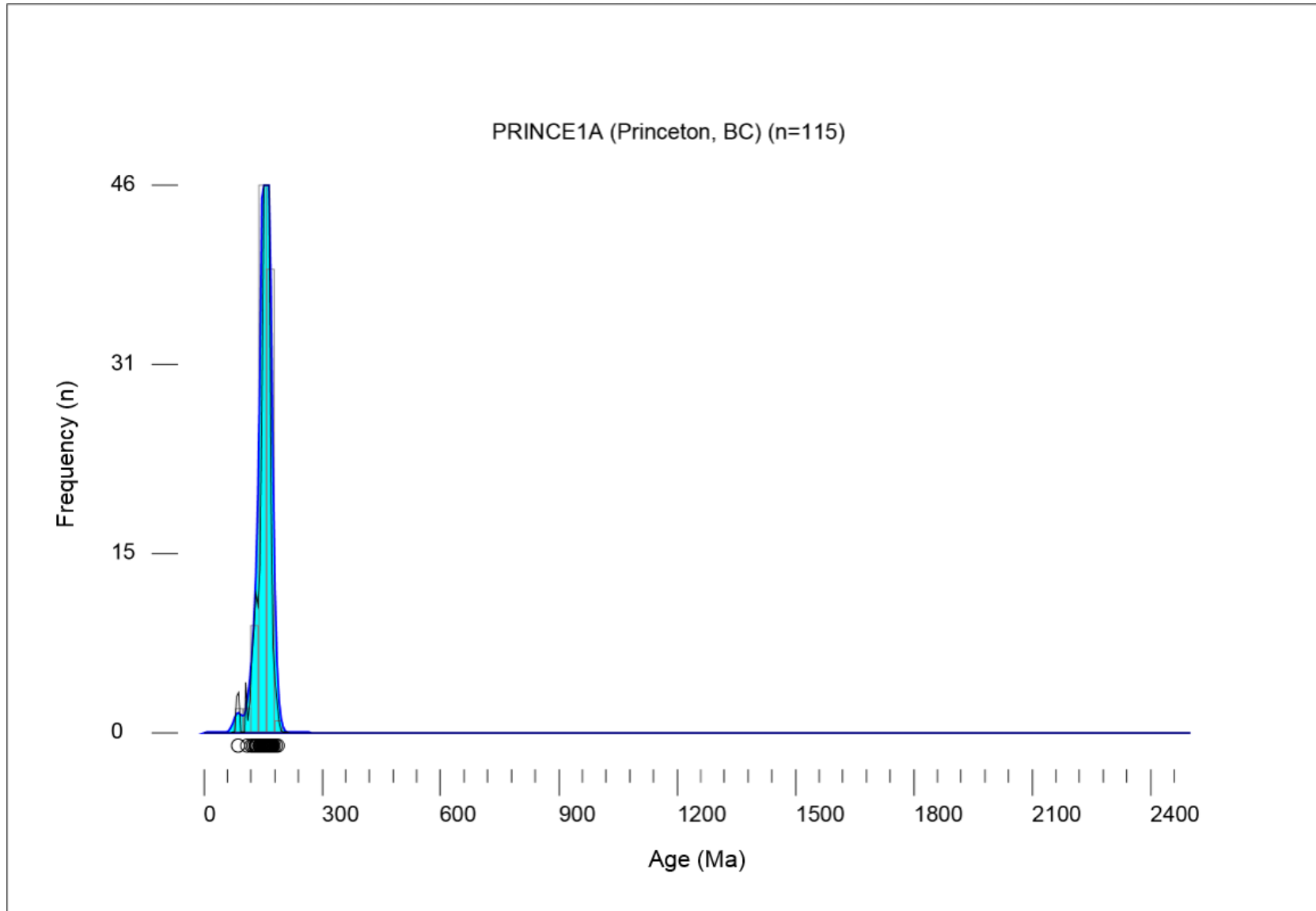


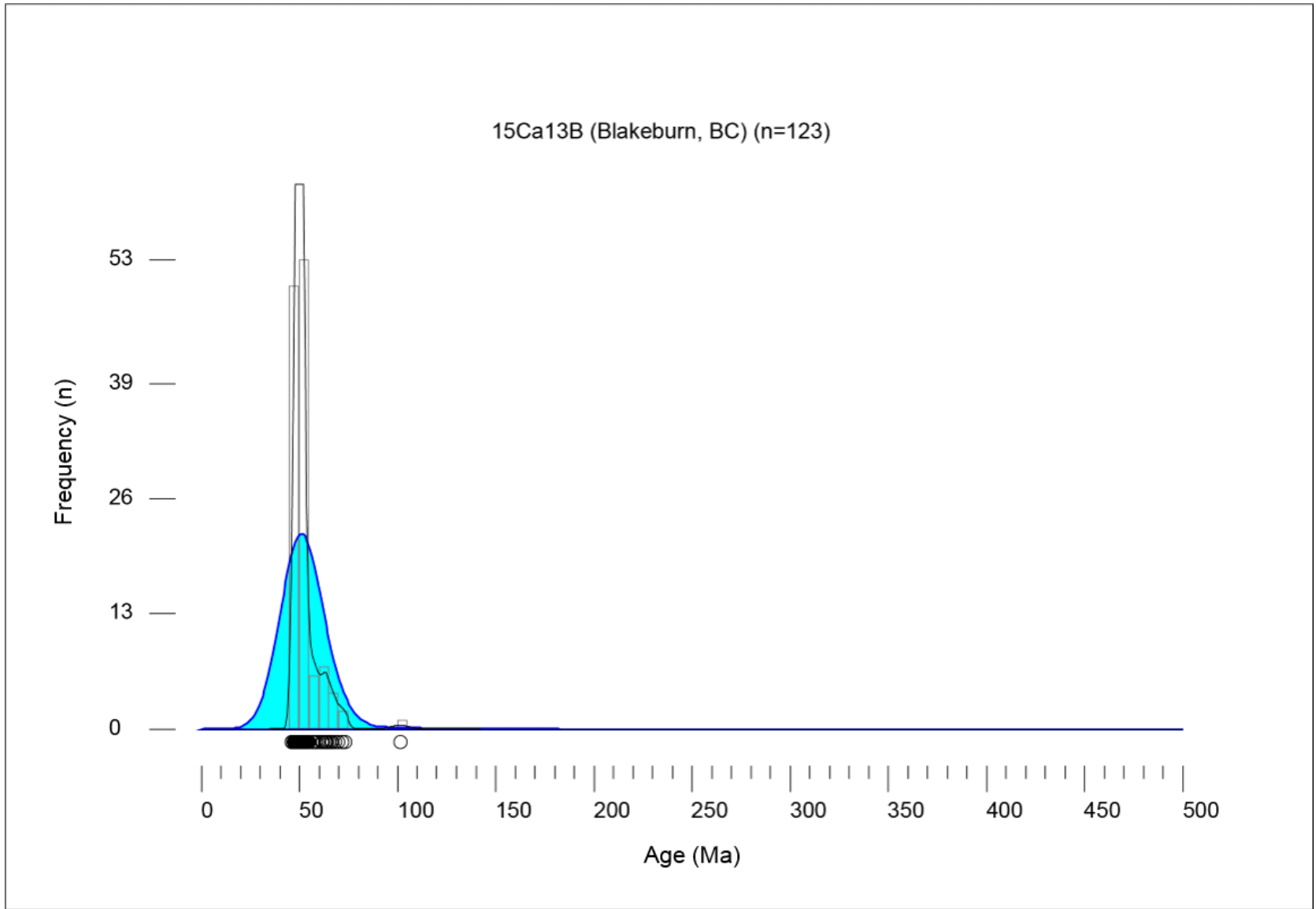


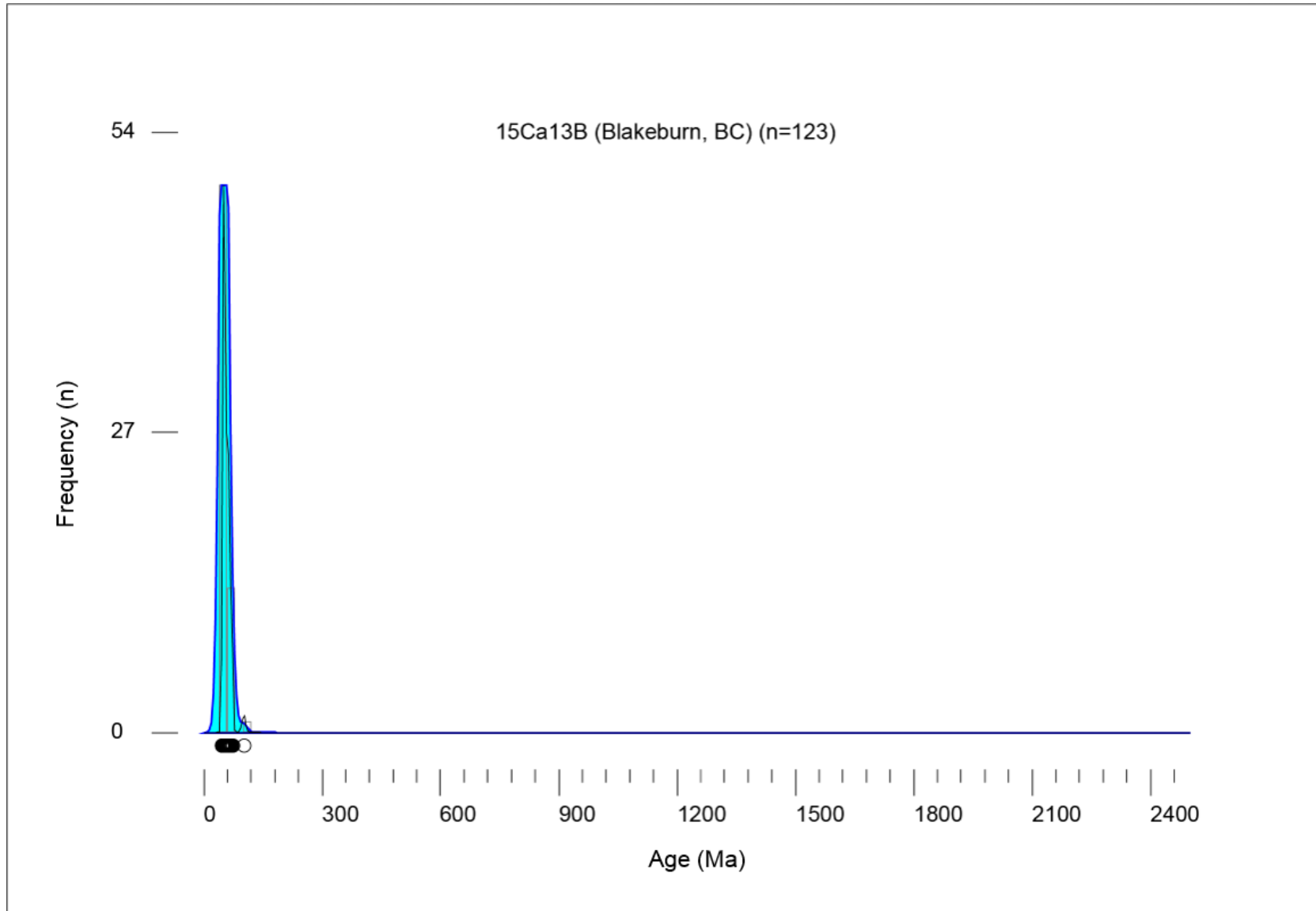


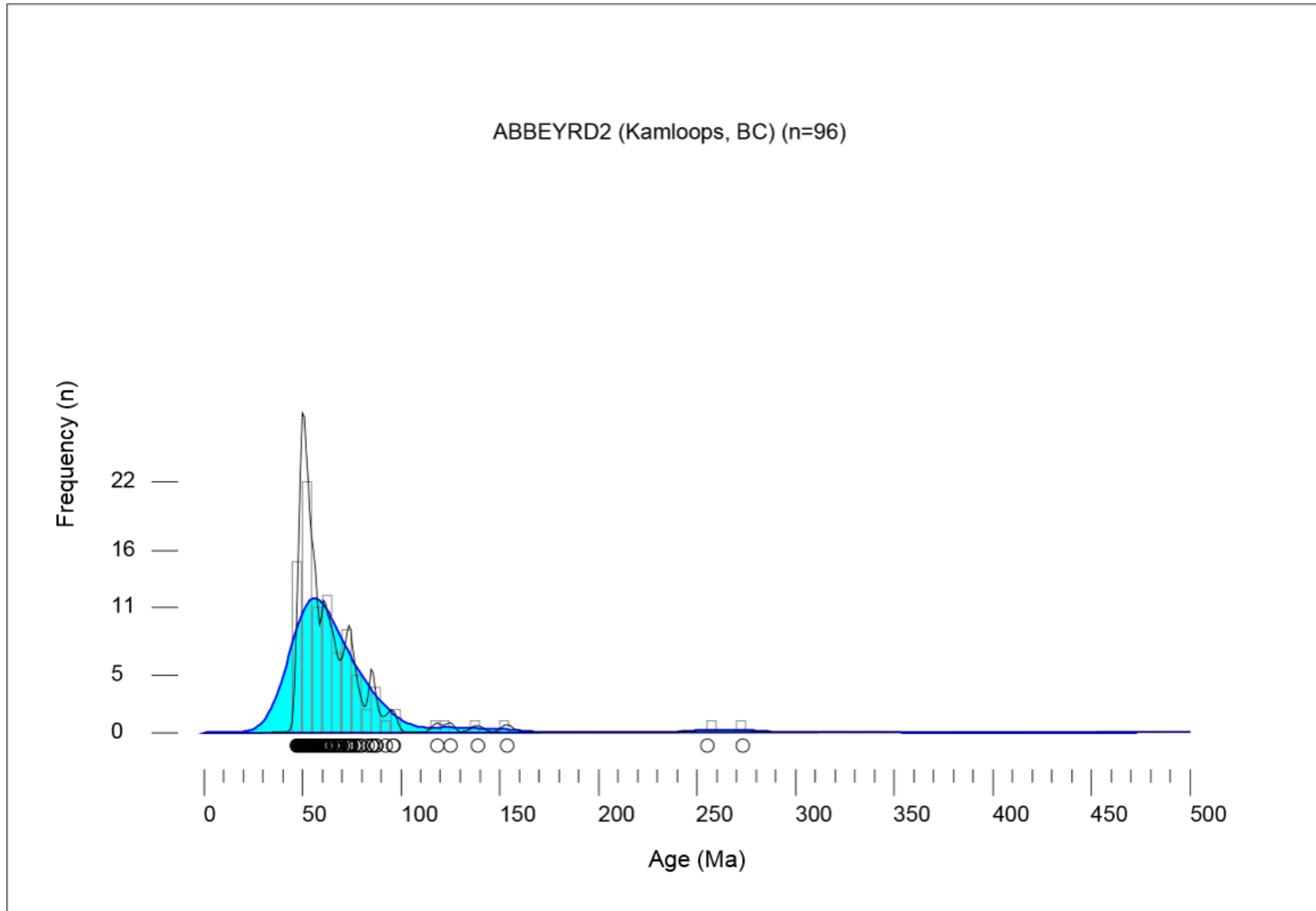


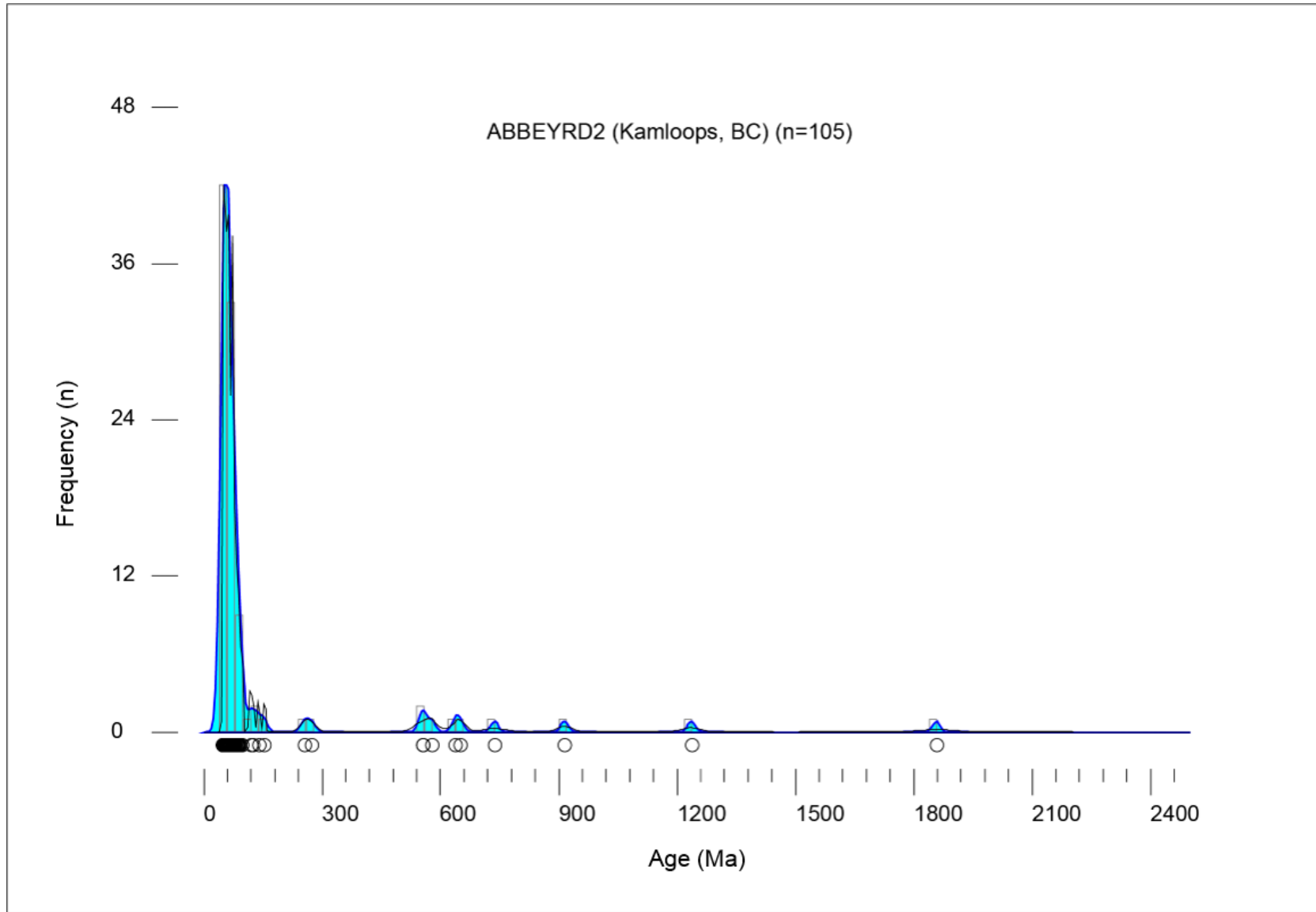


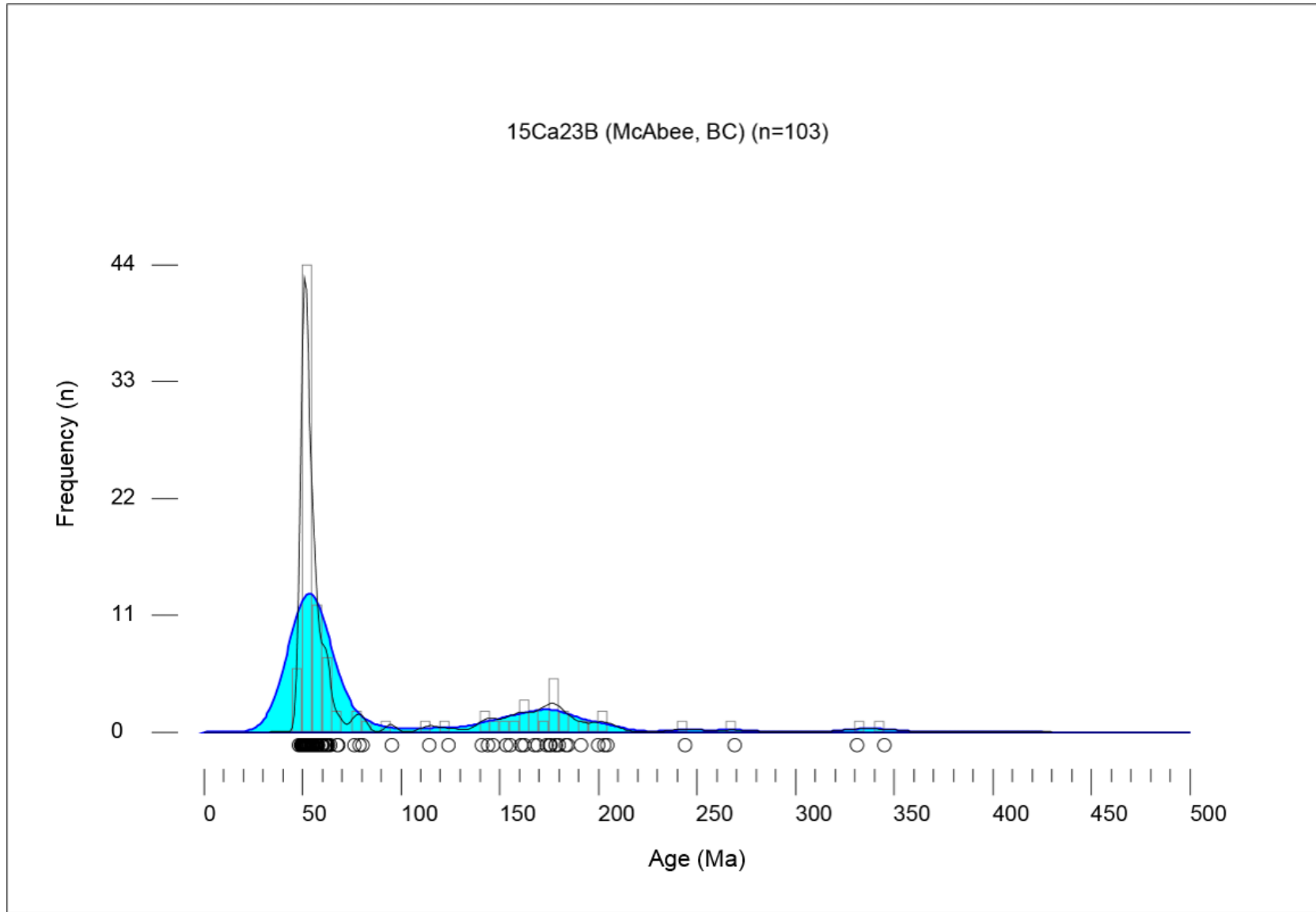


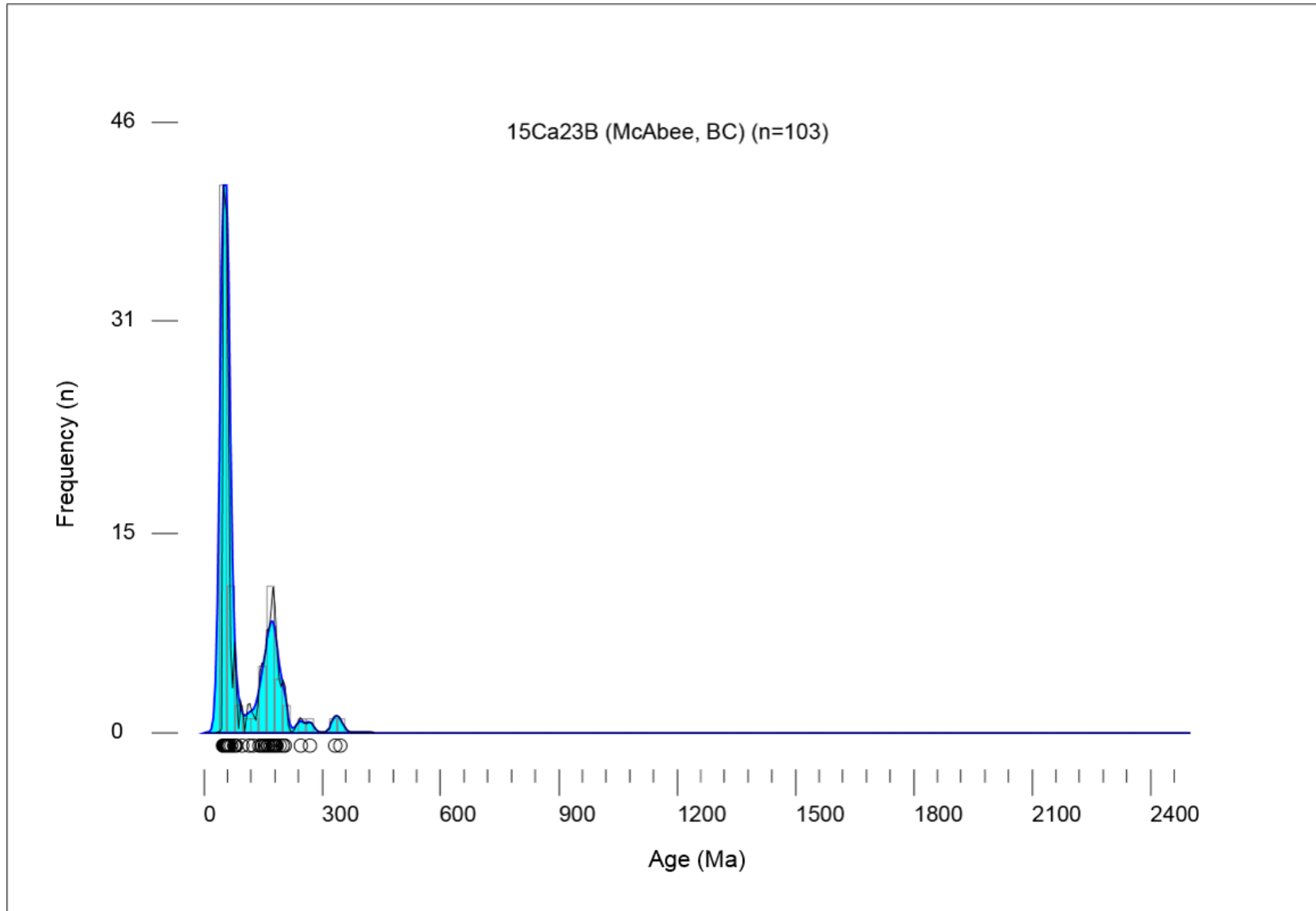


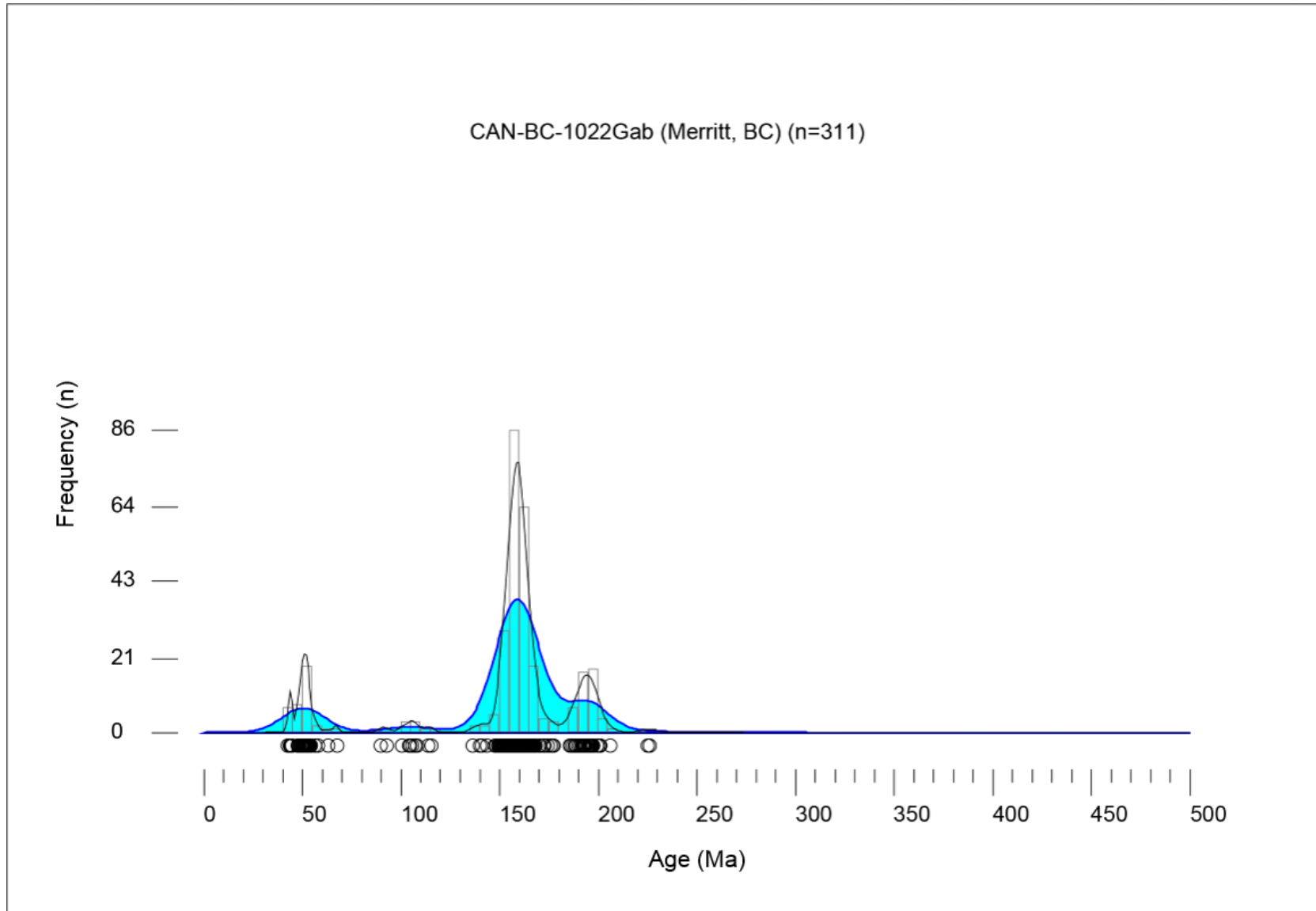


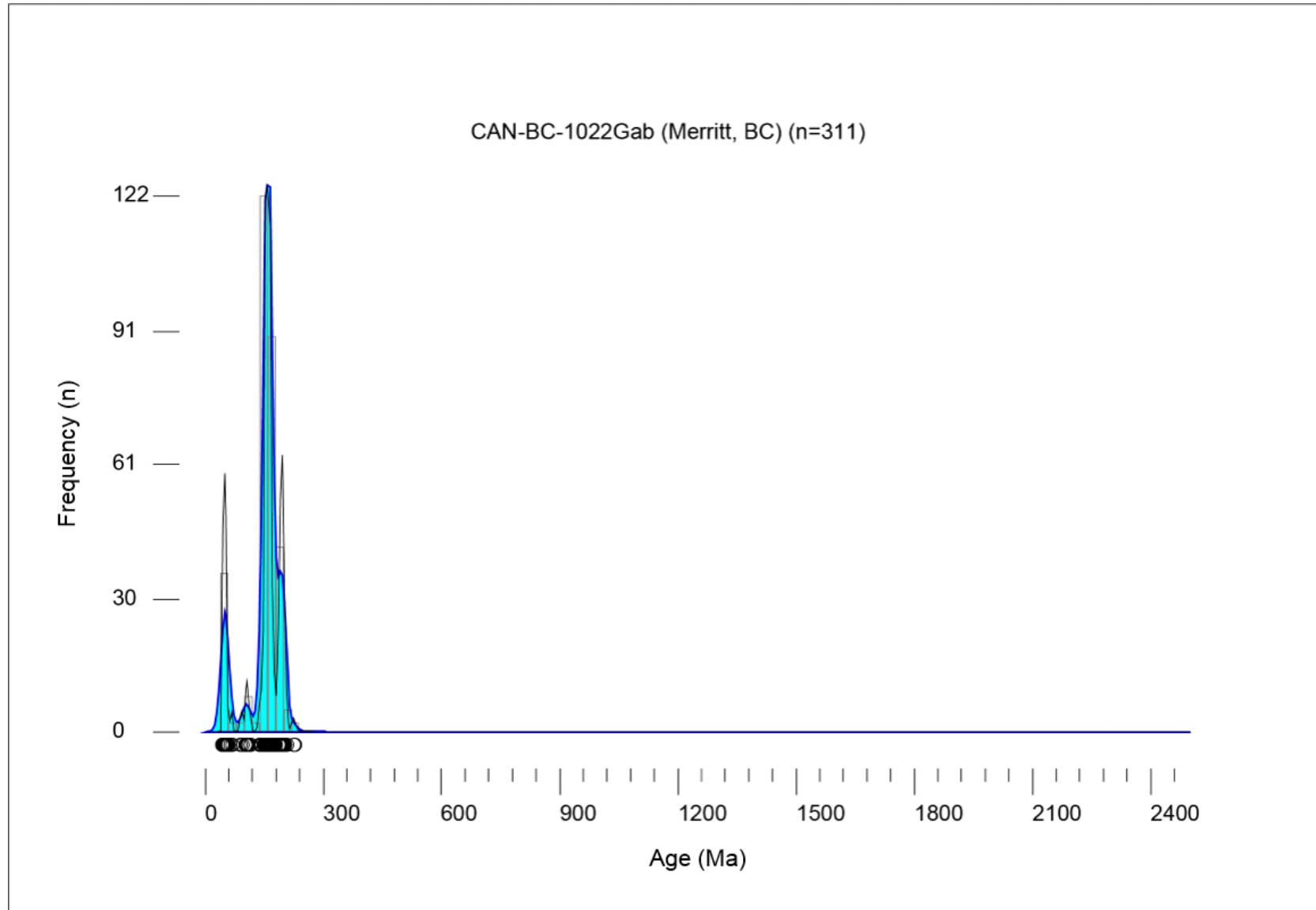


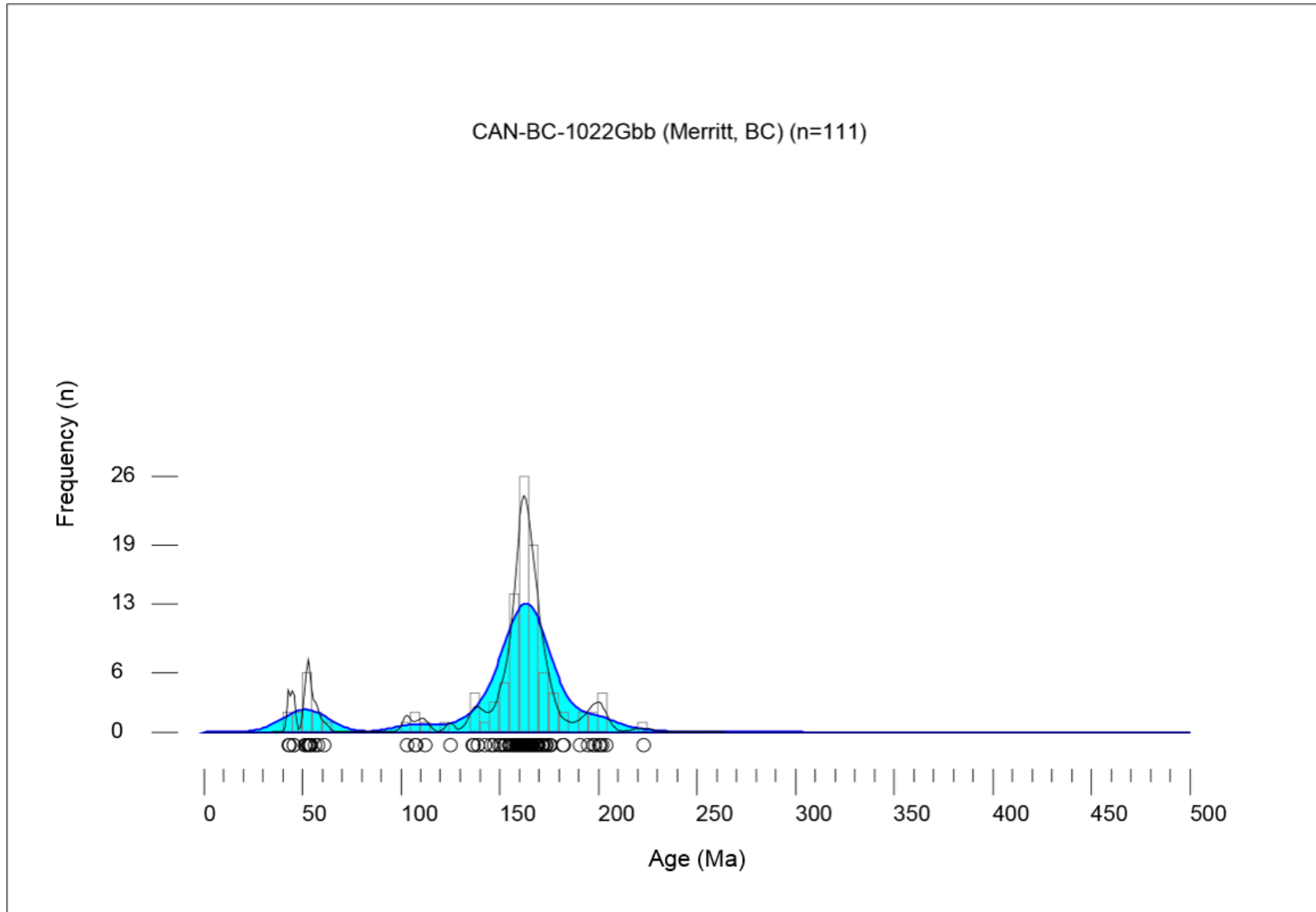


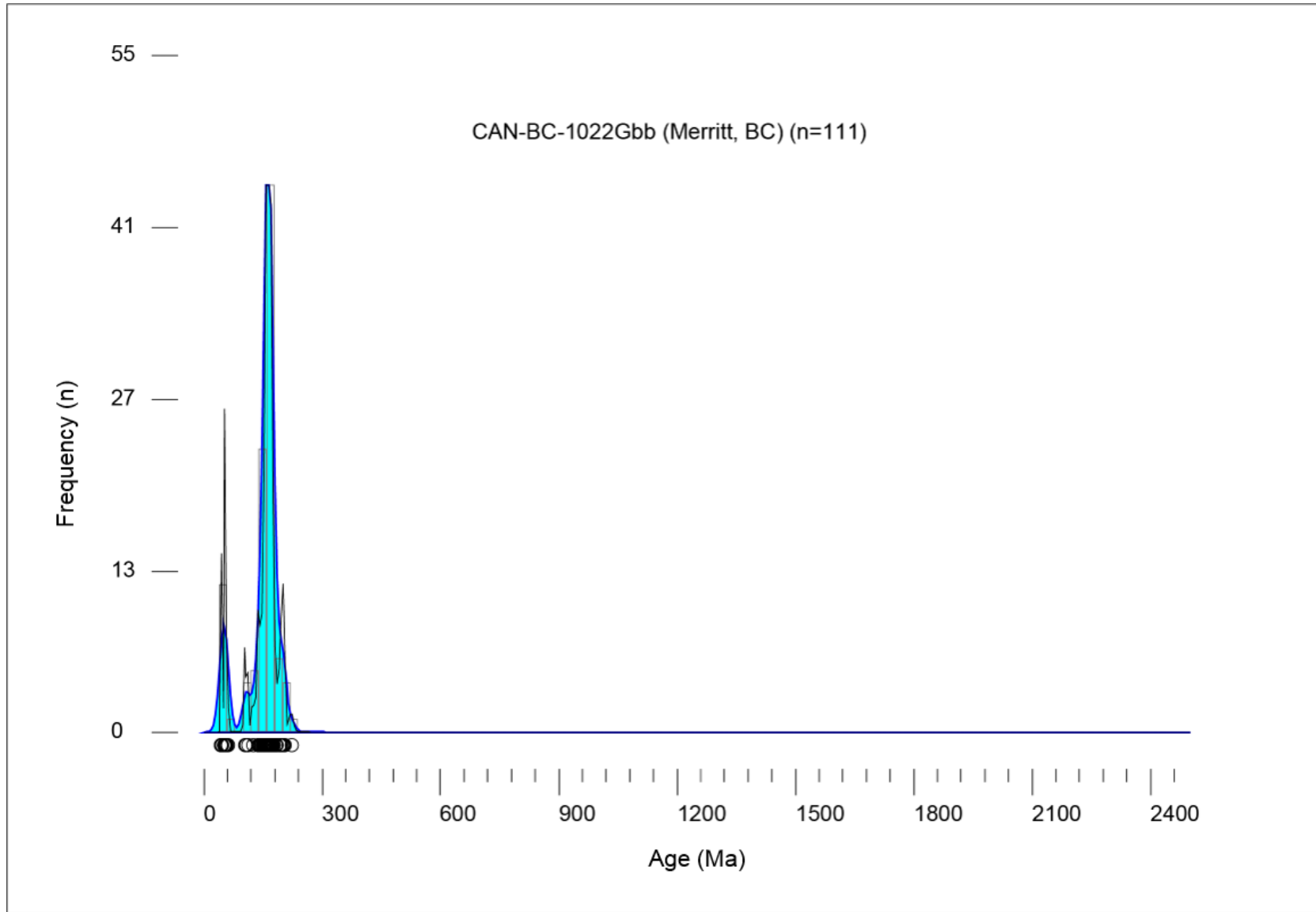


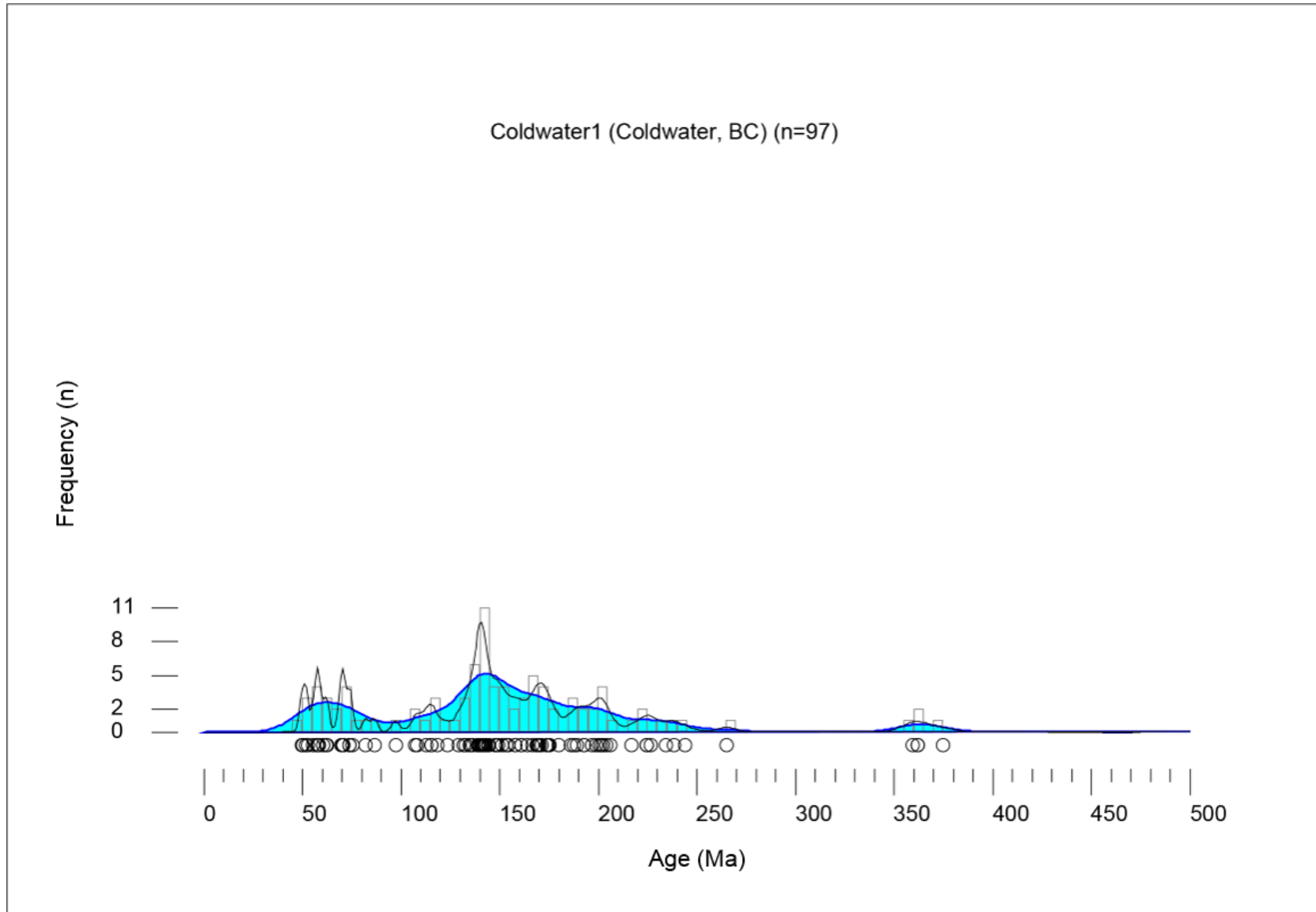


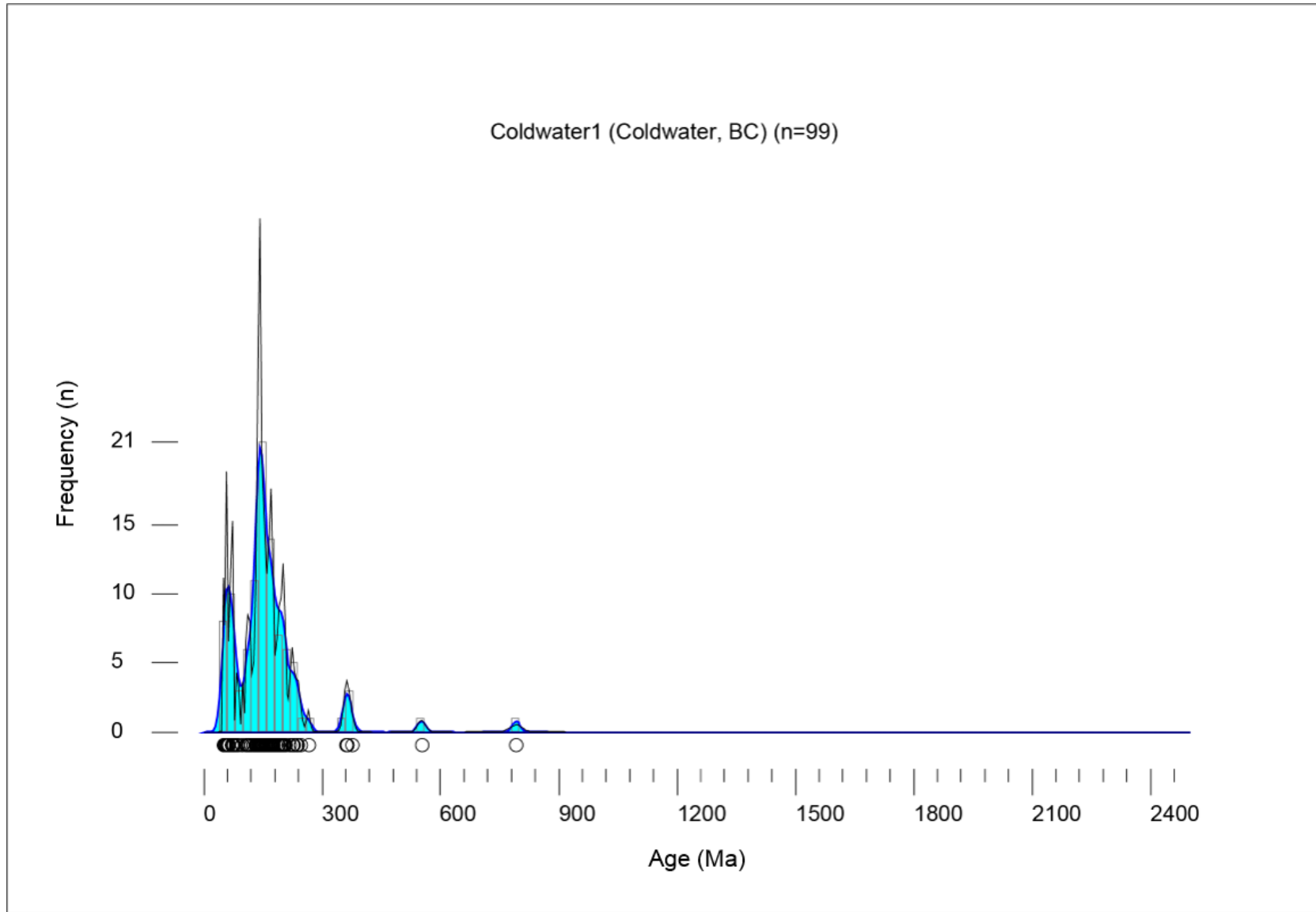








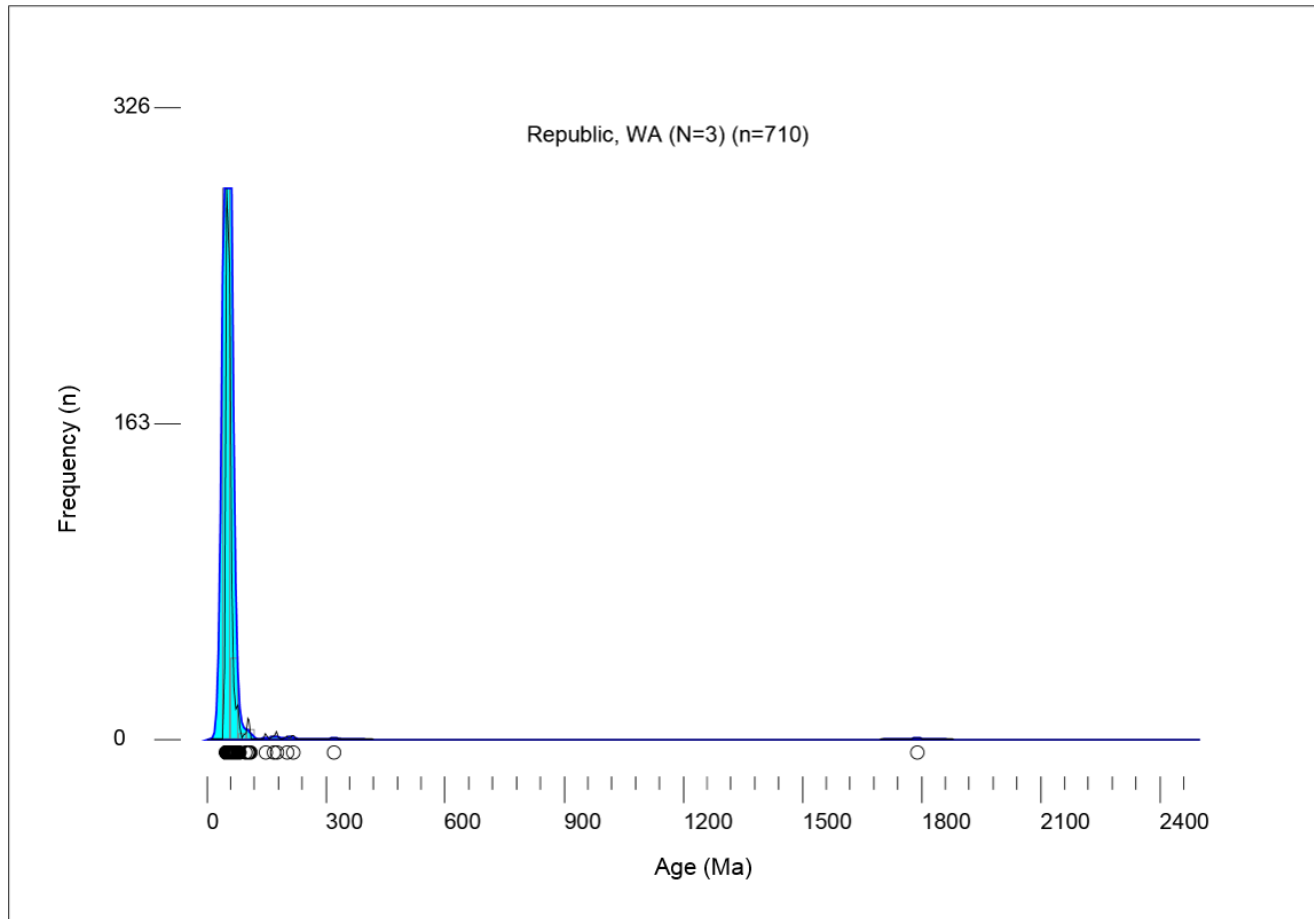


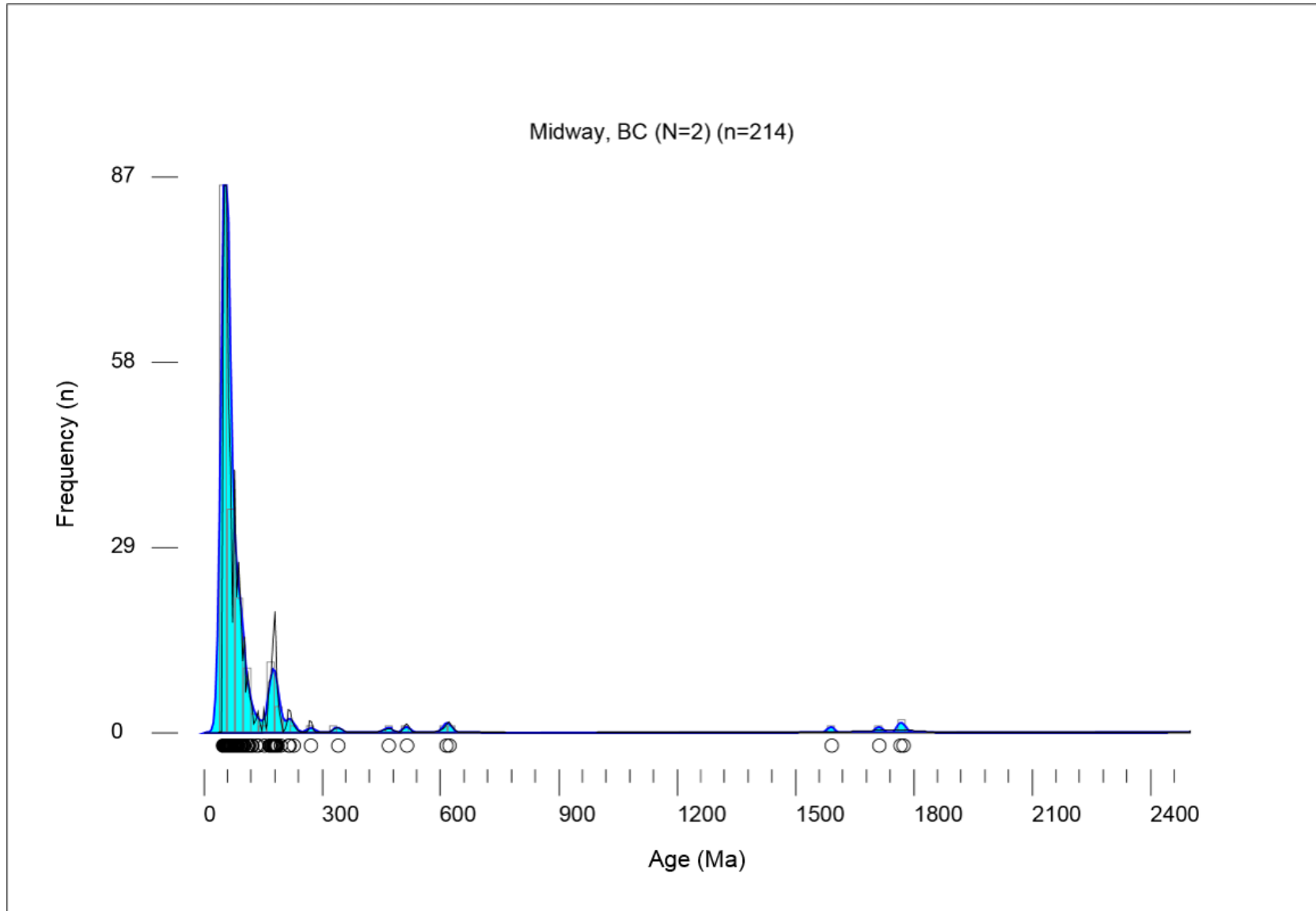


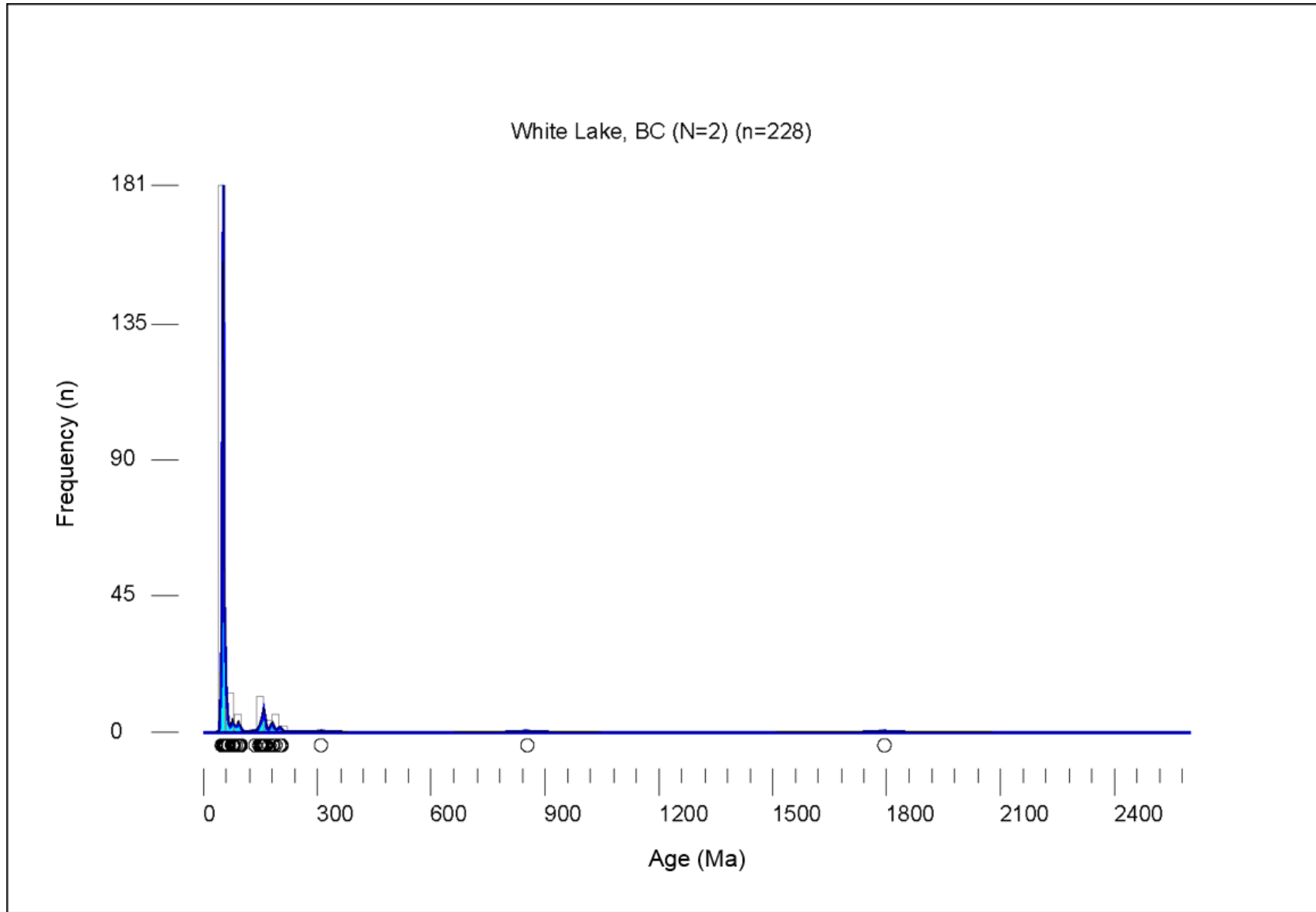
APPENDIX D

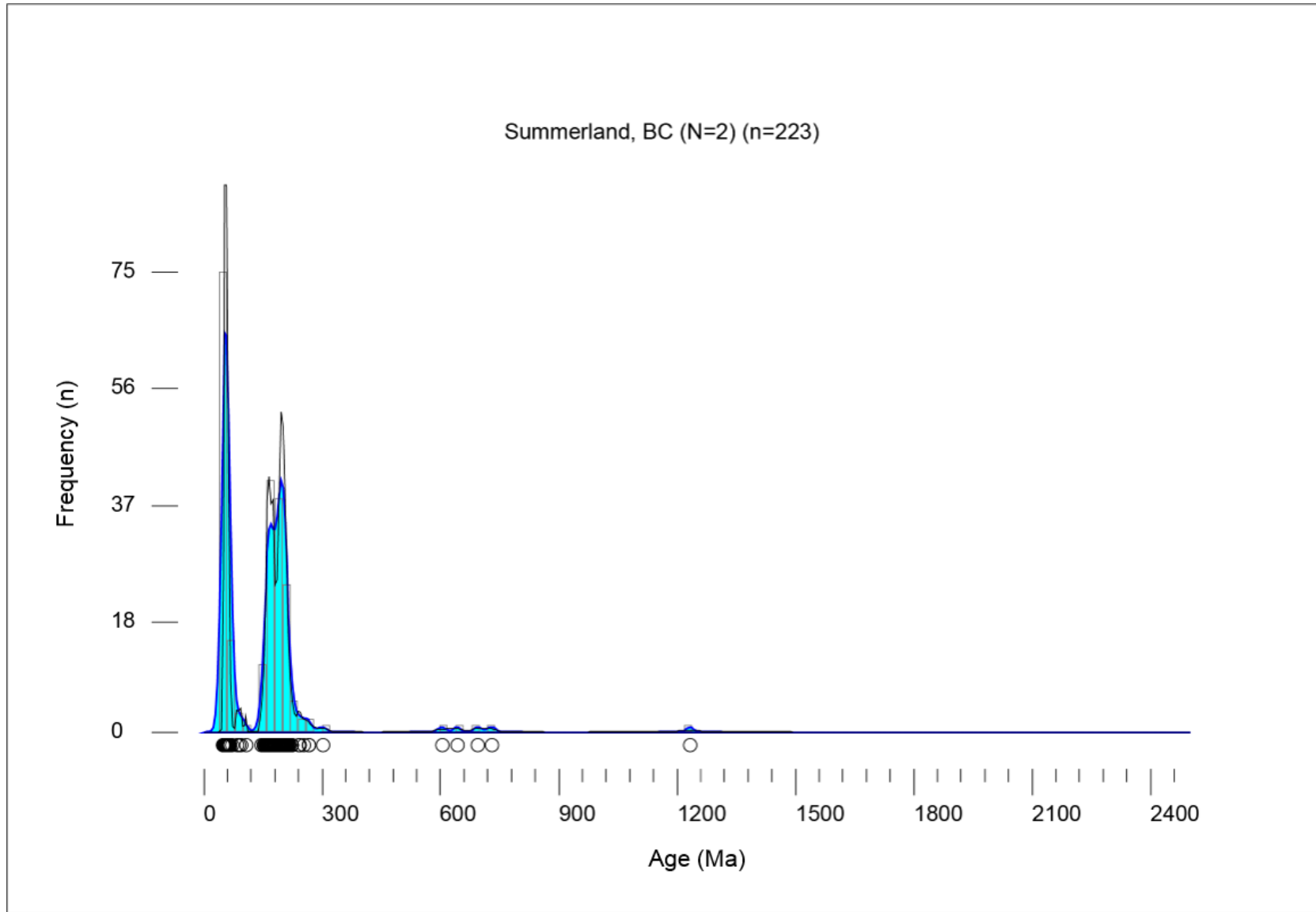
DETRITAL ZIRCON U-PB KDE (BLUE) AND PDP (BLACK) PLOTS

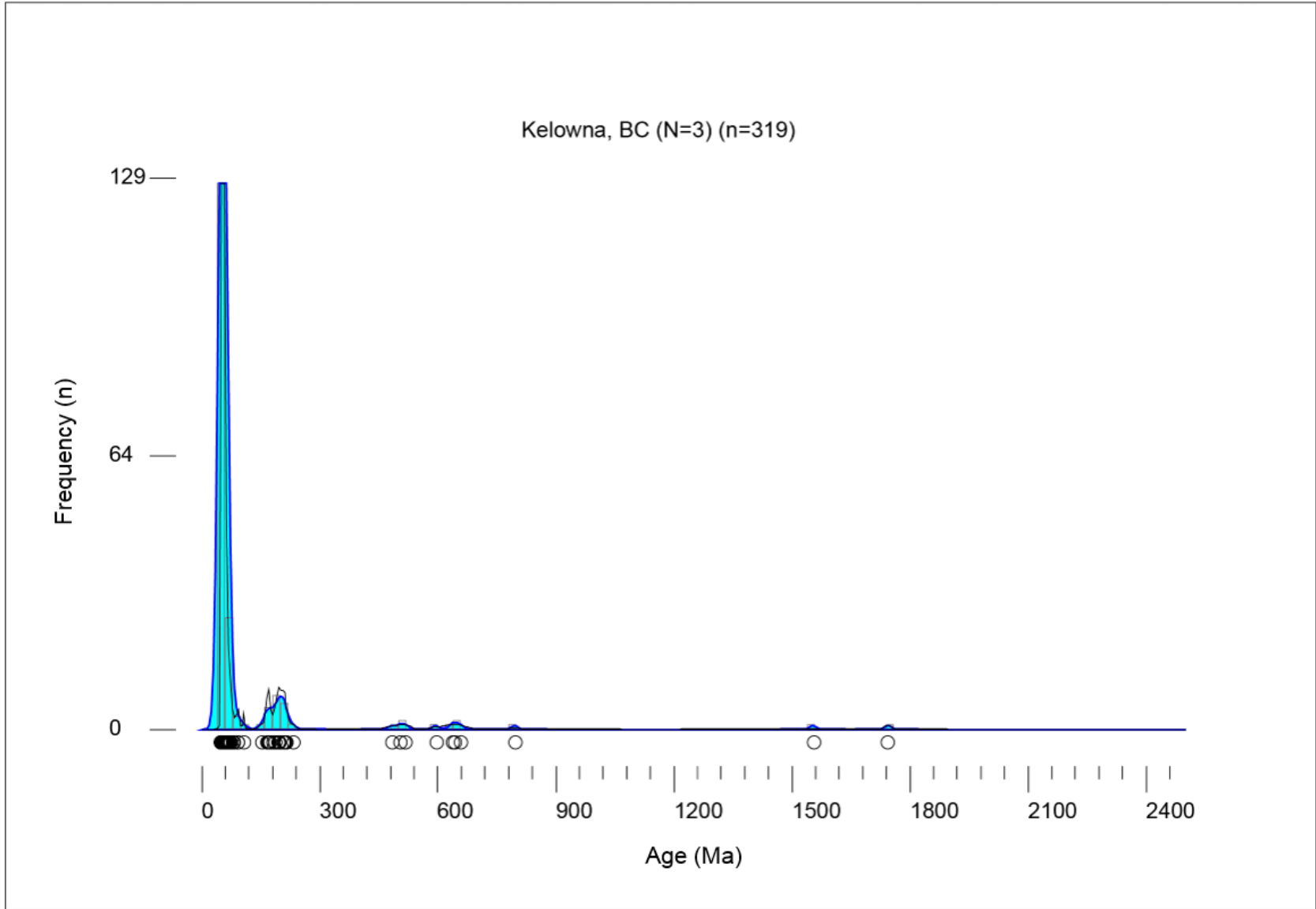
SEPARATED BY LOCATION (0-2,400 MA)

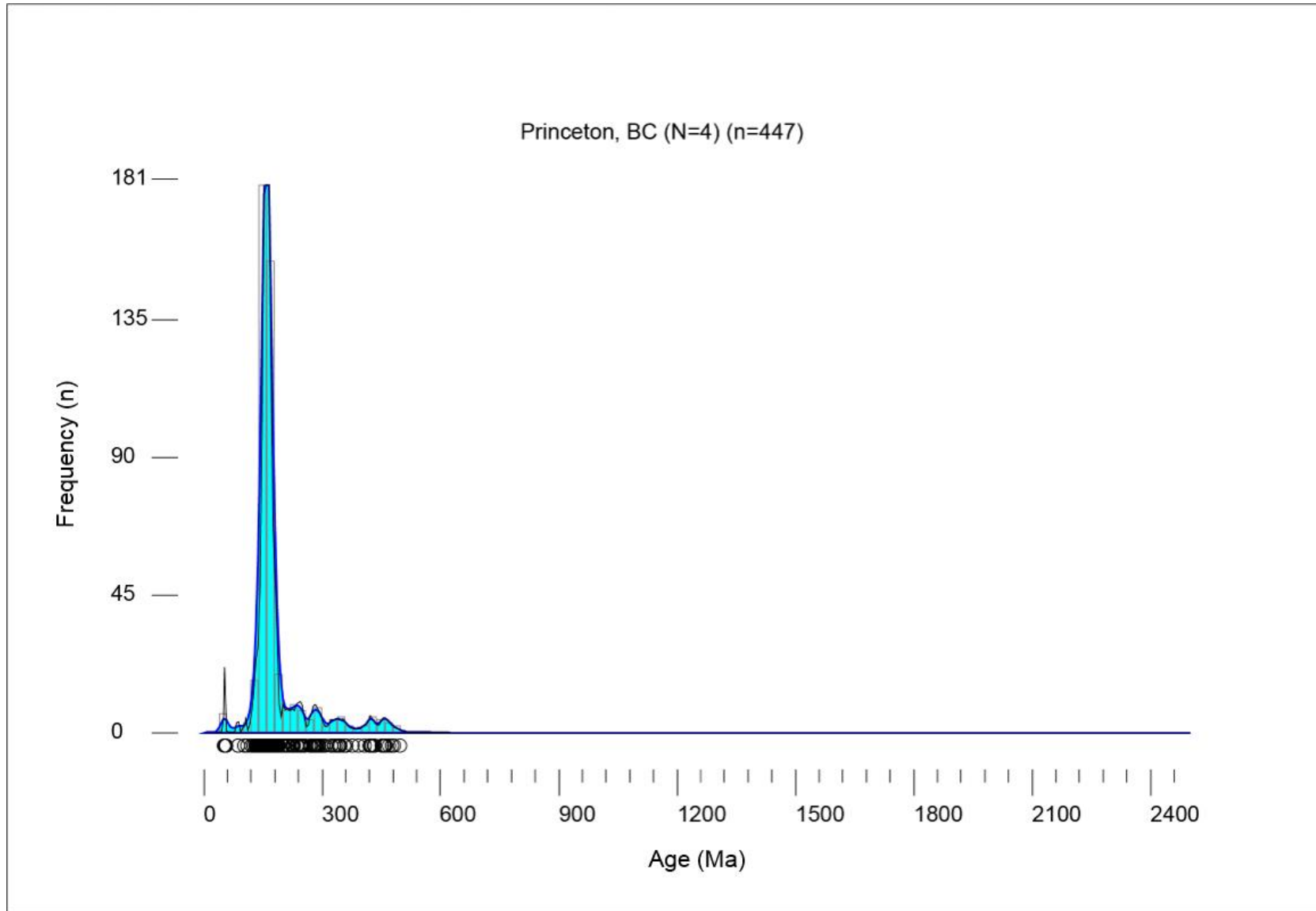


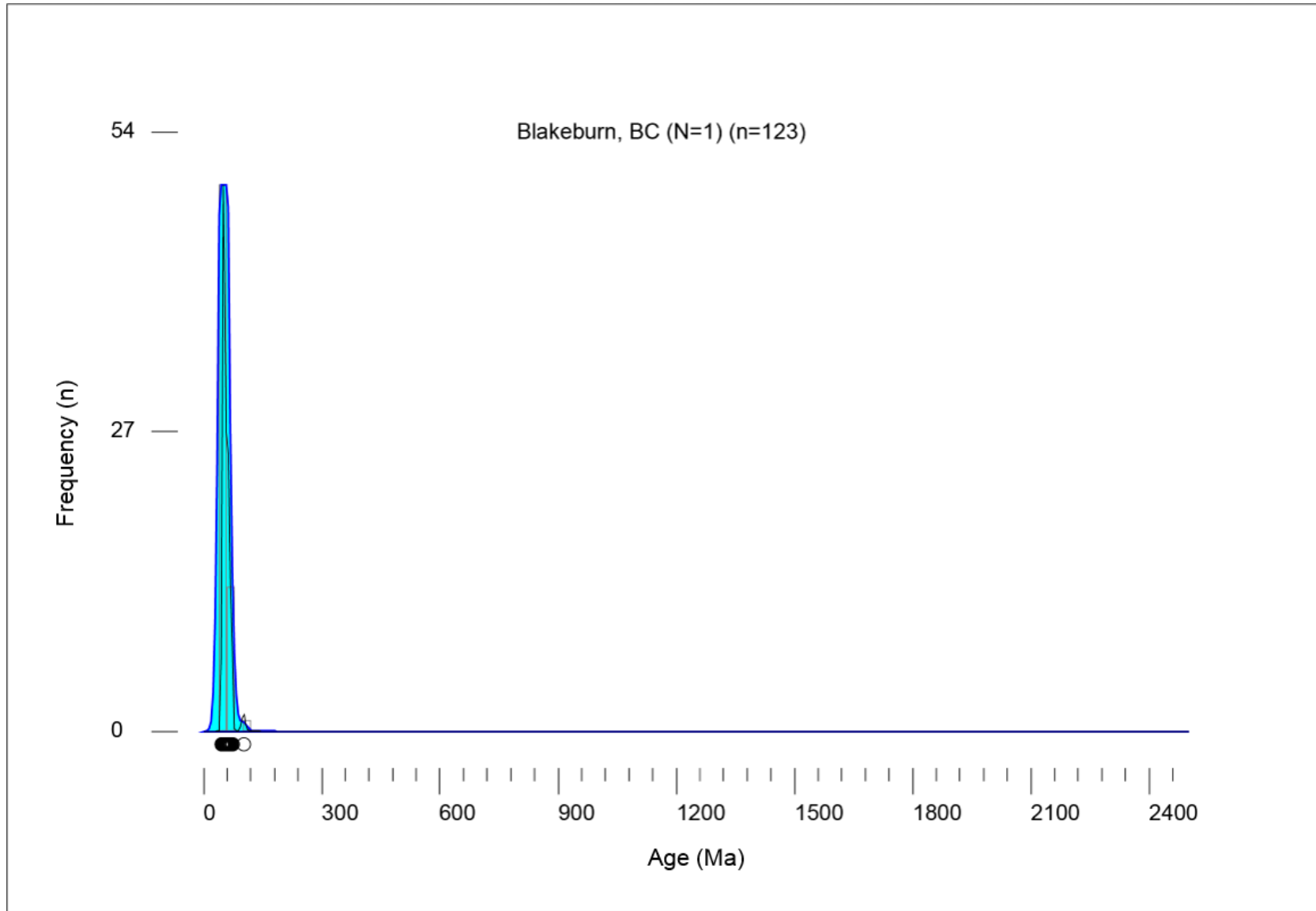


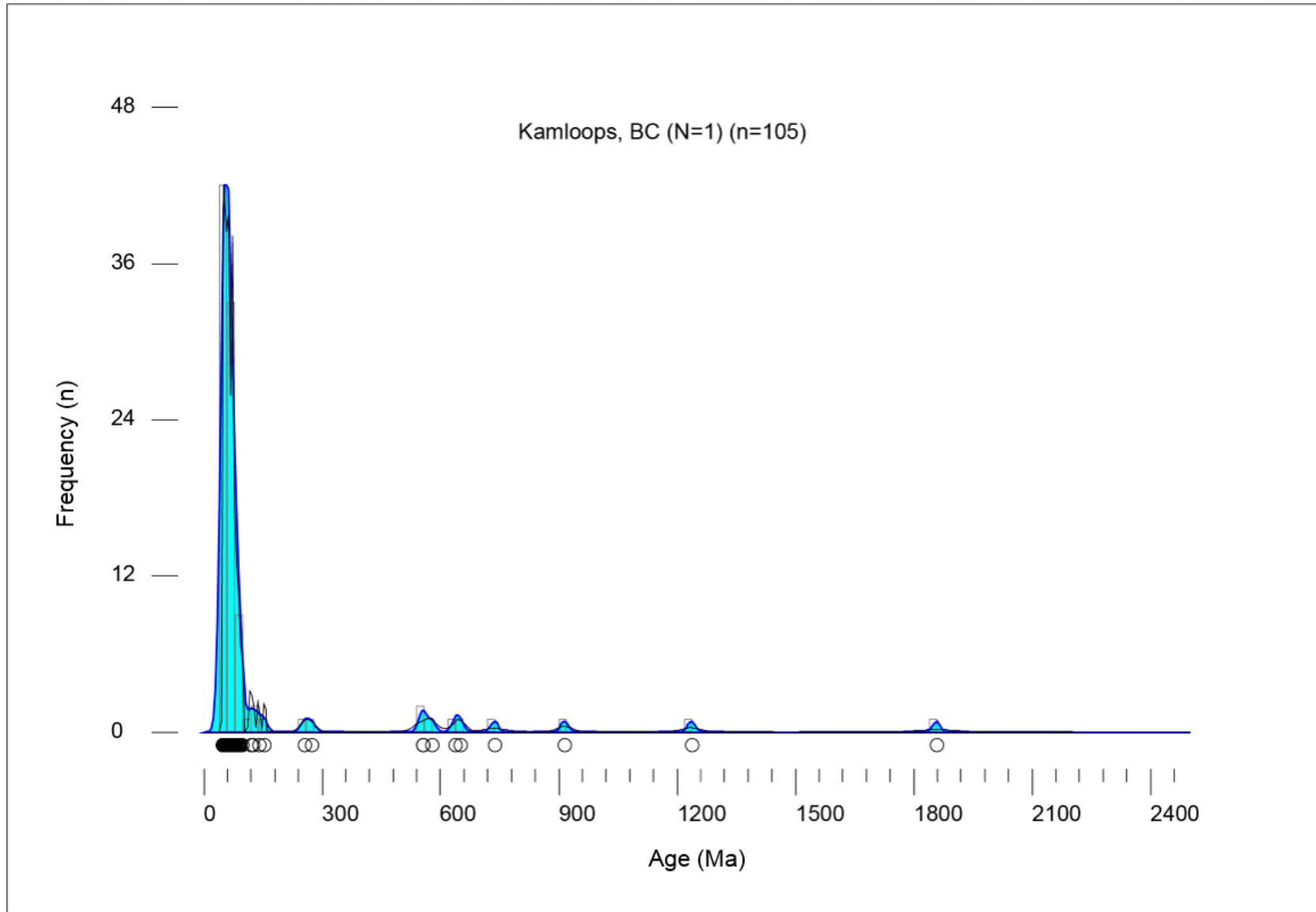


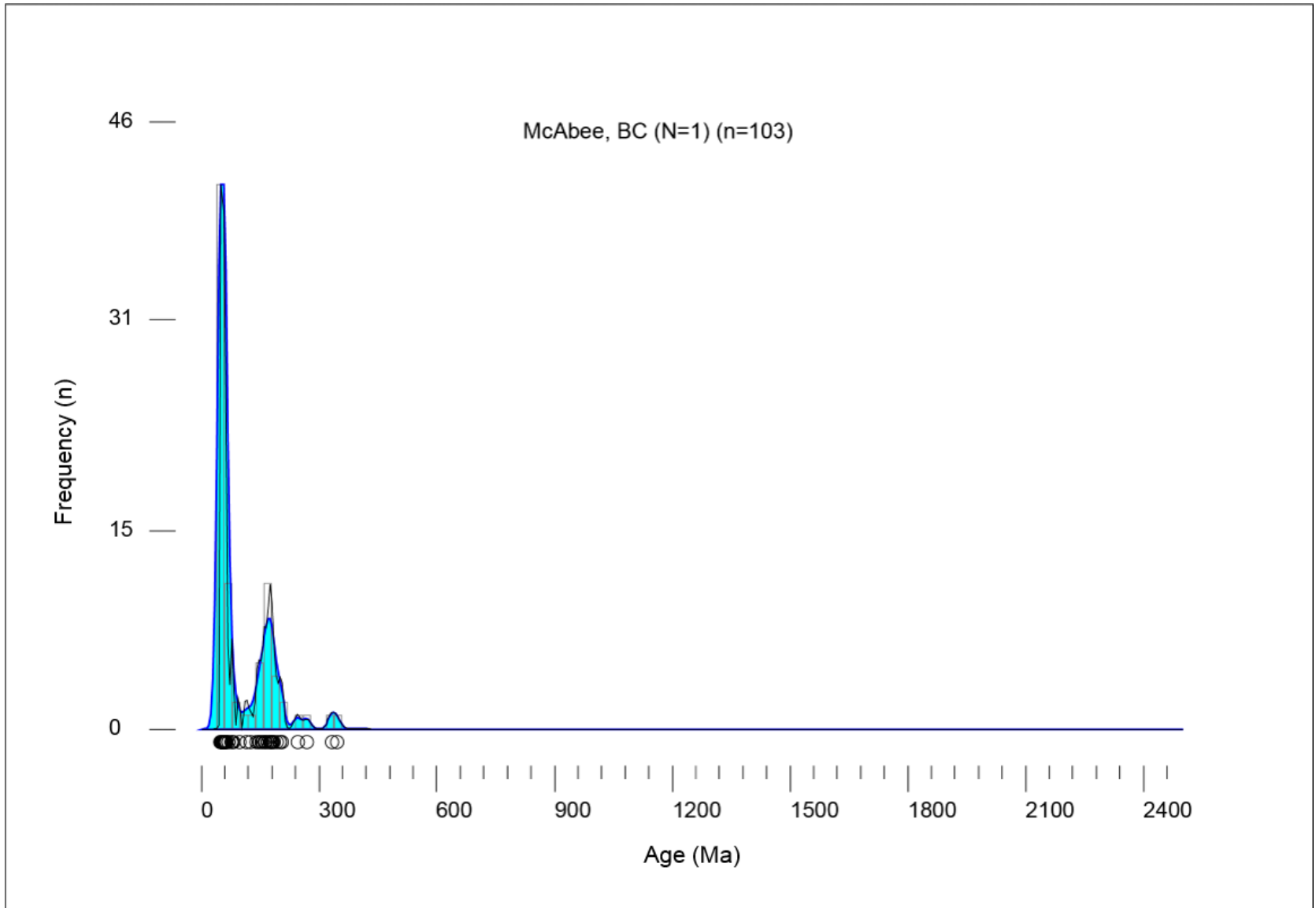


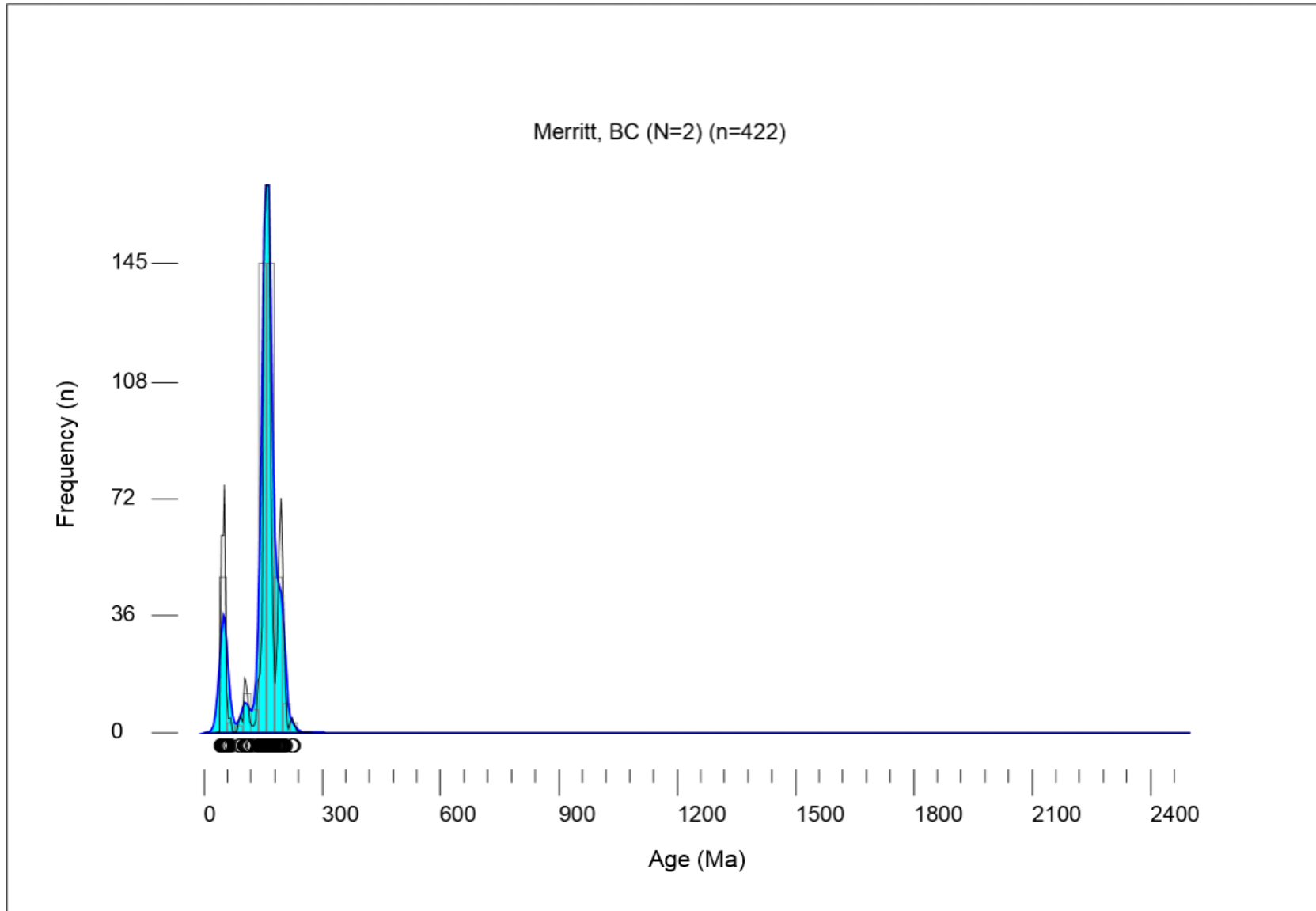


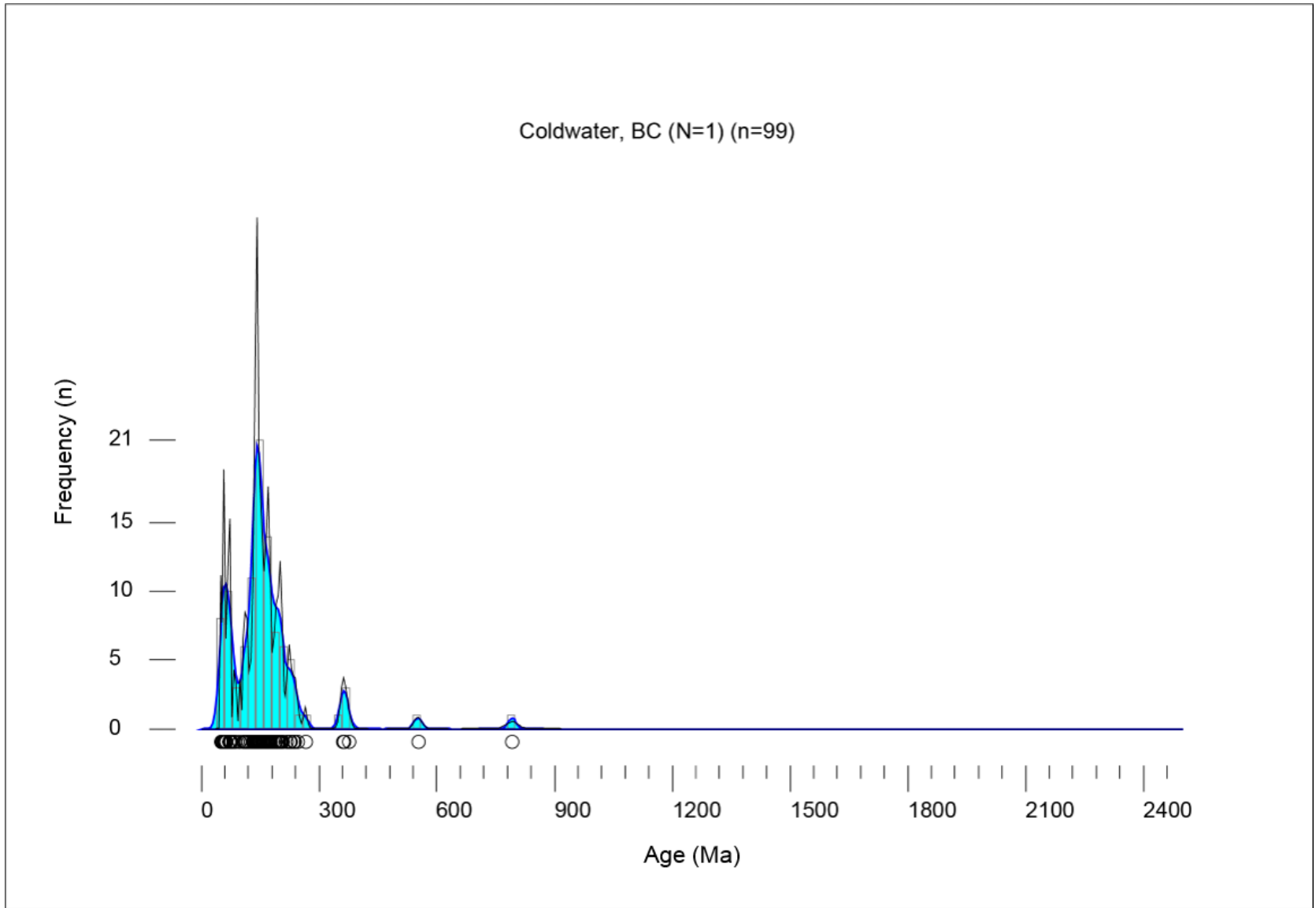












APPENDIX E

ARIZONA LASERCHRON CENTER U-PB & HF ANALYSES

The following sections on U-Pb geochronologic analyses of detrital zircon (Nu HR ICPMS) and Hf analytical methods at the Arizona LaserChron Center (ALC) were provided by the ALC and edited to accurately express processes provided by ALC. Prior to being sent to the ALC, zircons from samples (n=4) were extracted by traditional methods of crushing and grinding, density separation with a water table, heavy liquids (LMT), and Frantz magnetic separator in the Rock Preparation Facility and Sedimentary Geology Laboratory at the University of South Carolina (USC).

E.1 U-PB GEOCHRONOLOGIC ANALYSES OF DETRITAL ZIRCON (NU HR ICPMS)

Zircon crystals extracted from samples are processed such that all zircons are retained in the final heavy mineral fraction. A large split of these grains (generally thousands of grains) is incorporated into a 1” epoxy mount together with fragments of our Sri Lanka standard zircon. The mounts are sanded down to a depth of ~20 microns, polished, imaged, and cleaned prior to isotopic analysis.

U-Pb geochronology of zircons is conducted by laser ablation multicollector inductively coupled plasma mass spectrometry (LA-MC-ICPMS) at the Arizona LaserChron Center (Gehrels et al., 2006, 2008). The analyses involve ablation of zircon with a Photon Machines Analyte G2 excimer laser (or, prior to May 2011, a New Wave

UP193HE Excimer laser) using a spot diameter of 30 microns. The ablated material is carried in helium into the plasma source of a Nu HR ICPMS, which is equipped with a flight tube of sufficient width that U, Th, and Pb isotopes are measured simultaneously. All measurements are made in static mode, using Faraday detectors with 3×10^{11} ohm resistors for ^{238}U , ^{232}Th , ^{208}Pb - ^{206}Pb , and discrete dynode ion counters for ^{204}Pb and ^{202}Hg . Ion yields are ~ 0.8 mv per ppm. Each analysis consists of one 15-second integration on peaks with the laser off (for backgrounds), 15 one-second integrations with the laser firing, and a 30 second delay to purge the previous sample and prepare for the next analysis. The ablation pit is ~ 15 microns in depth.

For each analysis, the errors in determining $^{206}\text{Pb}/^{238}\text{U}$ and $^{206}\text{Pb}/^{204}\text{Pb}$ result in a measurement error of $\sim 1-2\%$ (at 2-sigma level) in the $^{206}\text{Pb}/^{238}\text{U}$ age. The errors in measurement of $^{206}\text{Pb}/^{207}\text{Pb}$ and $^{206}\text{Pb}/^{204}\text{Pb}$ also result in $\sim 1-2\%$ (at 2-sigma level) uncertainty in age for grains that are > 1.0 Ga, but are substantially larger for younger grains due to low intensity of the ^{207}Pb signal. For most analyses, the cross-over in precision of $^{206}\text{Pb}/^{238}\text{U}$ and $^{206}\text{Pb}/^{207}\text{Pb}$ ages occurs at ~ 1.0 Ga.

^{204}Hg interference with ^{204}Pb is accounted for measurement of ^{202}Hg during laser ablation and subtraction of ^{204}Hg according to the natural $^{202}\text{Hg}/^{204}\text{Hg}$ of 4.35. This Hg correction is not significant for most analyses because our Hg backgrounds are low (generally ~ 150 cps at mass 204).

Common Pb correction is accomplished by using the Hg-corrected ^{204}Pb and assuming an initial Pb composition from Stacey and Kramers (1975). Uncertainties of

1.5 for $^{206}\text{Pb}/^{204}\text{Pb}$ and 0.3 for $^{207}\text{Pb}/^{204}\text{Pb}$ are applied to these compositional values based on the variation in Pb isotopic composition in modern crystal rocks.

Inter-element fractionation of Pb/U is generally ~5%, whereas apparent fractionation of Pb isotopes is generally <0.2%. In-run analysis of fragments of a large zircon crystal (generally every fifth measurement) with known age of 563.5 ± 3.2 Ma (2-sigma error) is used to correct for this fractionation. The uncertainty resulting from the calibration correction is generally 1-2% (2-sigma) for both $^{206}\text{Pb}/^{207}\text{Pb}$ and $^{206}\text{Pb}/^{238}\text{U}$ ages.

Concentrations of U and Th are calibrated relative to our Sri Lanka zircon, which contains ~518 ppm of U and 68 ppm Th.

The analytical data are reported in Appendix F. Uncertainties shown in these tables are at the 1-sigma level, and include only measurement errors. Analyses that are >20% discordant (by comparison of $^{206}\text{Pb}/^{238}\text{U}$ and $^{206}\text{Pb}/^{207}\text{Pb}$ ages) or >5% reverse discordant are not considered further.

The resulting interpreted ages are shown on Pb*/U concordia diagrams and relative age-probability diagrams using the routines in Isoplot (Ludwig, 2008). The age-probability diagrams show each age and its uncertainty (for measurement error only) as a normal distribution, and sum all ages from a sample into a single curve. Composite age probability plots are made from an in-house Excel program (see Analysis Tools for link) that normalizes each curve according to the number of constituent analyses, such that each curve contains the same area, and then stacks the probability curves.

E.2 HF ANALYTICAL METHODS AT THE ARIZONA LASERCHRON CENTER

Hf isotope analyses are conducted with a Nu HR ICPMS connected to a New Wave UP193HE laser (2009-2010) or a Photon Machines Analyte G2 excimer laser (2011). Instrument settings are established first by analysis of 10 ppb solutions of JMC475 and a Spex Hf solution, and then by analysis of 10 ppb solutions containing Spex Hf, Yb, and Lu. The mixtures range in concentration of Yb and Lu, with $^{176}(\text{Yb}+\text{Lu})$ up to 70% of the ^{176}Hf . When all solutions yield $^{176}\text{Hf}/^{177}\text{Hf}$ of ~ 0.28216 , instrument settings are optimized for laser ablation analyses and seven different standard zircons (Mud Tank, 91500, Temora, R33, FC52, Plesovice, and Sri Lanka) are analyzed. These standards are included with unknowns on the same epoxy mounts. When precision and accuracy are acceptable, unknowns are analyzed using exactly the same acquisition parameters.

Laser ablation analyses are conducted with a laser beam diameter of 40 microns, with the ablation pits located on top of the U-Pb analysis pits. CL images are used to ensure that the ablation pits do not overlap multiple age domains or inclusions. Each acquisition consists of one 40-second integration on backgrounds (on peaks with no laser firing) followed by 60 one-second integrations with the laser firing. Using a typical laser fluence of $\sim 5 \text{ J/cm}^2$ and pulse rate of 7 Hz, the ablation rate is ~ 0.8 microns per second. Each standard is analyzed once for every ~ 20 unknowns.

Isotope fractionation is accounted for using the method of Woodhead et al. (2004): βHf is determined from the measured $^{179}\text{Hf}/^{177}\text{Hf}$; βYb is determined from the

measured $^{173}\text{Yb}/^{171}\text{Yb}$ (except for very low Yb signals); βLu is assumed to be the same as βYb ; and an exponential formula is used for fractionation correction. Yb and Lu interferences are corrected by measurement of $^{176}\text{Yb}/^{171}\text{Yb}$ and $^{176}\text{Lu}/^{175}\text{Lu}$ (respectively), as advocated by Woodhead et al. (2004). Critical isotope ratios are $^{179}\text{Hf}/^{177}\text{Hf} = 0.73250$ (Patchett and Tatsumoto, 1980); $^{173}\text{Yb}/^{171}\text{Yb} = 1.132338$ (Vervoort et al. 2004); $^{176}\text{Yb}/^{171}\text{Yb} = 0.901691$ (Vervoort et al., 2004; Amelin and Davis, 2005); $^{176}\text{Lu}/^{175}\text{Lu} = 0.02653$ (Patchett, 1983). All corrections are done line-by-line. For very low Yb signals, βHf is used for fractionation of Yb isotopes. The corrected $^{176}\text{Hf}/^{177}\text{Hf}$ values are filtered for outliers (2-sigma filter), and the average and standard error are calculated from the resulting ~58 integrations. There is no capability to use only a portion of the acquired data.

All solutions, standards, and unknowns analyzed during a session are reduced together. The cutoff for using βHf versus βYb is determined by monitoring the average offset of the standards from their known values, and the cutoff is set at the minimum offset. For most data sets, this is achieved at ~6 mv of ^{171}Yb . For sessions in which the standards yield $^{176}\text{Hf}/^{177}\text{Hf}$ values that are shifted consistently from the known values, a correction factor is applied to the $^{176}\text{Hf}/^{177}\text{Hf}$ of all standards and unknowns. This correction factor, which is not necessary for most sessions, averages 1 epsilon unit.

The $^{176}\text{Hf}/^{177}\text{Hf}$ at time of crystallization is calculated from measurement of present-day $^{176}\text{Hf}/^{177}\text{Hf}$ and $^{176}\text{Lu}/^{177}\text{Hf}$, using the decay constant of ^{176}Lu ($\lambda = 1.867e^{-11}$) from Scherer et al. (2001) and Söderlund et al. (2004). No capability is provided for

calculating Hf Depleted Mantle model ages because the $^{176}\text{Hf}/^{177}\text{Hf}$ and $^{176}\text{Lu}/^{177}\text{Hf}$ of the source material(s) from which the zircon crystallized is not known.

E.3 REFERENCES

- Amelin, Y., and Davis, W.J., 2005, Geochemical test for branching decay of ^{176}Lu : *Geochimica et Cosmochimica Acta*, v. 69, p. 465-473.
- Bahlburg, H., Vervoort, J.D., and DuFrane, S.A., 2010, Plate tectonic significance of Middle Cambrian and Ordovician siliciclastic rocks of the Bavarian facies, Armorican terrane assemblage, Germany -- U-Pb and Hf isotope evidence from detrital zircons: *Gondwana Research*, v. 17 (2-3), p. 223-235.
- Gehrels, G.E., Valencia, V., Ruiz, J., 2008, Enhanced precision, accuracy, efficiency, and spatial resolution of U-Pb ages by laser ablation–multicollector–inductively coupled plasma–mass spectrometry: *Geochemistry, Geophysics, Geosystems*, v. 9, Q03017, doi:10.1029/2007GC001805.
- Gehrels, G.E., Valencia, V., Pullen, A., 2006, Detrital zircon geochronology by Laser-Ablation Multicollector ICPMS at the Arizona LaserChron Center, in Loszewski, T., and Huff, W., eds., *Geochronology: Emerging Opportunities*, Paleontology Society Short Course: Paleontology Society Papers, v. 11, 10 p.
- Ludwig, K.R., 2008, *Isoplot 3.60*. Berkeley Geochronology Center, Special Publication 4, 77 p.
- Patchett, P.J., 1983, Importance of the Lu-Hf isotopic system in studies of planetary chronology and chemical evolution: *Geochimica et Cosmochimica Acta*, v. 47, p. 81-91.
- Patchett, P.J., and Tatsumoto, M., 1980, A routine high-precision method for Lu-Hf isotope geochemistry and chronology: *Contributions to Mineralogy and Petrology*, v. 75, 263-267.

- Scherer, E., Münker, C., and Mezger, K., 2001, Calibration of the Lutetium-Hafnium Clock: *Science*, v. 293, p. 683–687.
- Söderlund, U., Patchett, P.J., Vervoort, J.D., and Isachsen, C.E., 2004, The ^{176}Lu decay constant determined by Lu-Hf and U-Pb isotope systematics of Precambrian mafic intrusions: *Earth and Planetary Science Letters*, v. 219, p. 311-324.
- Stacey, J.S., and Kramers, J.D., 1975, Approximation of terrestrial lead isotope evolution by a two-stage model: *Earth and Planetary Science Letters*, v. 26, p. 207-221.
- Vervoort, J.D., 2010, Hf analysis in zircon by LA-MC-ICPMS: Promise and pitfalls: *Geological Society of America Abstracts with Programs*, v. 42 (5), p. 667.
- Vervoort, J.D., Patchett, P.J., Söderlund, U. & Baker, M., 2004, The isotopic composition of Yb and the precise and accurate determination of Lu concentrations and Lu/Hf ratios by isotope dilution using MC-ICPMS. *Geochem Geophys Geosyst*. DOI 2004GC000721RR.
- Wieser, M.E., 2006, Atomic weights of the elements 2005 (IUPAC Technical Report): *Pure and Applied Chemistry*, v. 78 (11), p. 2051–2066. doi:10.1351/pac200678112051
- Woodhead, J., Hergt, J., Shelley, M., Eggins, S., and Kemp, R., 2004, Zircon Hf-isotope analysis with an excimer laser, depth profiling, ablation of complex geometries, and concomitant age estimation: *Chemical Geology*, v. 209, p. 121-135.

APPENDIX F

ARIZONA LASERCHRON CENTER

DETRITAL ZIRCON U-PB ANALYSES DATA TABLE

Sample: 15CA01B	U-Pb geochronologic analyses				Isotope ratios				Apparent ages (Ma)									
	Analysis	U (ppm)	²⁰⁶ Pb/ ²⁰⁴ Pb	U/Th	²⁰⁶ Pb/ ²⁰⁷ Pb ^a	±	²⁰⁷ Pb/ ²³⁵ U ^b	±	²⁰⁶ Pb/ ²³⁸ U ^c	±	error	²⁰⁶ Pb/ ²³⁸ U ^d	±	Best age	±			
15CA-01B 29Feb-Spot 1	127	1320	1.4	11.8953	5.9	0.1444	6.4	0.0125	2.4	0.38	79.8	1.9	137.0	8.1	1294.1	114.4	79.8	1.9
15CA-01B 29Feb-Spot 2	83	1016	1.3	16.7681	7.7	0.0764	8.7	0.0093	3.9	0.45	59.6	2.3	74.8	6.2	590.4	167.7	59.6	2.3
15CA-01B 29Feb-Spot 3	42	547	1.1	7.7287	7.3	0.1611	9.8	0.0090	4.1	0.58	57.9	2.8	151.7	12.4	2089.7	128.7	57.9	2.8
15CA-01B 29Feb-Spot 4	100	485	0.5	8.8234	6.2	0.1413	7.1	0.0090	3.4	0.48	56.1	2.0	134.2	8.9	1852.3	112.6	56.1	2.0
15CA-01B 29Feb-Spot 5	26	693	1.1	26.6187	23.5	0.0403	24.1	0.0078	5.6	0.23	50.0	2.8	40.1	9.5	515.7	633.5	50.0	2.8
15CA-01B 29Feb-Spot 6	42	988	1.0	13.8749	7.4	0.0870	8.5	0.0088	4.1	0.48	56.2	2.3	84.7	6.9	988.0	150.6	56.2	2.3
15CA-01B 29Feb-Spot 7	26	395	1.1	60.1790	84.8	0.0179	84.9	0.0078	4.9	0.06	50.1	2.5	18.0	15.1	0.0	892.8	50.1	2.5
15CA-01B 29Feb-Spot 8	35	1236	1.0	24.8959	5.7	0.0444	7.6	0.0080	5.0	0.66	51.4	2.6	44.1	3.3	340.2	146.9	51.4	2.6
15CA-01B 29Feb-Spot 9	56	697	1.2	29.1384	5.2	0.0376	6.9	0.0079	4.4	0.65	51.0	2.2	37.4	1.8	163.2	147.6	51.0	2.2
15CA-01B 29Feb-Spot 10	90	550	0.6	7.9367	23.8	0.1624	24.2	0.0089	4.4	0.19	57.4	2.5	152.8	34.3	2119.9	422.9	57.4	2.5
15CA-01B 29Feb-Spot 11	152	2074	0.6	15.0647	3.2	0.0749	4.2	0.0082	2.8	0.66	52.5	1.5	73.3	3.0	818.4	66.3	52.5	1.5
15CA-01B 29Feb-Spot 12	70	2534	0.7	26.1762	4.0	0.0410	5.1	0.0078	3.1	0.62	50.0	1.6	40.8	2.0	471.1	104.8	50.0	1.6
15CA-01B 29Feb-Spot 13	139	1955	1.0	22.4170	4.3	0.0488	5.3	0.0079	3.1	0.58	50.9	1.6	48.4	2.5	76.9	104.6	50.9	1.6
15CA-01B 29Feb-Spot 14	84	630	1.1	33.7542	31.2	0.0341	31.3	0.0083	3.1	0.10	53.6	1.6	34.1	10.6	1187.6	894.4	53.6	1.6
15CA-01B 29Feb-Spot 15	52	779	1.1	23.4667	10.7	0.0480	11.4	0.0082	3.8	0.34	52.4	2.0	47.6	5.3	190.1	268.2	52.4	2.0
15CA-01B 29Feb-Spot 16	30	1629	0.8	28.1721	4.3	0.0396	5.8	0.0081	3.9	0.67	51.9	2.0	39.4	2.2	669.6	117.8	51.9	2.0
15CA-01B 29Feb-Spot 17	41	500	0.8	15.0954	7.0	0.0759	8.1	0.0083	4.1	0.51	53.3	2.2	74.3	5.8	814.2	145.6	53.3	2.2
15CA-01B 29Feb-Spot 18	250	2480	0.6	20.2215	3.3	0.0546	4.6	0.0080	3.1	0.68	51.4	1.6	53.9	2.4	169.3	78.1	51.4	1.6
15CA-01B 29Feb-Spot 19	41	620	0.7	25.2079	7.7	0.0457	11.2	0.0084	8.1	0.72	53.6	4.3	45.4	5.0	372.4	200.6	53.6	4.3
15CA-01B 29Feb-Spot 20	238	1598	0.5	23.2148	2.4	0.0478	3.8	0.0080	2.9	0.77	51.6	1.5	47.4	1.8	163.2	147.6	51.6	1.5
15CA-01B 29Feb-Spot 21	31	209	0.9	24.6467	6.9	0.0459	8.3	0.0082	4.6	0.55	52.6	2.4	45.5	3.7	314.3	178.0	52.6	2.4
15CA-01B 29Feb-Spot 22	44	2010	1.1	19.4196	5.1	0.0568	7.0	0.0080	4.9	0.69	51.4	2.5	56.1	3.8	263.0	116.1	51.4	2.5
15CA-01B 29Feb-Spot 23	70	445	0.8	7.8027	3.0	0.1566	4.4	0.0089	3.3	0.75	56.9	1.9	147.7	6.1	2072.9	52.2	56.9	1.9
15CA-01B 29Feb-Spot 24	37	340	0.8	202.4902	46.6	0.0052	46.9	0.0076	5.1	0.11	48.7	2.5	5.2	2.4	0.0	48.7	2.5	2.5
15CA-01B 29Feb-Spot 25	51	466	1.0	49.8604	27.3	0.0217	27.5	0.0079	3.5	0.13	50.3	1.8	21.8	6.3	2605.7	706.5	50.3	1.8
15CA-01B 29Feb-Spot 26	59	712	1.4	12.4523	14.2	0.0572	14.8	0.0088	1.0	0.28	56.2	2.3	94.2	13.3	1204.4	280.5	56.2	2.3
15CA-01B 29Feb-Spot 27	47	917	0.9	16.8853	4.9	0.0673	6.4	0.0082	4.2	0.65	52.9	2.2	66.1	4.1	575.3	107.9	52.9	2.2
15CA-01B 29Feb-Spot 28	105	2515	1.1	24.4160	3.3	0.0444	4.8	0.0079	3.5	0.73	50.5	1.7	44.1	2.1	290.3	83.7	50.5	1.7
15CA-01B 29Feb-Spot 29	52	653	1.3	28.6689	8.5	0.0390	9.4	0.0081	4.1	0.44	52.0	2.2	38.8	3.6	718.1	236.1	52.0	2.2
15CA-01B 29Feb-Spot 30	43	1478	1.0	7.4415	4.3	0.1668	6.3	0.0090	4.6	0.73	57.8	2.7	156.6	9.2	2156.0	75.2	57.8	2.7
15CA-01B 29Feb-Spot 31	813	2453	0.4	19.2933	6.7	0.0724	7.4	0.0080	3.2	0.43	51.6	1.6	71.0	5.1	786.8	140.8	51.6	1.6
15CA-01B 29Feb-Spot 32	64	401	0.8	37.6318	15.8	0.0282	16.5	0.0077	4.6	0.28	49.5	2.3	28.3	4.6	1548.5	534.7	49.5	2.3
15CA-01B 29Feb-Spot 33	40	1341	1.0	25.6167	4.7	0.0453	6.8	0.0084	4.9	0.72	54.1	2.6	45.0	3.0	414.3	123.2	54.1	2.6
15CA-01B 29Feb-Spot 34	59	501	0.9	61.9186	28.1	0.0174	28.4	0.0078	3.6	0.13	50.1	1.8	17.5	4.9	0.0	1076.7	50.1	1.8
15CA-01B 29Feb-Spot 35	32	618	0.8	6.3219	5.6	0.2101	7.6	0.0096	5.2	0.68	61.8	3.2	193.7	13.5	2436.3	95.0	61.8	3.2
15CA-01B 29Feb-Spot 36	72	1027	1.1	27.8190	14.8	0.0398	15.3	0.0080	3.9	0.26	51.5	2.0	39.6	5.9	635.0	407.0	51.5	2.0
15CA-01B 29Feb-Spot 37	33	324	0.9	51.2238	6.7	0.0217	6.4	0.0079	4.9	0.46	51.0	2.0	21.5	3.8	1204.4	280.5	51.0	2.0
15CA-01B 29Feb-Spot 38	39	4084	0.8	21.0991	4.8	0.0527	6.7	0.0081	4.7	0.70	51.8	2.4	52.1	3.4	69.2	113.6	51.8	2.4
15CA-01B 29Feb-Spot 39	29	3637	0.9	3.1547	3.7	0.5517	6.3	0.0126	5.1	0.81	80.9	4.1	446.1	22.7	3555.3	57.2	80.9	4.1
15CA-01B 29Feb-Spot 40	86	952	1.1	25.7402	6.3	0.0419	7.0	0.0078	3.1	0.44	50.2	1.5	41.7	2.9	426.9	166.0	50.2	1.5
15CA-01B 29Feb-Spot 41	88	4571	0.9	23.1059	3.4	0.0479	5.2	0.0080	3.9	0.75	51.6	2.0	47.5	2.4	151.5	85.5	51.6	2.0
15CA-01B 29Feb-Spot 42	61	4347	0.5	20.4803	3.5	0.0555	4.9	0.0083	4.3	0.59	52.9	1.6	54.9	3.1	69.6	83.5	52.9	1.6
15CA-01B 29Feb-Spot 43	149	179186	1.3	19.8278	2.5	0.0575	3.5	0.0083	2.5	0.70	53.1	1.3	56.8	1.9	215.0	57.9	53.1	1.3
15CA-01B 29Feb-Spot 44	45	1995	0.9	21.3863	4.9	0.0528	6.0	0.0082	3.4	0.57	52.6	1.8	52.2	3.0	36.9	117.2	52.6	1.8
15CA-01B 29Feb-Spot 45	34	470	1.1	13.9521	13.2	0.0835	14.0	0.0084	4.6	0.33	54.2	2.5	81.4	10.9	97.7	270.1	54.2	2.5
15CA-01B 29Feb-Spot 46	60	1095	0.8	28.0777	8.1	0.0376	9.1	0.0076	4.2	0.46	49.1	2.0	37.4	3.3	660.4	222.6	49.1	2.0
15CA-01B 29Feb-Spot 47	102	1997	0.7	22.9269	9.0	0.0476	9.8	0.0079	3.9	0.40	50.8	2.0	47.2	4.5	132.3	222.1	50.8	2.0
15CA-01B 29Feb-Spot 48	26	316	1.2	251.9378	165.3	0.0043	165.4	0.0078	5.3	0.63	50.3	2.7	4.3	7.2	0.0	9.0	60.3	2.7
15CA-01B 29Feb-Spot 49	63	935	0.7	24.9302	3.8	0.0438	5.1	0.0079	3.4	0.67	50.9	1.7	43.6	2.2	342.7	97.3	50.9	1.7
15CA-01B 29Feb-Spot 50	88	881	0.9	19.1317	5.8	0.0598	6.8	0.0083	3.6	0.53	53.3	1.9	59.0	3.9	297.2	132.1	53.3	1.9
15CA-01B 29Feb-Spot 51	45	1107	0.8	28.9634	9.8	0.0380	11.0	0.0080	5.0	0.45	51.2	2.5	37.8	4.1	746.7	275.8	51.2	2.5
15CA-01B 29Feb-Spot 52	27	209	1.0	138.6437	11.8	0.0081	12.6	0.0081	4.5	0.36	52.0	2.3	8.2	1.0	0.0	0.0	52.0	2.3
15CA-01B 29Feb-Spot 53	217	10537	0.8	17.5990	3.9	0.0625	5.3	0.0080	3.5	0.66	51.2	1.8	61.6	3.1	484.8	87.1	51.2	1.8
15CA-01B 29Feb-Spot 54	82	1406	0.9	19.3156	6.0	0.0726	8.4	0.0081	3.5	0.66	51.6	1.8	71.2	3.7	783.8	84.8	51.6	1.8
15CA-01B 29Feb-Spot 55	89	1958	1.0	23.1560	6.0	0.0463	7.0	0.0078	3.6	0.51	49.9	1.8	45.9	3.1	156.9	148.6	49.9	1.8
15CA-01B 29Feb-Spot 56	39	574	1.0	9.6369	8.5	0.1243	9.5	0.0087	4.2	0.44	56.8	2.3	119.0	10.7	1692.6	157.8	56.8	2.3
15CA-01B 29Feb-Spot 57	58	10319	1.3	21.9785	3.8	0.0514	5.8	0.0082	4.4	0.76	52.6	2.3	50.9	2.9	288	90.9	52.6	2.3
15CA-01B 29Feb-Spot 58	87	1340	0.6	25.5983	6.8	0.0423	7.6	0.0079	3.3	0.43	50.4	1.6	42.1	3.1	412.4	176.5	50.4	1.6
15CA-01B 29Feb-Spot 59	37	1003	0.7	21.7815	7.2	0.0500	9.7	0.0079	4.9	0.45	50.8	2.5	49.6	4.2	7.1	174.4	50.8	2.5
15CA-01B 29Feb-Spot 60	75	2361	0.7	22.5823	4.3	0.0500	5.8	0.0082	3.9	0.67	52.6	2.0	49.5	2.8	94.9	106.4	52.6	2.0
15CA-01B 29Feb-Spot 61	52	4142	0.9	11.0059	10.7	0.1069	11.6	0.0085	4.3	0.37	54.8	2.3	103.1	11.3	1443.7	205.1	54.8	2.3
15CA-01B 29Feb-Spot 62	44	328	1.0	52.4641	16.1	0.0205	16.8	0.0078	4.5	0.27	50.1	2.3	20.6	3.4	2852.6	1055.0	50.1	2.3
15CA-01B 29Feb-Spot 63	31	6943	0.9	18.8001	5.3	0.0595	6.6	0.0081	3.9	0.60	52.1	2.0	58.7	3.7	337.0	119.2	52.1	2.0
15CA-01B 29Feb-Spot 64	100	858	1.1	30.0126	13.7	0.0352	14.1	0.00										

Sample: 15CA01B		U-Pb geochronologic analyses					Isotope ratios					Apparent ages (Ma)						
Analysis	U (ppm)	206Pb/204Pb	U/Th	206Pb*/207Pb*	± (%)	207Pb/235U	± (%)	206Pb*/238U	± error	206Pb*/238U corr.	206Pb*/235U	± (Ma)	207Pb*/235U	± (Ma)	206Pb*/207Pb*	± (Ma)	Best age (Ma)	± (Ma)
15CA-01B 29Feb-Spot 92	112	1859	0.9	24.9790	3.1	0.0432	4.7	0.0078	3.5	0.75	50.2	1.7	42.9	2.0	348.8	80.3	50.2	1.7
15CA-01B 29Feb-Spot 94	53	1490	0.8	22.4712	5.5	0.0488	6.7	0.0079	3.8	0.56	51.0	1.9	48.4	3.2	82.8	135.5	51.0	1.9
15CA-01B 29Feb-Spot 95	36	510	0.9	48.7927	25.7	0.0221	25.1	0.0078	4.6	0.18	50.3	2.3	22.2	5.7	2529.6	712.7	50.3	2.3
15CA-01B 29Feb-Spot 96	49	4575	1.0	16.7778	5.5	0.0691	6.7	0.0084	3.7	0.56	54.0	2.0	67.8	4.4	589.2	119.8	54.0	2.0
15CA-01B 29Feb-Spot 97	149	88798	1.3	20.7975	3.1	0.0538	4.5	0.0081	3.3	0.73	52.1	1.7	53.2	2.3	103.3	72.8	52.1	1.7
15CA-01B 29Feb-Spot 98	49	426	1.3	48.4078	46.0	0.0218	46.1	0.0077	3.6	0.08	49.2	1.8	21.9	10.0	2495.9	234.8	49.2	1.8
15CA-01B 29Feb-Spot 99	48	1447	1.0	21.9967	4.4	0.0508	6.2	0.0081	4.3	0.70	52.1	2.2	50.3	3.0	30.8	106.5	52.1	2.2
15CA-01B 29Feb-Spot 100	54	15400	0.8	19.9887	3.9	0.0551	5.6	0.0080	4.0	0.71	51.3	2.0	54.5	3.0	196.3	91.4	51.3	2.0
15CA-01B 29Feb-Spot 101	30	9361	1.0	6.9718	7.5	0.1749	9.1	0.0088	5.1	0.56	56.8	2.9	163.7	13.7	2269.1	129.5	56.8	2.9
15CA-01B 29Feb-Spot 102	108	989	0.5	18.3992	8.7	0.0605	9.3	0.0081	3.5	0.37	51.9	1.8	59.7	5.4	385.6	195.0	51.9	1.8
15CA-01B 29Feb-Spot 103	114	783	0.7	27.4662	6.5	0.0403	7.2	0.0080	3.3	0.45	51.5	1.7	40.1	2.8	600.1	175.9	51.5	1.7
15CA-01B 29Feb-Spot 104	73	10101	1.0	21.0592	2.9	0.0528	4.5	0.0081	3.5	0.78	51.7	1.8	52.2	2.3	73.7	67.9	51.7	1.8
15CA-01B 29Feb-Spot 105	42	1361	1.1	15.7493	8.8	0.0688	9.7	0.0079	4.1	0.42	50.5	2.0	67.6	6.3	724.8	186.8	50.5	2.0
15CA-01B 29Feb-Spot 106	34	981	1.0	29.8186	8.5	0.0365	9.8	0.0079	4.8	0.49	50.6	2.4	36.4	3.5	829.0	244.4	50.6	2.4
15CA-01B 29Feb-Spot 107	44	870	0.8	33.3448	6.5	0.0337	7.6	0.0082	3.9	0.51	52.4	2.0	33.7	2.5	1159.9	200.5	52.4	2.0
15CA-01B 29Feb-Spot 108	38	259	0.9	1521.9178	166.2	0.0007	166.2	0.0075	5.0	0.03	48.0	2.4	0.7	1.1	0.0	0.0	48.0	2.4
15CA-01B 29Feb-Spot 109	53	1403	0.8	25.7745	5.3	0.0437	5.7	0.0082	3.7	0.65	52.5	1.9	43.4	2.4	430.3	113.2	52.5	1.9
15CA-01B 29Feb-Spot 110	41	410	1.0	29.3090	36.1	0.0386	36.4	0.0082	4.6	0.13	52.6	2.4	38.4	13.7	780.1	1048.0	52.6	2.4
15CA-01B 29Feb-Spot 111	56	1229	1.0	26.8005	4.6	0.0404	8.0	0.0078	6.5	0.82	50.4	3.3	40.2	3.1	533.9	123.1	50.4	3.3
15CA-01B 29Feb-Spot 112	130	2043	0.8	19.9323	8.2	0.0560	8.9	0.0080	3.5	0.39	51.2	1.8	54.4	4.7	195.9	191.6	51.2	1.8
15CA-01B 29Feb-Spot 113	331	21004	7.1	9.9339	2.5	0.0336	4.6	0.0510	3.9	0.85	320.4	12.2	541.0	19.4	1627.1	45.1	320.4	12.2
15CA-01B 29Feb-Spot 114	56	435	0.8	88.8641	8.0	0.0119	8.8	0.0077	3.5	0.40	49.2	1.7	12.0	1.0	0.0	0.0	49.2	1.7
15CA-01B 29Feb-Spot 115	27	229	1.1	-79.8596	147.1	-0.1030	147.2	0.0076	5.1	0.03	48.5	2.5	13.3	19.8	0.0	773.4	48.5	2.5
15CA-01B 29Feb-Spot 116	56	678	1.3	29.7564	7.7	0.0367	8.6	0.0079	3.9	0.45	50.8	2.0	36.6	3.1	823.1	220.5	50.8	2.0
15CA-01B 29Feb-Spot 117	41	685	1.1	26.8321	30.3	0.0412	30.7	0.0080	5.1	0.17	51.5	2.6	41.0	12.3	537.1	827.3	51.5	2.6
15CA-01B 29Feb-Spot 118	24	249	1.0	-72.9343	103.3	-0.1146	103.4	0.0077	4.5	0.04	49.6	2.2	14.9	15.5	0.0	1983.7	49.6	2.2
15CA-01B 29Feb-Spot 119	28	702	0.9	23.0630	25.8	0.0503	26.3	0.0084	5.0	0.19	54.1	2.7	49.9	12.8	146.9	648.1	54.1	2.7
15CA-01B 29Feb-Spot 120	65	4894	1.1	20.9157	3.9	0.0534	4.9	0.0081	2.9	0.60	52.1	1.5	52.9	2.5	89.9	93.3	52.1	1.5
15CA-01B 29Feb-Spot 121	62	2140	1.0	24.8035	3.5	0.0456	4.8	0.0082	3.2	0.67	52.6	1.7	45.2	2.1	330.6	90.7	52.6	1.7
15CA-01B 29Feb-Spot 122	42	722	1.0	22.2842	23.4	0.0494	23.7	0.0080	3.8	0.16	51.2	1.9	48.9	11.3	62.4	578.0	51.2	1.9
15CA-01B 29Feb-Spot 123	35	531	0.9	45.3854	57.5	0.0236	57.7	0.0078	4.5	0.08	49.8	2.3	23.7	13.5	2231.6	138.9	49.8	2.3
15CA-01B 29Feb-Spot 124	129	1137	0.8	29.9927	4.5	0.0366	5.5	0.0080	3.1	0.57	51.1	1.6	36.5	2.0	845.7	128.5	51.1	1.6
15CA-01B 29Feb-Spot 125	33	556	1.1	40.4003	56.2	0.0270	56.4	0.0079	4.3	0.08	50.8	2.2	27.1	15.1	1794.2	237.2	50.8	2.2
15CA-01B 29Feb-Spot 126	28	673	1.2	17.7609	6.7	0.0617	7.7	0.0079	3.8	0.49	51.0	1.9	60.8	4.5	464.4	148.9	51.0	1.9
15CA-01B 29Feb-Spot 127	54	1681	1.0	21.6138	4.5	0.0519	7.0	0.0081	5.4	0.77	52.3	2.8	51.4	3.5	11.5	107.5	52.3	2.8
15CA-01B 29Feb-Spot 128	35	846	0.9	31.8672	8.7	0.0339	9.9	0.0078	4.7	0.47	50.3	2.4	33.8	3.3	1022.8	260.3	50.3	2.4
15CA-01B 29Feb-Spot 129	48	421	0.8	43.0665	79.5	0.0248	79.6	0.0077	4.4	0.06	49.8	2.2	24.9	19.6	2028.6	927.1	49.8	2.2
15CA-01B 29Feb-Spot 130	47	371	1.0	34.2268	14.0	0.0312	14.6	0.0080	4.0	0.28	49.8	2.0	31.2	4.5	1240.8	440.6	49.8	2.0
15CA-01B 29Feb-Spot 131	46	1021	1.1	25.4584	5.0	0.0411	6.9	0.0079	4.8	0.69	50.7	2.4	40.9	2.8	502.5	132.2	50.7	2.4
15CA-01B 29Feb-Spot 132	106	11985	0.8	20.3002	3.1	0.0536	4.7	0.0079	3.6	0.76	50.7	1.8	53.0	2.4	160.3	72.3	50.7	1.8
15CA-01B 29Feb-Spot 133	41	337	0.9	107.8531	33.5	0.0097	33.7	0.0076	3.6	0.11	48.7	1.7	9.8	3.3	0.0	0.0	48.7	1.7
15CA-01B 29Feb-Spot 134	42	2145	0.8	5.7296	6.8	0.2196	7.8	0.0091	3.8	0.49	58.6	2.2	201.6	14.2	2601.6	113.2	58.6	2.2
15CA-01B 29Feb-Spot 135	53	561	1.1	44.4552	58.9	0.0240	59.1	0.0077	4.2	0.07	49.7	2.1	24.1	14.1	2150.2	201.4	49.7	2.1
15CA-01B 29Feb-Spot 136	76	67510	0.9	19.4807	3.4	0.0554	4.7	0.0078	3.2	0.68	50.2	1.6	54.7	2.5	255.8	78.4	50.2	1.6
15CA-01B 29Feb-Spot 137	40	943	1.1	24.3607	13.5	0.0452	14.1	0.0080	3.9	0.28	51.3	2.0	44.9	6.2	284.5	345.5	51.3	2.0
15CA-01B 29Feb-Spot 138	62	680	1.3	25.3064	6.2	0.0436	7.3	0.0080	3.8	0.53	51.4	2.0	43.3	3.1	382.5	160.4	51.4	2.0
15CA-01B 29Feb-Spot 140	47	639	1.1	21.7163	9.2	0.0501	10.1	0.0079	4.1	0.40	50.7	2.1	49.7	4.9	0.1	222.2	50.7	2.1
15CA-01B 29Feb-Spot 141	53	6184	1.2	18.8227	4.8	0.0582	5.7	0.0079	3.1	0.54	51.0	1.6	57.4	3.2	334.2	108.5	51.0	1.6
15CA-01B 29Feb-Spot 142	46	1240	1.2	24.8473	4.9	0.0448	6.0	0.0081	3.5	0.58	51.8	1.8	44.5	2.6	335.1	125.6	51.8	1.8
15CA-01B 29Feb-Spot 143	55	447	0.8	77.1003	135.5	0.0139	135.6	0.0077	4.6	0.03	49.7	2.3	14.0	18.8	0.0	0.0	49.7	2.3
15CA-01B 29Feb-Spot 144	56	5990	0.7	19.1053	4.4	0.0575	6.5	0.0080	4.7	0.73	51.1	2.4	56.7	3.6	300.4	100.8	51.1	2.4
15CA-01B 29Feb-Spot 145	82	718	1.1	35.7630	10.3	0.0292	11.0	0.0076	3.9	0.35	48.7	1.9	29.3	3.2	1380.6	335.0	48.7	1.9
15CA-01B 29Feb-Spot 146	47	2205	1.1	23.7957	4.4	0.0478	6.0	0.0082	4.1	0.68	52.9	2.2	47.4	2.8	225.1	111.2	52.9	2.2
15CA-01B 29Feb-Spot 147	55	6886	0.6	21.9557	3.8	0.0500	5.5	0.0080	3.9	0.72	51.1	2.0	49.6	2.8	26.3	92.5	51.1	2.0
15CA-01B 29Feb-Spot 148	43	573	0.9	44.4754	4.9	0.0246	6.4	0.0079	4.2	0.65	50.9	2.1	24.7	1.6	2152.0	190.5	50.9	2.1
15CA-01B 29Feb-Spot 149	58	2102	1.1	22.6804	8.1	0.0495	9.1	0.0081	4.0	0.44	52.3	2.1	49.1	4.3	105.6	200.6	52.3	2.1
15CA-01B 29Feb-Spot 150	89	2910	0.9	8.8044	2.0	0.1418	4.7	0.0091	3.5	0.75	58.3	2.1	134.6	5.9	1857.5	54.6	58.3	2.1
15CA-01B 29Feb-Spot 151	61	269	1.0	51.0788	3.1	0.0206	4.8	0.0076	3.9	0.77	49.0	1.8	20.7	1.0	2730.4	137.6	49.0	1.8
15CA-01B 29Feb-Spot 152	53	414	1.0	72.3179	29.4	0.0144	29.7	0.0076	4.4	0.15	48.6	2.1	14.5	4.3	0.0	1363.6	48.6	2.1
15CA-01B 29Feb-Spot 153	82	544	1.1	7.6606	15.1	0.1607	15.5	0.0089	6.5	0.40	57.3	3.7	151.3	23.2	2105.2	267.4	57.3	3.7
15CA-01B 29Feb-Spot 154	164	447	0.7	4.3513	10.7	0.3107	11.5	0.0098	4.2	0.36	62.9	2.6	274.7	27.8	3050.7	172.6	62.9	2.6
15CA-01B 29Feb-Spot 155	107	430715	0.7	20.0100	3.2	0.0547	4.4	0.0079	3.1	0.69	50.9	1.5	54.0	2.3	193.9	73.5	50.9	1.5
15CA-01B 29Feb-Spot 156	41	2112	1.0	20.5961	4.2	0.0523	6.4	0.0078	4.7	0.75	50.1	2.4	51.7	3.2	126.3</			

Sample: 15CA01B		U-Pb geochronologic analyses					Isotope ratios					Apparent ages (Ma)						
Analysis	U (ppm)	²⁰⁶ Pb/ ²⁰⁴ Pb	U/Th	²⁰⁶ Pb* ± 207Pb*	± [%]	²⁰⁷ Pb/ ²³⁵ U ± [%]	²⁰⁶ Pb* ± error	± corr.	²⁰⁶ Pb* ± 238U*	± error	Apparent ages (Ma) 235U	± error	²⁰⁶ Pb* ± 207Pb*	± error	Best age (Ma)	± error		
15CA-01B 29Feb-Spot 186	42	217	1.0	-80.1593	5.1	-0.0125	6.8	0.0073	4.5	0.67	46.8	2.1	12.8	0.9	0.0	46.8	2.1	
15CA-01B 29Feb-Spot 187	151	9516	0.7	21.8520	2.8	0.0509	4.2	0.0081	3.2	0.75	51.8	1.6	50.5	2.1	14.9	67.1	51.8	1.6
15CA-01B 29Feb-Spot 188	37	290	0.9	16.5814	11.3	0.0675	12.2	0.0091	4.5	0.37	52.2	2.3	66.4	7.9	144.6	244.9	52.2	2.3
15CA-01B 29Feb-Spot 189	41	2114	1.0	20.0075	5.4	0.0567	6.7	0.0082	4.0	0.60	52.8	2.1	56.0	3.7	194.1	125.1	52.8	2.1
15CA-01B 29Feb-Spot 190	101	1655	1.2	25.8000	10.6	0.0416	11.2	0.0078	3.5	0.31	50.0	1.7	41.4	4.5	432.9	279.4	50.0	1.7
15CA-01B 29Feb-Spot 191	63	2306	1.0	23.4328	3.2	0.0472	4.9	0.0080	3.6	0.74	51.5	1.9	46.9	2.2	186.5	81.2	51.5	1.9
15CA-01B 29Feb-Spot 192	104	4633	1.2	21.9182	3.9	0.0509	5.0	0.0081	3.3	0.64	52.0	1.7	50.4	2.5	22.2	93.4	52.0	1.7
15CA-01B 29Feb-Spot 193	54	10022	0.9	20.4230	3.7	0.0556	5.1	0.0082	3.4	0.68	52.9	1.8	55.0	2.7	146.1	87.8	52.9	1.8
15CA-01B 29Feb-Spot 194	34	243	1.1	-50.6293	56.5	-0.0200	56.6	0.0074	3.9	0.07	47.3	1.8	20.6	11.8	0.0	47.3	1.8	
15CA-01B 29Feb-Spot 195	34	810	1.0	29.6058	24.7	0.0375	25.3	0.0080	5.3	0.21	51.7	2.7	37.4	9.3	808.6	710.5	51.7	2.7
15CA-01B 29Feb-Spot 196	27	1021	0.8	28.4428	6.4	0.0382	7.6	0.0079	4.2	0.55	50.5	2.1	38.0	2.8	696.1	176.3	50.5	2.1
15CA-01B 29Feb-Spot 197	59	1572	0.9	7.8173	16.2	0.1580	17.3	0.0090	6.0	0.35	57.5	3.4	148.9	23.9	2069.6	287.5	57.5	3.4
15CA-01B 29Feb-Spot 198	66	3259	0.8	13.6576	7.0	0.0823	8.1	0.0082	4.0	0.50	52.3	2.1	80.3	6.3	1020.0	142.6	52.3	2.1
15CA-01B 29Feb-Spot 199	96	1815	0.7	19.9676	4.1	0.0548	5.3	0.0079	3.3	0.62	50.9	1.7	54.1	2.8	198.7	95.7	50.9	1.7
15CA-01B 29Feb-Spot 200	70	373	0.6	141.8868	38.5	0.0073	38.7	0.0075	3.9	0.10	48.1	1.9	7.4	2.8	0.0	48.1	1.9	
15CA-01B 29Feb-Spot 201	38	398	0.9	89.2283	9.3	0.0122	10.3	0.0079	4.4	0.42	50.9	2.2	12.4	1.3	0.0	50.9	2.2	
15CA-01B 29Feb-Spot 202	52	1678	1.2	22.0410	6.6	0.0498	7.5	0.0080	3.7	0.49	51.1	1.9	49.3	3.6	35.7	159.2	51.1	1.9
15CA-01B 29Feb-Spot 203	55	3055	0.7	17.4929	5.2	0.0653	6.6	0.0083	4.1	0.62	53.2	2.2	64.2	4.1	497.9	113.8	53.2	2.2
15CA-01B 29Feb-Spot 204	47	527	0.7	8.3709	7.0	0.1421	7.9	0.0086	3.7	0.47	55.4	2.0	134.9	10.0	1948.2	124.9	55.4	2.0
15CA-01B 29Feb-Spot 205	28	455	1.0	20.5698	7.0	0.0544	8.6	0.0081	5.1	0.59	52.1	2.6	53.8	4.5	129.3	163.7	52.1	2.6
15CA-01B 29Feb-Spot 206	51	734	1.0	19.0106	10.6	0.0583	11.3	0.0080	3.7	0.33	51.6	1.9	57.5	6.3	311.7	242.8	51.6	1.9
15CA-01B 29Feb-Spot 207	339	9924	0.4	18.3898	1.9	0.0602	3.4	0.0080	2.9	0.83	51.5	1.5	59.3	2.0	386.7	43.3	51.5	1.5
15CA-01B 29Feb-Spot 208	116	1525	0.7	21.0958	3.5	0.0518	4.6	0.0079	2.9	0.64	50.9	1.5	51.3	2.3	69.6	83.6	50.9	1.5
15CA-01B 29Feb-Spot 209	35	808	1.2	31.8411	6.0	0.0340	8.0	0.0079	5.3	0.67	50.5	2.7	34.0	2.7	1020.4	177.4	50.5	2.7
15CA-01B 29Feb-Spot 210	104	684	0.7	38.8478	32.1	0.0279	32.3	0.0079	3.4	0.11	50.5	1.7	28.0	8.9	1656.8	1131.4	50.5	1.7
15CA-01B 29Feb-Spot 211	118	3440	0.6	16.5780	3.1	0.0684	4.1	0.0082	2.6	0.64	52.4	1.7	67.2	2.7	615.1	67.8	52.4	1.7
15CA-01B 29Feb-Spot 212	59	3835	0.7	21.7023	3.5	0.0515	4.8	0.0081	3.3	0.69	52.1	1.7	51.0	2.4	1.7	83.5	52.1	1.7
15CA-01B 29Feb-Spot 213	91	8473	0.8	15.3611	3.5	0.0708	4.7	0.0079	3.2	0.67	50.7	1.6	69.5	3.2	777.5	74.1	50.7	1.6
15CA-01B 29Feb-Spot 214	29	451	0.9	39.5686	8.0	0.0278	9.9	0.0080	5.8	0.59	51.3	3.0	27.9	2.7	1719.8	282.0	51.3	3.0
15CA-01B 29Feb-Spot 216	28	3708	1.1	22.5198	5.1	0.0501	7.3	0.0082	5.3	0.72	52.6	2.8	49.7	3.6	88.1	124.9	52.6	2.8
15CA-01B 29Feb-Spot 217	111	527	0.5	21.0651	4.2	0.0526	5.3	0.0080	3.4	0.63	51.6	1.7	52.0	2.7	73.0	98.9	51.6	1.7
15CA-01B 29Feb-Spot 218	33	691	0.9	33.4919	7.2	0.0322	8.5	0.0078	4.5	0.54	50.2	2.3	32.2	2.7	1173.5	220.6	50.2	2.3
15CA-01B 29Feb-Spot 219	44	769	1.1	34.2037	34.4	0.0314	34.6	0.0078	3.7	0.11	50.0	1.9	31.4	10.7	1238.8	1101.0	50.0	1.9
15CA-01B 29Feb-Spot 220	47	362	0.8	21.2320	30.7	0.0525	30.9	0.0081	3.3	0.11	51.9	1.7	52.0	16.7	54.2	748.4	51.9	1.7
15CA-01B 29Feb-Spot 221	48	344	1.3	114.5949	31.0	0.0092	31.4	0.0076	4.6	0.15	48.9	2.3	9.3	2.9	0.0	48.9	2.3	
15CA-01B 29Feb-Spot 222	40	276	0.7	15.5833	26.1	0.0754	26.3	0.0085	3.3	0.13	54.7	1.8	73.8	18.8	747.3	561.3	54.7	1.8
15CA-01B 29Feb-Spot 223	29	206	0.9	7.6991	20.8	0.1329	21.5	0.0074	5.6	0.26	47.7	2.6	126.7	25.7	2096.4	370.0	47.7	2.6
15CA-01B 29Feb-Spot 224	44	1976	0.8	25.7547	4.4	0.0435	5.4	0.0081	3.2	0.60	52.1	1.7	43.2	2.3	428.3	114.2	52.1	1.7
15CA-01B 29Feb-Spot 225	479	20245	6.0	13.3233	1.6	0.3271	3.6	0.0316	3.2	0.89	200.6	6.4	287.4	9.1	1070.0	32.8	200.6	6.4
15CA-01B 29Feb-Spot 226	43	1688	1.0	26.3096	12.2	0.0441	13.2	0.0081	5.2	0.39	52.0	2.7	43.8	5.7	382.8	317.8	52.0	2.7
15CA-01B 29Feb-Spot 227	102	3526	0.6	22.0303	3.1	0.0525	4.3	0.0084	2.9	0.68	53.8	1.5	52.0	2.2	34.5	76.3	53.8	1.5
15CA-01B 29Feb-Spot 228	42	483	0.7	52.3618	13.1	0.0207	13.9	0.0078	4.2	0.34	50.4	2.4	20.8	2.9	2843.6	1120.9	50.4	2.4
15CA-01B 29Feb-Spot 229	88	4746	0.8	17.2453	4.0	0.0649	5.2	0.0081	3.2	0.63	52.1	1.7	63.8	3.2	529.3	88.8	52.1	1.7
15CA-01B 29Feb-Spot 230	43	1625	0.8	23.5980	4.9	0.0459	6.5	0.0079	4.2	0.65	50.5	2.1	45.6	2.9	204.1	123.1	50.5	2.1
15CA-01B 29Feb-Spot 231	54	484	0.8	41.2656	21.4	0.0260	21.7	0.0078	4.0	0.18	50.0	2.0	26.1	5.6	1870.5	782.3	50.0	2.0
15CA-01B 29Feb-Spot 232	42	697	1.1	22.8320	5.6	0.0492	7.4	0.0081	4.9	0.66	52.3	2.5	48.7	3.5	122.0	137.3	52.3	2.5
15CA-01B 29Feb-Spot 233	59	3484	1.0	23.3547	4.2	0.0483	6.1	0.0082	4.4	0.73	52.5	2.3	47.9	2.9	178.2	104.7	52.5	2.3
15CA-01B 29Feb-Spot 234	66	296	0.9	3.1649	3.6	0.5353	6.7	0.0123	5.7	0.85	57.7	4.4	435.3	23.7	3550.3	54.7	78.7	4.4
15CA-01B 29Feb-Spot 235	58	804	1.2	32.8258	12.5	0.0327	13.1	0.0078	3.8	0.29	50.1	1.9	32.7	4.2	1112.0	382.3	50.1	1.9
15CA-01B 29Feb-Spot 236	32	312	1.1	24.7739	13.5	0.0456	14.0	0.0082	3.7	0.27	52.5	1.9	45.2	6.2	327.5	347.1	52.5	1.9
15CA-01B 29Feb-Spot 237	38	1027	0.8	30.1549	6.5	0.0381	7.7	0.0083	4.2	0.55	53.6	2.3	38.0	2.9	861.2	185.6	53.6	2.3
15CA-01B 29Feb-Spot 238	67	8266	0.9	9.9859	2.8	0.1219	4.8	0.0088	3.9	0.81	56.7	2.2	116.8	5.3	1626.7	52.6	56.7	2.2
15CA-01B 29Feb-Spot 239	73	1515	1.3	27.9319	7.7	0.0394	8.6	0.0080	3.9	0.45	51.3	2.0	39.3	3.3	646.1	210.4	51.3	2.0
15CA-01B 29Feb-Spot 240	62	1448	0.7	23.4000	5.9	0.0471	6.8	0.0080	3.4	0.50	51.3	1.7	46.7	3.1	183.0	147.6	51.3	1.7
15CA-01B 29Feb-Spot 241	59	683	0.7	40.2045	13.8	0.0279	14.4	0.0081	4.0	0.28	52.2	2.1	27.9	4.0	1776.9	492.6	52.2	2.1
15CA-01B 29Feb-Spot 242	127	1864	1.0	24.6623	6.4	0.0442	7.2	0.0079	3.4	0.47	50.8	1.7	43.9	3.1	315.9	163.2	50.8	1.7
15CA-01B 29Feb-Spot 243	36	8740	0.7	19.9731	5.5	0.0561	7.1	0.0081	4.4	0.62	52.3	2.3	56.4	3.8	198.1	129.2	52.3	2.3
15CA-01B 29Feb-Spot 244	36	729	1.0	-66.9885	25.8	-0.0155	26.4	0.0075	5.7	0.22	48.2	2.8	15.8	4.2	0.0	48.2	2.8	
15CA-01B 29Feb-Spot 245	31	502	1.0	35.6137	26.5	0.0312	27.0	0.0081	5.4	0.20	51.8	2.8	31.2	8.3	1367.0	865.6	51.8	2.8
15CA-01B 29Feb-Spot 246	35	376	1.0	69.1854	37.6	0.0155	37.8	0.0078	3.8	0.10	49.8	1.9	15.6	5.8	0.0	49.8	1.9	
15CA-01B 29Feb-Spot 247	62	768	1.1	32.5316	9.0	0.0337	9.7	0.0080	3.5	0.36	51.1	1.8	33.7	3.2	1084.7	273.7	51.1	1.8
15CA-01B 29Feb-Spot 249	64	1859	0.8	22.6848	9.9	0.0488	10.7	0.0080	4.0	0.38	51.6	2.1	48.4	5.1	106.1	244.3	51.6	2.1
15CA-01B 29Feb-Spot 250	35	481	0.9	49.5173	14.5	0.0226	15.2	0.0081	4.6	0.30	52.1	2.4	22.7	3.4	2593.2	631.4	52.1	2.4
15CA-01B 29Feb-Spot 251	29	441	0.8	28.9060	13.0	0.0375	13.6	0.0079	4.1	0.30								

Sample: 15CA01B		U-Pb geochronologic analyses					Isotope ratios					Apparent ages (Ma)						
Analysis	U (ppm)	²⁰⁶ Pb/ ²⁰⁴ Pb	U/Th	²⁰⁶ Pb* ± 207Pb*	± 207Pb* 235U*	± 206Pb* 238U*	± error corr.	²⁰⁶ Pb* ± 238U*	± error corr.	²⁰⁶ Pb* ± 238U*	Apparent ages (Ma) 235U*	± 206Pb* (Ma)	± 207Pb* (Ma)	± Best age (Ma)	± (Ma)			
15CA-01B 29Feb-Spot 279	85	498	0.8	59.5735	49.0	0.0180	49.2	0.0078	4.0	0.08	50.0	2.0	18.2	8.9	0.0	440.3	50.0	2.0
15CA-01B 29Feb-Spot 280	45	932	1.0	23.3019	6.5	0.0478	7.3	0.0081	3.3	0.45	51.9	1.7	47.5	3.4	172.5	161.5	51.9	1.7
15CA-01B 29Feb-Spot 281	87	935	1.0	30.8692	24.5	0.0352	24.7	0.0079	2.6	0.11	50.6	1.3	35.1	8.5	929.0	724.6	50.6	1.3
15CA-01B 29Feb-Spot 282	34	7810	1.1	17.5228	5.6	0.0628	7.3	0.0080	4.7	0.64	51.3	2.4	61.9	4.4	494.2	123.3	51.3	2.4
15CA-01B 29Feb-Spot 283	62	2080	0.7	22.9684	8.3	0.0484	9.1	0.0081	3.8	0.42	51.7	2.0	48.0	4.3	136.7	205.4	51.7	2.0
15CA-01B 29Feb-Spot 284	42	4394	0.7	21.7987	4.9	0.0497	6.9	0.0079	4.9	0.70	50.5	2.4	49.3	3.3	9.0	118.9	50.5	2.4
15CA-01B 29Feb-Spot 285	34	1001	1.1	28.3155	4.9	0.0402	7.5	0.0083	5.6	0.75	53.0	3.0	40.0	2.9	683.7	136.0	53.0	3.0
15CA-01B 29Feb-Spot 286	55	368	1.1	10.2593	12.3	0.1156	12.8	0.0086	3.4	0.27	55.2	1.9	111.1	13.4	1576.3	231.1	55.2	1.9
15CA-01B 29Feb-Spot 287	36	1310	0.9	27.8616	8.1	0.0384	9.9	0.0078	5.7	0.57	49.8	2.8	38.3	3.7	639.2	222.8	49.8	2.8
15CA-01B 29Feb-Spot 288	63	1012	1.0	28.7431	6.9	0.0372	7.7	0.0078	3.4	0.45	49.9	1.7	37.1	2.8	725.3	191.7	49.9	1.7
15CA-01B 29Feb-Spot 289	37	336	0.8	222.8371	19.8	0.0048	20.2	0.0078	3.9	0.19	49.8	1.9	4.9	1.0	0.0	0.0	49.8	1.9
15CA-01B 29Feb-Spot 290	50	1615	0.9	7.4435	6.5	0.1683	7.9	0.0091	4.5	0.57	58.3	2.6	158.0	11.5	2155.5	113.1	58.3	2.6
15CA-01B 29Feb-Spot 291	172	98984	0.7	21.0587	2.2	0.0519	3.2	0.0079	2.3	0.73	50.9	1.2	51.4	1.6	73.8	51.6	50.9	1.2
15CA-01B 29Feb-Spot 292	31	1333	1.0	16.5884	7.9	0.0651	9.1	0.0078	4.5	0.49	50.3	2.2	64.0	5.6	613.7	171.0	50.3	2.2
15CA-01B 29Feb-Spot 293	45	2960	1.2	20.2103	4.5	0.0543	7.1	0.0080	5.5	0.77	51.1	2.8	53.7	3.7	170.6	106.1	51.1	2.8
15CA-01B 29Feb-Spot 294	55	708	1.0	33.9424	18.0	0.0307	18.4	0.0076	3.8	0.21	48.6	1.8	30.7	5.6	1214.9	562.6	48.6	1.8
15CA-01B 29Feb-Spot 295	36	568	0.7	37.9736	9.9	0.0285	11.0	0.0078	4.8	0.44	50.4	2.4	28.5	3.1	1579.0	337.1	50.4	2.4
15CA-01B 29Feb-Spot 296	36	675	1.0	34.1784	39.1	0.0313	39.4	0.0077	4.9	0.13	49.8	2.4	31.3	12.1	1236.5	1261.5	49.8	2.4
15CA-01B 29Feb-Spot 297	60	5016	0.6	10.4230	8.0	0.1205	9.2	0.0091	4.7	0.51	58.5	2.7	115.6	10.1	1546.6	150.0	58.5	2.7
15CA-01B 29Feb-Spot 298	47	1116	1.0	15.0307	4.4	0.0744	5.6	0.0081	3.5	0.63	52.1	1.8	72.8	4.0	823.1	91.3	52.1	1.8
15CA-01B 29Feb-Spot 299	340	36238	0.6	21.3023	1.9	0.0500	3.5	0.0077	2.9	0.83	49.6	1.4	49.6	1.7	46.3	45.8	49.6	1.4
15CA-01B 29Feb-Spot 300	30	278	0.9	-144.9651	56.1	-0.0072	56.4	0.0076	5.6	0.10	48.7	2.7	7.4	4.2	0.0	0.0	48.7	2.7
15CA-01B 29Feb-Spot 301	33	248	0.9	66.4064	30.4	0.0158	30.8	0.0076	5.2	0.17	48.8	2.5	15.9	4.9	0.0	1151.9	48.8	2.5
15CA-01B 29Feb-Spot 302	79	236	0.9	3.6977	13.2	0.4145	15.9	0.0111	8.9	0.56	71.3	6.3	352.1	47.3	3308.6	207.7	71.3	6.3
15CA-01B 29Feb-Spot 303	36	416	1.2	61.8934	64.3	0.0175	64.6	0.0079	6.7	0.10	50.5	3.4	17.6	11.3	0.0	22.2	50.5	3.4
15CA-01B 29Feb-Spot 304	54	2084	0.9	23.4827	4.1	0.0476	5.9	0.0081	4.2	0.72	52.1	2.2	47.3	2.7	191.8	101.6	52.1	2.2
15CA-01B 29Feb-Spot 305	167	952	0.8	31.9285	25.6	0.0342	25.9	0.0079	3.9	0.15	50.8	2.0	34.1	8.7	1028.5	773.9	50.8	2.0
15CA-01B 29Feb-Spot 306	312	8953	3.2	21.6540	1.7	0.0628	2.8	0.0099	2.2	0.80	63.3	1.4	61.9	1.7	7.1	40.4	63.3	1.4
15CA-01B 29Feb-Spot 307	55	678	0.8	18.2578	20.6	0.0621	20.9	0.0082	3.5	0.17	52.8	1.8	61.2	12.4	402.9	465.5	52.8	1.8
15CA-01B 29Feb-Spot 309	41	731	1.1	23.1510	9.1	0.0463	10.2	0.0078	4.5	0.44	49.9	2.2	45.9	4.6	156.4	226.5	49.9	2.2
15CA-01B 29Feb-Spot 310	23	306	1.2	539.6268	541.9	0.0021	541.9	0.0081	6.0	0.01	51.7	3.1	2.1	11.3	0.0	0.0	51.7	3.1
15CA-01B 29Feb-Spot 311	47	2837	1.0	15.3102	4.5	0.0703	5.7	0.0078	3.4	0.60	50.2	1.7	69.0	3.8	784.5	95.1	50.2	1.7
15CA-01B 29Feb-Spot 312	52	848	0.8	29.8499	6.1	0.0357	7.4	0.0077	4.3	0.58	49.6	2.1	35.6	2.6	832.0	173.3	49.6	2.1
15CA-01B 29Feb-Spot 313	67	611	1.1	42.7684	15.8	0.0248	16.2	0.0077	3.8	0.23	49.4	1.9	24.9	4.0	2002.5	594.3	49.4	1.9
15CA-01B 29Feb-Spot 314	41	1529	1.0	24.7240	5.0	0.0444	6.6	0.0080	4.3	0.65	51.1	2.2	44.1	2.9	322.4	128.5	51.1	2.2
15CA-01B 29Feb-Spot 315	75	563	0.8	42.2618	31.0	0.0252	31.1	0.0077	3.0	0.10	49.7	1.5	25.3	7.8	1958.0	1171.5	49.7	1.5

Sample: 15CA03A	U-Pb geochronologic analyses					Isotope ratios					Apparent ages (Ma)							
	Analysis	U	206Pb	U/Th	206Pb*	±	207Pb*	±	206Pb*	±	error	206Pb*	±	207Pb*	±	Best age	±	
		(ppm)	204Pb		207Pb*	(%)	235U*	(%)	238U	corr.	238U*	(Ma)	235U	(Ma)	(Ma)	(Ma)		
15CA-03A 29Feb-Spot 1	60	272	0.9	978.4126	40.5	0.0010	40.6	0.0074	3.3	0.08	47.6	1.6	1.1	0.4	0.0	47.6	1.6	
15CA-03A 29Feb-Spot 2	82	1464	1.1	26.4767	3.5	0.0414	4.5	0.0080	2.9	0.64	51.1	1.5	41.2	1.8	501.4	92.6	51.1	1.5
15CA-03A 29Feb-Spot 3	67	5752	0.9	21.1838	4.2	0.0540	5.3	0.0083	3.2	0.60	53.3	1.7	53.4	2.8	59.7	100.6	53.3	1.7
15CA-03A 29Feb-Spot 4	152	2183	0.7	17.1370	3.9	0.0623	4.5	0.0077	2.3	0.51	49.7	1.2	61.4	2.7	543.0	84.7	49.7	1.2
15CA-03A 29Feb-Spot 5	44	5373	0.8	12.3199	10.6	0.0944	11.7	0.0084	5.1	0.43	54.1	2.7	91.6	10.3	1225.5	208.3	54.1	2.7
15CA-03A 29Feb-Spot 6	64	1213	1.1	28.9280	4.2	0.0388	5.6	0.0081	3.7	0.66	52.2	1.9	38.6	2.1	743.2	118.4	52.2	1.9
15CA-03A 29Feb-Spot 7	69	1563	0.8	23.2054	6.3	0.0491	6.7	0.0083	2.1	0.32	53.1	1.1	48.7	3.2	162.2	157.4	53.1	1.1
15CA-03A 29Feb-Spot 8	115	894	1.1	27.3653	6.0	0.0402	6.5	0.0080	2.6	0.39	51.2	1.3	40.0	2.6	590.1	163.7	51.2	1.3
15CA-03A 29Feb-Spot 9	48	953	1.1	26.3747	6.5	0.0428	7.8	0.0082	4.3	0.55	52.6	2.2	42.5	3.2	491.1	171.9	52.6	2.2
15CA-03A 29Feb-Spot 10	45	3773	1.3	22.1366	4.3	0.0521	5.8	0.0084	3.9	0.67	53.7	2.1	51.5	2.9	46.2	104.5	53.7	2.1
15CA-03A 29Feb-Spot 11	33	1378	1.2	24.4285	5.8	0.0471	6.6	0.0083	3.2	0.49	53.6	1.7	46.8	3.0	291.6	148.2	53.6	1.7
15CA-03A 29Feb-Spot 12	65	695	1.2	9.5291	18.5	0.1291	19.5	0.0089	6.0	0.31	57.3	3.4	123.3	22.6	1713.3	343.7	57.3	3.4
15CA-03A 29Feb-Spot 13	60	4673	0.8	22.5079	3.7	0.0489	5.2	0.0080	3.7	0.70	51.2	1.9	48.4	2.5	86.8	90.5	51.2	1.9
15CA-03A 29Feb-Spot 14	61	4490	1.0	23.3503	3.7	0.0479	4.9	0.0081	3.1	0.64	52.1	1.6	47.5	2.3	177.7	93.4	52.1	1.6
15CA-03A 29Feb-Spot 15	52	3194	0.8	20.5593	5.0	0.0562	6.2	0.0084	3.8	0.60	53.8	2.0	55.5	3.4	130.5	117.1	53.8	2.0
15CA-03A 29Feb-Spot 16	54	2784	1.1	21.0735	4.2	0.0546	5.3	0.0083	3.2	0.61	53.6	1.7	54.0	2.8	72.1	99.3	53.6	1.7
15CA-03A 29Feb-Spot 17	84	10398	1.0	18.9863	3.7	0.0598	4.6	0.0081	2.8	0.60	52.0	1.4	58.0	2.6	314.7	83.5	52.0	1.4
15CA-03A 29Feb-Spot 18	82	474	1.0	58.6843	96.4	0.0181	96.4	0.0077	3.3	0.03	49.5	1.6	18.2	17.4	0.0	2070.3	49.5	1.6
15CA-03A 29Feb-Spot 19	42	719	1.3	28.4866	11.1	0.0380	11.7	0.0078	3.8	0.32	50.4	1.9	37.8	4.3	700.4	308.2	50.4	1.9
15CA-03A 29Feb-Spot 20	44	435	1.2	62.6619	8.9	0.0176	9.4	0.0080	3.1	0.33	51.3	1.6	17.7	1.6	0.0	1633.7	51.3	1.6
15CA-03A 29Feb-Spot 21	47	548	1.2	48.0517	31.0	0.0222	31.3	0.0077	3.9	0.12	49.6	1.9	22.2	6.9	2464.7	570.2	49.6	1.9
15CA-03A 29Feb-Spot 22	73	3977	1.1	22.8429	3.8	0.0489	5.1	0.0081	3.4	0.66	52.1	1.8	48.5	2.4	123.2	94.6	52.1	1.8
15CA-03A 29Feb-Spot 23	95	1711	1.0	24.6450	8.3	0.0441	8.7	0.0079	2.8	0.32	50.6	1.4	43.8	3.7	314.1	212.5	50.6	1.4
15CA-03A 29Feb-Spot 24	640	31325	0.9	21.1664	1.7	0.0514	2.3	0.0079	1.5	0.66	50.7	0.8	50.9	9.1	61.6	40.4	50.7	0.8
15CA-03A 29Feb-Spot 25	76	2987	0.9	24.1110	3.9	0.0473	5.4	0.0083	3.7	0.68	53.1	1.9	46.9	2.5	258.3	99.8	53.1	1.9
15CA-03A 29Feb-Spot 26	62	7233	1.2	19.1992	5.2	0.0595	6.4	0.0083	3.8	0.59	53.2	2.0	58.7	3.7	289.2	118.8	53.2	2.0
15CA-03A 29Feb-Spot 27	53	3677	1.0	22.1097	4.1	0.0498	5.5	0.0080	3.6	0.66	51.3	1.8	49.4	2.6	43.3	99.3	51.3	1.8
15CA-03A 29Feb-Spot 28	38	1027	1.1	27.1532	5.3	0.0400	6.9	0.0079	4.3	0.63	50.5	2.2	39.8	2.7	569.1	143.5	50.5	2.2
15CA-03A 29Feb-Spot 29	75	1352	1.2	26.4977	4.0	0.0425	5.0	0.0082	2.9	0.59	52.4	1.5	42.2	2.1	503.5	107.5	52.4	1.5
15CA-03A 29Feb-Spot 30	94	1435	0.9	25.3967	5.2	0.0443	6.1	0.0082	3.1	0.51	52.4	1.6	44.0	2.6	391.8	136.5	52.4	1.6
15CA-03A 29Feb-Spot 31	109	2581	1.4	24.2065	3.5	0.0447	4.4	0.0079	2.6	0.59	50.4	1.3	44.4	1.9	268.3	89.9	50.4	1.3
15CA-03A 29Feb-Spot 32	92	1074	0.7	27.4226	3.4	0.0398	4.3	0.0079	2.7	0.63	50.9	1.4	39.7	1.7	595.8	91.5	50.9	1.4
15CA-03A 29Feb-Spot 33	30	288	1.3	-472.8295	1323.4	-0.0022	1323.4	0.0077	4.7	0.00	49.4	2.3	2.3	30.2	0.0	0.0	49.4	2.3
15CA-03A 29Feb-Spot 34	33	10679	1.2	12.3376	11.2	0.0952	12.6	0.0085	5.7	0.45	54.7	3.1	92.3	11.1	1222.7	221.5	54.7	3.1
15CA-03A 29Feb-Spot 35	44	318	0.9	-202.3688	456.5	-0.0054	456.5	0.0079	3.2	0.01	50.5	1.6	5.5	25.0	0.0	0.0	50.5	1.6
15CA-03A 29Feb-Spot 36	38	1099	1.2	24.4451	5.7	0.0455	7.1	0.0081	4.3	0.60	51.8	2.2	45.2	3.1	293.3	144.6	51.8	2.2
15CA-03A 29Feb-Spot 37	38	502	1.0	29.4563	29.2	0.0391	29.4	0.0084	3.6	0.12	53.6	1.9	38.9	11.2	794.3	841.7	53.6	1.9
15CA-03A 29Feb-Spot 38	635	13824	1.2	17.8564	1.7	0.1252	2.2	0.0162	1.4	0.65	103.7	1.5	119.8	2.5	452.4	36.9	103.7	1.5
15CA-03A 29Feb-Spot 39	100	973	1.0	28.2190	12.3	0.0383	12.5	0.0078	2.5	0.20	50.3	1.2	36.1	4.7	674.2	339.3	50.3	1.2
15CA-03A 29Feb-Spot 40	40	656	1.2	55.0198	44.3	0.0200	44.5	0.0080	3.3	0.08	51.2	1.7	20.1	8.8	3079.7	453.2	51.2	1.7
15CA-03A 29Feb-Spot 41	163	1425	0.7	27.0063	12.8	0.0397	13.0	0.0078	2.3	0.18	50.0	1.2	39.6	5.0	554.3	345.2	50.0	1.2
15CA-03A 29Feb-Spot 42	100	28958	1.8	20.6679	3.4	0.0623	4.8	0.0093	3.4	0.71	59.9	2.1	61.4	2.9	118.1	79.7	59.9	2.1
15CA-03A 29Feb-Spot 43	168	2121	0.9	16.4071	5.2	0.0704	5.7	0.0084	2.4	0.42	53.8	1.3	69.1	3.8	637.5	111.1	53.8	1.3
15CA-03A 29Feb-Spot 44	64	2720	1.0	24.1230	4.4	0.0443	5.5	0.0078	3.3	0.60	49.8	1.7	44.1	2.4	259.6	112.5	49.8	1.7
15CA-03A 29Feb-Spot 45	146	1440	0.8	25.6980	2.9	0.0429	3.7	0.0080	2.3	0.62	51.3	1.2	42.6	1.6	422.6	76.8	51.3	1.2
15CA-03A 29Feb-Spot 46	59	71586	0.9	21.9885	3.9	0.0507	5.3	0.0081	3.6	0.68	51.9	1.9	50.2	2.6	29.9	94.8	51.9	1.9
15CA-03A 29Feb-Spot 47	51	517	0.8	44.6174	24.0	0.0232	24.2	0.0075	3.4	0.14	48.0	1.6	23.2	5.6	2155.6	945.5	48.0	1.6
15CA-03A 29Feb-Spot 48	53	575	1.2	46.7614	14.8	0.0232	15.4	0.0077	4.1	0.26	49.4	2.0	23.3	3.5	2264.4	596.2	49.4	2.0
15CA-03A 29Feb-Spot 49	54	2400	1.1	6.9740	17.7	0.1811	18.3	0.0092	4.3	0.24	58.8	2.5	169.0	28.4	2268.5	308.6	58.8	2.5
15CA-03A 29Feb-Spot 50	74	3691	0.9	21.3685	3.7	0.0502	5.0	0.0078	3.3	0.66	49.9	1.6	49.7	2.4	38.9	88.8	49.9	1.6
15CA-03A 29Feb-Spot 51	66	1961	0.7	20.7644	4.4	0.0518	5.8	0.0078	3.8	0.65	50.1	1.9	51.3	2.9	107.1	104.0	50.1	1.9
15CA-03A 29Feb-Spot 52	62	1992	1.0	25.1117	4.4	0.0446	5.5	0.0081	3.3	0.60	52.1	1.7	44.3	2.4	362.5	115.0	52.1	1.7
15CA-03A 29Feb-Spot 53	600	5220	0.6	21.6505	1.5	0.0510	2.2	0.0080	1.7	0.75	51.2	0.9	50.5	1.1	18.6	35.7	51.2	0.9
15CA-03A 29Feb-Spot 54	45	1076	1.1	27.9269	4.8	0.0390	5.9	0.0079	3.4	0.58	50.7	1.7	38.8	2.2	645.6	131.3	50.7	1.7
15CA-03A 29Feb-Spot 55	77	2573	0.7	22.7915	3.4	0.0499	4.5	0.0082	2.8	0.64	52.9	1.5	49.4	2.1	117.6	84.8	52.9	1.5
15CA-03A 29Feb-Spot 56	71	378	1.2	83.1842	38.1	0.0129	38.4	0.0078	4.0	0.10	50.0	2.0	13.0	5.0	0.0	1381.7	50.0	2.0
15CA-03A 29Feb-Spot 57	57	3047	1.2	22.9257	4.3	0.0476	5.4	0.0079	3.4	0.62	50.8	1.7	47.2	2.5	132.1	105.6	50.8	1.7
15CA-03A 29Feb-Spot 58	888	44637	4.1	21.2154	1.0	0.0511	1.7	0.0079	1.4	0.80	50.5	0.7	50.6	0.8	56.1	24.5	50.5	0.7
15CA-03A 29Feb-Spot 59	76	766	1.0	31.5414	20.7	0.0344	21.0	0.0079	3.6	0.17	50.6	1.8	34.4	7.1	992.3	618.9	50.6	1.8
15CA-03A 29Feb-Spot 60	58	4830	0.9	20.2666	3.6	0.0571	5.0	0.0084	3.4	0.68	53.9	1.8	56.4	2.7	164.1	85.1	53.9	1.8
15CA-03A 29Feb-Spot 61	98	117935	0.9	19.0979	4.1	0.0572	5.0	0.0079	2.9	0.58	50.9	1.5	56.5	2.7	301.3	92.4	50.9	1.5
15CA-03A 29Feb-Spot 62	52	858	1.1	32.6509	5.2	0.0327	6.2	0.0077	3.4	0.54	49.7	1.7	32.6	2.0	1095.8	158.8	49.7	1.7
15CA-03A 29Feb-Spot 63	98	3020	0.6	19.7939	4.1	0.0551	5.1	0.0079	2.9	0.58	50.8	1.5	54.5	2.7	219.0	95.8	50.8	1.5
15CA-03A 29Feb-Spot 64	140	4442	0.8	22.0937	2.3	0.0497	3.4	0.0080	2.5	0.73	51.1	1.3	49.2</					

Sample: 15CA03A		U-Pb geochronologic analyses					Isotope ratios					Apparent ages (Ma)						
Analysis	U (ppm)	206Pb/204Pb	U/Th	206Pb*/207Pb*	±	207Pb*/235U (%)	±	206Pb*/238U (%)	±	error	206Pb*/238U* (Ma)	±	207Pb*/235U (Ma)	±	206Pb*/238U (Ma)	±	Best age (Ma)	±
15CA-03A 29Feb-Spot 91	61	1073	1.1	26.4265	8.2	0.0416	8.5	0.0080	2.4	0.28	51.1	1.2	41.3	3.5	496.4	218.4	51.1	1.2
15CA-03A 29Feb-Spot 92	92	2152	1.4	20.4692	3.2	0.0526	4.0	0.0078	2.4	0.61	50.2	1.2	52.1	2.0	140.9	74.5	50.2	1.2
15CA-03A 29Feb-Spot 93	49	40143	0.7	6.0347	3.4	0.2213	5.8	0.0097	4.7	0.82	62.1	2.9	203.0	10.7	2514.7	56.5	62.1	2.9
15CA-03A 29Feb-Spot 94	62	802	1.2	26.1908	16.5	0.0420	16.8	0.0080	3.0	0.18	51.2	1.5	41.7	6.9	472.6	440.5	51.2	1.5
15CA-03A 29Feb-Spot 95	67	1258	1.1	24.0141	4.8	0.0456	5.9	0.0079	3.3	0.57	51.0	1.7	45.2	2.6	248.1	122.4	51.0	1.7
15CA-03A 29Feb-Spot 96	42	1443	1.1	25.5733	5.2	0.0440	6.5	0.0092	3.9	0.60	52.4	2.1	43.7	2.8	409.8	136.1	52.4	2.1
15CA-03A 29Feb-Spot 97	54	1215	1.2	28.0461	4.5	0.0389	5.4	0.0079	3.0	0.56	50.8	1.5	38.8	2.0	41.6	106.4	50.8	1.5
15CA-03A 29Feb-Spot 98	57	3636027	1.3	21.3450	4.4	0.0527	5.8	0.0082	3.7	0.64	52.4	1.9	52.2	2.9	41.6	106.4	52.4	1.9
15CA-03A 29Feb-Spot 99	45	570	1.1	44.3390	8.7	0.0241	9.7	0.0077	4.3	0.44	49.7	2.1	24.1	2.3	2140.0	337.9	49.7	2.1
15CA-03A 29Feb-Spot 100	74	4591	0.8	20.8285	3.1	0.0519	3.9	0.0078	2.5	0.63	50.4	1.2	51.4	2.0	99.8	72.7	50.4	1.2
15CA-03A 29Feb-Spot 101	126	499	0.6	8.7394	20.3	0.1349	20.7	0.0085	3.5	0.17	54.9	1.9	128.5	24.9	1870.8	371.0	54.9	1.9
15CA-03A 29Feb-Spot 102	85	2658	1.1	22.1759	5.7	0.0484	6.7	0.0078	3.5	0.52	50.0	1.7	48.0	3.1	50.6	138.4	50.0	1.7
15CA-03A 29Feb-Spot 103	56	644	1.0	21.3478	8.2	0.0574	12.1	0.0089	8.9	0.74	57.0	5.1	56.7	6.7	41.3	195.8	57.0	5.1
15CA-03A 29Feb-Spot 104	43	1574	0.9	8.3406	16.5	0.1470	17.3	0.0089	5.1	0.29	57.1	2.9	139.3	22.5	1947.7	296.8	57.1	2.9
15CA-03A 29Feb-Spot 105	78	667	1.0	36.5928	17.4	0.0303	17.6	0.0080	2.9	0.16	51.6	1.5	30.3	5.3	1455.4	575.3	51.6	1.5
15CA-03A 29Feb-Spot 106	86	7017	0.9	21.2635	3.8	0.0504	5.0	0.0078	3.3	0.66	50.0	1.6	50.0	2.5	50.7	91.1	50.0	1.6
15CA-03A 29Feb-Spot 107	68	585	1.0	38.5801	60.9	0.0273	51.0	0.0077	2.8	0.06	49.1	1.4	27.4	13.8	1633.0	160.5	49.1	1.4
15CA-03A 29Feb-Spot 108	146	36685	0.9	20.8945	2.2	0.0522	3.4	0.0079	2.5	0.75	50.8	1.3	51.7	1.7	92.3	52.7	50.8	1.3
15CA-03A 29Feb-Spot 109	41	1477	1.2	25.0769	13.6	0.0453	14.3	0.0082	4.4	0.31	52.9	2.3	45.0	6.3	358.9	351.9	52.9	2.3
15CA-03A 29Feb-Spot 110	25	584	1.1	43.1159	16.9	0.0254	17.8	0.0079	5.6	0.32	51.0	2.9	25.5	4.5	2032.9	642.5	51.0	2.9
15CA-03A 29Feb-Spot 111	58	390	0.7	21.9413	21.3	0.0503	21.6	0.0080	3.4	0.16	51.4	1.8	49.8	10.5	24.7	521.4	51.4	1.8
15CA-03A 29Feb-Spot 112	82	921	0.7	27.2597	8.4	0.0389	8.9	0.0077	3.0	0.34	49.4	1.5	38.8	3.4	579.7	227.6	49.4	1.5
15CA-03A 29Feb-Spot 113	75	1157	1.3	29.4203	4.9	0.0369	5.6	0.0079	2.7	0.48	50.6	1.4	36.8	2.0	790.8	137.9	50.6	1.4
15CA-03A 29Feb-Spot 114	52	647	1.1	31.5669	10.6	0.0352	11.0	0.0081	3.0	0.27	51.8	1.5	35.1	3.8	994.7	315.2	51.8	1.5
15CA-03A 29Feb-Spot 115	50	353	0.9	330.2544	144.7	0.0031	144.8	0.0074	4.0	0.03	47.6	1.9	3.1	4.5	0.0	0.0	47.6	1.9
15CA-03A 29Feb-Spot 116	75	616	0.8	37.6234	19.1	0.0288	19.3	0.0079	3.0	0.16	50.5	1.5	28.9	5.5	1547.7	646.9	50.5	1.5
15CA-03A 29Feb-Spot 117	49	548	1.2	34.2236	13.4	0.0322	13.8	0.0080	3.3	0.24	51.3	1.7	32.1	4.4	1240.6	420.6	51.3	1.7
15CA-03A 29Feb-Spot 118	54	777	1.0	32.4382	7.5	0.0340	8.6	0.0080	4.2	0.49	51.3	2.2	33.9	2.9	1076.0	226.8	51.3	2.2
15CA-03A 29Feb-Spot 119	57	993	1.1	24.0321	4.7	0.0445	6.1	0.0078	3.8	0.63	49.8	1.9	44.2	2.6	250.0	120.2	49.8	1.9
15CA-03A 29Feb-Spot 120	66	1044	2.1	23.7893	16.3	0.0555	16.6	0.0096	3.3	0.20	61.5	2.0	54.9	8.9	224.4	412.6	61.5	2.0
15CA-03A 29Feb-Spot 121	59	703	1.2	28.4367	6.4	0.0375	7.3	0.0077	3.5	0.48	49.6	1.7	37.3	2.7	695.5	177.2	49.6	1.7
15CA-03A 29Feb-Spot 122	34	524	1.2	43.0656	8.7	0.0259	7.7	0.0081	3.9	0.49	51.9	2.0	26.0	3.0	2028.6	251.6	51.9	2.0
15CA-03A 29Feb-Spot 123	33	571	1.2	48.3667	17.0	0.0227	17.6	0.0079	4.6	0.26	51.0	2.3	22.7	4.0	4492.3	725.3	51.0	2.3
15CA-03A 29Feb-Spot 124	101	24600	1.3	16.6840	4.5	0.0654	5.5	0.0079	3.1	0.57	50.8	1.6	64.3	3.4	601.3	98.3	50.8	1.6
15CA-03A 29Feb-Spot 125	123	1306	0.7	27.3098	4.6	0.0402	5.4	0.0080	3.0	0.54	51.1	1.5	40.0	2.1	584.6	123.8	51.1	1.5
15CA-03A 29Feb-Spot 126	140	23482	0.6	12.4216	1.7	0.0886	3.2	0.0080	2.7	0.84	51.3	1.4	86.2	2.6	1209.4	33.4	51.3	1.4
15CA-03A 29Feb-Spot 127	47	948	0.9	24.6409	6.2	0.0445	7.1	0.0080	3.3	0.47	51.1	1.7	44.2	3.1	313.7	159.8	51.1	1.7
15CA-03A 29Feb-Spot 129	97	480	0.8	10.3825	8.1	0.1121	8.5	0.0084	2.6	0.31	54.2	1.4	107.9	8.7	1553.9	152.7	54.2	1.4
15CA-03A 29Feb-Spot 130	54	3696	1.1	19.7821	5.1	0.0563	6.1	0.0081	3.4	0.56	51.8	1.8	55.6	3.3	220.4	117.5	51.8	1.8
15CA-03A 29Feb-Spot 131	84	855	0.8	36.2801	6.4	0.0287	7.3	0.0076	3.5	0.48	48.5	1.7	28.7	2.1	1427.2	208.4	48.5	1.7
15CA-03A 29Feb-Spot 132	83	1084	0.9	26.9991	11.5	0.0399	11.9	0.0078	3.2	0.27	50.2	1.6	39.7	4.7	553.7	310.4	50.2	1.6
15CA-03A 29Feb-Spot 133	56	373	1.2	131.5643	187.5	0.0082	187.6	0.0078	3.9	0.02	50.2	2.0	8.3	15.5	0.0	0.0	50.2	2.0
15CA-03A 29Feb-Spot 134	140	2171	0.8	23.5994	4.2	0.0453	4.9	0.0077	2.6	0.53	49.7	1.3	44.9	2.2	204.2	104.3	49.7	1.3
15CA-03A 29Feb-Spot 135	251	2451	0.8	21.9192	6.7	0.0490	7.1	0.0078	2.1	0.30	50.0	1.0	48.6	3.3	22.3	163.4	50.0	1.0
15CA-03A 29Feb-Spot 136	49	672	1.3	38.8961	8.2	0.0274	8.9	0.0077	3.4	0.39	49.7	1.7	27.5	2.4	1661.1	282.6	49.7	1.7
15CA-03A 29Feb-Spot 137	92	958	0.8	31.0371	9.2	0.0348	9.6	0.0078	2.7	0.28	50.2	1.3	34.7	3.3	944.8	270.4	50.2	1.3
15CA-03A 29Feb-Spot 138	38	1032	1.0	22.9135	17.4	0.0484	17.9	0.0080	4.1	0.23	51.6	2.1	47.9	8.4	130.8	433.1	51.6	2.1
15CA-03A 29Feb-Spot 139	72	3348	1.1	21.4824	5.0	0.0518	5.6	0.0081	2.5	0.46	51.8	1.3	51.3	2.8	26.2	119.0	51.8	1.3
15CA-03A 29Feb-Spot 140	368	1462736	2.4	9.1486	0.6	4.5021	1.8	0.2987	1.7	0.93	1685.0	24.5	1731.4	14.7	1787.9	11.6	1787.9	11.6
15CA-03A 29Feb-Spot 142	87	802	0.8	29.8353	6.1	0.0372	7.1	0.0081	3.7	0.52	51.7	1.9	37.1	2.6	802.6	173.7	51.7	1.9
15CA-03A 29Feb-Spot 143	36	413	1.3	51.8533	15.9	0.0204	16.6	0.0077	4.9	0.30	49.3	2.4	20.5	3.4	2798.7	1037.9	49.3	2.4
15CA-03A 29Feb-Spot 144	42	719	1.1	47.3843	17.9	0.0229	18.2	0.0079	3.3	0.18	50.5	1.7	23.0	4.1	2406.3	746.4	50.5	1.7
15CA-03A 29Feb-Spot 145	47	730	1.2	31.5794	5.9	0.0357	7.1	0.0082	4.0	0.56	52.4	2.1	35.6	2.5	995.8	175.4	52.4	2.1
15CA-03A 29Feb-Spot 146	154	1622	0.8	9.4833	10.5	0.1214	10.8	0.0083	2.4	0.22	53.6	1.3	116.3	11.9	1722.1	194.1	53.6	1.3
15CA-03A 29Feb-Spot 147	40	362	1.1	237.0356	68.8	0.0044	69.0	0.0075	4.8	0.08	48.0	2.3	4.4	2.6	0.0	0.0	48.0	2.3
15CA-03A 29Feb-Spot 148	42	14349	1.1	19.0154	4.9	0.0598	6.8	0.0082	4.7	0.69	52.9	2.5	58.9	3.9	311.1	110.8	52.9	2.5
15CA-03A 29Feb-Spot 149	839	55725	2.2	16.8931	2.4	0.2159	4.2	0.0266	3.5	0.62	159.1	5.8	189.4	7.7	574.3	52.9	169.1	5.8
15CA-03A 29Feb-Spot 150	83	2503	1.0	22.2613	4.6	0.0489	5.3	0.0079	2.7	0.51	50.7	1.4	48.5	2.5	59.9	111.4	50.7	1.4
15CA-03A 29Feb-Spot 151	42	855	1.0	27.3508	6.6	0.0376	8.8	0.0075	5.8	0.66	47.9	2.8	37.5	3.2	588.7	178.6	47.9	2.8
15CA-03A 29Feb-Spot 152	37	3947	1.3	20.0504	5.6	0.0562	6.7	0.0082	3.7	0.55	52.5	1.9	55.5	3.6	189.1	129.2	52.5	1.9
15CA-03A 29Feb-Spot 153	55	520	0.9	51.8086	77.9	0.0199	78.0	0.0075	3.4	0.04	48.1	1.6	20.0	15.5	2794.7	685.0	48.1	1.6
15CA-03A 29Feb-Spot 154	64	1226	1.0	23.1502	4.9	0.0460	5.6	0.0077	2.6	0.47	49.6	1.3	45.7	2.5	156.3	122.2	49.6	1.3
15CA-03A 29Feb-Spot 156	72	1826	1.0	20.8675	4.7	0.0531	5.6	0.0080	2.9	0.53	51.6	1.5	52.5	2.8	54.4	112.1	51.6	1.5
15CA-03A 29Feb-Spot 157	48	525	0.9	42.5486	24.7	0.0251	25.0	0.0078										

Sample: 15CA03A													U-Pb geochronologic analyses				Isotope ratios				Apparent ages (Ma)			
Analysis	U		U/Th	206Pb*		±	207Pb*		±	error	206Pb*		±	207Pb*		±	Best age	±						
	(ppm)	204Pb		206Pb*	207Pb*		(%)	235U*			(%)	238U*		238U*	(Ma)				235U*	(Ma)				
15CA-03A 29Feb-Spat 184	42	853	1.3	34.1647	9.2	0.0318	9.9	0.0079	3.5	0.35	50.6	1.8	31.8	3.1	1235.2	288.6	50.6	1.8						
15CA-03A 29Feb-Spat 185	78	986	1.3	30.2988	16.2	0.0358	16.4	0.0079	2.5	0.15	50.5	1.2	35.7	5.7	874.9	468.9	50.5	1.2						
15CA-03A 29Feb-Spat 186	81	685.1	1.3	20.1671	2.6	0.0548	4.1	0.0080	3.2	0.77	51.4	1.6	54.1	2.2	175.6	61.3	51.4	1.6						
15CA-03A 29Feb-Spat 187	43	2288	1.2	24.7199	4.7	0.0449	6.5	0.0081	4.5	0.70	51.7	2.3	44.6	2.8	321.9	120.3	51.7	2.3						
15CA-03A 29Feb-Spat 188	33	599	1.1	36.5198	6.1	0.0300	7.1	0.0079	3.6	0.50	51.0	1.8	30.0	2.1	1448.8	201.3	51.0	1.8						
15CA-03A 29Feb-Spat 189	40	976	1.2	28.8613	6.3	0.0390	8.2	0.0079	5.3	0.64	50.7	2.7	37.9	3.1	717.4	175.6	50.7	2.7						
15CA-03A 29Feb-Spat 190	111	2194	0.8	23.4752	2.9	0.0471	4.7	0.0080	3.7	0.78	51.5	1.9	46.8	2.2	191.0	73.6	51.5	1.9						
15CA-03A 29Feb-Spat 191	283	726.9	0.5	22.1396	2.0	0.0496	3.0	0.0078	2.2	0.73	50.0	1.1	48.1	1.4	46.6	49.6	50.0	1.1						
15CA-03A 29Feb-Spat 192	155	2285	3.9	23.7051	3.6	0.0645	4.5	0.0111	2.9	0.62	71.1	2.0	63.5	2.8	215.5	89.7	71.1	2.0						
15CA-03A 29Feb-Spat 193	55	1382	0.9	27.2562	5.8	0.0397	7.0	0.0078	4.0	0.57	50.4	2.0	39.5	2.7	579.3	155.6	50.4	2.0						
15CA-03A 29Feb-Spat 194	54	550	1.1	30.0516	7.1	0.0366	8.2	0.0080	4.1	0.50	51.2	2.1	36.5	2.9	851.3	202.9	51.2	2.1						
15CA-03A 29Feb-Spat 195	55	1297	1.3	27.8075	4.8	0.0407	5.7	0.0082	3.1	0.55	52.6	1.6	40.5	2.3	633.8	131.7	52.6	1.6						
15CA-03A 29Feb-Spat 196	49	241	1.1	-60.2263	9.3	-0.0172	10.5	0.0075	4.9	0.46	48.2	2.3	17.6	1.9	0.0	0.0	48.2	2.3						
15CA-03A 29Feb-Spat 197	46	3257.7	1.1	19.0359	4.9	0.0594	6.3	0.0082	4.0	0.64	52.6	2.1	58.6	3.6	308.7	111.3	52.6	2.1						
15CA-03A 29Feb-Spat 198	47	1599	1.1	26.2432	6.4	0.0426	7.0	0.0081	2.8	0.40	52.0	1.4	42.3	2.9	477.9	170.4	52.0	1.4						
15CA-03A 29Feb-Spat 199	99	6571	1.0	20.1291	3.6	0.0543	4.4	0.0079	2.5	0.57	50.9	1.3	53.7	2.3	180.0	84.9	50.9	1.3						
15CA-03A 29Feb-Spat 200	49	215	0.9	-41.4141	4.3	-0.0241	5.6	0.0072	3.7	0.65	46.4	1.7	24.7	1.4	0.0	0.0	46.4	1.7						
15CA-03A 29Feb-Spat 201	40	1922.7	1.1	9.0998	11.0	0.1216	12.3	0.0080	5.4	0.44	51.5	2.8	116.5	13.5	1797.6	201.2	51.5	2.8						
15CA-03A 29Feb-Spat 202	149	3344	0.8	22.0800	2.9	0.0496	3.3	0.0079	1.5	0.45	51.0	0.7	49.1	1.6	40.0	71.1	51.0	0.7						
15CA-03A 29Feb-Spat 203	73	2132	1.3	22.1918	3.9	0.0505	4.8	0.0081	2.8	0.58	52.2	1.4	50.0	2.3	52.3	95.4	52.2	1.4						
15CA-03A 29Feb-Spat 204	41	381	1.0	60.1191	67.6	0.0179	67.7	0.0078	4.7	0.07	50.1	2.3	18.0	12.1	0.0	127.5	50.1	2.3						
15CA-03A 29Feb-Spat 206	110	5072	1.1	20.7624	2.9	0.0533	4.4	0.0080	3.4	0.76	51.6	1.7	52.8	2.3	107.4	68.1	51.6	1.7						
15CA-03A 29Feb-Spat 207	102	3259	1.0	10.6402	7.0	0.1091	7.8	0.0084	3.5	0.44	54.0	1.9	105.1	7.8	1507.8	133.0	54.0	1.9						
15CA-03A 29Feb-Spat 208	40	376	1.3	90.0452	75.6	0.0121	75.8	0.0079	5.6	0.07	50.7	2.8	12.2	9.2	0.0	14.9	50.7	2.8						
15CA-03A 29Feb-Spat 209	94	12465	0.9	21.9173	2.7	0.0512	3.9	0.0081	2.9	0.72	52.3	1.5	50.7	2.0	22.1	66.0	52.3	1.5						
15CA-03A 29Feb-Spat 210	42	1217	1.2	25.7168	6.6	0.0434	7.9	0.0081	4.3	0.54	52.0	2.2	43.1	3.3	424.5	173.4	52.0	2.2						
15CA-03A 29Feb-Spat 211	92	2895	0.9	22.4801	2.7	0.0494	4.2	0.0080	3.2	0.76	51.7	1.6	48.9	2.0	83.8	67.4	51.7	1.6						
15CA-03A 29Feb-Spat 212	46	2859	1.1	23.6798	4.7	0.0464	5.8	0.0080	3.5	0.60	51.2	1.8	46.1	2.6	212.8	117.2	51.2	1.8						
15CA-03A 29Feb-Spat 213	40	1514	1.3	21.7807	5.3	0.0500	6.9	0.0079	4.4	0.64	50.7	2.2	49.5	3.3	7.0	128.0	50.7	2.2						
15CA-03A 29Feb-Spat 215	222	2716	1.3	22.9615	2.7	0.0474	3.6	0.0079	2.4	0.67	50.7	1.2	47.0	1.7	136.0	66.5	50.7	1.2						
15CA-03A 29Feb-Spat 216	63	793	1.1	30.4202	4.6	0.0344	6.5	0.0076	4.5	0.70	48.7	2.2	34.3	2.2	896.4	132.6	48.7	2.2						
15CA-03A 29Feb-Spat 217	200	1910	0.8	23.1292	3.6	0.0470	4.1	0.0079	3.0	0.49	50.6	1.0	45.7	1.9	154.1	88.4	50.6	1.0						
15CA-03A 29Feb-Spat 218	42	1142	1.4	26.2360	6.5	0.0415	7.6	0.0079	3.9	0.52	50.7	2.0	41.2	3.1	477.2	172.3	50.7	2.0						
15CA-03A 29Feb-Spat 219	44	572	1.0	31.3401	42.1	0.0356	42.2	0.0081	2.9	0.07	51.9	1.5	35.5	14.7	973.4	1288.3	51.9	1.5						
15CA-03A 29Feb-Spat 220	57	414	0.8	36.6276	32.3	0.0293	32.5	0.0078	3.7	0.11	49.9	1.8	29.3	9.4	1458.5	1086.5	49.9	1.8						
15CA-03A 29Feb-Spat 221	43	243159	1.2	16.4190	5.6	0.0671	6.5	0.0080	3.5	0.53	51.3	1.8	69.9	4.2	635.9	118.9	51.3	1.8						
15CA-03A 29Feb-Spat 222	54	412	1.1	37.9302	71.6	0.0287	71.6	0.0079	3.1	0.04	50.7	1.6	28.7	20.3	1575.1	741.6	50.7	1.6						
15CA-03A 29Feb-Spat 223	55	776	1.4	26.2493	10.3	0.0406	11.0	0.0077	3.8	0.34	49.6	1.9	40.4	4.4	478.5	274.3	49.6	1.9						
15CA-03A 29Feb-Spat 224	46	781	1.1	30.3717	27.3	0.0366	27.6	0.0081	3.6	0.13	51.8	1.9	36.5	9.9	881.8	801.5	51.8	1.9						
15CA-03A 29Feb-Spat 225	69	3890.9	1.1	14.0985	2.9	0.0797	4.1	0.0082	2.9	0.71	52.3	1.5	77.9	3.0	955.0	58.5	52.3	1.5						
15CA-03A 29Feb-Spat 226	33	879	1.1	23.8870	5.7	0.0449	7.3	0.0078	4.5	0.62	50.0	2.3	44.6	3.2	234.7	143.4	50.0	2.3						
15CA-03A 29Feb-Spat 227	71	363	1.2	12.5131	13.5	0.0902	14.0	0.0082	3.7	0.26	52.6	1.9	87.7	11.8	1194.9	267.5	52.6	1.9						
15CA-03A 29Feb-Spat 228	55	3413	1.3	22.1431	4.2	0.0522	5.8	0.0084	3.9	0.68	53.8	2.1	51.6	2.9	47.0	102.5	53.8	2.1						
15CA-03A 29Feb-Spat 229	90	11452	1.0	18.9462	4.2	0.0591	4.9	0.0081	2.5	0.51	52.2	1.3	58.3	2.8	319.4	96.0	52.2	1.3						
15CA-03A 29Feb-Spat 230	187	1967	0.8	25.0683	3.1	0.0432	3.9	0.0078	2.2	0.58	50.4	1.1	42.9	1.6	358.0	81.4	50.4	1.1						
15CA-03A 29Feb-Spat 231	48	729	1.3	30.1639	11.2	0.0357	11.7	0.0078	3.5	0.30	50.2	1.7	35.6	4.1	862.0	322.3	50.2	1.7						
15CA-03A 29Feb-Spat 232	80	1822	0.8	14.5153	9.0	0.0793	9.5	0.0084	2.9	0.31	53.6	1.6	77.5	7.1	895.5	186.9	53.6	1.6						
15CA-03A 29Feb-Spat 233	511	12240	1.0	21.8932	1.7	0.0506	2.4	0.0080	1.8	0.72	51.6	0.9	50.1	1.2	19.4	41.1	51.6	0.9						
15CA-03A 29Feb-Spat 234	132	2264	0.8	17.3704	4.1	0.0647	4.7	0.0082	2.3	0.49	52.3	1.2	63.7	2.9	513.4	89.8	52.3	1.2						
15CA-03A 29Feb-Spat 235	81	2176	1.5	24.8846	5.0	0.0459	5.7	0.0083	2.9	0.50	53.2	1.5	45.6	2.6	339.0	127.6	53.2	1.5						
15CA-03A 29Feb-Spat 236	48	5078	1.5	23.6521	3.8	0.0472	5.7	0.0081	4.3	0.75	51.9	2.2	46.8	2.6	209.8	95.2	51.9	2.2						
15CA-03A 29Feb-Spat 237	34	295	1.1	4.9854	8.8	0.2647	9.9	0.0096	4.4	0.45	61.4	2.7	238.4	21.0	283.0	144.3	61.4	2.7						
15CA-03A 29Feb-Spat 238	93	1617	1.0	25.7661	12.5	0.0427	12.9	0.0080	3.2	0.25	51.3	1.7	42.5	5.4	429.5	328.8	51.3	1.7						
15CA-03A 29Feb-Spat 239	40	291	1.1	127.9823	108.8	0.0085	108.9	0.0079	3.7	0.03	50.4	1.9	8.6	9.3	0.0	0.0	50.4	1.9						
15CA-03A 29Feb-Spat 240	71	800	1.1	33.7701	4.4	0.0318	5.5	0.0078	3.3	0.60	50.0	1.6	31.7	1.7	1199.1	136.4	50.0	1.6						
15CA-03A 29Feb-Spat 241	75	1131	1.6	27.3549	3.5	0.0399	9.9	0.0079	2.8	0.28	50.8	1.4	39.7	3.9	589.1	259.3	50.8	1.4						
15CA-03A 29Feb-Spat 242	63	1771	0.8	22.2114	4.5	0.0491	5.2	0.0079	2.7	0.52	50.8	1.4	48.7	2.5	54.4	108.8	50.8	1.4						
15CA-03A 29Feb-Spat 243	77	780	1.2	31.0827	5.3	0.0358	6.3	0.0081	3.3	0.53	51.9	1.7	35.8	2.2	949.1	156.3	51.9	1.7						
15CA-03A 29Feb-Spat 244	81	1621	0.9	21.2993	7.9	0.0514	8.6	0.0079	3.2	0.38	51.0	1.6	50.9	4.2	46.7	189.7	51.0	1.6						
15CA-03A 29Feb-Spat 245	141	2133	1.0	21.7056	8.2	0.0504	8.6	0.0079	2.6	0.31	50.9	1.3	49.9	4.2	1.4	197.5	50.9	1.3						
15CA-03A 29Feb-Spat 246	25	302	1.4	220.1437	115.0	0.0050	115.1	0.0080	5.8	0.05	51.7	3.0	5.1	5.9	0.0	0.0	51.7	3.0						
15CA-03A 29Feb-Spat 247	77	1089	0.7	30.0844	8.9	0.0358	9.4	0.0078	2.9	0.31	50.1	1.5	35.7	3.3	854.4	255.5	50.1	1.5						
15CA-03A 29Feb-Spat 248	51	320	1.1	1105.6382	64.8	0.0010	64.9	0.0077	3.1	0.06	49.3	1.5	1.0	0.5	0.0	0.0	49.3	1.5						
15CA-03A 29Feb-Spat 249	69	3318	0.9	17.4080	6.4	0.0650	7																	

Sample: 15CA03A		U-Pb geochronologic analyses										Isotope ratios										Apparent ages (Ma)									
Analysis	U	206Pb	U/Th	206Pb*	±	207Pb*	±	206Pb*	±	error	206Pb*	±	207Pb*	±	206Pb*	±	207Pb*	±	206Pb*	±	207Pb*	±	206Pb*	±	207Pb*	±	Best age	±			
	(ppm)	204Pb		207Pb*	(%)	235U*	(%)	238U	(%)	corr.	238U*	(Ma)	235U	(Ma)	207Pb*	(Ma)	207Pb*	(Ma)	207Pb*	(Ma)	207Pb*	(Ma)	207Pb*	(Ma)	207Pb*	(Ma)	(Ma)	(Ma)			
15CA-03A 29Feb-Spat 276	38	3676	1.1	20.0716	5.7	0.0549	7.2	0.0080	4.4	0.62	51.3	2.3	54.3	3.8	186.7	132.0	51.3	2.3	54.3	3.8	186.7	132.0	51.3	2.3	51.3	2.3					
15CA-03A 29Feb-Spat 277	110	4501	1.3	20.9817	3.4	0.0529	4.4	0.0080	2.7	0.63	51.6	1.4	52.3	2.2	82.4	80.6	51.6	1.4	52.3	2.2	82.4	80.6	51.6	1.4	51.6	1.4					
15CA-03A 29Feb-Spat 278	41	1754	1.2	21.1563	6.0	0.0501	8.0	0.0077	5.3	0.66	49.3	2.6	49.6	3.9	62.7	143.4	49.3	2.6	49.6	3.9	62.7	143.4	49.3	2.6	49.3	2.6					
15CA-03A 29Feb-Spat 279	44	1468	1.3	25.1795	11.6	0.0441	12.1	0.0081	3.4	0.28	51.7	1.7	43.8	5.2	369.4	302.1	51.7	1.7	43.8	5.2	369.4	302.1	51.7	1.7	51.7	1.7					
15CA-03A 29Feb-Spat 280	82	1079	1.3	29.4671	6.1	0.0362	7.7	0.0077	4.7	0.61	49.6	2.3	36.1	2.7	795.3	173.2	49.6	2.3	36.1	2.7	795.3	173.2	49.6	2.3	49.6	2.3					
15CA-03A 29Feb-Spat 281	47	718	1.2	31.0656	12.7	0.0354	13.5	0.0080	4.6	0.34	51.2	2.3	35.3	4.7	947.5	373.6	51.2	2.3	35.3	4.7	947.5	373.6	51.2	2.3	51.2	2.3					
15CA-03A 29Feb-Spat 282	61	1047	1.1	29.5885	5.6	0.0368	7.1	0.0079	4.4	0.61	50.9	2.2	36.7	2.8	816.6	160.9	50.9	2.2	36.7	2.8	816.6	160.9	50.9	2.2	50.9	2.2					
15CA-03A 29Feb-Spat 283	62	1296	1.2	21.9781	11.2	0.0524	11.6	0.0083	2.8	0.25	53.6	1.5	51.8	5.8	28.9	272.2	53.6	1.5	51.8	5.8	28.9	272.2	53.6	1.5	53.6	1.5					
15CA-03A 29Feb-Spat 284	70	1490	1.1	17.1492	6.8	0.0711	7.5	0.0088	3.1	0.41	56.8	1.8	69.8	5.1	541.5	149.6	69.8	1.8	69.8	5.1	541.5	149.6	69.8	1.8	69.8	1.8					
15CA-03A 29Feb-Spat 285	45	456	0.7	54.4721	18.4	0.0200	18.9	0.0079	4.4	0.23	50.7	2.2	20.1	3.8	3030.8	1075.9	50.7	2.2	20.1	3.8	3030.8	1075.9	50.7	2.2	50.7	2.2					
15CA-03A 29Feb-Spat 287	80	530	0.7	20.6425	10.3	0.0541	10.7	0.0081	3.1	0.28	52.0	1.6	53.5	5.6	121.0	243.1	52.0	1.6	53.5	5.6	121.0	243.1	52.0	1.6	52.0	1.6					
15CA-03A 29Feb-Spat 288	51	1378	1.1	23.5070	3.8	0.0477	5.7	0.0081	4.3	0.75	52.2	2.2	47.3	2.6	194.4	94.1	52.2	2.2	47.3	2.6	194.4	94.1	52.2	2.2	52.2	2.2					
15CA-03A 29Feb-Spat 289	78	430	1.2	50.6819	34.5	0.0215	34.7	0.0079	3.4	0.10	50.8	1.7	21.6	7.4	2695.5	573.4	50.8	1.7	21.6	7.4	2695.5	573.4	50.8	1.7	50.8	1.7					
15CA-03A 29Feb-Spat 290	448	19920	0.5	21.2984	1.5	0.0521	2.3	0.0080	1.7	0.74	51.7	0.9	51.5	1.1	46.8	36.2	51.7	0.9	51.5	1.1	46.8	36.2	51.7	0.9	51.7	0.9					
15CA-03A 29Feb-Spat 291	60	547	1.1	37.0549	16.5	0.0289	16.7	0.0078	2.8	0.16	49.8	1.4	28.9	4.8	1496.8	551.5	49.8	1.4	28.9	4.8	1496.8	551.5	49.8	1.4	49.8	1.4					
15CA-03A 29Feb-Spat 292	44	370	1.1	56.4542	115.1	0.0190	115.1	0.0078	3.6	0.03	50.0	1.8	19.1	21.8	3208.3	0.0	50.0	1.8	19.1	21.8	3208.3	0.0	50.0	1.8	50.0	1.8					
15CA-03A 29Feb-Spat 293	55	574	0.8	25.0701	10.6	0.0438	11.1	0.0080	3.1	0.28	51.2	1.6	43.6	4.7	358.2	275.6	51.2	1.6	43.6	4.7	358.2	275.6	51.2	1.6	51.2	1.6					
15CA-03A 29Feb-Spat 294	500	9737	0.5	21.4598	1.4	0.0496	2.3	0.0077	1.8	0.79	49.6	0.9	49.1	1.1	28.7	33.4	49.6	0.9	49.1	1.1	28.7	33.4	49.6	0.9	49.6	0.9					
15CA-03A 29Feb-Spat 295	85	638	0.7	37.6338	6.5	0.0293	7.2	0.0080	3.0	0.42	51.4	1.5	29.4	2.1	1548.6	219.2	51.4	1.5	29.4	2.1	1548.6	219.2	51.4	1.5	51.4	1.5					
15CA-03A 29Feb-Spat 296	48	3425	1.2	17.7663	4.8	0.0623	5.9	0.0080	3.5	0.58	51.5	1.8	61.3	3.5	463.7	106.6	51.5	1.8	61.3	3.5	463.7	106.6	51.5	1.8	51.5	1.8					
15CA-03A 29Feb-Spat 297	78	1527	0.8	23.7956	4.6	0.0466	5.7	0.0080	3.3	0.58	51.6	1.7	46.2	2.6	225.0	116.4	51.6	1.7	46.2	2.6	225.0	116.4	51.6	1.7	51.6	1.7					
15CA-03A 29Feb-Spat 298	32	1550	1.3	21.8107	5.7	0.0500	7.3	0.0079	4.6	0.63	50.8	2.3	49.6	3.6	10.3	137.9	50.8	2.3	49.6	3.6	10.3	137.9	50.8	2.3	50.8	2.3					
15CA-03A 29Feb-Spat 299	33	909	1.2	4.3439	34.0	0.3317	34.2	0.0105	3.8	0.11	67.0	2.5	290.9	86.7	3053.5	562.8	67.0	2.5	290.9	86.7	3053.5	562.8	67.0	2.5	67.0	2.5					
15CA-03A 29Feb-Spat 300	75	642	1.0	38.6654	4.2	0.0288	5.2	0.0081	3.2	0.60	51.8	1.6	28.8	1.5	1640.6	143.8	51.8	1.6	28.8	1.5	1640.6	143.8	51.8	1.6	51.8	1.6					
15CA-03A 29Feb-Spat 301	56	333	1.1	144.4013	60.5	0.0074	50.7	0.0078	3.8	0.07	49.9	1.9	7.5	3.8	0.0	0.0	49.9	1.9	7.5	3.8	0.0	0.0	49.9	1.9	49.9	1.9					
15CA-03A 29Feb-Spat 302	78	1794	0.9	25.1860	4.2	0.0432	5.0	0.0079	2.8	0.56	50.7	1.4	43.0	2.1	370.1	108.3	50.7	1.4	43.0	2.1	370.1	108.3	50.7	1.4	50.7	1.4					
15CA-03A 29Feb-Spat 303	38	324	1.1	526.6092	348.1	0.0021	348.1	0.0078	3.9	0.01	50.3	2.0	2.1	7.2	0.0	0.0	50.3	2.0	2.1	7.2	0.0	0.0	50.3	2.0	50.3	2.0					
15CA-03A 29Feb-Spat 304	95	2504	0.8	23.6998	6.6	0.0469	7.2	0.0081	2.8	0.38	51.8	1.4	46.6	3.3	214.9	167.1	51.8	1.4	46.6	3.3	214.9	167.1	51.8	1.4	51.8	1.4					
15CA-03A 29Feb-Spat 306	56	2617	1.3	22.4047	5.0	0.0502	5.8	0.0082	3.1	0.52	52.4	1.6	49.7	2.8	75.6	121.7	52.4	1.6	49.7	2.8	75.6	121.7	52.4	1.6	52.4	1.6					
15CA-03A 29Feb-Spat 308	36	1433	0.8	28.1869	6.3	0.0362	7.3	0.0078	3.5	0.49	50.2	1.8	38.1	2.7	671.1	175.0	50.2	1.8	38.1	2.7	671.1	175.0	50.2	1.8	50.2	1.8					
15CA-03A 29Feb-Spat 309	62	429	1.0	57.2059	25.8	0.0189	26.1	0.0078	3.9	0.15	50.3	1.9	19.0	4.9	3276.1	987.4	50.3	1.9	19.0	4.9	3276.1	987.4	50.3	1.9	50.3	1.9					
15CA-03A 29Feb-Spat 310	41	232	1.1	-42.9807	4.8	-0.0244	6.8	0.0076	4.8	0.71	48.7	2.3	25.1	1.7	0.0	0.0	48.7	2.3	25.1	1.7	0.0	0.0	48.7	2.3	48.7	2.3					
15CA-03A 29Feb-Spat 311	237	7410	0.7	20.2855	2.3	0.0546	2.8	0.0080	1.7	0.61	51.5	0.9	54.0	1.5	161.9	52.7	51.5	0.9	54.0	1.5	161.9	52.7	51.5	0.9	51.5	0.9					
15CA-03A 29Feb-Spat 312	40	3207	1.2	20.9464	4.8	0.0548	6.5	0.0083	4.4	0.67	53.5	2.3	54.2	3.4	86.5	114.8	53.5	2.3	54.2	3.4	86.5	114.8	53.5	2.3	53.5	2.3					
15CA-03A 29Feb-Spat 313	53	1069	1.1	32.1623	4.2	0.0339	5.8	0.0079	4.0	0.68	50.7	2.0	33.8	1.9	1050.3	126.7	50.7	2.0	33.8	1.9	1050.3	126.7	50.7	2.0	50.7	2.0					
15CA-03A 29Feb-Spat 314	96	1866	1.1	24.0746	3.8	0.0454	4.8	0.0079	3.0	0.62	50.9	1.5	45.1	2.1	254.5	95.7	50.9	1.5	45.1	2.1	254.5	95.7	50.9	1.5	50.9	1.5					
15CA-03A 29Feb-Spat 315	56	4777	0.9	17.9365	6.1	0.0642	7.4	0.0084	4.2	0.56	53.6	2.2	63.2	4.5	442.5	136.1	53.6	2.2	63.2	4.5	442.5	136.1	53.6	2.2	53.6	2.2					

Sample: CANBC1022Gab	U-Pb geochronologic analyses										Isotope ratios										Apparent ages (Ma)									
	Analysis	U (ppm)	206Pb 204Pb	U/Th	206Pb* 207Pb*	±	207Pb* 235U*	±	206Pb* 238U	±	error corr.	206Pb* 238U*	±	207Pb* 235U	±	206Pb* 207Pb*	±	Best age (Ma)	±	Best age (Ma)	±									
																						(%)	(%)	(%)	(%)	(%)	(%)	(%)	(%)	(%)
Leier-CAN-BC-1022ab-Spot 1	239	6327	1.1	21.3117	1.7	0.1642	3.4	0.0254	3.0	0.888	1615	4.7	154.3	4.9	45.3	41.3	1615	4.7												
Leier-CAN-BC-1022ab-Spot 2	478	13893	2.1	20.8794	0.9	0.1690	2.4	0.0253	2.2	0.92	1614	3.5	159.5	3.5	116.8	22.9	1614	3.5												
Leier-CAN-BC-1022ab-Spot 3	521	21846	1.6	20.3318	1.1	0.1728	2.1	0.0255	1.8	0.86	1623	2.9	161.9	3.1	156.6	24.7	1623	2.9												
Leier-CAN-BC-1022ab-Spot 4	607	1519	3.8	27.0173	1.6	0.0344	2.8	0.0087	2.3	0.83	43.3	1.0	34.4	0.9	555.5	42.4	43.3	1.0												
Leier-CAN-BC-1022ab-Spot 5	155	6779	1.9	20.7646	1.5	0.1719	2.6	0.0259	2.1	0.81	164.7	3.4	161.0	3.9	107.1	36.5	164.7	3.4												
Leier-CAN-BC-1022ab-Spot 6	141	4968	2.8	21.5197	2.9	0.1873	4.0	0.0292	2.7	0.68	185.8	5.0	174.4	6.4	22.0	70.6	185.8	5.0												
Leier-CAN-BC-1022ab-Spot 7	475	23606	1.3	20.1250	0.8	0.1701	2.0	0.0248	1.9	0.92	158.1	2.9	159.5	3.0	180.5	19.1	158.1	2.9												
Leier-CAN-BC-1022ab-Spot 8	563	4996	1.2	22.8553	1.6	0.0470	2.5	0.0078	1.9	0.78	50.1	0.9	46.7	1.1	124.5	39.5	50.1	0.9												
Leier-CAN-BC-1022ab-Spot 9	132	2376	1.7	21.7193	1.7	0.1611	2.9	0.0254	2.3	0.79	181.5	3.6	151.6	4.0	0.2	42.1	181.5	3.6												
Leier-CAN-BC-1022ab-Spot 10	282	6403	2.3	21.2438	1.3	0.1605	2.3	0.0247	1.9	0.82	137.4	2.9	151.1	3.2	52.9	31.4	137.4	2.9												
Leier-CAN-BC-1022ab-Spot 11	532	74335	2.2	20.5736	1.2	0.1700	2.3	0.0254	2.0	0.86	161.4	3.2	159.4	3.5	128.9	28.3	161.4	3.2												
Leier-CAN-BC-1022ab-Spot 12	3868	40726	3.2	20.1804	0.6	0.1497	2.0	0.0219	1.8	0.94	139.7	2.5	141.6	2.6	174.1	15.1	139.7	2.5												
Leier-CAN-BC-1022ab-Spot 14	438	67252	2.9	20.0803	1.1	0.1753	2.6	0.0255	2.3	0.90	162.5	3.7	164.0	3.9	165.7	25.6	162.5	3.7												
Leier-CAN-BC-1022ab-Spot 15	342	3103	2.7	22.5091	2.2	0.0504	3.1	0.0082	2.1	0.69	52.8	1.1	49.9	1.5	87.0	54.6	52.8	1.1												
Leier-CAN-BC-1022ab-Spot 16	680	27028	1.8	20.2956	0.7	0.1700	2.2	0.0250	2.0	0.94	159.3	3.2	159.4	3.2	160.8	17.1	159.3	3.2												
Leier-CAN-BC-1022ab-Spot 17	1007	35364	1.0	20.0090	0.7	0.1747	2.1	0.0254	2.0	0.95	161.4	3.1	163.5	3.1	194.0	15.7	161.4	3.1												
Leier-CAN-BC-1022ab-Spot 18	202	6489	3.1	21.0447	1.3	0.2007	2.4	0.0308	2.1	0.85	194.5	4.0	185.7	4.1	75.3	30.4	194.5	4.0												
Leier-CAN-BC-1022ab-Spot 19	602	15886	2.0	19.9514	0.9	0.1691	2.0	0.0245	1.8	0.89	155.8	2.9	158.6	3.0	200.6	2.9	155.8	2.9												
Leier-CAN-BC-1022ab-Spot 20	647	18245	2.3	20.4066	0.9	0.1634	2.6	0.0242	2.4	0.94	154.0	3.6	153.7	3.6	148.0	20.7	154.0	3.6												
Leier-CAN-BC-1022ab-Spot 21	1055	30188	1.8	20.0061	1.4	0.1680	2.5	0.0244	2.1	0.83	155.3	3.2	157.7	3.7	194.3	33.0	155.3	3.2												
Leier-CAN-BC-1022ab-Spot 22	921	148649	2.4	20.2230	0.8	0.1703	2.1	0.0250	1.9	0.93	159.0	3.0	159.6	3.1	169.1	17.8	159.0	3.0												
Leier-CAN-BC-1022ab-Spot 23	778	73448	1.5	20.3540	1.1	0.1739	2.6	0.0257	2.3	0.91	163.4	3.7	162.8	3.8	154.0	25.4	163.4	3.7												
Leier-CAN-BC-1022ab-Spot 24	189	184871	1.9	19.5862	1.3	0.1838	2.7	0.0261	2.3	0.86	166.1	3.8	171.3	4.2	243.4	30.8	166.1	3.8												
Leier-CAN-BC-1022ab-Spot 25	617	51689	2.8	20.3501	0.8	0.1774	1.9	0.0262	1.7	0.91	166.6	2.8	165.8	2.9	154.5	17.8	166.6	2.8												
Leier-CAN-BC-1022ab-Spot 26	1959	248596	3.0	20.1613	0.6	0.1639	1.9	0.0240	1.8	0.94	152.7	2.8	154.1	2.8	170.3	15.1	152.7	2.8												
Leier-CAN-BC-1022ab-Spot 27	641	21949	2.9	20.5531	1.0	0.1642	2.1	0.0245	1.9	0.89	155.9	2.9	154.4	3.1	131.1	22.6	155.9	2.9												
Leier-CAN-BC-1022ab-Spot 28	245	11214	2.0	20.8948	1.5	0.1655	2.6	0.0251	2.2	0.83	152.7	3.4	155.5	3.7	92.3	34.4	152.7	3.4												
Leier-CAN-BC-1022ab-Spot 29	563	19442	2.4	20.5340	0.9	0.1761	2.7	0.0262	2.6	0.95	166.9	4.3	164.7	4.2	133.4	20.2	166.9	4.3												
Leier-CAN-BC-1022ab-Spot 30	1592	68265	13.3	19.9623	0.7	0.2134	2.0	0.0309	1.9	0.94	196.2	3.7	196.4	3.6	199.4	16.3	196.2	3.7												
Leier-CAN-BC-1022ab-Spot 31	431	23271	4.5	19.9887	1.0	0.2132	2.4	0.0309	2.1	0.90	196.4	4.1	196.3	4.2	195.2	24.2	196.4	4.1												
Leier-CAN-BC-1022ab-Spot 32	256	5932	2.1	13.7312	6.1	0.2775	6.5	0.0276	2.0	0.31	175.8	3.5	248.7	14.2	1009.1	124.3	175.8	3.5												
Leier-CAN-BC-1022ab-Spot 33	232	10426	2.1	20.2685	1.6	0.2074	2.6	0.0305	2.1	0.80	193.6	4.0	191.4	4.5	163.9	36.4	193.6	4.0												
Leier-CAN-BC-1022ab-Spot 34	311	15303	0.9	20.5203	1.4	0.1655	2.7	0.0248	2.3	0.88	156.9	3.5	155.5	3.6	135.0	32.0	156.9	3.5												
Leier-CAN-BC-1022ab-Spot 35	232	20011	3.3	20.3868	1.0	0.2083	2.3	0.0309	1.9	0.85	195.6	3.7	194.6	3.1	150.3	28.3	195.6	3.7												
Leier-CAN-BC-1022ab-Spot 36	324	10006	2.1	19.1141	1.2	0.2275	2.2	0.0315	1.8	0.84	200.1	3.6	208.1	4.1	299.3	27.4	200.1	3.6												
Leier-CAN-BC-1022ab-Spot 38	778	22647	2.0	20.5051	0.8	0.1753	1.6	0.0261	1.4	0.86	165.9	2.3	164.0	2.4	136.7	19.0	165.9	2.3												
Leier-CAN-BC-1022ab-Spot 39	221	6970	2.2	21.2592	1.2	0.1678	2.6	0.0259	2.2	0.88	164.7	3.7	157.5	3.7	51.2	29.0	164.7	3.7												
Leier-CAN-BC-1022ab-Spot 40	140	62225	3.7	20.1410	1.3	0.2101	2.7	0.0307	2.4	0.88	194.9	4.6	193.6	4.8	178.6	30.5	194.9	4.6												
Leier-CAN-BC-1022ab-Spot 41	265	10074	3.0	20.7529	1.7	0.2054	2.8	0.0309	2.3	0.80	196.3	4.4	189.7	4.9	108.4	39.7	196.3	4.4												
Leier-CAN-BC-1022ab-Spot 42	257	9875	2.7	20.1922	1.4	0.2017	2.2	0.0295	1.8	0.80	187.7	3.3	186.6	3.8	172.7	31.7	187.7	3.3												
Leier-CAN-BC-1022ab-Spot 43	1314	35198	1.5	20.4306	0.8	0.1676	2.0	0.0248	1.8	0.93	158.2	2.9	157.4	2.9	145.2	18.3	158.2	2.9												
Leier-CAN-BC-1022ab-Spot 44	586	78006	1.8	20.1318	1.0	0.1682	2.3	0.0246	2.1	0.90	158.4	3.4	157.8	3.4	179.7	24.1	158.4	3.4												
Leier-CAN-BC-1022ab-Spot 45	277	208146	1.4	20.4872	1.5	0.1716	2.8	0.0255	2.4	0.85	162.3	3.8	160.8	4.1	138.7	34.2	162.3	3.8												
Leier-CAN-BC-1022ab-Spot 46	117	3319	2.1	22.5004	2.5	0.1034	3.4	0.0169	2.4	0.69	107.9	2.5	99.9	3.3	86.0	61.3	107.9	2.5												
Leier-CAN-BC-1022ab-Spot 47	601	2292	1.9	24.6807	2.1	0.0419	2.9	0.0075	2.0	0.68	48.2	0.9	41.7	1.2	317.9	54.5	48.2	0.9												
Leier-CAN-BC-1022ab-Spot 48	1528	24431	2.3	19.5204	1.0	0.1679	2.0	0.0238	1.8	0.88	151.5	2.7	157.6	3.0	251.1	22.5	151.5	2.7												
Leier-CAN-BC-1022ab-Spot 49	556	26382	0.9	20.3135	1.2	0.1730	2.1	0.0255	1.7	0.83	162.2	2.8	162.0	3.1	158.7	27.2	162.2	2.8												
Leier-CAN-BC-1022ab-Spot 50	990	69606	2.0	19.8116	0.6	0.1745	1.9	0.0251	1.8	0.95	159.7	2.9	163.3	2.9	217.0	14.0	159.7	2.9												
Leier-CAN-BC-1022ab-Spot 51	642	69399	2.0	20.1358	0.7	0.1780	2.0	0.0260	1.9	0.93	185.4	3.1	186.3	3.1	179.2	16.8	185.4	3.1												
Leier-CAN-BC-1022ab-Spot 52	1033	29760	1.8	20.1846	0.9	0.1707	2.4	0.0250	2.2	0.93	159.4	3.4	160.0	3.5	175.9	19.9	159.4	3.4												
Leier-CAN-BC-1022ab-Spot 53	1416	182192	1.7	20.2306	1.0	0.1691	1.9	0.0248	1.6	0.85	158.0	2.6	158.7	2.8	168.3	24.1	158.0	2.6												
Leier-CAN-BC-1022ab-Spot 54	655	6325	0.8	22.9692	1.5	0.0424	3.2	0.0069	2.8	0.88	44.2	1.2	42.2	1.3	71.7	37.7	44.2	1.2												
Leier-CAN-BC-1022ab-Spot 55	768	14347	2.5	20.6888	0.8	0.1693	2.0	0.0254	1.9	0.92	161.7	3.0	158.8	3.0	116.0	18.5	161.7	3.0												
Leier-CAN-BC-1022ab-Spot 56	769	12667	0.6	20.5435	1.2	0.1627	2.7	0.0242	2.5	0.90	154.4	3.7	153.1	3.9	132.3	28.3	154.4	3.7												
Leier-CAN-BC-1022ab-Spot 57	296	19699	2.2	20.0543	1.3	0.2108	2.1	0.0307	1.7	0.81	194.7	3.3	194.2	3.8	188.7	29.2	194.7	3.3												
Leier-CAN-BC-1022ab-Spot 58	112	3108	0.7	21.5558	2.8	0.1612	4.0	0.0252	2.9	0.72	160.5	4.6	151.8	5.7	18.0	67.4	160.5	4.6												
Leier-CAN-BC-1022ab-Spot 59	492	13232	3.2	20.2496	1.2	0.2082	2.2	0.0307	1.9	0.85	195.0	3.6	192.8	3.6	166.1	27.0	195.0	3.6												
Leier-CAN-BC-1022ab-Spot 60	389	126428	1.6	19.8928	1.3	0.1738	2.3	0.0251	1.9	0.82	159.7	3.0	162.7	3.4	207.5	29.9	159.7	3.0			</									

Sample: CANBC1022Gab	U-Pb geochronologic analyses											Isotope ratios											Apparent ages (Ma)											Best age (Ma)										
	Analysis	U (ppm)	206Pb/204Pb	U/Tn	206Pb*/207Pb*	±	207Pb*/235U*	±	206Pb*/238U	±	error corr.	206Pb*/238U*	±	207Pb*/235U*	±	206Pb*/207Pb*	±	Best age	±	Best age	±	Best age	±																					
																								±	±	±	±	±	±	±	±	±	±	±	±									
Leier-CAN-BC-1022ab-Spot 100	294	10963	3.3	20.7315	1.2	0.1998	2.3	0.0300	2.0	0.88	190.7	3.7	184.8	3.9	110.8	27.3	180.7	3.7																										
Leier-CAN-BC-1022ab-Spot 101	282	17796	3.6	20.255	1.4	0.2110	2.1	0.0410	1.6	0.78	196.8	3.0	194.4	3.1	105.4	33.4	196.8	3.0																										
Leier-CAN-BC-1022ab-Spot 102	497	13574	1.7	20.4939	1.1	0.1868	2.3	0.0449	2.0	0.86	157.8	3.1	156.8	3.1	138.0	27.0	157.8	3.1																										
Leier-CAN-BC-1022ab-Spot 103	384	39787	1.7	20.1820	1.4	0.1440	2.3	0.0167	1.9	0.80	106.7	2.0	109.6	2.4	173.9	32.7	106.7	2.0																										
Leier-CAN-BC-1022ab-Spot 104	382	92963	1.3	20.1324	1.2	0.1684	2.6	0.0246	2.3	0.89	156.6	3.6	158.0	3.8	179.6	26.9	156.6	3.6																										
Leier-CAN-BC-1022ab-Spot 105	457	64295	1.6	20.2462	1.1	0.1680	2.4	0.0247	2.2	0.88	157.1	3.3	157.7	3.6	166.5	26.8	157.1	3.3																										
Leier-CAN-BC-1022ab-Spot 106	1165	7490	1.6	19.0561	1.7	0.1545	2.8	0.0214	2.2	0.79	136.2	3.0	145.9	3.8	306.2	39.4	136.2	3.0																										
Leier-CAN-BC-1022ab-Spot 107	796	79279	1.8	20.3431	0.7	0.1699	1.9	0.0251	1.7	0.92	159.6	2.7	159.3	2.8	168.8	15.9	159.6	2.7																										
Leier-CAN-BC-1022ab-Spot 108	827	52092	2.2	19.1391	1.3	0.1787	2.0	0.0248	1.5	0.78	158.0	2.3	167.0	3.0	296.3	29.2	158.0	2.3																										
Leier-CAN-BC-1022ab-Spot 109	222	6125	1.0	21.7698	2.2	0.1569	3.1	0.0348	2.2	0.71	157.8	3.4	148.0	4.3	5.7	52.8	157.8	3.4																										
Leier-CAN-BC-1022ab-Spot 110	715	29560	2.9	20.5005	0.9	0.1891	2.0	0.0251	1.9	0.91	180.0	2.9	158.6	3.0	137.3	20.1	180.0	2.9																										
Leier-CAN-BC-1022ab-Spot 111	241	6349	1.5	20.5195	1.6	0.1658	2.9	0.0247	2.4	0.83	157.1	3.7	155.7	4.2	135.1	38.3	157.1	3.7																										
Leier-CAN-BC-1022ab-Spot 112	437	20177	1.8	20.1020	1.1	0.1630	2.3	0.0238	2.0	0.88	151.4	3.0	153.3	3.3	183.1	25.8	151.4	3.0																										
Leier-CAN-BC-1022ab-Spot 113	971	1016476	2.2	20.0356	0.8	0.1676	2.1	0.0244	1.9	0.92	155.2	2.9	157.4	3.0	190.9	18.8	155.2	2.9																										
Leier-CAN-BC-1022ab-Spot 114	1174	11255	0.5	21.1135	1.2	0.0507	2.0	0.0078	1.6	0.80	49.8	0.8	50.2	1.0	67.6	29.0	49.8	0.8																										
Leier-CAN-BC-1022ab-Spot 115	1195	10257	1.5	21.1134	1.0	0.0503	2.3	0.0077	2.1	0.91	49.5	1.0	49.9	1.1	67.6	23.4	49.5	1.0																										
Leier-CAN-BC-1022ab-Spot 116	274	12531	2.9	19.9454	1.4	0.2082	2.5	0.0301	2.1	0.84	191.3	4.0	192.0	4.4	201.3	31.8	191.3	4.0																										
Leier-CAN-BC-1022ab-Spot 117	1156	57870	1.5	20.1737	0.7	0.1681	2.0	0.0246	1.6	0.84	156.6	2.9	157.8	2.9	175.0	15.3	156.6	2.9																										
Leier-CAN-BC-1022ab-Spot 118	201	75920	1.6	17.5620	1.6	0.1760	4.0	0.0241	2.4	0.61	153.4	3.7	175.8	6.4	489.5	69.7	153.4	3.7																										
Leier-CAN-BC-1022ab-Spot 119	178	55848	2.4	19.8877	1.5	0.1815	3.2	0.0262	2.8	0.87	166.6	4.6	169.4	4.9	208.0	35.6	166.6	4.6																										
Leier-CAN-BC-1022ab-Spot 120	466	26455	3.4	20.2970	1.0	0.1735	2.2	0.0255	2.0	0.88	162.6	3.1	162.4	3.3	160.6	24.4	162.6	3.1																										
Leier-CAN-BC-1022ab-Spot 121	171	23841	2.0	19.1188	1.7	0.1762	3.1	0.0244	2.5	0.83	155.6	3.9	164.8	4.6	298.7	39.4	155.6	3.9																										
Leier-CAN-BC-1022ab-Spot 122	300	16965	2.8	20.1819	1.1	0.2101	2.4	0.0308	2.1	0.88	195.3	4.0	193.6	4.2	173.9	26.7	195.3	4.0																										
Leier-CAN-BC-1022ab-Spot 123	788	52226	2.5	20.1412	0.8	0.1722	2.1	0.0252	1.9	0.92	160.2	3.1	161.3	3.2	178.6	19.8	160.2	3.1																										
Leier-CAN-BC-1022ab-Spot 124	426	11810	3.4	20.0473	1.0	0.2061	2.0	0.0300	1.7	0.88	190.3	3.3	190.3	3.5	199.5	24.3	190.3	3.3																										
Leier-CAN-BC-1022ab-Spot 125	304	6032	1.9	21.328	1.3	0.1689	2.5	0.0261	2.1	0.85	186.3	3.5	158.5	3.6	43.9	31.1	186.3	3.5																										
Leier-CAN-BC-1022ab-Spot 126	633	12913	4.2	20.2769	0.9	0.1760	2.3	0.0259	2.1	0.91	164.8	3.4	164.6	3.4	162.9	21.4	164.8	3.4																										
Leier-CAN-BC-1022ab-Spot 127	784	40716	2.2	20.2438	0.8	0.1706	1.9	0.0250	1.8	0.91	159.5	2.8	159.9	2.9	166.7	18.8	159.5	2.8																										
Leier-CAN-BC-1022ab-Spot 128	110	2135	3.7	22.1219	1.5	0.2225	3.1	0.0357	2.6	0.86	226.1	5.9	204.0	5.6	44.6	37.3	226.1	5.9																										
Leier-CAN-BC-1022ab-Spot 129	118	796	3.1	33.8054	7.3	0.0303	8.0	0.0074	3.2	0.40	47.6	1.5	30.3	2.4	1202.3	226.6	47.6	1.5																										
Leier-CAN-BC-1022ab-Spot 130	758	26443	2.0	20.4361	0.8	0.1688	2.0	0.0250	1.9	0.92	159.3	2.9	158.3	3.0	144.6	18.8	159.3	2.9																										
Leier-CAN-BC-1022ab-Spot 131	926	51892	1.9	20.3546	0.9	0.1662	2.0	0.0245	1.8	0.90	156.3	2.8	156.1	2.9	154.6	21.1	156.3	2.8																										
Leier-CAN-BC-1022ab-Spot 132	964	91079	1.8	19.9910	0.8	0.2015	2.2	0.0292	2.0	0.93	185.6	3.7	186.4	3.7	196.1	19.3	185.6	3.7																										
Leier-CAN-BC-1022ab-Spot 133	208	5313	1.3	21.3725	2.5	0.1635	3.3	0.0084	2.3	0.93	53.7	1.2	51.8	1.7	28.2	59.6	53.7	1.2																										
Leier-CAN-BC-1022ab-Spot 134	440	4251	1.4	20.425	1.8	0.0524	2.6	0.008	2.8	0.08	51.8	0.9	51.8	0.7	51.8	42.7	51.8	0.9																										
Leier-CAN-BC-1022ab-Spot 135	829	20845	2.2	20.2639	0.8	0.1728	2.3	0.0254	2.1	0.94	161.6	3.4	161.8	3.4	164.4	18.2	161.6	3.4																										
Leier-CAN-BC-1022ab-Spot 136	910	47103	2.0	20.2298	0.8	0.1704	2.2	0.0250	2.0	0.93	159.2	3.2	159.8	3.2	168.3	18.8	159.2	3.2																										
Leier-CAN-BC-1022ab-Spot 137	290	3090	1.1	22.3681	2.2	0.0489	2.9	0.0079	1.9	0.66	51.0	1.0	48.5	1.4	71.6	52.8	51.0	1.0																										
Leier-CAN-BC-1022ab-Spot 138	253	4291	1.6	20.7473	1.5	0.1656	2.5	0.0249	2.0	0.79	158.7	3.1	155.6	3.6	109.0	36.0	158.7	3.1																										
Leier-CAN-BC-1022ab-Spot 139	1443	522280	1.6	19.8954	0.7	0.1666	1.9	0.0240	1.8	0.93	153.1	2.7	156.4	2.7	207.2	16.1	153.1	2.7																										
Leier-CAN-BC-1022ab-Spot 140	303	4888	1.2	20.6495	2.7	0.1652	3.3	0.0247	1.8	0.54	157.5	2.8	155.2	4.7	120.2	64.5	157.5	2.8																										
Leier-CAN-BC-1022ab-Spot 141	650	23149	2.0	20.2077	1.1	0.1672	2.7	0.0245	2.4	0.91	156.1	3.8	157.0	3.9	170.9	28.6	156.1	3.8																										
Leier-CAN-BC-1022ab-Spot 142	229	4934	2.7	21.5000	1.1	0.1566	3.2	0.0244	2.4	0.75	155.4	3.7	147.6	4.4	24.2	50.9	155.4	3.7																										
Leier-CAN-BC-1022ab-Spot 143	334	10969	1.7	20.7282	1.2	0.1634	2.5	0.0246	2.3	0.89	156.4	3.5	153.7	3.6	111.2	27.3	156.4	3.5																										
Leier-CAN-BC-1022ab-Spot 144	117	1650	0.7	22.9879	3.9	0.0470	4.6	0.0078	2.6	0.55	50.4	1.3	48.7	2.1	138.8	95.6	50.4	1.3																										
Leier-CAN-BC-1022ab-Spot 145	352	22277	1.6	20.4317	1.0	0.1666	2.4	0.0247	2.1	0.90	157.2	3.3	156.4	3.4	145.1	24.2	157.2	3.3																										
Leier-CAN-BC-1022ab-Spot 146	341	28420	2.9	20.1576	1.2	0.2115	2.6	0.0309	2.3	0.89	196.3	4.5	194.8	4.7	176.7	28.3	196.3	4.5																										
Leier-CAN-BC-1022ab-Spot 147	599	16846	2.1	21.1627	1.6	0.0431	3.1	0.0066	2.6	0.85	42.5	1.1	42.8	1.3	62.1	39.1	42.5	1.1																										
Leier-CAN-BC-1022ab-Spot 148	237	3587	1.7	21.4732	1.3	0.1618	2.6	0.0252	2.3	0.87	160.5	3.6	152.3	3.7	27.2	30.7	160.5	3.6																										
Leier-CAN-BC-1022ab-Spot 149	227	6317	1.5	16.9068	1.8	0.1732	2.8	0.0261	2.1	0.75	166.4	3.6	166.2	3.6	572.5	40.4	166.4	3.6																										
Leier-CAN-BC-1022ab-Spot 150	433	11989	0.9	20.5895	0.8	0.1612	2.7	0.0241	2.2	0.82	153.3	3.3	151.7	3.8	127.2	36.4	153.3	3.3																										
Leier-CAN-BC-1022ab-Spot 151	609	4253	2.8	22.3975	1.8	0.0483	2.6	0.0079	1.9	0.74	50.4	1.0	47.9	1.2	74.8	42.9	50.4	1.0																										
Leier-CAN-BC-1022ab-Spot 152	671	40126	3.1	19.9133	1.2	0.1728	2.1	0.0250	1.7	0.82	158.9	2.7	161.8	3.2	205.1	27.7	158.9	2.7																										
Leier-CAN-BC-1022ab-Spot 153	577	72766	2.0	19.7600	0.7	0.1770	1.9	0.0254	1.7	0.92	161.4	2.8	165.4	2.9	223.0	16.8	161.4	2.8																										
Leier-CAN-BC-1022ab-Spot 154	175	64228	1.6	20.4248	1.7	0.1736	2.8	0.0257	2.2	0.79	163.6																																	

Sample: CANBC1022Gab	U-Pb geochronologic analyses										Isotope ratios										Apparent ages (Ma)									
	Analysis	U (ppm)	206Pb/204Pb	U/Tn	206Pb*/207Pb*	± (%)	207Pb*/235U*	± (%)	206Pb*/238U	± error	206Pb*/238U*	±	207Pb*/235U	±	206Pb*/207Pb*	±	Best age (Ma)	±	Best age (Ma)	±										
																					±	±	±	±	±	±	±	±	±	±
Leier-CAN-BC-1022ab-Spot 198	155	5720	1.9	19.3401	2.1	0.1813	3.6	0.0254	2.9	0.80	181.9	4.6	189.2	5.6	272.4	4.8	181.9	4.6												
Leier-CAN-BC-1022ab-Spot 199	117	7992	1.7	20.3475	1.9	0.1812	2.2	0.0244	1.9	0.89	155.2	3.0	151.7	3.1	97.7	3.7	155.2	3.0												
Leier-CAN-BC-1022ab-Spot 200	1097	47729	5.2	20.5720	0.9	0.0872	2.4	0.0145	2.3	0.93	92.6	2.1	94.2	2.2	129.1	20.7	92.6	2.1												
Leier-CAN-BC-1022ab-Spot 201	703	12285	1.8	19.4658	0.7	0.1797	2.1	0.0254	2.0	0.94	161.5	3.2	167.8	3.3	257.6	16.3	161.5	3.2												
Leier-CAN-BC-1022ab-Spot 202	1253	229584	1.9	20.3759	0.8	0.1808	2.4	0.0238	2.3	0.94	151.4	3.4	151.4	3.4	151.4	3.4	151.4	3.4												
Leier-CAN-BC-1022ab-Spot 203	442	3765	1.3	21.8066	1.9	0.0567	3.1	0.0090	2.4	0.79	57.5	1.4	56.0	1.7	9.8	45.1	57.5	1.4												
Leier-CAN-BC-1022ab-Spot 204	1353	267897	1.6	20.1316	0.8	0.1651	1.6	0.0241	1.5	0.89	153.5	2.2	155.1	2.4	179.7	17.8	153.5	2.2												
Leier-CAN-BC-1022ab-Spot 205	951	6035	1.7	21.3873	1.7	0.0446	2.3	0.0069	1.6	0.67	44.4	0.7	44.3	1.0	36.8	41.8	44.4	0.7												
Leier-CAN-BC-1022ab-Spot 206	645	76903	1.8	18.9415	1.2	0.1840	2.4	0.0263	2.1	0.87	160.9	3.3	171.5	3.8	320.0	26.8	160.9	3.3												
Leier-CAN-BC-1022ab-Spot 207	132	5752	2.0	21.3977	1.9	0.1791	3.1	0.0278	2.4	0.79	176.8	4.3	167.2	4.7	36.3	44.9	176.8	4.3												
Leier-CAN-BC-1022ab-Spot 208	617	21831	2.0	20.4011	1.1	0.1637	2.3	0.0242	2.0	0.86	154.3	3.0	153.9	3.3	148.8	25.9	154.3	3.0												
Leier-CAN-BC-1022ab-Spot 209	370	9188	0.8	20.3332	1.8	0.1680	2.6	0.0248	1.9	0.72	157.7	2.9	157.6	3.8	156.5	41.7	157.7	2.9												
Leier-CAN-BC-1022ab-Spot 210	154	4673	3.9	20.5345	2.8	0.1727	3.8	0.0257	2.5	0.66	163.7	4.1	161.7	5.7	133.4	66.6	163.7	4.1												
Leier-CAN-BC-1022ab-Spot 211	401	54871	1.1	20.3719	1.1	0.1653	2.6	0.0244	2.4	0.91	155.6	3.7	155.4	3.8	152.0	25.8	155.6	3.7												
Leier-CAN-BC-1022ab-Spot 212	995	33595	1.6	17.9569	1.7	0.1916	2.4	0.0250	1.7	0.70	158.9	2.6	178.0	3.9	440.0	38.1	158.9	2.6												
Leier-CAN-BC-1022ab-Spot 213	946	20273	1.9	19.8138	0.8	0.1840	1.8	0.0264	1.6	0.89	168.2	2.6	171.8	2.6	216.7	19.1	168.2	2.6												
Leier-CAN-BC-1022ab-Spot 214	332	14220	2.4	20.5413	1.3	0.1793	2.9	0.0267	2.6	0.89	169.9	4.3	167.5	4.4	132.5	30.4	169.9	4.3												
Leier-CAN-BC-1022ab-Spot 215	1673	32801	2.3	20.3620	0.8	0.1601	1.8	0.0236	1.6	0.89	150.8	2.4	150.8	2.6	153.2	19.9	150.8	2.4												
Leier-CAN-BC-1022ab-Spot 216	381	4683	2.2	22.5420	2.5	0.0459	3.1	0.0079	1.9	0.61	69.0	1.0	69.0	1.0	69.0	60.3	69.0	1.0												
Leier-CAN-BC-1022ab-Spot 217	1128	15423	1.3	18.5450	1.7	0.1860	2.9	0.0250	2.3	0.80	159.3	3.6	173.2	4.6	367.8	38.9	159.3	3.6												
Leier-CAN-BC-1022ab-Spot 218	248	8503	2.5	21.0549	2.6	0.0530	3.5	0.0081	2.3	0.67	52.0	1.2	52.5	1.8	74.2	61.9	52.0	1.2												
Leier-CAN-BC-1022ab-Spot 219	1270	21926	0.4	19.8868	0.8	0.1621	1.7	0.0234	1.5	0.90	148.9	2.3	152.5	2.4	208.1	17.6	148.9	2.3												
Leier-CAN-BC-1022ab-Spot 220	426	71472	1.1	20.4698	1.1	0.1635	2.6	0.0243	2.3	0.91	154.6	3.5	153.8	3.6	140.8	24.9	154.6	3.5												
Leier-CAN-BC-1022ab-Spot 221	967	84518	2.1	19.2667	0.8	0.1706	1.5	0.0238	1.4	0.87	151.8	2.0	159.9	2.3	281.2	17.2	151.8	2.0												
Leier-CAN-BC-1022ab-Spot 222	808	32017	2.2	20.3488	0.9	0.1728	2.2	0.0255	2.0	0.92	162.1	3.2	161.6	3.3	154.7	20.2	162.1	3.2												
Leier-CAN-BC-1022ab-Spot 223	359	27370	1.5	20.0763	1.1	0.1709	2.4	0.0249	2.2	0.90	158.4	3.4	160.1	3.6	186.1	24.6	158.4	3.4												
Leier-CAN-BC-1022ab-Spot 224	573	24037	2.5	19.9511	2.0	0.1855	2.1	0.0255	1.8	0.86	162.2	2.9	172.7	3.4	318.8	24.7	162.2	2.9												
Leier-CAN-BC-1022ab-Spot 225	200	22352	1.8	20.8400	2.0	0.1090	3.1	0.0165	2.3	0.75	105.3	2.4	105.1	3.1	98.4	47.8	105.3	2.4												
Leier-CAN-BC-1022ab-Spot 226	924	48219	1.8	19.3222	0.8	0.1815	2.3	0.0254	2.1	0.94	161.9	3.4	169.4	3.5	274.5	17.6	161.9	3.4												
Leier-CAN-BC-1022ab-Spot 227	964	33222	2.5	20.3876	0.9	0.1649	2.5	0.0244	2.4	0.93	155.3	3.6	155.0	3.6	150.2	21.9	155.3	3.6												
Leier-CAN-BC-1022ab-Spot 228	556	16319	5.8	20.5121	0.9	0.1193	2.1	0.0177	1.9	0.90	113.4	2.1	114.4	2.2	135.9	21.1	113.4	2.1												
Leier-CAN-BC-1022ab-Spot 229	237	30061	4.1	19.0089	1.4	0.2292	2.6	0.0316	2.2	0.84	200.6	4.3	209.5	4.9	311.9	31.7	200.6	4.3												
Leier-CAN-BC-1022ab-Spot 230	1747	27600	2.1	19.9440	0.8	0.1640	1.9	0.0237	1.7	0.94	151.1	2.6	154.2	2.7	201.5	15.0	151.1	2.6												
Leier-CAN-BC-1022ab-Spot 231	586	27385	1.7	20.0285	1.1	0.1657	2.1	0.0241	1.4	0.85	162.3	2.9	156.7	3.1	182.1	25.9	162.3	2.9												
Leier-CAN-BC-1022ab-Spot 232	4111	18934	2.8	20.3129	1.1	0.1785	2.0	0.0283	1.6	0.83	167.4	2.7	158.8	2.7	158.8	26.7	167.4	2.7												
Leier-CAN-BC-1022ab-Spot 233	555	23531	1.0	19.9722	0.8	0.1683	1.8	0.0244	1.6	0.90	155.3	2.5	158.0	2.7	188.2	18.7	155.3	2.5												
Leier-CAN-BC-1022ab-Spot 234	939	18775	2.0	20.8154	0.6	0.1714	1.8	0.0259	1.7	0.93	164.7	2.7	160.7	2.6	101.3	15.0	164.7	2.7												
Leier-CAN-BC-1022ab-Spot 235	572	10541	2.8	20.6962	0.9	0.1637	1.8	0.0246	1.6	0.86	156.5	2.4	153.9	2.6	114.8	21.7	156.5	2.4												
Leier-CAN-BC-1022ab-Spot 236	1019	54673	1.7	20.1066	0.9	0.1721	1.9	0.0251	1.7	0.89	159.7	2.7	161.2	2.8	182.6	20.0	159.7	2.7												
Leier-CAN-BC-1022ab-Spot 237	125	6439	1.3	20.8641	1.9	0.1678	2.9	0.0254	2.2	0.76	161.6	3.6	157.5	4.3	95.8	45.0	161.6	3.6												
Leier-CAN-BC-1022ab-Spot 238	257	10241	1.8	18.0518	4.8	0.2168	5.3	0.0252	3.3	0.43	160.7	3.6	199.3	9.5	684.4	101.5	160.7	3.6												
Leier-CAN-BC-1022ab-Spot 239	1141	124238	1.9	20.2248	0.8	0.1670	1.6	0.0245	1.4	0.89	156.0	2.2	156.8	2.4	169.0	17.8	156.0	2.2												
Leier-CAN-BC-1022ab-Spot 240	492	30344	1.3	19.7749	1.1	0.1719	2.2	0.0247	1.9	0.85	157.0	2.9	161.0	3.2	221.2	26.2	157.0	2.9												
Leier-CAN-BC-1022ab-Spot 241	130	12345	2.9	19.6719	1.6	0.1834	3.3	0.0282	2.9	0.87	166.5	4.8	170.9	5.2	233.3	37.1	166.5	4.8												
Leier-CAN-BC-1022ab-Spot 242	2135	98959	1.5	20.4003	0.7	0.1517	2.2	0.0220	2.1	0.95	140.6	2.9	143.4	2.9	160.3	15.5	140.6	2.9												
Leier-CAN-BC-1022ab-Spot 243	401	88112	1.9	19.5815	1.1	0.1814	2.6	0.0258	2.4	0.91	163.9	3.9	169.2	4.1	243.9	25.2	163.9	3.9												
Leier-CAN-BC-1022ab-Spot 244	514	3004	1.9	24.0996	1.9	0.0397	2.8	0.0069	2.1	0.75	44.5	0.9	39.5	1.1	257.1	47.1	44.5	0.9												
Leier-CAN-BC-1022ab-Spot 245	136	7417	2.0	20.3192	1.3	0.1715	3.3	0.0253	3.1	0.92	160.9	4.9	160.7	5.0	158.1	29.7	160.9	4.9												
Leier-CAN-BC-1022ab-Spot 246	541	6143	1.8	22.2819	1.4	0.0471	2.5	0.0076	2.0	0.83	48.9	1.0	46.8	1.1	62.2	33.9	48.9	1.0												
Leier-CAN-BC-1022ab-Spot 247	431	12141	4.6	20.8579	1.2	0.1782	2.4	0.0180	2.1	0.87	115.2	2.4	114.3	2.6	96.6	28.8	115.2	2.4												
Leier-CAN-BC-1022ab-Spot 248	561	41889	1.4	20.0632	1.0	0.1744	2.3	0.0250	2.0	0.90	161.6	3.2	163.3	3.4	187.6	23.0	161.6	3.2												
Leier-CAN-BC-1022ab-Spot 249	578	12619	1.9	20.5346	1.1	0.1683	2.2	0.0251	1.9	0.86	159.6	3.0	158.0	3.2	133.3	26.8	159.6	3.0												
Leier-CAN-BC-1022ab-Spot 250	384	86754	1.1	19.8710	0.9	0.1654	2.4	0.0238	2.2	0.93	151.9	3.3	155.5	3.4	210.0	20.5	151.9	3.3												
Leier-CAN-BC-1022ab-Spot 251	232	9677	1.1	20.7102	1.4	0.1647	2.8	0.0247	2.4	0.87	157.6	3.8	154.8	4.0	113.3	32.3	157.6	3.8												
Leier-CAN-BC-1022ab-Spot 252	948	238868	3.1	19.5262	1.0	0.1787	2.0	0.0253	1.7	0.86	161.1	2.7	166.9	3.1	250.4	23.5	161.1	2.7												
Leier-CAN-BC-1022ab-Spot 253	75	713	3.3	40.8472	22.3	0.0234	22.7	0.0069	3.7	0.17	44.6	1.7	23.4	5.2	1842.4	813.7	44.6	1.7												
Leier-CAN-BC-1022ab-Spot 254	422	10552	2.3	20.4306	1.0	0.1654	2.5	0.0245	2.2	0.91	156.1	3.5	155.4	3.6	145.2	23.8	156.1	3.5												
Leier-CAN-BC-1022ab-Spot 255	230	71267	3.5	19.3979	2.1	0.1778	3.1	0.0306	2.3	0.73	144.6	4.3	200.1	5.6	285.8	49.1	144.6	4.3												
Leier-CAN-BC-1022ab-Spot 256	412	19040	0.7	20.1981	0.9	0.1718	1.6	0.0252	1.3	0.82	160.2	2.1	161.0	2.4	172.0	21.1	160.2	2.1												
Leier-CAN-BC-1022ab-Spot																														

Sample: CANBC1022Gab		U-Pb geochronologic analyses																				
Analysis	U (ppm)	206Pb/204Pb	U/Tn	Isotope ratios							Apparent ages (Ma)							Best age (Ma)	± (Ma)			
				206Pb*/207Pb*	± (%)	207Pb*/235U*	± (%)	206Pb*/238U	± error corr.	206Pb*/238U*	± (Ma)	207Pb*/235U	± (Ma)	206Pb*/207Pb*	± (Ma)							
Leier-CAN-BC-1022ab-Spot 296	252	450974	2.7	19.6880	1.3	0.2162	2.9	0.0309	2.6	0.90	196.0	5.1	198.7	5.2	231.4	29.0	196.0	5.1				
Leier-CAN-BC-1022ab-Spot 297	144	3359	3.9	21.9231	1.8	0.1907	3.2	0.0303	2.7	0.83	192.8	5.1	177.3	5.2	23.7	43.0	192.8	5.1				
Leier-CAN-BC-1022ab-Spot 298	529	1847	0.4	11.9326	10.4	0.0954	11.0	0.0093	3.8	0.34	53.0	2.0	92.5	9.8	1289.0	202.4	53.0	2.0				
Leier-CAN-BC-1022ab-Spot 299	648	7508	2.9	21.3343	1.0	0.1587	2.5	0.0247	2.3	0.92	157.3	3.6	150.4	3.5	42.8	33.2	157.3	3.6				
Leier-CAN-BC-1022ab-Spot 300	178	32062	1.3	16.3913	2.0	0.2090	2.8	0.0249	1.9	0.68	168.2	3.0	192.7	4.9	639.5	44.0	168.2	3.0				
Leier-CAN-BC-1022ab-Spot 301	839	28062	2.0	20.5995	0.9	0.1669	1.9	0.0249	1.7	0.87	158.8	2.6	156.7	2.8	125.9	22.0	158.8	2.6				
Leier-CAN-BC-1022ab-Spot 302	796	16487	1.8	20.3733	0.9	0.1613	1.7	0.0238	1.5	0.84	151.8	2.2	151.8	2.4	151.8	21.7	151.8	2.2				
Leier-CAN-BC-1022ab-Spot 303	225	1674	0.8	24.7503	2.7	0.0460	3.5	0.0083	2.3	0.64	53.0	1.2	45.6	1.6	325.1	69.1	53.0	1.2				
Leier-CAN-BC-1022ab-Spot 304	119	2751	1.2	21.8994	5.5	0.0524	6.0	0.0083	2.6	0.42	53.4	1.4	51.8	3.1	20.1	132.5	53.4	1.4				
Leier-CAN-BC-1022ab-Spot 306	391	52376	2.1	19.9494	1.9	0.1705	2.9	0.0243	2.2	0.74	154.8	3.3	159.9	4.3	235.9	44.5	154.8	3.3				
Leier-CAN-BC-1022ab-Spot 307	220	117211	4.2	20.1800	1.4	0.2069	2.5	0.0303	2.0	0.82	192.3	3.9	190.9	4.3	174.1	33.4	192.3	3.9				
Leier-CAN-BC-1022ab-Spot 308	353	700755	3.1	19.5640	1.2	0.2101	2.2	0.0298	1.8	0.83	189.4	3.4	193.7	3.8	246.0	27.5	189.4	3.4				
Leier-CAN-BC-1022ab-Spot 309	926	25651	2.4	20.2942	0.9	0.1671	1.9	0.0246	1.7	0.89	156.6	2.6	156.9	2.8	161.0	20.4	156.6	2.6				
Leier-CAN-BC-1022ab-Spot 310	356	38002	2.0	20.0799	1.2	0.1621	1.9	0.0236	1.5	0.79	150.4	2.2	152.5	2.7	185.7	27.0	150.4	2.2				
Leier-CAN-BC-1022ab-Spot 311	1437	39762	1.9	20.3610	0.6	0.1647	2.1	0.0243	2.0	0.96	154.9	3.1	154.8	3.1	153.2	13.8	154.9	3.1				
Leier-CAN-BC-1022ab-Spot 312	206	31945	0.8	22.2403	2.7	0.0507	3.3	0.0092	2.0	0.59	52.6	1.0	50.3	1.6	57.6	65.8	52.6	1.0				
Leier-CAN-BC-1022ab-Spot 313	145	31167	1.7	20.4300	0.8	0.1659	1.8	0.0246	1.6	0.90	156.5	2.5	155.8	2.6	145.3	18.7	156.5	2.5				
Leier-CAN-BC-1022ab-Spot 314	516	11814	2.6	21.0088	1.1	0.1664	2.3	0.0254	2.1	0.85	161.4	3.3	156.3	3.4	79.4	26.3	161.4	3.3				
Leier-CAN-BC-1022ab-Spot 315	1339	162433	2.1	20.3117	0.5	0.1623	1.7	0.0239	1.6	0.95	152.3	2.4	152.7	2.4	158.9	12.1	152.3	2.4				

Sample: CANBC1023H	U-Pb geochronological analyses					Isotope ratios					Apparent ages (Ma)								
	Analysis	U	206Pb	U/Th	206Pb*	±	207Pb*	±	206Pb*	±	error	206Pb*	±	207Pb*	±	206Pb*	±	Best age	±
		(ppm)	204Pb	207Pb*	(%)		236U*		(%)		238U*	(%)		238U*		(Ma)		(Ma)	
Leier-CAN-BC-1023H_29Feb-Spot 1	3229	49156	1.0	20.6112	1.3	0.0526	2.1	0.0079	1.6	0.78	50.5	0.8	52.0	1.1	124.5	30.7	50.5	0.8	
Leier-CAN-BC-1023H_29Feb-Spot 2	319	7400	3.2	19.9848	3.3	0.0529	3.8	0.0077	1.8	0.48	49.2	0.9	52.3	1.9	196.8	76.9	49.2	0.9	
Leier-CAN-BC-1023H_29Feb-Spot 3	129	1284	1.1	24.1808	5.3	0.0455	5.8	0.0080	2.3	0.39	51.2	1.2	45.2	2.6	265.6	135.4	51.2	1.2	
Leier-CAN-BC-1023H_29Feb-Spot 4	105	4204	1.1	16.7536	3.2	0.0682	4.1	0.0083	2.6	0.62	53.2	1.4	66.9	2.7	592.3	70.2	53.2	1.4	
Leier-CAN-BC-1023H_29Feb-Spot 5	2779	17982	0.7	21.2274	0.8	0.0525	1.5	0.0081	1.2	0.83	51.9	0.6	52.0	0.8	54.8	20.1	51.9	0.6	
Leier-CAN-BC-1023H_29Feb-Spot 6	119	1223	1.7	19.9211	5.9	0.0785	6.5	0.0111	2.7	0.42	70.9	1.9	74.9	4.7	204.1	137.2	70.9	1.9	
Leier-CAN-BC-1023H_29Feb-Spot 7	314	2191	2.8	14.9637	6.2	0.0780	7.0	0.0095	3.2	0.45	54.3	1.7	76.2	5.1	832.5	130.1	54.3	1.7	
Leier-CAN-BC-1023H_29Feb-Spot 9	3849	9268	0.6	18.0137	2.4	0.0626	3.6	0.0082	2.7	0.75	52.5	1.4	61.7	2.2	432.9	52.9	52.5	1.4	
Leier-CAN-BC-1023H_29Feb-Spot 10	643	4551	1.0	20.1880	3.8	0.0533	4.3	0.0078	1.9	0.45	50.1	1.0	52.7	2.2	173.2	88.6	50.1	1.0	
Leier-CAN-BC-1023H_29Feb-Spot 12	307	2779	2.6	23.1601	2.2	0.0460	2.9	0.0077	1.9	0.67	49.6	1.0	45.6	1.3	157.3	53.5	49.6	1.0	
Leier-CAN-BC-1023H_29Feb-Spot 13	1420	9791	0.8	11.7969	4.6	0.0920	4.8	0.0079	1.2	0.25	50.5	0.6	89.4	4.1	1310.2	90.0	50.5	0.6	
Leier-CAN-BC-1023H_29Feb-Spot 14	403	7134	1.0	20.4220	1.8	0.0511	2.3	0.0078	2.1	0.76	48.6	1.0	50.6	1.4	146.3	43.1	48.6	1.0	
Leier-CAN-BC-1023H_29Feb-Spot 15	300	3756	0.8	21.3641	2.6	0.0501	3.2	0.0078	1.8	0.57	49.8	0.9	49.6	1.5	39.4	62.5	49.8	0.9	
Leier-CAN-BC-1023H_29Feb-Spot 16	990	74769	31.1	20.2492	1.5	0.0840	2.4	0.0084	1.8	0.78	80.3	1.1	63.0	1.4	166.1	34.8	80.3	1.1	
Leier-CAN-BC-1023H_29Feb-Spot 17	631	4617	3.7	21.1762	1.6	0.0520	2.2	0.0080	1.5	0.69	51.2	0.8	51.4	1.1	60.5	37.0	51.2	0.8	
Leier-CAN-BC-1023H_29Feb-Spot 18	3453	66893	0.5	21.0779	0.7	0.0528	1.5	0.0081	1.3	0.88	51.8	0.7	52.3	0.7	71.6	16.1	51.8	0.7	
Leier-CAN-BC-1023H_29Feb-Spot 19	793	15256	1.0	19.6483	1.9	0.0564	2.6	0.0080	1.8	0.69	51.6	0.9	55.7	1.4	236.1	43.2	51.6	0.9	
Leier-CAN-BC-1023H_29Feb-Spot 20	232	12981	1.4	20.1974	2.2	0.0539	3.3	0.0079	2.5	0.75	50.7	1.2	53.3	1.7	172.1	50.7	50.7	1.2	
Leier-CAN-BC-1023H_29Feb-Spot 21	2701	75679	0.8	21.2195	0.9	0.0525	1.8	0.0081	1.6	0.86	51.9	0.8	52.0	0.9	55.6	22.0	51.9	0.8	
Leier-CAN-BC-1023H_29Feb-Spot 22	2396	306198	0.7	20.8330	0.7	0.0534	1.6	0.0081	1.4	0.89	51.8	0.7	52.8	0.8	99.3	16.8	51.8	0.7	
Leier-CAN-BC-1023H_29Feb-Spot 23	504	513693	3.5	18.2024	2.0	0.0591	2.7	0.0078	1.8	0.66	50.1	0.9	58.3	1.5	409.7	45.1	50.1	0.9	
Leier-CAN-BC-1023H_29Feb-Spot 24	671	26458	1.9	17.6089	3.6	0.0633	4.0	0.0081	1.8	0.46	51.9	0.9	62.3	2.4	483.4	78.9	51.9	0.9	
Leier-CAN-BC-1023H_29Feb-Spot 25	277	18053	23.0	19.8260	2.2	0.0712	3.0	0.0102	2.0	0.67	65.6	1.3	69.8	2.0	215.3	51.8	65.6	1.3	
Leier-CAN-BC-1023H_29Feb-Spot 26	98	2976	1.2	21.6366	3.7	0.0496	4.5	0.0078	2.6	0.58	50.0	1.3	49.2	2.2	9.0	86.6	50.0	1.3	
Leier-CAN-BC-1023H_29Feb-Spot 27	122	7344	2.0	16.5284	3.9	0.0648	4.6	0.0078	2.4	0.53	49.9	1.2	63.8	2.8	621.6	83.3	49.9	1.2	
Leier-CAN-BC-1023H_29Feb-Spot 28	361	9638	0.5	21.2990	1.4	0.0507	2.6	0.0078	2.2	0.84	50.3	1.1	50.3	1.3	46.7	33.8	50.3	1.1	
Leier-CAN-BC-1023H_29Feb-Spot 29	577	10703	3.2	20.5954	1.5	0.0511	2.3	0.0076	1.7	0.75	49.0	0.8	50.6	1.1	126.4	35.7	49.0	0.8	
Leier-CAN-BC-1023H_29Feb-Spot 30	311	7107	3.1	20.8057	2.5	0.0583	3.5	0.0088	2.5	0.72	56.4	1.4	57.5	2.0	102.4	58.2	56.4	1.4	
Leier-CAN-BC-1023H_29Feb-Spot 31	400	13747	2.9	20.7884	1.5	0.0521	2.5	0.0078	1.9	0.78	50.4	1.0	51.5	1.2	104.4	36.5	50.4	1.0	
Leier-CAN-BC-1023H_29Feb-Spot 32	3255	50982	0.5	20.9198	0.7	0.0536	1.4	0.0081	1.2	0.86	52.2	0.6	53.0	0.7	89.5	17.1	52.2	0.6	
Leier-CAN-BC-1023H_29Feb-Spot 33	193	6535	1.8	19.8980	2.4	0.0542	3.4	0.0078	2.4	0.70	50.2	1.2	53.5	1.8	206.9	56.2	50.2	1.2	
Leier-CAN-BC-1023H_29Feb-Spot 34	3118	9241	0.7	19.3712	0.8	0.0571	1.8	0.0080	1.6	0.89	51.5	0.8	56.4	1.0	268.7	18.5	51.5	0.8	
Leier-CAN-BC-1023H_29Feb-Spot 35	2731	21053	0.1	20.7762	1.0	0.0529	1.9	0.0080	1.6	0.86	51.2	0.8	52.4	1.0	105.7	22.6	51.2	0.8	
Leier-CAN-BC-1023H_29Feb-Spot 36	380	4910	25.5	21.1016	2.1	0.0622	3.6	0.0095	2.9	0.80	61.1	1.8	61.3	2.1	69.9	50.6	61.1	1.8	
Leier-CAN-BC-1023H_29Feb-Spot 37	440	105695	2.7	19.7623	1.5	0.0553	2.3	0.0079	1.8	0.76	50.9	0.9	54.7	1.2	222.7	35.5	50.9	0.9	
Leier-CAN-BC-1023H_29Feb-Spot 38	495	11295	2.6	20.0038	2.9	0.0558	3.3	0.0081	1.5	0.46	51.9	0.8	55.1	1.7	194.6	67.3	51.9	0.8	
Leier-CAN-BC-1023H_29Feb-Spot 39	626	32947	0.9	18.5258	3.1	0.0600	3.5	0.0081	1.8	0.50	51.8	0.9	59.2	2.0	370.1	69.3	51.8	0.9	
Leier-CAN-BC-1023H_29Feb-Spot 40	347	3840	1.0	20.8538	1.6	0.0523	2.5	0.0079	1.9	0.78	50.8	1.0	51.8	1.3	96.9	37.2	50.8	1.0	
Leier-CAN-BC-1023H_29Feb-Spot 41	448	5801	2.8	14.3044	3.2	0.0803	3.9	0.0083	2.2	0.57	53.5	1.2	79.5	3.0	925.7	66.5	53.5	1.2	
Leier-CAN-BC-1023H_29Feb-Spot 42	627	34070	3.6	20.5138	1.1	0.0524	1.7	0.0078	1.2	0.75	50.1	0.6	51.9	0.8	135.7	25.7	50.1	0.6	
Leier-CAN-BC-1023H_29Feb-Spot 43	1654	512071	1.0	20.7195	0.9	0.0530	1.6	0.0080	1.4	0.85	51.2	0.7	52.5	0.8	112.2	20.3	51.2	0.7	
Leier-CAN-BC-1023H_29Feb-Spot 44	2003	74084	0.8	20.6086	1.1	0.0544	1.8	0.0081	1.4	0.78	52.2	0.7	53.7	0.9	124.8	26.0	52.2	0.7	
Leier-CAN-BC-1023H_29Feb-Spot 45	316	2568	1.7	22.0604	3.9	0.0481	4.3	0.0077	1.7	0.39	49.5	0.8	47.7	2.0	37.9	95.0	49.5	0.8	
Leier-CAN-BC-1023H_29Feb-Spot 46	2269	53946	0.6	21.0146	0.8	0.0531	1.6	0.0081	1.4	0.86	52.0	0.7	52.5	0.8	78.7	19.3	52.0	0.7	
Leier-CAN-BC-1023H_29Feb-Spot 47	2282	19399	1.4	21.2340	0.9	0.0526	1.6	0.0081	1.3	0.83	52.0	0.7	52.0	0.8	54.0	21.5	52.0	0.7	
Leier-CAN-BC-1023H_29Feb-Spot 49	1073	22726	0.4	20.8089	1.0	0.0544	1.6	0.0082	1.3	0.78	52.8	0.7	53.8	0.9	102.0	24.5	52.8	0.7	
Leier-CAN-BC-1023H_29Feb-Spot 50	146	121530	0.9	9.3743	0.5	3.8859	1.9	0.2642	1.9	0.97	1511.3	25.4	1610.8	15.7	1743.3	9.4	1743.3	9.4	
Leier-CAN-BC-1023H_29Feb-Spot 51	251	6670	0.7	19.8916	2.7	0.0569	3.2	0.0081	1.8	0.55	52.2	0.9	56.2	1.8	231.0	62.3	52.2	0.9	
Leier-CAN-BC-1023H_29Feb-Spot 52	2940	19301	0.7	21.8455	1.4	0.0518	4.3	0.0081	4.0	0.95	52.2	2.1	51.3	2.1	8.0	33.4	52.2	2.1	
Leier-CAN-BC-1023H_29Feb-Spot 53	397	7140	3.0	2.8565	19.1	0.3715	19.2	0.0077	1.7	0.09	49.4	0.8	320.8	52.8	370.7	29.3	49.4	0.8	
Leier-CAN-BC-1023H_29Feb-Spot 54	270	3454	1.3	14.5215	4.4	0.0789	4.8	0.0083	1.8	0.37	53.4	0.9	77.1	3.6	894.7	91.8	53.4	0.9	
Leier-CAN-BC-1023H_29Feb-Spot 55	605	14539	1.1	20.1407	1.1	0.0560	2.0	0.0082	1.7	0.85	52.5	0.9	55.3	1.1	178.7	24.5	52.5	0.9	
Leier-CAN-BC-1023H_29Feb-Spot 56	294	6984	3.3	19.3390	3.5	0.0564	4.1	0.0079	2.2	0.53	50.8	1.1	55.7	2.2	272.5	80.6	50.8	1.1	
Leier-CAN-BC-1023H_29Feb-Spot 58	72	1760	3.4	20.8834	9.5	0.0611	9.9	0.0093	2.8	0.28	59.4	1.6	60.2	5.8	93.6	224.7	59.4	1.6	
Leier-CAN-BC-1023H_29Feb-Spot 59	3767	47879	0.8	20.8906	0.8	0.0541	1.4	0.0082	1.1	0.82	52.6	0.6	53.5	0.7	92.8	18.6	52.6	0.6	
Leier-CAN-BC-1023H_29Feb-Spot 60	761	144946	4.2	19.7907	0.7	0.1886	1.8	0.0271	1.6	0.91	172.2	2.8	175.5	2.9	219.4	17.1	172.2	2.8	
Leier-CAN-BC-1023H_29Feb-Spot 61	728	8411	1.3	21.2339	1.5	0.0524	2.2	0.0081	1.6	0.74	51.8	0.8	51.8	1.1	54.0	34.9	51.8	0.8	
Leier-CAN-BC-1023H_29Feb-Spot 62	192	4405	1.9	20.7337	2.6	0.0542	3.3	0.0082	2.1	0.64	52.3	1.1	53.6	1.7	110.6	60.6	52.3	1.1	
Leier-CAN-BC-1023H_29Feb-Spot 63	461	10708	1.0	15.2992	2.1	0.0755	2.4	0.0084	1.1	0.45	53.8	0.6	73.9	1.7	786.0	44.6	53.8	0.6	
Leier-CAN-BC-1023H_29Feb-Spot 64	179	28587	1.5	19.6833	2.7	0.0574	3.4	0.0082	2.1	0.61	52.6	1.1	56.7	1.9	231.9	61.9	52.6	1.1	
Leier-CAN-BC-1023H_29Feb-Spot 65	60	523	1.3	5.7036	23.3	0.2099	23.6	0.0087	3.9	0.17	55.7	2.2	193.5	41.6	2609.2	393.3	55.7	2.2	
Leier-CAN-BC-1023H_29Feb-Spot 66	153	1663	1.6	14.2911	9.4	0.0777	9.9	0.0081	3.0	0.31	51.7	1.6							

Sample: CANBC1023H	U-Pb geochronologic analyses										Isotope ratios					Apparent ages (Ma)															
	U		206Pb		U/Th		206Pb*		±		207Pb*		±		206Pb*		±		207Pb*		±		Best age		±						
	(ppm)	204Pb					(%)	235U*	(%)	238U	(%)	corr.	238U*	(Ma)	235U	(Ma)	238U*	(Ma)	235U	(Ma)	238U*	(Ma)	235U	(Ma)	238U*	(Ma)					
Leier-CAN-BC-1023H_29Feb-Spot 88	284	1987	3.0	22.0787	3.5	0.0492	4.1	0.0079	2.0	0.50	50.5	1.0	48.7	1.9	39.9	85.7	50.5	1.0	48.7	1.9	39.9	85.7	50.5	1.0	48.7	1.9	39.9	85.7	50.5	1.0	
Leier-CAN-BC-1023H_29Feb-Spot 89	683	4818	0.4	21.9275	1.6	0.0504	2.2	0.0080	1.5	0.67	51.5	0.8	49.9	1.1	23.2	39.0	51.5	0.8	49.9	1.1	23.2	39.0	51.5	0.8	49.9	1.1	23.2	39.0	51.5	0.8	
Leier-CAN-BC-1023H_29Feb-Spot 90	504	23318	30.1	20.5876	1.3	0.0669	2.4	0.0100	2.0	0.84	64.0	1.3	65.7	1.5	127.3	30.2	64.0	1.3	65.7	1.5	127.3	30.2	64.0	1.3	65.7	1.5	127.3	30.2	64.0	1.3	
Leier-CAN-BC-1023H_29Feb-Spot 91	3606	38137	0.6	20.7153	0.7	0.0546	1.4	0.0082	1.2	0.88	52.6	0.7	53.9	0.7	112.7	15.8	52.6	0.7	53.9	0.7	112.7	15.8	52.6	0.7	53.9	0.7	112.7	15.8	52.6	0.7	
Leier-CAN-BC-1023H_29Feb-Spot 92	3665	57074	0.5	21.1750	0.7	0.0528	1.4	0.0081	1.2	0.86	52.0	0.6	52.2	0.7	60.7	17.6	52.0	0.6	52.2	0.7	60.7	17.6	52.0	0.6	52.2	0.7	60.7	17.6	52.0	0.6	
Leier-CAN-BC-1023H_29Feb-Spot 93	144	390	0.3	6.5181	1.4	0.2134	2.7	0.0101	2.3	0.86	64.7	1.5	196.4	4.8	2384.4	23.0	64.7	1.5	196.4	4.8	2384.4	23.0	64.7	1.5	196.4	4.8	2384.4	23.0	64.7	1.5	
Leier-CAN-BC-1023H_29Feb-Spot 94	1529	16095	0.7	21.0887	1.1	0.0499	1.5	0.0078	1.1	0.71	49.0	0.5	49.4	0.7	70.4	26.0	49.0	0.5	49.4	0.7	70.4	26.0	49.0	0.5	49.4	0.7	70.4	26.0	49.0	0.5	
Leier-CAN-BC-1023H_29Feb-Spot 95	1600	81846	1.0	20.4579	1.8	0.0508	3.4	0.0075	2.9	0.85	48.4	1.4	50.3	1.7	142.1	43.0	48.4	1.4	50.3	1.7	142.1	43.0	48.4	1.4	50.3	1.7	142.1	43.0	48.4	1.4	
Leier-CAN-BC-1023H_29Feb-Spot 96	329	3702	3.9	19.0472	3.4	0.0579	4.1	0.0080	2.3	0.53	51.4	1.1	57.2	2.3	307.3	78.4	51.4	1.1	57.2	2.3	307.3	78.4	51.4	1.1	57.2	2.3	307.3	78.4	51.4	1.1	
Leier-CAN-BC-1023H_29Feb-Spot 97	31	276	1.1	70.9367	34.4	0.0146	34.7	0.0075	4.4	0.13	48.2	2.1	14.7	5.1	0.0	1164.9	48.2	2.1	14.7	5.1	0.0	1164.9	48.2	2.1	14.7	5.1	0.0	1164.9	48.2	2.1	2.1
Leier-CAN-BC-1023H_29Feb-Spot 98	456	27999	2.8	19.0172	2.5	0.0575	3.1	0.0079	2.0	0.62	50.9	1.0	56.7	1.7	310.9	55.9	50.9	1.0	56.7	1.7	310.9	55.9	50.9	1.0	56.7	1.7	310.9	55.9	50.9	1.0	
Leier-CAN-BC-1023H_29Feb-Spot 99	358	3874	2.4	21.3798	1.8	0.0515	2.8	0.0080	2.2	0.77	51.2	1.1	50.9	1.4	37.6	42.6	51.2	1.1	50.9	1.4	37.6	42.6	51.2	1.1	50.9	1.4	37.6	42.6	51.2	1.1	
Leier-CAN-BC-1023H_29Feb-Spot 100	2177	26243	0.9	20.8885	0.7	0.0528	1.8	0.0080	1.6	0.93	51.4	0.8	52.3	0.9	93.0	15.7	51.4	0.8	52.3	0.9	93.0	15.7	51.4	0.8	52.3	0.9	93.0	15.7	51.4	0.8	
Leier-CAN-BC-1023H_29Feb-Spot 101	3572	6949	0.8	18.0826	2.5	0.0627	2.9	0.0062	1.5	0.52	52.8	0.8	61.7	1.7	424.4	55.3	52.8	0.8	61.7	1.7	424.4	55.3	52.8	0.8	61.7	1.7	424.4	55.3	52.8	0.8	
Leier-CAN-BC-1023H_29Feb-Spot 102	324	1822	3.8	25.0492	2.2	0.0430	2.8	0.0078	1.7	0.62	50.1	0.9	42.7	1.2	356.0	56.0	50.1	0.9	42.7	1.2	356.0	56.0	50.1	0.9	42.7	1.2	356.0	56.0	50.1	0.9	
Leier-CAN-BC-1023H_29Feb-Spot 103	1257	40834	0.9	20.1200	1.8	0.0550	2.2	0.0080	1.2	0.57	51.5	0.6	54.4	1.1	181.0	41.2	51.5	0.6	54.4	1.1	181.0	41.2	51.5	0.6	54.4	1.1	181.0	41.2	51.5	0.6	
Leier-CAN-BC-1023H_29Feb-Spot 104	33	511	0.9	22.5935	18.2	0.0480	18.7	0.0079	4.1	0.22	50.5	2.1	47.6	8.7	96.2	450.0	50.5	2.1	47.6	8.7	96.2	450.0	50.5	2.1	47.6	8.7	96.2	450.0	50.5	2.1	
Leier-CAN-BC-1023H_29Feb-Spot 105	208	4519	1.3	21.7675	4.1	0.0501	4.7	0.0079	2.2	0.46	50.8	1.1	49.6	2.3	5.5	99.8	50.8	1.1	49.6	2.3	5.5	99.8	50.8	1.1	49.6	2.3	5.5	99.8	50.8	1.1	
Leier-CAN-BC-1023H_29Feb-Spot 106	2883	19224	0.9	21.3188	0.7	0.0525	1.6	0.0081	1.5	0.92	52.1	0.8	52.0	0.8	44.5	15.6	52.1	0.8	52.0	0.8	44.5	15.6	52.1	0.8	52.0	0.8	44.5	15.6	52.1	0.8	
Leier-CAN-BC-1023H_29Feb-Spot 107	1094	59517	0.7	21.0089	1.0	0.0535	1.9	0.0081	1.7	0.87	52.3	0.9	52.9	1.0	79.4	22.9	52.3	0.9	52.9	1.0	79.4	22.9	52.3	0.9	52.9	1.0	79.4	22.9	52.3	0.9	
Leier-CAN-BC-1023H_29Feb-Spot 108	156	5745	1.6	21.6042	3.0	0.0512	3.9	0.0080	2.4	0.62	51.5	1.2	50.7	1.9	12.6	72.8	51.5	1.2	50.7	1.9	12.6	72.8	51.5	1.2	50.7	1.9	12.6	72.8	51.5	1.2	
Leier-CAN-BC-1023H_29Feb-Spot 109	1807	30018	0.7	20.9664	0.9	0.0532	1.7	0.0081	1.5	0.85	51.9	0.8	52.6	0.9	84.2	21.5	51.9	0.8	52.6	0.9	84.2	21.5	51.9	0.8	52.6	0.9	84.2	21.5	51.9	0.8	
Leier-CAN-BC-1023H_29Feb-Spot 110	60	11535	0.9	19.7288	3.3	0.0565	4.1	0.0081	2.5	0.60	51.9	1.3	55.8	2.2	226.6	76.4	51.9	1.3	55.8	2.2	226.6	76.4	51.9	1.3	55.8	2.2	226.6	76.4	51.9	1.3	

APPENDIX G

ARIZONA LASERCHRON CENTER DETRITAL ZIRCON HF ANALYSES DATA TABLE

Table x. Hf Isotopic Data													
Sample	Sample Location	Analysis	$^{176}\text{Yb} + ^{176}\text{Lu}/^{176}\text{Hf}$ (%)	Volts Hf	$^{176}\text{Hf}/^{177}\text{Hf}$	$\pm (1\sigma)$	$^{176}\text{Lu}/^{177}\text{Hf}$	$^{176}\text{Hf}/^{177}\text{Hf}$ (T)	E-Hf (0)	E-Hf (0) $\pm (1\sigma)$	E-Hf (T)	Age (Ma)	
CAN-BC-1022Gab	Merritt, BC	CAN-BC-1022ab 196	73.56891291	1.637648134	0.282974104	4.31577E-05	0.003567	0.282970953	6.687206238	1.526166463	7.626315871	47.3	
CAN-BC-1022Gab	Merritt, BC	CAN-BC-1022ab 151	19.2558974	2.386800578	0.282842651	3.8381E-05	0.000693	0.282841744	2.038695697	1.35724858	3.125547051	50.4	
CAN-BC-1022Gab	Merritt, BC	CAN-BC-1022ab 312	14.5572636	2.623672455	0.282684679	3.7038E-05	0.000694	0.282683997	-3.547600121	1.309759012	-2.404582775	52.6	
CAN-BC-1022Gab	Merritt, BC	CAN-BC-1022ab 246	102.5947067	1.377545556	0.28307924	7.70676E-05	0.004600	0.283075038	10.40506393	2.725308508	11.34299032	48.9	
CAN-BC-1022Gab	Merritt, BC	CAN-BC-1022ab 115	13.60827141	2.633529255	0.282865314	4.14615E-05	0.000866	0.282864513	2.840103138	1.466184472	3.910788841	49.5	
CAN-BC-1022Gab	Merritt, BC	CAN-BC-1022ab 205	7.557462546	3.377613578	0.283111075	3.47382E-05	0.000486	0.283110671	11.53083046	1.228433082	12.50315672	44.4	
CAN-BC-1022Gab	Merritt, BC	CAN-BC-1022ab 215	20.19015323	2.808153674	0.282881112	2.68729E-05	0.001287	0.282877488	3.398776362	0.950292921	6.618328367	150.6	
CAN-BC-1022Gab	Merritt, BC	CAN-BC-1022ab 96	25.08439669	2.156002453	0.282833356	4.63499E-05	0.001260	0.28282975	1.70997488	1.639050531	4.985294158	153.1	
CAN-BC-1022Gab	Merritt, BC	CAN-BC-1022ab 20	29.22043802	1.937530657	0.282850838	5.65468E-05	0.001517	0.28284647	2.328186921	1.999638862	5.596796363	154	
CAN-BC-1022Gab	Merritt, BC	CAN-BC-1022ab 208	27.32721246	2.211798434	0.282835273	4.52784E-05	0.001628	0.282831033	1.793953527	1.601158358	5.057413391	154.3	
CAN-BC-1022Gab	Merritt, BC	CAN-BC-1022ab 311	18.60028998	2.671077619	0.282837262	4.67071E-05	0.001163	0.282833894	1.848109331	1.651684139	5.171988678	154.9	
CAN-BC-1022Gab	Merritt, BC	CAN-BC-1022ab 227	50.49423453	2.525739261	0.282804955	3.42555E-05	0.003182	0.282795715	0.705675479	1.21136361	3.830312658	155.3	
CAN-BC-1022Gab	Merritt, BC	CAN-BC-1022ab 95	25.91195205	2.8684763	0.282910162	3.51055E-05	0.001623	0.282905427	4.426048925	1.241418442	7.726936066	156	
CAN-BC-1022Gab	Merritt, BC	CAN-BC-1022ab 309	17.14849993	2.449109562	0.283032219	3.8893E-05	0.001075	0.283029073	8.742312771	1.375356147	12.11426655	156.6	
CAN-BC-1022Gab	Merritt, BC	CAN-BC-1022ab 194	12.04304258	2.731465691	0.282869765	3.69108E-05	0.000744	0.282867573	2.997514421	1.30526175	6.423476317	157.6	
CAN-BC-1022Gab	Merritt, BC	CAN-BC-1022g ab 209	77.85312508	1.172115131	0.282810542	6.4659E-05	0.003846	0.282799201	0.90323127	2.286509083	4.007050373	157.7	
CAN-BC-1022Gab	Merritt, BC	CAN-BC-1022g ab 267	25.45245224	1.703667918	0.282879504	4.72731E-05	0.001507	0.282874187	3.341898406	1.671699008	7.35034416	188.7	
CAN-BC-1022Gab	Merritt, BC	CAN-BC-1022g ab 265	32.22968942	1.400714633	0.283056526	5.84102E-05	0.001690	0.283050564	9.601862524	2.065532944	13.59008711	188.7	
CAN-BC-1022Gab	Merritt, BC	CAN-BC-1022g ab 124	22.27263104	1.571019539	0.283015078	4.69897E-05	0.001266	0.28301057	8.136142935	1.661676785	12.21090288	190.3	
CAN-BC-1022Gab	Merritt, BC	CAN-BC-1022g ab 57	20.99915151	1.662261842	0.283001411	5.31532E-05	0.001232	0.282996925	7.652850087	1.879632722	11.82628811	194.7	
CAN-BC-1022Gab	Merritt, BC	CAN-BC-1022g ab 30	12.47978547	1.730181642	0.282977411	5.21758E-05	0.000766	0.282974598	6.804149476	1.845070812	11.06986212	196.2	
CAN-BC-1022Gab	Merritt, BC	CAN-BC-1022g ab 31	11.06688675	1.432498997	0.282982249	5.35692E-05	0.000611	0.282980004	6.975216269	1.89434258	11.26557765	196.4	
CAN-BC-1023H	Kelowna, BC	CAN-BC-1023H 45	55.57592374	2.726995524	0.283083409	4.23333E-05	0.002811057	0.28308081	10.55250132	1.497013553	11.56044482	49.5	
CAN-BC-1023H	Kelowna, BC	CAN-BC-1023H 15	52.12429209	2.094197646	0.28272474	4.8039E-05	0.002538031	0.282722379	-2.130964423	1.698780955	-1.109328719	49.8	
CAN-BC-1023H	Kelowna, BC	CAN-BC-1023H 28	57.85698356	1.641222386	0.28251242	5.34993E-05	0.002877121	0.282509717	-9.639109343	1.891871878	-8.619315927	50.3	
CAN-BC-1023H	Kelowna, BC	CAN-BC-1023H 88	13.47577274	3.344640791	0.283017776	2.89231E-05	0.000724985	0.283017092	8.231542772	1.022794191	9.329192904	50.5	
CAN-BC-1023H	Kelowna, BC	CAN-BC-1023H 17	14.76979541	3.316378813	0.283098689	3.21651E-05	0.000826381	0.283097899	11.09286124	1.137441502	12.20263097	51.2	
CAN-BC-1023H	Kelowna, BC	CAN-BC-1023H 85	105.6138283	1.424051097	0.282593515	6.34806E-05	0.005161735	0.282588549	-6.771414736	2.24483776	-5.804675973	51.5	
CAN-BC-1023H	Kelowna, BC	CAN-BC-1023H 73	62.12190055	2.274192023	0.282515831	4.60121E-05	0.00282905	0.282513094	-9.518487692	1.627103809	-8.466605902	51.8	
CAN-BC-1023H	Kelowna, BC	CAN-BC-1023H 61	55.7305908	1.963650904	0.28256725	4.40721E-05	0.00268805	0.282564649	-7.700210092	1.558501541	-6.643294241	51.8	
CAN-BC-1023H	Kelowna, BC	CAN-BC-1023H 21	72.4443502	2.687747525	0.282561168	3.82821E-05	0.0034716	0.282557803	-7.915254216	1.353751745	-6.883186262	51.9	
CAN-BC-1023H	Kelowna, BC	CAN-BC-1023H 5	27.30474548	3.712557813	0.282567142	4.18586E-05	0.001210395	0.282565968	-7.704020418	1.480227634	-6.594400635	51.9	
CAN-BC-1023H	Kelowna, BC	CAN-BC-1023H 47	73.49813507	1.826025808	0.282518343	5.01908E-05	0.003524183	0.28251492	-9.429670969	1.774875868	-8.397594383	52	
CAN-BC-1023H	Kelowna, BC	CAN-BC-1023H 92	61.54456271	2.92222493	0.28247241	2.92732E-05	0.002996552	0.282469499	-11.05399561	1.035173691	-10.00398131	52	
CAN-BC-1023H	Kelowna, BC	CAN-BC-1023H 84	26.86432258	3.266651303	0.282537268	2.75263E-05	0.001334836	0.282535969	-8.760448353	0.973401223	-7.65095521	52.1	
CAN-BC-1023H	Kelowna, BC	CAN-BC-1023H 106	88.20103551	1.469431824	0.282691291	5.26492E-05	0.004117739	0.282687284	-3.313773565	1.861808699	-2.299432811	52.1	
CAN-BC-1023H	Kelowna, BC	CAN-BC-1023H 83	35.84692203	2.172026997	0.282576628	3.9217E-05	0.001767536	0.282574894	-7.368580632	1.38681256	-6.26540906	52.5	

Table x. Hf Isotopic Data

Sample	Sample Location	Analysis	$(^{176}\text{Yb} + ^{176}\text{Lu})/^{176}\text{Hf}$ (%)	Volts Hf	$^{176}\text{Hf}/^{177}\text{Hf}$	$\pm (1\sigma)$	$^{176}\text{Lu}/^{177}\text{Hf}$	$^{176}\text{Hf}/^{177}\text{Hf}$ (T)	E-Hf (0)	E-Hf (0) $\pm (1\sigma)$	E-Hf (T)	Age (Ma)
15Ca01B	Republic, WA	15CA-01B 178	14.31962322	2.712094618	0.28230172	3.02049E-05	0.000768678	0.28230101	-17.09003009	1.068120932	-16.02050513	49.4
15Ca01B	Republic, WA	15CA-01B 299	37.35265325	2.621034033	0.282340499	3.67436E-05	0.001847991	0.282338786	-15.71870769	1.299346488	-14.68006357	49.6
15Ca01B	Republic, WA	15CA-01B 158	22.53975074	2.393744546	0.282378166	3.4093E-05	0.001214224	0.282377028	-14.38668576	1.205614373	-13.31430458	50.2
15Ca01B	Republic, WA	15CA-01B 284	15.59539547	2.682224683	0.282437566	3.83065E-05	0.000804547	0.282436807	-12.28616176	1.354614866	-11.1934657	50.5
15Ca01B	Republic, WA	15CA-01B 13	19.07127027	2.444246909	0.282311291	3.53117E-05	0.000986033	0.282310354	-16.75155611	1.248710647	-15.65680691	50.9
15Ca01B	Republic, WA	15CA-01B 278	13.54372383	2.897911275	0.282377573	3.51108E-05	0.000700552	0.282376907	-14.40766414	1.241606971	-13.30305086	50.9
15Ca01B	Republic, WA	15CA-01B 147	23.28456248	2.46266638	0.282448832	3.54755E-05	0.001185079	0.282447701	-11.88774332	1.254503165	-10.79485754	51.1
15Ca01B	Republic, WA	15CA-01B 217	27.78228284	2.990645452	0.282425682	3.6562E-05	0.001294129	0.282424435	-12.7064004	1.292924347	-11.60662568	51.6
15Ca01B	Republic, WA	15CA-01B 104	21.38884166	2.661601719	0.282397612	3.17217E-05	0.001136708	0.282396515	-13.69901637	1.121759111	-12.59184642	51.7
15Ca01B	Republic, WA	15CA-01B 192	8.308620976	3.001504135	0.282380823	3.99441E-05	0.000437861	0.282380397	-14.29274057	1.412523931	-13.15520389	52
15Ca01B	Republic, WA	15CA-01B 99	20.55178171	2.462321684	0.282357568	3.70365E-05	0.001385335	0.28235622	-15.11509361	1.309705634	-14.00807341	52.1
15Ca01B	Republic, WA	15CA-01B 277	19.06869423	2.634105396	0.282431074	3.21475E-05	0.001030497	0.282430071	-12.51572528	1.136818252	-11.39619164	52.1
15Ca01B	Republic, WA	15CA-01B 44	19.19061731	2.425486911	0.282375636	3.71225E-05	0.000995816	0.282374657	-14.47616654	1.31274819	-13.34490606	52.6
15Ca01B	Republic, WA	15CA-01B 57	16.67263379	2.939751644	0.28229673	3.12659E-05	0.000877117	0.282295868	-17.26646981	1.105643376	-16.13141046	52.6
15Ca01B	Republic, WA	15CA-01B 75	13.35114549	2.947196139	0.282331432	3.17636E-05	0.000712901	0.282330726	-16.0393263	1.123240952	-14.88973598	53
15Ca03A	Republic, WA	15-CA-03A 59	15.64886634	2.657568978	0.282966077	4.2174E-05	0.00086773	0.282965259	6.403349342	1.49138188	7.496032524	50.5
15Ca03A	Republic, WA	15-CA-03A 70	19.05356113	2.079740272	0.282434153	4.04787E-05	0.001015728	0.282433193	-12.40683989	1.431428913	-11.31905144	50.6
15Ca03A	Republic, WA	15-CA-03A 25	35.08938913	2.283014565	0.282309445	3.94247E-05	0.001761086	0.282307777	-16.81683294	1.394159264	-15.75235378	50.7
15Ca03A	Republic, WA	15-CA-03A 150	17.83916846	2.429950689	0.282425436	4.83537E-05	0.000989773	0.282424499	-12.7150958	1.70991084	-11.6243217	50.7
15Ca03A	Republic, WA	15-CA-03A 242	11.7599072	1.975032411	0.282358015	3.95858E-05	0.000675007	0.282357375	-15.0992757	1.399855351	-13.99605457	50.8
15Ca03A	Republic, WA	15-CA-03A 202	16.40144028	2.154617782	0.282422783	4.05646E-05	0.000821436	0.282422001	-12.80890459	1.434466262	-11.70601158	51
15Ca03A	Republic, WA	15-CA-03A 65	25.79938025	1.870472533	0.282405138	5.80335E-05	0.001243812	0.282403951	-13.43288892	2.052211708	-12.34216108	51.1
15Ca03A	Republic, WA	15-CA-03A 13	23.49325552	1.436856051	0.282497691	4.73552E-05	0.001357406	0.282496393	-10.15998185	1.674599617	-9.070588395	51.2
15Ca03A	Republic, WA	15-CA-03A 28	14.32650675	2.280272727	0.282367899	4.10285E-05	0.000796372	0.282367135	-14.74977351	1.450871498	-13.63976064	51.3
15Ca03A	Republic, WA	15-CA-03A 255	18.5233956	1.740815009	0.282446126	4.58089E-05	0.000922663	0.282445245	-11.98345662	1.619920626	-10.88172329	51.1
15Ca03A	Republic, WA	15-CA-03A 203	16.81555662	2.272168929	0.282397668	3.20155E-05	0.000926834	0.282396764	-13.69704937	1.13215141	-12.57192776	52.2
15Ca03A	Republic, WA	15-CA-03A 258	19.04916487	1.96331332	0.282510301	4.69299E-05	0.001089666	0.282509237	-9.714042412	1.659560533	-8.591927593	52.3
15Ca03A	Republic, WA	15-CA-03A 98	16.90444681	2.164259612	0.282363583	4.19585E-05	0.000934467	0.282362669	-14.9023657	1.483760568	-13.77333508	52.4
15Ca03A	Republic, WA	15-CA-03A 66	23.52794527	2.382702666	0.282363744	4.22487E-05	0.001242328	0.282362526	-14.89667489	1.49402248	-13.77616506	52.5
15Ca03A	Republic, WA	15-CA-03A 84	10.48754274	3.050401204	0.282529108	4.07485E-05	0.000513643	0.282528536	-9.048992061	1.440971505	-7.747375742	59.6

APPENDIX H

DETRITAL ZIRCON U-PB

MAXIMUM DEPOSITIONAL AGE DATA AND GRAPHS

Sample	Location	Analysis	Age	2 σ
15CA01B	Republic, WA	ALC	46.8	2.1
			47.1	2.2
			47.2	1.6
15Ca 03A	Republic, WA	ALC	46.4	1.7
			47.6	1.6
			47.6	1.9
15Ca04A	Republic, WA	CEMS	48.1	1.8
			50.9	1.75
			51.2	0.7
CAN-BC-1024K	Midway, BC	CEMS	48.5	1
			49.4	1.1
			49.5	1
CAN-BC-1024L	Midway, BC	CEMS	52.1	0.95
			52.4	1.25
			52.5	1.25
WLR1	White Lake, BC	CEMS	46.1	1.4
			46.2	1.5
			47.2	1.7
WLR2	White Lake, BC	CEMS	45.5	1.05
			45.9	1.1
			46.7	0.95
SKEL1	Summerland, BC	CEMS	50.6	0.85
			51.4	1.05
			51.5	0.75
SKEL2	Summerland, BC	CEMS	47.8	1.6
			48.9	1.5
			49.1	1.4

Sample	Location	Analysis	Age	2σ
CAN-BC-1024H	Kelowna, BC	ALC	48.2	2.1
			48.4	1.4
			48.6	1.0
SAWMILL1	Kelowna, BC	CEMS	49.4	1.35
			50.2	1.3
			51.2	1.75
15Ca18A	Kelowna, BC	CEMS	50	1.25
			50.1	1.2
			50.2	1.1
PB2	Princeton, BC	CEMS	140.9	2.6
			142.5	2.4
			143	1.85
15CAN10B	Princeton, BC	CEMS	52.6	0.7
			52.9	0.65
15Ca15A	Princeton, BC	CEMS	50.1	1.15
			53.3	1.35
			53.9	2.4
PRINCE1A	Princeton, BC	CEMS	85.5	1.45
			85.9	1.85
15Ca13B	Blakeburn, BC	CEMS	45.7	1.2
			46.1	1.2
			46.8	1.2
ABBEYRD2	Kamloops, BC	CEMS	47	1.1
			47.1	1.45
			47.5	1
15Ca23B	McAbee, BC	CEMS	48	1.4
			48.8	1.65
			49.4	1.6
CAN-BC-1022Gab	Merritt, BC	ALC	42.5	1.1
			43.3	1.0
			44.1	0.9
CAN-BC-1022Gbb	Merritt, BC	CEMS	42.8	0.9
			43.3	1
COLDWATER1	Coldwater, BC	CEMS	49.3	1.15
			50.1	1.25
			51.5	1.05

